AGRICULTURAL RESEARCH INSTITUTE
PUSA

PROCEEDINGS

OF THE

INDIAN ACADEMY OF SCIENCES

VOL. XXIV

SECTION A

BANGALORE CITY
PRINTED AT THE BANGALORE PRESS, MYSORE ROAD
1947

CONTENTS

SECTION A—Vol. XXIV

No. 1—July, 1946

		PAGE
The Crystal Forms of Diamond and their Significance	SIR C. V RAMAN AND S RAMASESHAN	1
The Second Order Raman Spectrum of Diamond	R S KRISHNAN	25 *
Thermal Expansion of Diamond	R S KRISHNAN	33
Temperature Variations of the Raman Frequencies in Diamond	R S. KRISHNAN	45
On the Crystal Symmetry of Diamond and Its X-Ray Reflections	G N. RAMACHANDRAN	58
On the Nature and Origin of the Laminations Observed in Diamond	G N. RAMACHANDRAN	65
The Luminescence of Diamond Excited by X-Radiation	G N RAMACHANDRAN	81
X-Ray Topographs of Diamond—Part II	G N RAMACHANDRAN	95
The Faraday Effect in Diamond	S RAMASESHAN	104
The Cleavage Properties of Diamond	S RAMASESHAN	114
A Theory of the Crystal Forms of Diamond	S RAMASESHAN	122
Variations in the Absorption of Infra-Red Radiation by Diamond	K G RAMANATHAN	130
The Absorption of Ultra-Violet Radiation by Diamond	K G. RAMANATHAN	137
The Absorption Spectrum of Diamond in the Visible Region	K G. RAMANATHAN	145
The Infra-Red Absorption Spectrum of Diamond	K G RAMANATHAN	150
Local Variations in the Photoconductivity of Diamond	K. ACHYUTHAN	162
Geometric Patterns of Fluorescence in Diamond	G. R. RENDALL	168
Luminescence as "Forbidden" Electronic Transitions in Diamond	G. N. RAMACHANDRAN AND V. CHANDRASEKHARAN	176

PAGE

Phosphorescence Patterns in Diamond . V. CHANDRASEKHARAN 182

The Thermoluminescence of Diamond V CHANDRASEKHARAN 187

The Phosphorescence of Diamond . . . . V CHANDRASEKHARAN 193

No. 2—August, 1946

Geology and Petrography of the Bezwada and Kondapalle Hill Ranges. Part I. Bezwada Gneiss and Associated Rocks . . . . . M SRIRAMA RAO 199

X-Ray Studies of Peaty Lignites and Anthracitic Coals . . . . . C MAHADEVAN 216

On Multiple Fourier Series . . K. CHANDRASEKHARAN 229

5:6:7.8-Hydroxyflavonols. Part II. A Total Synthesis . . V. V SREERAMA MURTI, L. RAMACHANDRA ROW AND T. R SESHADRI 233

5:6 7·8-Hydroxyflavonols. Part III A Simplified Synthesis . . V D NAGESWARA SASTRI AND T R SESHADRI 238

Synthesis of 5:7:8-Hydroxyflavones and Their Derivatives . . V D NAGESWARA SASTRI AND T. R SESHADRI 243

Kinetics of the Hydrolysis of Anilides . . . . . D D. KARVE AND B W KELKAR 254

No. 3—September, 1946

Equilibrium Surface Tension of Aqueous Solutions of Nekal Bx and the Effect of Salts . . . T KRISHNAPPA, K S GURURAJA DOSS AND BASRUR SANJIVA RAO 261

Aging of Surfaces of Solutions. Part VI. Surface Aging of Casein Solutions . G. N. SUBBA RAO, K. S. GURURAJA DOSS AND . . . . BASRUR SANJIVA RAO 277

Studies in Inorgano-Organic Gels in Pinene. Part V. Gel-Strength Measurements of Gels of Sodium Stearate in Pinene . . . . . MATA PRASAD, S. S DHARMATTI AND G. S. HATTIANGDI 287

Studies in Inorgano-Organic Gels in Pinene. Part VI. Viscosity Changes with Time and Shear during the Gelation of Some Soap Systems in Pinene . . G. S. HATTIANGDI AND S. P ADARKAR 295

No. 4—October, 1946

PAGE

The Electrolytic Preparation of Hydrogen Peroxide Part I. The Intermediate Production of Sodium Persulphate . . . . D. N SOLANKI AND I. S KAMATH 305

Studies in Charnockites from St Thomas Mount, Madras—Part I . . . . . C RAJAGOPALAN 315

Studies in the Naphthalene Series Part XI The Condensation of 2-Acetyl-1-naphthol and Methyl 1-hydroxy-2-naphthoate with Stearyl, Palmityl and Lauryl Chlorides . . . . . R D DESAI AND W S WARAVDEKAR 332

Studies in the Naphthalene Series. Part XII The Preparation and Properties of 4-Stearyl-, 4-Palmityl- and 4-Lauryl-1-Naphthols R D DESAI AND W S WARAVDEKAR 338

Chemical Examination of Plant Insecticides. Part I Chemical Components of *Derris feruginea* . . . . . N V SUBBA RAO AND T R SESHADRI 344

5, 6, 7, 8-Hydroxy-Flavonols. Part IV A Synthesis of Calycopterin . . . . . T R SESHADRI AND V VENKATESWARLU 349

Colouring Matter of the Flowers of *Hibiscus vitifolius* . . . . . K VISWESWARA RAO AND T R SESHADRI 352

The Bitter Principle of *Phyllanthus niruri* . . . . . G. V KRISHNAMURTI AND T R SESHADRI 357

Chemical Examination of Plant Insecticides Part II. Chemical Components of *Derris scandens* . . . . . N V SUBBA RAO AND T R SESHADRI 365

Constitution of Gossypin—Part I . . . . . K VISWESWARA RAO AND T R SESHADRI 375

Studies in Naphthalene Series. Part XIII The Preparation and Properties of 6-Acy-2-naphthols containing Short and Long Chain Alkyl Groups . R. D. DESAI AND W. S WARAVDEKAR 382

Studies in Naphthalene Series: Part XIV. The Preparation and Properties of 2: 4-Distearyl-, 2:4-Dipalmityl- and 2: 4-Dilauryl-1-Naphthols . . . . R. D. DESAI AND W. S. WARAVDEKAR 389

No. 5—November, 1946

PAGE

On Fluctuations of Pressure and Temperature in the Atmosphere . . . . . R. ANANTHAKRISHNAN 393

Determination of the Magneto Optic Anomaly of Some Glasses . . . . . S RAMASESHAN 426

Umbilical Projection . . SAHIB RAM MANDAN 433

A Congruence Property of $\tau(n)$. HANSRAJ GUPTA 441

Some Congruence Properties of the ϕ-Function P. KESAVA MENON 443

Determination of Magnesium and Residual Manganese in Rocks and Minerals with 8-Hydroxy-Quinoline . . . . . C KARUNAKARAN AND K. NEELAKANTAM 448

Conditions of Plane Orbits in Classical and Relativistic Fields . . . . . V. V NARLIKAR AND K R KARMARKAR 451

Constitution of Populnin P RAMACHANDRA RAO AND T R. SESHADRI 456

Chemical Examination of Plant Insecticides Part III Chemical Components of *Derris Robusta* . . . . . N V. SUBBA RAO AND T. R SESHADRI 465

No. 6—December, 1946

A New Band System (Cordes Bands) of Iodine P VENKATESWARLU 473

Emission Bands of Halogens Part I. Iodine Bands arising in 0_N^1 State at 51683 cm. ^{1} . . . . . P VENKATESWARLU 480

Condensation of Aldehydes with Amides Part XII. Condensation of Benzaldehyde and o-Chlorobenzaldehyde . . . . . GUR SARAN BHATNAGAR AND KANTI LAL C. PANDYA 487

Chemical Examination of the Fixed Oil Derived from the Wood of *Pterocarpus Marsupium* Roxb.—Part I . . . . . PRITHWI NATH BHARGAVA 496

Chemical Examination of the Fixed Oil Derived from the Wood of *Pterocarpus Marsupium* Roxb. Part II. Isolation of Pterocarpol A and Petrocarpol B . . . . . PRITHWI NATH BHARGAVA 501

PAGE

Chemical Examination of the Unsaponifiable Matter of the Fat from the Fleshy Arils of *Celastrus paniculata* . . . . . PRITHWI NATH BHARGAVA 506

Overtone and Combination Lines in the Raman Spectrum of Chloroform . . . M. VISWESWARA RAO 510

Production of *Joshi-Effect* under *Uni-* and *Bi-*Electrode Excitation . B B PRASAD 514

A New Identical Equation for Multiplicative Functions of Two Arguments and its Applications to Ramanujan's Sum $C_M^{(N)}$ . . . . . C S. VENKATARAMAN 518

THE CRYSTAL FORMS OF DIAMOND AND THEIR SIGNIFICANCE

By Sir C V Raman and S. Ramaseshan

(From the Department of Physics, Indian Institute of Science, Bangalore)

Received for publication, June 4, 1946

CONTENTS

1. Introductory Statement 2 General Descriptive Characters. 3. Some Theoretical Considerations 4 Geometric Preliminaries. 5 The Configuration of the Edges. 6. The Crystal Symmetry of Diamond 7. Classification of the Crystal Forms 8 The Haidinger Diamond. 9. The Triangular Twins 10 Some Descriptive Notes. 11 The Allotropic Modifications of Diamond. 12 Summary. References Plates.

1. Introductory Statement

The crystallography of diamond presents problems of peculiar interest and difficulty. The material as found is usually in the form of complete crystals bounded on all sides by their natural faces, but strangely enough, these faces generally exhibit a marked curvature. The diamonds found in the State of Panna in Central India, for example, are invariably of this kind. Other diamonds—as for example a group of specimens recently acquired for our studies from Hyderabad (Deccan)—show both plane and curved faces in combination. Even those diamonds which at first sight seem to resemble the standard forms of geometric crystallography, such as the rhombic dodecahedron or the octahedron, are found on scrutiny to exhibit features which preclude such an identification This is the case, for example, with the South African diamonds presented to us for the purpose of these studies by the De Beers Mining Corporation of Kimberley. From these facts it is evident that the crystallography of diamond stands in a class by itself apart from that of other substances and needs to be approached from a distinctive standpoint. It is essential, at the very outset, to emphasise the point—seemingly obvious but often overlooked—that a crystal which exhibits curved faces cannot properly be described in the usual terminology which is based on the existence of plane faces obeying the crystallographic law of rational indices.

One of the most firmly established results of physics is the dependence of the physical properties of a crystalline solid on the symmetry of its structure of which the external form is an indication. There can be little

doubt, therefore, that a study of the crystal forms of diamond, pursued from an appropriate standpoint, would prove most helpful in understanding and interpreting the many remarkable properties of this substance These considerations and the availability of the material referred to above—some 72 specimens in all—encouraged us to undertake a critical examination of the subject The investigation had for its object the discovery of the factors determining the general shape and other distinctive features of the crystal forms, and of the connection between them and the internal architecture of the crystal The studies have enabled us to establish some definite propositions concerning these matters which are stated below The evidence on which our conclusions are based will be set out fully in the course of the paper

I Both the internal architecture of diamond and its external form are determined by the quadrivalence of the carbon atom and its intrinsic tetrahedral symmetry in the crystal

II. The sharply defined edges appearing on the curved surface of the crystal are its intersections with the six symmetry planes of the fundamental tetrahedron, each containing two of the valence directions.

III. The general shape of a diamond crystal stands in the closest relation with the configuration of the edges on its surface.

IV. An edge is most pronounced when it coincides exactly with a valence direction and becomes less conspicuous as it deviates from the same.

V The vertices of the crystal are the points where four or six edges meet.

VI The crystal symmetry of diamond as revealed by the edges on its surface is in the majority of cases that of the tetrahedral class only.

VII. While many diamonds exhibit the features characteristic of tetrahedral symmetry, there is a manifest tendency towards the assumption of forms which are common to the tetrahedral and octahedral symmetry classes.

VIII. The crystal forms of diamond exhibit a recognizable sequence on which it is possible to base a theory of their formation.

2. General Descriptive Characters

The Panna Diamonds:—Forty-three of our specimens are from the State of Panna in Central India. They are of widely differing shape, size and quality and may be considered as fairly representative of the diamonds mined in that area. As stated in the Introduction, the Panna diamonds invariably exhibit curved faces. During the senior author's two visits to the Panna State Treasury, he had the opportunity of examining several hundreds of

these diamonds, including several very large and exceptionally fine specimens and never once came across a crystal showing plane faces either alone or in combination with the usual curved forms. It is very remarkable also that though the Panna diamonds are found in conglomerate beds of obviously sedimentary origin, it is exceptional to find a specimen exhibiting signs of having undergone any wear and tear during the transit from the original site of formation to its final resting place in those beds. Indeed, amongst our 43 specimens, there are only two which give any indication of having suffered in this manner Most of our specimens, in fact, exhibit a remarkable transparency and smooth lustrous faces on which the details are seen beautifully clear and sharp. There cannot therefore be any doubt that the Panna diamonds exhibit precisely the same form as that in which they originally crystallised.

In an earlier symposium, a paper appeared by one of us (Ramaseshan, 1944) describing and depicting the forms of the Panna diamonds At that time, our Panna collection was not so extensive as it is now, having since been enriched by the addition of fourteen specimens of great interest from the scientific point of view. Further, at that time, we did not recognise as fully as we do now, the futility of describing curved crystal forms in the usual language of geometric crystallography. At that time also we had not discovered the physical significance of the details seen on the surface of these diamonds. The shortcomings arising from these circumstances, however, do not affect the scientific value of the diagrams, photographs and descriptive detail set out in the earlier paper It was, in fact, the attempt to explain the facts described in that paper which led us to the present investigation.

We may here briefly recapitulate the main facts which emerged from the earlier studies. The curved surface of a Panna diamond is not a single continuous sheet, but consists of distinct sections meeting sharply along well-defined edges These edges appear elevated above the general level of the surface to an extent depending on the angle between the sections on either side of them This angle and the prominence of the edge vary enormously. An edge may at one part of the surface be so pronounced as to form a visible ridge, while elsewhere it may be so little conspicuous as to be seen only on careful examination under suitable illumination. The points on the surface where four or six prominent edges meet appear as protuberances or vertices of the crystal form On the other hand, regions where the edges are inconspicuous are areas of relatively small curvature of the surface, even at points where they intersect. In a general way and subject to certain variations determined by the general shape of the diamond, the pattern of edges may be described by the statement that it divides the superficies of the crystal into

24 triangular sectors. These sectors are approximately similar to each other if the diamond is of fairly symmetric shape, while on the other hand, the sectors may differ greatly in size and shape if the diamond is of unsymmetrical form.

The Hyderabad Diamonds:—Eleven of the diamonds having their natural form as crystals included in our collection are a recent addition. They were picked out and purchased from the stock of unset stones in the possession of a firm of jewellers at Hyderabad (Deccan). No information was available regarding the origin of these stones beyond the statement that they had been detached for sale from some ancient jewellery Since the city of Hyderabad is the nearest market to various places in the Deccan where diamonds are found, it is not improbable that the stones are of South Indian origin All the eleven specimens are small, but they are of particular interest, being, with one exception, quite different from the Panna diamonds in their general features. They represent a combination of plane and curved forms, but the proportion of plane to curved surface varies in the different specimens. Taken together, the ten stones illustrate the successive stages of the transition from the curved faces and edges of the Panna diamonds to the form having eight plane faces separated by grooves which is the nearest approach made by diamond to the standard forms of geometric crystallography.

The South African Diamonds—The sixteen specimens presented to us by De Beers of Kimberley for the purpose of this investigation have proved very useful in enabling us to compare the South African forms with the Indian ones and determine the relationships between them. Two items of particular interest in the collection may be mentioned here One is a remarkably perfect example of the form of diamond first described by Haidinger, illustrations of which are to be found in the standard texts on mineralogy The other is a triangular twin of flat tabular form with beautifully sculptured edges, presenting an interesting comparison with the rounded contours of the triangular twins found at Panna We shall have occasion to refer to both of these specimens later in the course of the paper.

3. Some Theoretical Considerations

Geometric crystallography is based on the fact that crystals exhibit plane faces bounded by straight edges, and the descriptions given of them specify the directions of the face-normals with reference to the crystallographic axes. The obvious advantages of this system are that the directions of the face-normals are readily determined by goniometry, and that no changes are necessitated in the description by reason of any unequal development in different directions—a very common feature in actual crystals. When,

however, we seek to depict a crystal by means of a figure, what we actually do is to delineate its edges It follows that a crystal can be described by specifying the directions of its edges instead of its face-normals, and that such a description should enable us to determine the symmetry class to which the crystal belongs quite as definitely as the orientation of its faces. In this connection, however, a minor complication which may arise has to be borne in mind, namely, that the unequal development of a crystal in different directions would not only alter the lengths of its edges, but may also bring into existence new edges along which faces which do not meet in a perfectly developed crystal intersect each other

When the faces of a crystal are curved, as in diamond, it becomes impossible to specify the directions of the face-normals by a finite set of numbers But it remains possible to depict the form of the crystal exactly by delineating its edges The edges would then naturally be curved, but it may very properly be assumed that if a crystal does exhibit a set of well-defined edges on its surface, the configuration of these edges must be related in some specifiable manner to its internal structure, and hence that a study of the same would enable us to determine the symmetry class of the crystal in an unequivocal manner.

X-ray studies have made it clear that the structure of diamond is essentially based on the quadrivalence of the carbon atom The four axes of trigonal symmetry of the crystal are, in fact, also the directions of the valence bonds which link each atom of carbon in the structure with its four nearest neighbours. It stands to reason therefore that the visible signs of crystallinity exhibited by diamond in its natural forms should also be related in some simple manner to these valence directions A specific indication as to the nature of such relationship is obtained by considering the form of the regular rhombic dodecahedron. It is readily proved that if a diamond had this form, every one of its 24 edges would coincide with one of the valence directions Many actual diamonds do roughly resemble a rhombic dodecahedron, but they also exhibit features which cannot be reconciled with such a description. Nevertheless, a simple examination shows that the observable edges on such diamonds do approximately coincide with the valence directions. A more exact statement would be that the edges lie in the planes which contain the valence directions taken two at a time. This statement immediately makes intelligible the features observed on such diamonds which are irreconcilable with a description of them as rhombic dodecahedra

We summarise the considerations set out above in the form of two propositions.

A. The configuration of the edges on the surface of a diamond is determined by the structure of the crystal and hence should exhibit its symmetry properties.

B The configuration of the edges is also related in a simple way to the valence directions

4. Geometric Preliminaries

Before we proceed to discuss the observed forms of diamond in the light of the two foregoing propositions, it is useful to recall the symmetry properties of the crystal classes belonging to the cubic system All five classes in that system have as a common feature the four axes of trigonal symmetry which are the cube body-diagonals Taking these axes in pairs and drawing planes through them, we obtain the six diagonal planes of the cube. If these are symmetry planes, the crystal would belong to the tetrahedral class. All the elements of symmetry appearing in that class are represented by drawing through the centre of a sphere the six diagonal planes The sphere then appears divided up into 24 equal spherical triangles.

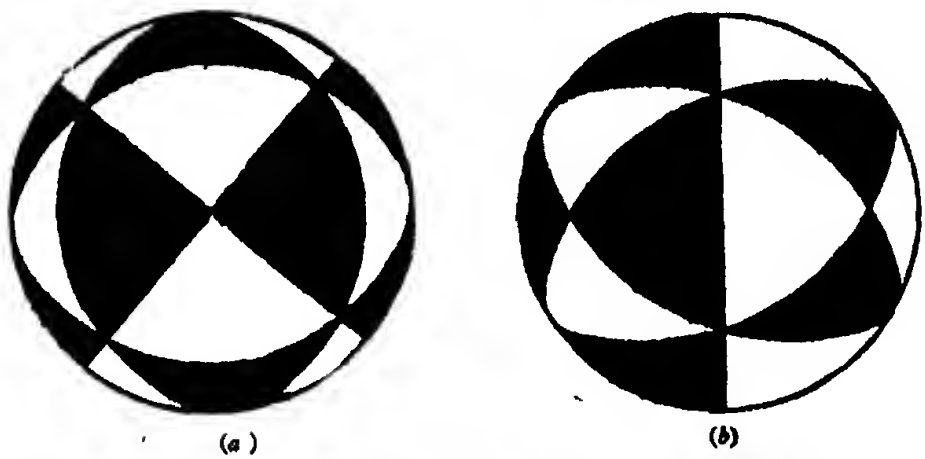

Figs 1 (*a*) and (*b*). Division of a spherical surface by the tetrahedral symmetry planes

Figs. 1 (*a*) and (*b*) represent two views of a spherical surface divided up in this way. It will be seen that there are six points on the surface where four sectors meet and eight points where six sectors meet There are respectively the intersections with the spherical surface of the three axes of diagonal symmetry and the four axes of trigonal symmetry. Any crystal of the tetrahedral class having a regular form, *viz*, a positive or a negative tetrahedron, a cube, a rhombic dodecahedron, a tetrakis-hexahedron or a hexakis-tetrahedron may be represented by its projection on the surface of

a sphere. The edges of the crystal would appear as the sharp dividing lines between the areas on the surface of the sphere, the number of distinct areas being the same as the number of faces in the crystal, *viz*, 4, 6, 12 or 24 as the case may be. To illustrate this, the case of the rhombic dodecahedron is represented in Figs 2 (*a*) and (*b*). The shorter diagonals of the rhombic faces have been retained in the figures so as to enable the similarity between Figs. 1 and 2 to be perceived.

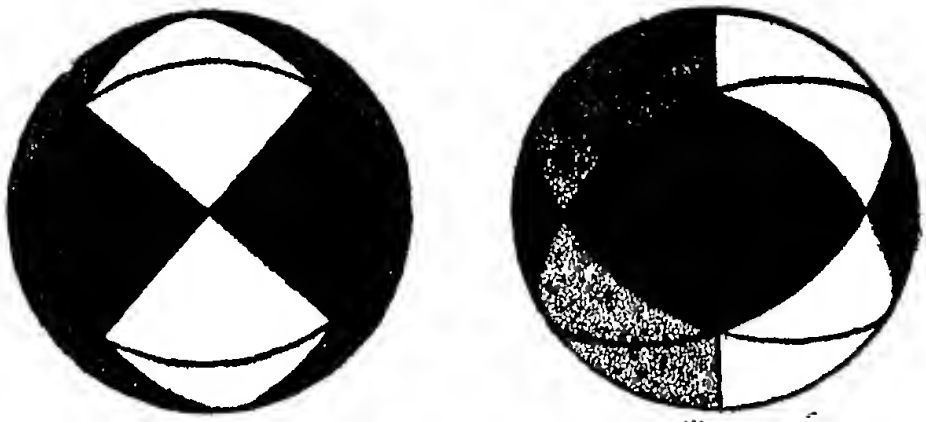

(*a*) (*b*)

FIGS. 2 (*a*) and (*b*) Rhombic dodecahedron projected on a sphere

If, besides the six diagonal planes, the three axial planes of the cube are also planes of symmetry, the crystal would belong to the octahedral class. The elements of symmetry appearing in that class may be represented by drawing all the nine planes through the centre of a sphere The surface of the latter would then appear divided up into 48 equal spherical triangles.

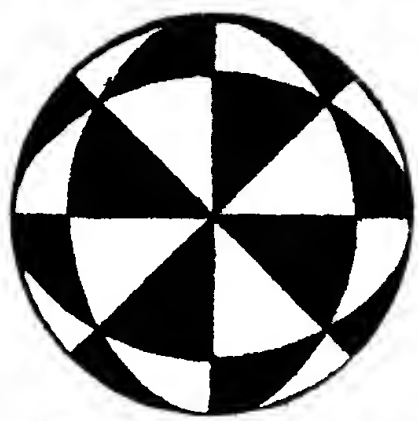

FIG. 3. Division of spherical surface by the octahedral symmetry planes

Fig. 3 illustrates the division of a spherical surface in this way by the symmetry planes of the octahedron. A regular crystal having the most

general form of this class with 48 similar faces could be represented by its spherical projection, the edges of the crystal appearing as the dividing lines between the sectors of the sphere. Particular cases of the class with a smaller number of similar faces could also be represented in the same way by the simple device of leaving out some of the dividing lines on the surface and thereby reducing the number of distinct areas into which it appears divided. For instance, a regular octahedron would be represented by Fig 3 with the six diagonal planes of symmetry omitted and only the three axial planes of symmetry retained, the surface of the sphere would then appear divided into 8 equal areas separated by sharp dividing lines It would, of course, be impossible to exhibit the form of an octahedral crystal with the aid of Fig. 1, since the three axial planes of symmetry are not present in that figure

5. The Configuration of the Edges

Even from the results of the earlier studies of the forms of the Panna diamonds referred to above (Ramaseshan, *loc. cit*), it is evident that the edges seen on the surface of these diamonds represent the division of the superficies of the crystal into 24 sections by the symmetry planes of the fundamental tetrahedron Many of the diamonds do indeed show marked deviations from the simplicity and regularity of the pattern depicted in Fig. 1. These deviations are however readily explained and do not represent any essential departure from the principles which determine the configuration of the pattern.

In the first place, the actual shape of the diamond has to be taken into consideration. The influence of this may be illustrated by considering the intersection of the symmetry planes of a tetrahedron with various surfaces other than a sphere, *e g*, a prolate spheroid, an oblate spheroid or an ovaloid of revolution, which roughly represent the shape of the smaller Panna diamonds In dealing with such cases, it is natural to suppose that the orientation of the tetrahedral axes with respect to the surface would not be arbitrary, but would be related to it in some specific fashion, *viz.*, one of the trigonal axes of symmetry would coincide with the rotation axis of the surface. It is noteworthy that this view is borne out by the actual facts, *viz.*, that the configuration of the edges on the surface of a diamond is very clearly related to the general shape of the crystal.

The division of the surface of a prolate spheroid into 24 sectors by the six diagonal planes of symmetry is shown in Fig 4. Fig. 4 (*a*) is a side view and Fig. 4 (*b*) is an end view. The sectors of the surface are still of roughly triangular form, but they are now of unequal area, those near the ends being considerably enlarged in relation to the others. A prolate spheroid has an

axis of rotation and a plane of symmetry bisecting that axis. But the pattern on its surface evidently does not exhibit these features

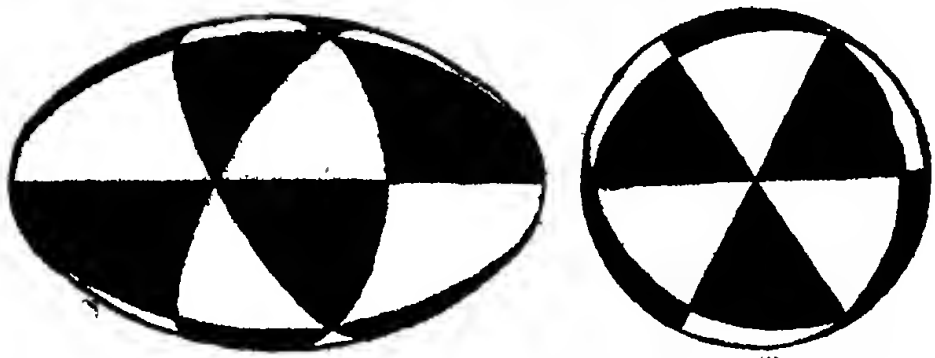

(*a*) (*b*)

FIGS. 4 (*a*) and (*b*) Division of a prolate spheroid by the tetrahedral symmetry planes

The division of the surface of an oblate spheroid into 24 segments by the six diagonal planes of symmetry is illustrated in Figs 5 (*a*) and (*b*), the

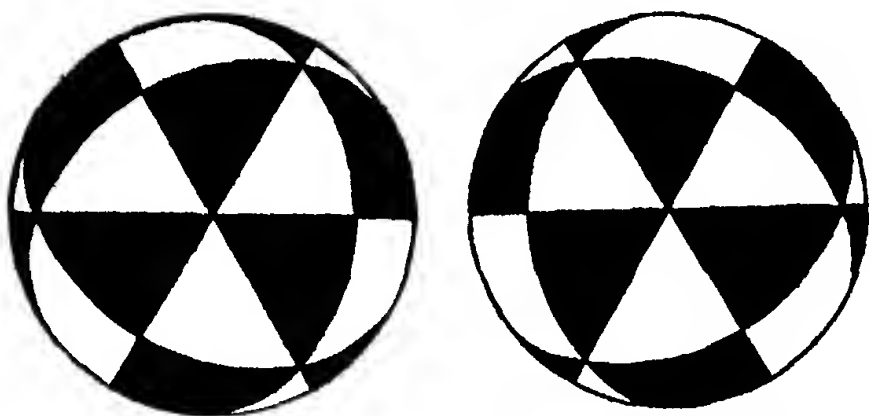

(*a*) (*b*)

FIGS. 5 (*a*) and (*b*). Division of an oblate spheroid by the symmetry planes of a tetrahedron

two figures being the front and back views of the surface It will be noticed that the front and back views are different and that one of them would require to be rotated through 180° to enable them to be brought into coincidence, thereby showing clearly that while the oblate spheroid has a plane of symmetry bisecting its axis of rotation, the pattern on its surface does not share that feature Later in the paper, we shall have occasion to consider the features appearing in Figs 5 (*a*) and (*b*) in relation to the theory of formation of the flat triangular twins of diamond

Fig. 6 illustrates the division of the surface of an ovaloid of revolution into 24 segments by the symmetry planes of a tetrahedron. The figure of

the ovaloid does not possess a centre of symmetry and hence a pattern drawn on its surface exhibits the tetrahedral symmetry in a more obvious fashion than similar patterns on the surface of a sphere or spheroid of revolution.

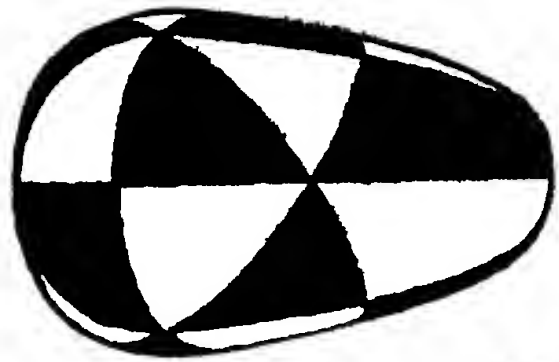

FIG 6 Division of an ovaloid of revolution by the symmetry planes of a tetrahedron

In the models illustrated in Figs 4, 5 and 6, the six diagonal planes of symmetry were drawn so as to pass through a single point within the surface, *viz.*, the centre of the spheroid or the centre of mass of the ovaloid As a consequence, the patterns are similar to that drawn on the surface of a sphere in their general features, *viz*, the division of the surface into 24 segments of triangular shape, four of which meet at six common points on the dyad axes and six at eight common points on the triad axes. The patterns are thus fundamentally related to the pattern of edges presented by a hexakis-tetrahedron or a tetrakis-hexahedron with 24 exactly similar faces. We know, however, that when the general shape of a crystal departs from regularity, the pattern of edges exhibited by it is substantially altered. While the *directions* of the edges which persist remain the same, their positions are altered, and new edges appear along the lines of intersection of the planes which did not previously meet A similar situation would arise in our present problem of the configuration of the edges on a curved surface, and similar results would naturally follow. Hence, the configuration of the edges in the vicinity of the dyad and triad axes would be altered to an extent varying with the general shape of the diamond and to different extents at the various points. The nature of such variations may be readily deduced by shifting the edges laterally while retaining their general directions and drawing intermediate edges connecting the broken ends together.

This has been done in Fig. 7 for the case of four edges which fail to meet exactly on a dyad axis, with the result that a fresh edge connecting up the broken ends appears on the surface. It may be remarked that this type of irregularity is seldom noticed in diamond The reason for this is that in the

vicinity of the dyad axes, the valence directions lie in two perpendicular planes and the edges meeting on these axes are usually very pronounced.

FIG. 7. Pattern of edges in the vicinity of a dyad axis

On the other hand, the six edges which run towards a triad axis often fail to meet exactly on that axis when they traverse a part of the surface which is very nearly flat. The various types of deviation which may be expected to occur are indicated by the diagrams in Fig 8. It may be remarked that they correspond closely to the features actually observed in our specimens

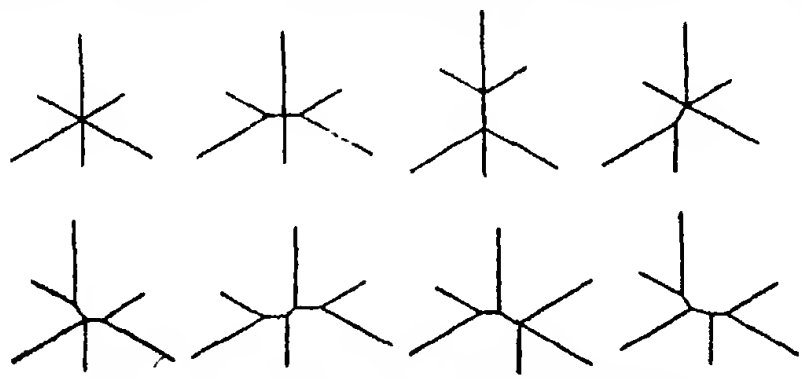

FIG. 8 Pattern of edges in the vicinity of a triad axis

All the Panna diamonds without exception exhibit on their surface a pattern of edges which may be described as its intersections with the tetrahedral planes of symmetry of the structure—subject to the modifications described and illustrated above This fact is all the more remarkable when it is recalled that some of the specimens in our collection bear no resemblance whatever to the conventional descriptions of a crystal. The actual configuration of the edges varies with the shape of the diamond and when this is irregular, the edges meander in their course. We shall refer to the points on the surface where four and six edges meet respectively as the dyad and triad vertices of the crystal. The actual shape of any particular specimen is closely connected with the configuration of the edges in the vicinity of the dyad and triad axes and the relative prominence of the two types of vertices. There are, of course, various possibilities, and many of them are illustrated

by the specimens in our collection. We shall return to these matters later in the paper, but meanwhile we may turn to the fundamental question—What is the crystal symmetry of diamond?

6. The Crystal Symmetry of Diamond

As illustrated in Fig 3, the planes of symmetry in the octahedral class divide the sphere into 48 equal sectors If diamond had octahedral symmetry of structure, we may expect it to exhibit such a subdivision, or at least the edges lying in the axial planes of symmetry. There is not the slightest hint or indication of any such edges in the Panna diamonds Geometric crystallography tells us that the tetrahedral and octahedral symmetry classes have some forms in common, *viz*, the cube, the rhombic dodecahedron, and the tetrakis-hexahedron If a substance crystallised exclusively in these forms, it would not be possible to decide between the two alternative possibilities A decision can only be based on the appearance or non-appearance of forms definitely indicative of the higher or the lower symmetry as the case may be. We are accordingly justified in applying similar tests in the case of diamond The non-appearance in the Panna diamonds of the edges lying in the axial symmetry planes is an indication that we are dealing with only the lower and not the higher symmetry But evidence of a more positive character is desirable We must however know what it is we have to look for Here, again, we may usefully draw upon the ideas and results of geometric crystallography

Fig 9 (*a*) represents a tetrakis-hexahedron viewed along a dyad axis in either direction, while (*b*) and (*c*) represent a hexakis-tetrahedron also viewed along a dyad axis in the two opposite directions respectively

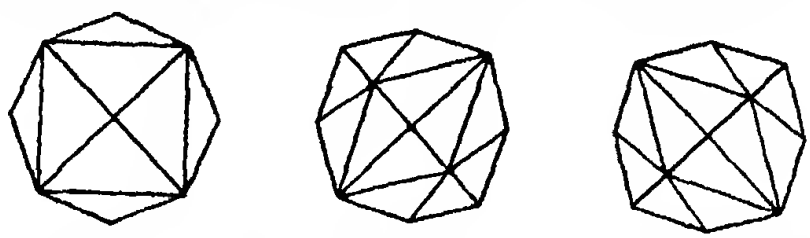

(*a*) (*b*) (*c*)

Figs. 9 (*a*), (*b*) and (*c*) (*a*) Tetrakis-hexahedron, (*b*) and (*c*) Hexakis-tetrahedron viewed along a dyad axis

Fig. 10 (*a*) represents a tetrakis-hexahedron viewed along a triad axis in either direction, while Figs. 10 (*b*) and (*c*) represent a hexakis-tetrahedron viewed along a triad axis in the two opposite directions respectively The forms illustrated in Figs. (9) and (10) both belong to the tetrahedral symmetry class, but the tetrakis-hexahedron can also be regarded as exhibit-

ing octahedral symmetry, the dyad axis then becoming a tetrad axis passing through a centre of symmetry. As can be seen from a comparison of the figures, the characteristic feature of tetrahedral symmetry is that the dyad vertices appear as ridges instead of as peaks, while the triad vertices appear as peaks and as domes respectively at the opposite ends of each axis instead of as peaks at both ends

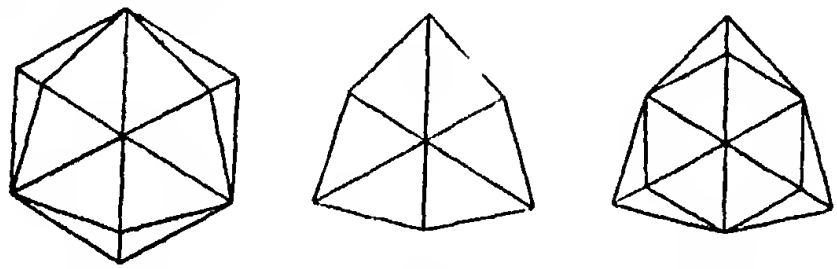

(*a*) (*b*) (*c*)

FIGS. 10 (*a*), (*b*) and (*c*) (*a*) Tetrakis-hexahedron, (*b*) and (*c*) Hexakis-tetrahedron viewed along a triad axis

Examination of our Panna collection discloses in numerous cases the specific features of tetrahedral symmetry indicated above It is a very common occurrence to find the dyad vertices appearing as elongated ridges formed by the meeting of two edges nearly parallel to each other, while the two other edges which are transverse to them go up and down the slopes of the ridge Then, again, one frequently finds the eight triad vertices falling clearly into two groups, one set of four forming fairly well-defined peaks, while the other set of four opposite to them appear as flattened domes. It is very significant also that such configurations of the dyad and triad vertices appear in association with each other In other words, it is the same diamonds that either show or do not show the stated features in respect of the dyad and triad vertices. Further, these features are clearly related to the general shape of the diamond. The crystals that do not exhibit these features are of highly symmetrical form. On the other hand, the specimens that do exhibit these features possess a symmetry of general shape which is obviously of a lower order. Some of the finest diamonds in our Panna collection —beautiful water-white crystals with smooth lustrous faces—present an external form which does not possess a centre of symmetry. It is impossible in the face of these facts to doubt the truth of the proposition that *the internal symmetry of the diamond structure is that of the tetrahedral class only and not that of the octahedral,* at least in all the cases now under consideration.

It remains to be explained, however, why diamond seems to prefer the forms whose symmetry may be indifferently assigned either to the lower or

the higher class, and why even in the forms in which the lower symmetry is observable, it does not appear as conspicuously as might have been expected. One possible explanation is that the more symmetric forms have a smaller surface per unit volume than the less symmetric ones If, as the curvature of the surfaces suggests, diamond was formed by solidification from carbon liquefied under pressure, the form having the smaller surface would have less surface energy and is therefore more likely to be assumed at the instant of solidification. The second possible answer, which is supported by much relevant evidence, is that the positive and negative tetrahedral forms appear intermingled in the crystal If this be the case, the crystal form would tend to imitate octahedral symmetry even if it does not exhibit the specific characters of that symmetry

7 Classification of the Crystal Forms

A survey of all the specimens in our collection indicates that in spite of the great variety of forms exhibited by diamond, it is possible to arrange them in a regular sequence which is evidently connected with the physical circumstances of their formation. The ordering of the forms in such a sequence is obviously an advantage It avoids the necessity for a minute description of all the individual specimens, and it also enables us, at least tentatively, to put forward a physical explanation of the features appearing in them. Indeed, we may advantageously reverse the order and derive from physical considerations an idea of what the forms of diamond should be and then proceed to fit the observed forms into a sequence based on such considerations.

It appears highly probable that diamond results from the solidification of carbon which has assumed the liquid state under conditions of high pressure and temperature. The state of the atoms in the liquid state is an important point needing consideration. The thermal agitation would certainly prevent a perfect ordering of the valence bonds within the liquid. Hence, it follows that the molten carbon would assume a rounded shape and this would be the more likely, the smaller the volume under consideration. Solidification is accompanied by a fixation of the valence bonds but not necessarily by any radical change of shape. On this basis, it is easy to understand why the crystals formed have curved faces. It may be remarked that the smaller diamonds in our Panna collection exhibit a highly marked curvature of the surface on which a pattern of edges appears as described earlier in the paper The formation of these patterns is readily explained. At the surface of the molten carbon there would be some free valences which may attach themselves to the surrounding material. The valences not thus

disposed of would link each carbon atom to its three nearest neighbours on the surface and hence would tend to align them with respect to its position in the valence directions. Accordingly, the first indication of the regular internal structure manifesting itself on the surface of the solidified material would be the formation of edges along the directions of the valence bonds, or in the planes containing them which are also the tetrahedral planes of symmetry of the structure

If the edges of the crystal could align themselves completely along the valence directions, the surfaces between them would be plane, and the form of the crystal would be that of the rhombic dodecahedron However, the curvature of the surfaces would prevent such a complete ordering of the edges In consequence, the form would only approximate to a rhombic dodecahedron; the edges would not stop at the triad vertices but would be continued along the shorter diagonals, thereby dividing the superficies into 24 parts and not 12. Since these " continuation edges " deviate considerably from the valence directions, they would be relatively inconspicuous and would also meander on the surface to fit its varying curvature These features are exhibited by several of our South African specimens. One of them (N C 26) is a beautiful crystal which might easily be mistaken for the regular rhombic dodecahedron of geometric crystallography, but is seen on a more careful examination to exhibit the features indicated above The other dodecahedroid diamonds are less symmetrical in shape and exhibit corresponding variations in the configuration of their edges These variations, however, are fully explicable on the same basis as in the case of the Panna diamonds already discussed in the foregoing pages.

If the valence bonds within the liquefied carbon have at least a semblance of the regular ordering which exists in the crystal, it would follow that the form assumed by the mass would deviate notably from a spherical shape. In a separate paper by Ramaseshan appearing in the present symposium, it is shown that the surface energy per unit area varies with the orientation of the surface in respect of the valence directions, being a minimum in the directions normal to the triad axes and a maximum in directions normal to the dyad axes. Accordingly, the liquid mass would tend to assume the shape of an octahedron with rounded edges, the largest proportion of the area appearing in the vicinity of the triad axes and the smallest near the dyad axes. On solidification, this general shape would be maintained but modified by the formation of the usual pattern of edges in the planes containing the valence bonds. Many of the larger Panna diamonds, including three examples in our collection (N.C. 2, N.C. 4, N.C. 8), have the shape indicated here. They may be referred to as " octahedroid " diamonds, but

are not true octahedra, since they do not exhibit any edges in the axial planes. It may be remarked that the edges in the vicinity of the triad axes are much less conspicuous in the octahedroid diamonds than in the dodecahedroids, since they necessarily deviate more from the valence directions.

A further stage in the sequence of the crystal forms of diamond is reached when the influence of the thermal agitation is diminished sufficiently to enable the surface of the molten carbon to adjust itself exactly to the condition of minimum surface energy This would exhibit itself by the surface in the immediate vicinity of the triad axes appearing as perfect planes in the solid crystal The subsequent stages in the sequence would correspond to increasing areas of such plane areas in the crystal and a corresponding contraction of the curved surfaces, until finally a crystal form is attained in which nearly the whole surface consists of optical planes normal to the triad axes of symmetry

The appearance of optically plane or "splendent" faces in combination with curved surfaces is represented in all its stages in our collection. The first indication of it to appear is a peculiar waviness or rippling of the surface in the vicinity of the triad vertices, often of a regular character and forming a hexagonal network of lines surrounding these vertices. The next stage in the sequence is the appearance of plane areas at and around these vertices. If these are continuous and of sufficient extent, they appear as a truncation or slicing off of the curved surface of the crystal and indeed have the form which would result from such a process, *viz*, a hexagon with three acute and three obtuse angles, the vertices appearing exactly at the points where the edges running across the curved surfaces meet the plane Not infrequently also, the planes appear at the top of a succession of terraces. These terraces run parallel to the perimeter of the plane area, and the edges which have traversed the curved surfaces can be traced through the whole series of terraces up to the plane surface before they finally disappear As the plane areas enlarge further in extent and the curved surfaces diminish correspondingly, the terraces or slopes—sometimes both terraces and slopes—fringing the plane areas persist, with the result that the crystal presents finally the appearance of an octahedron with deep grooves along its edges. The successive stages by which this result is reached can be followed in the Hyderabad specimens in our collection, thereby making it evident that it is not an accidental circumstance but a specific feature of the crystal forms of diamond.

8. The Haidinger Diamond

As mentioned earlier, our South African collection includes a magnificent example (N.C. 25) of the particular form of diamond originally

observed and figured by Haidinger and of which illustrations are to be found in the standard treatises on mineralogy. The general form is that of an octahedron, but the octahedral edges are absent In their place, we have the special feature of the form, namely, conspicuous V-shaped grooves with smooth surfaces which widen from the middle outwards Four of these grooves meet at each vertex of the octahedron and terminate in four sharp straight edges converging to a point on the symmetry axis *These edges lie in the planes containing the valence bonds, and our measurements indicate that they are parallel to the valence directions* They form part of the system of edges lying in the valence planes characteristic of all diamonds. Continuations of them, though much less conspicuous, may be traced running up the terraces on the faces of the octahedron and disappearing at the vertices with acute angles on each face Another set of edges can be seen cutting across each groove and dividing it at its narrowest part into two parts sharply inclined to each other. These same edges can also be traced climbing the terraces and meeting the plane octahedral faces at the vertices with obtuse angles

Apart from the fact that the particular specimen is a remarkably perfect one, the features which it exhibits can also be seen in several of our Hyderabad diamonds It is therefore clear that the Haidinger diamond is not a rare or accidental occurrence but is a typical form of deep significance in the crystallography of this substance The appearance of grooves or re-entrant edges is a characteristic feature of twinning, and in view of the independent evidence showing that the crystal symmetry of diamond is ordinarily that of the tetrahedral class, the only reasonable description of the Haidinger form is that it is an interpenetration twin of positive and negative hexakis-tetrahedra truncated by planes normal to the trigonal axes. Further, since the form mimics octahedral symmetry, it furnishes an excellent example of the result of such interpenetration in suppressing the external manifestation of the inherent tetrahedral symmetry of diamond

9 The Triangular Twins

The ideas developed in the preceding pages enable us to offer a simple explanation of the formation and peculiar shape of the well-known " macles " or twin diamonds of triangular form and of small thickness, examples of which are often forthcoming. Referring again to Figs 5 (*a*) and (*b*) on an earlier page in which the front and back views of an oblate spheroidal model were represented, the remark may be recalled that for these two views to become identical, it would be necessary to rotate one through 180° with respect to the other. In the figures, the pattern of edges is represented as

lying on the surface of the model. Actually, however, the dyad vertices would appear elevated above the surface, while the triad vertices would tend to be suppressed and become relatively inconspicuous, as is indeed the case in the majority of diamonds for reasons already explained. Hence, an oblate spheroidal diamond would tend to assume a triangular shape having its vertices on the dyad axes of the pattern, but the triangles on the two faces would be set oppositely, *viz.*, vertex to base and base to vertex Indeed, some of the specimens in our Panna collection (N C 6, N C 12) show such a form The thinner the diamond, however, the greater would be the probability that this incompatibility between the front and the back of the same crystal would be redressed during its formation by one half of the form swinging round through 180° with respect to the other, thereby resulting in the formation of a triangular twin in which the two halves fit each other perfectly, vertex to vertex and base to base

The pattern of edges formed by the intersections of the tetrahedral symmetry planes with the two surfaces of a model twin of triangular form is represented in Fig 11 Only one side of the model is shown, since the other would be identical in the twin Examination of the triangular twins in our Panna collection (N C. 9 and N C 23) reveals a pattern of edges on their faces and their edges which corresponds closely with that represented in Fig. 11.

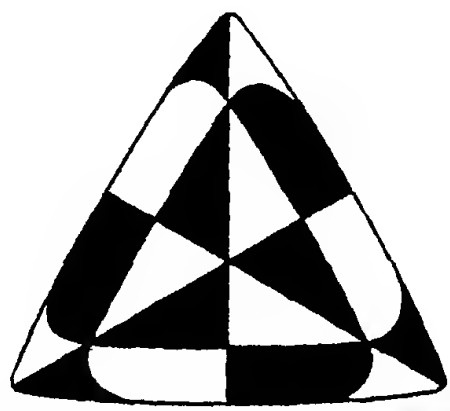

Fig. 11 Intersection of the tetrahedral symmetry planes with the surfaces of a triangular twin

One of the South African specimens in our collection (N C. 30) is also a triangular twin, but of a different type. It is much thicker, and also much more " like a crystal ", that is to say the faces are much flatter and the edges much steeper than in the Panna examples. Examination of this specimen reveals the remarkable fact that its two faces and also the edges up to a third

of the way down from each face exhibit a close similarity to the Haidinger form of diamond We have the same triangular faces with terraces, the same steep grooves below them and the same set of four sharp edges in the valence planes meeting near the vertices of the form. These features are incompatible with the usual description of the triangular diamonds as "spinel twins" obtained by cutting an octahedron in two and rotating one half through 180°. On the other hand, the specimen does exhibit in the vicinity of its median plane, the characteristic features of the form obtained in that way It may accordingly be described as a remarkable but only partially successful attempt by a crystal of the tetrahedral class to mimic one of the characteristic forms of octahedral symmetry

10 Some Descriptive Notes

In the paper by Ramaseshan in the 1944 symposium, descriptions, drawings and photographs have already been given of several of our Panna diamonds There is little need for reproducing the same or similar material here, especially as the numerous figures in the text of the present paper represent the theoretical counterparts of the features described in the earlier one. Since, however, several additions have been made to our collection, some of which are of special interest, it appears desirable to include descriptive notes and illustrations of a few of the new acquisitions

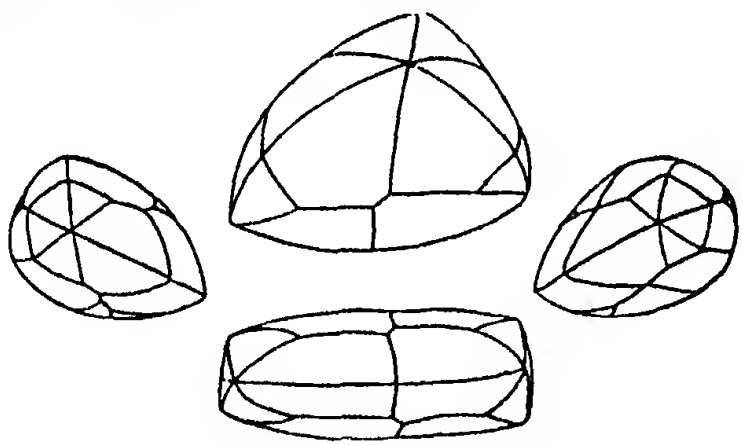

Fig 12. *Front and Side views of N C* 14

N.C. 14.—This diamond from Maharajpur (Panna) weighs 143 milligrams, and is water-white in colour, but exhibits a faint greenish surface tinge of the kind which is fairly common in the Panna diamonds. This is the specimen in our collection which makes the nearest approach in its shape to the regular hexakis-tetrahedron of geometric crystallography and hence most clearly demonstrates that diamond is a crystal of the

tetrahedral symmetry class. The form is obviously lacking in a centre of symmetry. The eight triad vertices of the form fall into two groups of four each; in one group of four vertices, the edges meet accurately, and on the ridges connecting these vertices appear the six dyad vertices of the form. The other triad vertices appear on the four nearly flat faces of the form In these vertices, the edges fail to meet and give rise to a pattern of broken lines as illustrated in Fig 8 on an earlier page. Two of the triad vertices of the former group appear as pointed triangular tips at which three prominent ridges and three fainter ones midway between them meet These tips are connected by an elongated ridge The two other triad vertices of the same group are less prominent and are connected by a much shorter ridge, and the dyad vertex appearing midway between them is a prominent feature of the form As a consequence of these features, both the general shape of the diamond and the details observed on it show only two of the planes of symmetry of the six which a perfect tetrahedron has The two planes of symmetry are mutually perpendicular and contain between them all the eight triad vertices—four on each Their intersection is a dyad axis of symmetry for the crystal

N C 18 —This diamond from Udasna (Panna) weighs 57 milligrams and is perfectly water-white in colour Being a relatively small diamond, the curvature of the faces is very marked Nevertheless, the specimen shows clearly enough the characters of tetrahedral symmetry The form lacks a centre of symmetry, and exhibits a trigonal axis at the two ends of which very different features are noticed One end of the axis

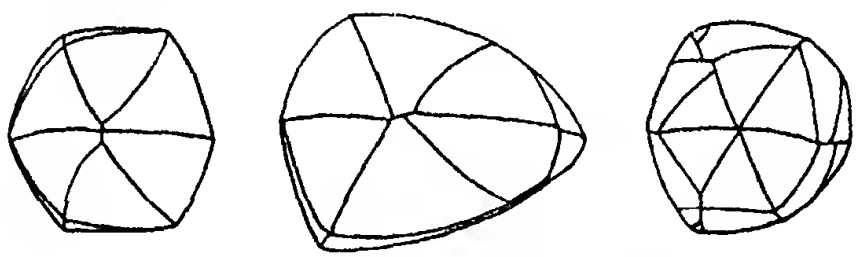

Fig 13 *Front and End views of N C 18.*

is a sharp triangular tip where six edges meet. The other end is a nearly flat dome with a hexagonal perimeter bounded by three dyad and three triad vertices, all of which are fairly prominent. The four other triad vertices—appearing respectively on the triangular faces of the tip and on the dome at its end—are of a different description, being zig-zag patterns of broken lines. Three of the dyad vertices appear

on the ridges which converge towards the triangular tip of the form, and the three others around the base of the dome.

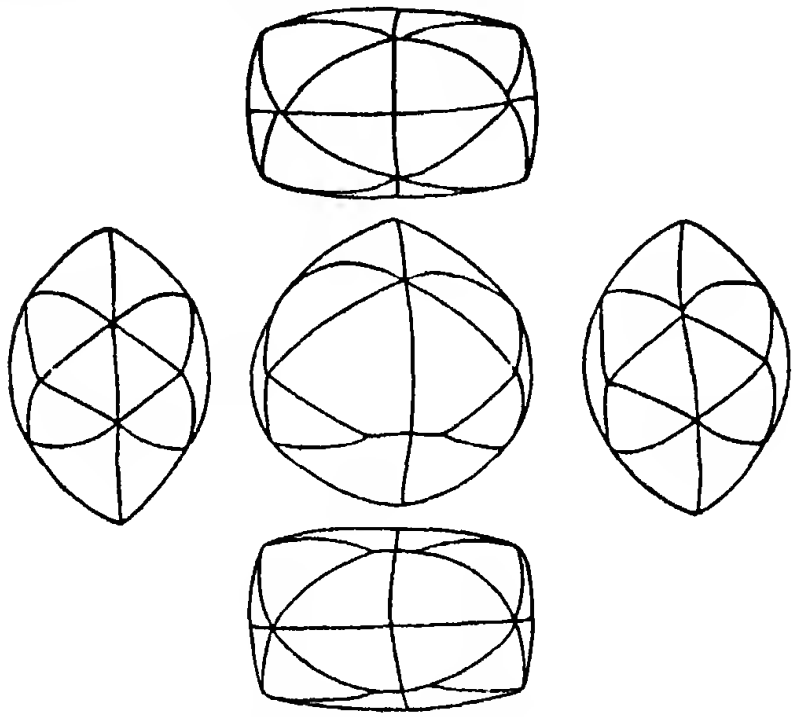

FIG 14 *Front and Side views of N C 10*

N C 10—This beautiful diamond from Maharajpur (Panna) weighing 182 milligrams, water-white in colour, with smooth lustrous faces, is well worthy of a detailed description as it illustrates a stage in the transition from the "tetrahedroid" to the "octahedroid" forms of diamond The crystal exhibits a perfect symmetry of shape and of detail about two planes which are perpendicular to each other These planes are two of the tetrahedral symmetry planes and the line along which they intersect is a dyad axis also for the actual shape of the crystal The two ends of this axis are prominent dyad vertices of the form and exhibit the tetrahedroid character, appearing as ridges rather than as peaks Since one of them is much more pronounced than the other, the crystal form has no centre of symmetry The four other dyad vertices come next in order of prominence and are all exactly alike each other They are peaks rather than ridges and thus exhibit an octahedroid character. The triad vertices form pairs, two of which appear in each of the two symmetry planes of the crystal The four pairs of vertices are of progressively diminishing prominence. They illustrate the successive stages

of the transformation of a triad vertex from a perfect meeting of six ridges to an elongated zig-zag of broken lines.

N C 25—This diamond from Bultfontein, South Africa, water-white in colour and weighing 211 milligrams, is the Haidinger form already described in some detail in Section 8 above A photograph with an accompanying sketch appear in Figs 1 and 2 in Plate I of this paper. Fig 10 in Plate III is a photograph of one of the faces of the form showing its characteristic hexagonal shape, the terraces surrounding it and the triangular depressions or "trigons" appearing on the same. Another photograph of the same diamond reproduced as a negative appears as Fig 11 in Plate III

N C 164—This is one of the Hyderabad diamonds whose forms were described and explained in Sections 2 and 7 above. It is a small diamond weighing 62 milligrams and is nearly water-white in colour It exhibits a combination of optically plane or "splendent" faces with curved surfaces separating them, the latter being smooth and lustrous and exhibiting edges analogous to those observed on the Panna diamonds. In this particular diamond, six of the plane faces are much larger than the other two The photograph reproduced as Fig 3 in Plate I shows the smallest of all the plane faces as a dark area Fig 9 in Plate III is an enlarged picture of the same face, showing clearly the curved surfaces surrounding it as well as the edges crossing them and meeting the vertices of the plane face The sketch reproduced in Fig. 4 in Plate I shows in addition two of the larger plane faces of the diamond and the curved surface lying between them and separated into sections by a system of curvilinear edges. See also Fig 12 in Plate III where the photograph is reproduced as a negative

N.C 26—This diamond from South-West Africa, weighing 191 milligrams and water-white in colour, is the "rhombic dodecahedron" the features observed on which have been described and explained in Section 7 above Photographs and sketches of it from two different points of view are reproduced as Figs. 5, 6, 7 and 8 in Plate II and in Figs. 13 and 14 in Plate III.

11 The Allotropic Modifications of Diamond

It is useful here to review our findings in so far as they have a bearing on the question of the symmetry of the internal structure of diamond. What the evidence indicates is that in the majority of the cases studied and possibly in all, the crystal symmetry is that of the tetrahedral class only and that none of the crystals appearing in our collection presents conclusive evidence of

its possessing a true octahedral symmetry. There is, however, a pronounced tendency towards the assumption of crystal forms which may be indifferently regarded as either tetrahedral or octahedral This tendency would result from an interpenetration of positive and negative tetrahedral forms, and there is crystallographic evidence that such interpenetration does occur. But it should not be forgotten that the same situation would arise from the existence of diamond having a truly octahedral symmetry of structure but formed under conditions unfavourable for the intrinsic symmetry expressing itself to the fullest extent in the external form The possibility has also to be borne in mind that the modifications of diamond having tetrahedral and octahedral symmetry of structure appear intertwinned with each other in the same crystal In all such cases, we could scarcely expect the crystal forms to exhibit either tetrahedral or octahedral symmetry exclusively It would then be necessary to rely on physical evidence, as for instance the infra-red absorption spectrum, to discriminate between the various possibilities and to establish the nature of any particular specimen

Summing up the situation, we may say that while the study of the crystal forms in our collection shows clearly enough that the majority of diamonds have only a tetrahedral symmetry of structure, the results do not exclude the possibility that diamond has in some cases a truly octahedral symmetry of structure which for one reason or another fails to manifest itself fully in the external form of the crystal.

12. Summary

The paper describes the conclusions reached from a critical examination of some 72 diamonds in their natural form obtained from various sources. The curvature of the faces and other special features exhibited by diamond invalidate a description of its forms in the standard terminology of geometric crystallography. The proper basis for description and classification is furnished by the configuration of the sharply-defined edges which appear dividing the superficies of the crystal into 24 distinct sections Subject to minor modifications, these edges lie along the intersections of the surface with the symmetry planes of a fundamental tetrahedron These planes also contain the directions of the valence bonds between the carbon atoms in the crystal and the sharpness of the edges is determined by the angle which they make with the valence directions. The configuration of the edges and the specific features exhibited by them in numerous specimens prove that in the majority of diamonds the crystal symmetry is that of the tetrahedral class only. The crystallographic evidence also shows that the positive and negative tetrahedral forms freely interpenetrate each other, and this explains the

frequent appearance of forms common to the tetrahedral and octahedral symmetry classes. That diamond may in some cases possess a true octahedral symmetry is however entirely consistent with the observed facts A physical theory of the formation of diamond is outlined which explains the observed features of the crystal forms and enables them to be classified in a regular sequence

References

Treatises

Dana, E S — "A System of Mineralogy," Wiley & Sons (1911), p. 3
"A Text-Book of Mineralogy," Wiley & Sons (1932), p 395

Groth, P — "Chemische Krystallographie" (1906), Erster Teil, p. 12

Hintze, C. — "Handbuch der Mineralogie" (1904), Erster Band, Erste Abteilung, p 14, 26

Miers, H A. — "Mineralogy," Macmillan (1902), p 291

Sinor, K P — "The Diamond Mines of Panna State," *Times of India* (1930)

Sutton, J R — "Diamond," Van Nostrand Co (1928)

Tutton, E. H — "Crystallography and Practical Crystal Measurement," Macmillan (1922), p 502

Papers

Goldschmidt, V — *Zeit fur Kryst*, 1912, 50, 460

Hirschwald, J — *Ibid.*, 1877, 1, 212

Martin, Weiss, etc — *Ibid*, 1882, 6, 103

Ramaseshan, S — *Proc Ind Acad*, *Sci*, 1944, 19 A, 334.

Sadebeck, A. — *Zeit fur Kryst*, 1878, 2, 13.

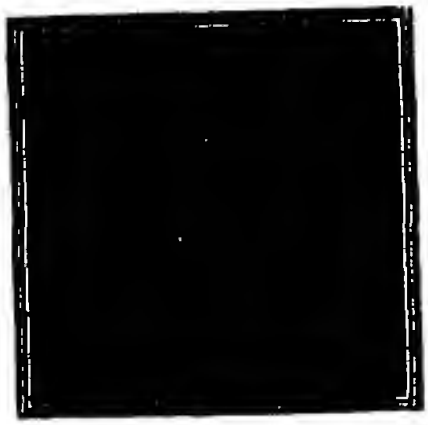

FIG 1

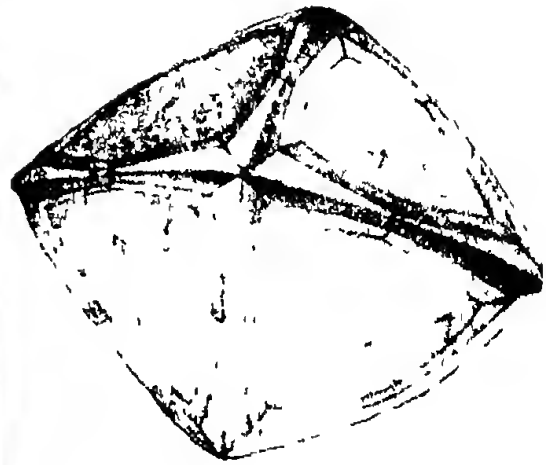

FIG 2

Hardinger Diamond (N C 25)

FIG 3

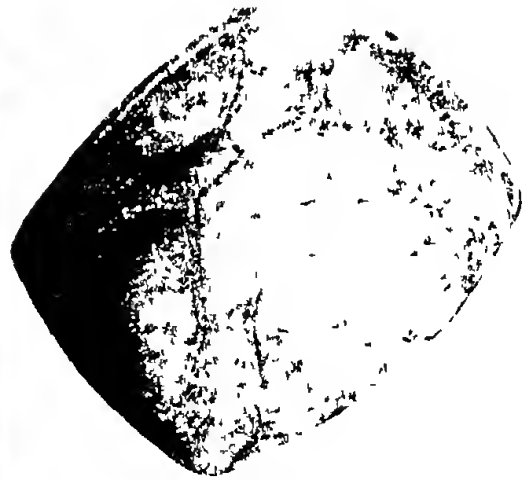

FIG 4

Hyderabad Diamond (N C 164)

Fig 5

Fig

Fig 7

Fig 8

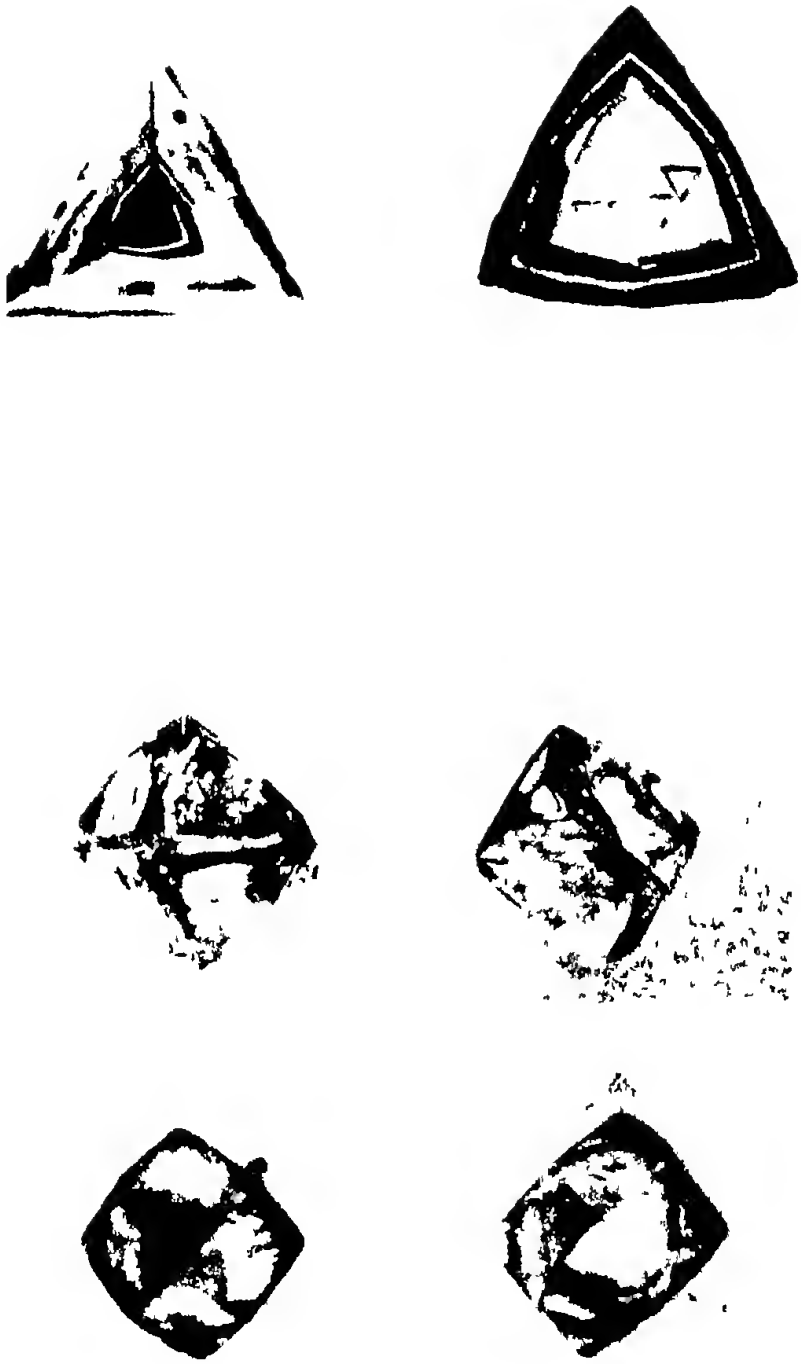

THE SECOND ORDER RAMAN SPECTRUM OF DIAMOND

By Dr R S Krishnan

(*From the Department of Physics, Indian Institute of Science, Bangalore*)

Received May 18, 1946

1 Introduction

The Raman effect in diamond has been studied by several investigators, *viz*, Ramaswamy (1930), Robertson and Fox (1930), Bhagavantam (1930), Robertson, Fox and Martin (1934) and Nayar (1941, 1942) They reported the existence of only a single sharp and intense Raman line with a frequency shift of 1332 cm^{-1} corresponding to the triply degenerate vibration of the two Bravais lattices of carbon atoms with respect to each other. Investigations by Robertson, Fox and Martin (1936) on the infra-red absorption spectrum and those by Nayar (1941 *a*, 1942 *a*) and by Miss Mani (1944) on the luminescence and absorption spectra of diamond, however, indicated that the lattice spectrum includes many more vibrations with discrete frequencies besides the one with the frequency shift of 1332 cm^{-1} so far recorded in the Raman spectrum It was therefore natural to expect that some of these vibrations would manifest themselves as second order Raman lines in an intensely exposed spectrum of diamond Accordingly, the author (Krishnan, 1944) undertook a re-examination of the Raman effect in diamond. The technique of using the visible and near ultra-violet radiations of the mercury arc as exciter has been exploited to the limits of its utility by the investigators already referred to, and consequently no further useful information regarding the second order spectrum of diamond would be got by employing the same. Using the extremely intense 2536 5 mercury resonance radiation from a water-cooled magnet-controlled mercury arc as exciter and diamonds of the ultraviolet transparent type, the author succeeded in recording a spectrum which exhibited besides the intense line with a frequency shift of 1332 cm.$^{-1}$, no fewer than ten Raman lines of comparatively feeble intensity. These constitute the Raman spectrum of the second order in diamond, the appearance of which was predicted on the basis of the Raman dynamics of crystal lattices In the preliminary investigation the results of which were published in the earlier symposium (Krishnan, 1944), the author had used a quartz spectrograph of small dispersion. Because of this and also due to imperfect reproduction, the second order Raman lines are not

seen clearly resolved from the background either in the spectrogram or in the microphotometric record Using a Hilger medium quartz spectrograph which had a higher dispersion than the one previously employed, fresh photographs were obtained, the best of which was published in *Nature* (Krishnan, 1945) Here also the reproduction was not quite satisfactory, as the picture was too small to bring out the real nature of the second order Raman spectrum of diamond, *viz*, a set of sharp lines appearing on a feeble continuum It was therefore thought desirable to investigate the problem afresh under more favourable conditions Improved experimental technique and the use of an exceptionally colourless plate of diamond belonging to the ultraviolet transparent type recently acquired by Sir C V Raman have enabled the author to record spectra of much greater intensity and much better resolved The results are presented in this paper

2 Experimental Details and Results

The catalogue number of the diamond used is N C 174 It was in the form of a semicircular disc about one centimetre in diameter and 2 millimetres thick It was held with its flat faces vertical and facing the most intense portion of a specially designed quartz mercury arc The arc was run under special conditions so as to emit the resonance radiation with exceptional intensity The light scattered through the straight edge of the diamond was focussed on the slit of a Hilger (E3) medium quartz spectrograph The diamond was kept cool with the aid of a fan The scattering from the specimen was so intense that the principal line could be recorded on the plate with an exposure of five seconds, while an exposure of the order of one hour was sufficient to bring out the essential features of the second order spectrum Numerous spectrograms were taken with exposures varying from 15 seconds to 15 hours Kodak B 20 Process Regular plates were used. It is interesting to record the fact that the second order spectrum becomes visible with an exposure of 15 minutes and the anti-Stokes of the principal line 1332 cm^{-1} appears with an exposure of 45 minutes

A microphotometric record of a moderately exposed spectrogram is reproduced together with the spectrum itself as Fig 1 (*a*) and 1 (*b*) in Plate IV The microphotometric record of the mercury arc is also included in Fig 1 (*c*) for purposes of comparison The photograph and the microphotometric record reproduced here represent a considerable improvement on the ones published earlier by the author. As is evident from the figures, the second order spectrum of diamond is mainly confined to a region extending to about 300 wave numbers on either side of λ 2698 9 It consists of a series of distinct Raman lines of which at least 7 can be dis-

tinguished without difficulty. Their positions have been marked in Fig 1 (*a*) The frequency shifts of these lines have been accurately determined by direct measurements made on the negative. Their values are 2176, 2253 2299, 2330, 2460, 2502 and 2666 cm^{-1} Three of them, namely the lines at 2176, 2460 and 2666 cm^{-1}, stand out prominently in the spectrum The line at 2460 cm^{-1} is the most intense one, while the sharpness of the line at 2666 cm.$^{-1}$ is comparable with that of a mercury line The line at 2502 cm.$^{-1}$ has an appreciable width extending from 2490 to 2514 cm^{-1} This line can be seen clearly separated from the intense line at 2460 cm^{-1} See Fig 1 (*b*) The line with the frequency shift 2253 cm^{-1} appears to have a finite width A careful examination of a lightly exposed spectrogram and its microphotometric record has shown that this line is made up of two closely spaced lines with frequency shifts 2245 and 2265 cm^{-1}

Besides the 7 lines described above, the presence of at least 3 other feeble lines with frequency shifts 2190, 2225 and 2430 cm^{-1} has been identified by a careful scrutiny of the spectrogram and its microphotometric record. The positions of these lines have also been indicated in Fig 1 (*a*) The frequency shifts of the 10 Raman lines belonging to the second order spectrum are listed in Table I, those of the prominent lines being shown in heavy type

TABLE I

Second Order Spectrum of Diamond

No	Frequency shifts of the observed Raman lines in cm^{-1}	Relative intensity	Frequencies of the observed infra red absorption maxima in cm^{-1}
1	2176	5	2170
2	2190		2186
3	2225		2217
4	2253	7	2240
5	2299	8	2290
6	2330	9	
7	2430		
8	2460	15	2452
9	2502	13	2506
10	2666	10	2666*

* Please see remarks in text The frequencies of the prominent peaks appearing in the infra-red absorption spectrum are also shown in heavy type

Superposed over the Raman lines there is a feeble continuum which extends from the Raman line 2253 cm.$^{-1}$ to the line 2666 cm^{-1} It is to be remarked that the line with the frequency shift of 2666 cm.$^{-1}$ has an individual

existence and is not merely the sharp cut off of the continuum See Figs. 1 (*a*) and 1 (*b*)

The values of the frequency shifts of the second order Raman lines reported earlier by the author were less accurate than the values presented now, as the former had to be evaluated from measurements made on the microphotometric record In the region between the mercury triplet and λ 2675 0 there is a sharp Raman line separated by about 1940 wave numbers from λ 2536 5 See Figs 1 (*a*) and 1 (*b*) This was wrongly assigned as a second order Raman line in the paper published in the earlier symposium It should, however, be assigned as the first order Raman line 1332 cm^{-1} excited by the mercury line λ 2576 3 The Raman line at λ 2749 seen in Figs 1 (*a*) and 1 (*b*) likewise corresponds to a first order line with the frequency shift 1332 cm^{-1} excited by the mercury line λ 2652

3 Intensity Measurements

In order to estimate the relative intensities of the second order Raman lines as well as the ratios of the intensities of the Stokes, the anti-Stokes and the octave of the principal Raman line 1332 cm^{-1}, the following procedure was adopted As already mentioned in the last section, a series of photographs of the Raman spectrum of diamond was taken with exposures varying from 15 seconds to 15 hours Standard developers were used throughout and the time and temperature of development was kept constant. A series of graded intensity marks was obtained on a separate Kodak B 20 plate by photographing the spectrum of a tungsten filament lamp provided with a quartz window with different slit-widths, but keeping the time of exposure constant A second series of photographs was taken on another plate varying the time of exposure but keeping the slit-width constant. These two negatives were put through the microphotometer With the aid of the microphotometric records, the density-log intensity and density-log time curves were plotted for the spectral region corresponding to the mean wave-length λ 2650 From these curves, the Schwarzschild correction factor appearing in the expression for the photographic density as exponent for time was evaluated For λ 2650 the Schwarzschild factor has the mean value of 0 8.

With the help of the density-log intensity curve and the microphotometric record of a moderately exposed spectrogram of the Raman effect in diamond, the relative intensities of the prominent second order Raman lines were evaluated in the usual way. Taking the intensity of the line 2666 cm.$^{-1}$ as 10 arbitrary units, the intensities of the other lines have been calculated and the values are listed in Table I. It is reasonable to assume that the

intensities of the lines 2176, 2460, 2502 and 2666 cm^{-1} are not affected to any appreciable extent by the presence of the feeble continuum and hence the values given in Table I may be taken to represent the actual peak intensities of these lines

With the aid of the microphotometer and using the series of photographs of the Raman spectrum taken with graded exposures, the density-log time curves were plotted for the Stokes line (1332 cm^{-1}), the anti-Stokes line ($-$ 1332 cm^{-1}) and the octave (2666 cm^{-1}) The time of exposure required to produce the same density (darkening) on the plate by each one of these lines was read off from the respective density-log time curve. Knowing the values of the exposure time for the three lines, their relative intensities were evaluated using the known value of the Schwarzschild factor. For the 1332 Raman line in diamond, the ratio of the intensities of the Stokes to the anti-Stokes is 575, while that of the fundamental to the octave is 290. In evaluating the former ratio it has been assumed that the density-log intensity curve is the same for the two regions of the spectrum, namely 2625 A U and 2453 A U where the Stokes and anti-Stokes lines fall

The ratio of the intensity of the Stokes to that of the anti-Stokes line to be expected on the basis of the Boltzmann formula was evaluated taking the temperature of the diamond to be 27° C It is equal to 590 which agrees fairly well with the observed value of 575

4 Infra-Red Spectrum of Diamond

The infra-red absorption spectrum of diamond was investigated in some detail by Robertson, Fox and Martin (1934). They reported the existence of three distinct regions of absorption in diamonds of the ultra-violet opaque type and two in diamonds of the transparent type The three groups of absorption which were denoted by letters A, B and C appeared respectively at 3 μ, 4–4 8 μ and 7–9 μ They could not detect any difference in the structure of the absorption bands given by the two types of diamond except for the absence of the absorption band C in diamonds of the ultra-violet transparent type. Robertson, Fox and Martin analysed the absorption in the region from 4–4 8 μ into three separate absorption bands denoted by the letters B′, B_α and B_β They noticed definite indications of structure in the absorption bands B_α and B_β See Fig 7 reproduced on page 482 of their paper.

Two years later, Robertson, Fox and Martin (1936) carried out further exploration of the fine structure of the absorption bands B_α and B_β with the aid of a grating. The absorption curve obtained thereby is reproduced in Fig 1 (*a*) on page 581 of their second paper The B_α band is bounded on

either side by a steep fall in absorption strength and exhibits a very sharp and prominent peak on its longer wavelength edge which forms a characteristic feature of this absorption band Robertson, Fox and Martin gave the value of 2170 cm^{-1} for the frequency of infra-red vibration corresponding to this peak This peak may be identified in its position with the Raman line 2176 cm^{-1} which stands out prominently in the observed second order spectrum.

The principal peak at 2170 cm^{-1} is followed by two others, then by a well-defined kink and finally by another peak. The positions of these have been estimated by the author from the curve reproduced by Robertson, Fox and Martin (1936) and their values in wave numbers are 2186, 2217, 2240 and 2290 These are included in Table I The positions of these peaks and kinks may be identified with those of the observed Raman lines 2190, 2225, 2253 and 2299 cm.$^{-1}$ Thus the fine structure of the infra-red absorption band B_a shows a very striking correspondence with the features observed in the second order spectrum

Robertson, Fox and Martin (1936) re-examined the absorption band at 4·1 μ also with the aid of a grating, but no new details except those already reported by them in their earlier paper were obtained In the absorption curves of the two types of diamond reproduced in Fig 7 on page 482 of their paper, the band at 4·1 μ exhibits some structure The existence of two rather broad peaks is easily noticeable in the absorption band of the ultra-violet transparent type of diamond The positions of these have been estimated by the author Their frequencies in wave numbers are 2452 and 2506 cm^{-1} Corresponding to these two infra-red absorption maxima, one observes two intense Raman lines with frequency shifts 2460 and 2502 cm^{-1} appearing prominently in the second order spectrum

The absorption curve for diamond of the ultra-violet opaque type shows a peak coinciding with the fundamental Raman frequency of 1332 cm^{-1} (K G. Ramanathan, 1946, see the paper appearing elsewhere in this symposium) The fine structure of the corresponding absorption band in the 4 1 μ region has not been investigated. The curve reproduced by Sutherland and Willis (1945), however, shows a precipitous fall of absorption strength beyond the 4 1 μ The point where the slope is greatest has the same frequency as that of the Raman line of frequency shift 2666 cm^{-1}

5. Comparison with Luminescence and Absorption Spectra

The luminescence and absorption spectra of diamonds have been studied in great detail by Nayar (1941 *a*, 1942 *a*) and by Miss Mani (1944). Associated with the principal electronic lines at λ 4152 and λ 5032 a set

lines appears at greater wavelengths in fluorescence and at diminished wavelengths in absorption The most clearly defined and prominent lattice frequencies appearing in luminescence and absorption spectra are in wave numbers 1332, 1251, 1149 and 1088 The Raman lines with frequency shifts 2666, 2502, 2299 and 2176 cm^{-1} appearing prominently in the second order spectrum are evidently the octaves of these lattice frequencies

6 Conclusion

According to the existing theories of Debye and Born, the vibration spectrum of a crystal is essentially a continuous distribution of frequencies ranging from zero upwards On this basis, the appearance of only a single sharp and intense line with the frequency shift of 1332 cm^{-1} in the Raman spectrum of the first order in diamond is scarcely intelligible In order to get over this obvious contradiction with the facts, it has been suggested that only the limiting frequencies of the lattice, *viz*, those having phase-wavelengths large compared with the lattice spacing could appear in the observed Raman spectrum It is further assumed that the frequencies of the vibrations of shorter phase-wavelengths disappear by reason of the optical interference of the effects due to them arising from different volume elements. There is no experimental justification for such an assumption Even if it were valid, the second order spectrum of diamond should likewise consist of a single sharp line corresponding to the octave of the limiting frequency of vibration, namely 2664 cm^{-1} What is actually observed is wholly different, *viz*, a set of Raman lines with discrete frequencies It is therefore impossible to reconcile the consequences of the Born theory with the experimental facts of the Raman effect in diamond

The appearance of a set of lines with discrete frequency shifts in the second order spectrum of diamond finds a natural explanation in the new theory of lattice dynamics put forward by Sir C V Raman (1943) According to the Raman dynamics the diamond lattice has a small number of fundamental modes of vibration with discrete frequencies The observed second order lines are the octaves and allowed combinations of some of these fundamental frequencies of oscillation of the diamond lattice

The author is grateful to Professor Sir C V Raman for the loan of the diamond used in the present investigation and for some useful discussions

7 Summary

Using an exceptionally colourless plate of diamond of the ultra-violet transparent type and the λ 2536 5 resonance radiation of mercury as exciter, the author has photographed the second order Raman spectrum of diamond

with greatly increased intensity and much better resolved than any recorded hitherto. The spectrum exhibits ten distinct Raman lines with frequency shifts 2176, 2190, 2225, 2253, 2299, 2330, 2430, 2460, 2502 and 2666 cm.$^{-1}$ The frequency shifts of the first five lines, in particular, correspond very closely with the positions of a set of five absorption peaks observed by Robertson, Fox and Martin while exploring the absorption band in the region 4–4 8 μ with the aid of a concave grating of the echelette type Of the ten observed second order Raman lines, the more intense and prominent ones have been identified as octaves of the prominent lattice frequencies of diamond appearing in the luminescence and absorption spectra These facts are irreconcilable with the consequences of the Born lattice dynamics. They can, however, be satisfactorily explained on the basis of the Raman dynamics of crystal lattices.

The relative intensities of the second order Raman lines, as well as the ratios of the intensities of the Stokes, the anti-Stokes and the octave of the principal Raman shift of 1332 cm^{-1} have been estimated by photographic photometry.

REFERENCES

Bhagavantam, S	*Ind Journ Phys*, 1930, **5**, 169 and 573
Krishnan, R S	*Proc Ind Acad Sci*, 1944, **19**, 216
	Nature, 1945, **155**, 171
Miss Mani	*Proc Ind Acad Sci*, 1944, **19**, 231
Nayar, P G N	*Ibid*, 1941, **13**, 284, 1942, **15**, 310
	Ibid, 1941 *a*, **13**, 483, 1942 *a*, **15**, 293
Raman, C V	*Ibid*, 1943, **18**, 237
Ramanathan, K G	*Ibid*, 1946, **24A**, 150
Ramaswamy C	*Nature*, 1930, **125**, 704
	Ind Journ Phys, 1930, **5**, 97
Robertson and Fox	*Nature*, 1930, **125**, 704
———, ——— and Martin	*Phil Trans Roy Soc*, A, 1934, **232**, 492
	Proc Roy Soc, A, 1936, **157**, 579
Sutherland and Willis	*Trans Faraday Soc*, 1945, **41**, 289

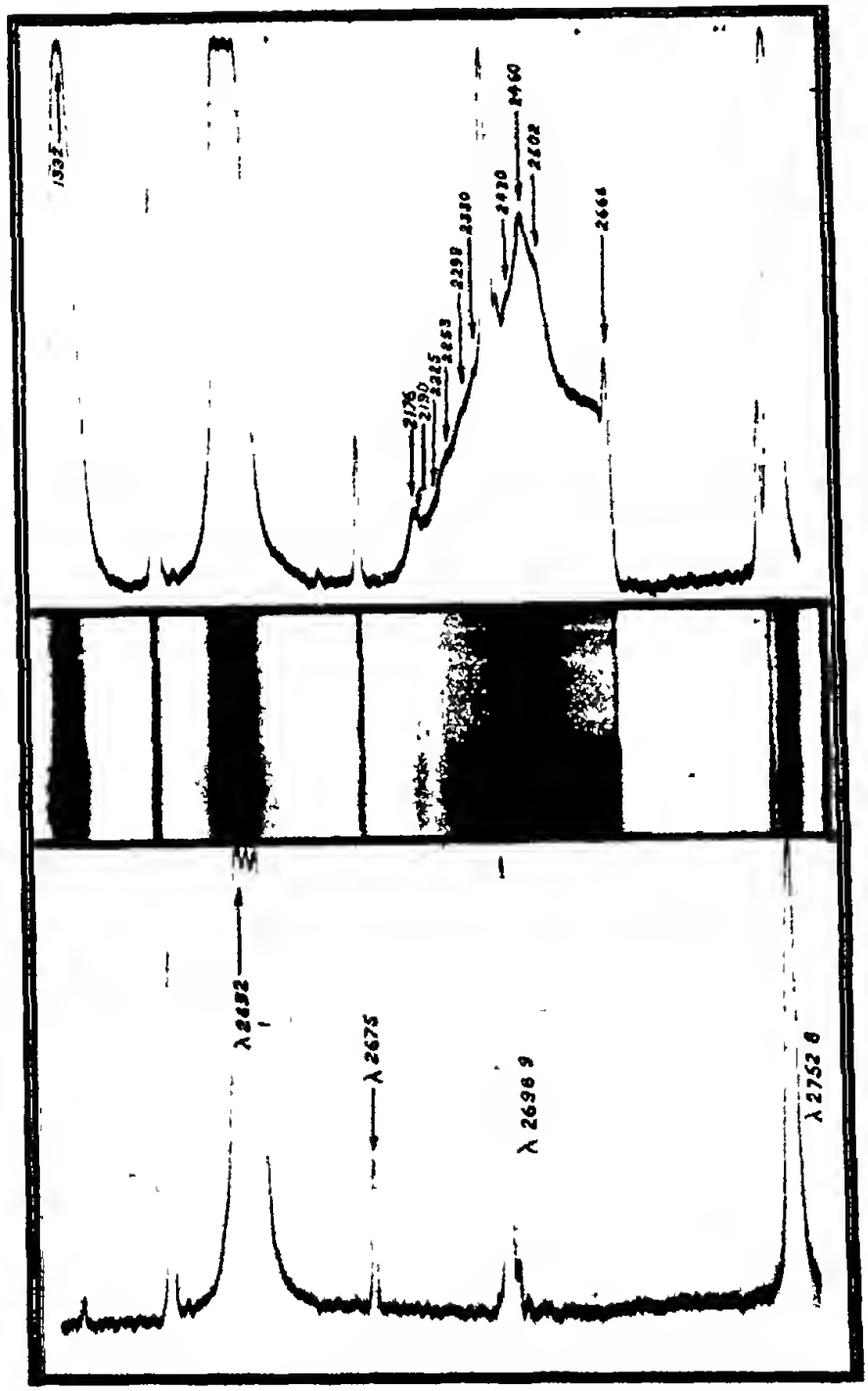

FIG. 1. (*a*) Microphotometer record of the second order spectrum of diamond
(*b*) The Raman spectrum of the second order in diamond
(*c*) Microphotometer record of the mercury spectrum

THERMAL EXPANSION OF DIAMOND

By Dr R. S Krishnan

(From the Department of Physics, Indian Institute of Science, Bangalore)

Received May 18, 1946

1 Introduction

It is well known that the coefficient of thermal expansion of a solid behaves qualitatively in the same manner as the specific heat, becoming constant at high temperatures, but reducing to zero as the temperature approaches the absolute zero Grüneisen (1912) who was the first to draw attention to this fact derived the following relation connecting the coefficient of thermal expansion α and the specific heat C_v of simple solids —

$$\alpha = \frac{\gamma \chi_0 C_v}{V_0}, \tag{1}$$

where χ_0 = the compressibility

V_0 = the atomic volume

and γ = a constant independent of temperature

Taking the value of γ as 1·1 for diamond and its specific heat values as given by a single Debye function corresponding to a characteristic temperature of 1860, Grüneisen (1926) satisfactorily explained the existing data on the thermal expansion of diamond due to Röntgen (1912) which covered the range of temperature from 84° T to 350° T Although the Grüneisen's relation is found to be valid over this range, a satisfactory test of the relation should require data over a wider range of temperature. Accurate measurements of the heat capacity of diamond have already been made by Pitzer (1938) over the range of temperature from 70° T to 300° T and by Magnus and Hodler (1926) from 273° T to 1100° T, while the thermal expansion of diamond does not appear to have been investigated above 350° T In view of the importance of the Grüneisen's relation in the theory of the solid state and its bearing on the nature of the vibration spectrum of a crystal, it was considered desirable to obtain data on the thermal expansion of diamond in order to test the validity or otherwise of the Grüneisen's relation for diamond at high temperatures In the present investigation* the thermal

* A preliminary report of the measurements of the coefficient of thermal expansion of diamond made by the author over the range of temperature from 28° to 680° C appeared in *Nature* (Vol 1944, 154, 486) The results obtained definitely established the dependence of γ on the temperature. The present paper deals with the results of new and more accurate measurements made by the author.

expansion of diamond has been studied over the range of temperature from 300° to 873° T

2. Technique of Study

As the expansion of diamond is rather small compared with that of ordinary solids and as the specimens available for study were in the form of thin plates, direct determination of the thermal expansion by the interferometric method could not obviously be made with any reasonable degree of accuracy The X-ray diffraction method was therefore employed and the variation of lattice spacings with increase of temperature was measured and the coefficient of thermal expansion calculated The technique of study was rather different from that usually adopted, being designed to enable the small expansion of diamond to be measured accurately It was based on the use of a beam of characteristic X-rays from a copper target diverging from a fine slit and falling on the crystal nearly at the Bragg angle for surface reflection The photographic film recording the reflections was kept at a considerable distance from the latter With a perfect crystal like some specimens of diamond, the characteristic X-ray reflections would appear as sharp lines, the width of which being nearly independent of the distance of the film from the crystal, would be determined by the fineness of the slit used. From the observed displacements of the $CuK\alpha_1$ and $K\alpha_2$ reflections when the temperature of the crystal was raised, the relative change in crystal spacing could be evaluated The observed shift being directly proportional to the crystal-film distance a very high degree of accuracy could be attained by increasing the latter.

3 Description of Apparatus

Camera—Fig 1 represents a horizontal cross-section of the X-ray camera employed in the present investigation It consisted of a fine lead slit S (4 mm high and 0 09 mm wide) which was kept facing and close to the window of a Coolidge demountable X-ray tube provided with a copper target At a distance of about 5 cm. from the slit was placed a single circle goniometer G The goniometer was so adjusted that its vertical axis was accurately parallel to the height of the slit To the axial rod of the goniometer was fixed a fused quartz tube with a drawn out end The crystal to be examined was held firmly in a slot at the drawn out end The quartz tube was long enough to ensure that its lower end was not sensibly heated up while the crystal itself was raised to the desired temperature by being enclosed in a small electrically heated chamber or furnace The latter which is not shown in Fig. 1 formed a separate unit which could be lowered over the crystal after all the necessary settings and adjustments have been made. To

the lower end of the goniometer axis were fixed two wooden arms about a meter in length, each one subtending an angle $2\theta_B$ with the line joining the slit to the crystal (see Fig. 1) θ_B is the Bragg angle for 111 reflection of diamond using CuKα radiations and has the value 21° 58′ Each arm carried a film holder (F_1 and F_2) which could be clamped at any desired distance from the crystal The films were always kept normal to the reflected beam A Hartmann diaphragm H provided with three holes was supported in front of each film holder as shown in the figure With the aid of this diaphragm three sets of X-ray reflections could be recorded in juxtaposition on the same film

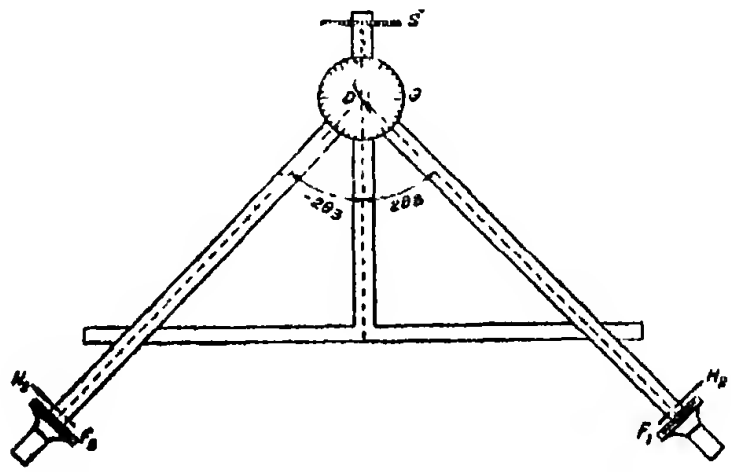

FIG 1 X Ray Camera

The Furnace—The constant temperature chamber consisted of a thin steel cylinder about 2½″ long and ½″ bore In order to permit free passage of X-rays over a wide angle through the centre of the heater, two segments about ¼″ high were cut away from the centre of the tube leaving two narrow ribs connecting the top and bottom halves of the tube To improve the uniformity of temperature within the chamber these segments were then closed by pieces of extremely thin aluminium foil (0 007 mm thick) The steel part of the tube was covered with a mica sheet and the heating coil was wound over the mica and set in position with the aid of a mixture of alumina and sodium silicate solution and finally covered over with asbestos Thick aluminium foil was then stuck on the outside of the furnace in order to minimise heat losses due to radiation The top of the furnace was closed by an iron disc to which was screwed a thin metal tube The latter was cemented on to a pyrex glass tube which was in turn fixed to the adjustable arm of a vertical stand. After placing the furnace in position above the crystal, it could be lowered vertically into the right position by means of a

rack and pinion arrangement The orifice at the bottom of the tube was partially closed by the quartz tube which supported the diamond to be studied The furnace had a low heat capacity so that the required temperature could be reached within a conveniently short time

4 Details of the Experiment

Calibration of the Furnace—As it was not possible to have a thermocouple inside the furnace to record the temperature of the crystal during exposures, the constant temperature chamber was calibrated beforehand A calibrated nichrome constantan thermocouple was supported vertically through a silica tube similar in size and shape to the one used for supporting the crystal in the actual experiment In order to measure the temperature of the air space within the furnace it was lowered over the silica tube containing the thermocouple such that the hot junction was at the position subsequently to be occupied by the crystal A steady current from a set of accumulators was then passed through the heating coil The current was measured on a good calibrated ammeter. The thermocouple was directly connected to a millivoltmeter When the steady state was reached which usually took about 15 to 20 minutes, the readings of the ammeter and the millivoltmeter were noted From the latter reading, the temperature of the chamber was evaluated On removing the furnace and replacing it, the temperature as recorded by the thermocouple was reproduced to $\pm 1°$ C As the temperature of the leads had no influence on the temperature recorded by the hot junction, it can be assumed that the thermocouple recorded the true temperature of the air space inside the furnace. The experiment was repeated with various heating currents and the steady temperature attained in each case was noted A curve showing the relation between the heating current and the steady temperature inside the furnace up to 650° C was drawn The furnace was recalibrated after a set of experiments and it was found that the calibration curve remained unaffected even after a lapse of six months. From the calibration curve the values of the heating current correct to the nearest readable division on the ammeter for temperatures as close to 100°, 200°, 300°, 400°, 500° and 600° C as could conveniently be arranged were read off The steady temperatures corresponding to these values of the heating current were accurately determined by experiment They were 105°, 205°, 300°, 405°, 505° and 605° C. While measuring the variation of the lattice spacings the crystal was maintained successively at these temperatures.

Selection and Mounting of the Diamond—As already remarked in Section 2, in order to attain a high degree of accuracy in the measurement

of the change of lattice spacing with temperature, it is necessary to use a piece of diamond which is the nearest approach to the perfect crystal Recent measurements of Ramachandran (1944) on the angular divergence of X-ray reflections in different diamonds have shown that diamonds which are opaque to the ultra-violet and which exhibit least fluorescence have the least angular divergence the value of which is just a little more than that for an ideal crystal Accordingly, diamond (N C 76) which had these characteristics was selected for the present investigation from Sir C V Raman's personal collection It was in the form of a triangular plate, about 0 9 mm thick, with its faces parallel to the octahedral cleavage planes

The mounting of the diamond on a suitable support presented some difficulty It was necessary to make the mounting sufficiently robust to withstand temperature changes without an accompanying change in the setting of the diamond Any displacement of the diamond caused by the yielding of the support when the temperature of the latter was raised would produce a spurious shift of the X-ray reflection After some trials, it was found that the use of a fused quartz tube for supporting the diamond and of a silicate dental cement for mounting it completely eliminated spurious effects up to a temperature of 500° C In the range of temperature from 500° to 600° C there was a slight effect which was corrected for by taking photographs of the X-ray reflections by rotating the crystal holder by twice the Bragg angle

The plate of diamond was mounted such that its surface (111) planes were exactly in the vertical plane and were parallel to the vertical axis of rotation of the goniometer It was then set roughly at the Bragg angle for surface reflection of copper $K\alpha$ radiations When the diamond was bathed in the divergent beam of X-rays, the characteristic $CuK\alpha$ line appeared in the distorted (111) X-ray topograph recorded on a film kept normal to the incident beam at a short distance from the crystal The film holder was moved away and kept normal to the incident beam at a distance of 80 cm from the diamond. A trial photograph was taken without the Hartmann diaphragm. The $CuK\alpha_1$ and $K\alpha_2$ reflections appeared on the film as sharp lines separated by about 0 9 mm The exposure time was adjusted so that the image recorded on the film was just clearly visible It was of the order of 10 minutes. No intensifying screen was used for photographing the reflections.

Using the Hartmann diaphragm, three sets of X-ray reflections were recorded in juxtaposition on the same film, the middle one with the diamond heated up to a known temperature and the top and bottom ones as controls

at room temperature. The room temperature photographs were taken one before and the other after the high temperature exposure During the experiment the camera was not disturbed The goniometer was then turned through twice the Bragg angle, *i e*, 43° 56′, so that reflections could occur at the second face of the diamond. With this setting and keeping another film at a distance of 80 cm from the crystal (see Fig 1), a series of three photographs were recorded in juxtaposition on it, the middle one with the diamond heated up to the same temperature as before and the top and bottom ones as controls at room temperature In this manner the experiment was repeated for temperatures 205°, 300°, 405°, 505° and 605° C As the shift of the X-ray reflection was smaller than the width when the temperature of the crystal was raised from 28° to about 100° C, it was evaluated in the following way. First the shift due to the rise of temperature from 28° to 300° was determined followed by that due to the rise of temperature from 105° to 300° C The difference gave the displacement due to an increase of temperature from 28° C. to 105° C The X-ray films were measured under a cross slide micrometer

5 Calculation of the Thermal Expansion Coefficient

When the temperature of the crystal is raised, its setting with reference to the camera might get altered giving rise to a spurious displacement of

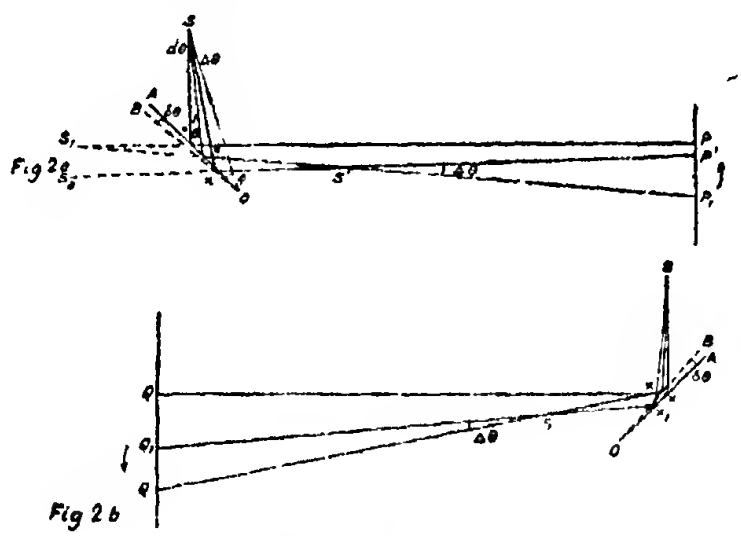

Figs. 2 *a* & 2 *b*

the X-ray reflection The observed shift would therefore be the sum of the displacement due to the change in the Bragg angle caused by the increase

in lattice spacing and the spurious displacement due to the change in the setting of the crystal. By taking measurements for two different goniometer settings as described in the previous section, the spurious effects are easily eliminated

S is the slit and OA the front surface of the diamond in the first setting At the room temperature the reflection appears at P or Q on the film (see Figs 2 *a* and 2 *b*) S_1 is the image of S in the plane of the diamond When the temperature is raised by $t°$ C, let the change in the lattice spacing be dl and the corresponding change in the *Bragg angle* $d\theta$

$$\text{since } 2l \sin \theta = \lambda, \quad d\theta = \frac{dl}{l} \tan \theta \tag{2}$$

This would produce a displacement x of the X-ray reflection on the photographic film x is equal to $(R + L)\, d\theta$, where R and L are the distances of the crystal from the slit and the film respectively Provided the setting of the crystal remains unchanged, the reflection will appear at P_1 and Q_1 for the two goniometer settings such that $PP_1 = QQ_1 = x = (R + L)\, d\theta$ (see Figs 2 *a* and 2 *b*)

Let us suppose that at the higher temperature the setting of the crystal with reference to the camera is altered Any vertical movement of the crystal in its own plane caused by the expansion of the support will not affect the horizontal displacement of the X-ray reflection Rotation of the plate about a vertical axis and/or a displacement normal to itself would, on the other hand, adversely affect the observed shift of the X-ray reflection Let us suppose that the diamond rotates through an angle $\delta\theta$ about the point 0 in the direction indicated in Figs 2 *a* and 2 *b*. A reference to the two figures shows at once that the displacements of the X-ray reflection for the $+\theta_B$ and $-\theta_B$ settings are given by x_1 and x_2.

where $$x_1 = (L + R)\, d\theta - (L - R)\, \delta\theta$$

and $$x_2 = (L + R)\, d\theta + (L - R)\, \delta\theta$$

$$x = \frac{\quad}{2} = (L$$

Thus the mean value of x_1 and x_2 gives the actual displacement due to the change in the Bragg angle

Similar results are also obtained for any displacement of the diamond normal to itself (see Figs 3 *a* and 3 *b*) It will be noticed that the displacements of the X-ray reflection due to the rotation or displacement of the diamond are in the same sense for both the settings while those due to the lattice spacing variation are in opposite directions for the two settings.

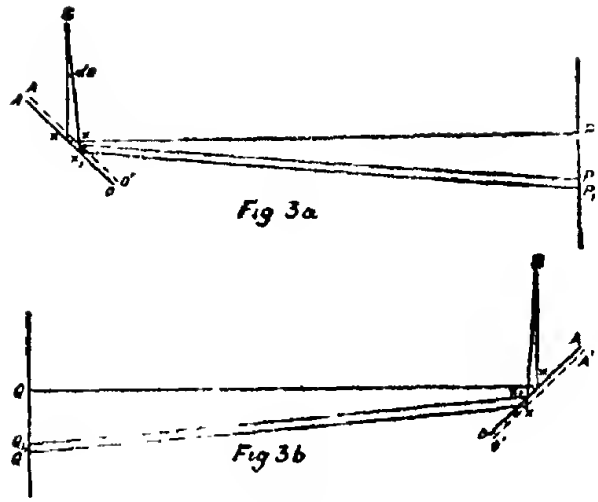

Fig 3a

Fig 3b

FIGS 3 a & 3 b

Let x_0 be the separation of $K\alpha_1$ and $K\alpha_2$ reflections Then

where l = the lattice spacing and $d\lambda$ is the wavelength separation of $CuK\alpha_1$ and $CuK\alpha_2$

$$\frac{x}{x_0} = \frac{d\theta\ 2l\cos\theta}{d\lambda}. \tag{3}$$

From equations (2) and (3) we get

$$\frac{x}{x_0} = \frac{dl}{l}\ \frac{\lambda}{d\lambda} \tag{4}$$

The increase in lattice spacing dl for a rise of temperature of t° is given by

$$dl = l\ \frac{x}{x_0}\ \frac{d\lambda}{\lambda} \tag{5}$$

and the mean coefficient of linear expansion is given by

$$\alpha = \frac{1}{t}\ \frac{dl}{l} = \frac{1}{t}\ \frac{x}{x_0}\ \frac{d\lambda}{\lambda}. \tag{6}$$

Thus the final expression for the coefficient of thermal expansion involves a term $\frac{x}{x_0}$ which could be accurately measured, λ the mean wavelength of the doublet and $d\lambda$ the wave-length separation The values of λ and $d\lambda$ have been accurately determined by the earlier workers. The expression for α does not, however, involve the distance of the film from the crystal or the slit.

6 Results

Typical photographs of the X-ray reflection showing the progressive displacement of the lines as the temperature is raised are reproduced in Plate V.

Table I

Temperature Range °T	Setting $(+\theta_2)$ $\frac{d_1}{x_0}$	Setting $(-\theta_2)$ $\frac{d_2}{x_0}$	Mean shift $\frac{d_1+d_2}{x_0} = \frac{x}{x_0}$	Change in lattice constant $da \times 10^3$
301–478	133	131	132	1 17 Å U
301–573	241	·239	24	2 13
301–678	382	·375	378	3 35
301–778	534	512	523	4 64
301–878	707	652	68	6 2
378–573	197	193	195	1 73
301–378	044	046	045	0 4

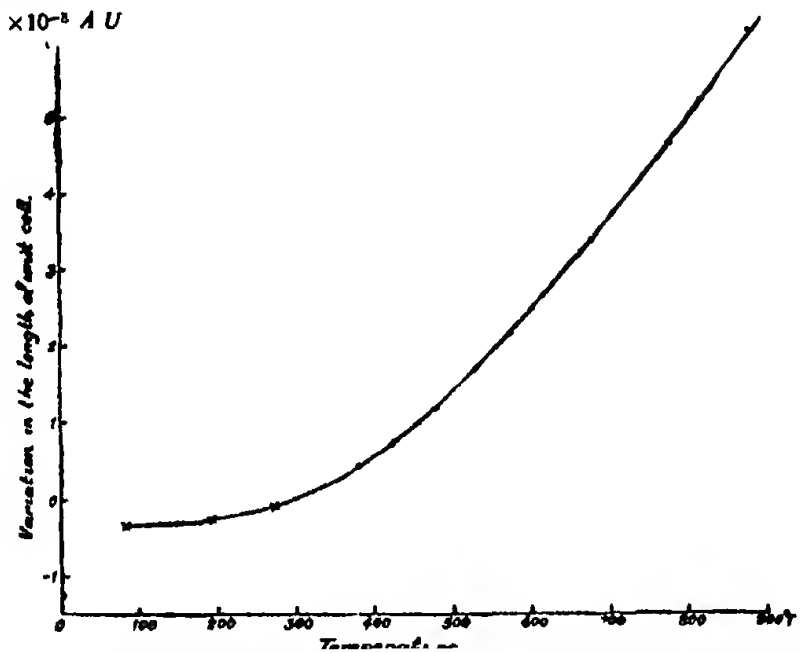

Fig 4 Change of lattice constant as a function of temperature Dots are author's values, and crosses are those calculated from the data of Röntgen

Table I gives the values of the displacements of the X-ray reflections in terms of the separation x_0 of the $K\alpha_1$ and $K\alpha_2$ lines As already indicated in Section 4, the displacements of the reflections are nearly the same for both the settings of the goniometer up to a temperature of 505° C, *i e*, 778° T The

increase of lattice-constant is calculated using equation (5) for the different temperature ranges and the values are given in column 5 of Table I. The lattice constant a at room temperature, *i e*, at 18° C (291° T) is taken as 3 55970 Å U. The wave-lengths of $CuK\alpha_1$ and $CuK\alpha_2$ are taken as equal to 1 537395 and 1 541232 Å U respectively. In Fig 3 the temperature of the diamond is plotted against the change of lattice-spacing taking the value at 28° C (301° T) as the standard. The portion of the curve below 301° T was drawn using the data on the thermal expansion coefficients for this region recorded by Röntgen (1912) and quoted by Grüneisen (1926).

Mean coefficient of cubic expansion (α) over the ranges of temperature of about 100° has been evaluated using equation (6). The results are shown in the 3rd column of Table II. Those above the dotted line are taken from the determinations of Röntgen (1912). The curve showing the variation of the mean coefficient of volume expansion with temperature is reproduced in Fig 4. The coefficient increases rapidly in the beginning and finally tends to a steady value at very high temperatures.

7 Discussion

The mean values of the atomic heat for the different ranges of temperature have been obtained by interpolation from the data of Pitzer (1938) below 273° T. and from the data of Magnus and Hodler (1926) above that temperature. These are given in column 5 of Table II.

Table II

Temperature Range °T	$\frac{x}{r_0}$	Mean value of $\alpha \times 10^6$	Calculated values of α using Grüneisen's value for γ	Mean value of Atomic Heat C_v	$\gamma = \frac{\alpha V_0}{A_0 C_v}$
84 8–104·1 ..		0 54	0 50	0 233	1 19
194·1–273 2 .		1 74	1 86	0 866	1 03
273 2–296 2		2 91	3 91	1 351	1·10
296·2–328 1 ..		3 51	3·45	1 605	1 12
328 1–351 1 ..		4 35	4 02	1 870	1 19
301–378 .	045	4·36	4 08	1·870	1·20
378–478 ..	087	6 51	5 8	2 627	1 27
478–573	·108	8 52	7 55	3 307	1·31
573–678 .	138	9 84	8 78	3 874	1·30
678–778 ..	·145	10 86	9 47	4·339	1·28
778–878 .	·157	11 76	10·03	4·657	1 29

Using the observed values of C_v and those of the coefficient of thermal expansion in equation (1), the values of γ for the different ranges of temperature have been evaluated. These are given in column 6 of Table II. The atomic volume V_0 is taken as equal to 3·42. The value of χ at 0° T. is not

known. The value of χ at 20° C given by Adams (1921) as 0 16 × 10^{-12} cm.²/dyne has been used in the evaluation of γ. The difference between χ_{293} and χ_0 would be very small for a crystal of extremely low compressibility like diamond The results presented in Table II go to show that γ, far from being independent of temperature, varies with temperature Its value increases steadily from about 1 03 in the temperature range 194–273° T to 1 31 in the range 478–573° T Above this temperature the value decreases slowly

Taking γ to be independent of temperature and equal to 1 1 as suggested by Grüneisen, Saksena (1944) has calculated the thermal expansion coefficients

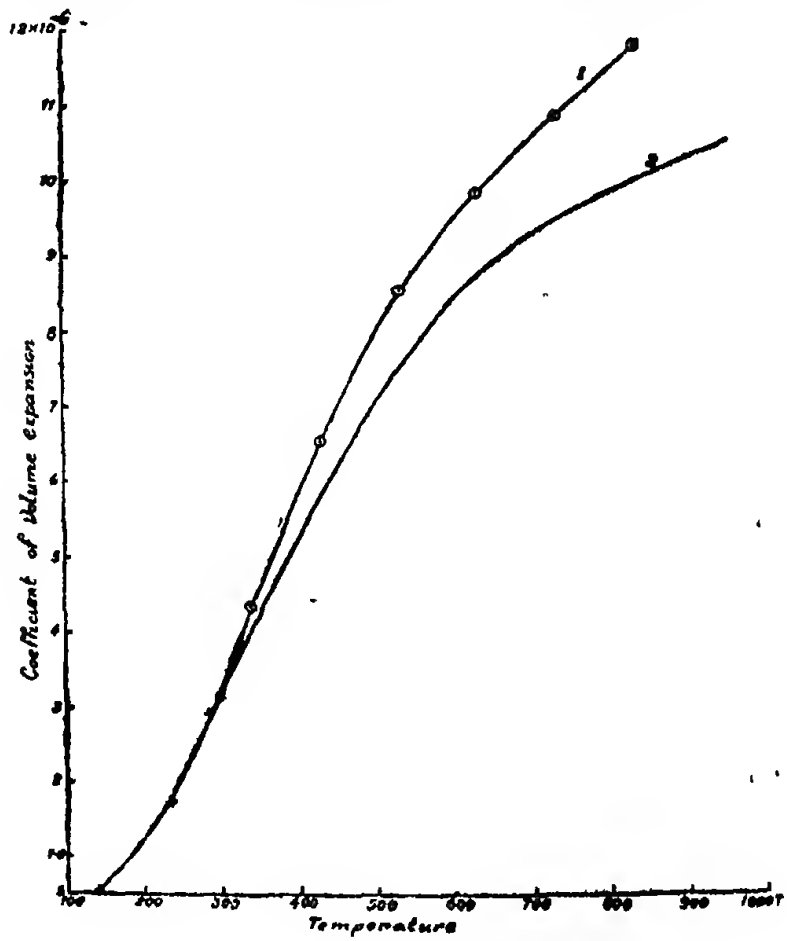

Author's observations
Röntgen's observations

FIG. 5. Mean coefficient of expansion as a function of temperature
Curve 1 Experimental, Curve 2 Theoretical on the basis of $\gamma = 1 \cdot 1$

of diamond for different ranges of temperature using equation (1) His results are given in column 4 of Table II The variation of the thermal expansion coefficient with temperature to be expected on the basis of Grüneisen's relation is graphically represented by curve 2 in Fig 5 There is fairly good agreement between the observed and calculated values of the coefficient of thermal expansion in the lower ranges of temperature, whereas at the higher temperatures the observed values are definitely higher, *e g*, to the extent of about 18% at about 600° C

The author wishes to express his grateful thanks to Sir C V Raman for the loan of the diamond and also for his kind interest in the work.

8 Summary

Using the X-ray method, the change in the lattice spacing of diamond with temperature has been measured over the range of temperature from 28° C to 605° C The technique employed is rather different from that usually adopted, being designed to enable the rather small expansion of diamond to be measured accurately The increase in the lattice constant at ordinary temperatures is small, while it is very rapid at higher temperatures From the observed changes in lattice constant, the mean coefficients of volume expansion for different ranges of temperature have been deduced The coefficient of volume expansion of diamond varies from $4\ 36 \times 10^{-6}$ in the range 301° – 378° T to $11\ 76 \times 10^{-6}$ in the range 778°–878° T Using the observed values of the coefficient of thermal expansion and the existing data on the atomic heat, the Gruneisen's constant γ which is the ratio $\frac{\alpha V_0}{\chi_0 C_v}$ has been evaluated V_0 is the atomic volume and χ_0 the compressibility of diamond It is shown that γ is not a constant, but increases from about 1 1 at low temperatures to about 1·3 at 600° T and falls again slowly as the temperature is raised

References

Grüneisen	*Ann d. Phys*, 1912, 39, 257
	Handbuch der Physik, 1926, 10, 41
Magnus and Hodler	*Ann d Phys*, 1926, 80, 808
Pitzer	*Journ Chem Phys*, 1938, 6 68
Ramachandran	*Proc Ind Acad Sci*, 1944, 20 A, 245
Röntgen	*Munch Ber*, 1912, 381
Saksena	*Proc Ind. Acad Sci*, 1944, 20 A, 92

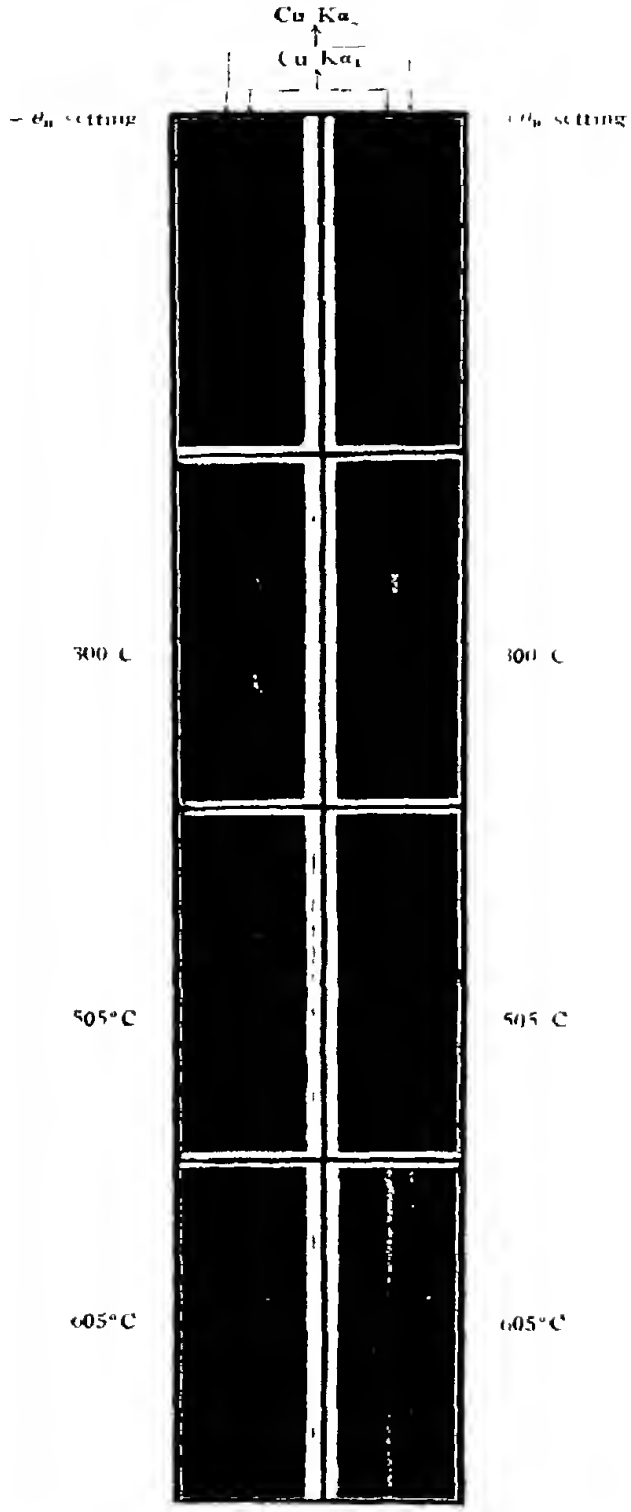
Cu Kα2
Cu Kα1
− θB setting
+ θB setting
300 C
300 C
505°C
505 C
605°C
605°C

FIG. 6

TEMPERATURE VARIATIONS OF THE RAMAN FREQUENCIES IN DIAMOND

By Dr R S Krishnan

(From the Department of Physics, Indian Institute of Science, Bangalore)

Received June 3, 1946

1 Introduction

When the temperature of a crystal is raised the atoms get less tightly packed resulting in an increase in the inter-atomic distances and a corresponding diminution of the forces acting on them The frequencies of atomic vibrations which are determined by the inter-atomic forces will therefore be decreased These frequency changes should in turn be related to the expansion of the crystal The actual form of the relationship will necessarily depend on the law of force between the atoms For constructing a simple theory of thermal expansion, G uneisen (1908) assumed that the relative change of any vibration frequency was directly proportional to the relative change in the volume In other words,

$$-\frac{\Delta \nu_i}{\nu_i} \times \frac{V}{\Delta V} = \frac{d(\log \nu_i)}{d(\log V)} =$$

where γ_i is a constant If we assume with Grüneisen (1912) that γ_i is the same for all the frequencies in the vibration spectrum of a crystal which is justified on the Debye theory, we then get from strictly thermodynamical considerations

where γ is the well-known Grüneisen constant V_0, χ_0 and C_v have the usual significance, namely volume, compressibility and specific heat of the crystal. Further, the quantity $\frac{d(\log \nu)}{d(\log V)}$ should be independent of temperature These conclusions have an important bearing on the theory of the solid state It is therefore necessary to see how far they are in agreement with facts in any particular case No attempt appears to have been made to test the validity of the above conclusions in any particular case. The present investigation was therefore undertaken with a view to get reliable data on the thermal variation of the Raman frequencies in diamond, the thermal expansion of which has already been studied in detail by the author (Krishnan, 1946 *a*)

2 Previous Work

Ramaswamy (1930) who was the first to photograph the Raman spectrum of diamond investigated the effect of temperature on the principal Raman frequency (1332 cm^{-1}) of diamond He reported that the Raman line was not perceptibly shifted or decreased in intensity and sharpness when the diamond was heated up to 250° C His negative result may be attributed either to the unsuitable way of heating the crystal or to the relatively small dispersion of the spectrograph employed by him Robertson, Fox and Martin (1934) reported similar negative results on cooling the crystal to − 180° C

Using the λ 4046 and λ 4358 excitation, Nayar (1941) measured the frequency shift of the principal line of diamond and its variation with temperature over the range of temperature from − 180° C to 860° C From the observed variation of the characteristic frequency, Nayar evaluated the thermal expansion coefficient of diamond and compared the same with the available data on thermal expansion which, however, covered only a short range of temperature The experimental value was definitely higher than the theoretical value Nayar's frequency-temperature curve in the region of high temperatures is not very reliable as it was based on observations made at three temperatures only in the range from 250° to 850° C

3 Details of the Experiment

As is well known, the first order Raman spectrum of diamond exhibits only a single, sharp and intense line with a frequency shift of 1332 cm^{-1} The other fundamental modes of oscillation of the diamond lattice are forbidden to appear in the first order spectrum Some of them manifest themselves as octaves and combinations in the second order Raman spectrum (Krishnan, 1944 *a*, 1946 *b*) The temperature variations of the frequencies of the forbidden modes have therefore to be estimated from the observed thermal behaviour of the Raman lines appearing in the second order spectrum As the second order lines are necessarily weak and not so sharp as the first order line (1332 cm^{-1}), it is not possible to determine their temperature variations with the same degree of accuracy and over short ranges of temperature as could be attained in the case of the principal line at 1332 cm^{-1} Two independent sets of experiments had therefore to be carried out In order to utilise the high resolving power of a quartz spectrograph in the ultra-violet and to take spectrum photographs with reasonably short exposures, the intense λ 2536·5 mercury resonance radiation was used for exciting the Raman spectrum. Diamonds of the ultra-violet transparent type were employed.

High Temperatures—For work above room temperature a specially designed heater was constructed It consisted of a thin rectangular steel tube (4" × ½" × ½") provided with three circular holes (¼" in diameter) covered with quartz windows on three of its sides in the central portion of the tube. These served for illumination of the crystal supported inside the tube and for observation of the scattered light The steel part of the heater was covered with a thin layer of mica and was closely wound over with nichrome wire set in a mixture of alumina and sodium silicate solution. To reduce losses due to radiation, an aluminium foil was stuck on to the outside of the furnace Steady current was supplied to the heater from a set of accumulators During an exposure the heater current was maintained at a constant value The top of the furnace was closed by a disc to which was attached a thin metal tube The tube supporting the furnace was clamped vertically to an adjustable stand

The specimen of diamond which was in the form of a thin plate (10 × 6 × 0 6 mm) was fixed on the top of a silica rod ¼" in diameter with its flat faces vertical and facing the most intense portion of a water-cooled magnet-controlled quartz arc The light scattered through one of the straight edges of the diamond in the end—on position was focussed on the slit of the spectrograph After the preliminary adjustments were made, the furnace was lowered into position To determine the temperature of the diamond during exposures, a calibrated nichrome-constantan thermocouple was fixed permanently inside the furnace almost touching the diamond Diamond being a good conductor of heat, its temperature was taken to be that of the air inside the furnace At the highest temperature used, namely, 700° C, after switching on the current, it took about 20-30 minutes for the furnace to come to a steady state

Low Temperatures—For work below room temperature a demountable vacuum flask with an inner vessel of metal and an outer vessel of glass was employed The lower end of the outer vessel was provided with two quartz windows Through one of these windows the diamond was irradiated with the light from the mercury arc, while the observation of the scattered light was made through the second window The thin plate of diamond was held in a copper block fixed to the bottom of the inner brass tube of the flask which formed the container for the refrigerant The flanged joint between the inner and outer tubes at the top was sealed with Apiezon sealing compound, "Q" The flask was kept evacuated continuously with the aid of a Cenco Hyvac pump.

Principal Raman Frequency (1332 cm^{-1})—For measuring the temperature variation of the principal Raman line, a Hilger El quartz spectrograph

having a dispersion of about 44 cm $^{-1}$/mm in the λ 2625 region was used. With a slit-width of 0 01 mm, exposures of the order of two hours were required to get the line recorded with a reasonable intensity. With the furnace in position, the temperature of the diamond was 55° C when no current was passed through the heater coil With the low temperature apparatus, the temperature of the diamond was the same as that of the room temperature, *viz*, 27° C, when no refrigerant was poured into the flask It was therefore necessary to make accurate measurements of the frequency shift of the principal Raman line for these two temperatures. For each temperature a couple of photographs of the Raman spectrum was taken with an iron arc comparison spectrum partially overlapping the Raman spectrum The plates were measured with a Hilger cross-slide micrometer reading up to 1/1000 mm The mean values of the frequency shift at 27° and 55° were evaluated in the usual way

Using a Hartmann diaphragm, two photographs of the Raman spectrum were recorded in juxtaposition on the same plate, one without any current passing through the heating coil, *i e*, the crystal being maintained at 55° C and the other with the crystal heated to a known temperature During the high temperature exposure, the furnace current was continuously regulated by hand in order to keep the temperature constant It did not vary by more than 2° from the desired temperature

The use of the high dispersion El spectrograph presented some difficulties in the beginning Being of an all-metal type, it was susceptible to small variations of temperature The spectrograph was housed in a separate double-walled cabin and the furnace, arc, etc, were placed outside In between two exposures, the cabin door had to be opened for shifting the Hartmann diaphragm While doing this, warm air from outside rushed into the cabin Consequently the temperature of the spectrograph varied to such an extent as to produce a noticeable drift of the mercury lines in the spectrogram recorded subsequently In order to minimise this trouble, the spectrograph was covered with two layers of woollen blankets which proved to be very effective As a further check, the frequency change of the 1332 line was evaluated not from the observed shift of this line, but from the relative shift with reference to the nearest mercury lines on either side

The frequency changes of the principal Raman line were determined for 13 different temperatures above 55° C, namely, 117° 152°, 211°, 242°, 285°, 345°, 396°, 452°, 500°, 550°, 600°, 654° and 703° C Two low temperature measurements were also obtained by using liquid air as refrigerant in one case and solid carbon dioxide-acetone mixture in the other case.

Second order Raman lines—Using a Hilger E3 medium quartz spectrograph which had a dispersion of about 140 cm^{-1}/mm, a heavily exposed Raman spectrum of diamond showing the second order lines was recorded with the specimen (N C 89) maintained at room temperature (30°) by fan cooling Similar photographs were also taken on different plates with the crystal maintained successively at 390° C and 620° C The constant temperature furnace described earlier in the section was used for this purpose The negatives were microphotometered, and from the microphotometric records the frequency shifts of the prominent second order lines were estimated

4 Results

The frequencies of the principal Raman line at different temperatures are given in Table I and the variation with temperature is graphically represented by the curve in Fig 1 The ordinates represent the decrease or

TABLE I

Frequencies of the principal Raman line in diamond at different temperatures

Temperature of	Frequency shift in cm^{-1}
85	1333·2
195	1332 7
300	1331 8
328	1331 5
390	1330 4
425	1329 6
484	1327 7
515	1327 3
558	1327 0
618	1325 6
669	1324 4
725	1323 1
773	1322 2
823	1320 8
873	1318 9
927	1317 6
976	1316 0

increase in frequency shift from the value at 300° T It will be noticed that the rate of decrease, *i e*, $-\frac{d\nu}{dT}$, is greater at higher temperatures As the temperature is lowered the curve tends to flatten up Comparing the results reported here with those of Nayar (1941), it is seen that although the general features of the ($\Delta\nu - T$) curve are similar in both cases, the actual values of the frequency shifts at higher temperatures are not in agreement For example, when the temperature of the diamond was raised from room

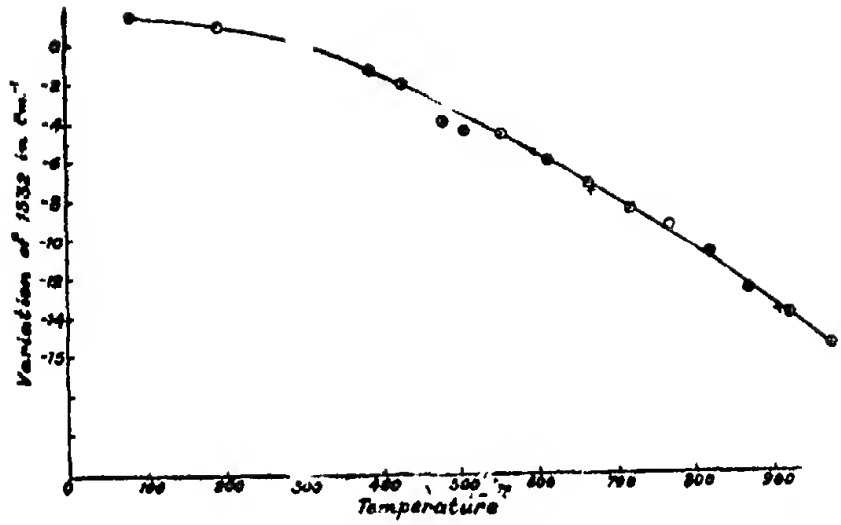

FIG 1

FIG 1 Frequency-Temperature curve for the principal Raman line of diamond

temperature to 632° C, Nayar recorded a change in the frequency equal to 10 2 wavenumbers Actually, for the same range of temperature the author has observed a frequency change of 13 4 wavenumbers The deviation increases with increasing temperature In order to be sure that the observed deviation had nothing to do with the type of diamond used in the present investigation, the experiment was repeated for two temperatures using the same specimen of diamond with which the thermal expansion measurements were made (Krishnan, 1946 *a*) and which belonged to the ultraviolet opaque type. In an earlier publication (Krishnan, 1944) the author had shown that at room temperature there is no difference in the frequency shifts of the principal Raman line for the two types of diamond. Using the constant temperature furnace described in the previous section, a Hilger two prism spectrograph and λ 4358 excitation, the frequency changes for the ultraviolet opaque diamond were measured for two ranges of temperature, namely, 55°-398° C and 55°-640° C The values are plotted in Fig 1. They are indicated by crosses and fall on the smooth curve, showing thereby that the temperature variations of the principal Raman frequency are the same for the two types of diamond in the range of temperature covered by the present investigation.

The smaller values for the frequency changes reported by Nayar (1941) may be attributed to the fact that in his experiments the thermo-couple might not have recorded the correct temperature of the diamond. As the specimen was kept at one end of the furnace, its temperature was in all

probability lower than the temperature inside the furnace. The thermo-couple which was supported inside the heater recorded the correct temperature of the latter and not of the crystal In the present experiment the diamond which was only 1 cm in length was supported inside the furnace which was about 4" long In order to eliminate air currents passing through the furnace, the top was completely closed by a metal disc, while the bottom was partially covered by the supporting quartz rod The calibration curve for the thermo-couple was checked against the readings taken with a standard thermometer

Table II gives the values of the frequency shifts of some of the prominent second order Raman lines at three different temperatures It is evident from the figures given in Table II that for the same increase of temperature,

TABLE II

Frequency shifts in wavenumbers of the prominent second order Raman lines in Diamond

30°	390°	620°
2666	2652	2640
2502	2494	2486
2460	2449	2438
2176	2171	2158

the proportional change in the frequency shift is different for different second order Raman lines

5 Discussion of Results

The quantity $\frac{d(\log \nu)}{d(\log V)}$ can be written in the form :—

$$\frac{d(\log \nu)}{d(\log V)} = \frac{d\nu}{\nu} \frac{V}{dV} \frac{\Delta \nu}{\nu} \frac{1}{\bar{a}(T_2 - T_1)}, \tag{3}$$

where $\Delta \nu$ is the diminution in frequency ν in the temperature range T_1 to T_2 and $\bar{a}$ is the mean coefficient of thermal expansion over the same range. In column 3 of Table III are given the observed values of the mean coefficient of thermal (volume) expansion for the different temperature ranges entered in column 1. The values below the horizontal line are those reported by the author (Krishnan, *1946 a*), while those above the horizontal line were taken from Röntgen's (1912) measurements The corresponding values of $\Delta \nu$ in wavenumbers for the principal Raman line (1332 cm.$^{-1}$) in diamond are read off from the curve reproduced in Fig 1 and are given in column 4.

The quantity $\gamma_{1332}\left\{=\frac{d(\log \nu)}{d(\log V)}\right\}$ has been evaluated using equation (3) The values for the different temperature ranges are entered in column 5 of Table III

TABLE III

Temperature range ° T	Mean Temperature ° T	$\bar{a} \times 10^6$	$\Delta\nu_{1332}$ in cm^{-1}	γ_{1332}	$\gamma = \frac{aV_0}{X_0 C_p}$
84 8–194·1	139 5	0 54	0 5	6 4	1 19
194 1–273 2	233 6	1 74	0 6	3·3	1·03
273 2–296 2	284 7	2 91	0 3	3 4	1·10
296 2–351 1	323	3 87	0 9	3 2	1·15
301–378	339 5	4 36	1 3	2 9	1 20
378–478	428	6 51	1 9	2·7	1·27
478–573	525	8 52	2 0	1·9	1 31
573–678	625	9 84	2 45	1 8	1·3
678–778	728	10 86	2 5	1 7	1 3
778–878	828	11 76	2 7	1 7	1 3

The last column in the above table gives the values of the Grüneisen number $\left(\frac{aV_0}{X_0 C_p}\right)$ taken from another paper by the author (Krishnan, 1946*a*) appearing in this symposium It is evident that γ_{1332} far from being a constant, *decreases* steadily from a value of 6 4 at 85° T to about 1 8 at 600° T Above 600° T its value remains constant The temperature dependence of γ_{1332} is graphically represented in Fig 2 The portion of the curve below

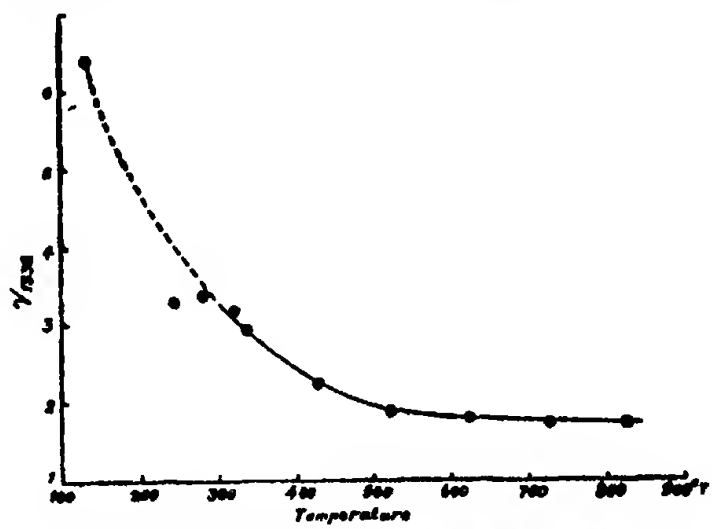

FIG 2 Temperature dependence of γ_{1332}, *i e*, the ratio of the relative change of frequency to the relative change of volume

273° T is shown by a broken line as the values of γ_{1332} are not so accurate as those at high temperatures owing to the small values of $\bar{a}$ and $\Delta\nu$ Comparing the values given in columns 5 and 6 in Table III one finds that throughout the range of temperature investigated here γ_{1332} is not equal to the Grüneisen number γ

The mean values of γ_i for the prominent second order Raman lines for the temperature ranges 30–390° C and 30–620° C have been evaluated from the observed displacements of the lines The results are entered in Table IV As is to be expected, γ_i is the same for the 1332 line and its octave at 2666 cm $^{-1}$ Different frequencies have in fact different γ_i's, that for the principal Raman line (1332 cm $^{-1}$) being the highest It is interesting to

TABLE IV

Raman line	$\bar{\gamma}_i$ 30–390°	$\bar{\gamma}_i$ 30°–620°
1332	2 0	1 9
2666	2 0	1 9
2502	1 2	1 2
2460	1 7	1 7
2176	0 3	1 6

note that γ_i for the line 2176 increases with temperature This line is evidently the octave of the prominent lattice line with a frequency shift of 1088 cm $^{-1}$ appearing in the luminescence and absorption spectra of diamond

Curves showing the relation between the increase of lattice spacing with increase of temperature and the corresponding decrease of frequency have been reproduced in Fig. 3 for the Raman lines 1332, 2502 2460 and 2176 cm $^{-1}$ The data on the lattice spacing variation were taken from the author's paper on the thermal expansion of diamond. Above room temperature, *i e*, 300° T the relationship is nearly linear for the lines 1332, 2460 and 2502 cm.$^{-1}$, but with different slopes The variation of the frequency of the 2176 line is represented by a more complicated curve. The relative decrease in frequency shift of this line is smaller at low temperatures, and increases rapidly above 400° C. The difference in the thermal behaviour of the Raman lines is due to the fact that the inter-atomic forces inside the diamond lattice are affected by temperature to varying extent On the basis of the lattice lines observed in luminescence, the Raman lines 2502 cm $^{-1}$ and 2176 cm $^{-1}$ can be assigned as the octaves of the fundamentals with frequency shifts 1251

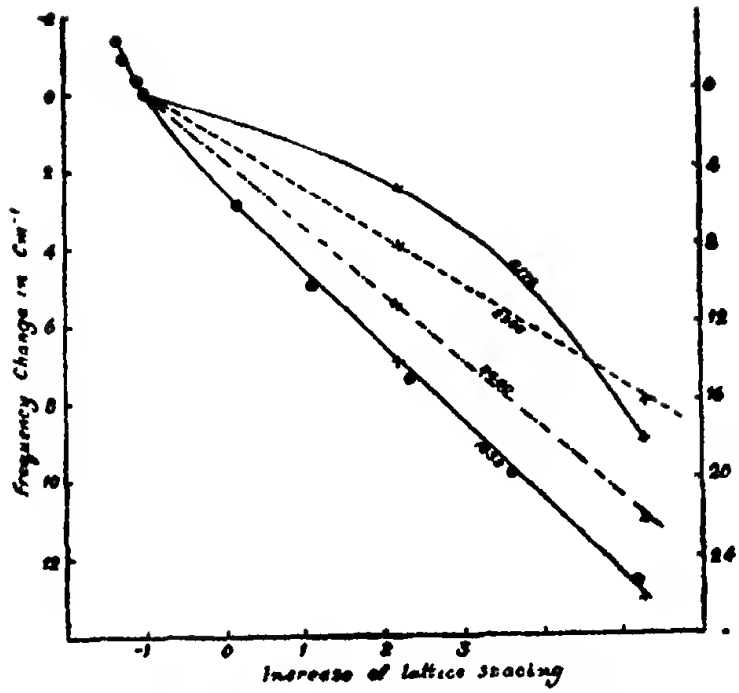

FIG 3 Dependence of frequency on lattice spacing

and 1088 cm^{-1} The lattice lines with frequency shifts 1332, 1251 and 1088 correspond to the modes F_2, H_4 and K_3 as designated by Bhagavantam (1943) The expressions for the frequencies are given in Table V.

TABLE V

Mode	$4\pi^2\nu^2$	Observed ν in cm^{-1}
F_2 ..	$\frac{8K \times 64K_e}{3m}$	1332
H_4 .	$\frac{8K \times 4K_e + 12K''}{3m}$	1251
K_3 .	$\frac{6K + 24K''}{3m}$	1088

K, K_e and K″ are the respective force constants arising from the primary valence bond, the directed valence bond and the repulsion between the next nearest neighbours. Their values are according to Dayal (1944) —

$$K = 0\ 314 \times 10^6 \text{ dynes/cm.}$$
$$K'' = 0{\cdot}039 \times 10^6 \quad ,,$$
$$K_e = 0\ 0197 \times 10^6 \quad ,,$$

From the observed variations of the frequencies of F_2, H_4 and K_3 with lattice spacing the corresponding changes in the force constants have been estimated When the temperature of the diamond is raised from 300° T to 800° T the values of K and K_a *decrease* by 3 7 × 10^2 dynes/cm and 2 5 × 10^2 dynes/cm. respectively, whereas the value of K″ increases by 3 4 × 10^2 dynes/cm The decrease in the value of K is of the same order of magnitude, but definitely greater than that of the force constant of the C—C bond with increase in the equilibrium nuclear distance as deduced from band spectrum data.

6 Width of the 1332 Line and its Interpretation

The author had remarked in one of the earlier papers (Krishnan, 1944 *b*) that the principal Raman line in diamond, though sharp, had a finite width at room temperature As the temperature is raised, this line is found to broaden, the aggregate intensity of the line being greater at the higher temperature The widths of the line at different temperatures have been estimated from the microphotometric records of the corresponding spectrograms. Typical microphotometric curves showing the variation of line width with

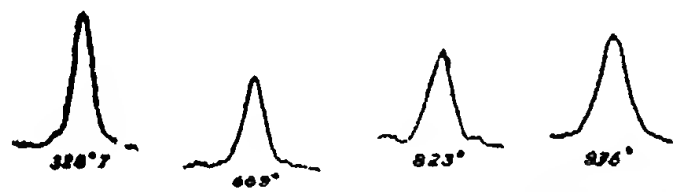

Fig. 4 Microphotometric records of the 1332 line at different temperatures

temperature are reproduced in Fig 4 The relation between the half width of the 1332 line at half intensity and the temperature of the diamond is illustrated by the curve reproduced in Fig 5 The values entered as ordinates are the measured half widths without making any allowance for the finite

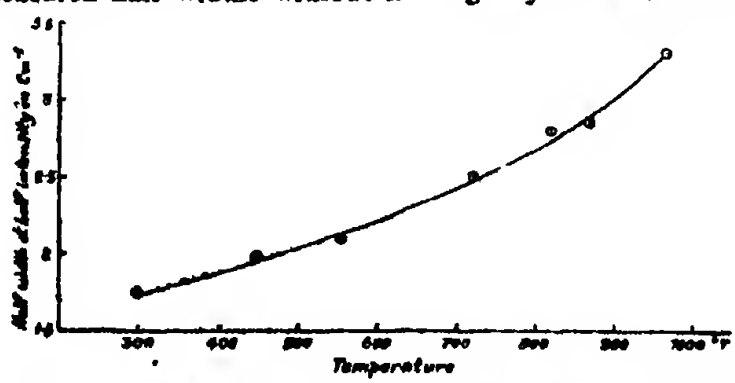

Fig. 5. Temperature dependence of the half width at half intensity of the 1332 line

width of the slit and other factors connected with the spectrograph A mercury line which was recorded on the plate with roughly the same intensity as the Raman line had a half width at half intensity of 1 5 wavenumbers The rate of increase of the breadth of the 1332 line increases with temperature The enhanced width of the 1332 line at high temperatures cannot be attributed to temperature variations of the furnace as the latter never exceeded 2° either way

The finite width of the Raman line at any particular temperature may be attributed to the thermal fluctuations in density inside the crystal On the basis of the new lattice dynamics, if the atoms within an element of volume in the crystal of sufficient extension are arranged with perfect regularity in the lattice, their vibrations would be strictly monochromatic But due to thermal agitation the lattice spacings undergo fluctuations As the domain gets compressed, the atomic vibration frequency increases and when it expands, the frequency gets diminished As the compressions and expansions are of varying magnitude, the frequency will vary continuously about the mean value, giving rise to a finite width for the Raman line The mean square of the fluctuations in volume is given by the well-known formula

$$(\Delta V)^2 = kT\chi V \tag{4}$$

where k is the gas constant, χ compressibility and V is the volume of the domain The relative mean fluctuation in volume is given by

$$\frac{\sqrt{(\Delta V)^2}}{V} = \sqrt{\frac{kT\chi}{V}} \tag{5}$$

From the observed variations of the frequency shift of the 1332 line with increase in lattice spacing, the half width of the line arising from the relative mean fluctuation in a volume element at any desired temperature can be evaluated The values of the half width for three different sizes of the volume element, namely, $V_1 = 8$ times, $V_2 = 64$ times and $V_3 = 512$ times the volume of the unit cube, and for different temperatures are given in Table VI

TABLE VI

Temperature °T	Calculated mean half width in cm.$^{-1}$			Observed value of half width*
	V_1	V_2	V_3	
300	10 8	4 3	1 7	1·7
500	13·7	5 1	2·1	2·1
700	16 4	6·1	2 5	2·4
900	18 0	8·9	2·8	2·9
970	18 8	7·1	2 9	2 6

* No correction has been made for the width arising from the finite width of the exciting line, width of slit used and other factors connected with the spectrograph.

Comparing the figures given in Table VI, it is evident that for a volume element which has 8 times the linear dimensions of the unit cubic cell, the calculated half width of the 1332 line is of the same order of magnitude as the observed half width at half intensity

In conclusion, the author wishes to express his grateful thanks to Professor Sir C V Raman for useful discussions during the progress of these investigations

Summary

With a high dispersion spectrograph, a diamond of the ultraviolet transparent type and the mercury λ 2536 5 excitation, the principal Raman frequency has been measured and is found to decrease from 1333 2 cm.$^{-1}$ at 85° T to 1316 0 cm^{-1} at 975° T Identical results are obtained with a diamond of the ultraviolet opaque type and the λ 4358 excitation The temperature dependence of the more prominent second order Raman frequencies has also been investigated The relative change of the principal frequency with relative change of volume decreases from a high value at 85° T to a constant small value above 500° T and differs greatly from the so-called Grüneisen constant The different lattice and superlattice frequencies behave differently in respect of their temperature variation and this has been explained as due to differences in the rate of change with temperature of the different force constants which determine the vibration frequencies of the diamond lattice

The 1332 line has a finite width which increases with temperature. This may be explained as due to the changes of lattice frequency arising from the thermal fluctuations of density in the volume elements of the crystal, if the effective linear dimensions of a volume element are assumed to be about 8 times as large as the edge of the unit cubic cell

References

Bhagavantam, S	*Proc. Ind Acad. Sci*, 1943, 18 A, 25
Dayal, B	*Ibid*, 1944, 19, 224
Grüneisen	*Ann der Phys*, 1908, 26, 211, 1912, 39, 266.
Krishnan, R. S	*Proc Ind Acad Sci.*, 1944 *a*, 19, 216, 1944*b*, 19, 298.
	Ibid, 1946 *a*, 24, 33, 1946 *b*, 24, 25
Nayar, P G N	*Ibid*, 1941, 13, 284.
Ramaswamy, C	*Ind Journ Phys*, 1930, 5, 97
Robertson, Fox & Martin	*Phil Trans.*, 1934, 232, 463
Röntgen, W C.	München Berichte, 1912

ON THE CRYSTAL SYMMETRY OF DIAMOND AND ITS X-RAY REFLECTIONS

By G N Ramachandran

(From the Department of Physics, Indian Institute of Science, Bangalore)

Received May 18, 1946

(Communicated by Sir C V Raman, Kt, F R S, N L)

§1 On the basis of the observed crystal forms of diamond, especially of grooved octahedra, duplex tetrahedra and such other typical twin forms, the earlier crystallographers assigned diamond to the hemimorphic hemihedral or the tetrahedral (Td) class of the cubic system (*vide* Groth, 1895, Liebisch, 1896, Miers, 1902, Hintze, 1904) That this is the case in the majority of diamonds is confirmed by observations of the infra-red absorption of diamond by a number of investigators (Ångstrom, 1892; Julius, 1893; Reinkober, 1911) and particularly by Robertson, Fox and Martin (1934), who found that a majority of diamonds exhibit a strong infra-red absorption in the region of 8μ, while in other diamonds, the absorption is absent. Applying the well-known selection rules for infra-red absorption (Placzek, 1934), it becomes obvious that the former class of diamonds should possess only tetrahedral (Td) symmetry, while the latter should possess the full octahedral (Oh) symmetry of the cubic system (Raman, 1944) An alternative explanation that the infra-red absorption arises from the presence of impurities or of structural imperfections is ruled out by the fact that the diamonds that show the absorption most prominently are precisely those that possess the maximum amount of crystal perfection (Ramachandran, 1944 *b*), while *per contra* diamonds that possess a large mosaic structure are transparent to the infra-red (Hariharan, 1944, Ramachandran, 1944 *a*) To explain these facts regarding infra-red absorption as well as a whole series of other phenomena exhibited by diamond, Sir C V Raman (1944) put forward considerations which indicate that there are four possible structures for diamond, two with tetrahedral symmetry and two others with octahedral symmetry, and in doing so remarked that the data regarding the X-ray reflections given by diamond are consistent with the existence of these four forms In the present paper, this question is considered in a formal and rigorous manner. The consequences of the difference in symmetry of the various structures

are worked out, and are compared with the observed X-ray behaviour of diamond *

We shall accept the results of X-ray analysis that the diamond structure consists of two interpenetrating face-centred cubic lattices, with the carbon atoms in the basis occupying the positions 000 and $\frac{1}{4}\frac{1}{4}\frac{1}{4}$ It may be pointed out that the main facts which led to this structure were the absence of the 200 and the 222 X-ray reflections observed by the earliest investigators (Bragg and Bragg, 1913) We shall accept the structure described above, since it fits in well with the quadrivalence of carbon, a well-known chemical result The questions to be decided are (*a*) what the symmetry of the electronic configurations of the individual carbon atoms is, and (*b*) what the relationship between the electronic structures of the two carbon atoms is In this connection, we have also to discuss the results of later experimenters, who have remarked that the 222 reflection is present feebly, *e g*, Bragg, 1921, Ehrenberg, Ewald and Mark, 1928

§2 On account of the special positions which the carbon atoms occupy in the space-lattice, they should possess a symmetry not lower than that of the point-group Td For the purpose of the following discussion, we shall take it that they possess that symmetry This means that if $\rho_1(xyz)$ is the electronic charge density at the point xyz, then it is the same at the following 24 equivalent points·

$$\begin{array}{llllll} xyz; & zxy, & yzx, & yxz, & zyx, & xzy, \\ x\bar{y}\bar{z}, & z\bar{x}\bar{y}, & y\bar{z}\bar{x}, & \bar{y}x\bar{z}, & \bar{z}y\bar{x} & x\bar{z}\bar{y}, \\ \bar{x}y\bar{z}, & \bar{z}x\bar{y}, & \bar{y}z\bar{x}, & \bar{y}x\bar{z}, & \bar{z}y\bar{x} & \bar{x}z\bar{y}, \\ \bar{x}\bar{y}z, & \bar{z}\bar{x}y, & \bar{y}\bar{z}x, & \bar{y}\bar{x}z, & \bar{z}\bar{y}x, & \bar{x}\bar{z}y, \end{array} \qquad (1)$$

This set may be represented by the symbol $\{xyz\}$ Similarly, the electronic charge densities at the points $\frac{1}{4}\frac{1}{4}\frac{1}{4}+\{xyz\}$ are all equal, which may be denoted by $\rho_2(xyz)$. Note that no assumption is made as to the relationship between ρ_1 and ρ_2 For the present, it is supposed that the two carbon atoms are different It is also to be noted that $\rho(xyz)$ is not necessarily equal to $\rho(\bar{x}\bar{y}\bar{z})$

We shall now derive an expression for the structure factor for the *hkl* reflection with such a structure Consider a set of 96 volume elements, each of magnitude dv, surrounding the points $\{xyz\}$, $\{\bar{x}\bar{y}\bar{z}\}$, $\frac{1}{4}\frac{1}{4}\frac{1}{4}$

* A preliminary report by the author (1945) appeared in *Nature*, in which some specific points raised by Mrs Lonsdale (1945) regarding the X-ray behaviour of the various forms of diamond were answered.

and $\frac{1}{4}\frac{1}{4}\frac{1}{4} + (\bar{x}\bar{y}\bar{z})$ Denoting by $\phi(hkl)$ the structure factor corresponding to these volume elements, it can be shown that

$$\phi(hkl) = \{\rho_1(xyz)(A + iB) + \rho_1(\bar{x}\bar{y}\bar{z})(A - iB) + \rho_2(xyz)(A + iB)$$
$$\exp 2\pi i(h + k + l)/4 + \rho_2(\bar{x}\bar{y}\bar{z})(A - iB)\exp 2\pi i(h + k + l)/4\}\, dv, \quad (2)$$

where
$$A = 16\cos 2\pi\frac{h-k}{4}\cos 2\pi\frac{k-l}{4}\cos 2\pi\frac{l-h}{4}.$$
$$\{\cos 2\pi lz(\cos 2\pi hx\cos 2\pi ky + \cos 2\pi kx\cos 2\pi hy)$$
$$+ \cos 2\pi hz(\cos 2\pi kx\cos 2\pi ly + \cos 2\pi lx\cos 2\pi ky)$$
$$+ \cos 2\pi kz(\cos 2\pi lx\cos 2\pi hy + \cos 2\pi hx\cos 2\pi ly)\} \quad (3)$$

and
$$B = -16\cos 2\pi\frac{h-k}{4}\cos 2\pi\frac{k-l}{4}\cos 2\pi\frac{l-h}{4}$$
$$\{\sin 2\pi lz(\sin 2\pi hx\sin 2\pi ky + \sin 2\pi kx\sin 2\pi hy)$$
$$+ \sin 2\pi hz(\sin 2\pi kx\sin 2\pi ly + \sin 2\pi lx\sin 2\pi ky)$$
$$+ \sin 2\pi kz(\sin 2\pi lx\sin 2\pi hy + \sin 2\pi hx\sin 2\pi ly)\}. \quad (4)$$

The crystal structure factor $F(hkl)$ can be obtained by integrating $\phi(hkl)$ over the appropriate volume From the above expressions, the elementary structure factors corresponding to the 200 and the 222 reflections are:

$$\phi(200) = A\,dv\,\{\rho_1(xyz) + \rho_1(\bar{x}\bar{y}\bar{z}) - \rho_2(xyz) - \rho_2(\bar{x}\bar{y}\bar{z})\} \quad (5)$$

$$\phi(222) = iB\,dv\,\{\rho_1(xyz) - \rho_1(\bar{x}\bar{y}\bar{z}) - \rho_2(xyz) + \rho_2(\bar{x}\bar{y}\bar{z})\} \quad (6)$$

Consequently, the condition that the 200 or the 222 reflection should vanish is that the quantity within the double brackets in Eq (5) or (6) respectively should be equal to zero

Let us now consider the circumstances under which the structure possesses octahedral symmetry This can occur in one of two possible ways: the individual carbon atoms can themselves possess octahedral symmetry, or the two carbon atoms can be tetrahedral, but possess identical configurations with the two tetrahedral atoms pointing in opposite directions. In the latter case, the structure has a centre of symmetry at $\frac{1}{4}\frac{1}{4}\frac{1}{4}$, and belongs to the space group O_h^7 The two conditions can algebraically be represented as follows:

$$(a)\quad \rho_1(xyz) = \rho_1(\bar{x}\bar{y}\bar{z}),\quad \rho_2(xyz) = \rho_2(\bar{x}\bar{y}\bar{z})$$
$$(b)\quad \rho_1(xyz) = \rho_2(\bar{x}\bar{y}\bar{z});\quad \rho_1(\bar{x}\bar{y}\bar{z}) = \rho_2(xyz) \quad (7)$$

A careful comparison of the conditions for the vanishing of the 200 and the 222 reflections with those for the existence of octahedral symmetry shows that there is really no interrelation between them, though if 7 (*b*) subsists, the 200 reflection automatically vanishes In other words, from the knowledge that the 200 or the 222 reflection is present or absent, one cannot uniquely conclude that the crystal has tetrahedral or octahedral symmetry and *vice versa*

§3 It is a fairly well-established experimental fact that the 200 reflection does not appear with diamond Taking this into consideration, let us consider what restrictions it imposes on the structure From (5), the condition that 200 should vanish is

$$\rho_1(xyz) + \rho_1(\bar{x}\bar{y}\bar{z}) = \rho_2(xyz) + \rho_2(\bar{x}\bar{y}\bar{z}), \tag{8}$$

i e, if we take two points in each of the atoms such that they are equidistant in opposite directions from the centre of the atoms, then the sum of the electronic charge densities at these two points should be the same for both the atoms. From this, it follows that the total charge in spherical shells surrounding the two atoms are equal, provided the radii of the two shells is the same, independent of the magnitude of the radius This explains why diamond is not a polar substance, and also makes it comprehensible why diamond does not exhibit any appreciable piezo- or pyro-electric properties. However, the condition (8) does not impose any restriction at all on the symmetry of the structure

We shall now consider the various structures that are possible, subject to the condition (8) In this connection, it will be convenient to use a special nomenclature It will be seen that if

$$\rho_1(xyz) = \rho_2(\bar{x}\bar{y}\bar{z}) \text{ and } \rho_1(\bar{x}\bar{y}\bar{z}) = \rho_2(xyz),$$

then the equation (8) is satisfied This is identical with (7 *b*), and the structure has a centre of symmetry mid-way between the two atoms. We shall therefore designate it as a symmetric structure On the other hand, we shall call a structure antisymmetric if

$$\rho_1(xyz) = \rho_2(xyz) \text{ and } \rho_1(\bar{x}\bar{y}\bar{z}) = \rho_2(\bar{x}\bar{y}\bar{z}) \tag{9}$$

It is obvious that this also satisfies Eq (8). It is easy to show that the ρ's in Eq (8) can always be split into a symmetric and an antisymmetric component, and that the manner in which this can be done is unique if the ρ's are known quantities. For let

$$\rho_1(xyz) = \alpha + \beta \quad \text{and } \rho_1(\bar{x}\bar{y}\bar{z}) = \alpha' + \beta' \tag{10}$$

where α and β are respectively the symmetric and the antisymmetric components Then, by the definitions above,

$$\rho_2(xyz) = \alpha' + \beta \qquad \text{and } \rho_2(\bar{x}\bar{y}\bar{z}) = \alpha + \beta' \qquad (11)$$

The four equations in (10) and (11) form a set of linear equations in the four unknown α, β, α', β' and can therefore be uniquely solved. If, on the other hand, it is only known that the 200 reflection is absent, then all that can be said about the electronic distribution is that it consists of a symmetric component α and an antisymmetric component β, the ratio of α to β being undetermined

Now, it is evident that if $\beta = \beta' = 0$, *i e*, if the antisymmetric component is entirely absent, then the structure possesses octahedral symmetry. But if the β's are finite, however small they might be, then the structure has only tetrahedral symmetry Since various physical properties of the tetrahedral and octahedral modifications of diamond do not differ notably (as, for example, the lattice spacing, the principal vibrational frequency of 1332 cm^{-1}, etc), the differences in the electronic configurations must be small In other words, the tetrahedral symmetry must arise from the presence of a relatively small proportion of an antisymmetric distribution. This would explain why the infra-red absorption observed in tetrahedral diamond is not very strong, a thickness of 1 mm producing only about 90% absorption (Ramanathan, 1946) in comparison with the practically cent per cent absorption of the alkali halides in extremely small thickness of the order of a few microns (Barnes, 1932).

§4 We shall now consider the various possibilities for the 222 reflection, *subject to the condition that the* 200 *reflection vanishes* From (6), 222 vanishes if

$$\rho_1(xyz) - \rho_1(\bar{x}\bar{y}\bar{z}) = \rho_2(xyz) - \rho_2(\bar{x}\bar{y}\bar{z}) \qquad (12)$$

Combining (12) with (8), the conditions that the 200 and the 222 reflections should simultaneously vanish can be put in the form

$$\rho_1(xyz) = \rho_2(xyz) \qquad \rho_1(\bar{x}\bar{y}\bar{z}) = \rho_2(\bar{x}\bar{y}\bar{z})$$

These are identical with (9), which means that 222 is absent if and only if the structure is completely antisymmetric. On the other hand, a symmetric distribution must necessarily give rise to a finite 222 structure amplitude. These statements however need a qualification In the special case, in which the individual carbon atoms possess octahedral symmetry, the distinction between the terms symmetric and antisymmetric disappears, since the electronic charge distribution satisfies the conditions for both, The 222 reflection would be absent for this structure.

We are now in a position to discuss the origin of the observed feeble 222 reflection referred to in §1 If we assume that this is a genuine Bragg reflection, then the octahedral diamond should have an electronic distribution of the symmetric type with no antisymmetric component whatsoever The tetrahedral modification must arise from the presence of a small proportion of an antisymmetric distribution as mentioned in §3 It can be shown that the structure amplitudes for reflections like 400 and 220 for which $h + k + l = 4n$ will be unaffected, while that for 222 will theoretically be different, the difference however being small, since it is proportional to the ratio of the antisymmetric to the symmetric component

Pisharoty (1941) has suggested that the 222 reflection is purely a modified or quantum reflection If this is the case, then, in the octahedral diamond, each of the carbon atoms should possess octahedral symmetry Here also, the tetrahedral modification must arise from the presence of a small proportion of the antisymmetric distribution. The 222 reflection is absent for both, and reflections *hkl* with $h + k + l = 4n$ are also unaffected.

My sincere thanks are due to Prof Sir C V Raman for the many illuminating discussions I had with him during the preparation of this paper

Summary

The problem of the symmetry of the diamond structure in relation to its X-ray behaviour is considered in a formal manner. It is shown that the presence or absence of the 200 or the 222 reflection cannot uniquely decide whether the symmetry is tetrahedral or octahedral The 200 reflection is shown to be absent if the structure is either completely symmetric or antisymmetric with respect to the centre of inversion at $\frac{1}{8}, \frac{1}{8}, \frac{1}{8}$ or if the two distributions are superposed in any arbitrary ratio The 222 reflection is, however, absent only in the fully antisymmetric case Making use of these results, the nature of the structures that are possible for the tetrahedral and the octahedral modifications of diamond are discussed.

References

1 Ångstrom, K . *Phys Rev*, 1892, **1**, 597
2 Barnes *Zeits f Phys*, 1932, **75**, 723
3 Bragg, W. H, and Bragg W L *Proc Roy Soc*, 1913, **89 A**, 277
4 Bragg, W H. *Proc. Phys Soc*, 1921, **33**, 304
5 Ehrenberg, W, Ewald, P P, and Mark, H . *Zeits f Krist*, 1928, **66**, 547
6 Groth, P, *Physikalische Kristallographie*, Engelmann, 1895, p 515

7. Hariharan, P S — *Proc. Ind. Acad Sci.*, 1944, 19 A, 261
8. Hintze, C — *Handbuch der Mineralogie*, Veit, 1904, Band 1, Abt. 1, p. 3
9. Julius — *Ann d Phys*, *Bieiblätter*, 1893, 17, 34
10. Liebisch, T — *Physikalische Kristallographie*, Veit, 1896, 88
11. Lonsdale, K — *Nature*, 1945, 155, 144
12. Miers, H. E — *Mineralogie*, MacMillan, 1902, 291
13. Pisharoty, P R — *Proc. Ind. Acad Sci*, 1941, 14 A, 377
14. Placzek, G. — *Handbuch der Radiologie*, 1934, Band 6, Teil II, 297
15. Ramachandran, G N — *Proc Ind. Acad Sci*, 1944 *a*, 19 A, 280
16. ——— — *Ibid*, 1944 *b*, 20 A, 245
17. ——— — *Nature*, 1945, 156, 83
18. Raman, C. V — *Proc Ind Acad Sci.*, 1944, 19 A, 189
19. Ramanathan, K G — *Ibid*, 1946, 24 A, 130.
20. Reinkober — *Ann d Phys*, 1911, 34, 343
21. Robertson, R, Fox, J J, and Martin, A. E — *Phil Trans Roy Soc*, 1934, 232 A, 482

ON THE NATURE AND ORIGIN OF THE LAMINATIONS OBSERVED IN DIAMOND

By G N. Ramachandran

(From the Department of Physics, Indian Institute of Science, Bangalore)

Received May 18, 1946

(Communicated by Sir C V Raman, Kt., F R S., N L)

1 Introduction

During their investigations on the birefringence exhibited by both crystals and cleavage plates of diamond, Raman and Rendall (1944) found that, quite apart from the irregular patches of restoration of light seen under crossed polaroids, many diamonds exhibit a " geometric pattern " consisting of bright streaks running in various directions They also found that the axes of birefringence of these coincided with the direction of the streaks and the direction perpendicular to them As a result of their studies, they came to the conclusion that the geometric birefringence is a photo-elastic effect occurring as a result of the juxtaposition of layers of diamond whose lattice spacing is slightly different from the rest of the crystal surrounding it The present paper mainly deals with more detailed investigations carried out by the author regarding these phenomena The studies were confined to cleavage plates of diamond, of which numerous examples were available in the personal collection of Sir C. V Raman.

In the experiments of Raman and Rendall, fine streaks and lines were found in only a few cases; in many others only broad bands running nearly parallel to one another were seen These differences must be attributed to an inherent defect in the method of observation that was employed, namely that the cleavage plates were always viewed normally. For, supposing that the intruding layers are not normal to the surface, but are inclined to it, then when viewed normally they would overlap one another and mutually obscure the details In favourable cases, in which the laminæ are not too fine and are small in number, the overlapping may not completely obliterate them, and they may still be observable But generally the details in the pattern will be washed out. It is obvious that the proper method of observation is to view them in such a position that the light traverses the crystal parallel to the laminæ. In the present investigation, this was achieved by using the Federov universal rotation apparatus in conjunction with a petrographic

microscope In addition, quantitative data regarding the sign and magnitude of the birefringence have been obtained by the use of a Babinet compensator, together with the above apparatus These studies have brought out new facts and have helped in understanding the nature and origin of the laminations

2 Experimental Procedure in General

The present investigation can be divided into two parts: (*a*) a detailed study of the birefringence exhibited by diamond with special reference to the orientation of the laminæ and of the axes of birefringence, and (*b*) a study of the magnitude of the birefringence and of the nature of the stresses that give rise to this

The experiments were all carried out with a Winkel-Zeiss petrological research microscope, model VI M, which had a large range of adjustments and had facilities for the use of a Federov universal stage and a Babinet compensator in conjunction with it On account of the fact that the birefringence phenomena were observed with a microscope which has a relatively small field of view, only sensibly parallel plates of diamond could be studied With wedge-shaped diamonds in which the two surfaces were appreciably inclined to each other, the incident light was refracted away so that it did not enter the microscope at all

The Federov stage was a large one capable of rotation about four axes, and was mounted on the rotating stage of the microscope The specimen of diamond was placed on the central glass disc of the Federov stage, with or without the pair of hemispherical glass segments For rapid comparison of different diamonds, and for studies where the crystal was not inclined very much, the glass segments were dispensed with The segments with a suitable immersion liquid were, however, useful in studying phenomena which could not be observed without them The spherical glass segments used had a refractive index $\mu = 1\ 649$ (the maximum that was available) and α-monobromonaphthalene with $\mu = 1\ 65$ was used as the immersion fluid.

The microscope was invariably used at a small magnification, the objective having a magnification 2 5 and the eye-piece 6, 9 or 12 as was found convenient With the glass spheres a special achromatic objective having a magnification 7 was sometimes used, with the same eye-pieces as before

The Babinet compensator was in a form in which it could be mounted on the microscope in place of the eye-piece. Measurements with this could be taken either visually using the micrometer screw of the instrument, or photographically Either method was used, as was found convenient,

A large number of visual observations were made with a variety of specimens of diamond Many of these were photographed A Microdak photographic equipment supplied by Eastman Kodak Co, was used for this purpose A selection of these photographs representing the main results of the investigation is reproduced in the plates accompanying the paper The magnification in each case is given in the legends describing the photographs

3 STUDIES ON THE GEOMETRIC CHARACTERS OF THE BIREFRINGENCE

As already remarked, observations of Raman and Rendall on the birefringence patterns of diamonds have brought to light the existence of 'geometric' birefringence in which lines or parallel striations are seen running at 60° or 90° It is therefore natural to suppose that these striations must be associated with the crystallographic planes of the crystal For instance, with plates of octahedral cleavage (most of the plates studied had this cleavage), the three other sets of octahedral planes intersect the surface along lines which run at angles of 60° to one another That the streaks in the birefringence pattern actually arise in this manner was recognised early in the course of the present investigation by determining the orientation of the crystal plate by means of X-rays It was then found that the directions of the lines in birefringence are invariably parallel to the intersections of one or more octahedral (111) planes with the surface of the diamond In less common cases, they were parallel to the intersections of some of the dodecahedral (110) planes with the surface.

An interesting point arises in this connection. Let us consider the intersections of the various octahedral and dodecahedral planes with the (111) plane These would be as shown in Fig. 1 Of these, the three directions *a a'*, *b b'*, and *c c'*, are those along each of which one octahedral and one dodecahedral plane intersects the surface, *e g.* $[01\bar{1}]$ is the intersection of the $(\bar{1}11)$ and the (011) planes with the surface (111) plane. However, A A', B B' and C C' can represent only the intersections of dodecahedral planes, these having the indices $(01\bar{1})$, $(10\bar{1})$ and $(1\bar{1}0)$ respectively. One thus sees that a knowledge of the azimuth α of the intersection (*viz.*, the angle made by the line with a reference line on the surface) alone is not sufficient to fix the orientation of the laminations completely. It is also necessary to know the inclination i of the laminæ to the normal to the surface. For dodecahedral planes intersecting along OA, OB and OC this angle is 0°, while for the other dodecahedral planes it is 35° 16'. For all the octahedral planes, the inclination is 19° 28'.

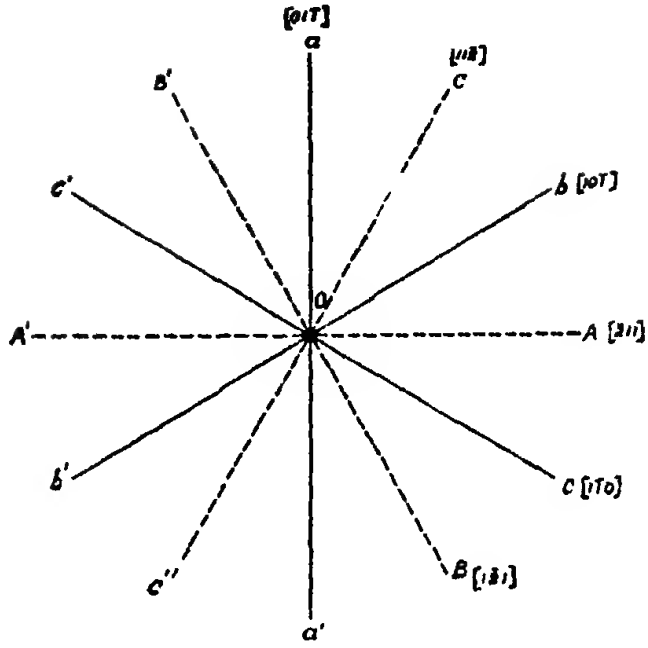

FIG 1

The determination of the azimuth and inclination is most accurately done by using the Federov stage The diamond was placed on the central glass plate of the Federov stage, and the birefringence pattern between crossed nicols was observed by means of the polarising microscope under low magnification The Federov stage was adjusted so that the principal horizontal axis was parallel to one of the cross-wires of the microscope. The axis of rotation of the tilting stage was also made parallel to the principal horizontal axis. Keeping the tilting stage horizontal, the inner glass disc on which the diamond was placed was rotated in such a way that the birefringence streak (or set of lines as the case may be) was parallel to the cross-wire of the microscope to which the axes of the Federov stage were parallel. (Hereafter, by the term cross-wire of the microscope, we shall always mean this cross-wire) The crossed nicols were also rotated together until the required set of lines in the birefringence pattern were seen most clearly Now on inclining the stage, it was found that the birefringence pattern either sharpened up or became more diffuse. If the latter happened, the stage was rotated in the opposite direction, when it sharpened up. It was generally found that the lines were sharpest at a certain angle, beyond which they became more and more diffuse.

The reason for the sharpening at certain inclinations is obviously that the laminations which give rise to the birefringence are oriented in a particular direction When the light passes parallel to these laminæ, the pattern is sharp and well resolved On the other hand, if the crystal is tilted away from this position, then the light traverses across a few of the laminæ, and the pattern overlaps portions of itself, thus becoming confused Hence, the position at which the birefringence pattern is clearest and most well-defined is that at which the light passes parallel to the laminæ inside the crystal From the measured inclination of the tilting stage, which should be the same as the angle which the light emerging from the crystal makes with the normal to the surface, the inclination i of the laminæ to the normal can be calculated The relation between i and θ is obviously

$$\sin \theta = \mu \sin i,$$

where μ is the refractive index of the diamond (2 417), or the relative refractive index between the diamond and the surrounding medium (1 466), if the glass spheres with homogeneous immersion is used. The azimuth of the laminæ could also be measured by adjusting the tilting stage of the Federov rotation apparatus horizontal, and measuring the angle between the cross-wire and the reference line, *viz.*, one of the edges of the diamond.

The remarkable way in which the sharpening occurs can be seen from Figs 2 (*a*) and (*b*) which represent the birefringence patterns of N C. 124 when the diamond plate is normal to the axis of the microscope and is at the best position respectively It will be seen that in the normal position there is practically no trace of the fine laminations, while on inclining the plate they come out prominently as fine sharp streaks These photographs were obtained with the glass spheres, the tilting angle being 24°, which corresponds to an inclination of 16° 7′ It may be mentioned that X-ray measurements gave a value 16° for the inclination of the corresponding octahedral plane to the surface. (The surface was slightly inclined to an octahedral plane due to errors in polishing)

The particular specimen of diamond referred to above was unique in that there was only one set of laminations shown in Fig 2 (*b*) In general however, many diamonds exhibited laminæ parallel to 2 or 3 sets of octahedral planes and also sometimes to the dodecahedral planes Details of these will be given in a later section on the results of the investigation.

Having thus determined the orientation of the laminations, the nature of the birefringence exhibited by them was next investigated. As already remarked, in the adjustments described above, the polariser and analyser were crossed, and they were rotated together until the required streaks in the

birefringence pattern were most clearly seen It was found that the axes of the nicols made an angle of 45° to the direction of the laminations when this happened If the nicols were now rotated together, a cycle of phenomena occurred, all the streaks vanishing when the axis of the polariser or analyser was parallel to them, and appearing in the intermediate positions These observations clearly showed that the principal axes of birefringence in all the laminæ were parallel, and were respectively parallel and perpendicular to the intersection of the laminæ with the plane normal to the axes of the microscope This phenomenon was found in all the cases of regular geometric birefringence An illustration of the vanishing of the parallel streaks is provided by Figs 3 (*a*) and (*b*) It will be seen that in both there is an irregular pattern which does not vanish at any setting of the nicols But the regular parallel streaks vanish completely when the axis of the polariser or analyser is parallel to them

To obtain more specific information regarding the nature of the birefringence in the laminæ, the following experiments were performed

(i) Having verified that the axes of birefringence were parallel and perpendicular to the cross-wires in the sharpest position, the tilting stage was rotated so that the pattern was no longer sharp Still the laminæ could be observed. Now also, on rotating the crossed nicols, extinction occurred four times in a revolution, respectively when the axes of the polariser and analyser were parallel to the cross-wire This was found to be the case whatever be the angle through which the tilting stage was rotated

(ii) The beam of light was also made to pass through the laminæ in different directions parallel to their plane, and the extinction directions were determined in each case For this, the axis of the tilting stage was set perpendicular to the cross-wire, and by rotating the glass disc and inclining the tilting stage, the birefringence pattern was obtained as before in the sharpest position, but with the streaks running perpendicular to the cross-wire. The Federov stage was then rotated through an angle (say of about 20°) about the principal horizontal axis The previous adjustments were repeated to obtain the streaks in the sharpest position and the effect of rotating the nicols was studied. It was found that now also the principal axes of birefringence were parallel and perpendicular to the lines in the birefringence pattern. The same was found to be the case for different settings of the crystal in which the light traversed it in various directions parallel to the laminæ.

From these experiments, one can conclude that *the laminæ behave like uniaxial crystals with the optic axis normal to them.*

4 Studies with the Babinet Compensator

The "order of birefringence" of the laminations, *viz*, the difference in the refractive indices for vibrations along directions parallel and perpendicular to the optic axis, was determined by means of a Babinet compensator, which was relatively a simple matter since the direction of the optic axis was known from the previous studies But the usual methods of determination with uniaxial crystals had to be modified to suit the purposes of the present investigation This was so because one is interested here in the *variations* of the order of birefringence from place to place *over the area of the crystal plate* The method employed could be described as follows The crystal plate was first adjusted by means of the Federov stage so that the laminations were seen most clearly by the method of the previous section The plane normal to the direction of propagation of the light within the crystal then contained the optic axis (which was perpendicular to the cross-wire, the laminations being parallel to it) The crossed polariser and analyser were rotated to extinguish the laminations, and were then set accurately at 45° from this position. By the transverse motion of the microscope stage the diamond plate was moved off the field of the microscope The Babinet compensator was put in with its length parallel to the cross-wire, the analysing nicol was removed and the eye-end nicol put on the compensator and adjusted to $-45°$ The bands in the compensator should then be at right angles to the cross-wire The diamond was then moved into the field, when *a focussed image of the diamond was thrown on the plane of the quartz wedge of the compensator* Then it was found that the bands in the field of view of the compensator were not straight, but assumed a zig-zag shape This occurs because the phase difference between the two polarised components varies from place to place, and the displacement of the Babinet fringes parallel to the cross-wire is a measure of this relative phase difference Fig 2 (*d*) is the photograph of what happens to the Babinet fringes with the diamond N C 124, the same specimen which was described in the last section in connection with the study of the laminations. This pattern might be called the "Babinet pattern" and gives a picture of the distribution of the magnitude of the birefringence over the area of the crystal plate. It may be mentioned that in this photograph, as well as in the photograph of the laminæ under crossed nicols [shown in Fig 2 (*b*)], the microscope could not be focussed sharply over the whole field of view on account of the inclination of the crystal. Only a portion was accurately focussed.

If t is the thickness of the plate, i the inclination of the laminations to the normal to the surface, and if ϵ is the phase difference and μ_1 and μ_2 the principal refractive indices, then

$$\epsilon = 2\pi(\mu_1 - \mu_2)\, t/\lambda \cos i \text{ or } \Delta\mu = \mu_1 - \mu_2 = \epsilon\lambda \cos i/2\pi t$$

$\Delta\mu$, the order of birefringence, is thus directly proportional to the phase difference and hence to the displacement of the Babinet fringes from their zero position

It will be noticed that the fringes have two types of displacements—one varying slowly over the length and breadth of the crystal, and the other having a rapid fine variation The former is irregular and on a large scale; it must be attributed to accidental strains, etc, which gives rise to the irregular birefringence. The latter is what we are interested in; in this diamond, it is characterised by the fact that the Babinet fringes alternately go one way and the other about the mean position This means that $\Delta\mu$ in the laminæ is alternately positive and negative, that is to say, the alternate laminæ behave as positive and negative uniaxial crystals Anticipating a little from a later section, it may be remarked that the obvious explanation of this is that the alternate layers are under tension and compression The fine variations assume different shapes in other diamonds; these and their interpretation will be discussed in the next section.

The effect of tilting the diamond away from the sharp position is much more pronounced with the Babinet pattern than with the birefringence pattern The fine variations all vanish and the appearance of the fringes with N.C 124 kept normal to the light is as shown in Fig. 2 (*d*) The contrast between this and Fig. 2 (*c*) is striking So also, the sharp peaks seen in Fig. 4 (*d*) vanish in Fig 4 (*b*) when the diamond is made normal This phenomenon explains why the birefringence pattern is so confused when viewed normally in many of the diamonds

5 Description of the Results

As a result of the observations on a number of diamonds, it was found that they could be divided into a few typical classes, as far as their behaviour in the polarisation microscope was concerned We shall briefly describe the properties of these in general, illustrating them by one or two examples.

(i) First, there is the variety of diamond completely transparent to the ultraviolet upto 2250 Å.U The birefringence patterns of these diamonds, when viewed normally, invariably show a large restoration of light and often contain sets of streaks running in different directions It is found that, in every case, laminations are present parallel to either octahedral or dodecahedral planes, or both, and that they can be brought out prominently by the technique described above There may be only one set of laminations, as for example in N C 124 shown in Fig. 2. The appearance of this diamond

when viewed normally under the polarisation microscope is shown in Fig 2 (*g*) It will be seen that, apart from the fact that all the broad bands run in the same direction, there is no suggestion of the fine laminæ brought out so strikingly in Fig 2 (*h*) by appropriate methods of observation. Figs 2 (*a*) and (*b*) are photographs of the same phenomenon under greater magnification using the glass spheres of the Federov stage This was the only diamond in the collection of Sir C V Raman which exhibited laminations in one direction only All the other diamonds of this type had laminæ running in different directions, *e g*, with N C 126 three such sets could clearly be seen These are illustrated in Figs 3 (*d*), (*e*), (*f*) when in their sharpest position, descriptions of which are given in the legends accompanying the photographs To illustrate the accuracy with which the orientation could be fixed, the table below gives the readings obtained for three diamonds with the microscope, which could be compared with the values to be expected for octahedral and dodecahedral planes from X-ray measurements The X-ray values for the azimuth are correct only to 5° while those for the inclination are correct to a degree.

TABLE I

	N. C 124		N C 125						N. C. 126			
	a	*i*	*a*	*i*	*a*	*i*	*a*	*i*	*a*	*i*	*a*	*i*
Birefringence ..	61°	15° to 17°	53°	18° to 21°	23°	−5° to 5°	48°	18° to 20°	−11°	18° to 21°	−42°	−5° to 5°
X ray ..	60°	16°	50°	19½°	20°	0°	50°	19½°	−10°	19½°	−40°	0°
Parallel to	(111)		(111)		(110)		(111)		(111)		(110)	

In every one of the cases, the axes of birefringence were parallel and perpendicular to the laminations The disappearance of the laminæ when the axis of the polariser or the analyser is made parallel to them is illustrated by Figs. 3 (*a*) and (*b*) It will be noticed that in Fig 3 (*b*) which was photographed with the polariser parallel to the laminæ, the bright streaks in Fig. 3 (*a*) have completely vanished

With all the diamonds, the Babinet pattern has the zig-zag shape described in the previous section It is most pronounced in N.C 124 which has only one set of laminæ

(ii) The birefringence patterns of some ultra-violet opaque diamonds consist of a dark field crossed by a small number of bright streaks An examination of such diamonds with the Federov stage showed that the streaks invariably had their origin in thin laminæ running parallel to octahedral planes. They sharpen up remarkably when tilted so that the light

passes parallel to them, as may be seen for example from Figs. 4 (*a*) and (*c*), which are the photographs of the appearance of one set of laminæ in N C 94 when viewed through the polarising microscope normally and in the sharpest position respectively. The axes of birefringence in laminæ of this type were also found to be parallel and perpendicular to the laminations The Babinet patterns are very interesting It is found that, corresponding to every one of the laminations, the dark fringe of the Babinet compensator has a sharp hump on one side or the other Two such humps towards the right hand side may be seen in Fig 4 (*d*) corresponding to the two bright streaks in Fig 4 (*c*) with diamond N C 94 There are six such sets of laminæ running along the sides of a hexagon in N C 94, and with every one of them the hump was towards the right However, with the lamina found in N C 99, illustrated in Fig 4 (*e*), the hump was to the left. It is not uncommon to find some laminations producing humps on one side and some on the other in the same diamond For example, in B I two laminæ quite close by produce displacements of the Babinet fringe on opposite sides The photograph of the laminæ in the sharpest position is shown in Fig. 4 (*g*) and their Babinet pattern is reproduced below them in Fig 4 (*h*)

The humps in the Babinet pattern disappeared when the diamond was tilted away from the correct orientation, as for example in Fig 4 (*b*) In general, it was found that the displacement of the Babinet fringe was greater with a thinner lamina than with a thicker one It may also be remarked that the broad lamina in N C 99 is ultra-violet transparent. Rendall (1944) has obtained a streak of transparency in this position in the ultra-violet transparency pattern Presumably, the streaks in the other diamonds are also transparent, but being very thin and lying obliquely to the surface of the diamond, it is difficult to verify whether they are transparent or not. By using a technique similar to that employed in the present investigation, *viz*, by holding the diamond at the appropriate angle to the beam of ultra-violet light, it may be possible to detect the transparency of these laminations.

(iii) In a large number of ultra-violet opaque diamonds, a restoration of light sometimes accompanied by one or more series of bands was found when viewed normally under crossed nicols These diamonds were generally yellow luminescent, the bands of yellow luminescence running parallel to those in birefringence (Rendall, 1946) These plates, when viewed at the proper angle with the Federov stage, exhibited a series of laminations running in one or more directions, generally parallel to the octahedral planes. The axes of birefringence were parallel and perpendicular to the laminæ The Babinet pattern had in general a number of humps,

some going one way and some the other way, the displacement, however, being smaller than with those classed under (i) These diamonds could be considered as being very similar to those in (ii), but in which a large number of laminæ occur

(iv) There were a few diamonds of the ultra-violet opaque class, which exhibited only pure blue luminescence and which produced very little restoration of light under crossed nicols These failed to show any laminations under the experimental conditions adopted by the author

It may not be out of place here to give some idea of the thickness of the laminæ as also of the order of birefringence produced by them. Both were variable, and it is only possible to give the order of magnitude of the quantities The laminæ had thicknesses varying from about 10μ to 100μ or a little more, being similar both in the ultra-violet transparent as well as the ultra-violet opaque diamonds By using a standard quartz plate, it was found that a shift of the Babinet fringes to the right meant that the refractive index for vibrations parallel to the laminæ, μ_h, was less than that perpendicular to it (μ_v), and *vice versa* for a displacement to the left Thus, if the laminæ behaves like a positive uniaxial crystal *i e*, $\Delta\mu = \mu_v - \mu_h$ is positive, then the shift will be to the right and *vice versa* As already remarked, the displacement was either to the right or to the left in diamonds of the types (ii) and (iii), the magnitude varying from 0 5 mm to about 2 5 mm Allowing for the thickness of the diamond and the inclination of the light to the surface, these correspond to orders of birefringence of 0 00006 to 0 00031 With ultra-violet transparent diamonds, in which the Babinet fringe alternately goes one way and the other, the maximum relative displacement is about 5 mm , nearly double that found in the opaque diamonds All these measurements are only rough and are intended only to give an idea of the orders of magnitude of the quantities concerned

6 Discussion and Interpretation of the Results

As already remarked, many diamonds exhibit an irregular birefringence pattern produced as a result of flaws and accidental strains in the crystal, which gives rise to a coarse and irregular displacement in the Babinet pattern. We shall leave this aside and consider only the fine laminations which may be observed by the techniques described above

The important points to be considered in this connection are that (*a*) the laminæ behave as uniaxial crystals with the optic axis along their normal and (*b*) as is seen from the behaviour of the Babinet fringes they may behave either as a positive or a negative uniaxial crystal In ultra-violet opaque

diamonds, the laminæ usually occur interspersed in the bulk of the crystal, these producing either a positive or a negative hump in the Babinet pattern On the other hand, ultra-violet transparent diamonds possess a laminated structure throughout their volume, the alternate laminæ being positive and negative. The obvious explanation for such a behaviour of the laminæ is that the birefringence is a photo-elastic effect produced as a result of stresses acting on them If the photo-elastic constant were known it would be possible to calculate the magnitude of the stresses. Even in the absence of such information, it is possible to have an idea of the nature of the stresses Assuming that the photo-elastic constant concerned is positive, it would mean that the positive laminæ are under compression and that the negative laminæ are under tension along a direction normal to them In any case, *it is clear that the laminæ that occur in the ultra-violet opaque diamonds are of two classes*, viz , *those that are under compression and those that are under tension* Similarly, the laminæ in the ultra-violet transparent diamonds are alternately under compression and tension

As was mentioned in the last section, there is strong reason to suppose that the laminations found in the ultra-violet opaque diamonds are transparent. Since the intrusion of this variety sets up stresses which may be either tensile or compressive, it is reasonable to suppose that there are really two variants of the transparent type, which are both in some way (probably in their lattice spacing) different from the opaque type and also from one another. This would immediately explain why the laminæ in the ultra-violet transparent diamonds are alternately under compression and tension —the alternate laminæ are composed of the two different variants of this type.

All these deductions are beautifully in accord with the theory put forward by Sir C V Raman (1944) regarding the structure of diamond According to this theory, diamond can have four possible structures, two of which, TdI and TdII, possess tetrahedral symmetry, while the other two, OhI and OhII, possess octahedral symmetry The former two are physically identical, but differ only in orientation. They are infra-red active and are also opaque to the ultra-violet below 3000 Å U The latter two are, however, transparent to the ultra-violet upto 2250 Å.U They are both geometrically and physically different from each other, as well as from the tetrahedral varieties. The differences, however, are so small that it is possible for the different structures to co-exist side by side in the same specimen of diamond.

If one studies these structures carefully (see for example Fig. 1 on p. 191 in the paper by Raman quoted above), it will be seen that the tetrahedral

structures are intermediate between the two octahedral structures Thus, designating the two interpenetrating lattices of carbon atoms in the diamond structure by A and B, then starting from OhI, if one reverses the direction of the axes of all the atoms in the B lattice, one gets TdI (or reversing the axes of all the atoms in the A lattice, one would get TdII) After this, if the axes of the atoms in the A lattice are reversed (or of those in the B lattice in the latter case), one now obtains the OhII structure Hence, it is reasonable to suppose that the two Td structures have properties intermediate between those of OhI and OhII

For example, the lattice spacing of the tetrahedral varieties would be less than that of one of the octahedral structures (say OhI) and greater than that of the other (OhII) This is exactly what is required to explain the phenomena observed with the laminations. Thus, if a lamina occurring in the midst of tetrahedral ultra-violet opaque diamond consists of the OhI variety only, then its lateral dimensions would be larger than the surrounding, there being thus stresses along the two boundaries tending to decrease the area of the lamina These stresses would be present along all directions in the plane of the lamina and are equivalent to a tensile stress normal to it. On the other hand, if the lamina consists of the OhII variety, then the stresses acting on it would be equivalent to a compressive stress normal to it. Thus, one of them would behave as a negative uniaxial crystal and the other as a positive one respectively, exactly as is found to be the case

In the ultra-violet transparent diamonds, however, the OhI and OhII structures alternate in the laminations giving rise to compressive and tensile stresses in alternate laminations, as is in fact found It also follows from the above argument that the difference in the birefringence and hence the relative shift of the Babinet fringes for an octahedral lamina in a tetrahedral diamond should be about half that between the two alternate laminæ in an octahedral diamond. That this is roughly the case is shown by the measurements reported in a previous section

The small magnitude of the birefringence, *viz*, less than 1 in 10,000, shows that the differences in the properties of the four diamond structures should be very small. This fits in with the results deduced by the author (1946) regarding such differences from X-ray and other data Thus it is in concordance with the fact that the infra-red absorption coefficient of the tetrahedral diamonds is very small compared with other infra-red active crystals (Ramanathan, 1946). So also, these ultra-violet opaque diamonds have a relatively small absorption coefficient upto 2250 Å.U, the transmission extending upto this wavelength with thin plates. The results of the present

investigation thus lend great support to Raman's theory In particular they show very clearly that there are two variants of octahedral diamond, a result which is a direct outcome of the theory

7 Laminations in Luminescence

Raman (1944 *b*) has pointed out that bands of yellow luminescence often appear sharp and clearly defined when viewed at certain angles and diffuse at others This must be due to the fact that the luminescence is located in laminæ having a definite orientation An attempt was made to see whether the technique of using the Federov stage can be used to bring out the laminæ in luminescence The difficulty was that the diamond had to be sufficiently luminescent to be seen under the microscope However, the phenomenon sought for was found Figs 5 (*a*) and (*b*) represent respectively the luminescence of diamond N C 154 when seen normally and in oblique position at which the bands are sharpest Owing to the depth of focussing being small, only a few sharp bands are seen in Fig 5 (*b*) The laminæ were verified to be parallel to a set of octahedral planes

In conclusion, I wish to thank Sir C V Raman for the encouraging interest that he took in the investigation

Summary

The birefringence patterns of many plates of diamond show sets of bright parallel streaks which have been attributed to the existence of definitely orientated laminations inside the crystal which are under strain These laminæ are most clearly seen when the light beam is made to pass parallel to them inside the crystal, which has been achieved in the present investigation by the use of a Federov stage and a polarising microscope By properly inclining the plate of diamond placed on the Federov stage, it is found possible to observe the laminary structure even in diamonds which do not exhibit any streaks when viewed normally From measurements made with the Federov stage and with X-rays, the orientation of the laminæ was fixed The laminæ are in general parallel to octahedral or dodecahedral planes The same specimen of diamond may possess laminations in more than one direction, each of which appears prominently when viewed properly Quantitative studies of the birefringence of the laminæ have also been made with a Babinet compensator The studies show that the laminæ behave either as a positive or a negative uniaxial crystal, with the optic axis normal to them They usually have a thickness between 10μ and 100μ and the order of birefringence varies from 0 00006 to 0 0003. In ultra-violet opaque diamonds, octahedral laminæ of the transparent diamond are found, which

have either positive or negative birefringence, laminæ of both types being sometimes present in the same specimen On the other hand, the ultra-violet transparent diamonds are completely laminated, the alternate laminæ being positive and negative These observations support the ideas of Raman that there are two varieties of the ultra-violet transparent diamond which are different from each other and from the opaque type Also, it is seen that one of them has a larger and the other a smaller lattice spacing than the opaque diamond Laminæ having a definite orientation have also been found to be exhibited in luminescence

References

1 Ramachandran, G N *Proc Ind Acad Sci*, 1946 **24** A, 60
2 Raman, Sir C V *Ibid*, 1944*a*, **19**, 189
3 ——— *Ibid*, 1944*b*, **19**, 199
4 ——— and Rendall, G R *Ibid*, 1944, **19**, 265
5 Ramanathan, K G *Ibid*, 1946, **24**, 130
6 Rendall, G R *Ibid*, 1946, **24**, 168
7 Rendall, G R *Ibid*, 1944 **19**, 293

Description of the Plates

Fig 2 (*a*) Birefringence pattern of N C 124 when viewed normally, taken with the glass hemispheres of the Federov stage × 28

(*b*) Ditto when viewed at the proper inclination × 28 Note that the laminæ which come out so prominently in this are practically unobservable in (*a*)

(*c*) Babinet pattern corresponding to (*a*) × 20

(*d*) Ditto corresponding to (*b*) × 20

(*e*) Babinet pattern of same diamond at smaller magnification, covering practically the whole of the diamond, at normal incidenc , taken without the glass spheres ×10.

(*f*) Same as (*e*) at the sharpest position × 10

(*g*) Birefringence pattern of N C 124 showing the whole diamond at normal incidence × 5

(*h*) Ditto at the proper inclination × 5

Fig 3 (*a*) Birefringence pattern of one of the laminations in N C 125 at the sharp position with the axes of polariser and analyser at 45° to the laminæ 10

(*b*) Ditto with the axis of the polariser parallel to the laminæ × 10 Note that the fine streaks have disappeared

(*c*) Babinet pattern corresponding to (*a*) × 25

(*d*) Photograph of a set of dodecahedral laminæ (the thin horizontal streaks) in N C 126 × 7·5

(*e*) Photograph of a set of octahedral laminæ × 7·5 These are the same as the coarse vertical bands seen in (*d*), but in the sharp position

(*f*) Photograph of a third set of laminæ parallel to the octahedral planes in this diamond × 7 5,

FIG. 4 (*a*) Birefringence pattern of a portion of N C 94 viewed normally × 10

(*b*) Babinet pattern of the same × 10

(*c*) Birefringence pattern at the proper inclination of the region shown in (*a*) × 10 Note the sharpness of the laminæ

(*d*) Babinet pattern of (*c*) × 10 Note the humps in the fringes going to the right

(*e*) A broad lamina in N C 99 at the sharp position × 10

(*f*) Babinet pattern of (*e*) × 10 The hump here goes to the left

(*g*) Two laminæ in diamond B 1 at the sharp position × 28

(*h*) Their Babinet pattern One hump goes to the right and the other to the left × 20

FIG 5 (*a*) Luminescence pattern of N C 154 when viewed normally × 10

(*b*) Ditto at the correct inclination for a set of octahedral planes × 10 A few laminæ are seen sharply

(a) (c) (e) (g)

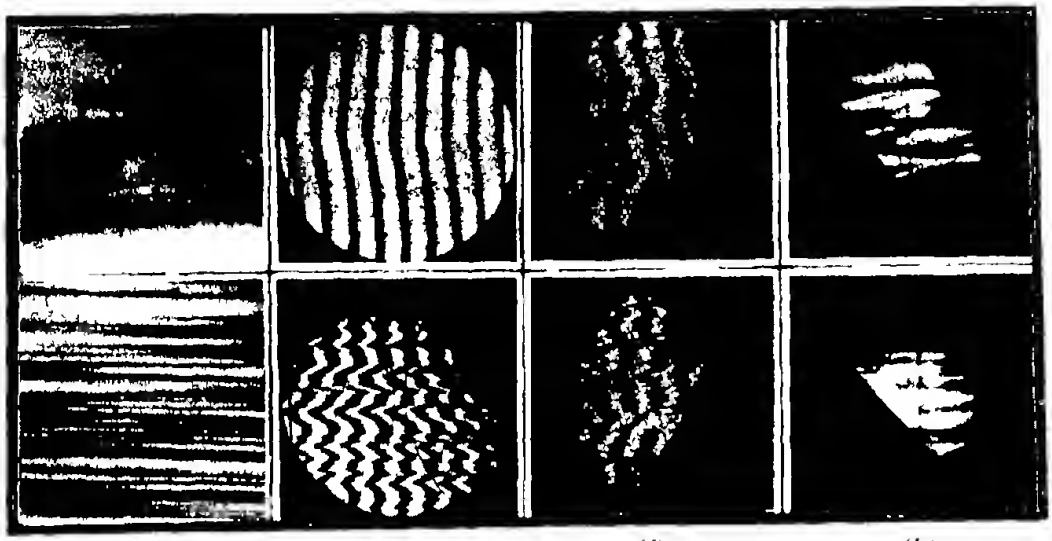

(b) (d) (f) (h)

FIG 2

(a)

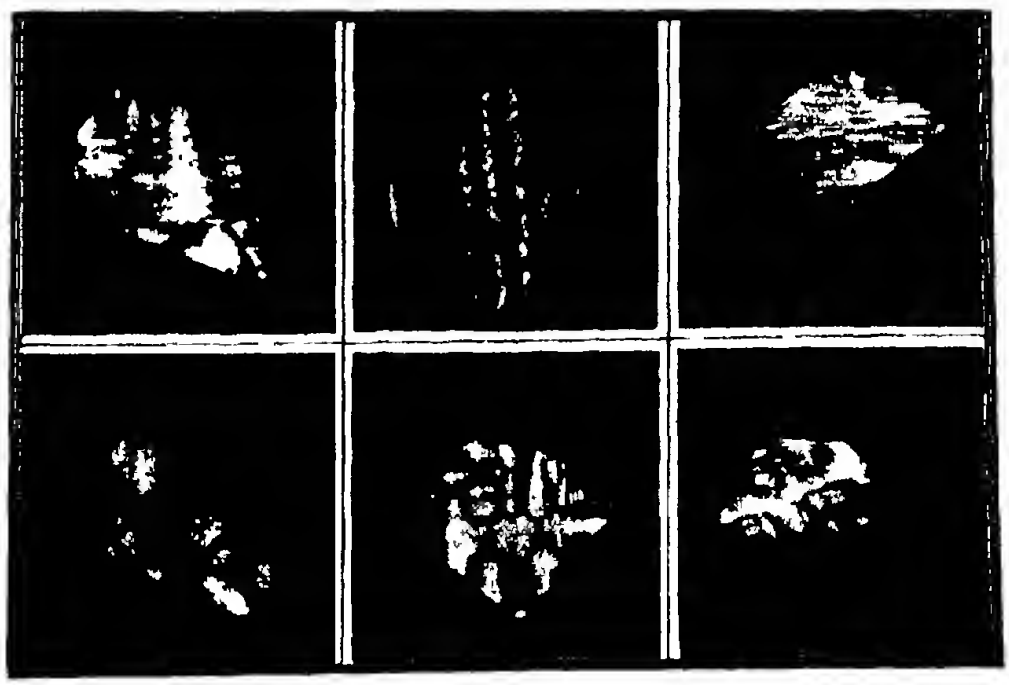

(b) (d) (f)

FIG 3

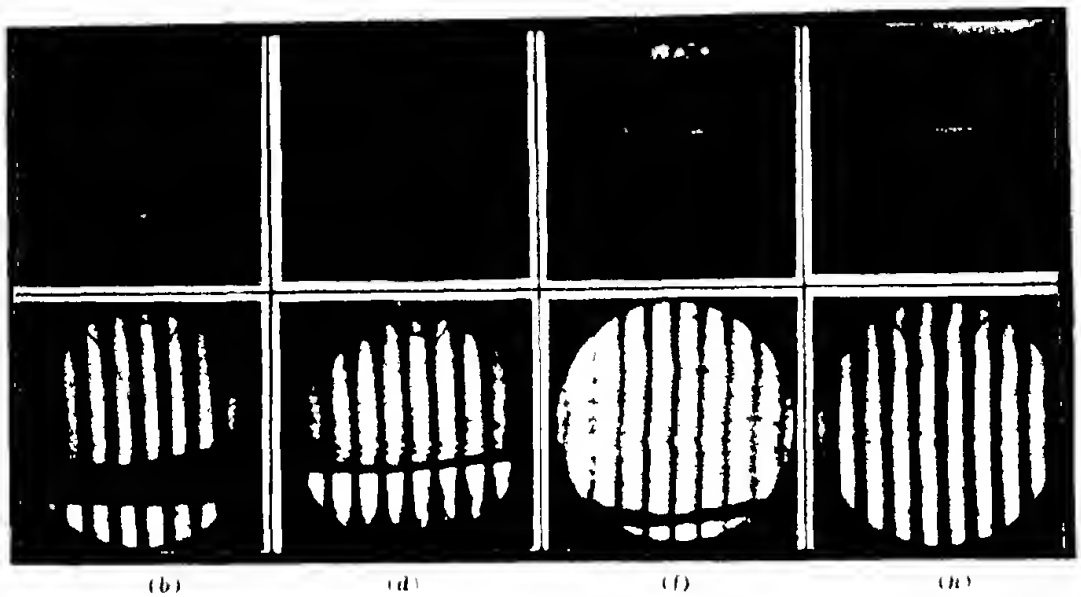

FIG 4

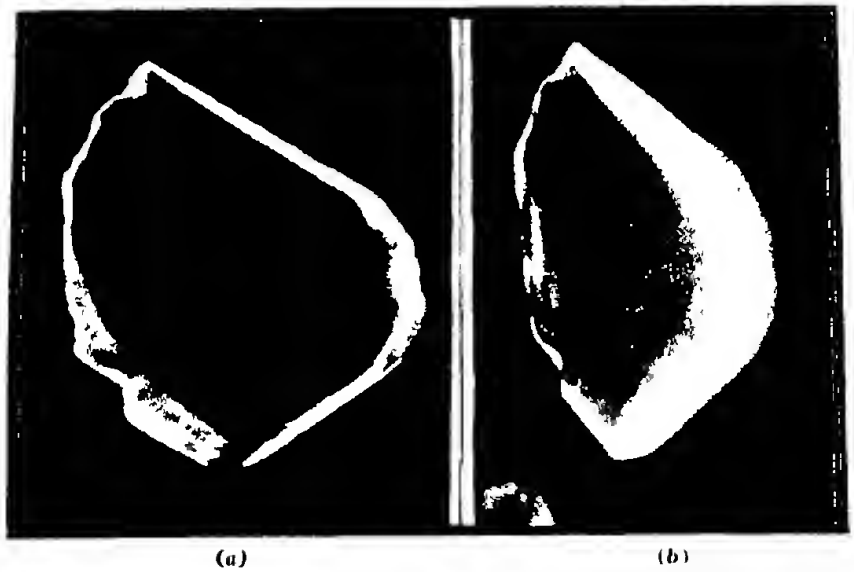

FIG 5

THE LUMINESCENCE OF DIAMOND EXCITED BY X-RADIATION

By G N Ramachandran

(*From the Department of Physics, Indian Institute of Science, Bangalore*)

Received May 18, 1946

(Communicated by Sir C V Raman, KT, F R S, N L)

1 Introduction

Diamond can be made to luminesce in a variety of ways, *e g*, by irradiating with ultra-violet rays, cathode rays or X-rays or by the action of heat or friction. The fluorescence spectra and various other properties associated with fluorescence, such as the local variations of colour and intensity, have been studied by a number of workers in this laboratory using ultra-violet excitation (Nayar, 1941, Mani, 1944, 1945, Sunanda Bai, 1944; Rendall, 1946) John (1930) has reported a study of the fluorescent spectrum when exposed to cathode rays The present paper describes the investigations made by the author on the fluorescence of diamond when irradiated with X-rays Among the various phenomena that were studied may be mentioned the fluorescence spectra, the fluorescence patterns, the correspondence or otherwise of these with those produced by ultra-violet excitation and the influence of the hardness and intensity of X-rays on the intensity of luminescence. A discussion is also included on the probable mechanism by which the luminescence is produced by the impact of X-rays

2 Colour and Intensity of Luminescence

The luminescence of diamond under X-ray irradiation is much weaker than that under ultra-violet irradiation The X-ray tube was generally run at 10 to 15 milliamperes with a peak voltage of 35 K V. Preliminary observations showed that increasing the voltage applied to the X-ray tube remarkably brightened up the luminescence Consequently, voltages up to 50 K.V were used for feebly luminescent diamonds A tungsten target was used in the X-ray tube to have a high efficiency of production of X-rays.

Visual observation with a large number of diamonds showed that the colour of luminescence in X-rays generally followed the colour as seen in the ultra-violet The diamonds which fluoresced blue in ultra-violet rays were also blue in X-rays, but the colour in X-rays had less of violet in it. The colour was blue to blue-green. Similarly, diamonds fluorescing green in ultra-violet also showed a green colour in X-rays The so-called non-

luminescent diamonds which emitted practically no light in ultra-violet rays were definitely luminescent in X-rays, although the luminescence was very feeble The colour could not be fixed definitely on account of the extreme feebleness, but appeared to be blue to blue-green

A striking fact that was obvious even on visual observation was that the range over which the intensity of luminescence varied from specimen to specimen with X-ray irradiation was much smaller than with ultra-violet irradiation This phenomenon was demonstrated in a qualitative manner by a series of photographs taken by the author and published in a paper by Sir C V Raman on the " Nature and Origin of Luminescence in Diamond " (Raman, 1944) The photographs were taken with a jewel containing a large number of diamonds which were known to fluoresce in ultra-violet rays with intensities varying in the ratio of about 1 1000 (Photographs illustrating this fact were also reproduced in Sir C V Raman's paper quoted above) With X-rays, the maximum range was certainly not more than 1 50 This phenomenon was quantitatively studied in a particular case of a purely blue-fluorescent diamond (N C 100) which showed patches of luminescence, which were sensibly uniform in intensity, but whose intensities were different Since the diamond was of uniform thickness, complications due to differences in thickness did not arise The diamond had at least three distinct areas whose intensities of luminescence were different (see Fig 6), which may be designated by A, the central bright patch, B, a small extension of this triangular patch to the right and C, the feebly luminescent surrounding area The relative intensities of luminescence of these three areas were determined by photographic photometry An absorption cell of a solution of sodium nitrite in water was always kept in front of the camera to absorb the ultra-violet rays scattered by the diamond. This cell was also kept when photographing the luminescence excited by X-rays, so that the comparison of intensities was restricted to the spectral region of luminescence in the visible. The results of photographic photometry gave intensity ratios of 12 5 0 1 with ultra-violet excitation, while with X-rays it was only 2 5. 1 6:1 The interpretation and explanation of this fact will be taken up in a later section.

3 Luminescence Patterns of X-ray Luminescence*

All diamonds which exhibited patterns of luminescence when excited by ultra-violet rays were found to exhibit patterns under X-ray excitation

* Hereafter, by the term 'X-ray luminescence' will be meant the luminescence under X-ray excitation, and similarly 'ultra-violet luminescence' will mean the visible luminescence excited by ultra-violet rays

also The patterns were photographed with some diamonds The technique was very simple The diamond was kept in a light-tight box, one side of which was closed by black paper, through which X-rays were incident The diamond was kept at an angle of about 30° to the X-ray beam and the pattern was photographed with a camera whose axis was kept normal to the diamond plate An examination of the appearance of the patterns in the focal plane of the camera confirmed the fact that the colour of the luminescence with X-rays is very much the same as with ultra-violet rays The luminescence patterns observed were also found to be remarkably similar to those in ultra-violet luminescence Hence, only a small number of photographs were taken to illustrate the patterns These are reproduced in Figs 5 and 6 in Plate VIII No attempts were made to separately photograph the blue and yellow luminescence patterns by the use of filters, as even the total luminescence took many hours to photograph and since the resemblance of these to the corresponding patterns in ultra-violet luminescence was so striking However, it was found that the X-ray luminescence patterns were less contrasty than the ultra-violet luminescence patterns of the same diamond. This will be evident on comparing the X-ray luminescence pattern of N C 100 (Fig. 6) with the corresponding ultra-violet luminescence pattern reproduced in a paper by Rendall (1946) in this symposium The origin of the difference must be found in the result described in the preceding section, namely that the ratio of intensities of luminescence had a much smaller range when X-rays are used than when ultra-violet rays are used The same phenomenon was also observed with other diamonds

It was observed that if the diamond plate was kept very nearly parallel to the X-ray beam so that the X-rays entered it at grazing incidence, then the details in the luminescence pattern became very much clearer and sharper than otherwise This will be evident from Fig 5 which is the luminescence pattern of N C 118 using X-rays falling at an angle of 5° on the diamond If one compares it with the corresponding pattern in ultra-violet light (reproduced as Fig 10, D 198 in Sir C V Raman's paper quoted earlier), it will be seen that the X-ray luminescence pattern is by far the clearer and the sharper of the two The origin of this sharpening must be traced to two causes Firstly, the bands of bright luminescence in diamond are generally found to be located in fairly narrow laminæ parallel to the octahedral planes (Ramachandran, 1946) In diamonds of octahedral cleavage, these laminæ do not run normal to the surface of the diamond, so that if the whole thickness of the diamond is luminescent, the luminescence pattern becomes somewhat confused when viewed normally. The second fact to be considered is that the luminescence with X-rays is largely caused by

the soft components which are absorbed in a relatively small distance from the surface The proof of this fact will be given in the next section. Therefore, when the diamond is kept obliquely to the X-ray beam, the intense part of the luminescence is confined to a thin layer near the front surface, and the confusion arising in the pattern due to overlapping is avoided The pattern thus comes out sharp and clear

As already remarked, diamonds which do not luminescence in ultraviolet light are definitely luminescent in X-rays The intensity is very small, about one-twentieth of the weakest blue-luminescent diamond, but it can be seen clearly In Fig 6 the X-ray luminescence pattern of such a diamond (N C 60) is reproduced. It will be seen that there is little variation in intensity The bright lines near the corners are due to bevelled edges, and the series of rings near the centre are interference fringes produced at the contact between the diamond and the plate on which it was kept

4 Effect of the Quality and Intensity of X-Rays on the Intensity of Luminescence

The influence of the applied voltage and the current through the X-ray tube on the intensity of fluorescence was investigated by photographic photometry All the photographs were taken with the same exposure time, and no assumptions were made as to the approximate validity of the reciprocity relation The time of development and other factors were carefully controlled The diamond employed for the investigation was N C 73, which exhibited uniform blue luminescence The density of the photographs was measured by a Moll microphotometer and the standards were obtained by varying the aperture of the camera. The results of the studies are given in Tables I to III below, which give respectively the effect of current and voltage applied to the X-ray tube and the effect of interposing aluminium filters of known thickness

Table I

Effect of current through the X-Ray tube on the fluorescence intensity Applied peak voltage 45 K V

Current m amp	Intensity of fluorescence in arbitrary units
1 0	1·0
2·5	2 4
5 0	5 1
8·0	7·9
10 0	10·0

TABLE II

Effect of the voltage applied to the X-Ray tube on the fluorescence intensity
Current 5 m amp

Peak voltage in K V	Fluorescence intensity I in arbitrary units	Log I
52 5	16 6	1 22
45 0	7 4	0 87
37 5	5·5	0 74
30 0	3 2	0 50
22 5	1 6	0 21
15·0	0 27	T 44

TABLE III

Effect of interposing aluminium foils in the X-Ray beam on the total intensity of fluorescence I of the diamond
Applied peak voltage 35 K V

Thickness t	I	Log I
mm		
0 0	5 0	0 70
0 2	2 2	0 34
0·4	1·35	0 13
0 55	1 0	0 00

It will be seen that the intensity of fluorescence varies linearly with current over the range of intensities studied It may be remarked that the absolute intensity was very much smaller than that excited by ultra-violet light, so that such an accurate linearity is to be expected The photometry confirms the visual observation that an increase in the applied voltage has an appreciable enhancing influence on the fluorescence intensity It will be seen that, in the range 25 to 50 K V, an increase in peak voltage of 7 5 K V nearly doubles the intensity of fluorescence If log I were plotted against the logarithm of the voltage, it will be found that the resulting curve is nearly a straight line with a slope of about 3, so that the fluorescence intensity varies roughly as the cube of the voltage This will be considered in greater detail in a later section. The results in Table III are very interesting since they throw much light on the relative capacities of X-rays of different wavelength to excite fluorescence in diamond The fact that the intensity is reduced to less than half by the interposition of only 0·2 mm. of aluminium, which transmits more than 60% of all wavelengths below 0 9 Å U, shows that components softer than this play a

predominant part in exciting the fluorescence This point is considered in greater detail in a later section where quantitative formulæ for the intensity of luminescence are developed

In order to confirm this fact, namely that most of the fluorescence is excited by soft X-rays, the following experiment was conducted A diamond (N C 71) which had a long straight edge was kept with this edge facing the X-ray tube and in such a way that the X-rays passed exactly parallel to the broad sides. In this way, the X-rays which excited the fluorescence entered through the edge over an area defined by the length and thickness of the crystal and proceeded inwards along its breadth If the diamond were viewed in a direction at right angles to the X-rays, a shading away of the luminescence from the front edge inwards was observed, as was expected The softer components of the X-rays were completely absorbed within the first millimetre or so, and the luminescence was very bright near the front edge As the X-rays progressed inwards they became harder and harder so that the intensity of luminescence steadily decreased The phenomenon was photographed and the photograph is reproduced in Fig 7 (*a*), Plate IX To further confirm the idea, aluminium foils of different thickness were introduced between the diamond and the X-ray tube It was then observed that the intensity of luminescence fell down progressively, as was to be expected from the results described in the previous para But what was more interesting was the fact that the fading away of the luminescence from the front surface inwards was also less and less prominent These are illustrated by Figs 7 (*a*) to (*d*), which were taken with aluminium foils of thicknesses 0 0, 0 1, 0 2 and 0 55 mm interposed The exposure times were 1 hr , 2 hrs , 4 hrs and 8hrs in order to obtain approximately the same initial intensity at the front edge. It will be seen that the fall of the luminescence intensity is less and less prominent as one passes from Fig 7 (*a*) to (*d*) The corresponding microphotometric traces are also reproduced in Fig. 1 which show very clearly that the rate of falling away of the intensity of fluorescence is smaller when the incident X-rays are made harder. Also, a study of the slope of the microphotometric traces at different distances from the front edge shows that this also becomes smaller and smaller as one goes away from this edge The reason for this becomes clear if one notes that the softer X-rays are also absorbed by the diamond, so that the X-ray beam becomes harder as it progresses into the crystal, and is consequently absorbed less The quantitative calculations are reserved to a later section.

The falling away of the intensity of luminescence as the X-rays penetrate the crystal was visually observed also with N C 60, a diamond of the ultra-violet transparent variety

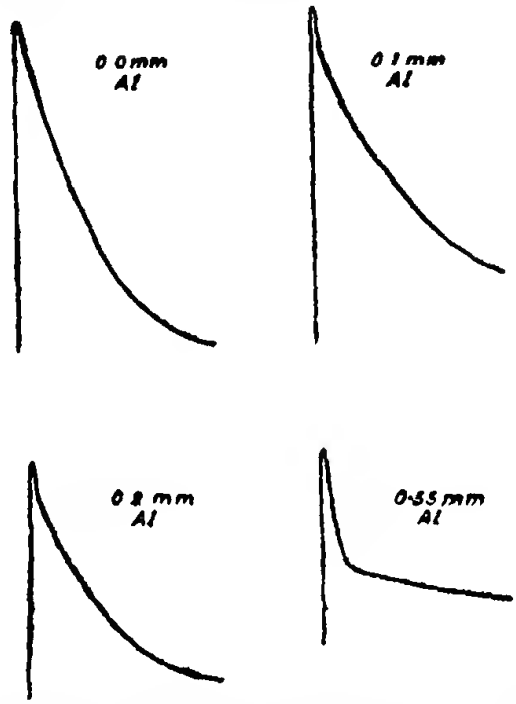

FIG. 1 Microphotometric traces of the fall of fluorescence intensity These were copied from the original traces to facilitate reproduction as line blocks

5 X-RAY LUMINESCENCE SPECTRUM OF DIAMOND

Since the luminescence of diamond under X-ray irradiation is extremely weak, a study of the spectrum was made with a fast spectrograph of small dispersion A somewhat detailed study has been made only with one diamond, N C 68, which is intensely blue-luminescent when excited by ultraviolet rays In X-rays, it was weakly luminescent, so that long exposures had to be given to obtain the spectrum An idea of the relative intensities in the two cases may be obtained from the fact that while 5 minutes sufficed to give a strong spectrum in the former case, an exposure of 20 hours was necessary to get a moderately strong spectrum with X-rays The two spectra have been taken side by side with a Hartmann diaphragm and are reproduced in Fig. 8 These were taken at room temperature. A comparison of the two spectra shows that, on the longer wave-length side of the principal electronic line at 4156 Å U , the spectrum is essentially the same in both the cases, namely consisting of four emission bands with maxima at 4278, 4387, 4514 and 4643 Å U The intensity of the bands are, however, different in the two cases. The spectrum of the X-ray luminescence in this region

appears as though the emission bands are superposed on a continuous spectrum The most interesting fact that comes out of the comparison of the two spectra is that, while the 4156 line itself comes out as an *emission* line in ultra-violet fluorescence, it occurs as an *absorption* line in X-ray fluorescence Also, there is an extension of the spectrum to the shorter wavelength side of 4156 Å U in X-ray fluorescence, which is absent with ultra-violet excitation This extension occurs as a continuous spectrum, in which the absorption bands occur with maxima of absorption at 4041, 3950 and 3850 Å U The continuous spectrum extends upto about 3600 Å U These details can be seen in Fig 8, Plate IX The spectrum of X-ray luminescence can thus be described as a combination of the absorption and the ultra-violet luminescence spectra It is a continuous spectrum, on which the absorption of diamond acts for wavelengths smaller than and including 4156 Å U and on which is superposed the ultra-violet fluorescence bands for longer wavelengths

That this description is essentially correct is shown by a study of the two spectra given by a weakly blue-fluorescent diamond, N C. 73 The ultra-violet fluorescence spectrum of this diamond is exactly similar to that of N.C 68, except for the fact that the whole spectrum is fainter. The X-ray luminescence spectrum, on the other hand, is strikingly different It consists of a continuous spectrum running from about 3600 to 5000 Å U with just a hint of an absorption line at 4156 Å U The continuous spectrum was recorded with nearly the same exposure as was required for N C 68 (*viz*, 20 hours), but no quantitative estimate was possible since the two diamonds had very different sizes and shapes Since this diamond (N C. 73) was feebly absorbing in the near ultra-violet, the absorption bands did not occur in the spectrum It thus appears as though X-rays give rise to a continuous spectrum in all diamonds of the blue-fluorescent class, and in addition give rise to the characteristic fluorescent bands with an intensity proportional to the intensity of ultra-violet fluorescence This idea fits in qualitatively with the results obtained for the two diamonds described above. For instance, it explains why the bands in the X-ray fluorescence spectrum are less clear than in the ultra-violet fluorescence spectrum with N C 68 and why they are absent in that of N C 73

A more quantitative verification of this idea is obtained in an entirely different manner, namely from the results described in section 2, in particular the values for the relative intensities of luminescence of different regions of N C 100 under X-ray and ultra-violet excitation. Let i_0 be the intensity of the continuous spectrum given by X-rays and let i be the intensity of the

fluorescent spectrum given by ultra-violet light Then the intensity of fluorescence under X-rays is

$$I = i_0 + ki \tag{1}$$

according to the above ideas If we denote by subscripts 1, 2, 3 the three areas of the diamond showing different intensities of luminescence, then

$$\frac{I_2}{I_1} = \frac{i_0 + ki_2}{i_0 + ki_1} = \frac{K + i_2}{K + i_1}, \text{ putting } \frac{i_0}{k} = K \tag{2}$$

In arbitrary units, we have $I_2/I_1 = 2\ 5$ and $i_2 = 5\ 0$, $i_1 = 1\ 0$, so that K comes out to be 6 33 Substituting the values for i_1 and i_2 and K in

$$\frac{I_2}{I_1} = \frac{K + i_2}{K + i_1}, \qquad \frac{I_2}{I_1} = 1\ 78 \tag{3}$$

which is in fairly good agreement with the experimentally determined value of 1 6 given in section 2 So also, this idea makes it intelligible why the maximum range of luminescence intensities is only 1 · 50 with X-rays while it is as large as 1 1000 with ultra-violet.

6 Mechanism of the Production of Luminescence by X-rays

In section 4, the results of experiments were described, which show how the intensity of luminescence varies with the intensity and hardness of the X-rays, the voltage applied to the X-ray tube and so on A quantitative explanation of these results must be sought for in a theory of the mechanism of the production of the luminescence It is obvious that the luminescence cannot be the direct outcome of the absorption of X-rays, for this results only in the ejection of photoelectrons which are of very high energy (of the order of tens of kilovolts) compared with energies of the order of a few volts associated with the luminescence. These photoelectrons are, however, rapidly absorbed in the medium as a result of the ionisation they produce. It is these low energy ions that are responsible for the production of luminescence

Using these ideas, it is possible to deduce an expression for the intensity of luminescence. Let $u_\lambda\, d\lambda$ be the intensity of X-rays at the point concerned in the spectral region λ to $\lambda + d\lambda$ and let a_λ be the fraction of this absorbed per unit length in the medium. a_λ is obviously equal to $\rho\mu_\lambda$, where ρ is the density and μ_λ the mass absorption coefficient Then the amount of X-rays absorbed per unit area in a thickness dt of the medium is clearly $a_\lambda i_\lambda d\lambda dt$, which is obviously proportional to the number of photoelectrons produced. This is not exactly true, since part of the X-rays absorbed is due to scattering and to the Compton effect. The assumption is, however, approximately true, particularly for the longer wavelengths Now, the photoelectrons

produced by the X-rays are absorbed within such a short distance (of the order of 0 01 mm) that it is reasonable to assume that they are absorbed as soon as they are produced* with the formation of low-energy ions. However, the number of ions so produced should depend on the energy of the photoelectron Since the production of each ion requires, on the average, a certain energy, we may suppose that the total number of ions produced is proportional to the energy of the photoelectron, *i e*, is inversely proportional to the wavelength of the X-ray, since the difference in energy between the X-ray and the photoelectron is only a few electron volts (the K absorption limit for carbon corresponds to an energy of 284eV), which is small ($< 2\%$) compared with energies of the order of thousands of electron volts for the X-ray Consequently, if one takes the intensity of fluorescence I at any point to be proportional to the number of ions per unit volume generated at that point, then

$$I = K \int_{\lambda_m}^{\infty} a_\lambda \frac{u_\lambda}{\lambda} \, d\lambda, \text{ where K is some constant} \tag{4}$$

We shall now apply this general formula to calculate the variation of the intensity of fluorescence with various factors and compare it with the experimental results described above The integral in (4) was evaluated by numerical integration, by dividing the range of wavelengths into a large number of sections and substituting the values of a_λ, u_λ and λ for each. The spectral variation in the intensity of white X-rays given out by a tungsten target has been studied by a number of investigators, but the only set of results covering a wide range of voltages which was found useful for the calculations were those given by Ulrey (1918) Although these have not been corrected for the variations in the structure factor of the crystal, etc, they form a fair basis for the calculations, which are themselves expected to be not very accurate Besides, no data as to the intensity of the characteristic radiation under the same conditions are available and so no account was taken of the characteristic radiation The data for white radiation were corrected for absorption in the window of the X-ray tube, which set the upper limit for λ at 3 Å U The values of the absorption coefficients were taken from standard tables (*e g*, Compton and Allison, 1935) and were obtained by interpolation

* This is easily proved If the X-rays are absorbed with an absorption coefficient a and the photoelectrons with a coefficient b with the formation of a tertiary product (ions), then the concentration of this tertiary product at a distance x from the boundary of the medium can be shown to be practically proportional to the intensity of the primary X-rays for values of $x > (\log b/a) / (b - a)$ Actually, for diamond this comes out to be 0·01 to 0·02 mm. for the X-rays used in these studies

(*a*) *Variation in the intensity of fluorescence with the distance from the front edge when the diamond is kept with its edge towards the X-ray tube* It is easily seen that the intensity at a distance x cms. from the edge is

$$I_x \propto \int \frac{i_\lambda a_\lambda}{\lambda} \exp(-a_\lambda x)\, d\lambda \tag{5}$$

where $i_\lambda d\lambda$ is the intensity of white X-rays emerging from the X-ray tube in the range λ to $\lambda + d\lambda$ The theoretically calculated values are represented as the continuous curve in Fig 2, while the circles are the experimetnal values obtained from the first microphotometric trace in Fig 1 The agreement is seen to be remarkably good, except for the first point, which is much above the theoretical curve This is obviously due to the presence of the characteristic L-radiation of tungsten in the region 1 0 to 1 5 Å, of which no account is taken in the theory These are absorbed to a very large extent in the first 0 1 cm and practically completely in 0 2 cm

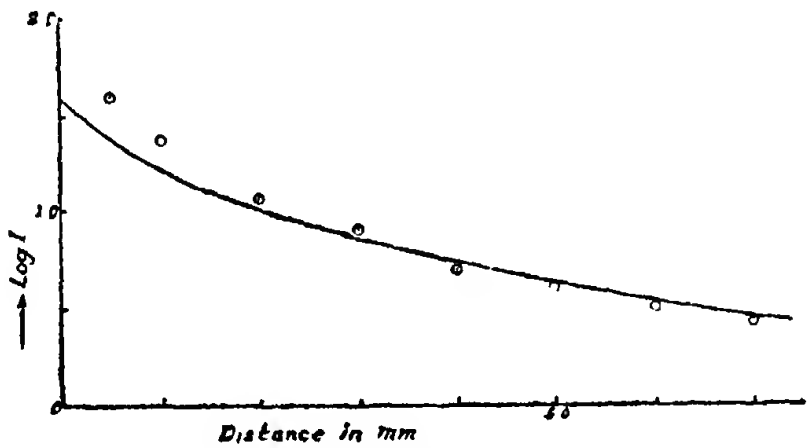

Fig 2

(*b*) *Variation of the intensity with voltage*—Under the experimental conditions, it is the total luminescence produced in the full thickness of the diamond that matters Consequently, one must consider the total amount of X-rays of each wavelength that is absorbed in the diamond while calculating the luminescence intensity Obviously this is proportional to $i_\lambda \{1 - \exp(-a_\lambda l)\}$, where l is the length of the path traversed by the X-rays in the medium. If the diamond is kept at an angle θ to the X-ray beam, $l = t \operatorname{cosec} \theta$ where t is the thickness of the crystal plate Hence,

$$I_V \propto \int_{\lambda_m}^{\infty} \frac{i_\lambda}{\lambda} \{1 - \exp(-a_\lambda l)\}\, d\lambda \tag{6}$$

Both the lower limit of integration and i_λ vary with the voltage The results of the calculations for a number of voltages are represented as a continuous curve in Fig 3, in which log I_V is plotted against log V The experimental data are shown by crosses against the corresponding values of the R M S voltage The agreement with theory is satisfactory For the lowest voltage, however, the experimental point is appreciably above the extrapolated theoretical curve This can be explained to be due to the presence of characteristic radiation, the relative proportion of which is larger for smaller voltages, as in the present case

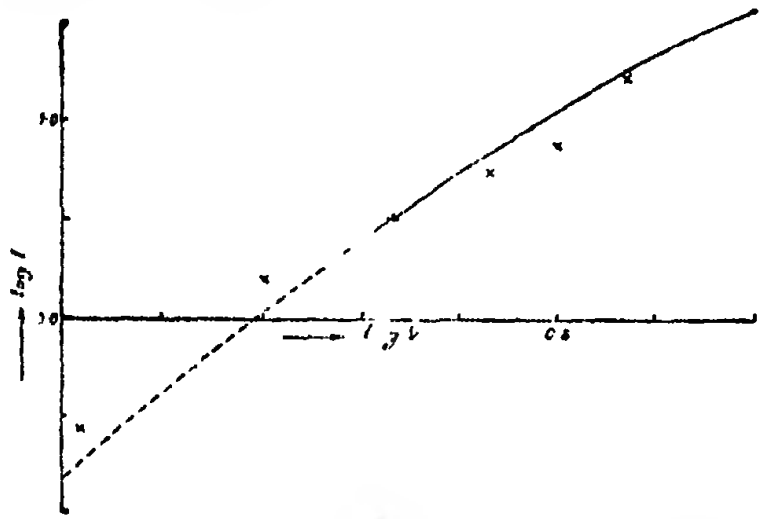

Fig 3

(c) *Reduction in the luminescence intensity when aluminium foils are introduced*—With an aluminium foil of thickness T introduced, the formula for the intensity is

$$I_T \propto \int_{\lambda_m}^{\infty} i_\lambda \{1 - exp(-a_\lambda l)\} exp(-b_\lambda T) d\lambda \qquad (7)$$

where b_λ is the linear absorption coefficient for aluminium The results of calculations made with formula (7) are shown in Fig 4 The agreement with experiment is reasonably good in this case also

These calculations thus support the idea that the production of luminescence by X-rays should be considered to be a tertiary phenomenon, namely, originating as a result of the ionisation produced by the photoelectrons ejected by the primary X-rays. Of course, the recoil electrons produced by the Compton scattering should also produce luminescence;

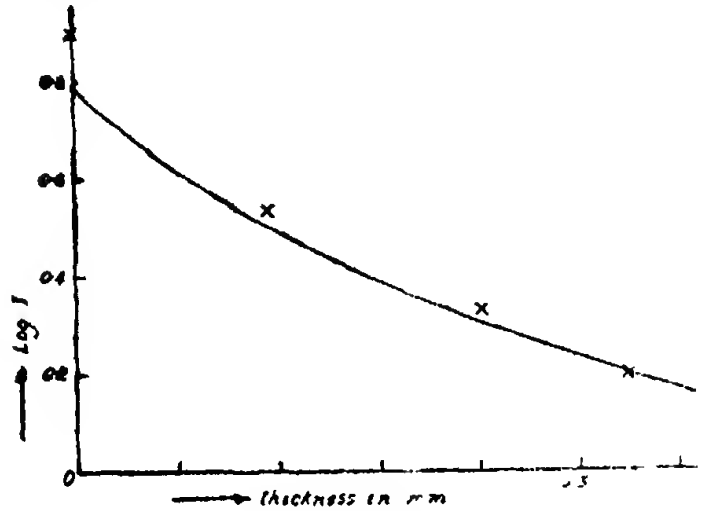

Fig 4

but the contribution due to these is comparatively small for X-rays which are not very hard, as were used in these experiments

My sincere thanks are due to Prof Sir C V Raman for the suggestion of the problem and for the discussions I had with him during the course of the investigation.

Summary

The paper deals with the investigations carried out by the author on various phenomena connected with the luminescence of diamond excited by X-rays The fluorescence generated by X-rays was found to be much weaker and also to vary over a smaller range of intensities than that excited by ultra-violet light The colour as well as the patterns of luminescence were the same as those excited by ultra-violet light, except that the patterns had less of contrast By photographic photometry, the fluorescence intensity was found to be directly proportional to the current through the X-ray tube and to vary roughly as the cube of the voltage Experiments are described which show that soft X-rays are more effective in producing luminescence than hard X-rays.

The luminescence spectrum of a brightly blue luminescent diamond excited by X-rays consisted of bands on the longer wavelength side of 4156 Å.U., these coinciding with those in the spectra excited by ultra-violet light, but there was a continuous spectrum on the shorter wavelength side, which was crossed by the absorption bands of diamond. The principal electronic line at 4156 Å.U. occurred as an absorption line. With a weakly blue-

fluorescent diamond, the spectrum was continuous, extending on either side of 4156 Å U with a trace of an absorption line at 4156 Å U A probable explanation for these is given, which also makes it intelligible why, with X-rays, the fluorescence intensity does not vary as much as with ultra-violet rays

It is suggested that the luminescence arises as a result of the ions produced by the photoelectrons which are ejected by the X-rays On this basis, quantitative formulæ are developed to explain the experimental data, and are found to hold fairly well

References

1 Compton and Allison — *X-Rays in Theory and Experiment*, Macmillan, 1935, p 799

2 John — *Ind J Phys*, 1931, **6**, 305

3 Mani, A — *Proc Ind Acad Sci*, 1944, 19A, 231, **20**, 117, 323, 1945, **21**, 280

4 Nayar, P G N — *Ibid*, 1941, **13**, 284

5 Ramachandran, G N — *Ibid*, 1946, **24**, 65

6 Raman, Sir C V — *Ibid*, 1944 **19**, 199

7 Rendall, G R — *Ibid*, 1946, **24**, 168

8 Sunanda Bai, K — *Ibid*, 1944, **19**, 274

9 Ulrey, C T — *Phys Rev*, 1918, **11**, 401

N C 115 N C 118 N C 82

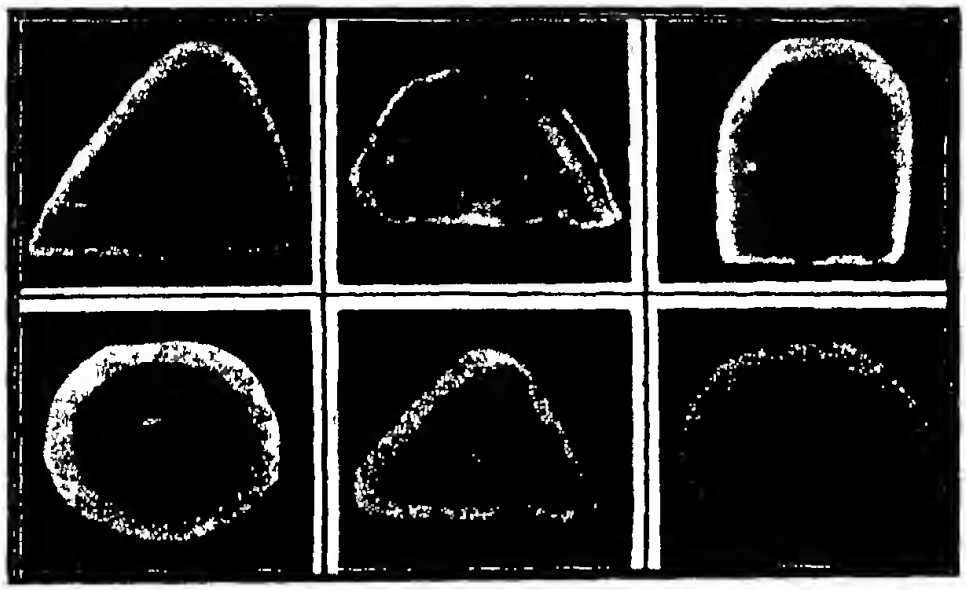

N C 80 N C 88 N C 99

FIG 5 X-Ray Luminescence Patterns

N C 127 N C 100 N C 122

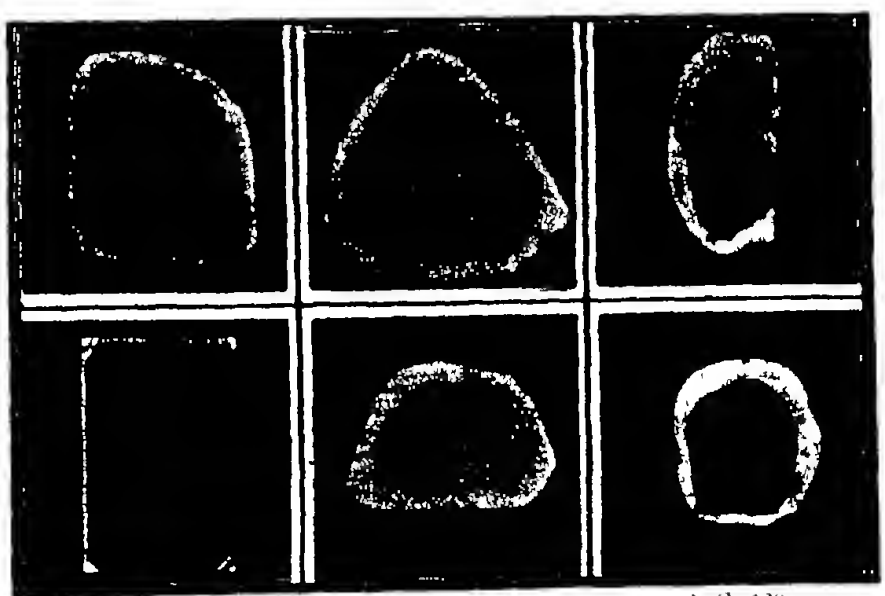

N C 60 N C 111 N C 120

FIG 6 X Ray Luminescence Patterns

(d)

(c)

(b)

(a)

(a)

(b)

→ λ increasing

Fig. 8

Luminescence Spectrum of NaCl (Z) with

(a) X Ray excitation and

(b) Ultra Violet excitation

X-RAY TOPOGRAPHS OF DIAMOND—PART II

By G N Ramachandran

(*From the Department of Physics, Indian Institute of Science, Bangalore*)

Received May 18 1946

(Communicated by Sir C V Raman, Kt, F R S, N L)

1 Introduction

In an earlier paper by the author (1944 *a*) bearing the same title, a method was described by which it is possible to obtain a photographic reproduction (X-ray topograph) of the variations in the X-ray reflecting power over the area of a cleavage plate of any crystal The method consists in using white X-rays diverging from a pinhole and obtaining Laue reflections from the full area of the cleavage plate The reflections may be obtained either from the internal or surface crystallographic planes In the former case, the crystal and the photographic plate have to be kept inclined at definite angles to the X-ray beam to obtain a non-distorted picture of the crystal, the values of which for any experimental arrangement could be obtained from formulæ given in the earlier paper When X-ray reflections are obtained from the surface cleavage plane, it is only necessary to keep the photographic plate parallel to the crystal to obtain a perfect reproduction A number of X-ray topographs obtained by the former method were reproduced in the paper quoted above and were discussed These topographs were, however, defective for two reasons Firstly, since duplitized X-ray films were used, two images were produced which were not in register on account of the oblique incidence of the X-ray beam on the film This seriously affected the clarity of the topographs It was found that the use of photographic plates eliminated this defect, although this necessitated the giving of fairly long exposures. Using this technique, some of the cleavage plates of diamond studied earlier have been reinvestigated and new specimens have also been studied. The other defect in the earlier photographs arose out of the use of fairly thick specimens. Since internal reflections were invariably involved, the reflections given by different layers of the diamond parallel to the surface were superimposed, thus obliterating many of the fine details (*e g*, lines and streaks) lying parallel to the plane of incidence and emphasizing those lying perpendicular to it. This defect was appreciably reduced by the use of thin plates Five such thin specimens, N.C 151, N C 155, N C. 156, N C 160 and N C 162 have been studied. The clarity of the photographs obtained

with the new technique makes more precise observations possible The present paper embodies the results of such further studies made on the X-ray topographs of diamond In particular, the crystallographic orientation of the various bands and streaks found in the X-ray topograph is discussed and the significance of the topographs in relation to the various other patterns exhibited by diamond is brought out.

Since the publication of the previous paper by the author on the subject, a note has appeared in *Nature* by N and W A Wooster (1945) describing their experiments for obtaining topographs using the principle of Bragg reflection from the surface The author wishes to point out that the possibility of obtaining topographs using the surface reflection from a stationary crystal was envisaged in the earlier paper (1944 a) where it was stated that, in this case, "the condition for no distortion is extremely simple, namely that the film must be parallel to the crystal" The surface reflection method was not used by the author since the reflected X-rays were even more obliquely incident on the film than in the other method and would completely mask all details if duplitized films were used. The method has later been tried with photographic plates, and the surface topographs thus obtained were essentially the same as those produced by internal reflection. An advantage of the ingenious modification of the method by N and W A Wooster, in which the crystal and film are simultaneously oscillated and the characteristic X-radiation is employed, is that the exposure times are reduced very much

2 Crystallographic Orientation of the Plates studied

Most of the specimens studied were of octahedral cleavage However, it is interesting to note that a few diamonds were found in the collection of Sir C. V Raman which were cleavage plates with their faces parallel to the (211) plane N C 82, for instance, whose topograph is reproduced in this paper, is one such diamond It is a fairly large plate (8 mm × 10 mm) having a thickness of about 2 mm N C 60 is a rectangular block 10 mm × 6 mm. × 1 5 mm whose broad faces are parallel to the $(\bar{2}11)$ plane, while the two edges are respectively parallel to (111) and $(01\bar{1})$ planes. N C 178 is another specimen whose broad faces are parallel to the (211) plane. The large size of these diamonds and the fact that the orientations of the surfaces were found to differ by less than 1° from those of the crystallographic planes suggest that these plates should have been obtained by cleavage. The slight deviations are to be explained as due to errors in polishing. These facts suggest that *diamond has a cleavage parallel to the* {211} *planes*, although this is not as often observed as the octahedral cleavage.

3 Interpretation of the Topographs

In the previous paper by the author (1944 *a*), it was mentioned that any increased reflection that is observed must be attributed to mosaic structure, arising from the angular deviation of fine crystallites in a sub-microscopic scale from their mean orientation It is a point of interest to find out whether this is really the case, or whether there is a misorientation of fairly large layers or blocks in the crystals In another investigation, the author (1944 *b*) has studied the angular divergence of the X-ray reflections given by blue-luminescent diamonds and has found that the reflection from the (111) planes had an angular half-width of nearly 60 seconds in an intensely luminescent diamond while it was only 3" with a feebly luminescent diamond The measurements were made on the Bragg reflections obtained from the surface of a stationary crystal using X-rays diverging from a very fine slit The line obtained on the photographic plate was very regular and of uniform width, showing that the mosaic structure is on a very fine scale When the same technique was tried with a non-luminescent diamond of the ultra-violet transparent variety, it was found that the line was very much distorted The width of the reflected X-ray beam was of the order of a few minutes of arc, and the distribution of intensity over the width was highly irregular, the $K\alpha_1$ and $K\alpha_2$ lines being not at all resolved These phenomena suggest that, in this variety of diamonds, misorientatio is on a fairly large scale also occur.

The question can also be settled in another way, namely by taking distortionless topographs at different distances from the crystal This is best accomplished by obtaining topographs using surface reflections and keeping the photographic plate parallel to the surface of the crystal, when one obtains a slightly enlarged non-distorted image In practice, this was done by having a long arm capable of rotating about the axis of the crystal, and setting this at double the angle of reflection to the direct beam of X-rays The film-holder was kept at the requisite angle to the arm and by moving it towards or away from the crystal along it, topographs at various distances were obtained It may be remarked that errors in the angular setting of the arm and the film holder would produce the same amount of distortion in all the pictures, so that the comparison can be done exactly If the relative distances of the various streaks remain the same in all the topographs, then there is no gross misorientation, while the measurement of differences in these relative distances, if any, would give the angular tilting

Actually, no such tilting could be found in the ultraviolet opaque diamonds showing blue luminescence, while a small angular tilting of a few minutes of arc was found in some ultraviolet transparent diamonds, This

probably explains why the latter class of diamonds give very much more intense X-ray reflections and why, in some cases, the Laue spots are drawn out into curious shapes The topographs reproduced do not give a true representation of the relative intensities of reflection given by different diamonds, for the exposure times were adjusted so as to get approximately the same density in all the cases An idea of the enormously greater intensity of reflection given by the ultraviolet transparent diamond may be obtained from the fact that N C 125 in Fig 1, which belongs to this class, required only an exposure of 15 minutes, while the topograph of N C 100 in the same figure, which is a diamond opaque to the ultraviolet, required as much as 10 hours' exposure

4 Discussion of the Topographs

For the purpose of this discussion, we shall consider not only the topographs reproduced in this paper, but also those reproduced in the earlier paper by the author (1944 *a*) Where reference is made to a diamond studied earlier, the new catalogue (N C) numbers are also given For a proper appreciation of the discussion below, it will be useful to compare the topographs with the luminescence, ultraviolet transparency and birefringence patterns of the same diamond reproduced in a paper by Rendall (1946) appearing in this symposium

It is convenient to divide the diamonds that were studied into three classes

(*a*) those exhibiting pure blue luminescence,

(*b*) those that are non-luminescent

and (*c*) those exhibiting both blue and yellow luminescence.

(*a*) As was remarked in the earlier paper, the topographs of purely blue-luminescent diamonds, which are opaque to the ultraviolet below 3000 Å U did not exhibit any streaks but only areas of varying intensity, these corresponding closely with those occurring in luminescence N C 100 whose topograph is shown in Fig 1, Plate X, is a good example The central bright portion here corresponds exactly with the bright region in the luminescence pattern The central bright area has, in addition, a weaker extension to the left in the luminescence pattern, which is also correspondingly reproduced in the X-ray topograph. In the case of other diamonds of this class like D 36 (N C 71), D 45 (N C 72) and D 221 (N C 73) studied earlier, both the luminescence pattern and the X-ray topograph are uniform. There is thus no doubt that, in diamonds of the blue-luminescent class, the X-ray reflecting power increases with increasing intensity of luminescence,

(*b*) In contrast to the above class of blue-luminescent diamonds, there is a class which transmits down to 2250 Å U, and which does not exhibit any luminescence, examples of which are N C 124, N C 125 and N C 126. A characteristic feature of the X-ray topographs of these diamonds is the existence of sets of parallel streaks

As has been shown by the author in another paper (Ramachandran, 1946) appearing in this symposium diamonds of this class possess a laminated structure, the laminations being generally parallel to octahedral planes and less often to dodecahedral planes It is of interest to know if the streaks found in the X-ray topographs also represent these laminæ A study of the directions of the streaks showed that they were invariably parallel to the intersection of either an octahedral or a dodecahedral plane with the surface However, if the laminæ observed optically are very fine and closely spaced, then the corresponding streaks are not found in the X-ray topograph This is the case, for example, with N C 124 (D 207) which reveals fine laminæ under the polarising microscope These lines, however, are absent in the topograph The reason why this happens is that the reflection takes place not only from the surface of the crystal plate but also from the interior Consequently, the streaks get superposed on one another and they disappear, if they are very fine For the same reason, details consisting of lines running perpendicular to the plane of reflection are lost, while those parallel to it come out clearly This is why only one set of streaks running at about 30° to the horizontal is found in the topograph of N C 125 in Fig 1 These correspond to dodecahedral laminations seen under crossed nicols Optically, octahedral laminations running perpendicular to these have been observed; but they are not found in the topograph since they are at right angles to the plane of reflection With N C 126 (D 209), only a coarse pattern is observed in the topograph, presumably due to misorientations The laminations are very fine and are not found in the topograph.

(*c*) The most interesting class of diamonds, in so far as the relationship between X-ray topographs and other patterns is concerned, is that which exhibits both blue and yellow luminescence A number of such diamonds have been studied in detail and most of the topographs reproduced in this paper belong to this class These diamonds can again be subdivided into two varieties, *viz.*, (i) those in which the blue and yellow luminescence patterns are identical and (ii) those in which they are different To the former class belong N C 113 shown in Fig 1, N C 156 and N C. 160 in Fig 2 and N C. 80 (D 38 of author's earlier paper). In all cases, it is found that the topograph and the birefringence pattern follow the luminescence pattern, parallel bands occurring in the topograph in the same places as in

luminescence In N C. 113, there are also large variations in ultraviolet transparency, the two margins being more transparent than the rest of the diamond These correspond with the bright bands seen in the topograph in the same regions

The latter class is even more interesting, typical examples of which are N C 115, N C 82, N C 108 and all the diamonds in Fig. 2 except N C. 156 and N C 160 As a result of a comparison of these topographs with the other patterns of the same diamonds, the following general results may be stated.

(1) The bands of yellow luminescence have their counterpart in the topograph

(2) Also, these bands correspond to the lines found in the birefringence pattern, the similarity between the topograph and the birefringence pattern being generally very striking

(3) Variations in blue luminescence are not generally reproduced in the topographs

(4) Although the blue luminescence pattern shows a great similarity to the ultraviolet transparency pattern, bright areas in the one corresponding to dark areas in the other, no particular similarity is observed between the topograph and the transparency pattern

These may be illustrated with special reference to the diamonds whose topographs are reproduced in Figs 1 and 2 The blue luminescence pattern of N C 115 consists of a central triangular bright patch with dark areas surrounding it near the margins The ultraviolet transparency pattern has an inverse relation to this, as described above The X-ray topograph does not show these differences, but the three bands found in the yellow luminescence pattern are beautifully recorded in it There is also some similarity to the birefringence pattern

N C 82 exhibits exactly similar features, the blue luminescence and transparency patterns corresponding inversely, while the yellow luminescence pattern is different, namely consisting of bands running diagonally. The latter are found both in the X-ray topograph and the birefringence pattern

The blue luminescence pattern of N C 155 is practically uniform, while parallel bands are seen in both the yellow luminescence and birefringence patterns These correspond exactly with the fine bands found in the X-ray topograph. (It may be noted that the diamond is inverted in the topograph with respect to the other patterns, right side here corresponding to left in the others and *vice versa*)

N C 151 is another typical case in which the blue and yellow patterns are quite different The birefringence pattern consists of bands running parallel to the yellow luminescence pattern and the topograph also shows these same bands As will be seen from the topograph, there is some sort of discontinuity in the middle of the diamond This could be seen visually in the birefringence pattern also when the nicols are oriented properly.

The patterns of N C 108 are rather confused, but still a general similarity is observable between the various patterns.

5 Interpretation of the Results

A theoretical background on the basis of which one may attempt to interpret the above results is furnished by Sir C V Raman's theory (1944) of the ultimate structure of diamond According to Sir C V Raman, diamond can have four different structures Two of these, called TdI and TdII, have tetrahedral symmetry, and by virtue of the selection rules exhibit an absorption for infra-red radiation in the region of 8 μ They are physically identical with each other, differing only in their geometrical orientation The other two structures, OhI and OhII, possess octahedral symmetry and are consequently transparent to the infra-red They are however, distinct from each other and also from the tetrahedral varieties The various structures may exist side by s de in the same specimen of diamond and it is the differences in the nature and the extent of interpenetration of the various structures that produces the amazing variations in the properties of diamond

The blue luminescent diamonds on account of their infra-red absorption, should consist solely of the TdI and TdII varieties According to Raman's theory, blue luminescence arises from the intermixture of these two varieties, the intensity being determined by the extent of their interpenetration Although the two structures are physically identical, nevertheless there would be discontinuities at the places where they join with each other, so that a sort of mosaic structure should result, the magnitude of the mosaicity being larger, the more intimately the two structures are mixed These considerations give a satisfactory explanation of the direct correlation observed between the intensity of X-ray reflection and that of blue luminescence.

The non-luminescent diamonds are transparent both to the ultra-violet below 3000 Å U and to the infra-red in the region of 8 μ These should therefore consist only of the OhI and OhII varieties The two structures are physically different and consequently one would expect the diamond to be subject to severe strains In fact, in another paper appearing in this symposium, the author (1946) has shown that the lattice spacings of the two

structures are different, that the diamond consists of laminæ alternately made of OhI and OhII structures and that these laminæ are alternately under compression and tension It is therefore not at all surprising that these diamonds possess a large mosaic structure and that they often show gross misorientations

The other type of intermixture that is possible is that between a Td and an Oh structure Raman supposes that, in this case, yellow luminescence results This is supported by the author's observations on the laminations in such diamonds If, in the midst of a blue-luminescent diamond, a yellow streak is observed, then it is found that birefringence is produced at this region and that the diamond composing the thin lamina has either a larger or a smaller spacing than the bulk of the specimen (For further details, see the paper by the author quoted above) Thus, at places where a band of yellow luminescence is observed, there should be a comparatively large mosaic structure, since the structure there has a spacing different from the rest of the crystal, in contrast with the areas of blue luminescence where the two intermingling structures are of identical lattice spacing This explains why yellow bands are invariably represented in the topograph as bright streaks while variations in blue luminescence are not represented.

The facts described in the previous section thus find a reasonable explanation on the basis of Raman's theory.

I wish to express my indebtedness to Sir C V Raman for the constant encouragement that he gave me during the course of this investigation

SUMMARY

X-ray topographs (*viz*, photographic representations of the variations in the X-ray reflecting power over the area of a crystal plate) of a number of diamonds have been obtained and studied Comparing these with the other patterns of the same diamonds, the following results emerge (1) In purely blue-luminescent diamonds, there is a direct correlation between the intensity of luminescence and the X-ray reflecting power (2) Topographs of non-luminescent diamonds show parallel bands, which often correspond with the bands in the birefringence patterns They also suggest that gross misorientations of fairly large crystalline blocks sometimes occur in these diamonds (3) In diamonds showing both blue and yellow luminescence patterns, the topograph exhibits a correspondence only to the yellow luminescence pattern if the two are different, and to both if they are similar. An explanation of these results is given on the basis of Raman's theory of the structure of diamonds.

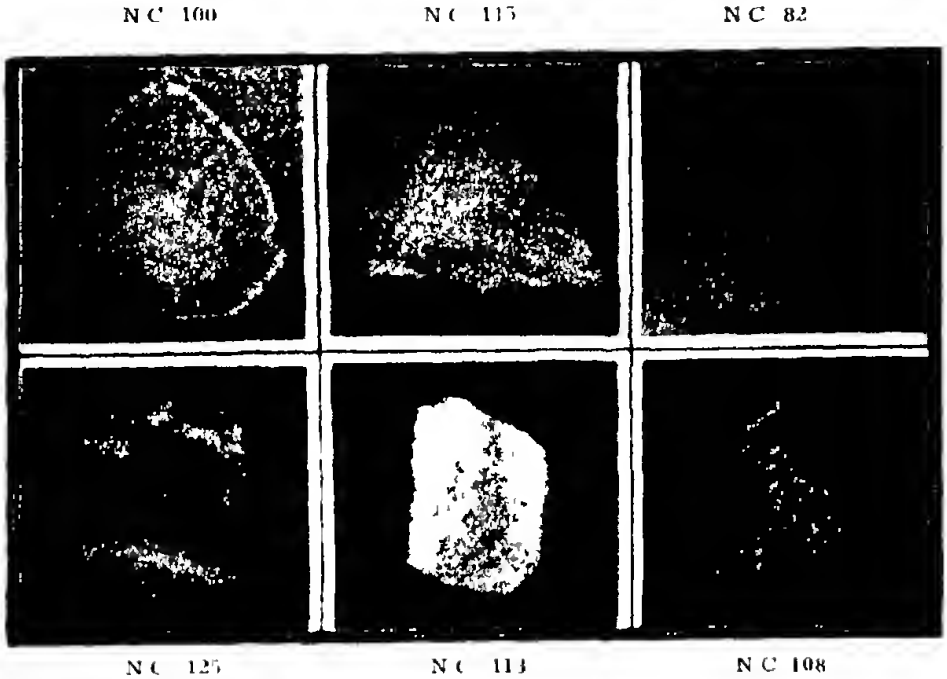

FIG 1 X-Ray Topograph of Diamond

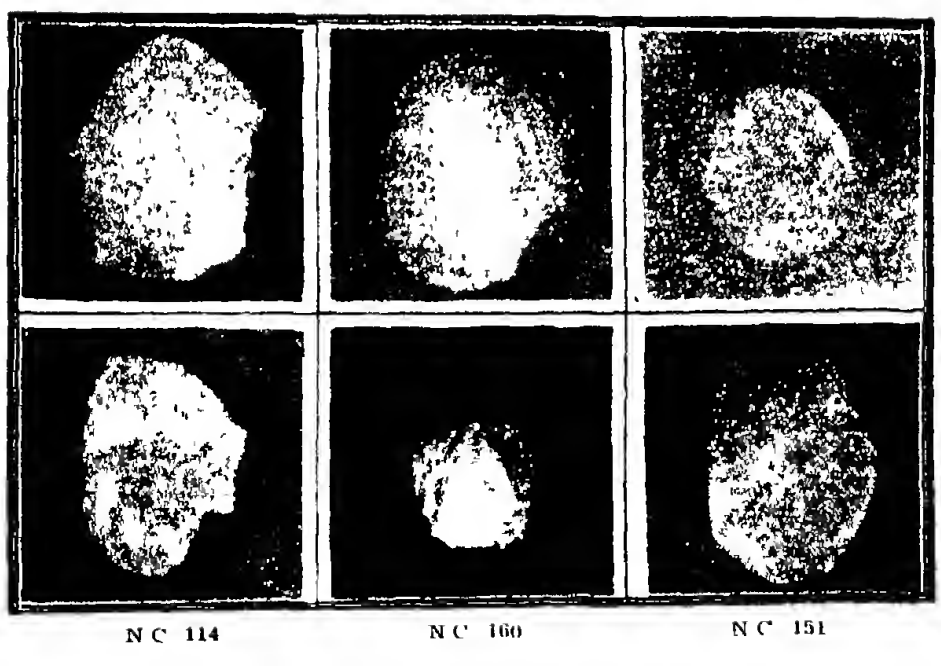

FIG 2 X-Ray Topographs of Diamond

A study of the orientation of a number of cleavage plates made in connection with this investigation showed that although most of them were of octahedral cleavage, at least 3 of the diamonds had their *large* faces parallel to the (211) plane, showing that diamond has also a direction of easy cleavage parallel to the {211} planes

Note added on 17th June 1946 —Since the above was written, it has been discovered by Ramaseshan (1946) that diamond possesses many other cleavages besides the new one (211) reported in section 2 of this paper Consequently, a systematic study of the orientation of a number of diamonds in the collection of Sir C V Raman was undertaken to see if any of the cleavage plates belonged to any of these new classes Out of a total of 48 diamonds studied, it was found that 42 were of octahedral cleavage Of the remaining, 3 diamonds (N C 60, 82 and 178) had their surfaces parallel to a {211} plane, N C 88 was parallel to a {322}, N C 123 to a {320} and N C 174 to a {431} plane The orientation of the last one was not very definite, since it was less than 5° away from a {331} or a {321} plane. The fact that such large cleavage plates having a surface area of 20 sq mm and above could be obtained parallel to these planes is very striking It shows that the cleavages are fairly well-defined, and thus supports the findings of Ramaseshan

References

1 Ramachandran, G N *Proc Ind Acad Sci*, A, 1944*a*, **19**, 280
2 ——— *Ibid*, 1944*b*, **20**, 245
3 ——— *Ibid*,, 1946, **24**, 66
4 Raman, Sir C V *Ibid* 1944, **19**, 189 199
5 Ramaseshan, S *Ibid*, 1946, **24**, 118
6 Rendall, G R *Ibid*, 1946, **24**, 168
7 Wooster, N and W A *Nature*, 1945, **155**, 786

THE FARADAY EFFECT IN DIAMOND

By S Ramaseshan

(From the Department of Physics, Indian Institute of Science, Bangalore)

Received May 18, 1946

(Communicated by Sir C V Raman, Kt, F R S, N L.)

1 Introduction

Since diamond is optically isotropic and has a large dispersive power, it may be expected to show an easily observable Faraday effect A search of the literature however reveals only a single observation on the Faraday effect of diamond recorded by H Becquerel (1877) in the following words, "In a remarkable crystal (octahedral) belonging to M Fizeau, we obtained a feeble rotation of near about 27 minutes in yellow light" The thickness of the specimen was 2 875 mm and the effective field was 7330 gauss The Verdet's constant for diamond calculated from these data comes out as 0 0128 minutes per centimeter per gauss. This is actually less than that constant for common crown glass and, as we shall see in the course of the paper, it is only one-half of the correct value The lack of any further observations with diamond in the century which has elapsed since Faraday's original discovery is evidently due to the difficulty of obtaining suitable specimens for study As is wellknown, diamond commonly exhibits birefringence in greater or less measure, and the restoration of light due to this effect when the crystal is observed between crossed nicols completely overpowers the feeble restoration due to the action of the magnetic field. That Becquerel could at least observe the Faraday effect shows that the particular specimen was better than most samples The low value obtained by him may be ascribed to the difficulty of measuring the Faraday effect in the presence of residual birefringence. Indeed, the Faraday rotation in isotropic bodies is known to be markedly diminished in the presence of birefringence induced by strain (Schutz, *Magneto Optik*, 1936)

However, contrary to the belief that has been frequently expressed in recent literature, birefringence is *not* always to be observed in diamond The observations of Raman and Rendall (1944) on this point indicate that it is present only when there is an admixture of physically different allotropic modifications of diamond and is absent when there is no such admixture In Sir C V Raman's collection of crystals and of cleavage plates, there are several specimens of diamond of which the birefringence is negligibly small.

Amongst these, the cleavage plates N C 157, N C 177 and N C 73 having approximately parallel faces were found on examination to be suitable for Faraday effect studies The thickness of these plates were however rather small (0 58, 0 85 and 0 68 mm respectively) Observations were also possible with a large diamond crystal in its natural form, N C 4, which gave an easily observable Faraday rotation on account of its considerable thickness (4 8 mm) Owing, however, to the curvature of the faces of this crystal and the consequent deviation of the rays in passing through it, the magnitude of the Verdet's constant deduced from it is not as trustworthy as that deduced from the observations on the other three plates in spite of their comparatively smaller thickness

Darwin and Watson (1927) have shown that the Faraday effect in most transparent bodies is accurately expressed by the modified Becquerel formula

$$V = \gamma \frac{e}{2mc^2} \lambda \frac{dn}{d\lambda}$$

where V is the Verdet's constant (rotation per cm per gauss), e and m are the electronic charge and mass respectively, c is the velocity of light, λ the wavelength of the light used and n the refractive index of the substance γ is a multiplying constant which may be called the *magneto-optic anamoly* (γ is usually expressed as a percentage) As has been shown by Darwin and Watson, γ remains constant over the whole of the visible and near ultra-violet spectrum, provided the part of the dispersion associated with the infra-red absorption is eliminated from the dispersive power appearing in the formula The value of γ for the great majority of carbon compounds lies between 40% and 60% Accordingly in the present investigation, the Faraday rotation has been determined for different regions in the visible spectrum to determine the magneto-optic anamoly of diamond and to ascertain whether or not it is independent of the wavelength of the light employed.

2 The Experimental Procedure

The magnetic field—A large electromagnet of the Rutherford type capable of giving fields upto 23,000 gauss was used for these investigations. Each of the two pole pieces supplied by the manufacturers had a longitudinal hole about 2 cms. in diameter When the pole pieces are brought quite close, the large size of the holes would result in the field between them being low and also sensibly non-uniform To eliminate this difficulty, specially designed soft iron plugs were introduced which reduced the diameter of the holes to 0 6 cm. The pole pieces after this modification, had a flat area of about 2 sq. cms They were kept at a distance of 0 95 cm. apart A

measurement of the field with a small search coil and fluxmeter over various regions in the space between the pole pieces showed that the variations in the field along the lines of force were not greater than 2 to 3 % The magnitude of the field with 6 amps current through the exciting coils was about 16,000 gauss

The source of light —An image of the tungsten bead of a powerful point-o-lite lamp was focussed on the slit of a constant deviation spectrograph, which was used as a monochromator A slit of width less than one mm selected out various regions of the spectrum The spectral band coming through the slit was not more than 50 Å in the green and blue regions and was about 100 Å in the red and yellow regions The mean wavelength of the band was determined with a calibrated direct vision spectroscope For accurate monochromatisation a mercury point-o-lite or a sodium lamp was substituted for the tungsten lamp Since a monochromator with a single prism was used, the scattered light gave a continuous background This was not considerable when the brighter regions of the spectrum, *i e*, from 6000 Å to 4800 Å are used, but became a serious source of error for wavelengths below 4800 Å The magnetic rotation of diamond was therefore studied only over a range of wavelengths between 6000 Å and 4800 Å where the background intensity did not affect the observations On certain occasions the monochromator was dispensed with, and sodium or mercury lamps with adequate filters were used

Two wide-angled nicols giving perfect extinction were used as polariser and analyser respectively The rotation of the analysing nicol was measured with a lamp and scale, the scale being at 80 cms from the mirror. The diamond plate was introduced between the pole pieces in a wooden holder and care was taken to see that the crystal was not strained thereby introducing birefringence The surface of the diamond was kept normal to the incident light, as otherwise, there would be a rotation of the plane of polarisation due to refraction at oblique incidence Although this scarcely affected the Faraday effect, it was more convenient to avoid such rotation

The general procedure of the experiment was as follows The light of the necessary wavelength was focussed on the slit and the diamond introduced in position and the nicols then accurately crossed. A large number of readings (usually 25) were taken for this crossed position. It was found that settings could be made within 1 5 mm when the scale was at 80 cms distance. The mean of these readings was taken as the position of extinction. The magnetic field was then put on by passing a current of 6 amps through the coils and the nicols crossed again. The mean of 25 readings gave the

position of extinction. Similarly, the extinction position when the field was reversed was found The rotation of the plane of polarisation was calculated by taking half the difference between the two extinction positions, the zero-reading acting as a check on the accuracy of measurement

Half-shades and other appliances for finding out the exact extinction position could not be successfully used in the case of diamond One seldom obtained complete extinction in all the regions of the diamond when it was observed between crossed nicols To get the correct extinction position it was, therefore, necessary to view only those regions which gave total extinction The half shade gave the mean extinction position for the whole plate of diamond and hence gave less accurate results than when ordinary nicols were used In fact when a half-shade was used, rotations of the same order as those observed with nicols were obtained, but the differences between individual readings were larger and hence the method was untrustworthy The numerous concordant values obtained when nicols were used bore testimony to the accuracy of this method

The absolute value of the Verdet's constant of diamond was determined by comparing the rotation produced by it with that produced by a thin crystal of rock salt placed exactly in the same position as the diamond This procedure was adopted so that if there was a minute rotation due to the effect of the magnetic field on the nicols, the cover slips protecting the nicols and other optical parts, the same could be eliminated Separate measurements of these spurious effects were made and they were found to be less than 5% of the rotation produced by diamond From the knowledge of the magnetic rotation due to a crystal of rock salt of known thickness and of the accurate Verdet's constant for it (from the International Critical Tables), it is possible to calculate the effective field Table I gives the effective fields calculated from the rotation by substances of different thicknesses The standard values of the Verdet's constant for these substances for the sodium 5890 line which were used for the calculation of the field are also given The value obtained with a search coil (0 7 cm long) is also given. These measurements were carried out for two different field strengths which were used in the determination of the magneto-optic rotation. The value of the field appears lower when the thickness of the substance used is small. This is, as already mentioned, due to the rotation produced (in the opposite direction) by the effect of the magnetic field on the optical system At the foot of the table has been entered the ratio of the Verdet's constant for water for the wavelengths 5890 Å and 5460 Å observed experimentally by the present writer and that given in the International Critical Tables.

The two values agree quite closely, indicating the accuracy with which the settings could be made.

TABLE I

Verdet's constant at 25°C for 5890A

NaCl 0 03585 mins per cm per gauss

Water 0 01306 " "

A Distance between pole pieces, 0 95 cms

Distance of scale from mirror, 79 cms

Substance	Thickness in cm	Wavelength in Å U.	Rotation in cms	Rotation in mins	Field in gauss
NaCl	0 046	5890	1 24	27 54	16700
	0 098	"	2 66	59·1	16820
	0 417	"	11 4	254 3	17010
Water	0 105	"	1 03	23 0	16720
	0 372		3 70	82 6	17010

Field determined with search coil 17100 gauss

B Distance between pole pieces, 1 05 cms

Distance of scale from mirror, 81 7 cms

Substance	Thickness in cm	Wavelength in Å U	Rotation in cms	Rotation in mins	Field in gauss
NaCl	0 043	5890	1 16	24·4	15810
	0 092	"	2 57	54 0	15880
	0 401		10 85	227 8	15890
Water	0·372	5890	3·37	70 8	15860
	0 372	5460	3·96	83 6	15890

$\frac{V_{5460}}{V_{5890}}$ for water at 25° 1 184 (I C T)

" " " 1 175 (Observed)

3 OBSERVATIONAL DATA

The cleavage plate N C 157 was used for the study of the variations of the Verdet's constant with wavelength Table II gives the Verdet's constant obtained for different wavelengths between 6000 Å and 4800 Å The last column in the table gives the magneto-optic anamoly, the method of calculation of which is indicated later Two monochromatic wavelengths 5890 Å (sodium) and 5460 Å (mercury) were used in the measurement of the Verdet's constant in N C 177 The values are given in Table III, each of them being a mean of 100 readings The ratio $\frac{V_{5460}}{V_{5890}} = 1\ 191$ and the ratio calculated from the Becquerel formula is 1 179 Table IV gives the results

obtained with N C 73 and N C 4 and also those obtained for a combination of N.C 157 and N C 73.

TABLE II

N C 157 Thickness of the plate 0 58 mm
Distance between pole pieces 0 95 cm Effective field 16700 gauss
Distance of scale from mirror, 79 cms

Wavelength in Å. U	Rotation in cms.	Rotation in mins	Verdet's constant in mins per cm per gauss	γ
5890	0 97	22 3	0 0230	27 4
5800	1·00	23 0	0 0237	28·1
5600	1 07	24 6	0 0254	27 9
5400	1 20	27 6	0 0285	28 9
5200	1 27	29 3	0 0302	28 2
5025	1 35	31 1	0 0321	27·8
4860	1·41	32 4	0 0335	26 9

TABLE III

N C 177 Thickness of the plate 0 85 mm Effective field 15800 gauss
Distance of the scale from the mirror, 81 7 cms

Wavelength in Å U	Rotation in cms	Rotation in mins	Verdet's constant mins. per cm per gauss	γ
5890 (Na)	1 36	31 3	0·0233	27 6
5461 (Hg)	1 62	37 3	0 0278	27·9

$$\frac{V_{5400}}{V_{5890}} = 1\ 191 \text{ (experimental)}$$
$$= 1\ 179 \text{ (from Becquerel's formula)}$$

TABLE IV

Effective field 16700 *gauss* *Distance of scale from mirror,* 79 *cms*

Diamond	Thickness in mms	Wavelength in Å U	Rotation in cms	Verdet's constant	γ
N. C. 73 ..	0·68	5800	1 20	0 0243	28 9
		5400	1 35	0 0273	27 5
		5025	1 54	0 0312	26 9
N C 73 and N C. 157	1 28	5800	2·22	0 0243	28 9
		5400	2 67	0 0292	29 6
N C 4 (Crystal) ..	4 8	5800	7 44	0 0209	25·4
		5400	9 08	0 0256	25 6

As already remarked, the result obtained with the crystal N.C 4 is not so trustworthy as that obtained with the cleavage plates

4 The Magneto-Optic Constants of Diamond

The value of γ was determined in the following way. Peter (1923) determined the refractive index of diamond from 6790 Å to 2265 Å and found the refractive index in this region to be well expressed by the formula

$$n^2 - 1 = \frac{\epsilon_1 \lambda^2}{\lambda^2 - \lambda_1^2} + \frac{\epsilon_2 \lambda^2}{\lambda^2 - \lambda_2^2}$$

where $\epsilon_1 = 0\ 3306$ $\lambda_1 = 1750$ Å

$\epsilon_2 = 4\ 3356$ $\lambda_2 = 1060$ Å

From this formula $\lambda \frac{dn}{d\lambda}$ was calculated for those wavelengths for which the magneto-optic rotation has been determined Using the relation

$$V = \gamma \frac{e}{2mc^2} \lambda \frac{dn}{d\lambda}$$

γ was found and is expressed as a percentage γ is thus the percentage ratio of the observed magnetic rotation to that calculated from the unmodified Becquerel formula The last columns of each of the Tables II, III and IV give the value of γ for the wavelengths indicated It may be noticed that for a range of wavelengths from 6000 Å to 4800 Å, the value of γ is, within the limits of experimental error, constant

From the examination of the above results, the following can be taken as the standard values of the various magneto-optic constants for diamond.

Verdet's constant	5890 Å	0 0233 mins per cm per gauss
	5460 Å	0 0278 ,, ,,

V_{5460} = 1 191 (observed)
V_{5890} = 1 179 (calculated from the Becquerel formula)

The mean value of γ for the visible spectrum = 27 8

Fig 1 gives the experimental values of the magnetic rotation for various wavelengths, as also the theoretical values, calculated from the Becquerel formula with $\gamma = 28\%$ It is estimated that in the measurement of the magnetic rotation, an error of not more than 4% could have crept in

5 The Magneto-Optic Constants of Zinc Blende

Since sphalerite (ZnS) has a crystal structure similar to that of diamond it was considered worthwhile to determine its Verdet's constant and the magneto-optic anamoly Using the same arrangement as that described for

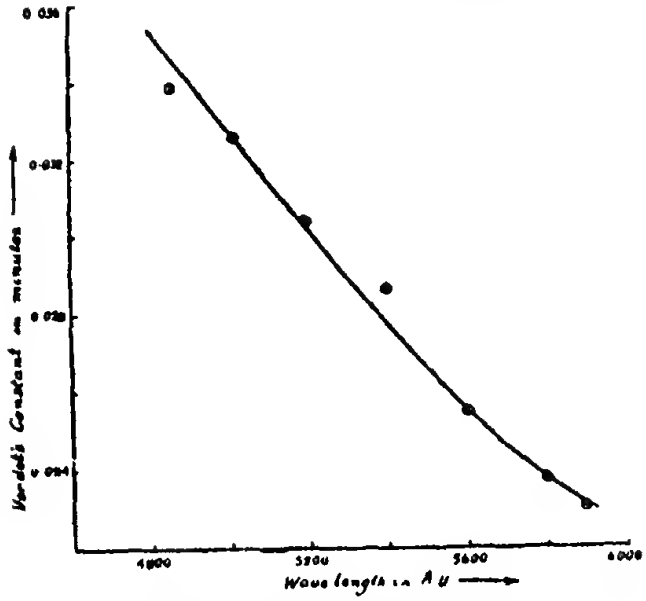

—— Theoretical curve from Becquerel's formula (γ = 28%)
○ Experimental points (N C 157)

Fig 1 Observed and Calculated Faraday Rotations of Diamond

diamond, the magnetic rotation for a beautiful transparent plate of sphalerite in the possession of Sir C V Raman was determined for different wavelengths Using the refractive index data of Maria Mull (1923) the magneto-optic anamoly for these wavelengths was determined The results are tabulated in Table V. Table VI compares the results obtained by the present writer with those obtained by different authors The agreement between these results is quite satisfactory

TABLE V

Sphalerite (ZnS) Effective field, 16700 gauss Thickness of the specimen, 5 55 mm

Wavelength in Å U	Rotation in degrees	Verdet's Constant	γ %
6100	32 7	0·211	91
5890 (Na)	35 0	0·226	91
5780 (Hg)	38 1	0·246	90
5600	40 4	0 261	90
5460 (Hg)	44 5	0 287	92
5400	45 6	0·294	92
5200	52·4	0 333	91 5
4360 (Hg)	90 25	0 582	91

TABLE VI

Sphalerite (ZnS)

Constant	Author	Other observers
Verdet's constant		
5890 A	0 226	0 225 (Becquerel) 1877
5460 A	0 287	0 286 (Cotton) 1932
$\frac{V_{4360}}{V_{5460}}$	2 03	2 057 (,,)
$\frac{V_{2750}}{V_{5460}}$	0 852	0 863 (,,)

6. DISCUSSION OF RESULTS

Table VII gives the optical and the magneto-optic constants of some cubic crystals of relatively simple structure The magneto-optic anamoly γ for all these crystals is constant over the range of the visible spectrum.

TABLE VII

Substance	Refractive Index 5890 Å	Dispersion 5890 Å	Verdet's constant 5890 Å	γ %
ZnS	2 3683	4611	0·226	91
NaCl	1 5443	669	0 03585	85
KCl	1 4904	586	0 02858	75
CaF_2	1 4338	242	0 00883	66
Diamond	2 4172	1298	0 0233	28

This indicates that the electrons which give rise to dispersion are also those responsible for the magneto-optic rotation The value of γ for atoms and ions having the inert gas configuration has been shown (Van Vleck, 1932) to be 100%, *i e*, they obey the unmodified Becquerel formula Hence we may legitimately infer that a deviation of γ from this value is an indication of the extent to which the electron configuration departs from the inert-gas state The low value of γ in the case of diamond finds a natural explanation on this basis The four electrons in the carbon atom are shared between the neighbouring atom and the electronic configuration is considerably different from that of the inert gas Rock salt and sylvine are usually considered to be typical examples of crystals with ionic binding In that case except for the slight perturbation produced by the crystal field, the sodium and chlorine ions in rock salt have the inert-gas structure and hence should have a value for γ approximating to 100% Actually, as we see in Table VII the value of γ for these crystals is considerably less. This can only mean

that the alkali and halogen structures in these alkali halides deviate from the inert-gas configuration by a considerable extent It seems possible that the binding between them may be at least partly covalent in nature. This is even clearer in the case of CaF_2 On this view, the fact that the value of γ for ZnS approaches that for an inert-gas configuration is significant It indicates that the binding between Zn and S is much nearer being an electro-valent than of a covalent nature, in spite of the geometrical structure of the crystal being similar to that of diamond Incidentally it may be remarked that in agreement with this view, ZnS is a strongly piezo-electric crystal.

In conclusion the author wishes to record his deep sense of gratitude to Professor Sir C V Raman, for his helpful interest and encouragement in this work

7 Summary

With three thin cleavage plates and a natural crystal of diamond, all of which had an almost negligible birefringence, the magnitude of the Faraday rotation was measured for a series of different wavelengths in the visible spectrum The magnetic rotation was proportional to the dispersion and the Verdet's constant for the wavelengths 5890 Å and 5460 Å were 0 0233 and 0 0278 minutes per cm per gauss respectively The magnetic rotation followed the modified Becquerel formula with the multiplying factor γ, which remains sensibly constant in the visible region, equal to 28% The value of this constant is much less than that for most carbon compounds available as liquids for which it is known The magneto-optic constants for sphalerite (ZnS) were also determined and it was found that γ, in this case, was 91% The significance of these results is discussed

References

Becquerel, H . *Annales de Phys et Chem*, 1877, **12**, 32
Cotton, A, Dupuy, G, and Scherer, M *Comptes Rendus*, 1932, **194**, 405
Darwin, C G, and Watson *Proc Roy Soc*, London, (A), 1927, **114**, 474
Maria Meli *Zeit fur Phys*, 1923, **16**, 244
Peter, F *Ibid*, 1923, **15**, 358
Raman, C. V, and Rendall, G R *Proc Ind Acad Sci*, 1944, **19A**, 265
Schutz *Handbuch der Experimental Physik*, 1936, **Band 16**, *Teil*, **1**, 49
Van Vleck *The Theory of Electric and Magnetic Susceptibility*, Oxford, 1932, 367

THE CLEAVAGE PROPERTIES OF DIAMOND

By S Ramaseshan

(From the Department of Physics, Indian Institute of Science, Bangalore)

Received June 5, 1946

(Communicated by Sir C V. Raman, Kt, F R S, N L)

1 Introduction

The easy and perfect cleavage of diamond along the (111) plane has long been known to the Indian lapidaries Cleavage plates of large area polished and slightly facetted at the edges were extensively used in jewellery, but this form of adornment has in recent years gone out of fashion In consequence, such plates can be purchased from the jewellers in the larger cities of India Sir C V Raman has in his collection several of these plates and they have proved extremely useful in the study of the different properties of diamond During his investigation of the X-ray topographs of diamond, Mr G N Ramachandran examined this material and found that three out of the fifty plates studied had a (211) cleavage Sutton (1928) in his book on the South African diamonds remarks that while the (111) cleavage is most common, the (110) is also occasionally found

In view of the facts stated above, it appeared desirable to undertake a systematic investigation of the cleavage properties of diamond A calculation of the cleavage energy of various planes in diamond indicated the possibility of numerous other cleavages besides those mentioned above. A careful goniometric study of 15 crystal fragments in Sir C V Raman's collection was accordingly made which resulted in a striking confirmation of this idea The paper records the results of these studies

2 The Nature of Cleavage

"Cleavage is not merely a tendency to fracture with the production of two more or less plane fracture surfaces along an approximately definite direction It is the facility for splitting along an absolutely *true* plane having an orientation within the crystal definitely fixed within one or two minutes of arc" (Tutton) The (111) cleavage of diamond is a striking example of the above definition Many writers (1932) have tried to give an explanation for the presence of the (111) cleavage. One set of authors attribute the perfection of the cleavage to the fact that the spacing is a maximum for the (111) planes, while others suggest that it is because the surface energy

is minimum for the (111) plane A calculation of the surface energies of different planes shows that this is indeed the case, but this energy is not greatly different from that for the other nearby planes Bearing in mind the fact that in the crude method used for cleaving diamonds the energies employed may be much in excess of what is required to effect cleavage in any direction, one would expect to have a fracture rather than a perfect cleavage From these facts it would seem that considerations of surface energy alone are not sufficient to explain the "atomic accuracy" of the (111) cleavage

An inspection of the diamond model shows that the (111) planes are not equally spaced, the ratio of the distances between alternate planes being 1 3 It is also found that the number of bonds cut per unit area depends on the place at which the two parts of the crystal are separated If cleavage is effected between the two octahedral layers which are farther apart, then one bond per atom will have to be cut On the other hand, if diamond is cleaved between the octahedral layers that are closer together, three bonds per atom will have to be ruptured It is, therefore, obvious that a cleavage in the former position requires only a third as much energy as for one in the latter position If, therefore, a cleavage starts parallel to the (111) plane between two layers which are farther apart, it will continue in the same plane since any slight deviation in the direction would involve a threefold increase in energy This sudden increase in energy which accompanies any deviations appears to be responsible for maintaining the (111) cleavage along a true geometric plane

3 The Calculation of the Energy of Cleavage

It is reasonable to assume that the energy required to cleave a diamond along a particular plane is equal to that required to rupture the bonds connecting atoms situated on either side of the plane The number of bonds cut per unit area thus gives a measure of the energy of cleavage for a particular plane Harkins (1942) has used this idea to calculate the surface energy of the (111) and (100) planes Since two surfaces are formed by cleavage, the surface energy should be equal to half the cleavage energy In this section we shall calculate the cleavage energy of a few planes in diamond

In the case of simpler planes such as (100), (111) and (110), the calculations can be made in a very simple manner In Fig 1 *a*, the area bounded by dotted lines represents the repetitive unit cell in the (100) plane which is a square whose side is $d = 3 \cdot 56$ Å, the length of the unit cubic cell in the diamond lattice There are two atoms per unit cell (one at the corner and one at the centre) so that the number of atoms per unit area is $2/d^2$. As

two bonds connect each atom with the atoms in the neighbouring plane, the number of bonds ruptured per unit area is $n_{100} = 4/d^2$

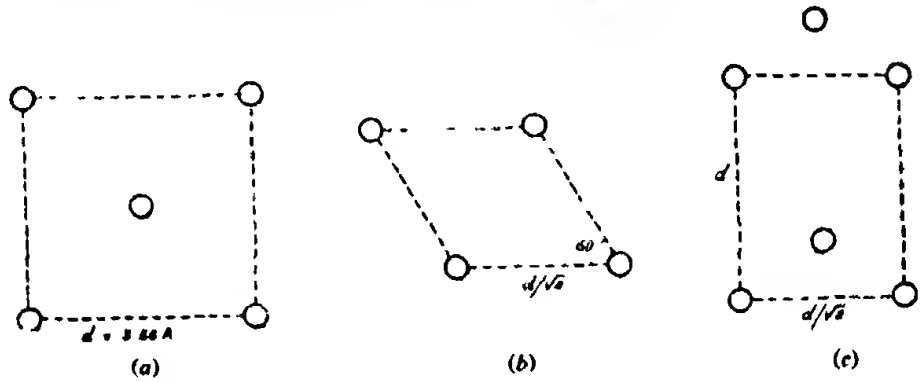

FIG 1

For the (111) plane the unit cell is a rhombus of side $d/\sqrt{2}$ and angle 60° which is shown in Fig 1 *b* There is only one atom per unit cell whose area is $d^2\sqrt{3}/4$ One bond connects each atom with an atom in the upper layer, while three connect it with atoms in the lower layer The number of bonds cut per unit area n_{111} is therefore, $4/d^2\sqrt{3}$ or $4\sqrt{3}/d^2$ according as the cleavage is above or below the plane under consideration

The unit cell in the case of (110) is shown in Fig. 1 *c* It is a rectangle of sides d and $d/\sqrt{2}$ containing two atoms Since each atom in this plane

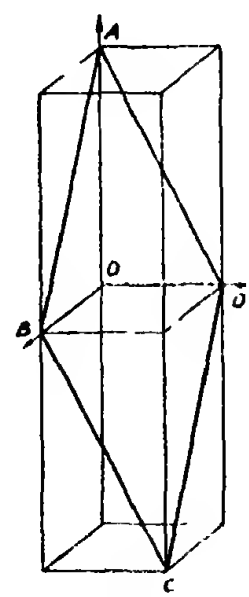

FIG 2

is connected by one bond to an atom in the neighbouring plane, the number of bonds cut per unit area n_{110} is $2\sqrt{2}/d^2$

For more complicated planes the following general analytical method is adopted Considering the (hkl) plane, let H, K and L be the corresponding indices in the Weiss notation (*i e*, H, K and L are the smallest integral intercepts made by the plane on the co-ordinate axes) In Fig 2 the unit cell in the (hkl) plane is represented by the parallelogram ABCD the area of which can be calculated from the condition OB $= Hd$, OD $= Kd$, and OA $= Ld$ The equation to this plane is

$$hx + ky + lz - p = 0$$

where $p = hH = kK = lL$ If the co-ordinates of an atom are substituted in the expression on the left hand side, the sign of the quantity obtained indicates the position of the atom with respect to the plane The atom lies on the same or the opposite side of the plane as the origin according as the sign is negative or positive Having thus found out the position of all the atoms in the diamond structure with respect to the plane (hkl), the number of bonds which connect atoms on opposite sides of the plane can be counted A difficulty arises when an atom lies on a plane In this case the plane of separation is slightly shifted away from or towards the origin and the number of bonds cut is counted in either case The two may either be equal or different If different the lower value is taken to calculate the cleavage energy As an example we shall take the (221) plane Here OB $= d$, OD $= d$ and OA $= 2d$ and the area of the cell is $3d^2$ It is found that the number of bonds cut per unit cell is 8 or 12 according as the cleavage takes place in the positive or the negative side of the plane ABCD Consequently $n_{221} = 8/3d^2$ Similar calculations have been made for other planes

The energy required to rupture a C—C bond has been calculated from thermo-chemical consideration to be $6\ 22 \times 10^{-12}$ ergs (Harkins, *loc cit*) Accepting this value the cleavage energy of various planes have been determined. The results are tabulated in Table I with the planes arranged in order of increasing energy It is found that the number of bonds cut per unit area can be given by the expression

$$\frac{4}{\ } \quad h$$

where h is the largest of the three indices.

A study of Table I shows that the energy of the (111) plane is the least and is an absolute minimum. The (111) plane must, therefore, be a plane

of easy cleavage The energy of the (100) plane is the largest and is about 80% higher than that for the (111) planes and the other planes have energies intermediate between these As has been mentioned above, the (110) and the (112) cleavages have been observed in diamond Table I shows that there are planes having energies less than these, and it is quite probable that

TABLE I

Plane	Angle between plane and the (111) plane	Expression for No of bonds cut per (3 56 Å)^2	$\frac{h}{\sqrt{h^2+k^2+l^2}}$	Cleavage energy in ergs per cm^2
111	0°	$4/\sqrt{3}$	$1/\sqrt{3}$	11330
332	10° 0′	$12/\sqrt{22}$	$3/\sqrt{22}$	12580
221	15° 48′	8/3	2/3	13080
331	22° 0′	$12/\sqrt{19}$	$3/\sqrt{19}$	13510
110	35° 16′	$4/\sqrt{2}$	$1/\sqrt{2}$	13880
322	11° 24′	$12/\sqrt{17}$	$3/\sqrt{17}$	14290
321	22° 12′	$12/\sqrt{14}$	$3/\sqrt{14}$	15730
211	19° 28′	$8/\sqrt{6}$	$2/\sqrt{6}$	16030
320	36° 48′	$12/\sqrt{13}$	$3/\sqrt{13}$	16330
210	39° 14′	$8/\sqrt{5}$	$2/\sqrt{5}$	17560
311	29° 30′	$12/\sqrt{11}$	$3/\sqrt{11}$	17750
100	54° 44′	4	1	19630

cleavages parallel to these might also occur under proper conditions One should expect the relative abundance of the cleavage planes to follow the order listed in Table I (111) being most frequent and (100) being almost absent From the general expression for the cleavage energy given above, it can be shown that the cleavage energy diminishes as the plane is tilted progressively towards a (111) plane. Consequently, curved cleavages or fractures could also be expected to occur in diamond If these curved fractures attain directions near about an octahedral plane, they might actually coincide with it and become plane cleavages

4 METHODS OF STUDY

To verify the deductions from theory, a systematic study of 15 fragments of diamond in Sir C V Raman's collection was made A visual examination with a pocket lens of these fragments revealed that most of them contained the usual (111) cleavages, but 9 of them appeared to have cleavages

other than the (111) Each of these nine was used for careful goniometric study, and it was found that while four crystals had planes other than the octahedral, the rest had very interesting fractures which were irregular and more or less curved A Mier's student goniometer with a collimator and telescope attachment capable of reading upto 1 minute of arc was used The crystal was attached to the instrument with soft wax and all adjustments of the crystal were made by hand The angles between the cleavage faces were measured with an accuracy not greater than 15 minutes of arc, but these were quite sufficient to identify the different planes The octahedral cleavages were very easy to recognise from the perfection and splendent lusture they exhibited While these planes gave extremely sharp signals in the telescope, the other planes did not give such sharp ones Only the angles between those surfaces which gave good signals were measured Care was always taken to see that curved surfaces were not used for observation When a low-power microscope was focussed on the diamond and the milled head of the goniometer rotated, reflections from the plane faces flashed into the microscope and they did not remain in the field of view for a rotation of more than 15 minutes of arc In the case of curved planes or faces, the reflection remained in the field of view even when the head was rotated through 2° It must also be mentioned that reflections from curved faces were extremely feeble and diffuse when observed with a telescope and could easily be distinguished from the reflection from plane faces

5 Observational Data

N C 42 had three large cleavage faces which were octahedral Two of these were absolutely plane The third showed the existence of two or three other cleavage faces. They lay in the [110] zone and measurement showed that two of them were (221) faces The third which gave a feeble but sharp signal was near about the (332) There were also some curved fracture faces on the surfaces of the crystal

N C 59 was a crystal fragment with a large number of cleavage faces on its surface The specimen is one of the collection of diamonds presented to Sir C V Raman by the De Beers Corporation of Kimberley In one of the [110] zones the following planes were identified 4 beautiful (111) planes, one (331), one (110), one (322) and one (211) In another perpendicular zone, two (111), one (221) one (331), one (110) and one (322) were found. Although all the planes were quite small, the signals obtained from (111), (221), (110) and (322) were extremely sharp One octahedral face which appeared to be very drusy was found on examination, to consist of hundreds of tiny (111) planes. In a third zone, one (111) and a tiny (322)

plane were found There were also some curved faces on the diamond, and some of the curved faces ended as tiny flat (111) cleavage faces

N C 45 was a natural crystal which had been broken on one side Three large prominent cleavage planes are visible on its surface Two of them were (111) and the third a (110) plane There was also another tiny (110) plane on the crystal The large (110) surface had large striations, which mainly consisted of fine (221) planes arranged in a step-like order

N C 174 was a thick flat polished plate with a few cleavage faces on the girdle Four of these were octahedral cleavages One (331), one (110), one (221) and a tiny (332) were also found The angles between the two large faces of the plate and the planes of known indices in the girdle were measured and it was found that the flat face was approximately a (431) plane In view of the fact that the surface is polished and the plate is quite thick, it is impossible to say whether the two flat faces are cleavage planes or not The other crystals examined had the (111) cleavage and also irregular and curved fractures N C 194 was a rectangular cleavage plate, all its six faces being perfect octahedral cleavages N C 49 had a large octahedral cleavage followed by a curved face with fine striations N C 39 was a yellowish crystal with two (111) faces and a fracture containing a large number of tiny octahedral faces N C 32 was a black diamond with two large (111) faces and with several tiny curved faces N C 50 had a good many cleavage faces and many of them were curved

Table II gives the collection of the results obtained The numbers in the vertical columns indicate the number of independent planes of a specific

TABLE II

Diamond Planes	N C 42	N C 59	N C 45	N C 174	N C 49	N C 39	N C. 32	N C 50	N.C 194
111	3/	6/	1/ 1t	4/	2/	3/	2/	3/	6/
332	1t			1t					
221	1s	2m	1s	1s					
331		2s		1s					
110		2m	1/ 1t						
322		3s							
211		2s							

index on a particular diamond All the planes which gave a common signal at a particular setting have been taken together and counted as one The letters accompanying each number indicate the size of the planes *l* (large) signifies planes having an area greater than two sq mm., *m* (medium) those with areas between one and two sq mm , *s* (small) those with areas between a half and one sq mm , while *t* (tiny) those with areas less than half a sq. mm

Table II can in no way be said to represent the relative abundance of different cleavages, as the number of cases examined has been too few. Even so, an idea of the relative frequencies of different planes can be obtained from the table The planes have been arranged in order of increasing energy and one could see that the lesser the energy of a plane the more frequent is its occurrence It may be mentioned here that amongst the planes of cleavage listed above, (111), (221), (331) and (322) belong to the category in which the distance between alternate layers of atoms are not equal

In conclusion, the author wishes to express his thanks to Sir C V Raman for his encouragement and interest in this investigation

Summary

Calculations of the cleavage energies of various planes in diamond indicated the presence of cleavages other than those already known A careful goniometric study of several crystal fragments in Sir C V Raman's collection revealed numerous other cleavages The presence of the following cleavage has been definitely established (111), (221), (110), (322), (331), (211) and (332) The (111) cleavage was found to be by far the most perfect and most abundant, while (221) and (110) cleavages were not uncommon It is suggested that the perfection of the (111) cleavage is not merely because that plane has the minimum cleavage energy but also due to the fact that on either side of the plane of easy cleavage lie layers of atoms having three times the cleavage energy. It was also found that diamond definitely has curved fractures and the theory developed in the earlier part of the paper accounts for the existence of these.

References

Harkins, W D — *Jour Chem Phys.*, 1942, **10**, 268

Sulton, J R. — *Diamond*, Van Nostrand, 1928, 16

Tutton, A E H. — *Crystallography and Practical Crystal Measurement*, MacMillan, 1922, **1**, 527

Wooster, N — *Science Progress*, 1932, **103**, 462.

A THEORY OF THE CRYSTAL FORMS OF DIAMOND

By S Ramaseshan

(From the Department of Physics, Indian Institute of Science, Bangalore)

Received for publication June 20, 1946

(Communicated by Sir C V Raman, Kt., F R S., N L.)

1 Introduction

The number of different kinds of planes permitted by the law of rational indices to appear as faces on a crystal is practically unlimited. The number of "forms" actually observed, however, is limited and there is a decided preference for a few amongst them This is one of the most striking facts of geometric crystallography and its explanation is obviously of importance Pierre Curie (1885) stressed the role played by the surface energy of the faces in determining the "forms" of the crystal According to him, the different faces of a crystal have different surface energies and the form of the crystal as a whole is determined by the condition that the total surface energy of the crystal should be a minimum According to W Gibbs (1877), on the other hand, it is the velocity of growth in different directions which is the determining factor, while the surface energy of the crystal plays a subordinate role and is only effective in the case of crystals of submicroscopic size

We have little direct knowledge as to how diamond is actually formed in nature It is necessary, therefore, to rely upon the indications furnished by the observed forms of the crystals One of the most remarkable facts about diamond is the curvature of the faces which is a very common and strongly marked feature. This is particularly noticeable in the case of the diamonds found in the State of Panna in Central India. Writing after a visit during which he had the opportunity of examining several hundreds of specimens, Sir C V. Raman (1942) drew attention to the remarkable beauty of the Panna crystals with their exquisitely perfect geometric forms, their smooth lustrous surfaces and the sharpness of the edges which divide the curved faces into distinct sections. Basing himself on the characters exhibited by the Panna diamonds, he outlined a theory of the crystal forms of diamond which may be usefully quoted here *in extenso*

"I wish to put forward tentatively a suggestion which seems to me to offer a reasonable interpretation of the facts stated above If carbon liquefied under suitable conditions of temperature and pressure when surrounded by molten silicious material, the form of the drops of the liquid diamond

would be determined by the interfacial tension and would be spherical, provided the valence bonds between the atoms of carbon in the liquid were oriented completely at random If, however, some measure of regularity in the orientation of the valence bonds could be assumed, the conditions within the liquid would roughly approximate to those in the solid crystal, in other words, *diamond in the molten state would be a liquid crystal* The interfacial tension would then vary with direction and the surfaces of minimum energy would not be spherical but would tend to show some resemblance to the forms exhibited by a cubic crystal If the shapes assumed by diamond in the liquid crystalline state persisted on solidification or else suffered only minor changes, we would have an explanation of the forms now observed "

The ideas expressed in the foregoing quotation have been made use of in the introductory paper of this symposium (Raman and Ramaseshan,

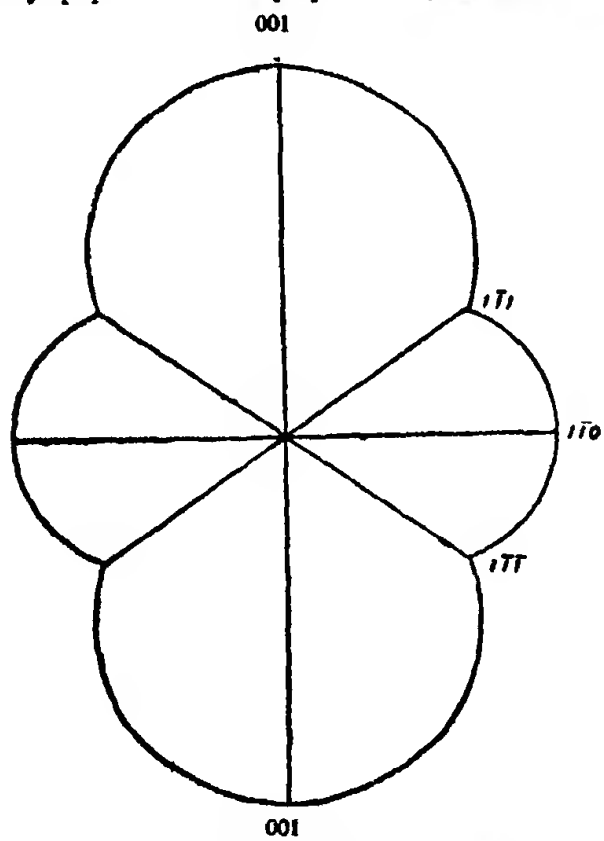

FIG 1 Surface Energies in the [110] zone

1946) in connection with the scheme of classification of the crystal forms of diamond adopted in that paper. In the present paper, the same ideas are

developed further and given a semi-quantitative form For this purpose, the calculation of the surface energy of the various crystallographic planes in diamond made by the present writer for a different purpose (Ramaseshan, 1946) are utilised The theory succeeds in explaining some of the principal facts which emerge from a study of the crystal forms

2 Surface Energies of the Crystal Planes

The surface energy of the different crystallographic planes in diamond is very large, being at least ten times as great as the surface tension of mercury at ordinary temperatures Hence, the surface tension may be expected to play a notable part in shaping the crystals of diamond under the conditions of their formation For a proper approach to the subject, it is necessary to evaluate the surface energy for numerous planes lying in different zones This has been already done by the present author in the paper on the cleavage properties of diamond appearing in the present symposium (Ramaseshan, 1946), and we may use the results here, taking the surface energy per unit area to be half the energy of cleavage In Figs 1 2 and 3 the surface energies of the various crystallographic planes in the [110], [100] and [111] zones have been represented in the form of polar diagrams.

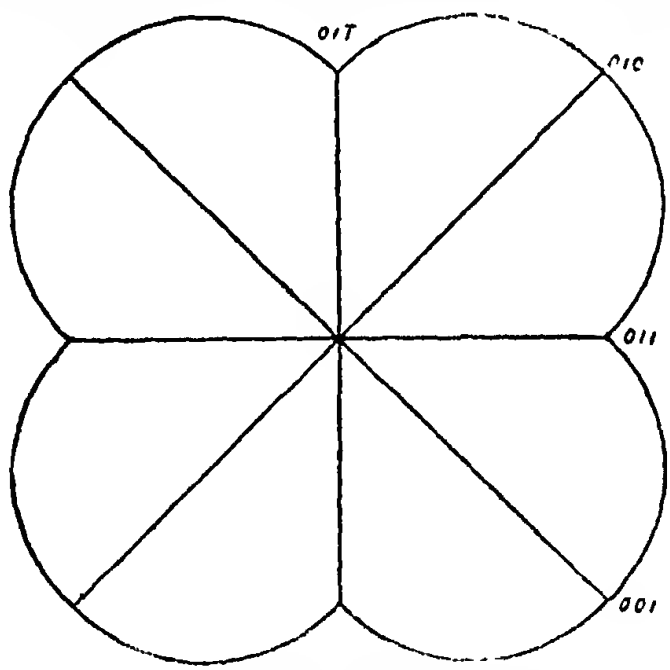

Fig 2 Surface Energies in the [100] zone

The following points emerge from a scrutiny of the figures The surface energy is an absolute minimum for the (111) planes, and an absolute maximum

for the (100) planes; in the [110] zone the surface energy is a minimum for the (111) planes and a maximum for the (100) planes, while there is an intermediate maximum for the (110) planes; in the [100] zone, the surface energy is a minimum for the (110) planes and a maximum for the (100) planes, in the [111] zone, the surface energy is a minimum for the (110) planes and a maximum for the (211) planes The situation thus described enables us at least qualitatively to understand the following empirically known facts·

(1) The plane faces which have been noticed to occur in diamond either by themselves or in combination with curved forms are, in the great majority of cases, if not in all, the (111) planes

(2) Curved forms *approximately* parallel to either to the (111) or the (110) planes are a common feature in diamond

(3) Curved forms parallel to the (100) planes are rarely, if ever, observed

(4) Many diamonds exhibit forms which may be *approximately* described as a combination of the (111) and (110) forms, these however exhibiting a marked curvature

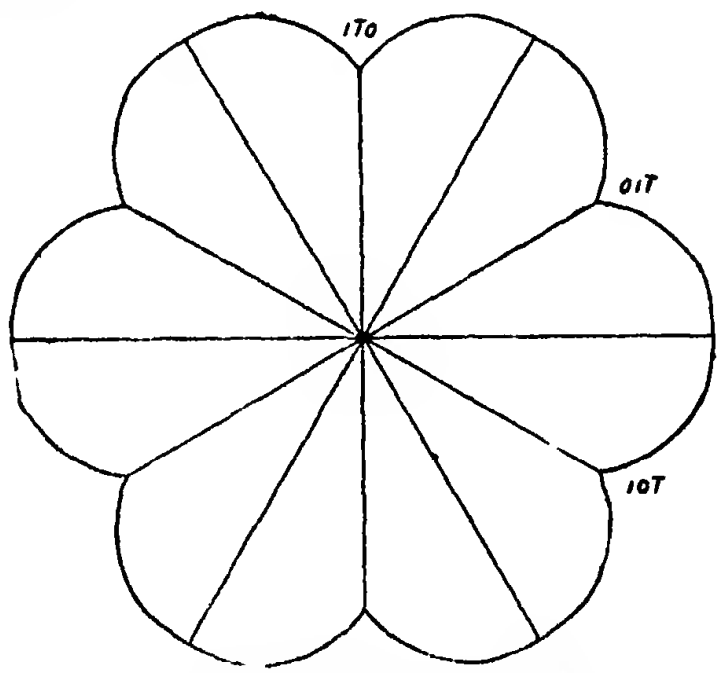

FIG 3 Surface Energies in the [111] zone

3 THE AGGREGATE SURFACE ENERGY

According to P Curie (*loc cit*), it is the total surface energy of the crystal that plays the determining role in respect of the forms assumed by

it. In the case of diamond, this would have to be found by integration over the curved areas and by addition of the surface energies of the plane areas (if any) appearing in combination with them. It is not without interest, however, to consider the purely hypothetical cases of the various regular forms, bounded by plane faces all of the same kind and to evaluate the surface energy of each of these It then becomes evident that forms which present faces with a relatively small surface energy may nevertheless have greater aggregate energies by reason of their presenting a larger area for the same volume

TABLE I

I	II	III	IV	V
Plane	Surface energy per unit area	Description	$\frac{\text{Area}}{(\text{Volume})^{2/3}}$	Product of II and IV
111	5665	Octahedron	5 718	32390
		Tetrahedron	7·204	40810
221	6545	Tris octahedron	5 26	34430
		Tris-tetrahedron	5 793	37910
110	6945	Dodecahedron	5 346	37130
321	7570	Hexakis octahedron	5 009	39430
		Hexakis tetrahedron	5 395	42460
210	8780	Tetrakis hexahedron	5 119	44940
100	9815	Cube	6	58890

The figures set out in Table I furnish us with some useful pointers If, for instance, we were concerned with forms of diamond exhibiting full octahedral symmetry, the simple octahedron with eight faces would be a more probable form than the others having that symmetry but exhibiting 24 or 48 faces On the other hand, if we are concerned with diamond having a tetrahedral symmetry of structure, its appearance in the forms specifically exhibiting that symmetry is not favoured In particular, the appearance of the form of the simple tetrahedron would be much less probable than that of the rhombic dodecahedron which is common to both the tetrahedral and octahedral symmetry classes It is also noticed that the appearance of the other forms common to the two symmetry classes, *viz*, the tetrakis-hexahedron and the cube, is much less probable than that of the dodecahedron. Similar considerations may also be applied to find the likelihood of appearance of various interpenetration forms. It is readily shown, for instance, that the Haidinger diamond or one similar thereto would have a surface energy for any given volume only slightly greater than that of a simple octahedron and hence that its appearance would be favoured,

4 Relation of Curvature to Surface Energy

A liquid drop composed of isotropic material would naturally assume the shape of a sphere Whether a liquid with anisotropic structure would show a similar behaviour depends on whether its surface energy is independent of orientation or not In the particular case of molten carbon, it would seem that a variation of surface energy with orientation is very probable and hence the liquid would tend to take up a configuration different from that of a sphere There would be clearly two opposing effects; areas having a smaller tension would tend to enlarge at the expense of areas having a greater, thereby diminishing the total energy, while on the other hand, the pressure within the drop would cause areas with a smaller tension to become more strongly curved, thereby diminishing their extent What the resulting configuration would be is a problem—and not a simple one—in the calculus of variations

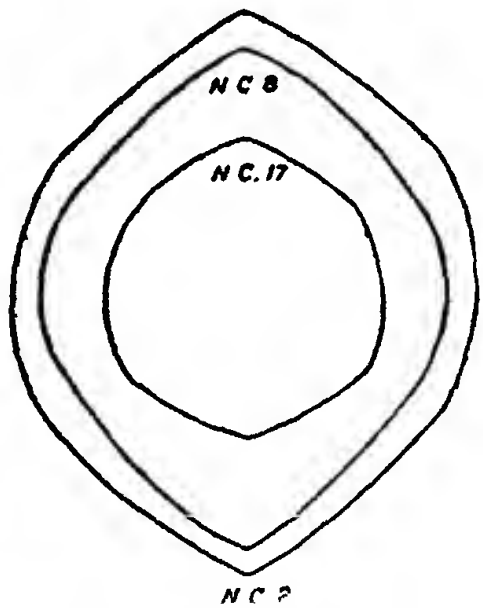

Fig 4 Form of N C 2, N C 8 and N C 17 in the [110] zone

For our present purpose, it is sufficient to draw attention to the obvious correlations which exist between the surface energy diagrams reproduced as Figs 1, 2 and 3 above with the observed forms of diamond in the respective zones. For this purpose, the outlines of three diamonds in the collection, N C 2, N C 8 and N C 17 of progressively diminishing size and having a fairly symmetrical shape have been photographically recorded for these zones. The outlines have been reproduced inside each other in Figs 4, 5 6 respectively in the same zones

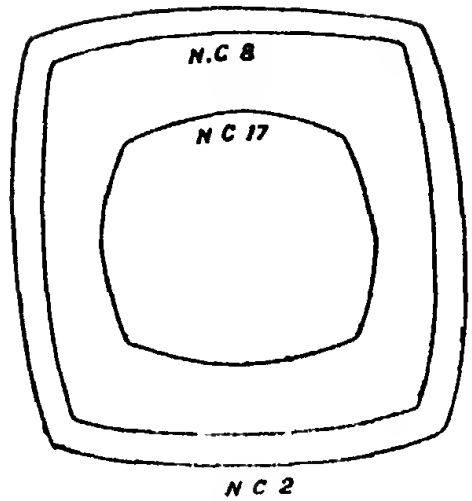

FIG 5. Form of N C 2, N C 8 and N C 17 in the [100] zone

Comparisons of Fig 4 with Fig 1, Fig 5 with Fig 2 and Fig 6 with Fig 3 are instructive In each case, the following features are noticed The smaller the diamond, the more marked is the curvature of its faces At the same time, the outlines of the form for the diamonds of different sizes tend to run parallel to each other The areas in the vicinity of the triad axis in the [110] zone are the flattest, while in the vicinity of the dyad axes, the surfaces present sharp edges; in the (110) directions, there is a marked curvature

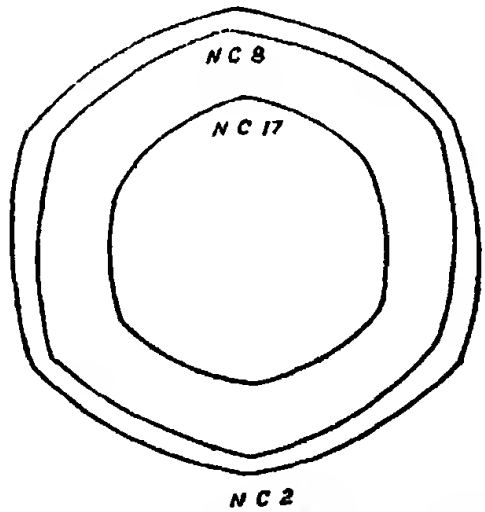

FIG. 6. Form of N C. 2, N.C 8 and N.C 17 in the [111] zone

In the [100] zone, the surface exhibits a relatively small curvature in the (110) directions and others adjacent to it, while in the (100) direction, the surface presents sharp edges In the [111] zone, the curvature is throughout very marked, but there are distinct kinks in the (112) directions, *viz*, those normal to which the surface tension is greatest in that zone

In conclusion the author wishes to thank Sir C V Raman for his kind interest and useful discussions

5 Summary

The calculations of the energies of different crystallographic planes of diamond made in another paper by the author have been utilised to give a semi-quantitative form to the theory of crystal shapes of diamond According to this theory (due to Sir C V Raman), diamond is formed by carbon liquified under pressure which retains the shape of the liquid drops with only minor modifications during solidification Accordingly, the shape of the crystal is controlled by the varying surface tension of the molten liquid in different directions due to the non-random orientation of the valence bonds between the carbon atoms contained in it It is found possible on this basis to explain various characteristic features of the crystallography of diamond, including especially the preference for certain forms, the influence of the size of the diamond on its shape, and the varying curvature in different zones of the crystal

References

Curie P — 'Oeuvres,' *Gauthier Villars*, 1908, 153
Gibbs, W — "Collected Works," Longmans, 1928, 1, 371
Raman, C V — *Current Science*, 1942, 11, 262
——— and Ramaseshan, S — *Proc Ind Acad Sci*, 1946, 24 A, 1
Ramaseshan, S — *Ibid*, 1946, 24 A, 114

VARIATIONS IN THE ABSORPTION OF INFRA-RED RADIATION BY DIAMOND

By K G Ramanathan

(From the Department of Physics, Indian Institute of Science, Bangalore)

Received May 18, 1946

(Communicated by Sir C V Raman, Kt, F R S, N L)

1 Introduction

The investigation by Reinkober (1911), of the infra-red absorption spectrum of diamond established that diamonds are not all alike with regard to their infra-red absorption He noticed the presence of the three bands at 3 0, 4 1 and 4 8 μ in the absorption spectrum of his diamond but failed to record the intense band at 8 μ previously registered by Angstrom (1892) and Julius (1893) More recently Robertson, Fox and Martin (1934), after a detailed investigation of the infra-red absorption of a large number of diamonds, were led to classify the substance into two types I and II, the type I showing the absorption band round about 8 μ which is absent in type II Recent investigations at this Institute (Raman, *et al*, 1944) of the various other physical properties of diamond, have however shown that they cannot be described as falling into one or the other of two types only, but show a more diversified behaviour It appeared probable therefore that the infra-red absorption of diamond should similarly show a diversified behaviour The present investigation was unde taken to test this idea, and also to obtain quantitative data on the strength of the 8 μ absorption band of diamond for numerous samples It was also desired to obtain quantitative data on the strength of the absorption band between 4 and 5 μ for some specimens and to see whether any variation, if present, was confined to the 8 μ region alone or also to the region between 4 and 5 μ The work was greatly facilitated by the use of the flat polished cleavage plates of diamond of which numerous examples were available in Sir C V Raman's collection The present investigation has shown that the strength of the 8 μ infra-red absorption band varies greatly from diamond to diamond, and that such variations are correlated with the behaviour of the specimen in respect of ultra-violet absorption and luminescence No such variation has, however, been noticed in the region 4-5 μ Another striking result established by the present research is the existence of patterns of infra-red transparency in individual cleavage plates of diamond closely analogous to the patterns of luminescence and of ultraviolet transparency (Raman, *et al.*, 1944) exhibited by them.

2 Experimental Arrangements

As a source of continuous infra-red radiation, an electrically heated globar element has been used. For detecting the radiation, a thermocouple with a receiver 1 5 millimetre square, which was made in this laboratory, was used in combination with a Hartmann and Braun galvanometer having a coil resistance of 5 ohms and sensitivity of 0 8 millimetre deflection on a scale at one metre distance for one microvolt In order to monochromatise the radiation for making measurements of absorption coefficients, two different arrangements (*a*) A Residual-ray apparatus and (*b*) An Infra-Red monochromator, have been used

(*a*) *The Residual Ray Apparatus* —In this arrangement which is useful only for investigating the 8μ region, the residual ray band of crystalline quartz which lies in the wavelength range 7 7–9 5μ is made use of The radiation from the globar source was reflected two times from surfaces of crystalline quartz at nearly 20° incidence The radiation thus partially monochromatised by reflections from quartz, was allowed to pass through a one-millimetre aperture before finally being focussed on the thermocouple The diamond was kept close to the aperture so that the radiation passed through it before falling on the aperture After passing through the aperture and before falling on the thermocouple the radiation was made to pass through a one-centimetre filter of clear, transparent fluorspar crystal which served to cut off the 20μ residual rays from quartz and also to further monochromatise the radiation The radiation finally obtained, occupies a position in the spectrum approximately the same as the 8μ absorption band of diamond

(*b*) *The Infra-Red Monochromator* —This is a rocksalt-prism spectrometer which was recently constructed in this laboratory The two concave spherical aluminized mirrors used in the instrument are of 9 centimetres clear aperture and 25 centimetres focal length The 54° prism of rocksalt also made in this laboratory, has got refracting faces about 5 centimetre square The instrument was used to determine quantitatively the absorption coefficients of a few representative specimens of widely different behaviour in the region 4–5μ and also to check up by an independent method the results obtained with the Residual-ray apparatus Using a wide slit (0 5 millimetre for 4–5 region and 1 5 millimetres for the 8μ region), the monochromator was first adjusted at the peak of either the 4–5μ band or the 8μ band of diamond whichever was to be investigated Then keeping the adjustments fixed, the absorption coefficients were determined for some representative specimens,

For focussing the radiation, wherever not stated, concave (spherical) aluminized mirrors having very high reflectivity for the infra-red were used. The deflections of the galvanometer, which, with both the apparatus, were of the order of a few millimetres could be conveniently measured with a travelling microscope to an accuracy of 0 05 millimetre The procedure for determining the absorption coefficients consisted in noting the deflections of the galvanometer with and without the diamond in the path of the radiation For diamonds which do not show appreciable variations of absorption within their areas, the transmission was taken to be the mean of three or more values obtained through different parts within the area of the specimens. Diamonds showing appreciable variations of transparency within their areas were investigated carefully by moving them before the one millimetre aperture of the Residual-ray apparatus between successive readings and noting the transmission and also the portion of the diamond which covered the aperture during each reading Altogether, thirty-seven cleavage plates of diamond have been examined for their absorption in the 8μ region

Reinkober (1911) has shown that the reflecting power of diamond for reflection from a single surface, is 16% ($r = 0$ 16) of the incident energy, for the entire infra-red region between 1 0 to 18 0μ The theoretical value of the reflecting power calculated from the expression derived on the basis of the electromagnetic theory is also 17% Hence it can be safely assumed that if infra-red radiation in the $4\text{-}5\mu$ or 8μ region is incident on a plate of diamond, 16% of the energy is lost at every reflection taking place from a diamond-air surface in a direction perpendicular to it If the diamond be considered to have a thickness t centimetres and an absorption coefficient k per centimetre, then the transmitted fraction of the incident energy σ is given by

$$\sigma = (1 - r)^2 e^{-kt},$$

considering the effect of two reflections only The quantities σ, r and t being known for a plate of diamond, the coefficient of absorption k per centimetre can be calculated Since the radiation used for the measurements is not strictly monochromatic, but has a varying intensity distribution in itself, k is the mean coefficient of absorption for this band

3 Results

The results obtained with different types of diamond are entered in Table I together with the ultraviolet transmission limits of the diamonds for short photographic exposure, and the nature of luminescence of the diamond. The results entered in the table can be summarised as follows:—

TABLE I

Absorption and Luminescence of Diamonds

New Catalogue Number	Thickness	Infra Red Absorption Coefficient in the 8μ Region	Ultraviolet Transmission Limit for short Photographic Exposures	Colour and Intensity of Luminescence
	mm	per cm	A U	
N C 93	0 56	16 5	2950	Weak Blue
N C 94	0 59	15 1	3030	Do
N C 98	0 47	14 9	—	Do
B_1	1 37	12 0	—	Do
N C 99	0 58	10 7	2900	Do
N C 78	1 39	10 2	3100	Moderate Blue
N C 177	0 82	10 0	—	Do
N C 77	0 97	9 2	3010	Weak Blue
N C 75	0 94	8 6	2950	Do
N C 71	0 79	8 2	2910	Moderate Blue
N C 80	0 89	7 6	-	Do
N C 157	0 59	7 6	—	Weak Blue
N C 176	1 18	7 0	—	Moderate Blue
N C 74	0 66	6 8	—	Weak Blue
N C 92	0 61	6 7	2910	Do
N C 70	2 20	6 5	2950	Intense Blue
N C 179	1 18	6 2	—	Moderate Blue
N C. 79	1 20	5 4	2800	Intense Blue
N C. 73	0 68	5 4	2830	Weak Blue
N C 62	1 50	5 0	2700	Intense Blue
N C 126	0 78	4 4	2270	Faint
N C 127	0 66	4 0	2660	Do
N C 117	0 87	3 3	2680	Do
N C 122	0 74	1 9	2700	Yellow
N C 120	0 78	1 7	2300	Do
N C 124	0 94	1 7	2260	Non fluorescent
N. C 121	0 54	1 5	2260	Strong Yellow
N C 89	1 10	1 3	2260	Non fluorescent
N C 125	0 66	0 6	2300	Do
N C 178	0 85	0 6	2250	Do
N C 174	1 62	0 4	2250	Do
N C 60	1 27	0 2	2250	Do
N C. 123	0 63	≤0	2260	Do

— indicates not investigated

(*a*) The diamonds which absorb most strongly in the region of the 8 μ band are those which show a weak blue fluorescence The infra-red absorption tends to be less for the strongly blue-luminescent diamonds The absorption coefficient exhibits a wide variation ranging between 5 0 per centimetre and 16 5 per centimetre.

(*b*) Diamonds showing a yellow luminescence or a mixed type of luminescence exhibit infra-red absorption coefficients which are much less than those of blue-luminescent diamonds, the values lying between 2 0 per centimetre and 4·0 per centimetre.

(*c*) Non-luminescent diamonds are highly transparent in the 8 μ region, the loss of energy when this radiation passes through a plate being mostly due to reflection

(*d*) Allowing for the effect of varying thickness, it is seen that the ultra-violet transmission limit of a diamond progresses further and further into the ultraviolet as the diamond becomes less and less absorbing in the 8 μ region of the infra-red

In the following Table (II) are reproduced the results of absorption coefficient measurements in the region 4–5 μ together with those obtained for the 8 μ region

TABLE II

Comparison of Infra-Red Absorptions in the 4–5 μ and 8 μ Regions

New Catalogue Number	4–5μ Region	8 μ Region	
	Monochromator	Monochromator	Residual Ray Apparatus
	cm^{-1}	cm^{-1}	cm^{-1}
N C 60	6 8	0 3	0 2
N C 174	7 0	—	0·4
N C. 73 ..	7 7	—	5 4
N C 74	7 6	8 7	6·8
N C 71	7·1	11 0	8 2
N C 77 .	7 0	—	9·2
B_8	6·8	13 0	12·0
N. C 94 .	7 5	—	15 1

— indicates not investigated

In Table II the values in the second column remain constant within the limits of experimental error In columns three and four containing the mean absorption coefficients for the 8μ region measured with the Infra-Red monochromator and the Residual-ray apparatus respectively, the values exhibit a wide range of variation It can be seen that due to the comparative narrowness of the band used with the monochromator, the values given there are higher than those obtained with the Residual-ray apparatus.

4 PATTERNS OF INFRA-RED TRANSPARENCY

Four diamonds out of the thirty-seven cleavage plates examined have been observed to show striking variations in their infra-red transparency within their area. An attempt has been made in Fig. 1 to represent the variations in infra-red transparency for the four diamonds together with their luminescence and ultraviolet transparency patterns The drawings of

infra-red transparency-variation, made from a visual examination of certain regions of the diamond chosen to cover their full area, are reproduced just to show their similarity to the luminescence and ultraviolet transparency patterns and are not to be regarded as an exact representation of the absorption patterns However, methods have been devised in this laboratory to obtain photographically the variations in infra-red transparency of diamonds, but as the details have not yet been fully worked out, it is hoped to investigate the question at some later date

Out of the four diamonds investigated at present, the cleavage plate N C 82 (see Fig 1) shows both blue and yellow luminescence The central

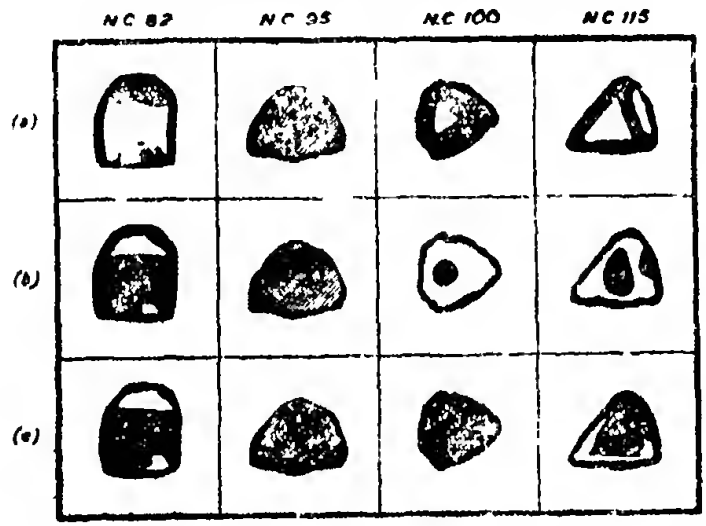

FIG 1

(a) Patterns of Luminescence (b) Patterns of Infra-Red Transparency
(c) Patterns of Ultraviolet Transparency

area of the plate shows a fairly bright blue luminescence covered by bands of yellow luminescence The two extremities of the diamond (top and bottom right-side corner) are non-luminescent and also more transparent to the ultraviolet in the 2536 Å region than the central area The infra-red absorption coefficient is 5 3 per centimetre in the central part and 1 9 per centimetre at the top non-luminescent area and varies between these values at other regions. N C 95 which also shows both blue and the yellow luminescence, has got a gradual variation in the intensity of its luminescence over its area. Observations on infra-red transparency show that the brighter regions in the luminescence photograph correspond to regions more transparent to the infra-red The diamond N C 100 has got a blue luminescent spot in the centre surrounded by non-luminescent area on all sides The

infra-red transmission through the central spot is lower than in the surrounding area, the coefficients of absorption being 10 0 per centimetre and about 7 0 per centimetre for the two regions respectively. Lastly, the diamond N C 115 is again of the mixed type, showing blue and yellow fluorescence. The central triangular area and the narrow strip at one of the sides which are luminescent and opaque to the ultraviolet at 2536 Å are found to be more opaque to the infra-red than the other regions It is thus quite clear that there is a close correlation with luminescence, and one of a different nature with the ultraviolet transparency A non-luminescent area must be carefully distinguished from either a weakly blue-fluorescent area or a weakly yellow-fluorescing area As was shown in Table I, a weakly blue fluorescent diamond is highly opaque in the 8 μ region, while a non-luminescent diamond or one showing weak yellow fluorescence is highly transparent All these features are shown by diamonds showing infra-red transparency patterns, sometimes one and the same diamond showing all the above-mentioned behaviours

I take this opportunity to express my heartfelt gratitude to Sir C V Raman under whose direction the present work was done I am also thankful to Dr R S Krishnan whose kind help was always available to me during the progress of this research

Summary

Using a Residual-ray apparatus, the infra-red absorption coefficients have been measured for 37 cleavage plates of diamond in the 8 μ region. While the absorption coefficients measured with an infra-red monochromator in the region 4-5 μ remain constant within the error of the measurement for all diamonds, those in the 8 μ region show a wide range of variation. The results are correlated with the behaviour of diamond in respect of luminescence and ultraviolet absorption Some cleavage plates of diamond have also been shown to exhibit patterns of infra-red transparency in the 8 μ region, closely analogous to the patterns of ultraviolet transparency and of luminescence.

References

1 Angstrom — Quoted by Reinkober

2 Julius — *Ibid*

3. Raman, *et al* — (Symposium on Structure and Properties of Diamond) *Proc Ind Acad Sci*, 1944, 19A, 189.

4 Reinkober — *Ann der Phys*, 1911, 34, 343

5 Robertson, Fox and Martin — *Phil Trans Roy Soc*, 1934, 232, 482

THE ABSORPTION OF ULTRAVIOLET RADIATION BY DIAMOND

By K G Ramanathan

(From the Department of Physics, Indian Institute of Science, Bangalore)

Received May 18, 1946

(Communicated by Sir C V Raman, Kt, F R S, N L.)

1 Introduction

The early work of Miller (1862) and the later investigation by Peter (1923) showed that while the majority of diamonds completely cut off the ultraviolet radiation below 3000 Å, there were a few which possessed high transparency up to 2250 Å. This finding has been confirmed by Robertson, Fox and Martin (1934) who made extensive investigations on the absorption spectra of both the absorbing and non-absorbing diamonds at different temperatures and discovered several interesting facts On the basis of their work they also classified diamonds into two categories, the absorbing diamonds showing complete cut-off below 3000 Å and the non-absorbing diamonds which possess high transparency up to 2250 Å Whereas the previous workers were of opinion that opacity below 3000 Å sets in because of the presence of impurities, these writers attributed it to the strain which they assumed to be present in such crystals It is however very unlikely that the presence of mechanical strain in any substance can give rise to observable changes in its spectroscopic behaviour Further, it has been shown very clearly by the investigations carried out recently in this laboratory [Raman and Rendall (1944) and Ramachandran (1944)] that it is precisely those diamonds which absorb strongly in the ultraviolet that are free from any mechanical strain and that form the nearest approach to crystal perfection The transparent diamonds on the other hand have been found to possess a readily observable mosaic structure. On the basis of these facts it is clear that the observed difference in absorption spectra can be ascribed neither to the presence of chemical impurities, nor to the presence of mechanical strain, but to basic difference in crystal structure.

The recent work of P G N Nayar (1941,' 42) and Miss Sunanda Bai (1944) on the above subject, carried out in this laboratory, have established that the results are of a more diversified character and cannot be described in terms of two alternatives only, as suggested by earlier observers Working with thin specimens, the thinnest of them being 0 76 millimetre thick,

and by suitably increasing the photographic exposures, Nayar showed that for the so-called ultraviolet opaque diamonds, there was no complete cut-off at 3000 Å and the spectrum could be progressively extended upto 2700 Å. Sunanda Bai found out that for blue-luminescent diamonds the extension of the spectrum transmitted in the ultraviolet depended not only on the thickness of the specimen and the photographic exposures employed but also on the intensity of luminescence For short photographic exposures, the diamonds showing the mixed type of luminescence transmitted up to 2700 Å, but as the exposure time was increased they showed transmission upto 2250 Å, the strength of absorption increasing rapidly as the limit was approached. The spectrum of the transmitted radiation, far from being continuous, is crossed by a number of absorption lines and bands throughout the recorded range Some of these were discovered by Robertson, Fox and Martin, many others by P G N Nayar, while some more were added to the list by Sunanda Bai The behaviour of these lines and bands depended greatly on the strength of luminescence of the diamond Nayar found that the absorption bands in the region 3000 to 3500 Å were strongest in weakly blue-fluorescent diamonds (*i e*, diamonds showing the visible absorption weakly) and *vice versa* On the other hand, in diamonds showing the mixed fluorescence, Sunanda Bai showed that the bands near 2360 Å behaved in just the opposite manner, appearing strong in strongly luminescent diamonds and weak when the visible luminescence was weak.

The fact that even the most highly absorbing diamonds show a definite photoconductivity with a maximum for exciting wavelength at 2300 Å just as for the highly transparent diamonds, suggests that these should also transmit the ultraviolet upto 2250 Å provided that sufficiently thin specimens are used. The present investigation was undertaken (*a*) to investigate the ultraviolet absorption by the thinnest plates of diamond, (*b*) to trace the variation of the absorption coefficient with wavelength in the range 3100 Å to 2570 Å of a typical blue-luminescent diamond and (*c*) to determine the ultraviolet transmission limits of a number of diamonds in order to correlate this property with the behaviour of the diamonds in the infra-red dealt with in another paper appearing elsewhere in the symposium It may at once be stated here that the thinnest diamonds of the so-called ultraviolet opaque type have been found, in this investigation, to exhibit transmission upto 2240 Å which is also the limit for the so-called ultraviolet transparent type Other results which have emerged out of this investigation will be dealt with in the course of the paper.

2 ULTRAVIOLET ABSORPTION SPECTRUM OF THE THINNEST DIAMONDS

One of the two blue-fluorescent specimens which were used for this work, was originally a flat, polished circular cleavage plate of thickness 1 39 millimetres It was made into a wedge of angle 10° 40′ by the firm of Surajmal. The thinnest portion of this wedge was only 0 12 millimetre thick and so could be used for absorption work to take advantage of its thinness The diamond, previous to making into a wedge had been shown to have a mean coefficient of absorption of 10 2 per centimetre in the 8 0 μ region of the infra-red (See paper on variations in the infra-red absorption spectrum of diamond appearing elsewhere in the symposium) It was also absorbing the ultraviolet below 3000 Å very highly so that spectra obtained with even long exposures extended little below 3000 Å The other piece which was used for this work is a rectangular plate N C 62 which is an intensely blue-fluorescent diamond with its thickness diminishing from 1 5 millimetre at the centre to nearly 0 2 millimetre at the edges by steps The edges of the plate are in the form of knife-edges with an angle of about 30° For photographing the absorption spectra through the thinnest portions of a wedge, continuous ultraviolet radiation from a hydrogen discharge tube was first focussed on the diamond attached to the moveable jaw of a slit, the screw cap of which carried a micrometer head The radiation, deviated by the prismatic wedge, was again focussed on the slit of a medium quartz spectrograph so that a focussed image of the wedge was formed in the plane of the slit. By turning the micrometer head, different portions of the diamond could be brought to focus on the slit The spectrograph had to be kept tilted by an angle equal to the deviation caused by the wedge The advantage in having a micrometer head is that absorption spectra can be obtained through different portions of the diamond wedge, beginning from one end and increasing or decreasing the thickness of the absorption path by known amounts.

Results —Transmission spectra obtained with N C 78 through its thinnest portion show clear transmission upto 2240 Å, both at room temperature of the diamond and when it is cooled with liquid air Beyond 2240 Å there is complete cut-off of the radiation All efforts to record the spectrum below 2240 Å with long exposures failed to extend the observable transmission beyond that limit It may be remarked here that the diamond N C 78 previous to being made into a wedge (when it was a cleavage plate of thickness 1·37 millimetres) gave transmission spectrum extending very little below 3000 Å

Transmission spectra obtained with the intensely blue-fluorescent diamond N C 62 through the centre of the plate 1 5 millimetres thick extend

upto 2400 Å only, even with very long exposures The spectra with different times of exposure show, as has been pointed out by Sunanda Bai, a series of step-like falls of intensity at 2900 Å, 2715 Å and 2570 Å, indicating steep rises in the absorption curve Of all these, the one at 2715 is the most prominent one The absorption spectrum of the same diamond (N C 62) obtained through the thinnest portion of the prismatic edge (about 25 mm) shows a transmission upto 2250 Å

3 Ultraviolet Absorption Bands of Diamond

The absorption spectra of the two diamonds N C 78 and N C 62 obtained with the specimens kept at room temperature show very intensely the absorption bands at 2364 Å, 2359 Å, 2310 Å and 2298 Å The former two have been recorded by Sunanda Bai (1944) in the room temperature pictures and all the four in spectra obtained at −180° C In the present investigation, the room temperature pictures of N C 78 in which the conditions were most favourable, have been found to show in addition to the above four bands, two others at 2258 Å and 2246 Å On cooling the diamond with liquid air, the band at 2298 Å undergoes resolution into two lines, a fainter component appearing on the shorter wavelength side The two new diffuse

Table I

Ultraviolet Absorption Bands of Diamond

Robertson, Fox and Martin (1934) λ in Å.U	Sunanda Bai (1944) λ in Å U		Present investigation λ in Å U.	
	29° C	−180° C	27° C	−180° C
		2405 (w)		
		2399 (s)		
		2396 (w)		
		2395 (w)		
		2388 (w)		
2365-2359	2364·5	2359 9 (v s)	2364 (v s)	2369 (v s.)
	2359 5	2356 5 (v s)	2359 (v s)	2355 9 (v s)
		2314 (w)		
2312-2300		2309 − (s)	2312 − (s)	2309 − (s)
		2306	2308	2306
		2300 − (s)	2302 — (s)	2301 − 2295 (s)
		2296	2294	
				2294 (w)
				2271·4 (w)
			2261 — (s)	2260 (w)
			2255	
			2248 − (s)	2252 8 (w)
			2244	2246 5 (w)

(v. s) —very strong , (s)—strong , (w)—weak

bands at 2258 Å and 2246 Å have also been found to undergo resolution, a set of four sharp lines appearing in their place All these features have been recorded for the first time. However, the five absorption bands between 2405 and 2388 Å obtained by Sunanda Bai in diamonds showing the mixed fluorescence could not be recorded in the absorption spectra of N C. 78 The results are entered above in the Table I

4 The Absorption Curve of Blue-Luminescent Diamond

Peter (1923) quantitatively determined the absorption coefficient of the highly transparent variety of diamond in the region beginning from the visible and extending into the ultraviolet upto 2250 Å where complete opacity sets in. The curve reproduced by him shows that the absorption coefficient increases continuously from 0 036 per millimetre at 3130 Å to 1 477 per millimetre at 2260 Å without showing any features Quantitative measurements on the absorption coefficient of the highly absorbing blue-fluorescing diamonds have not been attempted till now

In the present work, for obtaining the variation of the absorption coefficient with wavelength of a typical blue-fluorescing diamond, the specimen N C 78 already referred to was used A number of spectra were photographed in the same plate by giving equal exposures and running the hydrogen discharge tube at constant current The diamond was successively moved by means of the micrometer head through equal distances between successive exposures. The distance through which the diamond is moved between two successive exposures is accurately determinable from the known value of the pitch of the micrometer screw Hence the increment in thickness between successive exposures can also be calculated

If x and $(x+t)$ centimetres are the thicknesses of the diamond in two successive spectra and if I_1 and I_2 are the intensities of transmitted light in the two cases, the incident light being I in the spectral region λ, the absorption coefficient k per centimetre is given by $I_1/I_2 = e^{kt}$

The values of I_1 and I_2 required to determine k, were obtained as follows: Absorption spectra were photographed for different thicknesses on a highly contrasting plate (Ilford process plates were used) together with a series of intensity marks given by the method of varying slit-widths Curves connecting photographic density and logarithm of intensity were drawn for different spectral regions between 2550 Å and 3030 Å The relative intensities of transmission I_1 and I_2 could be then obtained by microphotometering the spectra and reading off the intensities from the calibration curves. Fig. 1 is a graphical reproduction of the absorption spectrum obtained in

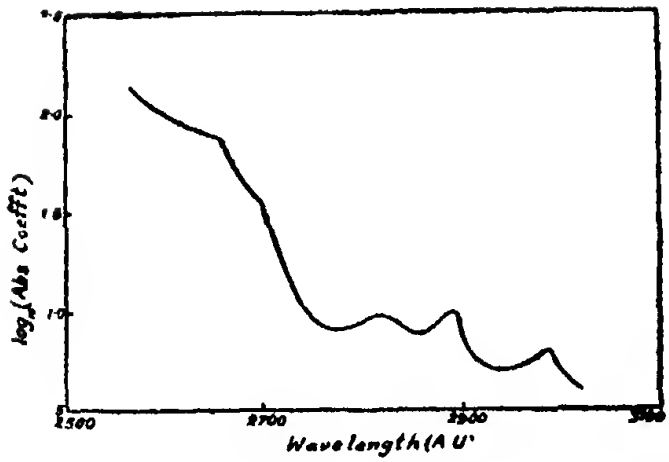

FIG 1

this manner where the logarithm$_{10}$ (Absorption coefficient) is plotted against wavelength It can be seen that corresponding to every step-like fall of intensity in the absorption spectrum, there is a steep rise in the absorption curve

5 Ultraviolet Transmission Limits of Diamonds

The transmission spectra were investigated of the diamonds, whose coefficients of absorption in the infra-red had been determined previously To establish the degree of correlation existing between ultraviolet and infra-red transparency, the spectra of the diamonds were photographed, giving different exposures for the same diamond on the same plate The ultraviolet transmission limits of the diamonds for two or three different exposure times together with the infra-red mean absorption coefficients in the 8 0μ region and their behaviour in respect of luminescence are reproduced in Table II It was stated in the introductory part of this paper that the thickness of a cleavage plate is an important factor in deciding the ultraviolet transmission limit of a diamond This fact was also brought to light in Section 2 of this paper where it was shown that even the most highly absorbing diamond could be made to transmit light upto 2250 Å While looking at Table II, though it shows in a general manner the correlation between mean infra-red coefficient, the ultraviolet transmission limit and luminescence, the thickness factor should always be borne in mind

In conclusion, I wish to record my grateful thanks to Sir C. V Raman under whose inspiring guidance, the present work was done. The diamonds used in this investigation were all from his personal collection,

TABLE II

New Catalogue Number	Thickness	Mean Infra Red Coefficient	Colour and Intensity of Luminescence	Ultra-violet Transmission Limits		
				Very short Exposures	Short Exposures	Long Exposures
	mm.	cm^{-1}		Å	Å	Å
N C 123	0 63	≲0	Non Luminescent	2260	2250	2240
N C 60	1·27	0 2	Do	2260	2250	2250
N. C. 125	0 66	0 6	Do	2300	2250	2240
N C 89	1 10	1 3	Do	2260	2250	2245
N C 121	0·54	1 5	Yellow	2260	2240	2240
N C 120	0 78	1 7	Do	2360	2255	2250
N. C 124	0 94	1 7	Non Luminescent	2260	2250	2250
N C 122	0 74	1 9	Yellow	2700	2270	2250
N C 117	0 87	3 3	Faint	2680	2310	2250
N C 127	0 66	4 0	Do	2660	2300	2260
N C 126	0 78	4 4	Do	2270	2250	2242
N C 62	1 50	5 0	Intense Blue	2700	2450	2380
N. C 62	0·25*	5·0	Do	—	—	2250
N C 73	0 68	5 4	Weak Blue	2830	2650	2400
N C 79	1 20	5 4	Intense Blue	2800	2650	—
N C 70	2 20	6 5	Do	2950	—	2400
N C 92	0 61	6 7	Weak Blue	2910	2740	2580
N. C. 157	0 59	7 6	Do	2870	2730	2650
N C 71	0·79	8 2	Medium Blue	2910	2780	—
N C. 75	0 94	8 6	Weak Blue	2950	2850	—
N C 77	0·97	9 2	Do	3010	2880	—
N C 78	1 39	10·2	Medium Blue	3100	2940	—
N C 78	0 12*	10 2	Do	—	2240	2240
N C. 99	0·58	10·7	Weak Blue	2900	2780	—
N C 94	0 59	15·1	Do	3030	2830	—
N C 93	0 56	16 5	Do	2950	2810	—

*—Approximate thickness — —Transmission limit not determined

SUMMARY

The thinnest diamonds of the so-called ultraviolet opaque type have been shown to exhibit transmission upto 2240 Å which is also the limit for the so-called ultraviolet transparent type In a diamond showing blue luminescence, five new absorption bands have been discovered for the first time in the region below 2300 Å The variation of absorption coefficient with wavelength for a typical blue-luminescent diamond has been determined for the first time in the region 3030 Å-2570 Å Finally, the ultraviolet transmission limits for a number of diamonds have been obtained for different photographic exposures and the data correlated with their luminescence and mean infra-red absorption coefficient in the 8 μ region.

References

1	Miller	(Quoted by Robertson, Fox and Martin)
2.	Nayar, P G N	*Proc Ind Acad. Sci*, 1941, **14A**, 1
3	———	*Ibid*, 1942, **15**, 293
4	Peter	*Z f Physik*, 1923, **15**, 358
5	Ramachandran, G N	*Proc Ind Acad Sci*, 1944, **19**, 304
6.	Raman, C V, and Rendall, G R.	*Ibid*, 1944, **19**, 265
7	Robertson, Fox and Martin	*Phil Trans Roy Soc*, 1934, **232A**, 482
8	Sunanda Bal, K	*Proc Ind Acad Sci*, 1944, **19A**, 253.

Description of Plates

Plate XI

Fig. 1 Ultraviolet Transmission Limits of Blue-Fluorescent Diamond (N C 78) for different thicknesses (*a*) 0 15 mm (*b*) 0 30 mm. and (*c*) 0 37 mm

Fig 2 Ultraviolet Transmission Limits of Strongly Blue-Fluorescent Diamond (N C 62) for (*a*) Very short photographic exposure, (*b*) Short photographic exposure, (*c*) Long photographic exposure and (*d*) Small absorption path 0 25 mm.

Plate XII

Fig 3. Micro-photometric curve of the Ultraviolet Absorption Spectrum of Blue-Fluorescent Diamond (N C. 78) at Liquid Air Temperature.

Fig 4 Ultraviolet Absorption Spectrum of Thin Blue-Fluorescent Diamond (N C 78) (*a*) At Room Temperature, (*b*) At Liquid Air Temperature

Fig 5 Ultraviolet Absorption Spectrum of (*a*) Green-Fluorescent Diamond N C 151 and (*b*) Non-Fluorescent Diamond N C 126

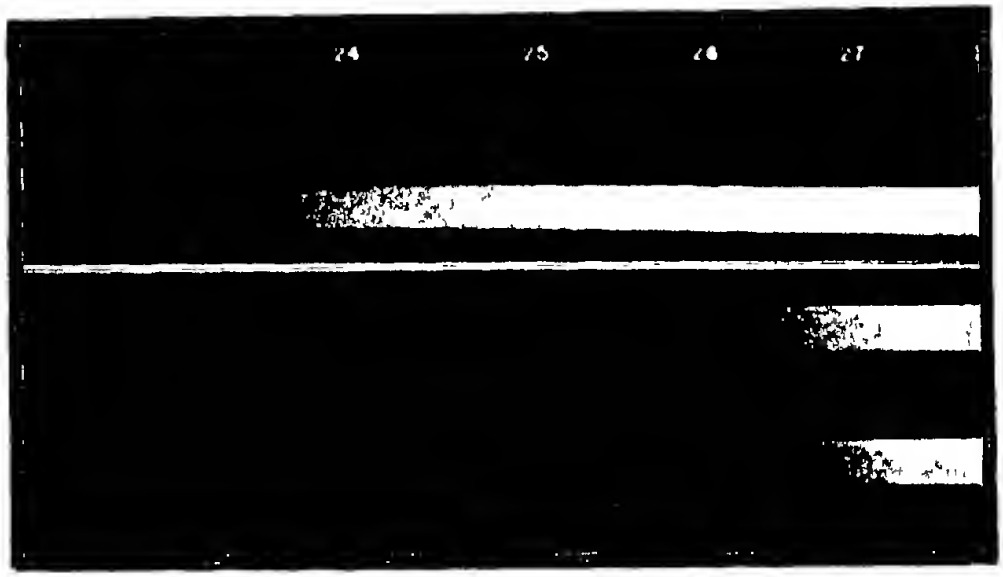

Fig. 1

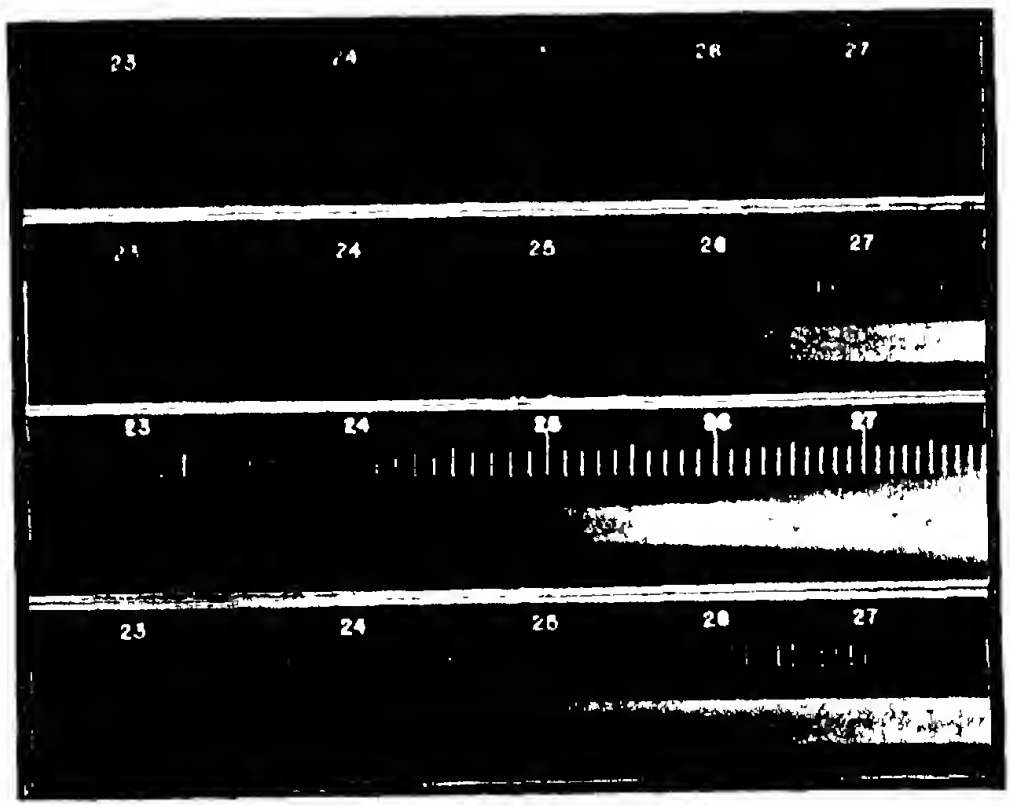

Fig. 2

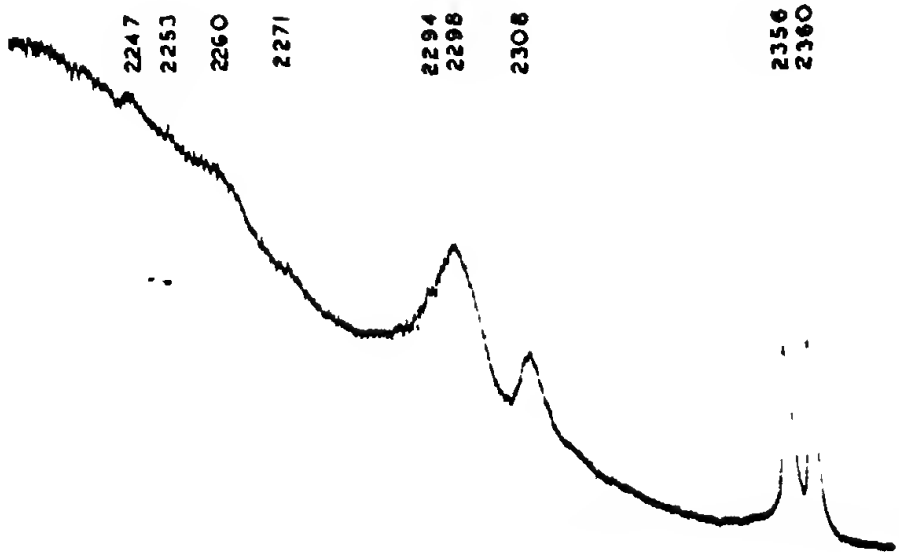

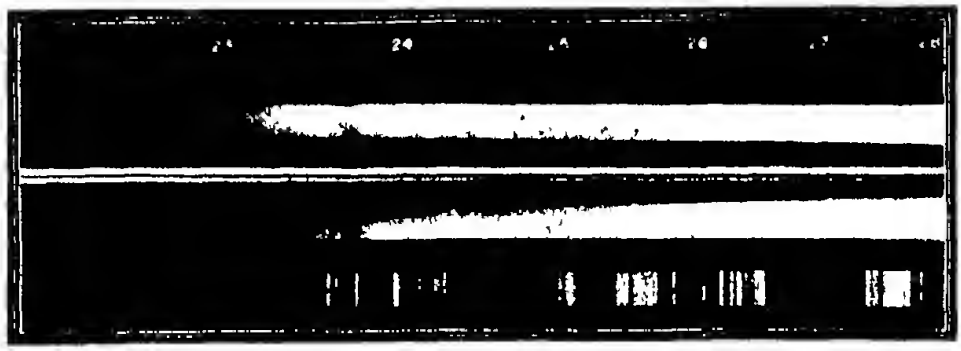

FIG. 4

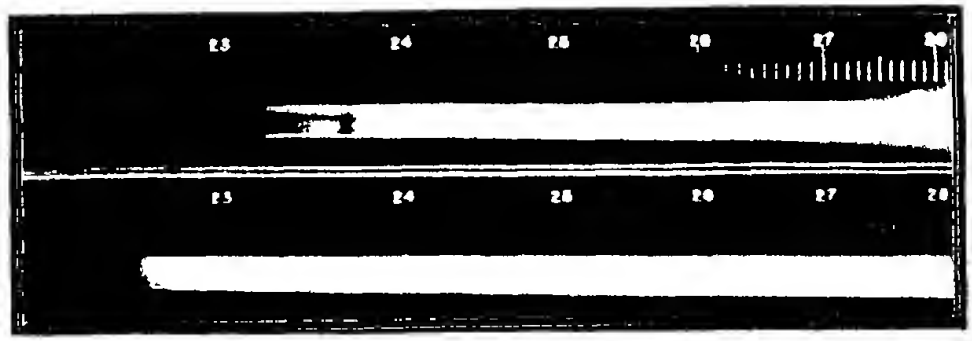

FIG. 5

THE ABSORPTION SPECTRUM OF DIAMOND IN THE VISIBLE REGION

By K G Ramanathan

(From the Department of Physics, Indian Institute of Science, Bangalore)

Received May 18, 1946

(Communicated by Sir C V Raman, Kt, F R S, N L)

1 Introduction

Walter (1891) who first noticed the line at 4155 Å in the absorption spectrum of diamond, attributed it to the presence of impurities A fluorescent emission at the same wavelength and hence presumably having the same origin was noticed by the early workers on the Raman spectrum of diamond Robertson, Fox and Martin (1934) who investigated the absorption spectra of numerous diamonds, detected the presence of the 4155 Å line in only one of their specimens and so were led to dismiss the fact as a rare occurrence not characteristic of diamond, but probably due to the presence of impurities That the situation is, in reality, quite different became evident from the investigations at liquid air temperatures made at this Institute P G N Nayar (1942) found that the 4152 Å line appeared both in emission and in absorption with all the diamonds examined by him, though with enormously different intensities in the different specimens, and that it is accompanied by a subsidiary set of lines and bands appearing at longer wavelengths in fluorescence and at diminished wavelengths in absorption The latter were interpreted as arising out of the combinations of the lattice frequencies of diamond with the most intense electronic line at 4152 Å Miss Mani (1944) investigated the behaviour of numerous diamonds including some non-luminescent ones and established by her studies that while non-luminescent diamonds show no absorption, the 4152 Å system is characteristic of blue fluorescence as shown by Nayar and that yellow fluorescence is characterised by an electronic emission at 5032 Å together with a subsidiary system due to lattice vibrations analogous to the 4152 Å system In addition to the 4152 Å and 5032 Å lines and the systems associated with them, Miss Mani showed that several electronic lines were present, some of them appearing in absorption while most of them appeared in fluorescence. Some of these lines were characteristic of blue fluorescence, others of yellow fluorescence, while there were some others appearing in both blue and yellow fluorescent diamonds

The intensity with which an electronic line appears in absorption depends both on the intrinsic strength of the absorption and the length of

path available. While it is possible to record even very weak electronic lines in emission by prolonging the exposure, such lines can be recorded in absorption only when the conditions are favourable. The results of Miss Mani suggested that by the use of large thicknesses of diamond for absorption work, one would probably be able to obtain all the electronic lines in absorption also The present work was undertaken to investigate the absorption spectra of large thicknesses of diamond and to see whether the many electronic lines observed in the spectrum of fluorescence could be observed in absorption also The work was greatly facilitated by the availability of four large, circular cleavage plates of diamond B_1, B_2, B_3 and B_4 each one of them being about a centimetre and a half in diameter and of thickness ranging between 1 2 and 1 6 millimetres. It may be mentioned here that as a result of the present investigation, several electronic lines appearing in the spectrum of blue fluorescence have been observed in absorption also; several new absorption lines have also been discovered which were not recorded previously either in fluorescence or in absorption Another interesting fact observed here is that by employing large thicknesses of diamond, the light is completely cut-off below the 4152 Å line

2. Method of Investigation

Nayar and Miss Mani used diamonds edgewise to obtain large absorption paths In the present investigation the use of the "Multiple Transmission Method" has enabled still larger paths to be obtained. The four plates of diamond were kept close together such that they formed an assembly of total thickness nearly 6 millimetres. The whole assembly was then sandwiched between two brass plates in which two small holes were cut so that light could be allowed to enter the system through one of the holes and after multiple transmission inside the diamonds, the emergent light could be made to come out through the second hole in the other brass plate. Aluminium foil was attached to the brass plates to reflect the radiation after each transmission through all the four plates in the system In this manner an absorption thickness of several centimetres (3 0 centimetres for four internal reflections) could be easily secured It would have required a Cullinan diamond to have secured such large absorption paths in the ordinary way. For working at low temperatures, the whole assembly was put inside a copper block and the block screwed on to the bottom of the brass inner vessel of a demountable Dewar flask The interspace was continually evacuated by a Cenco Hyvac pump and liquid air was poured in the inner vessel to cool the diamonds to $-180°$ C

As a source of continuous radiation, an incandescent lamp with a straight filament was used. A medium quartz spectrograph was first used

to photograph the spectra, but later when higher dispersion seemed desirable, a Fuess glass spectrograph was used The results obtained are described below

3 Experimental Results

(*a*) *Limit of Transmission.*—At room temperature, the absorption spectra showed a complete cut-off of all radiations with wavelengths below 4160 Å The cut-off was not sharp, but the transmitted intensity decreased gradually as 4160 Å was approached Even with long photographic exposures the spectrum could not be extended below 4160 Å When the diamonds were cooled with liquid air, the cut-off at 4160 Å became very sharp as can be seen from the photograph reproduced [Fig 1 (*b*) in Plate XIII]

(*b*) *Sharp Electronic Lines.*—The second column of Table I gives a list of the electronic absorption lines and bands recorded in spectra obtained at – 180° C The third, fourth, fifth and sixth columns show the results of Miss Mani and are given here for comparison Most of the lines observed by Miss Mani in the fluorescence spectrum of blue-luminescent diamonds have been recorded in the present work. In addition, several other electronic lines which could not have been observed in the fluorescence because of their overlapping with the lattice spectrum accompanying the 4152 Å line have also been recorded in the absorption spectra obtained with a large thickness of diamond On the other hand, the 5032 Å absorption line and the whole system associated with it, have not appeared in these spectra even under these favourable conditions The intense electronic line at 4277 Å, which has been identified by Miss Mani as characteristic of yellow fluorescence has also not been recorded here It must be mentioned here that all the diamonds used in this work except one are purely blue-luminescent specimens One of the four diamonds shows some yellow fluorescent patches in addition to its blue fluorescence

(*c*) *Broad Absorption Bands* —Miss Mani observed in a single diamond N C 70 three broad absorption bands at 4516 Å, 4652 Å and 4776 Å In the absorption spectra obtained in this investigation with large thicknesses of diamond, these three bands appear very intense This suggests that the three broad bands are characteristic of all blue-fluorescing diamonds and not the peculiarity of an exceptional specimen.* The measurements of the bands are contained in Table II

* Miss Mani has reproduced in her paper, the absorption and fluorescence spectra of this specimen D 32 (N C 70) While the 4152 Å line appears with great strength in absorption, it is scarcely noticeable in the emission spectrum reproduced, its intensity being evidently reduced almost to vanishing point by self-reversal This supports the inference made from the present investigation that the three bands are characteristic of blue fluorescence, but are observable only when the absorption is of adequate strength.

TABLE I

Sharp Electronic Absorption Lines observed at − 180° C in Thick Diamonds

Description of line	Wavelength	Blue-Fluorescing Diamonds		Yellow-Fluorescing Diamonds	
		Luminescence	Absorption	Luminescence	Absorption
	A U	A. U	A U	A U	A U
Band { edge	4141				
Band { peak	4151	4152	4152	4152	4152
Band { edge	4162				
Weak	4168	—	—	—	—
	—	—	—	4175	—
Medium	4186	4189	4189	—	—
Do	4196	4197	4197	—	—
Strong	4206	4206	4206	—	—
Weak	4216	—	—	—	—
Medium	4223	—	—	4222	—
—	—	†4227	—	4227	—
Medium	4233	—	—	4232	—
Strong	4250	—	—	—	—
—	—	—	—	4277	—
Strong	4307	—	4304	—	—
Weak	4317	—	—	—	—
Medium	4335	—	—	—	—
Do.	4354	—	—	—	—
Strong	4378	—	4380	—	—
—	—	*4388	—	4388	—
Medium (Diffuse)	4397	—	—	—	—
Medium	4621	—	—	—	—
—				4907	4907
No absorption observed in the region between 4900 A U and 6500 A U		†4959	†4959	4959	4959
		†5032	†5032	5032	5032
		—	—	5359	5359
		—	—	5558	—
		—	—	5695	—
		—	—	5758	—
		—	—	6177	—
		—	—	6265	—
		—	—	6358	—

*—Observed in one diamond only

†—Observed in some diamonds but not in other typically blue-fluorescent specimens

TABLE II

Absorption Bands in Blue-Fluorescing Diamonds

Description	Wavelength	Measurement of Bands by Miss Mani
	A U	A.U
Medium { edge	4466	4494
Medium { peak	4512	4516
Medium { edge	4558	4538
Weak { edge	4586	4602
Weak { peak	4625	—
Weak { edge	4682	4701
Intense { edge	4754	4759
Intense { peak	4776	—
Intense { edge	4797	4794

FIG. 1. Absorption of Visible Light by Thick Diamond

(a) At Room Temperature

(b) At Liquid Air Temperature

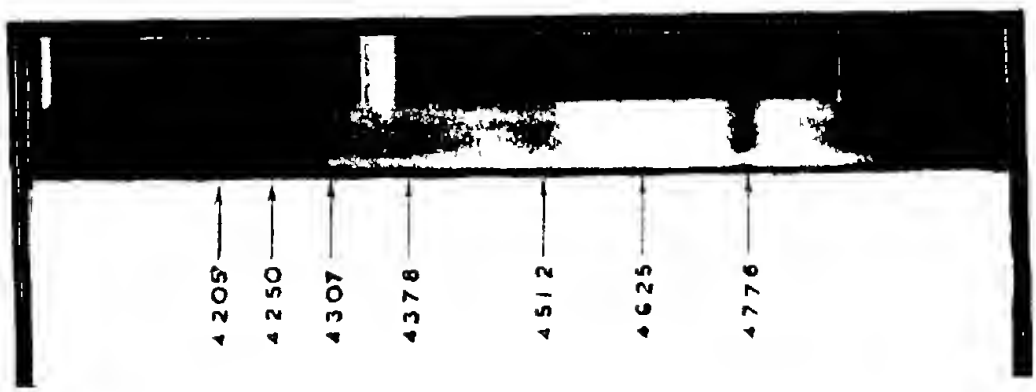

FIG. 2. Absorption of Visible Light by Thick Diamond under High

In conclusion, I wish to record my grateful thanks to Sir C V Raman for the able guidance and kind encouragement he gave me during the progress of the work.

Summary

The absorption spectrum of diamonds exhibiting a weak blue fluorescence has been investigated in the visible region with large absorption paths secured by the method of multiple transmission With thicknesses of the order of a few centimetres, the radiation is completely cut-off below 4160 Å At the temperature of liquid air, a whole series of electronic absorption lines have been observed in the visible spectrum, several of them for the first time Three absorption bands centred at 4512 Å, 4625 Å and 4776 Å have also been recorded which had been previously noticed only in one specimen having an exceptionally strong absorption

References

1 Mani, Miss Anna *Proc Ind Acad Sci*, 1944, 19, 231
2 Nayar, P G N *Ibid*, 1942, 15, 293
3 Robertson, Fox and Martin *Phil Trans Roy Soc*, 1934, 232, 482
4 Walter *Wied Ann*, 1891, 42, 505

THE INFRA-RED ABSORPTION SPECTRUM OF DIAMOND

By K G Ramanathan

(From the Department of Physics, Indian Institute of Science, Bangalore)

Received for publication June 4, 1946

(Communicated by Sir C V Raman, Kt, F R S, N L)

1 Introduction

In a paper (Ramanathan, 1946) appearing earlier in this symposium, it is shown that the infra-red absorption of diamond exhibits a diversified behaviour in the 8μ region of the spectrum On the basis of quantitative measurements contained therein, diamonds have been broadly classified as falling into one or the other of four groups related to the behaviour of diamond in respect of luminescence, *viz*, (*a*) Weakly blue-fluorescent diamonds exhibiting a high coefficient of absorption in the 8μ region, (*b*) Strongly blue-fluorescent diamonds in which the absorption comes down; (*c*) Diamonds showing blue and yellow fluorescence in which the absorption is still less; and (*d*) Non-fluorescent diamonds, which, after correcting for reflection, are non-absorbing in the 8μ region The need for investigating the absorption spectrum in the near infra-red of typical specimens representing each one of the above four groups, was felt because of the lack of previous work on the subject relating it to the property of luminescence Also, with our present knowledge of the several other physical properties of diamond, it is easy to see that the investigations on the infra-red absorption spectrum of diamond carried out till now have been made with unsatisfactory specimens The so-called Type II diamonds (D 2 and D 22) of Robertson, Fox and Martin (1934) show photoconductivity maxima at 3300 Å which is characteristic of their Type I diamonds. In the ultraviolet region, D 2 begins to absorb appreciably even at 2350 Å It is not surprising therefore, that in the 8μ region of the infra-red, the so-called transparent diamond D 2, for which a curve has been reproduced by the above authors, shows only about sixty per cent transmission. Sutherland (1945) remarks that his three so-called transparent diamonds were 'admittedly of a "rough" nature', all of them showing a complete black-out in the region 4·5 to 5 0μ and less than one or two per cent transmission in other regions

For the present work, a large number of cleavage plates of diamond, excellently suited for work of this kind, was available for choice in Sir C. V.

Raman's collection Even with very short photographic exposures, the spectrum transmitted in the ultraviolet by the typical non-luminescent diamonds extend upto 2250 Å In what follows, the investigation of the infra-red absorption spectra of four typical diamonds, each one representing one of the abovementioned four groups is described in detail It may be mentioned here, that as a result of the present investigation the principal lattice vibration of diamond with a frequency of 1332 cm^{-1} has been recorded in absorption for the first time in the luminescent diamonds investigated and has been found to be absent in the non-luminescent diamond. Also, the non-luminescent diamond after allowing for reflection, is found to be hundred per cent transparent in the region between 770–1400 cm^{-1} Other interesting observations made in this investigation will be described in the course of the paper

2 Experimental Technique

The source of continuous infra-red radiation and the rock-salt prism spectrometer have already been described in the paper referred to in the introduction In the present investigation a Boy's radiomicrometer constructed in this laboratory has been used for detecting the radiation. The instrument was fitted with a rock-salt window for making it air-tight The use of a fairly thick quartz fibre for the suspension resulted in steady working of the instrument The deflections in the 8 μ region with a slit-width of a quarter of a millimetre were of the order of 6 centimetres and could be read to an accuracy of 0 05 centimetre For calibrating the instrument, the well-known absorption peaks of diamond at 1285 and 1208 cm^{-1} have been used as standards During the present work, more care was devoted in obtaining a correct contour of the 8 μ absorption band in the different diamonds than in determining the exact positions of the absorption peaks

The procedure for obtaining the absorption curve of a diamond consisted in traversing the spectrum before the exit slit of the instrument by setting the spectrometer at frequent intervals of wavelength At each setting of the spectrometer, the percentage of radiation cut-off by the diamond was obtained by taking the mean of eight readings which gave a value for the percentage cut-off correct within half a per cent in the 8 μ region of the spectrum A very simple lever mechanism served to bring the diamond in the path of the radiation always to the same position before the entrance slit of the spectrometer With regard to the wavelength measurements, the accuracy can be judged from the positions at which the other well-known absorption peaks at 1376, 1105 and 1013 cm^{-1} appear in three of the curves reproduced. The results obtained in the investigation are described below.

3 Experimental Results

Nature of the 8 μ Band —

(*a*) *Weakly Blue-Fluorescent Diamond* —The absorption curve (Fig 1) for the diamond N C 71 (thickness 0 78 mm) shows that the 8 μ band is a little more intense than the band appearing at 5 μ (2000 cm^{-1}). The general nature of the curve is very similar to the absorption curves obtained by previous investigators for the so-called Type I diamonds, except for the fact that there is evidence of two new absorption peaks at 1330 cm.$^{-1}$ and 1150 cm.$^{-1}$ in the curve reproduced for N C 71

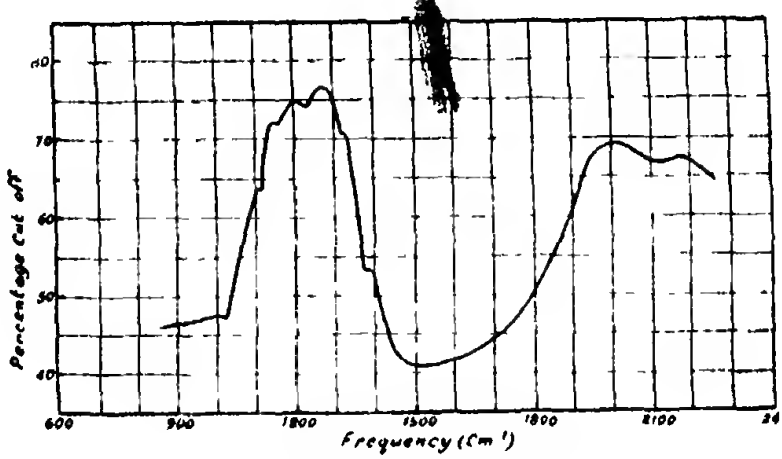

Fig 1. Infra-Red Absorption Spectrum of N.C 71

(*b*) *Non-Luminescent Diamond* —The absorption curve (Fig. 2) of N C 60 (thickness 1 27 mm) shows a uniform transmission of 74% in the region between 7 μ and 13 μ Accepting Reinkober's (1911) value of the reflection coefficient ($r = 0$ 16) we should expect a transmission of only 72% even for completely transparent diamonds As the difference of 2% is not within the error of the measurements, the discrepancy is likely to be due to the slight focussing action of light which the diamond possessed probably due to the curvature of its faces.

(*c*) *Intensely Blue-Luminescent Diamond* —In Fig 3 is shown the absorption curve of N C 79 (thickness 1 20 mm). The peak value of the absorption in the 8 μ region is slightly lower than the value in the 5 μ (2000 cm^{-1}) region While some of the individual peaks come out very prominently in the absorption spectrum of this diamond, the two well-known maxima at 1208 and 1285 cm^{-1} are weaker in intensity than 1332 cm.$^{-1}$

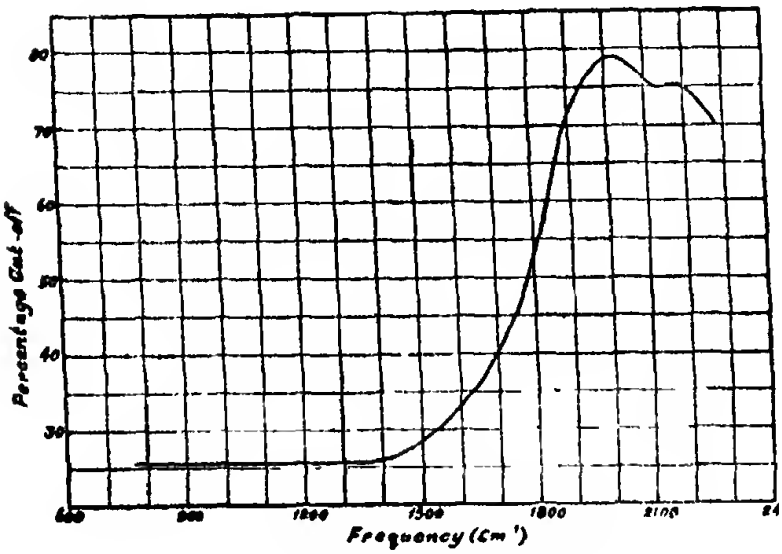

FIG 2 Infra-Red Absorption Spectrum of N C 60

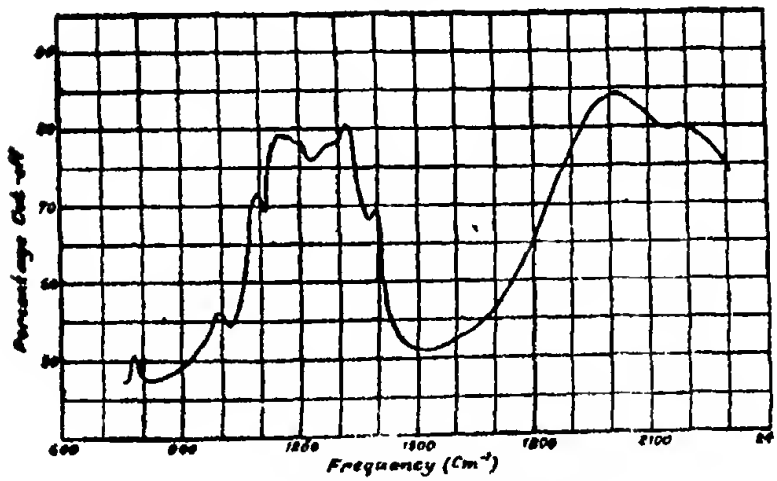

FIG 3 Infra-Red Absorption Spectrum of N C. 79

(*d*) *Diamond Luminescing Blue and Yellow with Great Intensity* —In this diamond with a thickness of 0 80 mm (Fig 4), the peak absorption in the 8 μ region is much less than the value in the 5 μ region. Here again there appears a change in the distribution of intensity in the band

Absorption Maxima —The principal lattice vibration with a frequency of 1332 cm.$^{-1}$ has been recorded for the first time in the luminescent diamonds investigated. As was mentioned in the introductory part of the paper, the

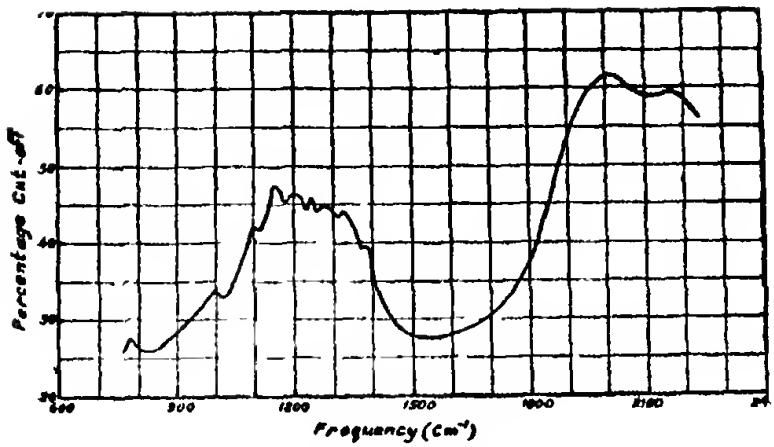

FIG 4 Infra-Red Absorption Spectrum of N C 110

failure to record the band previously might be due to the use of unsatisfactory specimens of diamond The difficulty in recording the band in a weakly blue-fluorescent diamond is that the band appears as a small kink in the curve which is likely to be mistaken for a fluctuation in the intensity of the source or some error in observation By the use of a globar which, in virtue of its large heat capacity, has got a very constant infra-red radiancy and by taking the mean of a number of observations for each setting of the spectrometer, the above sources of error have been eliminated in the present work In addition to the 1332 cm^{-1} absorption peak, a few other peaks have been observed to be present in the absorption spectra of the intensely luminescent diamonds The values of the frequencies of these peaks, which are not claimed to be very accurate, are entered in Table I together with the results of previous workers

TABLE I

Frequencies observed in Infra-Red Absorption in the 8 μ Region

Robertson, Fox and Martin (1934)	Sutherland and Willis (1945)	Present Work
cm^{-1}	cm^{-1}	cm^{-1}
—	784	780
—	1013	1000
—	1105	1100
—	—	1150
—	—	1170
1208	1208	1208
—	—	1245
1289	1285	1280
—	—	1325
1372	1376	1385

The 5 μ Band —

The absorption curves for the four diamonds are identical in contour in the 5 μ region Also, apart from minor deviations, they are positioned according to the requirements of the thicknesses of the diamonds In all the three luminescent diamonds it can be seen that the minimum of absorption between the 5 μ and the 8 μ bands is roughly at about 1550 cm $^{-1}$ This is due to the overlapping of the 5 μ and the 8 μ bands and it can also be seen from Fig 2 where the 8 μ band is completely absent, that the 5 μ band starts really at about 1400 cm $^{-1}$ This position is a little less than double the fundamental lattice frequency at 780 cm $^{-1}$ observed in two of the diamonds The two peaks appearing at 2010 cm $^{-1}$ and 2180 cm $^{-1}$ are undoubtedly the octaves of the next two vibrations appearing in Table I with frequencies 1000 cm $^{-1}$ and 1100 cm $^{-1}$ Hence we are justified in concluding that the absorption peaks appearing in the 8 μ band are the fundamental frequencies and those appearing in the 5 μ band the octaves and combinations of the same frequencies Due to the inadequacy of the resolving power of the instrument used, the measurements could not be pushed beyond 2200 cm $^{-1}$ with any advantage Also, for the same reason, the finer details observed by Robertson, Fox and Martin (1936) in the 5 μ region, could not be recorded here

4 Interpretation of Results The 8 μ Band

(*a*) *Principal Lattice Vibration* —The fundamental vibration of the diamond structure with a frequency of 1332 cm $^{-1}$ represents the oscillation of the two interpenetrating lattices of carbon atoms against each other. If we regard the unit cell containing two non-equivalent atoms to possess either tetrahedral or octahedral symmetry, then the activity of the lattice vibration in Raman effect and infra-red absorption can be obtained by an application of the principles of group theory If the symmetry is tetrahedral, then as can be seen from Table II, the triply degenerate mode F_2 which represents the lattice vibration, will be active both in Raman effect and infra-red absorption

If, on the other hand, the symmetry is octahedral (Table III), then the triply degenerate mode F_{2g} which represents the same lattice vibration will be active in Raman effect but inactive in infra-red absorption In fact for the octahedral symmetry, the selection rules for Raman effect and infra-red absorption are complementary, the modes appearing in scattering being inactive in absorption and *vice versa* The non-luminescent diamond investigated here for which the absorption curve is reproduced in Fig. 2 is found to be completely non-absorbing in the region between 770 cm.$^{-1}$

TABLE II

** Symmetry operations pertaining to the Td group are*
E, $8C_3$, $3C_2$, 6σ and $6S_4$

T_d	E	$8C_3$	$3C_2$	6σ	$6S_4$	n_i	n_i'	Selection Rules Raman	Selection Rules Infra-Red
A_1 ..	1	1	1	1	1	0	0	—	—
A_2 .	1	1	1	−1	−1	0	0	—	—
E ..	2	−1	2	0	0	0	0	—	—
F_1 ..	3	0	−1	−1	1	0	0	—	—
F_2 ..	3	0	−1	1	−1	2	1	Active	Active
U_R ..	2	2	2	2	2				
$h_j x_j$.	6	0	−6	12	−12				
$h_j \phi_j^0$.	0	0	0	12	−12				

* The symbols used in this and in the following table are the same as those given in *Scattering of Light and Raman Effect*, by Prof S Bhagavantam (Andhra University Publication, 1940).

TABLE III

The symmetry operations pertaining to the O_h group are
E, $8C_3$ $3C_2$ 6σ, $6S_4$, i, $8S_6$ 3σ, $6C_2$ and $6C_4$

O_h	E	$8C_3$	$3C_2$	6σ	$6S_4$	i	$8S_6$	3σ	$6C_2$	$6C_4$	n_i	n_i'	Selection Rules Raman	Selection Rules Infra Red
A_{1g} .	1	1	1	1	1	1	1	1	1	1	0	0	—	—
A_{2g} ..	1	1	1	−1	−1	1	1	1	−1	−1	0	0	—	—
E_g ..	2	−1	2	0	0	2	−1	2	0	0	0	0	—	—
F_{1g} .	3	0	−1	−1	1	3	0	−1	−1	1	0	0	—	—
F_{2g}	3	0	−1	1	−1	3	0	−1	1	−1	1	1	Active	Inactive
A_{1u}	1	1	1	1	1	−1	−1	−1	−1	−1	0	0	—	—
A_{2u} ..	1	1	1	−1	−1	−1	−1	−1	1	1	0	0	—	—
F_u ..	2	−1	2	0	0	−2	1	−2	0	0	0	0	—	—
F_{1u} ..	3	0	−1	−1	1	−3	0	1	1	−1	0	0	—	—
F_{2u} ..	3	0	−1	1	−1	−3	0	1	−1	1	1	0	—	—
U_R ..	2	2	2	2	2	0	0	0	0	0				
$h_j x_j$ ..	6	0	−6	12	−12	0	0	0	0	0				

and 1400 cm.$^{-1}$ At the same time, it shows a sharp line at 1332 cm^{-1} in Raman effect We are therefore justified in assigning the octahedral symmetry to the non-luminescent diamonds which show a triply degenerate Raman-active frequency in light scattering but no corresponding infra-red absorption maximum. All the luminescent diamonds investigated (Figs. 1, 3 and 4) show an absorption peak at 1332 cm.$^{-1}$, this being strongest in the weakly blue-fluorescent diamond. Since the triply degenerate mode appears both in Raman effect and infra-red absorption in the luminescent diamonds,

the appearance of the 1332 cm^{-1} peak should be ascribed to the tetrahedral symmetry of the crystals

That diamond may be either tetrahedral or octahedral in symmetry is not an *ad hoc* hypothesis. One has only to study the crystallographic evidence set out in the introductory paper of the present symposium to appreciate the position in this respect correctly. Further, it is an indisputable fact that the diamonds which show the infra-red absorption in the 8 μ region are precisely those which are most nearly free from chemical impurities and which form the nearest approach to crystal perfection, while the diamonds which do not show this absorption band exhibit characteristic irregularities of structure. Hence, the appearance of the absorption band and its absence respectively in the two cases cannot be ascribed to crystal imperfections or other adventitious circumstances, and must be due to fundamental difference in *crystal symmetry*

When interpenetration of the positive and negative tetrahedral forms occurs, the crystal structure must, in strictness, be considered as deviating from tetrahedral towards octahedral symmetry to an increasing extent as the interpenetration is on an increasingly finer scale. Such interpenetration would also result in an appreciable inhomogeneity of structure which would be favourable for the development of luminescence As is shown in other papers appearing in the symposium, this explanation of the origin of blue luminescence is confirmed by various other lines of experimental evidence. Hence, also, we should expect that with increasing intensity of blue luminescence, the infra-red absorption should show a distinct weakening. The fact that for the strongly blue-fluorescent diamond N.C. 79, the absorption in the 8 μ region shows a lower value than what we should expect if it were weakly blue-fluorescent, thus affords support for the interpenetration theory of blue luminescence (Raman, 1944). If a diamond is a mixture of tetrahedral and octahedral varieties, then it should show even a still lower value of absorption in the 8 μ region, and that is what is actually observed for the specimen N C. 110 (Fig 4). Hence the infra-red data for the yellow luminescent diamonds provide independent evidence that the tetrahedral and octahedral varieties appear intertwinned in such diamonds

(*b*) *Superlattice Vibrations*—An application of the group theory to a superlattice having twice the dimensions (eight times the volume) of the unit cell (Bhagavantam, 1943) results in eight modes of vibration of which one is the same as the lattice vibration 1332 cm.$^{-1}$ The seven other superlattice frequencies are disallowed in Raman effect and infra-red absorption irrespective of whether the symmetry of the crystal is tetrahedral or octahedral.

Working at liquid air temperatures, Nayar (1942) and Miss Mani (1944) have observed these superlattice frequencies in the absorption and emission spectra of diamonds in the visible region, these appearing in combination with the two principal electronic lines at 4152 and 5032 Å In the infra-red absorption spectrum of the non-luminescent (octahedral) diamond investigated, the principal lattice frequency 1332 cm^{-1} as well as the superlattice frequencies are absent as fundamentals. This is in perfect accord with the selection rules On the other hand, several discrete absorption maxima are found to be present in the absorption curves of the luminescent diamonds in addition to the 1332 cm.$^{-1}$ peak The positions of most of these peaks agree reasonably well with the superlattice frequencies obtained by Nayar and Miss Mani Still, we cannot completely identify them with the vibration frequencies of the superlattice unless and until the infra-red absorption measurements are carried out at the temperature of liquid air In the following table (Table IV) are reproduced the positions of the infra-red absorption maxima together with the frequencies observed by Miss Mani in absorption and luminescence in the visible region The figures within brackets refer to those which are very weak

TABLE IV

Superlattice Frequencies of Diamond

Infra Red Absorption	Luminescence and Visible Absorption
cm^{-1}	cm^{-1}
—	565
780	784
—	(848)
—	(946)
1000	1013
1100	1088
—	1131
1150	1149
1170	—
1208	1218
1245	1252
1280	1284
1325	1330
—	1341
—	1361
1385	1387

It will be seen from the table that the observed infra-red absorption maxima agree fairly well with those observed in luminescence and visible absorption The position regarding the superlattice frequencies can be stated as follows: (1) They appear in infra-red absorption when the fundamental lattice vibration (1332 cm^{-1}) is active (2) They are absent when the

1332 cm.$^{-1}$ vibration is inactive. (3) Their intensities are roughly of the same order of magnitude as that of the 1332 cm.$^{-1}$ vibration. (4) Those superlattice frequencies appear most strongly which are nearest to the principal lattice frequency, while those which are remote from it appear only weakly (5) The entire absorption is of an order of magnitude very small compared with that observed in polar crystals. (6) The 5 μ band due to the octaves of the superlattice frequencies is about as strong or even stronger than the 8 μ band, in which they appear as fundamentals, instead of being much weaker as is usually the case with overtone and combination frequencies in crystals. As remarked above, according to the ordinary selection rules, the superlattice frequencies should be inactive in infra-red absorption as fundamentals The facts recited above indicate that the activity actually observed is connected with the activity of the 1332 cm^{-1} vibration and is in the nature of a resonance effect.

5 Interpretation of Results The 5 μ Band

As was mentioned in the previous section, an application of the principles of group theory to a superlattice having twice the linear dimensions of the unit cell (eight times the volume) leads in the case of diamond to the result that the atomic vibration spectrum of this crystal should exhibit eight distinct monochromatic frequencies Of these, the mode of highest frequency (1332 cm.$^{-1}$) corresponds to the triply degenerate vibration of the two Bravais lattices of carbon atoms with respect to each other. The other seven frequencies which form the superlattice vibrations, represent oscillations of the layers of carbon atoms parallel to the faces of the octahedron or the cube occurring normal or tangential to these planes, with the phase reversed at each successive equivalent layer By the nature of the case, such oscillations should be inactive in the infra-red absorption as fundamentals under the ordinary selection rules But owing to anharmonicity the octaves of these frequencies should be capable of appearing in infra-red absorption Besides the octaves, various combinations of these frequencies would also be active in infra-red absorption.

A detailed exploration of the infra-red absorption band exhibited by diamond in the regions of wavelengths between 4 μ and 5 μ was made by Robertson, Fox and Martin, using a concave grating of one metre focus of echelette type in conjunction with a prismatic instrument. The investigation showed that the band had an observable fine structure; indeed a whole series of sharply defined peaks of absorption maxima was noticed, the positions of which were capable of exact measurement within a few wave-numbers. As Robertson, Fox and Martin have catalogued only four of the

most prominent absorption maxima, careful measurements of the wavelengths and frequencies of all the absorption peaks and kinks made from their published absorption curve are reproduced in Table V.

TABLE V

Infra-Red Absorption Maxima in the 5 μ Region

Description	Wavelength	Wavenumber	Probable Assignment	
	μ	cm.$^{-1}$	cm^{-1}	
Kink ..	5·230	1912	2 × 565 + 784	$2M_2 + H_2$
Peak .	5 172	1933	784 + 1149	$H_2 + H_1$
Kink ..	5·126	1951	1170 + 784 ?	
$B\beta_2$ Peak	5·061	1976		
Peak	5 000	1996	1208 + 784	
$B\beta_1$ Peak ..	4 931	2028	2 × 1012	$2K_1$
Kink	4 885	2047		
Kink	4·835	2068	784 + 1284	$H_2 + M_1$
Peak .	4·763	2099	1013 + 1088	$K_1 + K_2$
Peak	4·721	2118	784 + 1332	$H_2 + F_2$
Kink .	4·673	2140	2 × 565 + 1013	$2M_2 + K_1$
Ba_2 Peak .	4·608	2170	2 × 1088	$2K_2$
Peak .	4 578	2184	1170 + 1013 ?	
Ba_1 Peak ..	4·511	2217	2 × 565 + 1088	$2M_2 + K_2$
Kink ..	4 474	2236	1088 + 1149	$K_2 + H_1$
Peak .	4·392	2277	2 × 565 + 1149	$2M_2 + H_1$
† Broad Peak	4·08	2482	2 × 1248	$2H_4$
† Kink ..	3·89	2573	2 × 1284	$2M_1$
† Centre of Steep Rise	*3 73	*2680	2 × 1332	$2F_2$

* Measurement Approximate

† These measurements were obtained from the earlier work of Robertson, Fox and Martin (1934).

Probable assignments for most of these frequencies are made in terms of the lattice and superlattice frequencies of diamond. It will be seen that most of the assignments fit within a few wavenumbers with the actual values of the frequencies of the absorption maxima These results should be considered surprising according to the early theories of crystal dynamics according to which the vibration spectrum of a crystal is essentially continuous. On the other hand they fit in naturally with the ideas regarding crystal dynamics recently put forward by Sir C. V. Raman (1943)

ACKNOWLEDGEMENT

I am greatly indebted to Sir C. V. Raman for the inspiring guidance and kind encouragement he gave me during this research.

Summary

The absorption spectra of four typical diamonds, three of them luminescent and the fourth non-luminescent, have been investigated in the infra-red in the wavelength range 4 5μ to 13μ with a rock-salt prism spectrometer and radiomicrometer Allowing for reflection, the non-luminescent diamond is found to be completely non-absorbing in the frequency range 770 cm^{-1} to 1400 cm.$^{-1}$ The luminescent diamonds show a band in this region with a number of absorption maxima whose frequencies may be identified with those of the lattice and superlattice vibrations The intensity of this band is greatest in the weakly blue-fluorescent diamond, somewhat weaker in the intensely blue-fluorescent diamond and still weaker in the diamond showing both blue and yellow fluorescence These results are accounted for on the basis of the crystal structure and symmetry of diamond in its various allotropic modifications The absorption peaks appearing in the region between 1400 to 2700 cm^{-1} are accounted for as octaves and combinations of the lattice and superlattice frequencies which are allowed by virtue of the anharmonicity of the vibrations The appearance of the superlattice frequencies in the 8μ band is closely associated with the infra-red activity of the fundamental lattice vibration and is in the nature of a resonance effect

References

1 Bhagavantam *Proc Ind Acad Sci*, 1943, **18 A**, 251
2 Mani, Miss Anna *Ibid*, 1944, **19**, 231
3 Nayar, P G N. *Ibid*, 1942, **15**, 293
4. Raman, C V *Ibid*, 1943, **18**, 237
5 ——— *Ibid*, 1944, **19**, 189.
6 Ramanathan, K. G *Ibid*, 1946, **24**, 130
7 Reinkober *Annalen der Physik*, 1911, **34**, 343
8. Robertson, Fox and Martin *Phil Trans.*, 1934, **232**, 465.
9 ——— *Proc Roy Soc*, 1936, **157 A**, 579
10. Sutherland and Willis *Trans Faraday Soc*, 1945, **41**, 289

LOCAL VARIATIONS IN THE PHOTOCONDUCTIVITY OF DIAMOND

By K Achyuthan

(*From the Department of Physics, Indian Institute of Science, Bangalore*)

Received May 29, 1946

(Communicated by Sir C V Raman, Kt, F R.S, N L)

1 Introduction

The important discovery that though diamonds are usually non-conducting, they conduct electricity under ultra-violet irradiation was first made by Gudden and Pohl (1921) These authors noticed that two of their diamonds showed remarkable differences in behaviour, both in respect of the magnitude of the effect as well as its spectral variation One non-fluorescent crystal which transmitted the ultraviolet spectrum down to λ 2300 was found to be much more photo-conducting than another which was fluorescent and absorbed ultra-violet radiations of lesser wavelength than λ 3000 Later workers, notably Robertson, Fox and Martin (1934) have investigated the problem in detail An examination of their data indicates that diamonds show a highly diversified behaviour, the photoconductivity ranging from a very high to a very low value, through successive stages. Pant (1944) who first drew attention to this situation studied the photoconductivity of thirty-six cleavage plates of diamond and arranged them in a regular sequence He found that the photoconductivity is closely correlated with similar variations in other properties of diamond, notably its ultraviolet transparency and the colour and intensity of its luminescence under ultraviolet irradiation

The present paper describes a new and hitherto unsuspected phenomenon, namely that the photoconducting power of diamond may show large variations over the area of a single specimen Such variations could have been expected and have actually been found in the present investigation, in cleavage plates of diamond which show variations in ultraviolet transparency over their area (Raman, Rendall, 1944) Surprisingly enough, however, noticeable variations have also been found in a polished cleavage plate which is completely transparent to ultraviolet radiation upto λ 2250 and also to infra-red radiation in the 8 μ region It appears that these variations are connected with variations in the degree of mosaicity of the crystal which is suggested by the varying nature of the birefringence pattern of the plate in different parts of it as seen between crossed polaroids

The diamonds examined were all cleavage plates with well polished faces, the thickness ranging from 0 8 mm. to 1·3 mm To study the photoconducting behaviour of a particular region in one of them, an electric field is applied across that region by means of two pointed metallic electrodes kept pressed on the faces of the plate. Light from a quartz mercury arc passing through a slit 2 mm wide is focussed by two quartz lenses at the particular region, the width of which was about 1 mm The current produced is amplified and measured For studying another region, the diamond is moved parallel to the plane faces till the region to be examined is illuminated Thus the whole surface of the diamond is surveyed by steps

2 Some Experimental Details

The diamond is clipped between two crocodile clips with all their teeth removed except the front three, so that the points of contact are quite sharp and defined The clips are mounted on two brass rods movable along a groove made on an ebonite base The diamond is illuminated on one side by the light of a quartz mercury lamp as explained above, and by the light of a 500 watt filament lamp filtered through a red filter on the other side The voltage to be applied is obtained from a set of 144 dry cells connected in series giving a total of 220 volts, any part of which could be tapped The current generated is amplified by a D C amplifier, constructed before by Ananthakrishnan (1934) and working under 120 volts, the amplified current being measured on a shunted galvanometer By measuring the change in output current for a known small change in input voltage, the current amplification factor is calculated as 3,500, giving an overall sensitivity of 2×10^{-11} amp in the input circuit for one division deflection on a scale at one metre from the galvanometer in the output circuit

Because of the pressure applied by the springs in the clips, good contact was obtained between them and the diamond This is clear from the fact that all the readings given below are reproducible to 2 mm of deflection, if proper care is taken to remove any polarisation formed inside the crystal Applying different voltages obtained from the dry battery set across the diamond and measuring the resultant currents in the output circuit, the exact linearity of amplification was tested. Also, irrespective of the fact whether the points of contact were illuminated or not, the photocurrent was strictly proportional to the area illuminated, thus indicating that no spurious charges were produced at the points of contact If was found that if the following two precautions were not strictly adhered to, highly erroneous results might be obtained (1) Before each reading, the diamond was cleaned with benzene to remove any surface impurities, dried in folds of filter-paper

and heated to 150° C. to remove any space charges that might have formed before (2) The sharp ends of the clips were occasionally cleaned to remove any non-conducting material which might get deposited there.

3 Results

The three diamonds N C 115, 82 and 127 give interesting ultraviolet transparency patterns Rough sketches of the patterns are shown in the accompanying figure, numbered as I *a*, II *a*, III *a* respectively The shaded regions in the other drawings are the regions illuminated and the points marked are the points of contact between the clips and the diamonds The voltage applied between the clips is 120 volts The currents corresponding to the different regions are tabulated in Table I

Table I

Voltage — 120 V at 1½ mm apart

Area studied	N C 115		N.C 82		N C 127	
	Deflection	Ph Current in 10^{-10} amp	Deflection	Ph Current in 10^{-10} amp	Deflection	Ph Current in 10^{-10} amp
1	116 mm	23 2	47	9·4	11	2 2
2	17	3 4	22	4·4	10	2·2
3	12	2 4	8	1 5	15	3 0
4	107	21 4	4 5	0 9	9	1·8
5	27	5 4	6·5	1 3	19	3 8
6	224	44·8	12	2 4	9	1·8
7	147	29·5	2	0 4	7	1·4
8	30	6 0	16	3 6		
9	35	7 0	5 5	1 1		
10	5·5	1·1	3 0	0·6		
11	4 0	0 8	4 0	0 8		
12	4 0	0 8	4·0	0 8		
13	5 5	1 1	5 5	1 1		
14	11 5	2 3	4·0	0 8		
15	2 0	0 4	3 5	0·7		
16	90	18	7 5	1·5		

Diamond N C 60 which transmitted ultraviolet uniformly throughout the surface was then studied A voltage of 1000 volts obtained by means of a rectifier was applied across the electrodes which were 2 5 mm. apart. The results are given in Table II. Though variations were not expected, Table II *a* corresponding to Fig. IV *b* clearly shows variations and hence a more thorough study by applying the field parallel to the shorter edge and moving the diamond mm by mm. along the longer edge, was made. The regions are numbered in Fig. IV *c* and the results given in Table II *b*. A sketch of the birefringence of the diamond as seen between crossed polaroids is given in Fig. IV *a*.

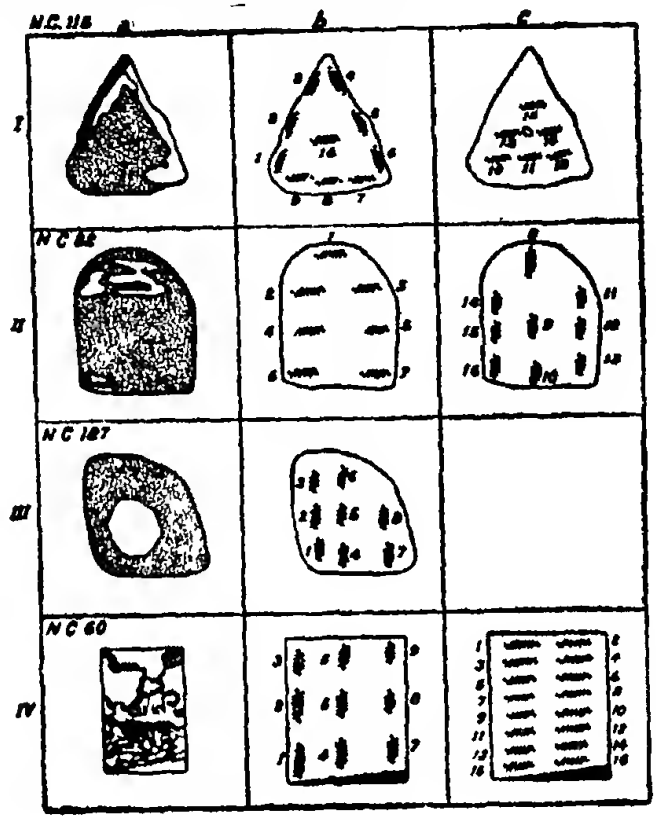

TABLE II

P D between electrodes 2 5 mm apart = 1000 volts

(a) See Fig 1V b			(b) See Fig 1V c	
Area studied	Deflection mm	Photo Curr in 10^{-10} amp.	Deflection mm	Photo Curr in 10^{-10} amp
1	57	11 4	29	5 8
2	43	8 6	44	8 8
3	30	6 0	25	5 0
4	50	10 0	28	5 6
5	55	11 0	36	7 2
6	40	8 0	30	6 0
7	64	12 8	38	7 6
8	50	10·0	50	10 0
9	47	9 4	31	6 2
10			50	10 0
11			42	8 4
12			50	10 0
13			49	9 8
14			45	9 0
15			58	11 6
16			39	7·8

4 Discussion of Results

A comparative study of the ultraviolet transparency patterns and of the variations in the photoconducting behaviour observed in the three diamonds N C 115, 82 and 127 shows that the transparent regions are much more photoconducting than the opaque parts It will be noticed that variations in photoconductivity are large in N C 115, rather smaller in N C 82 and still less in N C 127 The behaviour of these diamonds in respect of ultraviolet transparency is very similar Parts of N C 115 are highly transparent; N C 82 is rather imperfectly transparent in parts. In N C 127 the central region is only slightly more transparent than the margin which is completely opaque, a long exposure being found necessary to bring out the difference

In N C 60, a study of the birefringence pattern in relation to the values of photoconductivity given in Table II reveals that the effect is greatest in regions where the birefringence pattern consists of fine streaks and least where it is full of patches

Any theory of the photoconductivity of diamond must necessarily consider the following factors; (1) the power of the activating ultraviolet radiation to penetrate into the crystal, (2) its power to set free electrons from the crystal lattice, and (3) the ability of the electrons so set free to move sufficient distances to transport a charge The striking dependence of photoconductivity on ultraviolet transparency is presumably explicable on the basis of the first factor itself The variations in photoconductivity shown by the different regions of N C 60 indicate, however, that the other two factors may also be variable and that such variations have also to be considered

N C 60, as mentioned above, shows variations in the nature of birefringence over its surface But birefringence as such is a macroscopic phenomenon and is not necessarily an indication of any variations in the fine structure of the crystal However, as has been shown by G N Ramachandran in another paper appearing in the present symposium, the X-ray topographs of such diamonds exhibit a close relationship to the birefringence patterns Since the varying intensity of X-ray reflection arises from mosaicity of crystal structure, variations in the nature of the birefringence pattern may be indicative of variations in the degree of mosaicity. At any rate, it is not improbable that over the region in N C 60 where the birefringence, pattern is streaky, the mosaicity of structure may be greater, thereby giving rise to a larger number of photoelectrically active centres *Per contra*, where the birefringence is patchy, the mosaicity may be less and consequently the

number of active centres may also be less Whether this is the correct explanation of the differences in photoconductivity or whether the variations are due to differences in the free paths of electrons in different parts in the plate, can only be established by further investigations

In conclusion, the author wishes to express his deep sense of gratitude to Sir C V Raman for the great interest he has taken in this work and for the constant encouragement given by him during the course of the work

Summary

Three cleavage plates of diamond showing variations of ultraviolet transparency over their area have been studied with respect to their photoconducting behaviour. It is found that the transparent regions are more photoconducting than the opaque, the actual value of the photocurrent in a region depending on the degree of ultraviolet transparency

A fourth plate of diamond which was completely transparent to the ultraviolet region above λ 2250 and also to the 8 μ infra-red region throughout its area, also showed variations of photoconductivity. It is suggested that such variations may arise from a variation in the degree of the mosaicity of the crystal structure in different parts of the plate and consequent differences in the number of active centres from which electrons could be released by the incident radiation.

References

1 Ananthakrishnan, R *Proc Ind Acad Sci*, 1934, 1, 205
2. Gudden and Pohl *Zeit, f Phys*, 1920, 3, 123.
3. Pant, D D *Proc. Ind Acad, Sci*, 1944, 19, 315
4 Raman, C. V *Ibid*, 1944, 19, 199
5. Rendall, G R *Ibid*, 1944, 19, 293
6. Robertson, Fox and Martin *Phil Trans Roy Soc*, 1934, 232, 463

GEOMETRIC PATTERNS OF FLUORESCENCE IN DIAMOND

By G R Rendall

(*From the Department of Physics, Indian Institute of Science, Bangalore*)

Received June 8, 1946

(*Communicated by Sir C V Raman, Kt, F R.S, N L*)

1 Introduction

Working with the polished cleavage plates of diamond in his collection, Sir C V Raman (1943) discovered that while several of them show a more or less uniform blue fluorescence under ultraviolet irradiation, others exhibit geometric patterns of fluorescent light with a varying intensity and in some cases also a varying colour over the area of the plate A detailed study of the phenomenon (Raman, 1944) showed clearly that there are two distinct types of luminescence with different characters designated respectively as "blue" and as "yellow", and that the pattern observed in any particular diamond might be of one or the other description, or of both simultaneously The "blue" and "yellow" patterns in a diamond might have entirely different configurations, thereby indicating that they have different origins. The geometry of the patterns is clearly related to the crystal structure, a circumstance which indicates that the phenomenon is characteristic of diamond and not a consequence of impurities present in it This conclusion is reinforced by the fact that cleavage plates showing such patterns also show variations over their area of other physical properties, *viz*, transparency in the ultraviolet region of the spectrum (Sunanda Bai, 1944 *a*), in the visible spectrum (Anna Mani, 1945), in the infra-red (8 μ) region (Ramanathan, 1946), of the X-ray reflection intensities (Ramachandran, 1944), and of photoconductivity (Achyutan, 1946) In the earlier symposium, photographs were reproduced showing for numerous plates, their luminescence patterns (Sunanda Bai, 1944 *b*), their ultraviolet transparency patterns (Rendall, 1944), their X-ray topographs (Ramachandran, *loc cit*) and their birefringence patterns (Raman and Rendall, 1944), and these exhibited highly significant resemblances and differences.

In the present study, considerable improvements have been effected in the technique of photographing the luminescence patterns and in presenting them for detailed scrutiny. As was remarked by Sunanda Bai herself (*loc cit*) in her paper on these patterns, a correct rendering of them would only

be possible if the "blue" and "yellow" types of luminescence were separately photographed by the use of appropriate light filters This has been done in the present investigation, and by attention to various details, *viz*, critical focussing, adequate magnification and suitable photographic exposures, a notable improvement has been made in recording the details visible in these patterns. In the earlier symposium, illustrations of the different patterns for the same diamonds appeared dispersed over several separate papers, and except in a very few cases it was not easy for the reader to compare them in detail This defect has been remedied in the present study. Four different patterns, *viz*, those of the blue luminescence, of the yellow luminescence, of the ultraviolet transparency and of the birefringence have been photographed for each of 19 different cleavage plates of diamond, and these are presented in juxtaposition in the Plates accompanying this paper All the four patterns have precisely the same magnification and also the identical setting, thereby making it easy for the reader to compare them in detail The present paper makes an advance over the previous work also in respect of the material studied 10 out of the 19 diamonds studied are new additions to Sir C V Raman's collection 8 of them are cleavage plates of the smallest available thickness The confusion which arises from the overlapping of the patterns at different depths which are not completely in register is minimised by the use of such plates Thin plates naturally require more intense illumination and longer exposures to yield satisfactory pictures. But the extra effort has been fully justified by the results

2 General Nature of the Patterns

The correlations which exist between luminescence, ultra-violet transparency and birefringence have already been stated by Sir C V Raman in his paper (1944) quoted above They may usefully be reproduced here.

(*a*) A blue-luminescent diamond is invariably of the ultraviolet opaque type, but the opacity diminishes with increasing intensity of luminescence.

(*b*) Non-luminescent diamonds are invariably of the ultraviolet transparent type.

(*c*) The diamonds which exhibit an yellowish-green luminescence are of the intermediate type, in other words, are neither perfectly transparent nor perfectly opaque to the λ 2536 radiations

(*d*) The foregoing statements are also valid in respect of the individual areas in a cleavage plate which exhibit a luminescence pattern.

(*e*) Diamond may be perfectly isotropic and strain-free; it is then invariably of the blue-luminescent type

(*f*) Non-luminescent diamond exhibits a characteristic and readily recognisable type of birefringence, consisting of closely-spaced parallel streaks running in several directions through the crystal.

(*g*) Diamond exhibiting the yellowish-green luminescence invariably shows a characteristic type of structural birefringence, consisting of parallel dark and bright bands, usually rather wider apart than those shown by non-luminescent diamonds

(*h*) Diamond in which the blue-luminescent and non-luminescent types, or the blue-luminescent and the yellowish-green luminescent types are simultaneously present invariably shows structural birefringence

The reader can easily test the correctness of the foregoing statements for himself by a careful study of the Plates accompanying this paper The Plates also serve to illustrate the geometric nature of the patterns and the variety of forms which they exhibit, *viz*, parallel bands, triangles, hexagons, irregular polygons, and spirals The present investigation also brings into relief the striking differences in geometric configuration or intensity distribution or both, of the "blue" and the "yellow" luminescence patterns The variations in the properties of diamond exhibited in these patterns have been explained by Sir C V. Raman as due to the existence of different allotropic modifications, *viz*, the positive and negative tetrahedral forms designated as Td I and Td II, and the two octahedral forms designated as Oh I and Oh II Interpenetration of these modifications gives rise to a wide diversity in behaviour So far as luminescence is concerned, we may again quote here from his paper on the subject

(*a*) Diamonds with tetrahedral symmetry of structure are, in general, blue-luminescent.

(*b*) Diamonds with octahedral symmetry of structure are non-luminescent.

(*c*) Diamonds in which the tetrahedral and octahedral types of structure are intimately mixed exhibit the yellowish-green type of luminescence.

Attention may here be drawn to the interesting fact that has emerged from the present studies, *viz*, that the interpenetration of the positive and negative tetrahedral forms gives rise to blue luminescence which may take the shape of parallel bands, straight or curved, as the case may be. The configurations of these bands may be the same or different or partly the same

and partly different from the banding of the yellow luminescence Instances of such behaviour are furnished by the various diamonds here studied N C 151 in Plate XVII is a particular interesting case showing parallel bands of blue luminescence and of yellow luminescence running in completely different directions.

3 The Diamonds Studied

B1, B2, B3, B4 are large cleavage plates of diamond, each about 5 carats in weight and about 1 5 millimetres thick. The pictures in their case have been magnified only about 2 diameters All the other cleavage plates are relatively small in size, and their photographs have been magnified from 3 to 10 diameters as necessary in each case N C 151, N C 152, N C 153, N.C 154, N C 155, N C 156, N C 159 and N C 160 are small thin plates N C 80, N C 82, N C 100, N C 108, N C 110, N C 111, N C 113, N C 114 and N.C 115 were figured in the earlier symposium, but they have been examined afresh for the reasons already explained N C 175 is a new acquisition showing some remarkable features in its patterns

4 Experimental Technique

Luminescence —The photographic filters used in the investigation were prepared by the author from suitable dyestuffs in the laboratory by staining a thin film of gelatine with them An unexposed photographic plate was fixed in a hypo bath and thus all the silver salts were removed from it In this way a thin clear gelatine film on a glass plate was obtained To stain the gelatine with the dye, the plate was placed in a flat dish containing an aqueous solution of the dyestuff The plate was then removed and dried in a dust proof chamber The filter was then bound with a clean glass plate so that the dyed gelatine was protected from being scratched Two such filters were prepared, such that one of them transmitted the blue luminescence and cut off the yellow one, while the other cut off the blue luminescence and transmitted the yellow one. Both of them transmitted the red beyond 6000 Å U , but this did not matter

The source of light employed for the thicker plates was a carbon arc run at 220 volts with about 8 amperes current The light of the arc, after passing through a water cell and a filter of Wood's glass is focussed by a short focus lens on to a quartz plate. The diamond was stuck on the quartz plate. The inclination of this plate to the incident beam was so adjusted as to secure a uniform irradiation of the diamond The diamond should be mounted in such a way that no reflections at the bevelled edges of the crystal are seen through the camera lens A rectangular glass cell containing a concentrated solution of sodium nitrite was placed in front of the camera

lens This served as a complementary filter cutting out all the ultraviolet rays transmitted by the Wood's glass The colour filter for isolating the blue or the yellow luminescence as desired was introduced in front of the camera lens The camera was fitted with a Zeiss Sonar lens of 5 cm focus The luminescence pattern under suitable magnification was very carefully focussed on the photographic plate Very fast Ilford H P 3 plates were used for obtaining the photographs, the time of exposure being varied according to the nature of luminescence. The blue luminescence patterns were obtained with exposures ranging from 15 minutes to 1 hour, but the yellow luminescence required longer exposures ranging from two hours to six hours.

For the thinner plates, sunlight and much longer exposures were employed, other details being the same

Ultraviolet Transparency—The procedure which has been developed and found to be simple and successful for the observation of the ultraviolet transparency patterns of diamond is based upon the use of the extremely intense radiation of wavelength 2536 Å U furnished by a water-cooled, magnet-deflected mercury arc in quartz. An image of the arc formed by this radiation is thrown on a plate of uranium glass and is made visible by the intense fluorescence of the latter If a piece of diamond is stuck on the front surface of the uranium glass, its behaviour in respect of transmission through it of the 2536 Å.U. radiation is immediately rendered evident by its screening effect on the fluorescence of the uranium glass The luminescence of the diamond itself excited by the 2536 Å U is of negligible intensity. As the 2536 Å U radiation penetrates very little into the glass, the fluorescence seen on its surface is an accurate representation of the variations of transparency of the diamond to that radiation Provided the plate of diamond is not very thick and it is in close contact with the uranium glass plate, all the details of the transparency patterns are shown up very clearly.

In this connection it should be pointed out that though the mercury arc in quartz when water-cooled and magnet-deflected predominantly gives the 2536 Å.U radiations, these are accompanied by numerous other radiations of both longer and shorter wavelengths Since diamond is transparent in every case to radiation of greater wavelengths than 3000 Å U, and since the latter also could excite the visible fluorescence of the uranyl glass, it is essential for the success of the method that they are eliminated when forming the image of the mercury arc on the uranium glass This is readily accomplished using an optical train composed of a quartz lens, a constant deviation quartz prism and a second quartz lens to form a mono-

chromatic image of the arc on the uranium glass. Even with this arrangement there is some parasitic illumination due to other radiations scattered at the surface of the lens and the prism and reaching the plate of uranium glass. This, however, gives no trouble, provided the plate is viewed by the fluorescent light alone in a slightly oblique direction and not by the parasitic light coming directly through it The success and efficiency of the method is entirely due to the extremely great intensity of the 2536 A U radiation emitted by the quartz mercury arc under the conditions stated already, in comparison with all such disturbing factors

The ultraviolet transparency pattern as made visible in the manner explained above can be readily photographed using a short focus camera lens and Ilford Selochrome plates Many diamonds appear at first quite opaque but when long exposures are given, the photographs exhibit faint patches where the 2536 radiations are weakly transmitted Careful focussing is needed to bring out the details of the pattern with the maximum of clearness.

Birefringence—The source of illumination used was a tungsten filament 100 watts, 220 volts lamp enclosed in a box with an aperture. Two polaroids were supported by platforms just above the aperture, the distance between them being 10 cm. The cleavage-plate of diamond under investigation was introduced between the polaroids supported on a strain-free glass plate and could be set in any desired orientation. The polaroids were mounted on circularly divided supports, so that they could be rotated with respect to each other. The birefringence pattern as seen through the crossed polaroids was photographed by using an achromatic camera objective of 5 cm. focus. Ilford Selochrome plates were used for photographing the patterns, the time of exposure depending on the particular case.

The nature of the pattern exhibited by the birefringence of diamond between crossed polaroids was in general found to vary in a remarkable manner when the setting of the diamond in its own plane was altered. The pattern observed repeated itself four times in each complete revolution of the diamond in its own plane while in intermediate positions it was, in general, different. The alterations produced in the birefringence pattern by rotating the diamond, however, were not usually the same at all parts of the diamond, thereby showing clearly that the axes of the birefringence varied from place to place. Photographs of the birefringence patterns different from each other could therefore be obtained by merely setting the diamond in different orientations with reference to the crossed polaroids At least two such photographs were obtained for each diamond. Only one of them, however,

has been reproduced in the accompanying plates, being that which showed the pattern most clearly in all the different parts of the plate

5 Description of the Plates

The pictures marked B1, B2, B3 and B4 in Plate XX are the birefringence patterns of these octahedral cleavage plates and have been reproduced in view of their remarkable hexagonal forms, the lines evidently following the intersections of the other octahedral planes in the crystal with the plane of the cleavage plate. All of them are blue-luminescent diamonds, and being also pretty thick are practically opaque to the λ 2536 radiations Their luminescence patterns show a set of diffuse hexagons, but as they are not very distinct except in the case of one of them B1, the patterns of B2, B3 and B4 have not been reproduced with the present paper

In all cases, the four patterns of each diamond have been set above each other as described in the explanation of the plates (see below) at the end of the paper The photographs have all been reproduced as positives. Comparing them with each other, various resemblances and differences are noticed. A very common and striking feature is that areas which appear as bright in the blue luminescence are reproduced as dark areas in the ultraviolet transmission This, of course, is because blue-luminescent diamond is ultraviolet opaque The converse feature, *viz*, that areas which appear bright in ultraviolet transmission are dark areas in blue luminescence is also noticed, but it is not quite so common nor always so striking. It is explained by the fact that diamond which is completely ultraviolet transparent is non-luminescent, while diamond which is yellow-luminescent is partially transparent to the ultraviolet rays. Cases of both kinds occur, the latter more frequently, the effect being then naturally less conspicuous There is often but little in common between the features observed in the blue luminescence and the birefringence patterns This is because blue-luminescent diamond is inherently non-birefringent. On the other hand, striking resemblances are observed between the yellow luminescence and the birefringence patterns. This is because yellow luminescent diamond is laminated in structure and is therefore necessarily birefringent. In some cases, however, the blue and yellow luminescence patterns resemble each other and in such cases both exhibit features analogous to those seen in the birefringence patterns.

In conclusion, the author wishes to express his sincere gratitude to Sir C. V Raman for his kind interest and guidance.

NC 159 NC 153 NC 760

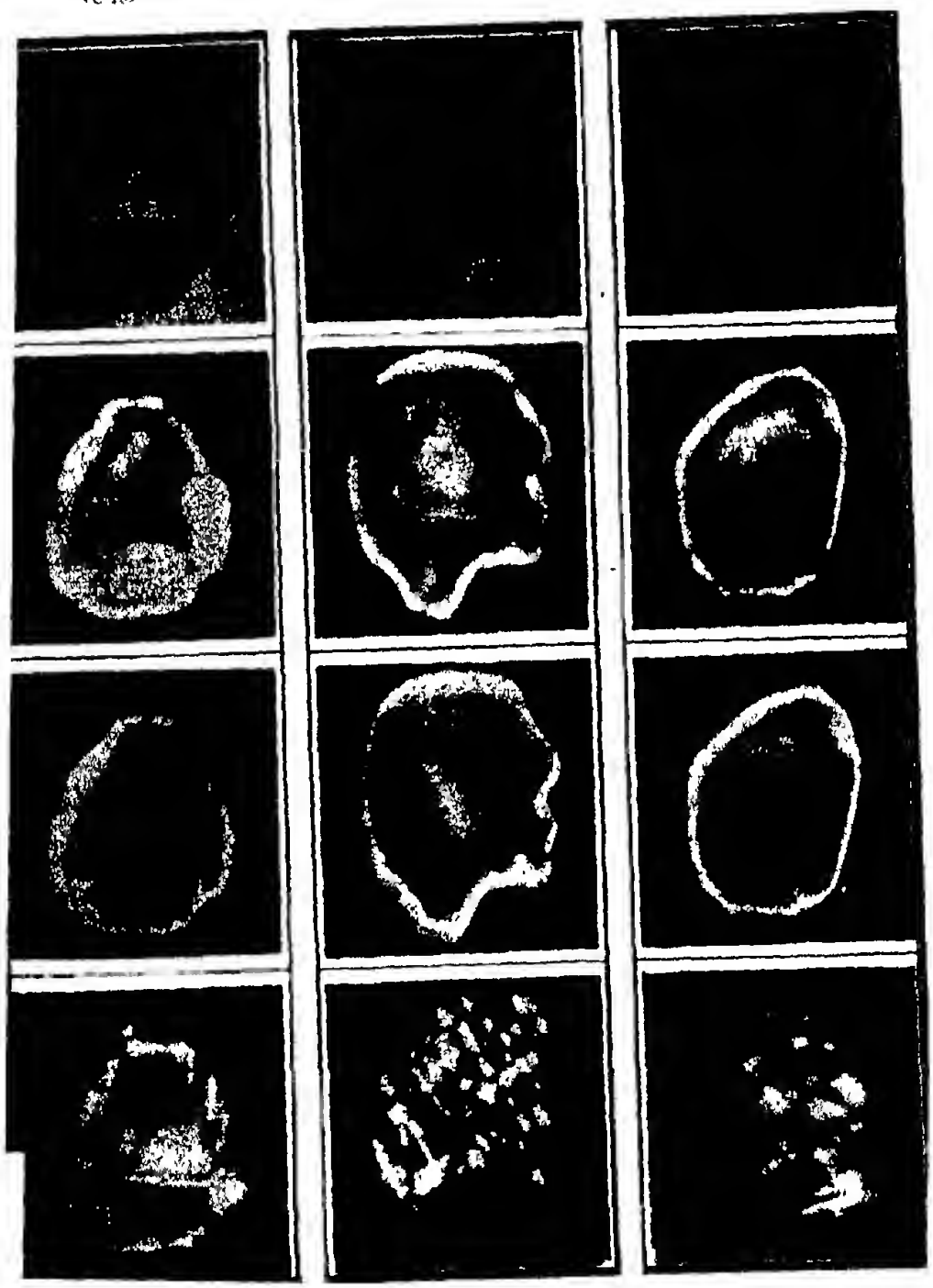

NC 108 NC 152 NC 82

(a)

(b)

(c)

(d)

NC 114 NC 115 NC 116

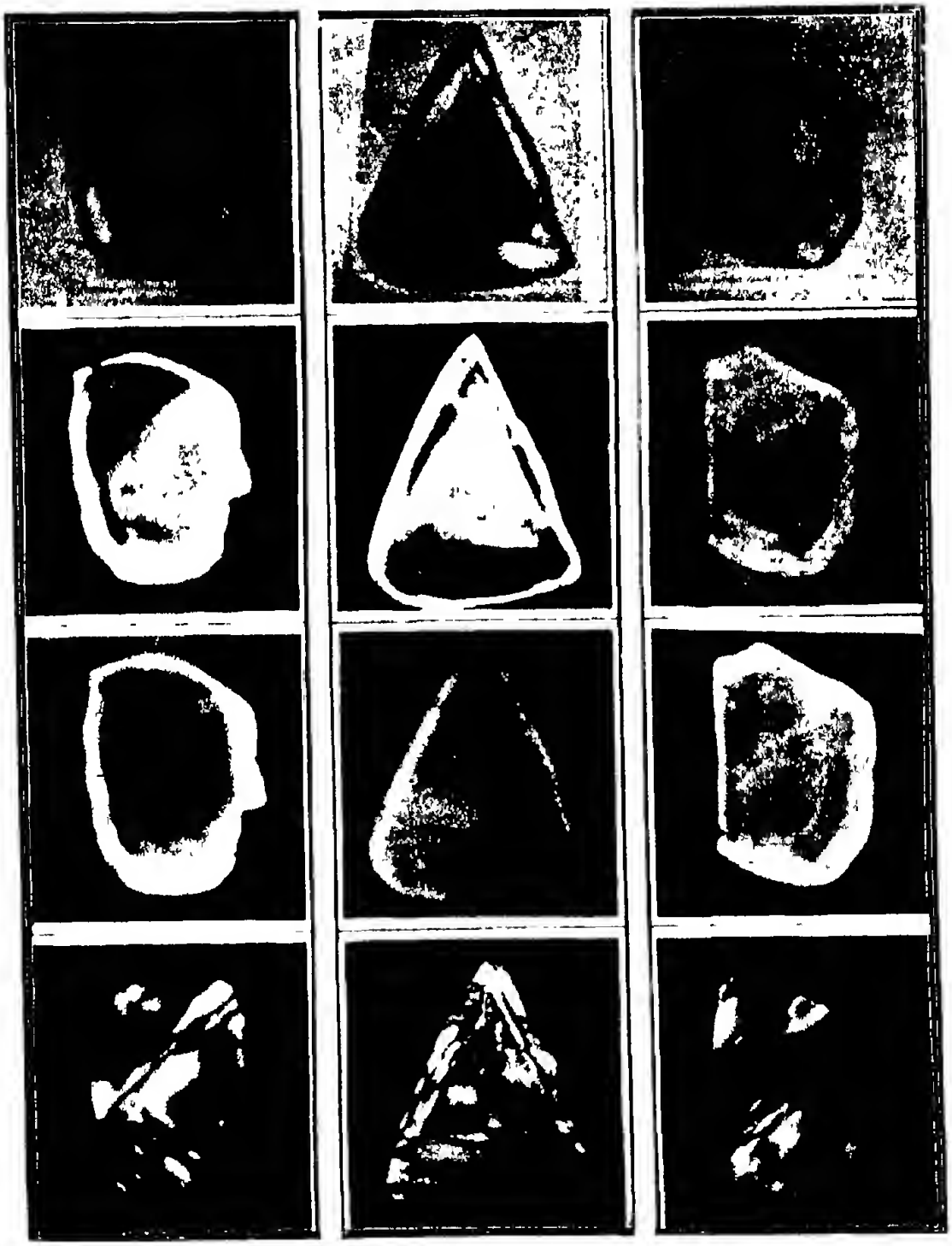

NC 110 NC 157 NC 100

(a) (a)

(b)

(c) (c)

d)

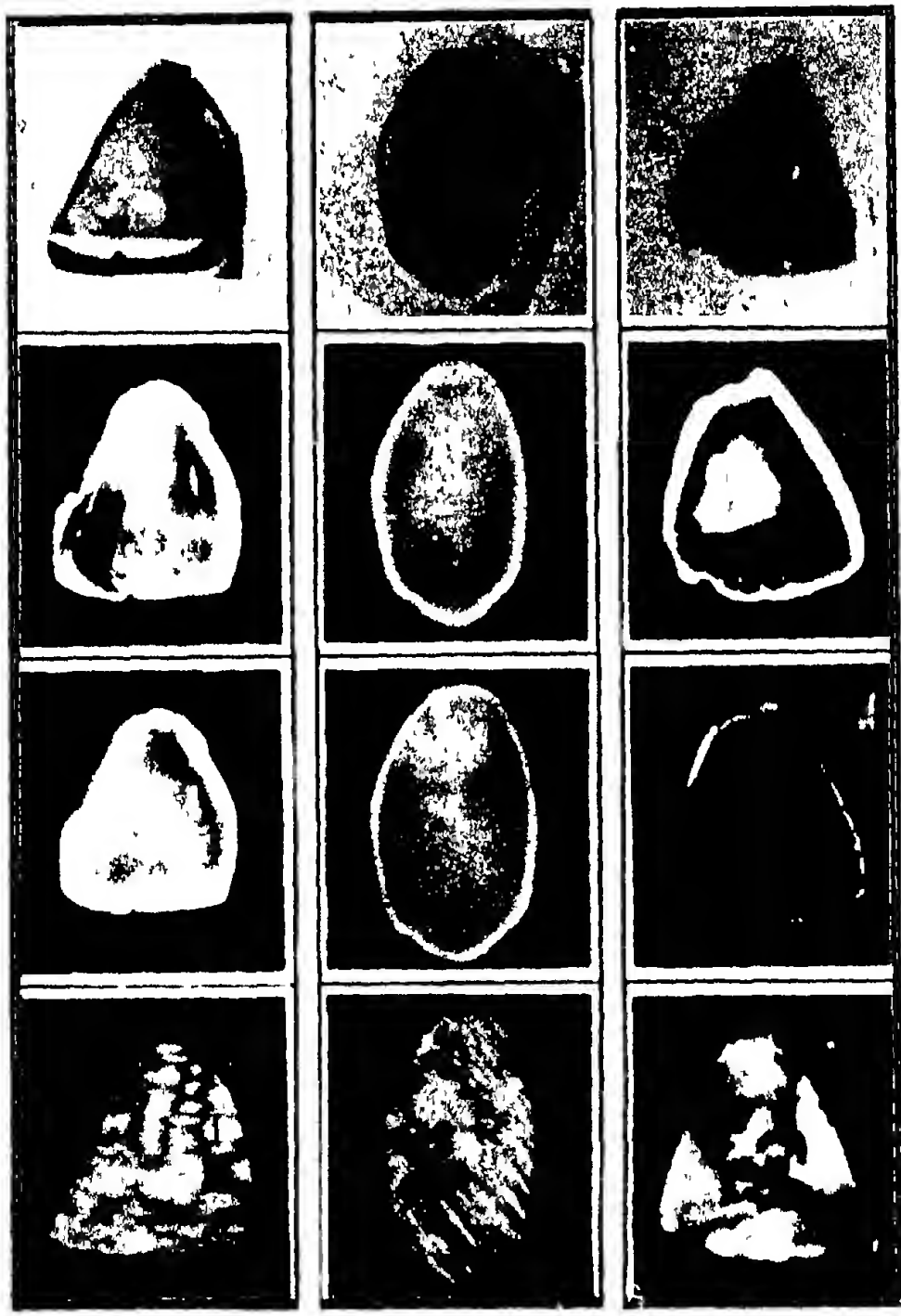

B 1 No. 111 No. 80

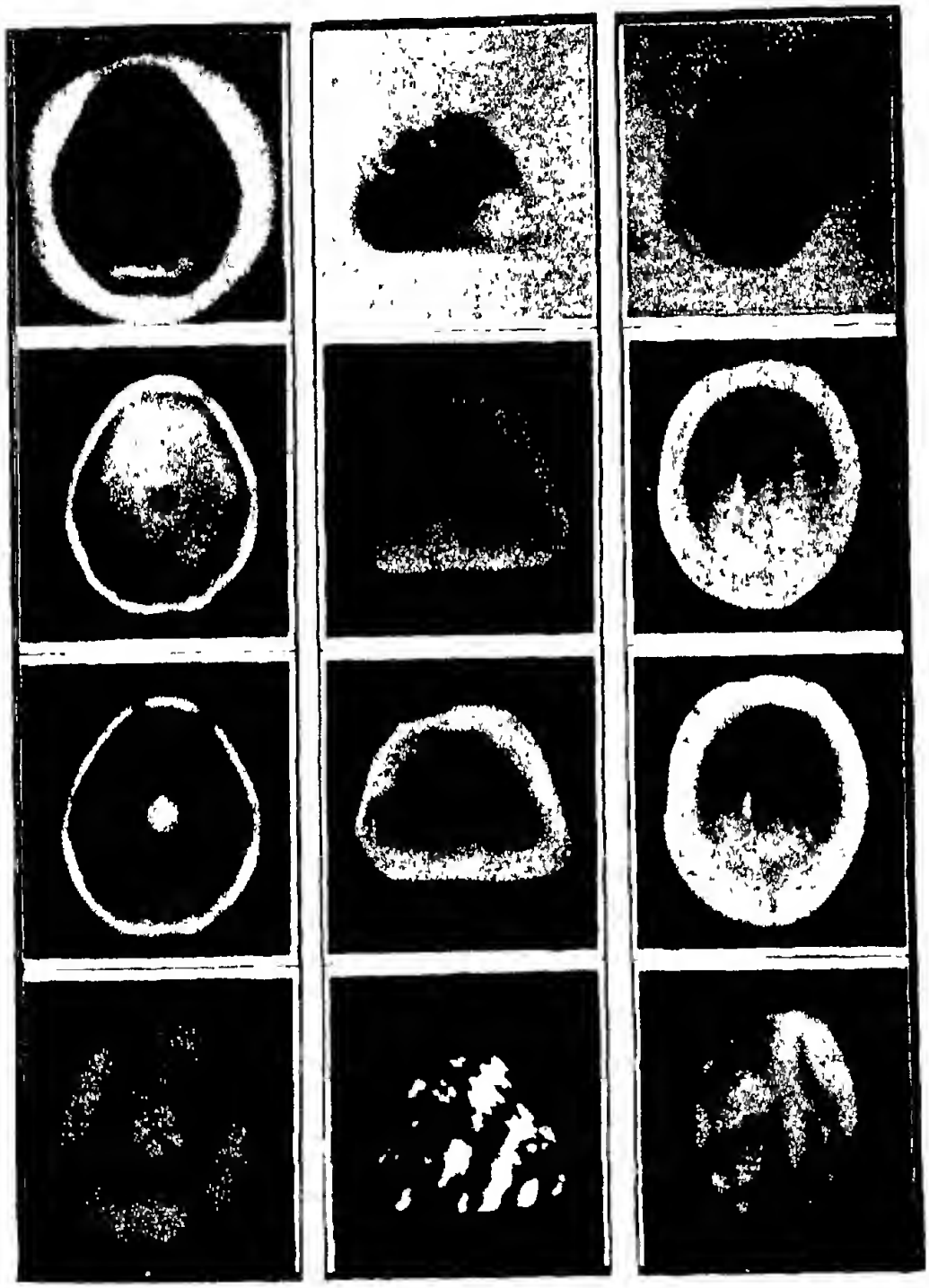

(a)

(b)

(d)

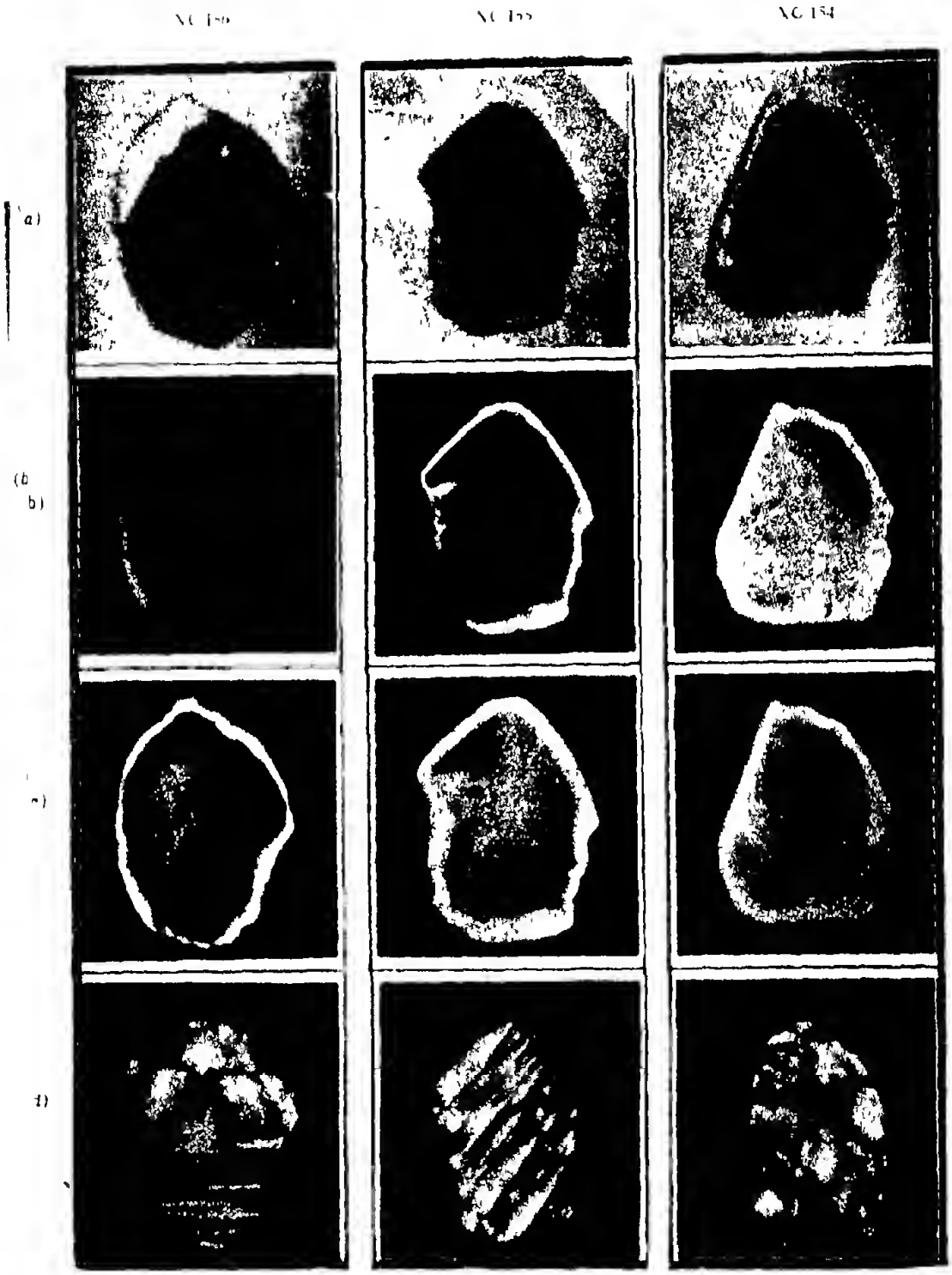
XC 150
XC 152
XC 154
(a)
(b)
(c)
(d)

XC 17

B1

Summary

The blue and yellow patterns of luminescence exhibited by 19 cleavage plates of diamond have been photographed separately using appropriate light filters, and are reproduced along with the patterns of transparency of the same plates to the λ 2536 radiation of the mercury arc and their birefringence patterns Study and intercomparison of the patterns enables the correlations between luminescence, ultraviolet transparency and birefringence to be readily perceived and interpreted with reference to the structure of the crystal The blue and yellow patterns are often strikingly different In some cases, they both appear as parallel bands, but running in different directions through the crystal

References

1 Achyutan, K *Proc Ind Acad Sci*, 1946, 24A, 165
2 Mani, Miss A *Ibid*, 1944, 20, 323
3 Ramachandran G N *Ibid*, 1944, 19, 280
4 Raman, Sir C V *Curr Sci*, 1943, 12, 33
5. ——— *Proc Ind Acad Sci*, A, 1944, 19 199
6 ——— and Rendall, G R *Ibid*, 1944, 19, 265
7 Ramanathan K G *Ibid*, 1946, 24, 135
8 Rendall, G R *Ibid*, 1944, 19, 293
9. Sunanda Bai, K *Ibid*, 1944*a*, 19, 253
10 ——— *Ibid*, 1944*b*, 19, 274

Explanation of Plates XIV to XX

(*a*) Ultraviolet Transparency Pattern
(*b*) Blue-luminescence Pattern
(*c*) Yellow-luminescence Pattern
(*d*) Birefringence Pattern.

Important Note—In the case of N C 151 on Plate XVII, (*b*) is yellow-luminescence and (*c*) is blue-luminescence pattern.

LUMINESCENCE AS "FORBIDDEN" ELECTRONIC TRANSITIONS IN DIAMOND

By G N Ramachandran and V Chandrasekharan

(*From the Department of Physics, Indian Institute of Science Bangalore*)

Received June 13, 1946

(Communicated by Sir C V Raman, KT F R S N L)

1. Introduction

The fluorescence spectrum of all diamonds at the room temperature exhibits an electronic line at 4156 Å, which also occurs in absorption, accompanied by vibrational bands on the longer wavelength side of it (Nayar, 1941) When the diamond is cooled to liquid air temperatures, the electronic line becomes sharp and is resolved into a doublet with a mean wavelength of 4152 Å The separation of the doublet is variable, depending on the specimen, but is not less than 2 Å or about 12 cm^{-1} A number of other electronic lines are also observed, of which one at 5032 Å is also accompanied by subsidiary bands (Mani, 1944) This, however, is very weak in blue-luminescing diamonds In this paper, we shall discuss the nature and origin of the doublet at 4152 Å, which is present in the spectrum of all fluorescing diamonds

The first question that arises in this connection is "What is the agent which gives rise to luminescence in diamond?" In the past, it has been generally supposed that some chemical impurity present in the diamond is responsible for the fluorescence As has been, however, shown by Sir C V Raman (1944), there are good reasons for believing that this is not the case. Blue fluorescence is a very general and characteristic property of diamond irrespective of its source of origin and especially of the diamonds which are chemically the purest and physically the most perfect Blue-fluorescing diamonds exhibit little or no birefringence, while the comparatively less common non-luminescent ones show a characteristic laminated structure accompanied by a strain pattern in the polariscope The X-ray studies made by one of the authors (Ramachandran, 1944, 1946) indicate, in agreement with this, that the non-luminescent diamonds possess a high degree of mosaicity of structure, while the blue-fluorescent ones make a near approach to the ideal of crystal perfection These considerations, as well as the close relationships observed between luminescence and other physical properties of diamond, make it highly improbable that it is due to extraneous impurities,

On the other hand, one is led to suppose that the electronic transition is really one occurring between levels belonging to the diamond structure itself There are, however, considerations to show that the transition is ordinarily forbidden, but that it has become allowed under the conditions existing in the fluorescing diamonds A study of the refractive index and dispersion of both ultraviolet opaque (fluorescing) and ultraviolet transparent (non-fluorescing) diamonds shows that these do not sensibly differ in the two cases (Martens, 1901, Peter, 1923) and that the variation of the refractive index with wavelength can be represented by a formula using two characteristic frequencies lying in the extreme ultraviolet, *viz*, at 1750 and 1060 Å respectively (Peter, *loc cit*) The contribution of the electronic transition at 4152 Å to the dispersion of diamond is negligible, except probably in the close neighbourhood of this wavelength, where no measurements have been made. This means that the probability of the transition is small, which is equivalent to saying that it is ordinarily forbidden

There are several cases known in which such forbidden transitions occur in crystals giving rise to both fluorescence and absorption In ruby, for example, the principal lines in fluorescence and absorption have been attributed to transitions between different levels in the normal configuration $3d^3$ of Cr^{+++} (Deutschbein, 1932) As is to be expected, the wave-numbers do not coincide exactly with those deduced from the energy levels of Cr IV, but are quite close to them Similarly, a large number of lines have been found in absorption in $KCr(SO_4)_2$ of which the sharpest and the most intense can be attributed to some of the forbidden transitions in Cr^{+++} (Spedding and Nutting, 1934) However, a study of the absorption spectra of a large number of chrome alums shows that the wave-numbers of the intense lines in the red vary appreciably with the compound concerned over a range of nearly 300 cm^{-1} (Kraus and Nutting, 1941) Similar results have also been found with the salts of the rare earth elements Ellis (1936) has given reasons to believe that the absorption lines observed in these are due to forbidden transitions taking place between low-lying levels belonging to the normal configuration of the atoms Calculations of the term values of such levels for Tm^{+++} made by Bethe and Spedding (1937) show remarkable agreement with experimental values. These observations suggest that we might reasonably look for a similar transition to explain the fluorescence in the case of diamond also.

2 Electronic Energy Levels in Diamond

In order to obtain an idea of the energy levels in diamond, it is useful to consider the case of the carbon atom and see if there are any levels in it,

transitions between which are ordinarily forbidden. The authors, however, do not wish to suggest that it is the carbon atom which gives rise to fluorescence in diamond The energy levels in the carbon atom are only brought in as an analogy in order to obtain an idea of where to look for other forbidden transitions, if any.

The normal configuration $2s^2 2p^2$ of the carbon atom consists of 3 levels, *viz*, a group of three levels ($^3P_0$, $^3P_1$, $^3P_2$) forming the ground state and two excited levels $^1D_2$ and $^1S_0$ The term values of these levels with respect to the ground state of C II can be obtained from standard tables (Bacher and Goudsmit, 1932) In Fig 1 (*a*) an energy level diagram is given with the term value of the $^3P_0$ state taken to be zero. The scheme of energy levels is identical with that in a number of other cases where forbidden transitions have been observed, *e.g.*, that of N II, O III and Pb I and that of O I, except for the inversion of the triplet levels of the ground state ^3P On the analogy of these cases (Bowen, 1936; Mrozowski, 1944), the transitions which might be expected to occur in C I are shown in Fig 1 (*a*) The lines $^3P_1$–$^1S_0$ and $^3P_2$–$^1S_0$ have been observed in Pb I by Mrozowski (*loc cit*) As will be seen from the diagram, these lines in the case of C I have wave-numbers 21632

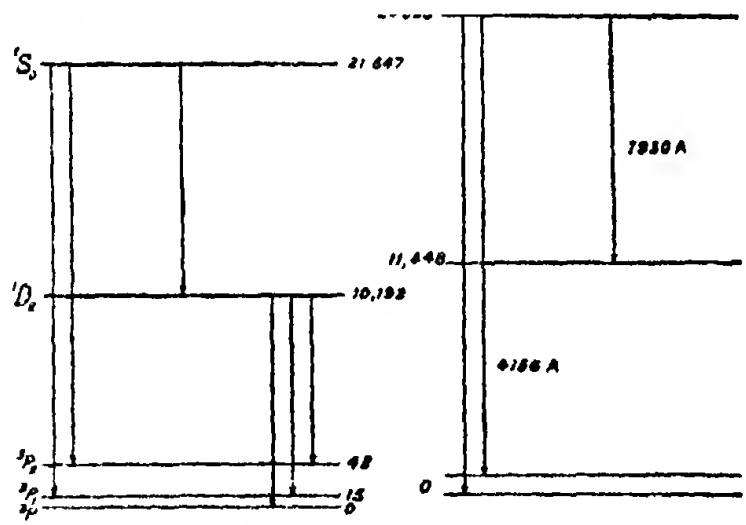

Fig 1*a* Energy levels in carbon atom Fig 1*b* Energy levels in diamond

and 21605 respectively, thus forming a doublet with a separation of 27 wave-numbers. As already remarked, the 4152 Å line is also a doublet. One may therefore take the above transitions in carbon to correspond to the 4152 Å line (24077 cm^{-1}) in diamond. It will be noticed that the wave-number of the diamond doublet is 1·114 times that in C I.

Following the analogy, one may expect an intermediate level in diamond corresponding to the $^1D_2$ level in C I A rough idea of the term value of this level can be obtained if we assume that this also is shifted in the same ratio as the one corresponding to the ^1S level in the carbon atom The value comes out to be 11340 cm.$^{-1}$ Now, transitions from the ^1D to the ^3P level have been observed in auroral and nebular spectra in the case of N II, O III and O I and in the laboratory in O I and Pb I Similarly, the transition ^1D–^1S has been found to occur in all the cases, except Pb I where it lies in the infra-red On the basis of these analogies, one may expect emission lines in diamond at about 7849 Å and 8816 Å An attempt was therefore made to discover whether any such lines actually occur

3 Search for the Emission Lines in the Infra-Red

An intensely blue-luminescent diamond (N C 67) was used for the purpose and was excited by ultraviolet radiation between 3600 and 4050 Å by using light from a carbon arc filtered through Wood's glass The red and the infra-red rays transmitted by this glass were cut out by means of a filter of copper sulphate solution In practice, a round-bottomed flask containing a 10% solution of copper sulphate was used to focus the carbon arc on the diamond. The fluorescence spectrum of the diamond was photographed with a Zeiss 3-prism spectroscope having an aperture of *f*/2 3 With this instrument, the 4152 spectrum could be obtained in 5 seconds, while it required nearly 3 hours to record the infra-red. The spectra were photographed on Kodak extra-rapid infra-red plates which were sensitive upto 8500 Å (See Plate XXI)

Actually, it was found that there was a sharp emission line in the fluorescence at 7930 Å This is clearly shown in Fig 2 (*a*) at the position indicated by the arrow The line has also been obtained with another brilliantly blue-fluorescent diamond N C 68, whose spectrum is shown in Fig 2 (*b*). It may be noticed that the line at 7930 Å is actually sharper than the one at 4152 Å indicated by the arrow in Fig. 2 (*d*) This is probably due to the very small dispersion of the spectrograph in the infra-red region The wavelength of the observed line agrees fairly closely with the expected value of 7849 Å. The other expected line was not recorded, being beyond the limit of sensitiveness of the photographic plate that was available

It is of interest to examine whether the line at 7930 Å arises from a transition from an upper level to an intermediate level, or whether it is an ordinary transition to the ground level, many examples of which are known For example Mani (1944) has recorded a number of such electronic lines, occurring both in emission and absorption by diamond, of which those at

5032, 4959, 5359 come out strongly. Two tests can be done to decide the issue If the transition were one ending in an intermediate level, then it should not occur in absorption and also it should not be emitted unless the exciting light has a wavelength smaller than 4152 Å The first test, of course, is not very sensitive since it depends on a negative result and may be affected by the fact that a sufficiently long column has not been used for absorption. However, the experiment was tried and it was found that although the absorption line at 4152 Å came out quite clearly, no trace of any absorption could be found in the neighbourhood of 7930 Å

The second condition for the emission of the infra-red line was also verified. Using the light from a carbon arc filtered through a green filter (which transmitted strongly from 4800 Å to 6000 Å and weakly upto 7000 Å) as the exciting radiation, an exposure of 3 hours only brought out the continuous spectrum in the infra-red weakly An exposure of 8 hours was required to record the continuous spectrum with about the same intensity as with ultraviolet excitation, but yet the line at 7930 Å was not recorded [see Fig. 2 (*c*)]

These observations strongly support the idea that the transition is one occurring from the higher excited level to an intermediate level. In Fig. 1 (*b*) are shown the energy levels in diamond as calculated from the results reported in this paper.

Our grateful thanks are due to Prof. Sir C V Raman for the kind interest that he took in this investigation

SUMMARY

Arguments are adduced to show that the doublet centred at 4152 Å occurring in the spectrum of all fluorescing diamonds arises from ' forbidden ' transitions analogous to the forbidden ^3P–^1S transitions in the spectrum of C I. On the basis of this analogy, fluorescence lines are also expected to occur at about 8816 Å and 7849 Å, analogous to the ^3P-^1D and ^1D–^1S transitions in C I Of these, the former should also occur in absorption, while the latter should not occur in absorption and should be emitted only if the exciting radiation has a wavelength shorter than 4152 Å A line has actually been found at 7930 Å, satisfying the latter conditions. The former line could not be recorded being outside the limit of sensitivity of the photographic plate,

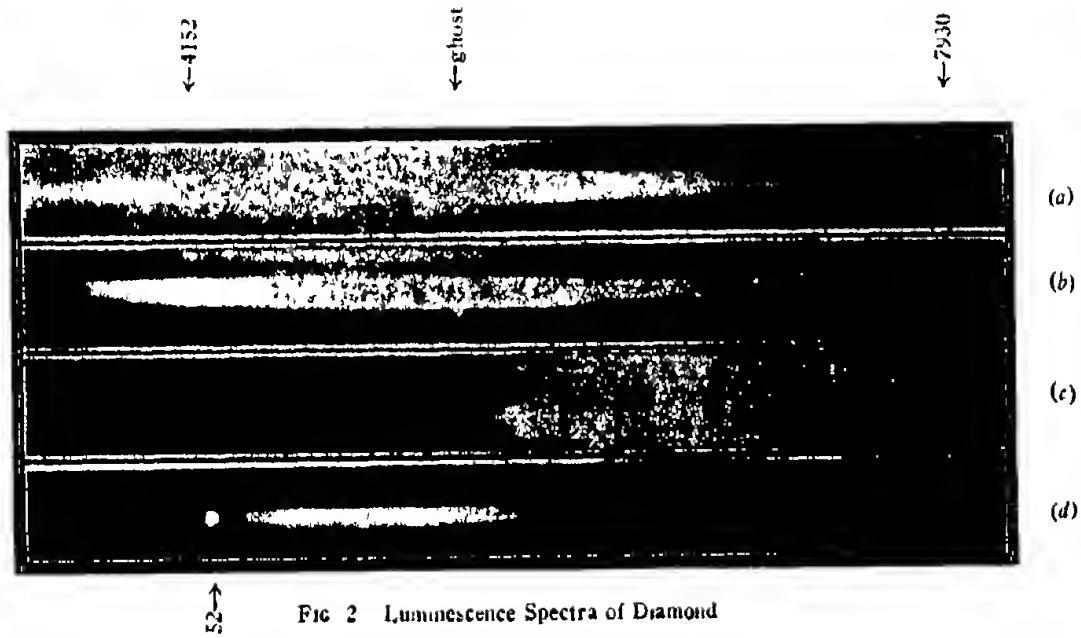

FIG 2 Luminescence Spectra of Diamond

REFFRENCES

1. Bacher and Goudsmit — " Atomic Energy States ", McGraw Hill, 1932
2. Bethe, H A , and Spedding, F H — *Phys Rev* , 1937, **52**, 454
3. Bowen, I. S. — *Rev Mod. Phys* , 1936, **8**, 55
4. Deutschbein, O — *Zeits f Phys* , 1932, **77**, 489
5. Ellis, C B — *Phys. Rev* , 1936, **49**, 875
6. Kraus, D L , and Nutting, G C — *Ibid* , 1941, **9**, 133
7. Mani, Miss A — *Proc Ind Acad Sci* , 1944, **19A**, 231
8. Martens — *Ann d Phys* , 1901 **6**, 605.
9. Mrozowski, S — *Rev Mod Phys* , 1944, **16**, 153
10. Nayar, P. G N — *Proc Ind Acad. Sci* , 1941, **13A**, 284
11. Peter — *Zeits f Phys* , 1923, **15**, 358
12. Ramachandran, G N — *Proc Ind. Acad Sci* , 1944, **20A**, 245 , 1946, **24**, 95
13. Raman, Sir C V — *Ibid* , 1944, **19**, 199
14. Spedding, F H , and Nutting, G C — *Journ Chem Phys* , 1934, **2**, 421

PHOSPHORESCENCE PATTERNS IN DIAMOND

By V Chandrasekharan

(From the Department of Physics, Indian Institute of Science, Bangalore)

Received June 5, 1946

(Communicated by Sir C V Raman, Kt, F R S, N L)

1 Introduction

That some diamonds continue to shine for a while in darkness after exposure to sunlight has long been known and to this phenomenon is applied the term phosphorescence The brightness of the phosphorescence varies enormously for different diamonds, and this variation is closely related to the strength of emission of visible light under ultraviolet irradiation which in general is known as fluorescence Brightly phosphorescent diamonds are also brightly fluorescent However, there is a striking difference in this respect between yellow-fluorescent and blue-fluorescent diamonds (Raman, 1944) The former have a short-lived and scarcely noticeable phosphorescence, while the latter have a bright glow lasting for several minutes The glow in both types of diamond is greenish yellow By viewing the diamond through a suitable violet filter, Sir C V Raman discovered that for a brief duration of a few seconds, there is blue light accompanying the greenish yellow glow in the case of brightly blue-fluorescent diamonds. But it is the latter that carries most of the energy emitted

Researches carried out at this Institute (Raman, 1943) have revealed that cleavage plates of diamond often exhibit patterns of fluorescence due to variations in *intensity* of the emitted light from various parts of the plate, and in many cases also variations of *colour* A detailed investigation of these patterns appears in a paper by G R Rendall (1946) in the present symposium. The results of the investigation show that while some diamonds exhibit only blue or yellow fluorescence patterns, others exhibit both of them, and these patterns may be entirely different. Visually it is noticed that cleavage plates which exhibit fluorescence patterns also exhibit phosphorescence paterns, that is, variations of the intensity of the phosphorescence. The object of the present investigations was to photograph such patterns so that they could be studied at leisure and compared in detail with the fluorescence pattterns The main difficulty in obtaining such patterns is the feebleness of the phenomenon requiring long exposures of more than 50 hours if a phosphoroscope and a camera are used. This has been successfully

overcome by the use of the ingenious method of contact photography suggested by Mr Hermann Yagoda in a letter to Sir C V Raman The method consists in placing the luminous plate of diamond in direct contact with a sensitive photographic plate in the dark and developing the plate subsequently The records obtained by this method are presented in this paper The interesting result has emerged that the yellow phosphorescence emission corresponds to the blue-fluorescence pattern, and that the yellow-fluorescence patterns are not recorded in phosphorescence

2 Experimental Technique

The technique used in getting the phosphorescence patterns was extremely simple The best source for exciting the phosphorescence in diamond was found to be sunlight between 10 A M and 2 P M Sunlight was reflected by a heliostat into a hollow brass tubing fixed in one of the walls of a dark room. Close to this tubing was fixed a lens of aperture 10 cms and focal length 15 cm Just in front of the lens was placed a Corning glass filter (3" × 3"), which allows only the ultraviolet light between 3500 and 4000 Å and a little red light above 7000 Å to pass through The filter also served the useful purpose of cutting off the long-wave radiations which would otherwise heat the diamond The specimens used in these experiments were cleavage plates of diamond in the collection of Sir C V Raman A hypersensitive panchromatic HP3 plate was kept in readiness inside a darkened chamber. The cleavage plate was held for about a minute in the path of the ultraviolet beam and transferred quickly into the chamber and placed in contact with the sensitive side of the photographic plate After half an hour, by which time the glow would have practically disappeared for even the most intensely blue-luminescent specimens, the diamond was removed and the photographic plate was developed A photograph showing great wealth of detail was obtained which may be called the phosphorescent pattern of the diamond, as the prints show at a glance the large variations in the intensity of the evanescent light over the different portions of the same diamond.

In the case of moderately luminescent specimens, the diamonds were placed in contact with a mirror silvered on the front and after excitation dropped along with the mirror on the photographic plate. Thus, a nearly fourfold increase in intensity was obtained as the phosphorescence is doubled up in intensity and the mirror reflects half the phosphorescent light back to the photographic plate. The clarity was not, however, lost as the diamonds were very thin, being rarely more than 1 mm thick Another method of obtaining an increase in intensity of the glow—employed especially for big

cleavage plates—was to hold the diamonds at the focus of the ultraviolet light and oscillate the diamonds quickly so that the whole area of the plate is excited uniformly to the maximum possible activation

One of the possible methods of obtaining the patterns in weakly luminescent diamonds would be to increase the aperture of the lens beyond $f/1$ 5 used in the experiments Alternatively, a big concave mirror could be used But the best method would be to make an arrangement by which the diamonds could be replaced in exactly the same position on the photographic plate By this method the procedure can be repeated a number of times and each time the exposure need only be for a short time of 2 or 3 minutes, as weakly phosphorescent diamonds have a short-lived glow.

In the case of the intensely blue-fluorescent diamond N C 79, it was dropped on the photographic plate half a minute after excitation (Fig 1 in Plate XXII) Also to show that the glow is mainly yellow and not blue, two more photographs of the glow were obtained by placing two thin gelatin filters respectively between the diamond and the HP3 plate. One of the filters was yellow and transmits wavelengths above 5000 Å, while the other was a violet filter transmitting wavelengths below 5000 Å and above 6300 Å From Fig. 2 in Plate XXII which was obtained with the yellow filter, it is clearly seen that the energy of phosphorescence is almost entirely in the yellow In the picture obtained with the violet filter (not reproduced), the outline of the diamond was barely visible.

The contact method of photography used in the present investigations might be suitably adapted for taking fluorescent patterns in very feebly fluorescent diamonds. Between the diamond whose pattern is required and the photographic plate a thin cellophane filter, which cuts off the ultraviolet light completely might be placed, ultraviolet light alone being incident on the diamond Thus the fluorescence pattern alone will be recorded on the photographic plate

3. Description of the Patterns

The phosphorescence patterns of 12 cleavage plates of diamond of different size and shape are reproduced in Plates XXII and XXIII and the prints have been made of the same size by a suitable enlargement of the negatives All the diamonds are strongly fluorescent, N C. 79 being the most intense blue-fluorescent one. The others exhibit varying colours in fluorescence due to mixing of the blue and yellow fluorescence in different proportions. N C. 110 and N C 107 are triangular and N C 85 is rod-shaped. N C 80 and N.C. 108, are circular, N.C 106, N C. 107 and N C. 114 are very small and thin, while B1, B2, B3 and B4 are large plates.

In most cases, geometric patterns of phosphorescence are obtained N C 110 shows nearly parallel bands, N C 80, N C. 85, N C 107 and N C 114 exhibit triangles, while B 1, B 2, B 3 and B 4 show hexagons N C 108 shows an interesting pattern which resembles a spider's web

4 COMPARISON OF PHOSPHORESCENCE AND FLUORESCENCE PATTERNS

The comparison of phosphorescence with the fluorescence patterns in the same diamond confirms the observation that brightly blue-fluorescent portions have bright phosphorescence Thus in the case of purely blue-fluorescent diamonds, both the patterns are exactly analogous As an example the case of N C 79 (old number D 34) might be cited The bright blue patch comes out brightly in the phosphorescence patterns also The fluorescence patterns of this and of N C 85 and N C 106 (old numbers D 42 and D 186 respectively) are given in the paper by Sunanda Bai (1944) in the earlier symposium

In the case of diamonds showing the mixed type of fluorescence, however, the phosphorescence patterns were compared with the blue and yellow fluorescence patterns recorded separately in the paper by Rendall (1946) which appears in the present symposium There, the fluorescence patterns of N C 80, N C 108, N C 110, N C 114 and B 1 are represented. The comparison at once reveals that it is the blue and not the yellow pattern that is recorded in the phosphorescence pattern in spite of the fact that the glow is yellow. Striking examples are N C 110 and N C 114 which show entirely different patterns in the yellow and blue as might be seen in the abovementioned paper. In the yellow fluorescence patterns of these diamonds there are straight parallel bands In the blue, N C 110 exhibits curved bands and a portion at the left bottom is comparatively weakly luminescent The phosphorescence pattern is identical with the blue-fluorescence pattern In the blue, N C 114 exhibits a patch at the right while the parallel bands appearing in the yellow are entirely missing. The phosphorescence pattern of this diamond shows a bright portion at the right and resembles the blue pattern. However a small portion at the bottom of the bright patch in the blue fluorescence is not recorded in phosphorescence These observations confirm the finding that yellow fluorescence has only a feeble and short-lived phosphorescence accompanying it. As further confirmation of this, a brightly green-fluorescent diamond was tried and gave an extremely feeble picture showing only the bare outline (not reproduced)

N C. 80 exhibits nearly the same patterns both in blue and yellow fluorescence and the phosphorescence pattern is similar to both. N C. 108 has a bright central spot in the blue fluorescence surrounded by a spiral,

while in the yellow the spot is absent In phosphorescence the central bright spot along with the spiral comes out

In all the photographs the edges of the diamond come out strongly as they have bright blue-fluorescence and hence strong phosphorescence. In the case of the phosphorescence pattern of B 1, there is a bright patch in the middle of the hexagon, while in the blue fluorescence pattern this is entirely absent In the cases of B. 2, B 3 and B 4, a larger number of concentric hexagons are obtained in phosphorescence than in fluorescence patterns. In these cases and that of N C 114 referred to above, therefore, there are slight departures from the exact identity of the phosphorescence patterns with the blue-fluorescence pattern.

In conclusion the author wishes to express his grateful thanks to Prof Sir C V Raman for suggesting the problem and for the invaluable guidance given during the investigations

Summary

Phosphorescence patterns in a dozen cleavage plates of diamond revealing the variations in intensity of phosphorescence in different portions of the same diamond have been successfully recorded by the method of contact photography. Comparison of these with the fluorescence patterns in the same diamond shows that the yellow phosphorescence emission corresponds to the blue fluorescence patterns, and that the yellow fluorescence patterns, if present, are not recorded in phosphorescence Geometric patterns such as parallel bands, triangles, hexagons and spirals have been obtained in many cases.

References

Raman, C. V — *Proc Ind Acad Sci.*, 1944, 19, 214
——— — *Current Science*, 1943, 12, 42
Rendall, G R — *Proc Ind Acad Sci.*, 1946, 24, 168
Sunanda Bai, K. — *Ibid*, 1944, 19, 278.

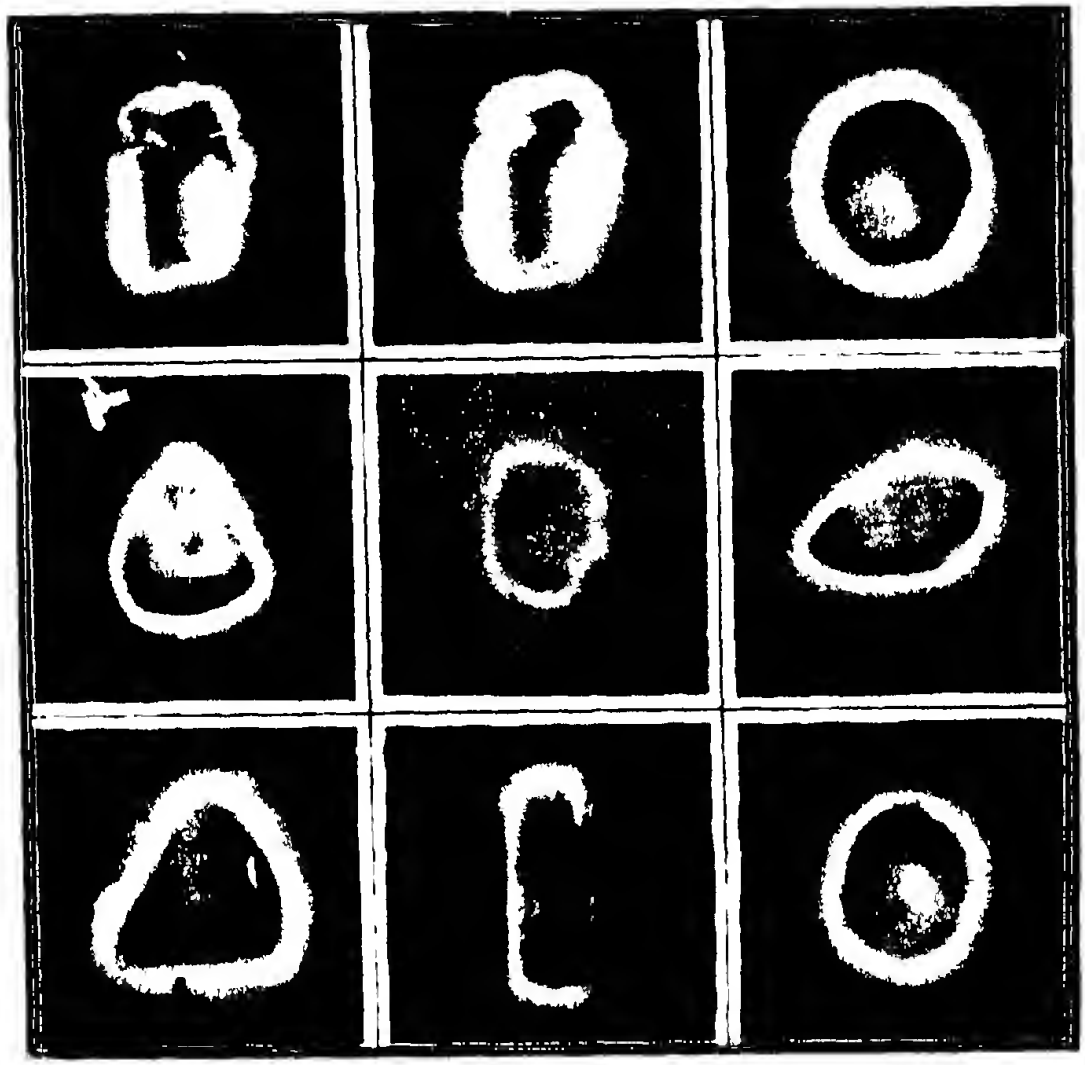

Fluorescence Patterns in Diamond

N.C. 79	N.C. 79	N.C. 80
N.C. 107	N.C. 114	N.C. 106
N.C. 110	N.C. 85	N.C. 108

B 1

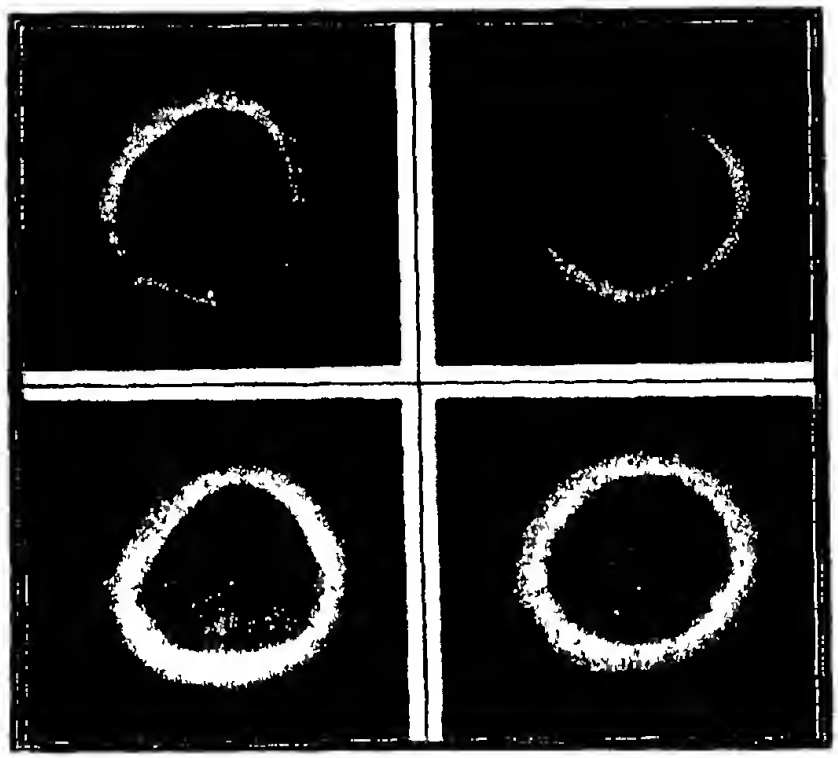

B 3 B 4

Phosphorescence Patterns in Diamond

THE THERMOLUMINESCENCE OF DIAMOND

By V. Chandrasekharan,

(From the Department of Physics, Indian Institute of Science, Bangalore)

Received June 13, 1946

(Communicated by Sir C V Raman, Kt., F R S., N L)

1 Introduction

Some substances have the property of storing up energy under suitable excitation which they later release The release of energy as visible light at the temperature of excitation is known as phosphorescence But, even after the afterglow has decayed, the substance may retain some of the stored-up energy which manifests itself as light on heating the substance in darkness. To this phenomenon is applied the term thermoluminescence That some diamonds exhibit thermoluminescence has long been familiar to several investigators in the past In the twelfth century, Albertus Magnus by placing the diamond in hot water noticed the glow, while in the seventeenth century, Robert Boyle held a diamond near a flame and observed its glimmering on removing it quickly to a distance However, there seems to be no recent work on the subject mentioned in the literature The present paper describes the results of a study of thermoluminescence undertaken by the author, and these are briefly enumerated below

Fluorescent diamonds, after exposure to ultraviolet of the sun, glow in darkness with a greenish-yellow colour In the case of brightly blue-fluorescent diamonds, Sir C V Raman discovered that for a brief duration of a few seconds, there is blue light accompanying the greenish-yellow glow which lasts for several minutes On raising the temperature of the diamond to 270° C., the colour of the visible afterglow changes to blue and it is very bright. This thermoluminescence is observed even if the diamond is heated a few days after activation, by which time the ordinary phosphorescence would have completely disappeared There is the yellow portion also in the blue thermoluminescence, as can be verified by viewing the diamond through an yellow filter. Another important result of the investigation is that the ultraviolet light below 3200 Å is able to excite thermoluminescence more efficiently than ultraviolet between 3500 and 4000 Å, even though the former excites little phosphorescence at room temperature. X-rays are also able to produce a slight activation. The effect of irradiation of the diamond with light of wavelength greater than 4200 Å is to practically remove the activa-

tion in diamonds even at or below room temperature Green fluorescent diamonds show a weak greenish-yellow thermoluminescence.

2 Phosphorescence

In order to facilitate an understanding of the thermoluminescence, the main facts about the phosphorescence of diamond are briefly stated below They will be dealt with in greater detail in a separate paper on the subject appearing in the present symposium The source of light used in the study was sunlight and the arrangement was that described in the paper on phosphorescence patterns also appearing in the present symposium

Blue-fluorescent Diamonds—The colour of the light emitted by blue-fluorescent diamonds under the ultraviolet of the sun changes suddenly to greenish yellow when the exciting radiation is cut off. The afterglow can be seen for about half an hour in darkness in the case of the strongly blue-luminescent diamonds Observation of the diamond through suitable light filters enables us to obtain an idea of the nature of the phosphorescence spectrum It is found that the glow can be seen with almost undiminished intensity through an yellow filter transmitting above λ 5000 for practically the whole of its duration On the other hand, through a violet filter cutting off between 4950 and 6300 Å the diamond is visible faintly for a relatively short duration of about 20 seconds Thus the energy of the phosphorescence is mainly in wavelengths above 5000 Å. This is further confirmed by viewing the diamond through a filter which has its cut-off between λ 5200 and λ 6250 The phosphorescence is then seen more brightly and for a longer duration of a few minutes On viewing the afterglow through a direct vision spectroscope, the spectrum is found to extend at first on both sides of λ 5000, but in a few seconds the spectrum on the violet side diminishes in intensity relatively to that on the green side However, the entire spectrum also becomes very feeble and it is not possible to continue its study after the first few seconds. There is no red phosphorescence, as the glow is invisible through a red filter transmitting above 6300 Å The brightness of the phosphorescence increases with the intensity of the ultraviolet light used. However, a variation of the time of irradiation from one second to several minutes produced no perceptible increase in intensity of the glow, and the time for which the diamond can be perceived through the various filters remains unaltered. The brightness of the glow in different diamonds increases with the intensity of their fluorescence

One of the diamonds was cooled by immersing it in liquid air contained in a Dewar flask and then irradiated with ultraviolet light. On shutting

off the light, a greenish-yellow glow was detected for 30 seconds, as has already been mentioned in a paper by Nayar (1941)

Green-fluorescent Diamonds—Green fluorescent diamonds in striking contrast with the blue ones exhibit a faint greenish-yellow glow which lasts for only 40 seconds even in the case of the most brightly fluorescent specimens As the glow is faint and of short duration, it cannot be examined through filters

General Remarks—In the fluorescence spectra of all diamonds, electronic lines at λ 4152 and λ 5032 with their accompanying bands at longer wavelengths are recorded In blue-fluorescent diamonds the λ 4152 system is strong but the λ 5032 is also recorded in many cases though weakly In green-fluorescent diamonds, the λ 5032 system is strong but is always accompanied by the λ 4152 system though with relatively much less intensity On the other hand, the phosphorescence spectra of strongly blue-fluorescing diamonds recorded by Nayar (1941) and Miss Mani (unpublished work) show both the λ 4152 and λ 5032 system with comparable intensity Their spectrograms were obtained with a time-interval of the order of a fraction of a second between excitation and observation The visual observations described in the present paper indicate that with longer time-intervals the λ 4152 grows gradually weaker and disappears after a few seconds and that the subsequent phosphorescence consists exclusively of λ 5032 and its accompanying band system. Further experimental work is necessary to confirm this finding and also to investigate how the duration of the phosphorescence of any diamond depends upon the relative and absolute intensities of the λ 4152 and λ 5032 systems as exhibited in its fluorescence

3 Thermoluminescence

A blue-fluorescent diamond N C 67 was activated by exposing it to the ultraviolet light of the sun and was then placed on a hot plate whose temperature was about 100° C The glow brightened up but the colour remained unaltered When the temperature of the diamond was raised to 270° C., the glow was very bright and *blue in colour* However, the diamond could be observed through the yellow filter indicating that the yellow portion must also be accompanying the blue glow The blue thermoluminescence was perceived for about 10 minutes.

In all the above described experiments, ultraviolet light between 3500 and 4000 Å has been used To use ultraviolet light below λ 3000, the light from an iron arc was focussed by a quartz lens on the diamond. After shutting off the incident light the diamond showed little phosphorescence,

However, on heating the diamond, bright blue thermoluminescence was observed When during irradiation, a glass plate was introduced between the diamond and the quartz lens, the intensity of thermoluminescence became extremely small, showing that wavelengths below 3000 Å produce very high activation compared to wavelengths between 3500 and 4000 Å As a further confirmation of this, the diamond was held close to a water-cooled low-pressure quartz mercury arc and then heated to 270° C in darkness A brilliant blue glow was observed

The diamond N C 67 was activated by means of the light of an iron arc and kept in darkness After 10 days the diamond was heated to 270° C and a blue glow was observable Thus some energy can be stored up in the diamond for any length of time It should be realised, however, that the heating does not produce, but only releases the energy 'frozen in' at room temperature, as the thermoluminescence glow is not persistent at the high temperature like fluorescence, but decays (Pringsheim and Vogel, 1943) Thermoluminescence is nothing but phosphorescence at a high temperature In support of this view the heated diamond at 270° C was irradiated with ultraviolet light and on shutting off the light, the phosphorescence was bright blue P G N. Nayar has similarly observed that the phosphorescence at room temperature could be quenched at any stage of its life by immersion in liquid air and the residual part of its life completed on regaining the room temperature

The effect of X-rays in producing the activation in the diamond was tried The diamond N.C. 67 was heated for several minutes at 270° C until no trace of glow was detected and after cooling, it was irradiated by X-rays It was then again heated to 270° C in darkness and a faint blue glow appeared which was visible for about a minute

In the case of a green-fluorescent diamond N C 41, a comparatively faint *greenish-yellow* glow was detected for about 10 minutes on heating it to 270° C.

4 The Effect of Red Light

It has been stated above that the activation in N.C 67 could be retained for several days and released on heating it The diamond after activation was exposed for about a minute to bright red light of the sun obtained by the use of a red filter, and on heating the diamond subsequently an extremely faint glow was detected. Thus the activation was practically removed. Similarly, when the phosphorescing diamond was exposed for a minute to red light, the brightness of the phosphorescence was much smaller than what it would otherwise have been. A careful study of the effect of red light will

be presented in a later paper. It was found by the use of various filters that any wavelength above 4200 Å was able to remove the activation in diamond. In fact, if the diamond after exposure to focussed ultraviolet light of the sun was taken out into bright daylight, the activation disappeared practically as was verified by heating the diamond subsequently

5 Discussion

The foregoing experiments have made it clear that there are two distinct types of phosphorescence, one blue and the other yellow The former is faint and observable only for a short time at and below room temperature, while the latter predominates in the glow and lasts for a long time At high temperatures, the glow is blue showing that the blue then prodominates The ultraviolet light below 3000 Å is able to excite thermoluminescence with greater efficiency than the very near ultraviolet, while the converse is true of phosphorescence at room temperature These facts have to be remembered in presenting any theory of the phosphorescence of diamond.

The blue phosphorescence and thermoluminescence may be identified with the λ 4152 system, while the yellow phosphorescence and thermoluminescence may be identified with the λ 5032 system However, the diamonds which show the latter system brightly in fluorescence compared to the former, show only feeble greenish-yellow phosphorescence and greenish-yellow thermoluminescence

In the fluorescence of diamond, principally two electronic lines λ 4152 and λ 5032 are found (Anna Mani, 1944) and as these come out in absorption also, there are three main energy levels, one ground and two upper ones, in diamond The usual explanation of phosphorescence is based on the idea that there are metastable levels near the upper levels in which some electrons are trapped Due to the thermal agitation, these slowly leak to the main levels and from there they drop to the ground state emitting light. This view is supported in the case of the after-glow of diamond as both the 4152 and 5032 lines are observed in phosphorescence. There must also, however, be some traps from which the electrons cannot escape at room temperature On raising the temperature, however, the electrons are enabled to escape from these levels.

In conclusion the author wishes to thank Sir C V Raman, Kt, F R.S., N.L, for suggesting the problem and for the encouragement given during this work.

6. Summary

Blue-fluorescent diamonds show a greenish-yellow glow at room temperature after exposure to ultraviolet light In this glow, there is also a blue component which however decays more rapidly. On heating to 270° C. the colour of the glow changes to blue and the glow brightens up This effect, known as thermoluminescence, can be observed even if the diamond is heated a few days after activation Remarkably enough, radiations below 3000 Å are able to produce an activation greater than that produced by radiations between λ 3500 and λ 4000, even though the former give rise only to slight phosphorescence Even X-rays are able to produce a slight activation In the case of the green-fluorescent diamonds, the phosphorescence is feeble and greenish yellow in colour The thermoluminescence of these diamonds is greenish-yellow and is much fainter than that of blue fluorescent ones Light of any wavelength greater than λ 4200 is able to remove the activation in both varieties of diamond

References

Anna Mani — *Proc Ind Acad Sci*, 1944, **19**, 231

Chandrasekharan, V — *Ibid*, 1946, **24**, 193

Mellor, J W — *Treatise on Inorganic and Theoretical Chemistry*, **5**, 768.

Nayar, P G N — *Proc Ind Acad Sci*, 1941, **13**, 534

Pringsheim, P, and Vogel, M — *Luminescence of Liquids and Solids and its Practical Applications*, 1943 17

THE PHOSPHORESCENCE OF DIAMOND

By V Chandrasekharan

(*From the Department of Physics, Indian Institute of Science, Bangalore*)

Received June 15, 1946

(Communicated by Sir C V Raman, Kt, F R S, N L)

1 Introduction

A remarkable property of many diamonds is their power to store up energy under ultraviolet irradiation, a portion of which is released as visible light on shutting off the exciting radiation This phenomenon, known as phosphorescence, has been remarked upon by several early workers like Robert Boyle, Crookes, Becquerel and others However, the rest of the energy is retained in the diamond even for several days and released as visible light on either heating or more effectively on re-illuminating the diamond with long wavelength radiations even at or below room temperature. The former effect of heating has been dealt with in the paper on thermoluminescence appearing in the present symposium, while the latter is mainly dealt with in this paper The main facts about phosphorescence already summarised in the paper referred to are also presented here more fully

Diamonds which show bright blue fluorescence under ultraviolet light exhibit a greenish-yellow afterglow for about 30 minutes in which there is also a blue component during the first few seconds Sir C V Raman discovered this fact by the use of a violet filter and this technique of viewing the diamond through filters has been found extremely useful in studying the effect of re-illumination The green-fluorescent diamonds show only a feeble phosphorescence When blue-fluorescent diamonds after exposure to ultraviolet light are re-illuminated with red light and viewed through a filter complementary to the red, a very bright blue flash is observed which dies away in a few minutes. In the case of green-fluorescent diamonds, the flash is green. Both varieties of diamonds on heating lose their activation in the form of thermoluminescence Ultraviolet light below 3000 Å produces activation several times greater than that produced by radiation between 3500 and 4000 Å X-rays are also able to produce a slight activation Any wavelength above 4200 Å is able to remove the activation in diamonds

2. Phosphorescence

The main facts about the phosphorescence of diamonds have already been stated in the paper on thermoluminescence appearing in the present symposium. As the specimens N.C 67, N C. 68, and N C. 41 have been

used in the study of re-illumination with long wavelength radiations, their phosphorescence is described below. The former two are small brilliants and are intensely blue-fluorescent, while N C 41 is a moderately large crystal which is brightly green-fluorescent. N C 67 and N C. 68 after exposure to ultraviolet light of the sun exhibit a greenish yellow glow and the change of colour from the blue fluorescence to greenish yellow phosphorescence is very striking To find whether any blue phosphorescence is present in the glow, the diamond is viewed through a violet filter having a cut-off between 4950 and 6300 Å; a faint glow is then detected lasting for about 20 seconds The main bulk of the emitted energy is, however, in the yellow, as the brightness of the glow is practically undiminished by the interposition of an yellow filter transmitting wavelengths greater than 5000 Å The green-fluorescent diamond shows a faint greenish yellow glow lasting for about 40 seconds which is, however, too faint to be studied with filters

It is found that the decay of the afterglow in all cases is extremely rapid in the first few seconds It is proposed to take up the exact nature of the decay in a further communication

The fluorescence spectra of diamonds taken by Miss Mani (1944) reveal mainly a line at λ 4152 and a system of bands associated with it and also another line at λ 5032 and an accompanying band system. In the phosphorescence spectrum of N C 68 taken by Miss Mani (unpublished work), both systems appeared. As the time interval between irradiation and exposure was only a fraction of a second, the violet phosphorescence was present and was recorded as the 4152 system The green glow may be identified with the 5032 system which presumably has a long lifetime in the phosphorescence of blue-fluorescent diamonds

3 The Effect of Red Light

In order to follow the effect of re-illumination, it is important to recall the Stokes law of fluorescence The wavelength of the exciting radiation should be near about or less than the wavelength of fluorescence. Thus red light is unable to excite any visible fluorescence, and similarly green light cannot produce any violet fluorescence.

Blue-Fluorescent Diamonds.—The diamond N C 67 is exposed to ultraviolet light of the sun for about a minute and after shutting it off, red light obtained by passing sunlight through a red filter transmitting above 6300 Å is focussed on it On viewing the diamond through a 3 cm. filter of saturated copper sulphate solution which is complementary to red light, a bright blue flash is observed which decays very rapidly in the beginning and is visible for about four minutes. As red light cannot produce an

fluorescence, the flash is due to the release of the stored-up energy in the diamond by red light Even though the colour of the flash is blue, it also contains wavelengths from 5000 to 6000 Å This is shown by the fact that the glow can be observed both through a blue filter of ammoniacal copper sulphate solution transmitting wavelengths less than 4600 Å and through a green filter transmitting 5000 to 6000 Å

On illuminating the activated diamond with green light (5000 to 6000 Å) of the sun and observing through a complementary violet filter, a bright violet flash is observed for about two seconds, and subsequently there is a persistent faint red colour due to fluorescence produced by the green light. The violet flash is, however, due to the release of activation energy by the green light as is indicated by the decaying of the flash

The effect of both green light and red light can be noticed even a few days after activation by ultraviolet light This indicates that the stored-up energy is retained by the diamond and is released by exposure to green light for a sufficient time, since red light has subsequently no effect; also, *vice versa* If similarly the activated diamond is exposed to blue light (4100 to 5000 Å) for about a minute, any flash occurring during the exposure cannot be observed through a complementary filter owing to the presence of a persistent green and red fluorescence produced by blue light However, after such exposure, the diamond no longer shows any flash on irradiation with red light, thereby indicating that blue light is able to remove the stored-up energy presumably as a flash Using a monochromator with sunlight as the source, a preliminary study of the efficiency of different wavelengths in removing the activation in the blue-fluorescent diamond N C 68 has been made Green light near about λ 5500 appears to be the most efficient, but a more thorough examination of the facts will be published later It is also found that for a given wavelength, the brightness of the flash increases with intensity of the light used while the duration of visibility diminishes, showing that the whole of the stored-up energy is released in a shorter interval of time by a more intense source of light

The activation in diamond is increased on increasing the intensity of the activating ultra-violet light. However, as in the case of phosphorescence, the time of irradiation need only be a second Increased exposure times do not result in an observable increase in the intensity of the flash which results from illuminating the diamond with a constant source of red light.

When the radiations from a low pressure quartz mercury arc are used for activation, it was found that the blue flash obtained by subsequent irradiation with red light (above 6800 Å) is much brighter than when the

near ultraviolet between 3500 and 4000 Å is employed for activation In fact, the blue colour is clearly seen for a few seconds even in the presence of the intense red light in the former case, while a filter of copper sulphate solution has to be used to cut out the red light if the blue flash is to be observed in the latter case A very large part of the high activation produced by the quartz mercury arc is due to radiations below 3000 Å. This is shown by the fact that when a glass plate which cuts off these wavelengths is interposed between the diamond and the mercury arc, the activation is reduced to a very small fraction of its former strength It is also found that subsequent exposure to light between 3500 and 4000 Å reduces the large activation produced by radiations below 3000 Å

During any part of a flash if the illuminating light is cut off, the flash disappears instantaneously as far as the eye can judge The remaining part of the flash can be completed at any later time by illuminating again with the light

X-rays are also able to produce a slight activation. This can be verified by removing all previous activation in the diamond by exposure to bright red light for about half an hour and then irradiating it with X-rays for a few seconds. Subsequently, when red light is allowed to fall on the diamond, a feeble blue flash is observed through the copper sulphate filter

Green-fluorescent Diamonds—The green fluorescent diamond N C 41 behaves in exactly the same way with regard to all the above effects except for the fact that the flash is green as observed through copper sulphate solution and not blue. The major portion of the energy of the flash is hence in the green

Spectrum of the Flash—The diamond N C 67 after activation by focussing the light of a quartz mercury arc on it with a quartz lens, was placed very close to the slit of a Zeiss three-prism spectrograph. The light of a carbon arc was passed through a red filter transmitting wavelengths greater than 6300 Å and focussed on the diamond After one minute of exposure, the diamond was activated again and the experiment repeated 30 times. A faint spectrum (not reproduced) was obtained in the violet part and showed the 4152 line and its system of bands. To prove that the spectrum was not due to fluorescence, a blank experiment was performed in which the diamond was not activated with the mercury arc but a continuous exposure of one hour and a half was given with red light focussed on the diamond as before In the spectrum, no trace of the violet portion was found and only the band in the red region due to the incident light appeared.

In the case of the brightly green-fluorescent diamond N C 41, the 5032 line and its bands were found faintly with an exposure repeated 50 times in the manner described above

4 The Effect of Heat

It has been stated that the diamonds retain energy for several days after activation The activated blue-fluorescent diamonds on heating to 270° C exhibit blue thermoluminescence as stated in the paper on thermoluminescence After a few minutes the glow disappears, and after cooling the diamond shows no longer any flash on irradiating with red light and observing through copper sulphate solution In the case of the green-fluorescent diamond N C 41, a faint greenish yellow thermoluminescence is observed on heating to 270° C and subsequently the usual flash with red light is absent Thus at 270° C the diamonds lose their activation

On cooling the diamonds by immersing in liquid air, they showed every one of the usual effects resulting from activation

In conclusion, the author wishes to express his deep gratitude to Professor Sir C V Raman for his inspiring guidance and for his helpful interest in the problem

5 Summary

Fluorescent diamonds retain some energy after ultraviolet irradiation, a part of which is released at room temperature as phosphorescence However, a greater part of the energy remains with the diamond for any length of time until it is illuminated with long wavelength radiations; it is then emitted as a flash of visible light This can be observed through a proper filter complementary to the illuminating light Any wavelength above 4200 Å is able to remove the activation in diamonds Ultraviolet light below 3000 Å produces activation several times greater than that produced by the very near ultraviolet between 3500 and 4100 Å X-rays are also capable of producing a weak activation All these effects are observed even at liquid air temperature. However, the activation in diamond can be removed by heating it to 270° C when thermoluminescence is observed In the case of blue-fluorescent diamonds, the stored-up energy is given out mainly as a blue flash on illuminating them with long wavelength radiations and the spectrum of the flash reveals mainly the 4152 system, while in green-fluorescent diamonds, green light is mainly emitted and the 5032 system is found in the spectrum of the flash.

References

Anna Mani .. *Proc Ind Acad Sci*, 1944, **19**, 231
Chandrasekharan, V. .. *Ibid.*, 1946 **24**, 187.

608-46 Printed at The Bangalore Press Bangalore City by G Srinivasa Rao, Superintendent,
and Published by The Indian Academy of Sciences, Bangalore

GEOLOGY AND PETROGRAPHY OF THE BEZWADA AND KONDAPALLE HILL RANGES

Part I. Bezwada Gneiss and Associated Rocks

By M Srirama Rao
(*Andhra University*)

Received April 5, 1946
(Communicated by Prof C. Mahadevan, F A Sc')

Introduction

Bezwada is a growing town on the east coast of India, situated roughly about midway between Madras and Vizagapatam with a great strategic importance Kondapalle is a village about ten miles north-west of Bezwada and is a place of great historic antiquity At both these places massive ranges of hills rise abruptly above the plains of the Kistna to considerable heights The geological features of these hill ranges are complex and highly interesting and form the subject-matter of the present studies by the author.

The area covered in this work comprises about 140 square miles (sheet No. 65 D/10 on 1 inch 1 mile scale, Survey of India) and is included between 16° 30′ and 16° 41′ N latitude and 80° 30′ and 80° 40½′ E longitude. It forms a part of the Bezwada taluk in the Kistna District

In the present paper are set forth the results of the field work, optical and chemical studies of the rocks and their correlation to other well-known rock suites.

Previous Literature

The area studied comes under the Eastern Ghats Province in the Non-Charnockite region described by Fermor (1935) This province has not so far been studied in detail. For the earlier reports on this area we are indebted to Heyne (1814), Benza (1837) and Newbold (1844) The first reliable geological record, perhaps, is that of R. Bruce Foote (1879), who distinguishes the gneisses in this region as an entirely distinct petrological entity characterised by some local peculiarities; but, his classification does not seem to be based on any close petrological study. W. King's contribution (1880) deals partly with the stratigraphical sequence of the rock formations in the Bezwada as well as the Kondapalle hills. He contends that the Bezwada gneiss is younger than the Kondapalle gneiss as evidenced by its less highly metamorphosed condition.

It is evident from a perusal of the memoirs of Foote and King that at that stage of our knowledge of Indian rock formations, they did not recognise the identity of the "Bezwada Series" with the khondalites, or of the "Kondapalle Gneiss" with the charnockites, as detailed work on these was only done early in this century. Even the stratigraphical sequence deduced by them is not fully borne out by the careful study as evidenced by their giving the granites, for instance, a basal position in the rock groups; whereas, in point of fact, they are distinctly intrusive into the khondalites.

Later, Middlemiss (1903) notes the thorough permeation of the Bezwada gneiss by acidic material and accounts it as a myrmekite Some petrological studies having reference to parts of this area are to be found in Walker's monograph (1902) on the geology of the Kalahandi State wherein are set forth the results of a fairly detailed study of an adjoining region whose rock formations have a great deal of similarity to those of the Bezwada area

A recent paper by Krishnan (1944) summarising his observations on the chromite deposits of Kondapalle is succinct and clear with a brief description of the geology of the area

Physical Features

The area under discussion is, on the whole, more or less hilly. The plains have an average elevation of 70 feet above sea-level The two ranges of hills—one to the east and the other to the west of the Bezwada town—and the very huge chain of mountains extending northwards from Ibrahimpatnam and lying west of the Kondapalle village—all rise abruptly from the plains of the Kistna Valley The hills are of the 'relict type' and the remarkably level character of the ridge tops is a striking feature The hills round Mogalrajpuram contain caves, said to have been Buddhist hermitages, and are of archæological interest

Except the rather low-lying hills round about the Bezwada town, the rugged high hills in the Kondapalle region are clothed with sparse forests; but, the valleys amidst them—erosion valleys—support dense vegetation containing useful timber There is generally a very heavy, practically impenetrable, thorny shrubby growth which renders field work rather difficult. Ordinarily, therefore, only some stream courses and footpaths are readily available for geological observations. The hills are very rugged and rise to over 1,000 feet above the level of the plains, the highest point with an altitude of 1,406 feet being situated just a few hundred yards north of the celebrated fort of Kondapalle, which is now in ruins.

The Kistna is the only river within the area under report. It has reached its base level of erosion. At Bezwada an anicut is built across it. It is one

of the perennial rivers in South India supporting an extensive canal system both for irrigation and transport. The climate is dry and hot for the most part of the year

GEOLOGY

The area consists essentially of archæan formations which include the following rock types, arranged in stratigraphical sequence as below —

Pegmatite and quartz veins

Pink Granite Gneiss

Charnockite Series —Acid Charnockite, Intermediate Charnockite; Norite, Pyroxenite, Basic garnetiferous norite, and Hornblende-hypersthene-granulite

Bezwada Series (Khondalite system) —Bezwada gneiss (quartz-sillimanite-garnet-graphite gneiss), Garnetiferous gneiss, Garnetiferous quartzite; Biotite schist; Garnetiferous mica schist, Crystalline Limestone; and Calciphyre

These archæan rocks are covered by laterite cappings and alluvium.

The members which constitute the metamorphosed sedimentary succession of the " Bezwada Series " of King are included in the broad division of the khondalite group. They are well developed in the group of hills east and west of the Bezwada town, though a few of them are of limited distribution in the plains and low mounds of the Kondapalle area. The Charnockite Series, as a whole, and the associated granite gneiss compose almost the whole of the Kondapalle ranges

In all the hills round about Bezwada the country rock is the Bezwada gneiss with preponderance of garnet and sillimanite and some disseminated graphite and showing dominant gneissic structure. It often grades into the variety—garnetiferous gneiss,—as also into garnetiferous quartzite Charnockites and granite gneiss are met with as intrusives, presumably in the order of sequence mentioned Cutting all these formations are the quartz veins and pegmatites

Bezwada Gneiss: Field Characters —The gneiss is the country rock of our area. It belongs to the khondalite series and due to its slight mineralogical difference from the typical khondalite—Kailassa gneiss of King—is considered as a phase of the latter. It constitutes the two hill ranges, east and west of the Bezwada town, the former extending eastward from Governorpet to Gunadala and the latter northward from the banks of the Kistna right upto the 335 milestone on the N S Ry The main mass of the detached hillocks towards the west of the railway station is also a similar gneiss The

strike disposition of the beds is generally NNE-SSW, though some local variations, as for example, a N-S strike are not uncommon; thus, Foote's observation that the Eastern Ghats have a run prallel to the Coromandel coast-line is broadly confirmed. Corresponding to the strike of the beds described, the dip direction too varies—from E to SE—but not very frequently The dips are fairly high and range from 50° to 70°. Structurally, the hills show intense folding, plication and flexures.

Megascopic and Microscopic Examination —The most striking character about this group of rocks is the gneissic structure and compactness They are mostly medium-grained They are seen to be abundantly studded with garnets—fresh and translucent to spongy and opaque varieties. In addition, needle-like sillimanite, quartz, reddish brown felspar, secondary micas and graphite can be identified.

The gneiss shows a wide range of alteration In the weathered state it simulates a ferruginous sandstone. Specimens were collected systematically in order of increasing alteration, and it has been found that the rocks of comparatively fresh nature at the bottom gradually weather and alter towards the top of the hills where they are found to be very much lateritic The specific gravity of some of the freshest specimens varies from 2 79 to 2·85, whereas, in the case of much altered and lateritic ones it varies from 2 60 to 2·70. Moreover, the extensive secondary alteration of these rocks is seen in the occurrence of kaolin, serpentine and limonite.

Under the polarising microscope, the gneiss presents a remarkable appearance It is medium-grained and displays parallel arrangement of the constituent minerals in the foliation planes. Garnet, sillimanite, quartz and felspar are the major constituents with graphite, scapolite and iron ore minerals as accessories Biotite derived from garnet and kaolin from felspar are sometimes recognised in microsection. Garnet is dominant, sillimanite slightly less in amount and both show banded arrangement and quartz and felspar form the intervening layers.

The detailed description of the mineral constituents of the different members of the khondalite group is given in a later chapter of this paper.

The mode of the rock determined by means of Shand's Recording Micrometer is as follows (figures per cent):—

Quartz	32 9	Sillimanite	12·9
Orthoclase	14 6	Graphite	2·8
Plagioclase	9·2	Mica	5·1
Garnet	22·1	Magnetite	0·4

The freshest of the specimens of gneiss from among the collection was chemically analysed, the results of which are shown, along with those of other comparable rocks, in Table I.

TABLE I *Analysis of Bezwada Gneiss and Khondalites*

	I	II	III	IV	V	VI	VII
SiO_2	63 30	57 04	57 96	64 79	63 41	60 08	74 17
Al_2O_3	21 07	33 10	24·01	18·14	17·81	12·38	17·16
Fe_2O_3	2·41	0 40	3·51	1·50	3·26	3·28	7 82
FeO	4 25	7 29	6·16	5 90	5·97	4·20	..
MnO	0·10	0 06	0·24	0 36	0·09	0·18	..
MgO	1 79	0 73	1 05	1·33	1 94	1·95	0 83
CaO	1 24	0 75	0 68	1 07	1 13	9 43	0·61
Na_2O	1 88	0 03	0·35	2 33	1 86	2 59	0·49
K_2O	3·72	0·47	2 13	2 92	3 81	3 06	..
TiO_2	0 16	0 10	1 38	0 89	0 25	0 65	.
H_2O+	0·20	0 44	2·17	0·05	0 22	1 80	.
H_2O-	0·18	0 16	0·40	0 02	0 05	0·22	
Others	..	0·16	0 15	0·13	0 19	0·78	..
Total	100·30	100 72	100 19	100 03	100 00	100 60	100 19
si	244·5	203 5	222 0	286·7	240 8	195·1	405 2
al	48 0	69 5	54 0	44 0	40 0	22 6	55·0
fm	31 0	26 6	30 5	34 3	39·4	29 2	28 7
c	5 0	2 6	2 8	4 7	4 6	32·8	2·6
alk	16·0	1 1	6 7	17·0	16 0	14 4	2·7
tl	0 5	.	4 0	2·7	..	1·5	..
k	0 67	..	0 79	0 46	0·58	0·43	.
mg	0 33	0 15	0 23	0 28	0 36	0·45	..

I. Bezwada gneiss, from the quarry adjoining the Bezwada—Ellore road and half a mile east of the town. Analyst M. Srirama Rao.

II Khondalite, from the road between Passara and Ella, m p 12, Ceylon Anal . R J C. Fabry, Adams · *Canadian Jour of Research*, Vol. 1, p. 489

III Khondalite, from the road between Passara and Ella, m p 9 5, Ceylon. Analyst E G. Radley, *Ibid*

IV Khondalite, from Passara, Ceylon Analyst R G Radley, *Ibid.*

V Khondalite, from the road between Kandy and Aluinuwara, m p 24·5, Ceylon Analyst R. J C. Fabry, *Ibid.*

VI Khondalite, from the road between Bandervala and Nuwara Eliya, m p 1, Ceylon Analyst M S Krishnan, *Rec G S I* Vol LXVIII, p 395

VII Khondalite, from Kalahandi State Analyst T L Walker, *Mem. G S I*, Vol XXXIII, pt. 3, p 9.

The Basis Composition of the rock, calculated from the chemical analysis, is shown below:

Kp	13 6	C	1 1
Ne	10·2	Fs	2 5
Cal	3·8	Q	51 0
Sp	7·5	Ru	0 1
Hz	10·2		

The Kata Molecular Norm and the C.I.P.W Norm of the gneiss are shown in Table II

TABLE II

	Kata Molecular Norm	C.I P W Norm
Q	17 20	30 24
Or	22 66	22 24
Ab	17 00	15 72
An	6 23	6 11
C		11 62
Hy		10 07
Cord	13 72	
Fe Cord	18 70	
Sillimanite	1 70	
Hm	1 70	
mg		3 48
il		0 30
ru	0·10	
H_2O		0 38

A comparison of the norm with the mode shows that there are some discrepancies Whereas, there are hypersthene and magnetite in the C.I.P.W Norm and cordierite and Fe cordierite in the kata molecular norm there is not even a vestige of these in the microsection, but, they appear to be represented by the complex mineral garnet So also, while there is nearly 45% of normative felspar, only 23 8% enters into the modal composition the remainder of it going partly into mica and partly into the garnet The corundum of the C I P W Norm transforms itself into sillimanite in the rock at the expense of some silica In the norm there is no place for an accessory like graphite, though as much as 2 8% of it may figure in the micrometric analysis.

From the megascopic and microscopic examination, as also the chemical analysis, of the gneiss, it is seen to be akin to the khondalites of Walker and Adams with local peculiarities

Garnetiferous Gneiss —This also belongs to the khondalite series and constitutes the main mass of the hillock 245, half a mile south of Kondapalle village.

Megascopically, the rock exhibits gneissic structure and coarse texture and consists of quartz and felspar in which are studded garnets—red, fairly big, spongy and mostly opaque

In thin section, the gneissic structure is quite distinct. The garnets have the same characters as described above. The felspar is mostly orthoclase, plagioclase being subordinate and untwinned. The one conspicuous feature

about this rock is the absence of sillimanite and graphite Referring to this feature, Krishnan (1944) remarks that there is little doubt that it is a phase of the khondalite.

Garnetiferous Quartzite —This is an important formation of our area. In the range west of the Bezwada town and on the side facing the Kistna towards the north of the range in the higher levels are seen beds of garnetiferous quartzite interbanded with the normal gneisses for a distance of about four furlongs In the same range, a little south of the above band, and just adjoining the Bezwada-Ibrahimpatnam road is another outcrop, roughly lenticular in shape, extending for a few hundred yards.

The rock is bluish-grey in colour and is coarse-grained It is made up almost wholly of quartz, the garnets being small in size and rose-red in colour. On close observation it can be said that there is a rough banding due to slight elongation of the quartz grains The quartz is bluish

Under the microscope, the small crystals of garnet are seen to stand in a mosaic of quartz, simulating the porphyroblastic texture The two minerals are not equidimensional but elongated in a definite direction Quartz contains several dark, minute, dust-like inclusions of rutile and the bluish tints are perhaps to be ascribed to this It shows strain polarisation. The occurrence of biotite at the contacts of quartz grains in the form of long trains is common. Graphite is an accessory found as small irregular pockets

Mica-Schist —Forming part of the geological succession are the schist members which include the biotite schists and the garnetiferous mica schists The schists occur, in most cases, in the typical Bezwada gneiss as bands of very narrow width extending only for a few yards They are ubiquitous in their distribution being found in all horizons. In the hill range west of the Bezwada town they are fairly common

The biotite-schist is buff to brownish in colour and always shows fine schistosity.

Under the microscope, biotite is found to be the principal constituent. It is brown occasionally containing minute zircons surrounded by pleochroic haloes and is very much chloritised The crystalloblasts of chlorite replace the biotite The pale green colour, the weak pleochroism, the low birefringence and the ultra-blue interference colours show this particular chlorite to be a variety penninite Quartz is subordinate and exhibits undulose extinction. Apatite is commonly present as an accessory, though traces of iron ores are not wanting.

Garnetiferous Mica-Schist —The mica-schists generally grade into the garnetiferous mica-schists The latter are well exposed in all the hills in the Bezwada area and also in the low mounds outside the Reserve Forest area and just west of ½ milestone on the Ibrahimpatnam-Kondapalle road. Here they are found in close association with the members of the Charnockite series.

The garnetiferous mica-schists are very fissile. The garnets in them are dark-red to brownish in hand specimens and form mostly irregular crystals ranging in size from small granules to large crystals measuring 3" across. Sometimes inclusions of quartz are met with. The garnets occur as distinct porphyroblasts. They are mostly altered and cracked, secondary materials filling the cracks.

Crystalline Limestone —The characteristic feature about this rock type is its mode of occurrence It is found as small pockets and lenses in the khondalite In many cases the material, due perhaps to its solubility, seems to have been leached away leaving behind empty cavities. In some of the low mounds east of and adjoining the Bezwada town and in the westernmost parts of the nearby ranges and also a few hundred yards north of the Kanakadurga temple in the range west of the town minor outcrops of this rock are observed.

Megascopically, the rock is a white, medium to coarse-grained crystalline limestone. Excepting calcite, other minerals are not visible to the naked eye. It has a specific gravity of 2 75

In thin section, the rock is seen to be almost wholly made up of a mosaic of calcite, the different grains being well interlocked In many crystals there are only two sets of cleavages The mineral is, as usual, distinguished by its twinkling and polarisation colours. Biotite and diopside are the accessory minerals

Calciphyre —The calciphyres are mainly distributed in the main range west of the Bezwada town as narrow irregular bands in the country rock.

They are generally white, coarse to fine-grained and spotted with grains of greenish minerals which on decomposition stain the calcite crystals reddish-brown. On weathered surfaces, the silicates stand out in relief.

Mineralogically, they consist of an equidimensional granular aggregate of calcite together with diopside, with quartz and acid plagioclase as accessories. The pyroxene is irregularly shaped and exhibits coarse cleavage.

The different members of the khondalite series described above are highly metamorphosed sediments and contain mineral assemblages

indicative of the grade of metamorphism to which they have been subjected. In addition to quartz and felspar, the most constant and commonly occurring mineral in these rocks is garnet Others in order of abundance are sillimanite, biotite, chlorite, graphite, calcite, diopside, enstatite, apatite, scapolite, and rutile. Of these, the garnets have been studied in great detail for the obvious reason that the molecules of the garnet group have an important significance in different types of rock groups. The other minerals have been studied in detail under the petrological microscope.

Garnet —As already pointed out, garnet is a constant accessory of the khondalites on account of which these rocks have often been named garnetiferous gneisses They occur not only in the normal gneisses but often in association with mica schists and quartzites

In Table III are given the results of analysis of a garnet from the Kondapalle area For purposes of comparison, analyses of garnets from Nellore mica-schists, khondalites of Kalahandi State and the almandite garnet from *Dana's System of Mineralogy* are also given.

TABLE III *Analysis of Garnets*

	I	II	III	IV
SiO_2	38 49	39 55	37 74	39 12
Al_2O_3	24 27	23 43	21 24	21 08
Fe_2O_3 ..	1·38	2 44	.	6 00
FeO .	25 34	25 69	34 06	27·28
MnO	0 26	0·21		0 80
MgO .	4 69	4 69	4 01	
CaO .	5 58	3 19	2 06	6 76
TiO_2 .	trace	0 92	.	..
Loss on ignition .	0·10	0 06	.	..
Total	100 11	100 09	100 00	100 04
si	77 6	83·0	75 5	83·2
al .	28·8	29 0	25·0	26·2
fm .	59·1	63 8	68 8	59 5
c	12·1	7 2	6·2	14·3
mg	0 25	0 25	0·18	.

I Garnet from garnetiferous gneiss, Kondapalle Analyst M Srirama Rao

II. Garnet from the Schist Complex of Nellore, Analyst N Jayaraman, *Proc Ind Acad Sci*, Vol. V, No. 2, 1937

III. Garnet from Khondalite, Kalahandi, Analyst · L. L. Fermor, *Rec. G S I*, Vol. LIX

IV Almandite from Zillerthal, *Dana's System of Mineralogy*, p. 441.

In Table IV, these analyses have been rearranged in terms of their constituent garnet molecules.

TABLE IV

	I	II	III	IV
Spessartite	0 50	0·50	.	1 89
Pyrope ..	15·78	15 68	13 31	
Almandite	59·89	62 22	78 80	75 56
Grossularite .	14 91	8·58	7 89	15 48
Total pure garnets	91 08	86 98	100·00	92 93
Sillimanite ..	7 29	7 45	.	2 75
Quartz	0 96	3 72		3 79
Loss on ignition calculated as H_2O	0·10	0 06		
Ilmenite ..		1 82		0 25
O_2	.	0 24	.	0 02

It may be seen that the total molecules from the Kondapalle area sum up only to 91 08 The excess over the garnet molecules has been shown as sillimanite and quartz Dr Fermor (1927) in his paper on the Indian garnets records a similar feature with regard to this mineral from the khondalites of the Kalahandi and Natan Barampur.

The garnet molecules are recalculated to 100 in Table V.

TABLE V. *Garnet Molecules Recalculated to* 100

	I	II	III	IV
Spessartite	0 55	0 57		2·00
Pyrope .	17 30	18 03	13 31	..
Almandite .	65 70	71 53	78 80	81 30
Grossularite .	10 45	9 87	7 89	16 17

It may be seen from Table V that the Kondapalle garnet approaches nearest to almandite. Its formula can be expressed by the method of Eskola and Ford as follows·

This result is in absolute conformity with Fermor's observation that the almandine garnet is characteristic of argillaceous crystalline schists

The garnet occurs as large porphyroblasts in these rocks. It is often fractured and crushed. Generally it is diablastic with inclusions of quartz and less frequently of sillimanite Under the microscope, the mineral is seen to be traversed in a few cases by parallel cloudy bands which apparently appear to be made up of some nearly isotropic material. The directional

structure of the rock seems to have influenced the growth of the mineral and this is particularly manifest in its elongation in the direction of schistosity. The garnet shows different stages of alteration, the most common product being chlorite, that to biotite being less frequent.

Sillimanite —After garnet this is the most abundantly occurring accessory mineral in the khondalites. It is found as very fine needles in the rock on account of which it is not quite as evident to the naked eye as the garnet

Under the microscope, it is readily recognised by its characteristic fibrous, elongated, slender prismatic nature frequently jointed and presenting a fluxional appearance. It is colourless and has high R I giving under crossed nicols second order pinks and greens It has straight extinction It is biaxial and has a positive sign with the optic axial angle (2V) varying two degrees on either side of 28° It is not easily altered but occasionally gives rise to pseudomorphous growths of biotite and muscovite

Biotite —Though not so abundant as the other two minerals, it is seen fairly frequently in these rock types It has an intense body colour and exhibits strong pleochroism according to the following scheme.

X Dark Yellow, Y and Z Reddish Brown

The biotite most commonly occurs as a grade mineral in metamorphism but instances of its secondary origin from the alteration of garnets are not uncommon It changes to chlorite without losing its shape or cleavage It occurs mostly as elongated laminæ with lengths twice or three times the breadth

Chlorite —It is always a secondary mineral derived from garnet, biotite and other ferromagnesian minerals Under the microscope, it occurs as irregular flakes with bent cleavages; it is pleochroic according to the scheme:

X and Y. Light Yellow Green; Z Green

Graphite —This occurs as disseminated flakes quite frequently in the khondalites. It is only when the khondalites are cut by quartz or pegmatite veins that streaks, pockets or lenses are met with Graphite and sillimanite which are constant accessories in the Bezwada area are conspicuously absent in the Kondapalle hills

Calcite —Its normal mode of occurrence is that of lenticular bands of crystalline limestone. It is also abundant in calciphyres. Occasionally it occurs as an accessory mineral in the normal gneisses It is recognised by its rhombohedral cleavage and its idioblastic relationship to quartz when it occurs in association with this mineral.

Diopside —This is a prominent mineral of the calciphyres. In hand specimen it is recognised by its pyroxenic cleavage, black colour and prismatic appearance. Under the microscope, it is colourless and has a rough cleavage and is subhedral. It is characterised by an oblique extinction, the angle $Z \wedge c$ being as much as 52° Its optic axial angle (2V) is $59° \pm 1°$ and with Z as acute bisectrix.

Enstatite —This was observed only in the calciphyres in colourless small grains. It exhibits extinction parallel to the cleavage, is biaxial and positive

Apatite —Is a commonly distributed accessory universally present in the mica schists and is recognised as rounded grains with high relief and polarisation colours of first order grays

Scapolite —This was occasionally met with in the gneisses and distinguished by its low R I , straight extinction, moderate birefringence and nearly right-angled cleavage

Rutile —Occurs as minute needles with no regular orientation as inclusions in quartz

Sphene —Is sometimes met with in calciphyres with its wedge shape, light-brown colour, faint pleochroism, high relief and marked polarisation colours.

Magnetite —Is recognised both in its primary and secondary phases.

Petrogenesis

To decipher the nature of metamorphic rocks, Grubenmann and Niggli (1924) have constructed tetrahedra using the four values *al, fm, c* and *alk* Taking into consideration the three values *al, alk,* and *c/fm* and with each one at the corner of a triangle, they were able to recognise the Eruptive Field running as a small band of very low width and corresponding roughly to the altitude of the triangle with *al-alk* as the base (Fig. 1). On either side of this Eruptive Field are the fields of " Ruckstande Sedimente ", " Tonige Sedimente " and " Chemische Sedimente ", the first two being towards the side of *al* and the third on the side of *alk*.

The *al, alk* and *c/fm* values of the Bezwada gneiss—(48 0, 16·0 and 0 16 respectively)—are plotted in the abovementioned diagram and their intersection point falls very well outside the Eruptive Field and in the region of Ruckstande and Tonige Sedimente.

This fact affords ample evidence in favour of the argillaceous parentage of the gneiss.

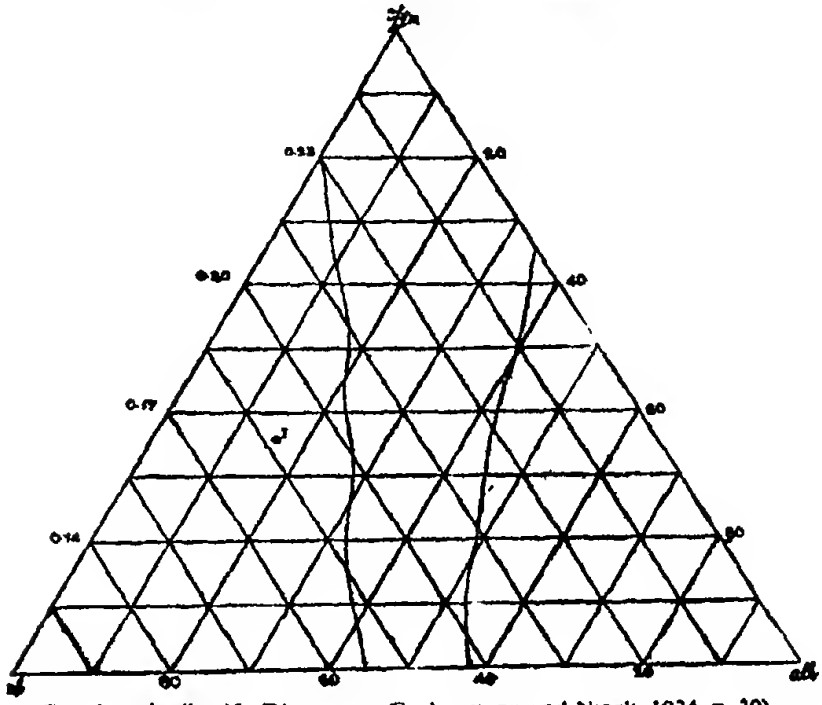

FIG 1 *al alk, c/fm* Diagram. (Grubenmann and Niggli, 1924, p 30)

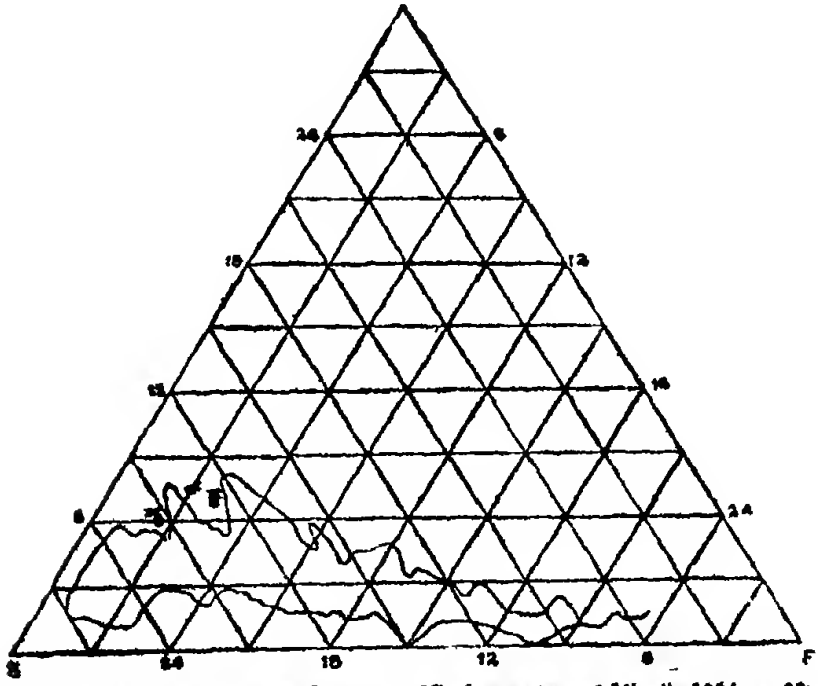

FIG. 2. S-Al-F Diagram of Osann. (Grubenmann and Niggli, 1924, p. 23).

In Figs 2 and 3 are represented Osann's diagrams The first one is the S-Al-F diagram. The three values represent respectively the proportions of SiO_2, Al_2O_3, and (Fe, Mn, Mg, Ca) O of the rock From the graph it will be seen that the area bounded by the irregular line and which is in the lower portion of the triangle represents the rocks of igneous parentage The

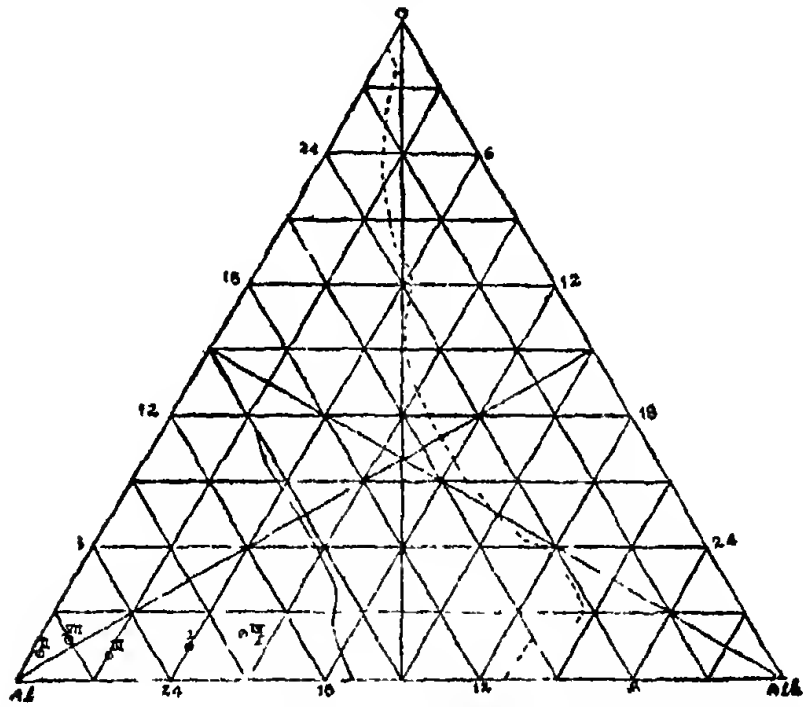

Fig 3 C-Al-Alk Diagram of Osann (Grubenmann and Niggli, 1924, p 23)

S-Al-F values of the gneiss and the khondalites shown in Table I are arranged in the following table.

TABLE VI

Rock Type No	S	Al	F
I ..	19·5	7 5	3 0
III ..	19 0	7·0	4·0
IV ..	21 5	6·0	2 5

The projection point of the gneiss, as also the points of two other khondalites, fall distinctly outside the igneous area, thereby indicating the original sedimentary nature.

The other diagram (Fig. 3) utilises the three values C, Al and Alk They stand for the proportions of CaO, Al_2O_3 and $(Na, K)_2O$ respectively.

The three values occupy the three corners of a triangle The field of igneous rocks comes into the centre of the figure The C-Al-Alk values of the gneiss and Khondalites are arranged in Table VII

TABLE VII

Rock Type No	C	Al	Alk
I	1 5	22 5	6 0
II	1 1	28 4	0 5
III	1 3	25 7	3 0
IV	2 1	20 0	7 9
V	2 2	19 9	7 9
VII	1 8	27 0	1 2

The projection points of the Bezwada gneiss and the other khondalites fall much outside the igneous region and are towards the Al corner, implying their original aluminous nature

The interpretation of the results of chemical analysis of the gneiss itself is sufficient to come to this conclusion For any rock, if originally undoubtedly a sediment, the relative proportions of the different oxides have to be as follows —

(i) excess of silica, figuring to a very great extent as normative quartz;

(ii) excess of alumina, as normative corundum and sillimanite;

(iii) slight excess of magnesia over lime, if not in equal proportions;

(iv) preponderance of potash over soda

All these conditions, it is seen, are satisfied by the Bezwada gneiss.

From a consideration of the facts detailed above, it is evident that the Bezwada gneiss is a typical metamorphosed argillaceous sediment.

DISCUSSION

The origin of the khondalites is a subject on which there seems to be perfect agreement among geologists Walker (1900) is of the opinion that they are ancient sediments metamorphosed by great mountain building forces and later intrusions. Middlemiss (1903) and Smith (1900) hold the view that they are metamorphosed rocks, the metamorphism being the result of intrusion of charnockites and granites, *i.e*, thermal metamorphism with some influence of stress Fermor (1935) asserts that they are the result of hypograde regional metamorphism Lacroix (1891), Adams (1929), Coomaraswamy (1900), Wadia (1943) and others who have studied the Ceylon occurrences have come to the conclusion that these rocks are undoubtedly metamorphosed sediments.

From a careful study of Niggli's and Osann's diagrams, the author has arrived at the conclusion that the Bezwada gneiss is a para-gneiss. Now, considering its field relationships, namely, its thorough permeation by felspathic material, the author is obliged to adopt Fermor's (1919) view of the hybrid nature of the gneiss It is thus surmised that the gneiss approaches in composition most of the khondalites of Ceylon which however appear to be more felspathic than the Indian ones.

Summary and Conclusion

The results of a detailed field and laboratory study on the different members of the khondalite group, *viz.*, gneisses, garnetiferous quartzites, micaschists, garnetiferous mica-schists, crystalline limestones and calciphyres, which are intruded by the charnockites and granites and which form the country rock of the area, are recorded here

From a study of the chemical composition of the formations, some minerals by advanced petrographic methods and the modal composition by Shand's Recording Micrometer and the plotting of these results in trilinear diagrams, it is seen that the khondalites were original argillaceous sediments which have been metamorphosed into their present form

Myrmekitisation of the Bezwada gneiss observed in the field is confirmed by the laboratory studies.

Acknowledgments

The author is greatly indebted to Prof. C Mahadevan for much helpful and constructive criticism and for facilities for work in the laboratories of the Andhra University and to Dr M S. Krishnan for valuable suggestions and for facilities for consulting the necessary literature. He is thankful to Mr. C Karunakaran for his keen interest in the work.

References

Adams, F. D. . "The Geology of Ceylon," *Canadian Jour. of Research*, 1929, 1, 425–511.

Beaza, P. M. .. "Notes, chiefly Geological, of a journey through the Northern Circars in the year 1835," *Mad. Jour. Lit Sci.*, 1837, 5.

Coomaraswamy, A K. .. "Ceylon Rocks and Graphite," *Quart Jour. Geol. Soc Lond.*, 1900, 56

——— .. "Crystalline Limestones of Ceylon,' *Ibid.*, 1902, 58, 399–424.

Crookshank, H. "The Western Margin of the Eastern Ghats," *Rec. G S. I.*, 1938, 73, 398–433

Fermor, L. L. "Some problems of Ore-genesis in the Archean of India," *Proc. Asiatic Soc. Bengal*, 1919, 15, N. S. clxx—cxcv.

——— .. "Manganese Ore Deposits of India," *Mem. G.S.I.*, 1909, 37.

FIG. 1

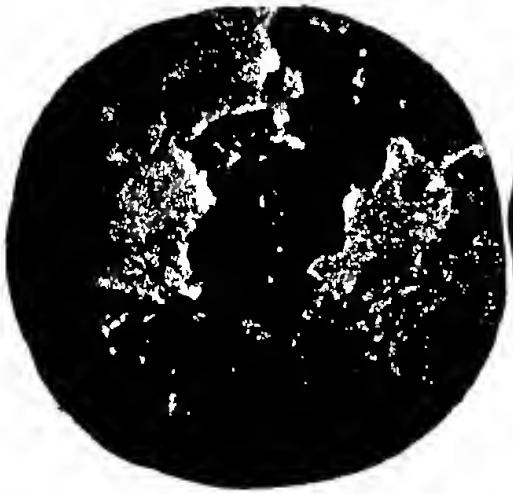

FIG. 2

FIG. 3

Fermor, L. L. — "On the composition of some Indian Garnets," *Rec G S I*, 1927, 59, 191–207

——— — "An attempt at the correlation of the ancient Schistose formations of Peninsular India,' *Mem. G S I*, 1935, 70, pts 1 and 2

Foote, R B — 'On the Geological Structure of the Eastern Coast from the latitude 15 Northwards to Masulipatam,' *ibid*, 1879, 16, pt 1

——— — Singareni Coalfield to the Kistna,' *Rec G S I*, 1885, 18, pt 1

Grubenmann, U, and Niggli, P — *Die Gesteinsmetamorphose*, 1924

Heyne, B — "Tracts, Historical and Statistical, on India, with journals of several tours through various parts of the Peninsula, also, an account of Sumatra, in a series of letters," 1814

Jayaraman, N — "The Mineralogy and Chemical Composition of Garnets from the Schist Complex of Nellore," *Proc Ind Acad Sci*, 1937, 5, Sec A, 148–60

King, W — "The Upper Gondwanas and other formations of the Coastal Region of the Godavery Dt," *Mem G S I*, 1880, 16, pt 3

Krishnan, M S — 'Lateritisation of Khondalite," *Rec G S I*, 1934, 68, 392

——— — 'Chromite in the Kondapalle Hills, Kistna District, Madras Presidency", *Fort St George Gazette*, 1944

Middlemiss, C S — 'General Report, 1901–02,' *G.S.I*, 1902, 21–23.

——— — 'General Report 1902–03," *ibid*, 23–25

Newbold, T J — "Notes, chiefly Geological, across the Peninsula from Masulipatam to Goa," *Jour As Soc Beng*, 1844, 13

Smith, F H. — "Preliminary Report on the Geology of the Ganjam District," *G S I Gen Rep*, 1899–1900, 1900

Wadia, D N — "A Brief Account of the Mineralogy of the Graphite Deposits of Ceylon—A Note on the Origin of Graphite," *Prof Paper No 1, Rec Dept of Mineralogy, Ceylon*, 1943

Walker, T L — "A Geological sketch of the eastern portion of the Jeypore Zamindari, Vizagapatam District," *ibid*, 1899–1900, 1900

——— — "The Geology of the Kalahandi State," *Mem G S I*, 1902, 33, pt 3.

Explanation of Microphotographs

1 *Bezwada Gneiss*—The gneissic structure is very well exhibited In the centre there are big, round grains of garnet with small inclusions and some cloudy bands Sillimanite as clusters of minute needles is to be seen. The colourless portion represents quartz and felspar. The dark patches are of graphite and biotite

2 *Garnetiferous Gneiss*—The band in the centre is made up of garnet which has irregular streaks in it and is crowded with inclusions The colourless area denotes quartz while the rest with a set of mines is felspar

3. *Garnetiferous Quartzite*—(Nicols Crossed) made up of a mosaic of quartz with a band of garnet in the centre.

X-RAY STUDIES OF PEATY LIGNITES AND ANTHRACITIC COALS

By Prof C Mahadevan, M A, D Sc, F A Sc.
(*Erskine College of Natural Sciences, Andhra University, Waltair*)

Received April 23, 1946

I Introduction and Experimental

Introduction —Results of the chemical studies of different specimens of Tertiary coals ranging from Peaty Lignites to Anthracitic Coal were published in an earlier paper.[1] It was found that at the early stages of coalification, the ratio of cellulose to lignin comes down rapidly, while at a certain stage it increases again It was inferred from these studies that at the early stages in coalification, lignin is more resistant than cellulose, while at a later stage, cellulose is relatively more resistant. The ratio of cellulose to lignin in a specimen is thus a good index of its actual stage in the process of coalification. Seshan[2] continued the work on other Indian, American and Bavarian coals and Anthracites, and confirmed and extended the above results. The chemical studies were extended to X-ray examination of the various members in the Tertiary coal series, as also of the products derived from the treatment of these coals by alkalis and acids In the present paper, the results of these investigations are recorded.

Materials Studied —The materials used in these investigations which were kindly supplied by Dr C S Fox are a peaty lignite from Palana in Rajputana, lignitic coals from Mach and Makerwal in Baluchistan, and anthracite from Jammu in Kashmir.

Simpson[3] and Fox[4] have recorded the geological history of the horizon from which these specimens were obtained Their observations may be summarised as follows: All the coals are from the same geological age and horizon, *i e.* (Laki stage, Eocene age).

The lignite beds of Rajputana (Palana) barely suffered any movement at all. The lignitic coals of Mach and Makerwall in Baluchistan were involved in the moderate movements of the Himalayan uprise, whereas the anthracitic areas in Jammu (Kashmir) were regions of great orogenic activity and compression, resulting in the uplifting of the Himalayas.

Experimental —The untreated coals and the products obtained in breaking them up by the chemical methods described[1] were studied by the X-ray diffraction methods.

The source of X-rays was a shearer tube with aluminium cathode and copper target The vacuum in the tube was obtained by using a Cenco-Hyvac as a backing pump and two mercury diffusion pumps on the high vacuum side. The X-ray tube was run with a secondary current of 5 mil amps

The camera consisted of a rectangular wooden box covered with a lead sheath 3 mm thick To one of the larger sides of this camera was soldered a lead cylinder with 3 slits aligned one behind the other The photographic plate holder could be slipped into a groove on the other side of the camera The substance was kept in the central hole of a brass disc 2 mm. thick which was held in place inside the camera by a suitable device When the coal and the products lost the power of coherence in some of the experiments, a thin " zig zag " tissue paper or a very thin flake of mica was used to hold the substance in position.

The beam of X-rays on emergence was passed through the lead cylinder and the diffraction pattern due to the substance contained in the brass holder was received on the photographic plate kept usually at a distance of 2·6 cm from the substance. The direct beam of X-rays was cut off on the photographic plate by a lead disc stop of suitable dimensions This device facilitated the observation of the details around the direct spot The time of exposure varied from 2 to 9 hours depending on the nature of the substance examined.

The tangent of the angle of diffraction is obtained by measuring the distance from the diffracting substance to the plate and the distance from the centre of the direct spot to a point on the diffraction halo where the intensity is at the maximum. The diffracting angle having been thus determined, we have next to calculate the spacing 'a' which give rise to the characteristic pattern on the photographic plate. This was obtained from the well-known Bragg formula.

$$a = \lambda/2 \sin \theta/2.$$

where λ = the wave-length of the X-radiation (being 1·54 Å U. due to the characteristic $K\alpha$ radiation in this case);

and θ is the diffracting angle noted above.

2. Results

The results of the study by the above methods are given below From Table I, it is seen that peaty lignite from Palana, lignite coals from Mach and Makerwal give two halos each The spacing 'a' for Palana lignite is 3·59 Å.U. for the inner and 2·43 Å U for the outer halo. The corres-

ponding values for the Mach and Makerwal coals are (inner) 3 53 Å U, (outer) 2 23 Å U., and (inner) 3·51 Å U., (outer) 2 23 Å U., respectively.

TABLE I. *Untreated coals*

	θ_1	θ_2	Å U a_1	Å U a_2	Description of the Patterns
Palana Peaty Lignite	24°43′	39°0′	3 59	2 43	
Mach Lignitic coal	25°11′	40°22′	3 53	2 23	Some central scattering and scattering at small angles (14½°) Inter-spaces not very clear
Makerwal Lignitic coal	25°19′	40°22′	3 51	2·23	General scattering pronounced. No definite central scattering

Jammu Anthracite (Untreated)

Rings	r_1	r_2	r_3	r_4	r_5	r_6	r_7	r_8
θ	13°14′	21°58′	26°4′	29°2′	35°8′	38°46′	44 36′	55°54′
a (in A° U).	6·68	4·04	3·39	3·06	2·50	2 56	2 03	1 64
	Very fair	Strong	Very strong	Fair	Fair	Faint	Faint	Faint

The Palana peaty lignites show an intense general scattering between the direct spot and the halos The edges of the inner halo are rather hazy, the outer edge showing greater diffuseness than the inner In the Mach coal, the general scattering between the direct spot and the halos is just as pronounced as in the next case (Makerwal coal) but a very definite scattering at small angles is seen here The Makerwal coal also shows a similar intense scattering between the direct spot and the halo. The edges of the halo are diffuse but not so much as in the case of Palana lignites.

The Jammu anthracite coal differs entirely from the above group in many respects Instead of the two diffuse edged halos met with in the coals described above, we see here quite a number of concentric rings, more or less well defined, with the interspaces fairly clear. The first halo is at 6·68 Å U and successive rings are seen at 3 39, 3 06, 2 50, 2·56, 2·03 and 1 64 Å U respectively. The identity of some of these rings with the halos due to graphitic carbon and others to the mineral matter usually associated with coals[5] can be easily made out.

The coals were dehydrated and then extracted with benzene. The patterns for the dehydrated specimens show a little clearing of the general scattering. The benzene extracts were also studied by the X-ray method.

Only the lignitic coals gave any extract with benzene The Jammu anthracite left the benzene almost uncoloured even after several hours of extraction In the X-ray pattern for the benzene extract of the Palana peaty lignite, a very intense halo with $a = 5\ 31$ Å U. having fairly well-defined edges, a second very diffuse but intense halo at $a = 3\ 91$ Å U and a last, faint halo (spacings not determinable due to the faintness) are observed. In Mach as well as in the Makerwal coals, a pattern nearly identical with the one just described was obtained. A fair amount of general scattering between the direct spot and the halos was observed in all these cases The great similarity of these benzene extract patterns to the 'gamma compound' pattern of coal[6] may be pointed out incidentally

The next series of examinations is of the "lignins" and residual products of the lignin extraction process The first group in this class was the study of the residue obtained by treating the coals with 72% H_2SO_4 for 20 hours and freeing them from acids

TABLE II. *Benzene soluble products of the coals*

Coal	θ_1	θ_2	θ_3	Å U a_1	Å U a_2	Å U a_3	Remarks
Palana peaty lignite	16° 42′	22° 44′	Faint	5 30	3 91	..	Inner halo sharp and very intense; 2nd halo diffuse and intense
Mach lignitic coal	16° 42′	22° 22′	42°6	5·30	3·00	2 14	Inner halo sharp and very intense; 2nd halo diffuse but intense
Makerwal lignitic coal	16° 6′	22°	Faint	5 50	4 08		Inner halo sharp and very intense, 2nd halo diffuse but intense
Jammu anthracite coal	No extract obtained for study						

The spacings obtained in the resulting diffraction pattern are tabulated in Table III.

TABLE III. "*Lignin*" *from* 72% H_2SO_4 *treatment*

	θ_1	θ_2	Å U a_1	Å U a_2	Remarks
Palana peaty lignite	24° 26′	41° 30	3 64	2 17	Very intense general scattering, edges not defined
Mach coal	24° 25′	Faint	3·64		Outer halo not clear. Edges fairly defined. Intense general scattering
Makerwal coal ..	24° 25′	41° 30	3·64	2·17	Intense general scattering, Edges somewhat defined
Jammu anthracite coal	No lignin extracted				

Only the first three coals indicated loss of weight as a result of this treatment Jammu coal was almost unattacked by the acid In the case of the Palana lignite, Mach and Makerwal coals, two halos were obtained in the diffraction pattern, one rather intense at $a = 3\ 54$ Å.U. and another at $a = 2\ 17$ Å U The patterns are thus more or less identical. The edges of the intense halo are fairly well defined. Appreciable general scattering is seen between the direct spot and the halo.

Then the lignins obtained from autoclaving the coals with 10% NaOH at 150° C for 10 hours and further purified were examined. For purposes of comparative study, lignin extracted from jute (flax) by the same process was examined The results are recorded below

TABLE IV. *Pure lignin from autoclaving with 10% KOH at 150°*

Coal	θ_1	θ_2	Å U a_1	Å U a_2	Remarks
Palana lignite	12° 35′	23° 30′	7 02	3 78	Two well defined halos outer more intense than the inner Very little inter halo scattering
Mach coal	12° 35′	23° 30′	7 02	3 78	
Makerwal coal	12° 35′	23° 30′	7 02	3·78	"
Jammu anthracitic coal	No lignin obtained for study				
Jute (Flax)	12° 35′	23° 30′	7 02	3·78	Same as above

Here too the Jammu anthracite gave almost no extract The lignin diagrams for all the three coals and the lignin diagram for the jute are seen to be nearly identical. In all the cases an inner distinct halo at $a = 7$ Å U. is seen The next halo is at 3 78 Å U The space between the direct spot and the halos are very nearly clear. The halos are sharp and well defined

The identity of the patterns for lignin from the three coals and the close resemblance of these to the lignin pattern from jute are extremely interesting

Finally, the residues of the Palana and the Makerwal coals after the NaOH extraction were subsequently treated with 72% H_2SO_4 and digested for 20 hours to destroy any cellulose or celluosic products left unattacked in the autoclaving process.

The residual products after throwing away the digested matter were washed, and dried and these were studied by the X-ray methods. (The coals used in the autoclave extraction were not benzene-extracted.)

TABLE V. *Residues not extracted by KOH or H_2SO_4*

Coal	θ_1	θ_2	θ_3	a_1 in Å U.	a_2 in Å.U.	a_3 in Å.U.	Remarks
Palana peaty lignite	16° 18′	20° 16′	41° 30′	5·43	3 98	2 17	Inner intense and well defined 2nd halo intense and diffuse, outer faint
Mach lignitic coal	23° 52′		Faint	3 72		Faint	One intense halo at 24° and outer, faint
Makerwal lignitic coal	20° 14′		41° 64	2 61		2 15	Very intense general scattering, diffuse edges
Jammu anthracitic coal	20° 14′		Faint	3·61		.	A very sharp (crystal powder) pattern

The results reveal some interesting features For the Palana peaty coal, 3 halos are obtained, the innermost very intense and well defined, with $a = 5\ 43$ Å U, the second halo at 3 98 Å U with fair intensity but with very diffuse edges; the outer halo faint with $a = 2\ 17$ Å U There is a fair amount of general scattering in the pattern The very close similarity of this pattern (for the Palana lignite) to the 'gamma compounds' pattern of coals[6] is very striking

In the Mach coal, the first halo, which is quite intense, has a spacing of 3 72 Å U No halo corresponding to the inner well-defined ring noted in the corresponding products from the Palana lignite is seen here The outer halo is rather faint.

For the Makerwal coal, the inner intense halo gives a spacing of 3 39 Å U and the outer halo is very faint at $a = 2{\cdot}13$ Å.U This pattern is very similar to the pattern obtained for graphite carbon in colloidal state.

In the case of Jammu anthracite, a very intense and perfectly sharp ring is obtained at $a = 3\ 39$ Å U The outer intense halos due to mineral matter observed in the untreated coals are somewhat faint Faint halos corresponding to 2 16 Å U and 2 01 Å U can also be identified in the photographic negative

3 DISCUSSION OF RESULTS

(*a*) *Geological age in relation to coal formation* —To understand the significance of the above results it is necessary to review briefly the classical investigations of Bergius on the artificial production of coal from cellulosic materials. Experimenters before Bergius who attempted to produce coal in the laboratory failed in their attempt, as no control could be exercised over the temperature due to exothermic reactions involved in the proces

which consequently converted the original substance into a product resembling coke rather than coal. The high-pressure technique developed by Bergius enabled water under great pressure to be kept in a liquid state and used as a thermostat to prevent local superheating This temperature control was of utmost importance in these experiments of Bergius.

Subjecting pure cellulose to this reaction at 340° C. for 12 hours, Bergius obtained a product identical with soft coal of 84% of carbon, 5% of hydrogen, and 11% of oxygen CO_2 was evolved in the reaction.

Various cellulosic substances such as peats were then subjected to this treatment for varying periods from 8 to 64 hours at temperatures from 250° C to 340° C These experiments showed that the carbon percentage rises with the length of the heating and with the temperature at which the reaction takes place It reaches, however, a final value at about 84% carbon above which it does not go even after prolonged heating As this substance is thus the stable end-product of the voluntary reaction of decomposition mentioned above, every further increase in the carbon value cannot represent a further decomposition caused by the same reaction in still greater periods of time. Only through reactions caused by new external conditions, could the carbon percentage be still further raised

The experimental methods of Bergius allowed not only the regulation but the variation of temperature The speed of the reactions at various temperatures was studied to calculate the rate at which the reaction takes place in nature. The experiments were carried out at 310° and 340° and the end product in both cases was found to be nearly identical according to analysis From the widely accepted theory of Potonic for chemical reactions, Bergius calculated from the above laboratory experiments, eighty million years as the period necessary for coal formation in nature—a result corroborated to the correct order of magnitude from independent geological data If the temperature and pressure are together raised, the end product is seen to resemble a substance much like anthracite The extreme high pressure is surmised to account for a new reaction taking place which gives rise to anthracite

Leaving out the effect produced by temperature, which was merely a means of accelerating in the laboratory the slow process of nature, a perfect analogy is found in the natural coal-fields with regard to the effect of pressure. Whenever a coal-field has been subjected to a compression as a result of tectonic disturbance, an increase in the carbon content of the coal and the conversion of the coal, to a greater or smaller degree, into anthracite may be expected. The formation of coal in nature is conceived by Bergius as

progressing on its own accord under ordinary pressure. Irrespective of the time elapsed, this end-product would not undergo anthracitisation unless forced by increased pressure giving rise to an altogether new reaction. He points out the error in attributing anthracite to older geological ages and refers to the well-known finds of anthracite in highly folded regions of tertiary period, whereas ordinary bituminous coal may be found in undisturbed palæozoic strata

These experiments are unique since the chemical observations have been sought to be co-ordinated with geological facts and results of a far-reaching nature, broadly acceptable to the geologist as well as to the chemist, have been obtained

The above laboratory records may be supplemented from geological data before we commence the discussion of the significance of the X-ray results in relation to these facts In an earlier part of the paper, the geological history of the horizon from where the coals were obtained was briefly narrated. The Palana (Bikanir) area was found to be undisturbed by tectonic forces; the Mach and Makerwal (Baluchistan) and Salt range fields showed a fair amount of folding, and the Jammu beds were seen to be located in a region of great orogenic activity Campbell[7] remarks on the Pennsylvanian anthracite region that these can be correlated by means of fossil plants to the great bituminous coals to the west and originally were of the same horizon and that the anthracites are now confined to the areas of great folds and faults which displaced and greatly disturbed the rocks Likewise he concludes that the anthracitic beds of Colarado are due to their having been subjected to great folds and faults.

The results of the X-ray study of the tertiary coals will be discussed here in the light of the views and facts mentioned above. As was pointed out in Section 2 peaty lignite from Palana gives two halos with intense general scattering, the peak intensity for the inner halo being at $a = 3 \cdot 59$ Å U and for the outer faint halo at 2 43 Å U In the case of the Mach and Makerwal coal, general scattering though intense, was not quite so much as that noted for the Palana lignites. The peak intensity of the inner maximum was at $a = 3$ 52 Å U and for the outer halo, the value was 2 23 Å.U. The Jammu anthracite, on the other hand, gave eight distinct halos of varying intensity, separated by fairly clear interspaces. In this connection, attention may be drawn to the earlier work of the author on peats[8] (1930), tertiary coals[9] (1930) and permocarboniferous coals[10] (1929). It was shown in these contributions that the peak intensity of the principal halo for the peats was 3 7 Å U., for the tertiary coals 3 5 Å U , and for the permo-

carboniferous coals 3·38 Å U. For the last type, more than ten coals were examined and they all gave consistently the value mentioned, *viz.*, 3 38 Å U. We see from the above that while a progressive change in dimensions of the halos of the X-ray patterns is observed from peats to peaty lignites and lignitic coals (Tertiary age), the corresponding halos for the permocarboniferous coals give a consistent value for the spacing corresponding to the peak intensity of the halo This is so, irrespective of the composition of the coal as determined by proximate analysis On the other hand, it happens that, though the proximate analysis for a tertiary coal may be very similar to that for a permocarboniferous coal, the influence of the geological age on the X-ray diffraction pattern is very distinct. The obvious inference suggested by the above facts is that the tertiary coals are still to reach the end mature product of coal-formation referred to by Bergius The process of formation of the end product evidently involves changes which are largely of a structural kind rather than compositional The method of X-ray analysis is very sensitive to changes of the former kind and this explains why the X-ray patterns show distinct differences where the proximate analysis yields results apparently alike

The peaty lignite from Palana gives intense general scattering and the intensity maxima of the principal halo of diffraction is at a smaller angle than what is obtained for the corresponding halo of Mach and Makerwal lignitic coals From the geological history of the region, we see that the Bikanir area was nearly completely free from pressure. Bergius has emphasised the importance of pressure in the process of coalification. Enough time has elapsed for the vegetable matter to be converted to lignite but not enough pressure was available for the complete obliteration of the peaty structure.

This is confirmed by the fact that the chemical analysis shows an appreciable percentage of cellulose for this specimen. It will be seen moreover that in this group of lignitic coals, the X-ray pattern shows greater relationship to the pattern for ordinary peat than to the pattern of the other members of the coal series; at the same time, indication is given of progression towards the coal stage.

In the case of the Mach and Makerwal coals, the peak intensity spacing for the principal halo corresponds nearly with the values obtained for other tertiary coals from different localities.[8] The pressure for the transformation of the vegetable matter to coal must have come from the weight of the superincumbent sediment or from other sources. Though Mach and Makerwal coals are now seen to be exposed profusely at the surface, they may not

have been long under heavy sediments; a part of the pressure necessary for coalification may have been derived from horizontal forces of compression which have acted on this region; sufficient geological time has however not elapsed for the lignites to reach the end-product or mature stage of coalification. It is of great interest to point out, from X-ray results, the similarity between the normal tertiary coals of other localities and the groups of coals discussed here Their deviation from the permocarboniferous coals, even where the proximate analysis in some cases are very similar, is another significant observation, and we seem to understand the soundness of the Bergius' conception of coal formation in nature from confirmatory evidence afforded by an independent field of study

We next come to the case of anthracitic coal from Jammu. From the geological history of the region from where these anthracitic coals were obtained, it was seen that Jammu area was subjected to intense mountain building activity Consequently, the coal strata were subjected to much pressure The second distinct process referred to by Bergius in his laboratory experiments for the formation of anthracites, *viz*, the existence of a great pressure, has been obtained in the Jammu area for the conversion of the bituminous coal to anthracite The X-ray pattern for this specimen is quite unique Distinct halos with fairly clear interspaces (testifying to the low content of moisture and volatile matter) are identified, of these, some are due to free graphitic carbon in fairly coarse state of division and a few other halos to the mineral matter in association with the coal. The specimen of anthracite looks, in a hand specimen, like a typical vitrain and shows its real nature only when subjected to physical and chemical tests The emphasis on this point seems very necessary in view of a somewhat similar pattern given by the dull variety of bituminous coal-durain.

The observations of Campbell[7] to which reference has been made earlier in this section, are in agreement with the conclusions of the Indian geologists for the Jammu anthracitic region, *viz*, that the same beds when subjected to great pressure, show local alterations of the beds to anthracite. The results of X-ray diffraction methods confirm completely the geological evidence.

A passing reference may be made here to a theory of Donath[11] that the formation of anthracite is due to a difference in the original vegetable matter, a particular type of decaying wood giving rise to bituminous coals and another type, to anthracite. From the evidence afforded by the Indian (and American) coal-fields cited in the paper, such a theory finds no support. The coals from the same geological horizon (and age) showing progressive

alteration from the peaty lignite in the undisturbed area (Palana, Bikanir) gradually to lignitic coals in moderately folded regions (Mach and Makerwal), and finally ending in semi-anthracites in places of great activity, indicate clearly the corresponding changes in the X-ray pattern The theory of Bergius on coal and anthracite formation finds good support from X-ray studies To attribute the differences in the stages observed to a difference in the original substance deposited seems not only artificial but is clearly contradicted by geological evidence

Reference was made to the X-ray patterns of the end and residual products of the coal after autoclaving with 10% KOH and the subsequent treatment of the residue with 72% H_2SO_4 for 20 hours. In the autoclaving process, the lignin was all extracted leaving the residue consisting partly of cellulosic and some non-cellulosic substances. Now, in the case of the Palana peaty lignite, the X-ray pattern obtained for the last residue is interesting The pattern is very similar to the 'gamma compound' patterns of bituminous coals [4] For Mach, Makerwal and Jammu anthracites, the end residual patterns are very much akin to the 'graphitic carbon' pattern.[5] The rapid degradation of cellulose to compounds having the aromatic or six carbon ring is now well established In these coals the cellulosic products have been changed into carbonaceous products not acted on by the alkali or the acid. These residual carbonaceous products being the more dominant we see only the pattern due to them The carbonaceous products may be partly due to the alteration of the cellulosic constituent and perhaps to a small extent also due to the alteration of some of the non-cellulosic derivatives.

4 Summary and Conclusion

Investigations were carried out with tertiary coals of the same geological age and horizon ranging from peaty lignites to anthracites by X-ray diffraction methods.

Lignins were isolated from the coals by digestion with alkali and purified. The X-ray patterns of all these lignins are practically identical and resemble the pattern for flax lignin. On a comparison of the X-ray patterns for the untreated flax and its lignin, it is seen that except for the observation of fibrous nature in the untreated flax, the halos in the two cases show great similarity.

In the case of lignite from Palana, the end residual products after alkali autoclaving and acid treatment give X-ray patterns very similar to the 'gamma compound' pattern of coals.

The X-ray patterns obtained with the peaty lignites and lignitic coals in the untreated state consist of two halos, one intense and the other somewhat fainter, the corresponding spacings for the two groups being 3 59 Å U (intense) and 2·43 Å U (faint) and 3 50 Å U (intense) and 2 23 Å U (faint) respectively The anthracitic coals give quite a different pattern showing unmistakable indications of the presence of free carbon in a fairly course state The spacings for the tertiary coals, *viz*, 3 50 Å U are distinctly different from the corresponding values, *viz*, 3 38 Å U for permocarboniferous coals, in spite of apparent similarity of the composition as determined by proximate analysis These observations are discussed in relation to the geological history of the coal-fields from where the specimens were obtained and in relation to the Bergius' theory of coal formation in nature

It is seen that in conformity with the field observations, the X-ray patterns show progressive alteration to anthracitic stage with increasing pressure. The Palana lignites which have not been subjected to much pressure show larger spacings for the halo similar to a pattern for peat. The next set of coals, Mach and Makerwal have been subjected to moderate pressure and they correspond closely to the normal tertiary coals studied from other horizons The anthracitic coals which are from a region of great tectonic activity give patterns characteristic of free carbon and mineral matter.

The distinct difference between the X-ray patterns of the tertiary and the upper palæozoic coals, especially the higher spacings for the former in spite of their similar proximate composition, points to a less compact structure of the fundamental coal substance in the tertiary specimens The palæozoic coals seem to have reached the final stage of maturity In normal (*i e*, unfolded) palæozoic strata, anthracite coals are absent. The existence of anthracites in highly folded regions is attributed to the great pressure to which these regions had been subjected The results of the X-ray study are in conformity with the above observations and support Bergius' theory of coal and anthracite formation in nature.

In conclusion, the author has much pleasure in acknowledging his grateful thanks to Prof Sir C. V Raman, F R S, N L, under whose inspiring guidance the work was carried out and to Prof. S Bhagavantam for valuable suggestions

References

1. Mahadevan, C — *Ind Jour Phys*, 1933, 8, 259–68
2. Seshan, P K — *Proc Ind Acad Sc*, 1935, 1, 536–41
3. Simpson, R R — *Mem G S I*, 1913, 51, 7
4. Fox, C. S — *Proc. Ind Sc. Cong.*, 1929, 256
5. Mahadevan, C — *Ind Jour Phys*, 1929, 4, 96 and 98
6. ——— — *Ibid.*, 1929, 4, 88, 89 and 97.
7. Campbell, M R — *International Conference on Bituminous Coal*, 1926, 47.
8. Mahadevan, C — *Ind Jour Phys*, 1930, 4, 460 62
9. ——— ——— *Ibid.*, 1930, 4, 533, 534 and 539.
10. ——— *Ibid.*, 1930, 4, 82 and 95
11. Donath — *Alts and Naus Zur Lignin Theorie Von Hans Bode Berlin*, 1930, Bd 11, H ft No 5, 81–100 "A review of the ligno-cellulose theory of the origin of coal from geological standpoint."

ON MULTIPLE FOURIER SERIES

By K. Chandrasekharan, *Madras*

Received June 4, 1946
(Communicated by Prof B S Madhava Rao)

§ 1 The object of this note is to announce some of the results obtained by the author on the *Spherical* Summation of Multiple Fourier Series, with an indication of the method of proof A complete account of these results will appear elsewhere, in due course

§ 2. *Notations and Definitons* Let $f(x) = f(x_1 \quad x_k)$ be a function of the Lebesgue class L, which is periodic in each of the k-variables, with period 2π.

Let

The Series

$$\Sigma\, a_{n_1 \quad n_k}\, e^{i(n_1x_1+\cdots+n_kx_k)} \tag{2 1}$$

is called the Multiple Fourier Series of the function $f(x)$

Let

$$S_R(x) = \sum_{\nu \leqslant R} a_{n_1 \quad n_k}\, e^{i(n_1x_1+\cdots+n_kx_k)},\ \nu^2 = n_1^2 + \quad + n_k^2 \tag{2 2}$$

denote the 'spherical' partial sum of the Series (2 1), that is, we shall consider (2 1) as a simple series

$$\sum_{j=0}^{\infty} \sum_{\nu = R_j} a_{n_1 \quad n_k}\, e^{i(n_1x_1+\cdots+n_kx_k)}, \tag{2 3}$$

where R_j^2 is the sequence of all integers that can be represented as sums of k-squares.

Let

$$\quad 2 \quad 2 \tag{2 4}$$

so that S_R^δ is the Riesz mean of the Series (2 1), of type ν^2 and order δ

If $\lim_{R\to\infty} S_R^\delta$ exists and is finite, then the Series (2 1) will be summable (ν^2, δ). If $S_R^\delta(x)$ is of bounded variation in $0 < R < \infty$, the Series (2 1) will be *absolutely* summable (ν^2, δ), or summable $|\nu^2, \delta|$

Let

$$f_p(x, t) = f_p(t) = \frac{c}{t^k} \int f(y) \left(1 - \frac{s^2}{t^2}\right)^{p-1} dy,$$

where dy is the k-dimensional volume element, $\sum_1^k (y_i - x_i)^2 = s^2 \leq t^2$, and c is a suitable constant If $p = 0$, we write $f_0(x, t) = f_x(t)$ $f_p(t)$ may be called the 'spherical mean' of order p of the function $f(x)$

We prove theorems connecting the behaviour of the spherical mean of a function at a point, with the summability of the corresponding Fourier Series at the point.

§ 3 *Theorems on Summability*

Theorem 1 If $f_p(t) \to l$ as $t \to 0$, then $\underset{R \to \infty}{lt}\, S_R^\delta(x) = L$, for $\delta > p + \frac{k-1}{2}$ and $L = 2^{\frac{k-2}{2}} \Gamma\left(\frac{k}{2}\right)$.

Theorem 2. If (i) $f_{p+1}(t) - l = o(1)$, $t \to 0$,

(ii) $t^{-k-2p} \int_0^t s^{k+2p-1} |f_p(t)|\, dt = O(1)$ as $t \to 0$,

or if

$$t^{-k-2p} \int_0^t s^{k+2p-1} |f_p(t)|\, dt = o(1),$$

then, $\underset{R \to \infty}{lt}\, S_R^\delta(x) = L$, for $\delta > p + \frac{k-1}{2}$

Theorem 3 If $f_p(t) - l = O(t^\alpha)$ as $t \to 0$, $0 < \alpha < 1$, then, for $\delta = p + \frac{k-1}{2} + \beta$, $0 < \beta$,

$$S_R^\delta(x) - L = \begin{cases} O(R^{-\alpha}), \text{ if } \beta > \alpha, \\ O(R^{-\alpha} \log R), \text{ if } \beta = \alpha, \\ O(R^{-\beta}), \text{ if } \beta < \alpha. \end{cases}$$

Theorem 4. If $\frac{f_p(t) - l}{t^\alpha} \to s_\alpha$,

then,

$$R^\alpha (S_R^\delta - L) \to l_\alpha, \text{ for } \delta > p + \frac{k-1}{2} + \alpha,$$

where

$$l_\alpha = s_\alpha \cdot \frac{2^{\frac{k-1+\alpha}{2}} \Gamma(\delta+1)\, \Gamma\left(p + \frac{\alpha}{2} + \frac{k}{2}\right) \Gamma\left(\frac{k}{2}\right)}{\Gamma\left(p + \frac{k}{2}\right) \Gamma\left(\delta + 1 - \frac{\alpha}{2}\right)}.$$

Theorem 5. If $S_R^\gamma(x) \to s$ as $R \to \infty$, then $f_p(y) \to s/2^{k/2-1}\,\Gamma\left(\frac{k}{2}\right)$, as $y \to 0$, provided $p > \max\left(1, \gamma - \frac{k-3}{2}\right)$.

Theorem 6. If $S_R^\gamma(x) - s = O(R^{-\alpha})$ as $R \to \infty$, $0 < \alpha < 2$, then,

$$f_p(y) - s/2^{\frac{k}{2}-1}\,\Gamma\left(\frac{k}{2}\right) = O(y^\alpha),$$

for $$p > \max\left[1, \gamma - \frac{k-3}{2} + \alpha\right]$$

Combining Theorems 1 and 5, we can state the following

Theorem 7. A necessary and sufficient condition that the Multiple Fourier Series of a function $f(x)$ should be summable (spherically) at a point is that the meanlimit, of some order, of the function exists at that point.

Combining Theorems 2 and 6, we can state the following.

Theorem 8 If $t^{-k-2p}\int_0^t s^{k+2p-1}\,|f_p(s)|\,ds = O(1)$ as $t \to 0$, or in particular, if $f_p(s) = O(1)$, then the Multiple Fourier Series of $f(x)$ is either summable (ν^2, δ) for every $\delta > p + \frac{k-1}{2}$ or for no δ; a necessary and sufficient condition for it to be summable is that $f_q(t) \to l$ as $t \to 0$, for $q > p + 1$.

Theorem 9. If $f_p(t)$ is of bounded variation in $0 < t < \infty$, then the Series (2·1) is summable $|\nu^2, \delta|$, for $\delta > p + \frac{k-1}{2}$

Theorem 10. If $S_R^\delta(x)$ is of bounded variation in $0 < R < \infty$, then $f_p(t)$ is of bounded variation in $0 < t < \infty$, for $p > \max\left(1, \delta - \frac{k-3}{2}\right)$

Theorem 11. If $f_p(t)$ is of bounded variation in $0 < t < \infty$, *and* $p \geqslant 1$, then the Series (2·1) is summable (ν^2, δ) for $\delta > p - 1 + \frac{k-1}{2}$

Theorem 12. Summability $|\nu^2, \delta|$, for $\delta > \frac{k+1}{2}$, of the Multiple Fourier Series of $f(x)$ at any point depends only on the behaviour of the function in the neighbourhood of that point.

The proof of the above Theorems is essentially based on the following fundamental formula of *Bochner·

* S. Bochner · "Summation of Multiple Fourier Series by Spherical Means," *Trans American Math. Soc.*, 40 (1936), 175–207.

$$S_R^\delta(x) = 2^\delta \Gamma(\delta+1) R^\delta \int_0^\infty t^{\delta-1} f_x(t) V_{\delta+\frac{k}{2}}(tR)\, dt, \tag{3·1}$$

for $\delta > \frac{k-1}{2}$, where $V_l(x) = J_l(x)/x^l$ and J_l denotes the Bessel function of order l.

By partial integration, we can generalize the formula (3·1) and prove its reciprocal. We accordingly obtain, on the one hand,

$$S_k^\delta(x) = \frac{2^{\delta-p}\, \Gamma(\delta+1)\, \Gamma\left(\frac{k}{2}\right)}{\Gamma\left(p+\frac{k}{2}\right)} R^{k+2p} \int_0^\infty t^{k+2p-1} f_p(t)\, V_{\delta+p+\frac{k}{2}}(tR)\, dt \tag{3·2}$$

if $\delta > h + \frac{k-1}{2}$, where h is the greatest integer less than p; and on the other,

$$f_p(y) = \frac{\Gamma\left(p+\frac{k}{2}\right)}{2^{\delta-p}\, \Gamma(\delta+1)\, \Gamma\left(\frac{k}{2}\right)} y^{2\delta+2} \int_0^\infty S_R^\delta\, R^{2\delta+1}\, V_{p+\delta+\frac{k}{2}}(yR)\, dR \tag{3·3}$$

if $p > 1$ and $\delta > \frac{k-1}{2}$.

Formulæ (3·2) and (3·3) enable us, on the application of appropriate arguments, to connect the behaviour of $\underset{R\to\infty}{lt}\ S_R^\delta$ with that of $\underset{t\to 0}{lt}\ f_p(t)$ and deduce all the results cited above.

5:6:7:8-HYDROXYFLAVONOLS

Part II. A Total Synthesis

By V. V. Sreerama Murti, L. Ramachandra Row
and T. R. Seshadri, F.A.Sc

(From the Department of Chemistry, Andhra University)

Received May 6, 1946

In a recent publication[1] which may now be considered as Part I of this series the preparation and properties of the four important members of this group of flavonols were described They were made from 2-hydroxy-ω·3 4·5 6-pentamethoxyacetophenone which was itself obtained by the fission of calycopterin-dimethyl ether. A method of total synthesis has now been worked out and it is described in this communication

ω : 3 : 6-Trimethoxy-2·4-dihydroxyacetophenone (I) was first prepared by Baker, Nodzu and Robinson[2] and its preparation was later simplified by Rao, Rao and Seshadri [3] It has now been subjected to partial methylation yielding 2-hydroxy-ω·3·4: 6-tetramethoxyacetophenone (II) This compound is also known as gossypetol tetramethyl ether and was obtained earlier by the fission of gossypetin hexamethyl ether[4] and herbacetin pentamethyl ether[5] with alkali. The synthetic sample is identical with the natural one and the present work constitutes the first synthesis of this compound Oxidation of this ketone with alkaline persulphate yields 2 5-dihydroxy-ω: 3 : 4 : 6-tetramethoxyacetophenone (III) Partial methylation of this dihydroxy compound has been found to be very difficult In only one of a number of experiments a very small yield of a crystalline sample agreeing in all its properties with 2-hydroxy-ω: 3. 4: 5 6-pentamethoxyacetophenone could be obtained. Efforts are being made to get consistent yields The dihydroxy ketone has been directly condensed with the sodium salt and anhydride of anisic acid and also of benzoic acid The products (IV) yield on methylation the fully methylated ethers of calycopteretin and 6 : 8-dihydroxygalangin respectively and on demethylation the free hydroxy flavonols.

The present synthesis yields as an important stage methyl ethers of the flavonols with a free hydroxyl in the 6-position. Possibilities exist of obtaining 5 : 6-dihydroxy and 3·5·6-trihydroxy compounds by partial demethylation using hydrobromic acid and aluminium chloride.

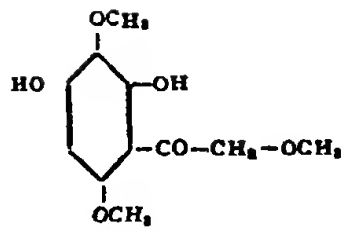

(I)

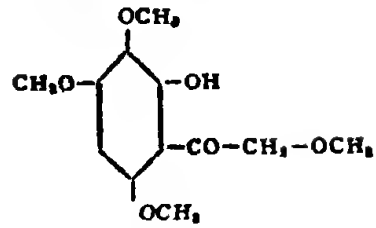

(II)

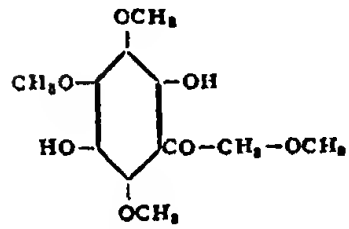

(III)

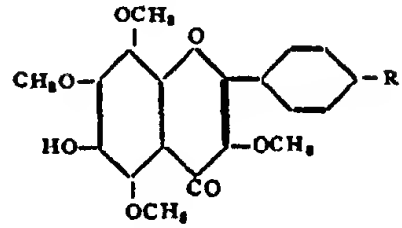

(IV)

R = H or OCH_3

EXPERIMENTAL

2.4-*Dihydroxy-ω* 3: 6-*trimethoxy-acetophenone* (I).—

In preparing this compound according to the method of Rao, Rao and Seshadri,[8] it is necessary to adhere very closely to the conditions prescribed in order to get a good yield of the main product and avoid as far as possible the by-product. The compound melted at 150-151° and had all the properties described in the literature

2-*Hydroxy-ω*· 3· 4: 6-*tetra-methoxy-acetophenone* (*Gossypetol-tetramethyl ether*) (*II*).—

Method I—The above dihydroxy ketone (2 4 g, 1·0 mol) was treated with dimethyl sulphate (1·3 g., 1 1 mol) and anhydrous potassium carbonate (2 0 g) in anhydrous acetone (75 c c). The resulting mixture was refluxed for 12 hours and then filtered hot. The residue on the filter (A) was washed thrice with warm acetone. The acetone filtrate and washings were then evaporated to dryness The solid residue was purified by dissolution in ether and extraction with aqueous alkali. The alkali extract on acidifying gave the 2-hydroxy-acetophenone free from the fully methylated derivative. It was crystallised from aqueous alcohol when it was obtained as short flat needles melting at 116-118°. Yield 1·6 g (Found: C, 56·6; H, 6·6; $C_{12}H_{16}O_6$ requires C, 56·2; H, 6·3%)

From the potassium salt residue (A), a portion of the original dihydroxy ketone (0 3 g) was recovered unchanged.

Method II—Gossypetol tetramethyl ether was obtained by subjecting hexamethyl gossypetin to hydrolysis with 8% absolute alcoholic potash. For this purpose, gossypetin was methylated by means of excess of dimethyl sulphate and anhydrous potassium carbonate in anhydrous acetone medium. The hexamethyl gossypetin was crystallised from ethyl acetate when it was obtained as almost colourless needles melting at 170-172°

Hexamethyl gossypetin (2 0 g) was refluxed with absolute alcoholic potash (8%, 45 c.c) for about 6 hours The alcohol was then removed under reduced pressure and the residue dissolved in water (75 c.c) and acidified with hydrochloric acid The turbid solution was repeatedly extracted with ether and the combined ethereal extracts shaken with aqueous sodium bicarbonate solution to remove the veratric acid which was a product of hydrolysis The ether layer was then washed with water, dried over anhydrous sodium sulphate and the solvent distilled off. The residue turned into a crystalline solid on cooling It crystallised from aqueous alcohol in the form of short flat needles melting at 116-118° Yield, 0 8 g It did not depress the melting point of the ketone obtained by method I

2-Hydroxy ω-. 3: 4: 6-tetramethoxy-acetophenone was soluble in aqueous alkali rather sparingly yielding an almost colourless solution. With ferric chloride, a reddish brown colouration was developed in alcoholic solution.

2. 5-*Dihydroxy-ω*: 3. 4. 6-*tetramethoxy-acetophenone* (*III*)—

To a mechanically stirred solution of gossypetol tetramethyl ether (2·6 g) in aqueous sodium hydroxide (1 5 g. in 50 c c) kept between 15-20°, was added potassium persulphate solution (3 0 g. in 50 c.c. of water) little by little during the course of three hours. The solution which was almost colourless at first, gradually changed through pale reddish brown to deep reddish brown during the course of the addition After leaving the solution overnight it was made neutral to litmus with dilute hydrochloric acid and extracted twice with ether to remove the unoxidised gossypetol tetramethyl ether (0·2–0·3 g.) The aqueous solution was then rendered strongly acidic by adding concentrated hydrochloric acid (10 c.c). Benzene (50 c.c) was then added to this liquid and the mixture refluxed on the water-bath for about half an hour. While still warm, the benzene layer was separated and the aqueous layer extracted twice with benzene. The combined benzene extracts were cooled and dried over sodium sulphate. After distilling off the benzene, the semi-solid residue was crystallised from benzene-petroleum ether mixture (1 : 1) when the 2: 5-dihydroxy-ketone was obtained as bright yellow rectangular plates melting at 102–103°. A

second crystallisation was also done from the same solvent; but there was no improvement in the melting point. Yield, 0·4 g. It dissolved readily in aqueous alkali yielding a reddish yellow solution. A transient green colour was obtained with ferric chloride in alcoholic solution, the colour changing rapidly to brown; after half an hour it was deep reddish brown. (Found: C, 53 0, H, 6·3; $C_{18}H_{16}O_7$ requires C, 52 9 and H, 5·9%)

6-Hydroxy-3:5 7.8.4'-Pentamethoxy-flavone (IV) —

The above dihydroxy ketone (0 8 g) was subjected to Allan and Robinson condensation with anisic anhydride (2 0 g) and sodium anisate (0 8 g.) by heating at 170–180° for about four hours. After hydrolysis with 10% alcoholic alkali, the alcohol was removed under reduced pressure and the solid product dissolved in water (125 c c.). After saturating the alkaline liquid with carbon dioxide, it was extracted repeatedly with ether When the ether extract was distilled, a bright yellow crystalline residue was obtained. It was crystallised twice from alcohol. The 6-hydroxy-flavone came out in the form of stout rectangular prisms melting at 160–161° with slight sintering at 159° Yield, 0 4 g It was easily soluble in aqueous alkali yielding a bright yellow solution It gave no marked colour with ferric chloride in alcoholic solution (Found: C, 61·8; H, 5·4; $C_{20}H_{20}O_6$ requires C, 61 8 and H, 5 2%)

Calycopterin-dimethyl ether.—

The above 6-hydroxy flavone (0·3 g.) was methylated with excess dimethyl sulphate (0·3 c.c) and anhydrous potassium carbonate (0·3 g.) in anhydrous acetone medium After refluxing for 20 hours, the acetone solution was filtered and the residue on the filter washed thrice with warm acetone. When the filtrate was evaporated, a colourless crystalline solid was left behind which was crystallised twice from aqueous alcohol. The methyl ether was thus obtained in the form of colourless long needle-shaped crystals melting at 131–132°. It did not depress the melting point of an authentic sample of calycopterin dimethyl ether. Yield, 0·2 g.

Calycopteretin.—

The above sample of calycopterin dimethyl ether (0·15 g.) was demethylated by refluxing for an hour with hydriodic acid (d. 1·7, 2·5 c.c.) and acetic anhydride (1·5 c.c). After demethylation, the liquid was cooled and diluted with sulphur dioxide water. The precipitated flavone was filtered and washed with water. The solid was yellow in the beginning but gradually turned greenish yellow. It was dried in a desiccator and crystallised twice from dry ethyl acetate. Calycopteretin was thereby

obtained in the form of deep yellow tiny rectangular plates melting with decomposition at 318–20° The mixed melting point with an authentic sample of calycopteretin was undepressed The colour reactions in alkaline buffer solutions were also identical (Found C, 56 6, H, 3·5, $C_{18}H_{16}O_8$ requires C, 56 6 and H, 3 2%).

3 : 5 . 6 : 7 : 8-*Pentamethoxy-flavone.*—

The dihydroxy ketone III (1 0 g) was condensed with benzoic anhydride (3 0 g) and sodium benzoate (1 0 g) using the conditions already described After hydrolysis, the alkaline liquid was saturated with carbon-dioxide and the flavone recovered by ether extraction It was pale yellow and gave brownish green colour with ferric chloride in alcoholic solution, indicating the presence of a free 5-hydroxyl The solid was therefore dried in a vacuum desiccator and methylated completely with dimethyl sulphate (1·0 c c.) and anhydrous potassium carbonate (1 0 g) in anhydrous acetone medium. After refluxing for 20 hours, the solution was filtered and the potassium salts washed with warm acetone (20 c c) On distilling off the solvent from the filtrate a colourless crystalline solid was obtained It gave no colour with ferric chloride in alcoholic solution. When further crystallised from aqueous alcohol it was obtained as colourless long needles melting at 81–82° The mixed melting point with an authentic sample of the pentamethoxy-flavone was undepressed. Demethylation of this ether with hydriodic acid yielded 6 : 8-dihydroxygalangin as yellow rectangular plates melting at 257–258° and identical with an authentic sample described already.[1]

Summary

A method of complete synthesis of 5 : 6 · 7 : 8-hydroxy flavonols is described It starts from ω · 3 : 6-trimethoxy-2 4-dihydroxy-acetophenone which is subjected to partial methylation (of the 4-hydroxyl group) and subsequently to persulphate oxidation The product, 2 : 5-dihydroxy-ω : 3 : 4 : 6-tetramethoxy-acetophenone is condensed with the anhydride and sodium salt of anisic acid and also of benzoic acid The resulting 6-hydroxy-flavones yield on further methylation the fully methylated ethers of calycopteretin and 6 : 8-dihydroxy-galangin and on demethylation, the free hydroxy-flavonols.

References

1. Venkateswarlu and Seshadri . *Proc Ind. Acad. Sci.*, A, 1946, 23, 192.
2. Baker, Nodzu and Robinson . *J C S.*, 1929, 77.
3. Rao, Rao and Seshadri .. *Proc Ind. Acad. Sci.*, A, 1944, 19, 88.
4. Perkin .. *J.C.S*, 1913, 103, 650.
5. Rao and Seshadri .. *Proc. Ind. Acad. Sci.*, A, 1945, 22, 162.

5:6:7:8-HYDROXYFLAVONOLS

Part III.A Simplified Synthesis

By V D Nageswara Sastri and T R. Seshadri, F A Sc

(From the Department of Chemistry, Andhra University)

Received May 6, 1946

A method of total synthesis of these highly hydroxylated flavonols and their derivatives was described in Part II [1] As an intermediate stage compounds with the 6-hydroxyl free and the others methylated could be obtained By suitable choice of the acid component used for the Allan-Robinson condensation and by partial demethylation of the product it is possible to have further free hydroxyl groups in the 3 and 5 positions and also in the side phenyl nucleus Since these flavonols occur mostly as partial methyl ethers, methods of preparing such ethers become important A method of total synthesis which is simpler and which further offers possibilities of having the hydroxyl in the 7-position free has now been successfully investigated and the results are presented in this paper.

In the preparation of 2 4-dihydroxy-ω:3 6-trimethoxy-acetophenone (II), the Hoesch condensation with the dibenzyloxydimethoxybenzene (I) gave rise to a by-product[2] which varied in amount depending on the conditions employed. This substance is now shown to be 2-hydroxy-ω.3:6 trimethoxy-4-benzyloxyacetophenone (III) It is possible by a suitable adjustment of the experimental conditions (using excess of ether and a shorter period of condensation) to effect only the debenzylation of the benzyloxy group ortho to the carbonyl and obtain the derivative (III) as the major product of the reaction Its constitution is definite, as it yields on further debenzylation in the usual manner the 2.4-dihydroxy-acetophenone (II) from which it differs in regard to its solubility in water and aqueous sodium carbonate The use of this benzyl ether (III) obviates the necessity for partial methylation as in the case of the 2·4-dihydroxyacetophenone (II) and by oxidation with potassium persulphate in alkaline solution, the pentahydroxybenzene derivative 2:5-dihydroxy-ω.3:6-trimethoxy-4-benzyloxyacetophenone (IV) is obtained from it in moderately good yields This constitution for the dihydroxyacetophenone is supported by analogy with compounds obtained in a similar manner. Further, there is only one available position for the new hydroxyl group to enter

and the persulphate oxidation of phenolic compounds is known to yield always the corresponding quinol derivatives provided the necessary para position is free.

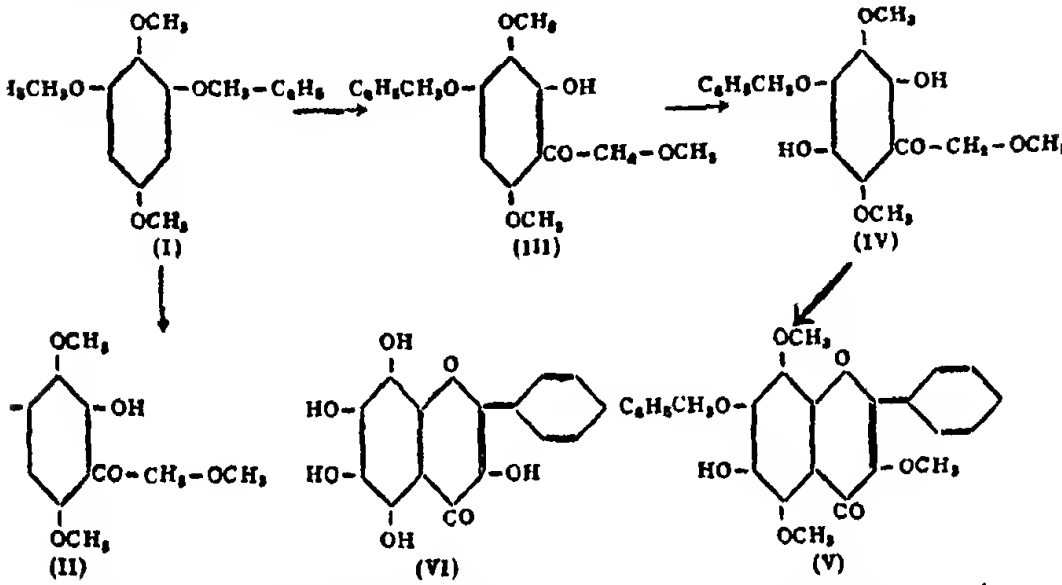

When condensed with benzoic anhydride and sodium benzoate according to the method of Allan and Robinson the acetophenone (IV) yielded the corresponding 6-hydroxyflavonol derivative (V) This compound dissolved in aqueous alkali with an yellow colour and gave no characteristic ferric reaction; in these properties it closely resembled similar flavone derivatives having the 6-hydroxyl alone free [1] On demethylation it yielded the pentahydroxyflavonol, 6 . 8-dihydroxy galangin (VI) whose identity was confirmed by comparison with a sample obtained by other methods[1, 3] and also by the preparation of the acetate

The synthesis of the flavonols of this group can thus be effected in a fewer number of stages and in fairly good yields Further by the debenzylation of the 6-hydroxyflavonol derivatives (V), it is possible to get the 6 : 7-dihydroxy compounds Again by adopting known methods of methylation and partial demethylation several partial methyl ethers of this group of flavonols could be obtained.

Experimental

2-Hydroxy-ω : 3 : 6-trimethoxy-4-benzyloxyacetophenone (III).—

1 : 4-Dimethoxy-2 : 6-dibenzyloxybenzene (5 g.) was brought into complete solution in enough dry ether and methoxyacetonitrile (4 c.c.) and finely

powdered fused zinc chloride (1 g.) were added A rapid stream of dry hydrogen chloride was passed through the solution which was cooled by means of ice-salt mixture In about an hour, the ketimine hydrochloride separated as an orange-red crystalline crust and the hydrogen chloride gas was passed for further two hours The container was then corked tight and left in the refrigerator for 24 hours. The supernatant ether solution was decanted off and the crystalline solid washed thrice with 20 c c. portions of dry ether Water (100 c c) was then added while cooling the flask under the tap and the hydrolysis effected by heating the mixture on the water-bath at 60–70° for half an hour with frequent stirring The ketimine hydrochloride gradually went into solution with the simultaneous separation of a pale yellow crystalline solid. Unless the hydrolysis was carefully conducted the product was a deep-brown semi-solid which did not easily solidify After cooling, the solid was filtered, washed and crystallised twice from dilute alcohol using a little animal charcoal Yield, 1·5 g. After a third crystallisation from the same solvent, 2-hydroxy-ω. 3 6-trimethoxy-4-benzyloxyacetophenone was obtained as narrow rectangular plates and prisms and it melted at 109–110° It was very sparingly soluble in hot water and dissolved in 10% aqueous sodium hydroxide from which a sparingly soluble sodium salt separated. Its solution in alcohol developed a brown-pink colouration with ferric chloride (Found· C, 65 2; H, 6 3 $C_{18}H_{20}O_6$ requires C, 65 1; H. 6 0%).

Debenzylation.—

The foregoing benzyl ether (0 5 g.) was dissolved in glacial acetic acid (4 c.c) and after the addition of hydrochloric acid (d, 1·16, 2 c.c.) the solution was heated on the boiling water-bath for one hour. Water (50 c.c.) was then added and the solution extracted twice with ether. The ether solution was washed with water and the solid obtained after removal of the solvent was crystallised from hot water It was obtained as long colourless needles and melted at 149–150° The melting point was not depressed on admixture with an authentic sample of 2 : 4-dihydroxy-ω · 3 : 6-trimethoxyacetophenone.

2 : 5-*Dihydroxy-ω 3 6-trimethoxy-4-benzyloxyacetophenone* (*IV*) —

To a constantly stirred solution of the above acetophenone (4 g.) in aqueous sodium hydroxide (75 c.c. containing 3 g of sodium hydroxide) was added dropwise during the course of 3 hours, a solution of potassium persulphate (4 g.) in water (75 c.c.), the temperature being maintained at 15–20° throughout the addition. After allowing to stand over-night, the

mixture was rendered just acid to litmus by adding concentrated hydrochloric acid, while cooling the flask under the tap The solution was filtered to remove the unchanged original ketone that was precipitated and extracted once with ether To the clear deep-red aqueous solution was added concentrated hydrochloric acid (10 c c) along with benzene (25 c c) and the mixture heated on the water-bath at 45–50° for half an hour. After cooling, it was thoroughly shaken, the benzene layer separated and the aqueous solution extracted twice with benzene The combined benzene extract was dried over sodium sulphate and distilled under diminished pressure The 2 5-dihydroxy-compound was thus obtained as a deep yellow viscous oil which did not solidify on keeping in the refrigerator for 48 hours and did not crystallise even after repeated attempts using benzene-petroleum ether mixture Yield, 0 4 g It was easily soluble in the ordinary organic solvents Its solution in alcohol gave a transient green colouration with a drop of ferric chloride and turned deep reddish-brown on the addition of a few more drops of the reagent, it deposited a brown precipitate after about an hour The dihydroxy compound dissolved in aqueous sodium carbonate and hydroxide to give orange-red solutions which turned reddish-brown on keeping No precipitate was obtained with lead acetate in alcoholic solution

3 · 5 : 6 . 7 · 8-*Pentahydroxyflavone* (6 : 8-*Dihydroxy galangin, VI*) · *Allan-Robinson Condensation.*—

To an intimate mixture of benzoic anhydride (2 g) and sodium benzoate (0·5 g) was added a solution of the above dihydroxy ketone (0 6 g.) in dry ether The solvent was carefully distilled off and the mixture heated at 175–180° for 4 hours in an oil-bath under diminished pressure After cooling, the pale brown cake was broken up, dissolved in alcohol (20 c.c.) and the mixture heated under reflux for 10 minutes. A solution of potassium hydroxide (3 g) in water (8 c c) was then gradually added and the refluxing continued for a further period of 20 minutes After distilling off the alcohol under reduced pressure, the brown residue was dissolved in water (50 c c), filtered to remove some insoluble matter, and saturated with carbon dioxide. The crude flavone was precipitated as a brown semi-solid and the mixture was therefore ether extracted and the ether solution dried over sodium sulphate. On distilling off the solvent, the substance was obtained again as a semi-solid and was directly used for demethylation. Yield, 0·4 g. It was readily soluble in alcohol, acetone and glacial acetic acid and dissolved in aqueous sodium hydroxide with an yellow colour. Its alcoholic solution gave no prominent characteristic colour with ferric chloride Its solution

in concentrated sulphuric acid was yellow and exhibited no fluorescence. With magnesium and hydrochloric acid it gave an orange-yellow colour in alcoholic solution.

Demethylation.—

The above product (0·3 g) was dissolved in acetic anhydride (5 c.c.) and cautiously treated with hydriodic acid (d. 1·7, 5 c c) The solution was then heated in an oil-bath at 135–140° for two hours, cooled, and diluted with water saturated with sulphur dioxide. The yellow solid that separated was collected, washed with water, dried and crystallised twice from ethyl acetate Yield, 0·2 g. On recrystallisation from the same solvent, the tetrahydroxyflavonol was obtained as yellow narrow rectangular plates which slowly turned greenish-brown on exposure to air It melted at 257–58°; it was identical in every respect with an authentic sample of 6 8-dihydroxy galangin obtained by other methods and the mixed melting point was undepressed (Found in material dried *in vacuo* at 120–125° for two hours C, 59 8; H, 3 6; $C_{15}H_{10}O_7$ requires C, 59·6, H. 3 3%)

3 : 5 : 6 : 7 · 8-*Pentaacetoxyflavone* —

The tetrahydroxyflavonol (0·1 g) was acetylated by boiling with acetic anhydride (2 c c) and a few drops of pyridine for 3 hours The penta-acetate crystallised from ethyl acetate as colourless flat needles and narrow rectangular plates and melted at 207–208° with slight sintering at 204° The melting point was undepressed on admixture with the penta-acetate of 6 : 8-dihydroxy galangin obtained by other methods (Found · C, 58 7; H, 3 9; $C_{25}H_{20}O_{12}$ requires C, 58 6; H, 3·9%)

Summary

A satisfactory procedure for the preparation of 2-hydroxy-ω : 3 · 6-trimethoxy-4-benzyloxy-acetophenone is described Oxidation of this to the 2 . 5-dihydroxyketone (IV), its condensation with the anhydride and sodium salt of benzoic acid and subsequent demethylation yield 6 : 8-dihydroxy-galangin This constitutes a simplified method for the synthesis of 5 . 6 · 7 : 8-hydroxyflavonols and their methyl ethers

References

1. Murti, Row and Seshadri . *Proc Ind. Acad. Sci*, A, 1946, 24, 233
2. Rao, Rao and Seshadri . *Ibid*, 1944, 19, 88
3. Seshadri and Venkateswarlu .. *Ibid.*, 1946, 23, 192

SYNTHESIS OF 5:7:8-HYDROXYFLAVONES AND THEIR DERIVATIVES

By V D. Nageswara Sastri and T. R Seshadri, F A Sc
(*From the Department of Chemistry, Andhra University*)

Received May 6, 1946

Though a number of flavonols with the 5:7:8-arrangement of hydroxyl groups have been isolated from plants, only one member of the corresponding flavone series has so far been found in them and that is wogonin It was first isolated by Takahashi[1] from the roots of *Scutellaria baicalensis* in which it occurs along with baicalein Its constitution was first investigated by Shibata, Iwata and Nakamura[2] and later by Hattori[3] It was found to have the formula $C_{16}H_{12}O_5$ and a methoxyl group By fission with alkali, benzoic acid and acetophenone were obtained These indicated that it was a flavone with the side phenyl nucleus unsubstituted Diazomethane effected only partial methylation and the monomethyl ether formed thereby gave reactions for the presence of a free hydroxyl group in the 5-position Complete methylation could be carried out by means of dimethyl sulphate and alkali and the product, O-dimethyl wogonin, was found to be different from baicalein trimethyl ether Further the trihydroxy-compound obtained by the demethylation of wogonin was not identical with baicalein Consequently wogonin was considered to be a monomethyl ether of 5·7 8-trihydroxyflavone From a study of the absorption spectrum Hattori[3] fixed the position of the methoxyl group as 8 (Formula I) The isolation of iretol (II) from the products of alkali degradation of wogonin (Hattori and Hayashi[4]) further supported the above conclusion

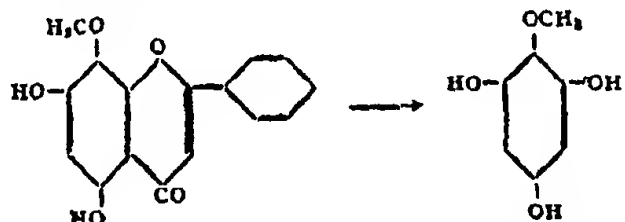

(I) (II)

In order to provide synthetic evidence in confirmation of the constitution of wogonin, Hattori[3] proceeded as follows 2:3·4:6-Tetramethoxyacetophenone (III) was treated with aluminium chloride and the product, considered to be 2-hydroxy-3:4.6-trimethoxyacetophenone (IV), was fused

with benzoic anhydride and sodium benzoate according to the method of Allan and Robinson. The trimethoxy flavone thus obtained was identical with wogonin dimethyl ether (V) and it yielded on demethylation a trihydroxyflavone different from baicalein and identical with norwogonin. The constitution of the ketone was, however, indefinite since demethylation with aluminium chloride could take place in either of the two ortho-positions. Further Nierenstein[5] claimed to have obtained the acetophenone (IV) with a different melting point. As a matter of fact Shibata and Hattori[6] at one time felt that the substance was in reality the isomeric 2-hydroxy-4 5:6-trimethoxyacetophenone (VI) Subsequently, however, Hattori[7] supplied indirect evidence in support of the earlier constitution (IV) for the ketone by the following series of reactions Antiarol (VII) was transformed into its ethyl ether (VIII) which underwent conversion into 2-hydroxy-3:4-dimethoxy-6-ethoxyacetophenone (IX) by the action of acetyl chloride and aluminium chloride The analogy is based on the assumption that the ethoxy and methoxy groups can be dealkylated with equal ease.

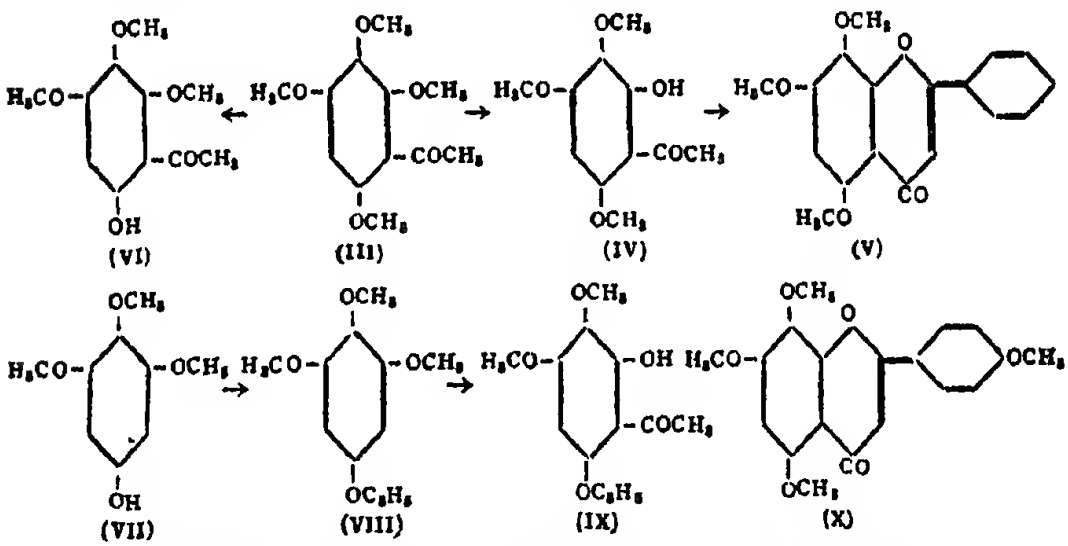

The Allan-Robinson method was also used for the synthesis of the higher member of the flavone series and Hattori[7] claimed the synthesis of 5 7.8:4'-tetramethoxyflavone (X) by the anisoylation of the ketone (IV).

Wessely and Moser[8] employed for their synthetic work 2:4-dihydroxy-3:6-dimethoxy-acetophenone (XI), a ketone with a definite constitution. However, the Allan-Robinson condensation using anisic anhydride and sodium anisate took an unexpected course resulting in partial demethylation and the formation of the dimethyl ether of scutellarein (XII); the expected

5 : 7 : 8-compound (XIII) was obtained in only one experiment out of a large number. This result was confirmed by Wessely and Kallab[9] who, however, noticed that the anisoylation of the ketone (IV) led to the formation of the 5 . 7 : 8-compound (X) in agreement with the observation of Hattori,[7] no demethylation interfering in this case with the normal course of the reaction

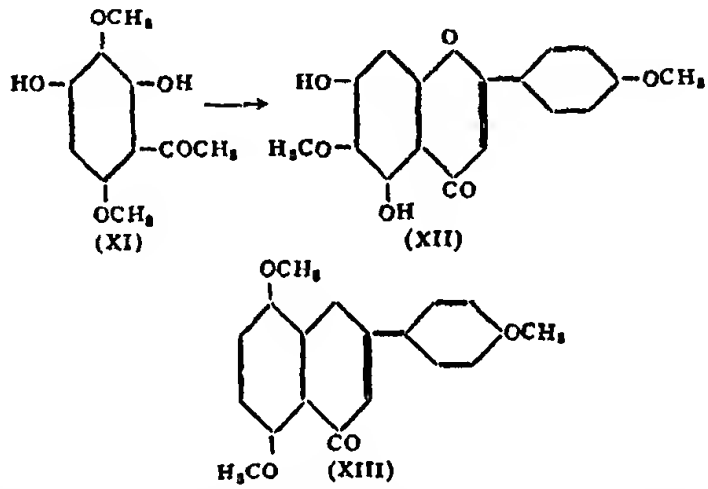

Contrary to the results of Wessely and Moser,[9] Furukawa and Tamaki[10] claimed that the anisoylation of the above dihydroxyketone (XI) proceeded normally to yield 5 8 4'trimethoxy-7-hydroxy flavone (XIII) The benzoylation was also reported to give the normal product (Shah, Mehta and Wheeler[11]) which in this case was 5 : 8 · dimethoxy-7-hydroxy-flavone (XIV). Wogonin (XV) was obtained from it by partial demethylation and wogonin dimethyl ether by methylation.

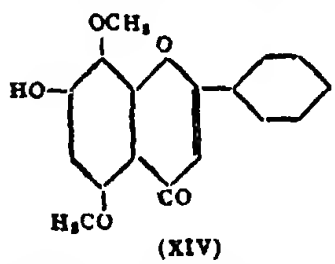

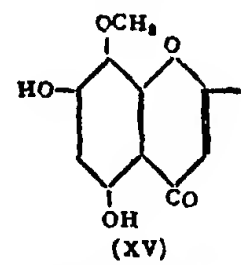

Obviously slight and ununderstood changes in the experimental conditions seem to bring about these differences in the nature of the products and the Allan-Robinson reaction has not yielded, in the case of these flavones, as consistent results as with the corresponding series of flavonols.[12] Since authentic samples of the 5 : 7 . 8-hydroxyflavones and their derivatives were required in connection with the study of plant colouring

matters in progress in these laboratories, it was found necessary to synthesise them by the Baker-Venkataraman method starting with a ketone of unambiguous constitution.

2-Hydroxy-3:4:6-trimethoxyacetophenone (IV) has now been prepared by a direct method which is free from ambiguity It involves partial methylation of 2·4-dihydroxy-3·6-dimethoxyacetophenone (XI) The product is, however, found to be identical with the sample obtained by the nuclear acetylation of 1·2:3:5-tetramethoxybenzene according to the improved method of Baker[12] which involves partial demethylation The preparation of the dihydroxy ketone itself has now been simplified It is obtained directly from 1·4-dimethoxy-2 6-dibenzyloxybenzene by the Hoesch reaction using acetonitrile, debenzylation and condensation taking place in one operation Its benzoate (XVI) undergoes smooth rearrangement in the presence of sodamide to form 2-hydroxy-3:4.6-trimethoxydibenzoylmethane (XVII) which subsequently yields 5 7.8-trimethoxyflavone (XVIII) when heated with acetic acid and sodium acetate This agrees in its properties with the dimethyl ether of wogonin[3] The higher member of this series, 5·7:8:4′-tetramethoxyflavone (XVIII, R = OCH_3) has also been prepared in a similar way using the O-anisoyl derivative of the ketone

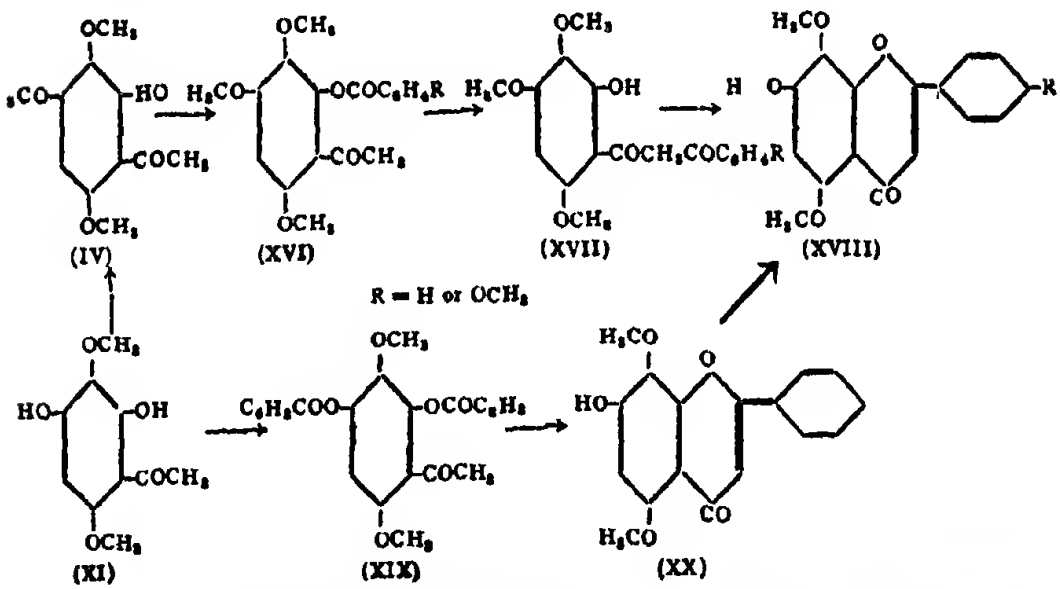

The dihydroxy ketone (XI) has also been directly used for this synthesis. The dibenzoate (XIX) undergoes migration and subsequent ring-closure to 5:8-dimethoxy-7-hydroxyflavone (XX) though the yields are poor. This

compound corresponds in its properties to the product obtained by Shah, Mehta and Wheeler[11] by adopting the Allan-Robinson method Its constitution is definite since it has yielded 5 7 · 8-trimethoxyflavone (wogonin dimethyl ether) (XVIII) on methylation

Discordant results have been reported in regard to the action of hydriodic acid on the methyl ethers of the 5 7 · 8-hydroxyflavones Hattori[9] and Furukawa and Tamaki[10] claimed to have obtained the normal products of demethylation from wogonin, wogonin dimethyl ether, 5-ethoxy-7 : 8-dimethoxyflavone and 7-hydroxy-5 8 . 4′-trimethoxyflavone On the other hand Wessely and coworkers [8, 9] noticed isomeric change into the 5 6 7-hydroxy compounds Shah, Mehta and Wheeler[11] also met with this difficulty in the use of hydriodic acid and hence they effected demethylation using aluminium chloride which was found to be free from this defect At a later stage Hattori,[14] reviewing the whole position, explained that these discrepancies were due to the different conditions used by the different workers and reported that, when employed under controlled conditions, hydriodic acid does not bring about isomeric change Our experiments using wogonin dimethyl ether indicate that by boiling for two hours with hydriodic acid, as is usually done in ordinary demethylations, almost complete conversion into baicalein takes place and this is obtained in a pure condition on crystallising the product It has also been characterised by the preparation of the acetate Though under the milder conditions prescribed by Hattori[14] the product consists essentially of norwogonin, the melting point is frequently found to be low even after repeated crystallisation and only under exceptional circumstances is a pure sample obtained It would appear that though the isomeric change is considerably minimised, it is not altogether avoided. Under these mild conditions sometimes the demethylation is not complete The behaviour of the higher member (tetramethoxy flavone) is quite similar Shah, Mehta and Wheeler[11] employed anhydrous aluminium chloride in nitrobenzene for the demethylation of 5 . 8-dimethoxy-7-hydroxy-flavone and obtained norwogonin For the demethylation of wogonin dimethyl ether we have now employed this reagent in benzene medium since a methoxyl in the 7-position of flavones is best demethylated in this solvent [15] Norwogonin thus obtained is a golden yellow crystalline solid melting at 257–59° and yielding an acetate melting at 225–6° Its properties are quite different from those of baicalein, the reactions with alkali, ferric chloride and *p*-benzoquinone being quite characteristic.

EXPERIMENTAL

2 : 4-Dihydroxy-3 : 6-dimethoxyacetophenone (XI) —

2 : 6-Dibenzyloxy-1 : 4-dimethoxybenzene[12] (3·5 g.) was treated with anhydrous ether (50 c c), freshly distilled acetonitrile (1·5 c c) and finely powdered fused zinc chloride (1 g.) A rapid stream of dry hydrogen chloride was passed through the mixture during the course of 5 hours, the reaction flask being cooled in ice-salt mixture. The ketimine hydrochloride began to separate as a dark brown semi-solid mass and the reaction was completed by keeping the tightly corked flask in a refrigerator for two days The ether was then decanted and the residue of the ketimine hydrochloride washed twice with 20 c c portions of dry ether It was dissolved in water (50 c c) and the hydrolysis effected by heating the solution on the boiling water-bath for ½ hour. On cooling, it deposited the crude ketone as a practically colourless crystalline mass with a small quantity of resinous matter It was filtered, washed and crystallised twice from hot water (charcoal) when the dihydroxy ketone was obtained as bunches of long colourless needles which melted at 128–129° (Wessely and Moser[8] give m p 129°): Yield, 1 5 g It was freely soluble in alcohol and dissolved with a pale yellow colour in aqueous sodium hydroxide and aqueous sodium carbonate Its alcoholic solution developed a violet-brown colouration with a drop of ferric chloride. (Found · C, 56 7; H, 5 9; $C_{10}H_{12}O_5$ requires C, 56 6, H, 5·7%)

2-Hydroxy-3 4 · 6-trimethoxyacetophenone (IV) —

A mixture of the above dihydroxyacetophenone (1 g), dry acetone (5 c c.), dry benzene (50 c.c), anhydrous potassium carbonate (3 g) and acid-free dimethyl sulphate (0 5 c.c.) was refluxed on the water-bath for 12 hours. The inorganic salts were then filtered off and washed with a small quantity of warm benzene The benzene filtrate was washed twice with water and then extracted with 5% aqueous sodium hydroxide On acidification with hydrochloric acid, the alkaline extract yielded the partially methylated ether as a pale brown solid. It was filtered, washed with water and crystallised twice from dilute alcohol Yield, 0·8 g. It was obtained as pale yellow stout rectangular prisms melting at 113–114°. It dissolved in aqueous sodium hydroxide to a pale yellow solution and gave a reddish brown colour with ferric chroride in alcoholic solution (Found: C, 58 6; H, 6·5; $C_{11}H_{14}O_5$ requires C, 58 4; H, 6·2%) For the substance obtained by the nuclear acetylation of 1 : 2 3 : 5-tetramethoxybenzene Baker[13] gave the melting point of 103–105° Its melting point could now be raised to 113–114° by repeated crystallisation and it is identical with the sample described above.

2-Benzoyloxy-3, 4·6-trimethoxyacetophenone (XVI, R = H) —

2-Hydroxy-3, 4, 6-trimethoxyacetophenone (2 g) was dissolved in dry pyridine (10 c c) and treated with benzoyl chloride (1 5 c.c) The mixture was heated on a boiling water-bath for 30 minutes and then added to ice-water containing a little dilute hydrochloric acid; the oil that first separated solidified to a crystalline solid on stirring It was filtered off, washed with very dilute hydrochloric acid and water and dissolved in sufficient quantity of ether The ether solution was washed with 5% aqueous sodium carbonate and 5% aqueous sodium hydroxide to remove any acid and unchanged hydroxyketone. After a final washing with water it was dried over calcium chloride and the solvent distilled. The colourless crystalline solid residue was recrystallised from alcohol and alcohol-benzene mixture when the benzoyl derivative was obtained as rhombohedral prisms and melted at 124–125° Yield, 2 5 g It was insoluble in aqueous alkali and gave no colour with ferric chloride in alcoholic solution (Found: C, 65 4, H, 5 5; $C_{18}H_{18}O_6$ requires C, 65 5, H, 5·5%)

2-Hydroxy-3 4 6-trimethoxydibenzoylmethane (XVII, R = H) —

The O-benzoyl derivative (3 g) was dissolved in dry toluene (30 c c) and treated with sodamide (10 g) finely powdered under toluene The mixture was heated on a steam-bath for five hours with frequent shaking and left overnight The yellow solid was then collected, washed well with warm benzene, dried and added in small quantities to crushed ice When all the unchanged sodamide was decomposed, the yellow solution was filtered to remove insoluble impurities and saturated with carbon dioxide The dibenzoylmethane separated as a deep orange-yellow oil which solidified in the course of about an hour It was collected, washed and crystallised from benzene-light petroleum mixture, yield, 1·5 g. On recrystallisation from the same solvent, the dibenzoylmethane was obtained as long, stout rectangular prisms and melted at 132–133°. It dissolved in aqueous sodium hydroxide to give a bright yellow solution and gave an intense reddish-brown colouration with ferric chloride in alcoholic solution. (Found: C, 65 7, H, 5 5; $C_{18}H_{18}O_6$ requires C, 65·5; H, 5 5%)

5 : 7 : 8-Trimethoxyflavone (wogonin dimethyl ether, XVIII, R = H) —

A mixture of the dibenzoylmethane (1 g.), glacial acetic acid (10 c c) and fused sodium acetate (2 g) was gently boiled over a wire-gauze for 4 hours. On dilution with water the trimethoxyflavone separated as a colourless crystalline solid which was collected, washed and crystallised twice from dilute alcohol It was obtained as colourless, long narrow rectangular plates

and prisms melting at 166–167°: yield, 0·7 g (Hattori[8] gives m p 167–168°). Its solution in concentrated sulphuric acid was yellow and exhibited no fluorescence (Found in material dried at 120° for two hours *in vacuo*: C, 69 3, H, 5·4; $C_{18}H_{16}O_5$ requires C, 69 2, H, 5 1%)

2·4-Dibenzoyloxy-3 6-dimethoxyacetophenone (XIX) —

A mixture of the dihydroxyketone (XI, 2 g), dry pyridine (10 c c) and benzoyl chloride (3 g) was heated on the water-bath for 30 minutes and then added to water containing hydrochloric acid The semi-solid product obtained, was worked up as in the previous benzoylation After crystallisation from alcohol, the dibenzoate was obtained as colourless prismatic rods and melted at 117-118° It was insoluble in aqueous sodium hydroxide and gave no colour with ferric chrloride in alcohol solution (Found: C, 68 6, H, 5 0, $C_{24}H_{20}O_7$ requires C, 68 6, H, 4 8%)

Rearrangement of (XIX) —

Sodamide (6 g) finely powdered under toluene, was added to the dibenzoate (2 g) in toluene (30 c c) and the mixture heated on the water-bath for 4 hours It was yellow in the initial stages and rapidly acquired a greenish tinge. The solid product was collected, washed with toluene, and dissolved in ice-water, the solution was filtered and saturated with carbon dioxide Not much solid, however, was precipitated in this case, and the entire mixture was therefore extracted with ether The ether solution, after drying over sodium sulphate, was distilled leaving an orange-yellow semi-solid which gradually solidified when left in the refrigerator for 24 hours. It was filtered and crystallised from benzene-light petroleum mixture when rhombic prisms were obtained: yield, 0·5 g It melted between 117–125° and appeared to be a mixture of 2-hydroxy-4-benzoyloxy- and 2:4-dihydroxy-3:6-dimethoxy-ω-benzoylacetophenones; it was used directly for the next stage in the synthesis. It dissolved in aqueous sodium hydroxide to an yellow solution and gave a reddish-brown colouration with ferric chloride in alcoholic solution

7-Hydroxy-5 8-dimethoxyflavone (XX) —

The foregoing product (0 4 g.) was dissolved in glacial acetic acid (5 c c.), freshly fused sodium acetate (1 g.) added and the whole gently boiled over a wire-gauze for 4 hours The mixture was diluted with water (50 c.c.) and the precipitated pale-brown crystalline solid filtered and washed with a small quantity of water and alcohol. It was dissolved in 5% aqueous sodium hydroxide and the bright yellow solution filtered to remove some insoluble residue. The flavone was then reprecipitated by passing carbon

dioxide into the clear alkaline solution. It was filtered, washed with hot alcohol, acetone and ether, and finally crystallised from ethyl acetate. 7-Hydroxy-5 8-dimethoxy-flavone was then obtained as long rombohedral plates and it melted at 286-287° (Shah, Mehta and Wheeler[11] record m p 287–288°)· yield, 0 3 g It was very sparingly soluble in the common organic solvents and dissolved in aqueous sodium hydroxide to a bright yellow solution It gave no colour with ferric chloride in alcoholic solution and dissolved in concentrated sulphuric acid to an yellow solution without any fluorescence (Found C, 68 3, H, 4 8, $C_{17}H_{14}O_5$ requires C, 68 5; H, 4·7%)

To a suspension of the above hydroxyflavone (0 2 g) in dry acetone (25 c c.) were added acid-free dimethyl-sulphate (1 c c.) and anhydrous potassium carbonate (2 g) The mixture was heated under reflux for 12 hours, the potassium salts filtered and washed with warm acetone The acetone filtrate was concentrated to small bulk and diluted with water The precipitated methyl ether was crystallised from dilute alcohol when it was obtained as colourless narrow rectangular plates and prisms melting at 166–167° and identical with authentic 5.7 8-trimethoxyflavone already described

5 7· 8-*Trihydroxyflavone (norwogonin)*

Wogonin dimethyl ether (0 2 g) was dissolved in dry benzene (12 c c) and freshly powdered anhydrous aluminium chloride (1 0 g) added and the mixture gently refluxed on a water-bath kept at 80-85° for one hour After cooling, the solvent was decanted and the orange coloured solid residue decomposed with ice and dilute hydrochloric acid. Finally, the mixture was diluted with water and heated on a boiling water-bath for 15 minutes. The colour of the solid turned golden yellow It was filtered and washed. The product appeared crystalline and melted at 252-254° sintering a few degrees earlier A recrystallisation from rectified spirits yielded golden yellow rectangular rods and prisms melting at 258-60° Further recrystallisation did not raise the melting point Shah *et al*[11] gave the melting point as 250–51° (Found OCH_3, nil, C, 66 8, H, 4·0; $C_{15}H_{10}O_5$ requires C, 66 7, H, 3·7%) When to an alcoholic solution of the substance a drop of ferric chloride solution is added, a brown colour is obtained which intensifies to a deep reddish-brown on further addition With a very dilute solution of the reagent and using just a drop it is possible to get a pale green colour, but further addition yields the deep reddish-brown. A similar deep reddish-brown solution results on adding an alcoholic solution of *p*-benzoquinone and a brown precipitate is slowly formed. With 2% aqueous alkali

it forms an immediate brownish-red solution which instantaneously changes into pale blue; this slowly fades to a very pale yellow With a buffer solution of pH 12·2 an orange-yellow solution is obtained which fades rapidly to a pale yellow colour in the course of a few minutes

The acetate of norwogonin was prepared by boiling the hydroxyflavone with acetic anhydride and a drop of pyridine for 3 hours It crystallised from ethyl acetate as colourless rectangular rods melting 225–226°. Hattori[7] gave the melting point as 216–17°. (Found. C, 63 5; H, 4 2; $C_{21}H_{16}O_6$ requires C, 63 6, H, 4 1%)

2-*Anisoyloxy*-3 4 : 6-*trimethoxyacetophenone* (*XVI*, $R = OCH_3$) —

A mixture of the acetophenone (IV, 2 g.), dry pyridine (10 c c) and anisoyl chloride (2 c.c.) was heated on the water-bath for 30 minutes. The pale-brown solid obtained by adding ice-water containing hydrochloric acid, was filtered, washed with very dilute hydrochloric acid and water, and treated thrice with 50 c.c portions of cold ether to remove unchanged original ketone. After two crystallisations from alcohol the anisoyl derivative was obtained as rombic prisms melting at 173–174°. Yield, 3·0 g. It was insoluble in aqueous sodium hydroxide and gave no ferric reaction. (Found. C, 63 3, H, 5 7; $C_{19}H_{20}O_7$ requires C, 63 3, H, 5 6%)

2-*Hydroxy*-3 · 4 : 6 4'-*tetramethoxydibenzoylmethane* (*XVII*, $R = OCH_3$) —

The O-anisoyl derivative (2·5 g), dry toluene (30 c c.) and finely powdered sodamide (8 g) were used for the rearrangement The dibenzoylmethane which was precipitated from the alkaline solution as a yellow solid, was crystallised twice from benzene-light petroleum mixture. It was thus obtained as yellow narrow rectangular plates melting at 155–156°: yield, 1·4 g It dissolved in aqueous alkali to give an yellow solution and its alcoholic solution developed a reddish-brown colouration with ferric chloride. (Found: C, 63·3, H, 5 6; $C_{19}H_{20}O_7$ requires C, 63 3; H, 5 6%)

5 . 7 : 8 . 4'-*Tetramethoxyflavone* (*XVIII*, $R = OCH_3$) —

A mixture of the above dibenzoylmethane (1 g.), glacial acetic acid (10 c.c.) and sodium acetate (2 g.) was gently boiled over a wire-gauze for 4 hours, and then diluted with water; the tetramethoxyflavone was precipitated as a colourless crystalline solid. It was twice crystallised from alcohol when long needles and narrow rectangular plates melting at 209–210° were obtained: Yield, 0·8 g. (Wessely and Kaliab[9] give 208°; Hattori[7] gives m p. 207–208°) It was moderately soluble in

alcohol, more so in acetone and acetic acid The yellow solution in concentrated sulphuric acid exhibited no fluorescence (Found: in material dried at 120-125° *in vacuo* for two hours: C, 66 6; H, 5 5; $C_{18}H_{18}O_6$ requires C 66 7; H, 5 3%).

Summary

Since there was an element of uncertainty in the methods employed in the past for the synthesis of 5. 7. 8-hydroxyflavone derivatives, an unambiguous method has now been worked out The required ketone, 2-hydroxy-3 : 4 6-trimethoxyacetophenone has been prepared by the partial methylation of 2 : 4-dihydroxy-3 : 6-dimethoxyacetophenone which is obtained directly from 1 · 4-dimethoxy-2. 6-dibenzyloxybenzene by the Hoesch reaction It has been converted into 5 7 : 8-trimethoxyflavone (wogonin-dimethyl ether) and 5 7 : 8 4'-tetramethoxyflavone by the Baker-Venkataraman procedure Even the above dihydroxyketone could be used for this purpose fairly satisfactorily and it yields as an intermediate stage 5 8-dimethoxy-7-hydroxyflavone Demethylation with hydriodic acid even under mild conditions is not satisfactory. Nor-wogonin is best obtained by employing anhydrous aluminium chloride in benzene solution for this reaction

References

1. Takahashi — *Chem Zentr*, 1889, ii, 620
2. Shibata, Iwata and Nakamura — *Acta Phytochim*, 1923, 1, 105.
3. Hattori — *Ibid*, 1930, 5, 99
4. ——— and Hayashi — *Ber*, 1933, 66, 1279
5. Nierenstein — *J C S*, 1917, 4
6. Shibata and Hattori — *J Pharm Soc. Japan*, 1931, 51, 15. *Chem Zentr*, 1931, i, 3358.
7. Hattori .. *Acta Phytochim*, 1931, 5, 219
8. Wessely and Moser — *Monatsh*, 1930, 56, 97
9. ——— and Kallab — *Ibid.*, 1932, 60, 26
10. Furukawa and Tamaki — *Bull Inst. Phy Chem. Research* (Tokyo), 1931, 10, 732.
11. Shah, Mehta and Wheeler — *J C S*, 1938, 1555
12. Baker, Nodzu and Robinson . *Ibid*, 1929, 74
    Goldsworthy and Robinson — *Ibid*, 1938 56.
    Rao, Rao and Seshadri — *Proc Ind Acad. Sci*, A, 1944, 19, 88
13. Baker — *J C.S*, 1941, 666
14. Hattori . *Ber*, 1939, 72, 1914.
15. Krishnaswamy and Seshadri — *Proc Ind Acad. Sci*, A, 1942, 15, 437.

KINETICS OF THE HYDROLYSIS OF ANILIDES

By D D Karve and B W Kelkar
(Chemistry Department, Fergusson College, Poona)

Received December 1, 1945

The hydrolysis of anilides has mainly been studied from the points of view of (i) the kinetics, and (ii) the influence of structure on the ease and the velocity of hydrolysis The work carried out so far has been mainly confined to the ease of saponification with regard to the position of the substituted groups in anilides, and the pH of the reacting medium One of the major difficulties experienced in these studies is that investigations on all the anilides could not be conducted in the same solvent for want of solubility

The authors have attempted a detailed study of the hydrolysis of sixteen anilides under varying conditions of temperature, solvent, concentration of catalyst, etc.

Experimental Technique

Among the anilides investigated, formanilide, form-*o*-toluidide, form-*p*-toluidide, *p*-nitroacetanilide, *p*-bromoacetanilide and benzoyl-*p*-toluidide were prepared in the laboratory according to standard methods Acet-*o*-toluidide, acet-*m*-toluidide, acet-*p*-toluidide, acet-α-naphthalide, acet-β-naphthalide, propionanilide, benzanilide and benzoyl-*o*-toluidide were products of the British Drug House Acetanilide was a product of Schering-Kahlbaum, whereas *o*-nitroacetanilide was a product of Messrs E Merck All these compounds were tested for their purity before use

The alcohol used was a product of the Government Distillery, Nasik, and it was distilled with alkaline permanganate, the portion between 77° and 78° C being used in this investigation Sulphuric acid used was an extra-pure compound. Barium hydroxide, used in the estimation of acid liberated during the reaction, was a product of the British Drug House

The hydrolysis was carried out in flasks fitted with ground-glass reflux condensers placed in a thermostat maintained at a constant temperature with a variation of 0 1° C. Equal volumes of anilide solutions and sulphuric acid solutions (catalyst) were mixed at any required temperature and the liberated acid was estimated from time to time by titrating 25 c.c. of the reaction mixture against 0·1 N barium hydroxide solution, using methyl red as an indicator. Where acetic acid was used as a solvent, separate test-tubes, fitted with reflux condensers, were used for carrying out the reactions,

the amine liberated at definite intervals of time being estimated in the contents of each test-tube. The infinity reading was calculated from the initial concentration of the anilide when alcohol was used as the solvent, while in other cases it was obtained experimentally.

As many of the anilides were insoluble or not sufficiently soluble in water, absolute alcohol, water-alcohol mixtures or acetic acid were used as solvents. The introduction of alcohol in the reaction system caused ester formation with the acid liberated by hydrolysis of the anilides to some extent.

The values of K_1, the velocity constants for the hydrolytic reactions carried out under different conditions, were calculated from the equation for a uni-molecular reaction In the case of reactions in 50% alcohol, the values of $(a - x)$ were corrected for the amount of the acid esterified and the values of K_1 are the corrected values excepting those marked with an asterisk. The various results obtained are given in the following tables under four different headings The reactivity of the different anilides has been taken to be proportional to the velocity constant.

Results

(A) Hydrolysis of Anilides in Water

Table I *Effect of Catalyst Concentration*

Temperature 30 °C — Concentration of Anilide 0·05 M

Anilide	Concentration of catalyst (H_2SO_4)	$K_1 \times 10^4$	$K_2 \times 10^4$
Formanilide	0 05 N	13 2	28·4
	0 10 N	24 7	24·7
	0·25 N	61·3	24·5
Form-o-toluidide	0 05 N	5·3	10·6
	0·25 N	27 3	10·9

Table II *Effect of Temperature*

Formanilide in aqueous medium (0·05 M)

Temp. (°C.)	$K_1 \times 10^4$ at different concentrations of catalyst		
	0·05 N	0·10 N	0·25 N
30	13·2	24·7	61·3
35	19·7	38 0	.
40	27·2	51·8	126 8
45	40·4	78·5	..
Q (calories)	13,820	14,340	13,860

TABLE III. *Effect of Temperature*

Form *o*-toluidide in aqueous medium (0 05 M)

Temp. (°C)	$K_1 \times 10^4$ at different concentrations of catalyst	
	0 05 M	0·25 N
30	5·35	27·3
35	7 68	..
40	11 43	59·16
45	16 24	..
Q (calories)	14,230	14,730

TABLE IV. *Effect of Temperature*

Concentration of catalyst 0·25 N Concentration of anilide (0·10 M)

Temp. (°C)	Values of $K_1 \times 10^4$ for			
	Acetanilide	Acet-*o* toluidide	Acet *m* toluidide	*o*-Nitro acetanilide
65	14·36	..		..
70	20·10	7·4	..	..
75	29·40	..	..	..
80	41 22	13·6	99·2	76·2
85	59 00	..		105 3
90	83 00	24 6	78 7	155·7
95	120·00	..	..	211 2
Q (calories)	17,940	15,020	18,110	17,730

TABLE V *Reactivity of Different Anilides*

Concentration of anilide 0·05 M Concentration of catalyst 0·15 N

Anilide	Temperature	$K_1 \times 10^4$
Formanilide ..	40	126 8
Form *p*-toluidide .	40	102 5
Form *o*-toluidide ..	40	59 2
o-Nitroacetanilide .	80	76·2
Acetanilide ..	80	41 2
Acet-*m* toluidide ..	80	39·2
Acet-*o*-toluidide ..	80	13 6

(B) Hydrolysis of Anilides in 50% Alcohol

Table VI *Effect of Catalyst Concentration*

Concentration of anilide 0·05 M

Anilide	Temperature (°C)	Concentration of catalyst (H_2SO_4)	$K_1 \times 10^4$	$K_2 \times 10^4$
Formanilide	30	0·045 N	7 1	158
		0·100 N	16 5	165
		0·250 N	40 25	161
		0 300 N	47·32	158
Form *o*-toluidide	30	0 050 N	4 1	82
		0 100 N	8 6	86
		0 250 N	19 0	76
		0 300 N	22 8	76
Form *p* toluidide	30	0 050 N	5 8	116
		0·100 N	12·1	121
		0 250 N	28 0	112
		0 300 N	36 0	120
Acetanilide	70	0·150 N	7 0	46
		0 250 N	12 0	48
		0 350 N	16·5	47

Table VII *Effect of Temperature*

Concentration of Anilide 0 05 M Concentration of catalyst 0·25 N

Temp (°C)	Values of $K_1 \times 10^4$				
	Formanilide	Form *o* toluidide	Form *p* toluidide	Acetanilide	*o*-Nitro acetanilide
20	21 9	9·7	14 6	..	.
25	33 3	14·9	22 0		.
30	47 2	21 0	31·6		.
35	73 7	31 5	46·0	.	.
40	103·1	44 0	67·2	..	.
45	161 3	64 5	96 6	.	..
60	.		..	8·7	16·8
70	..		..	17·78	35·5
Q (calories)	12,720	13,600	12,990	14,560	15,210

Table VIII *Effect of Concentration of Anilide*

Concentration of catalyst 0·25 N Temperature 70° C.

Concentration of acetanilide (M)	0 025	0 050	0·10	0·15	0·20
$K \times 10^4$ ..	12·8	12 0	10·3	9·4	8·9

TABLE IX *Reactivity of Different Anilides*

Concentration of anilides 0·05 M Concentration of catalyst 0 25 N

Anilide	Temperature (°C)	$K_1 \times 10^4$
Formanilide	40	103 1
Form *p*-toluidide	40	67 0
Form-*o*-toluidide	40	44·0
p-Nitroacetanilide	70	42 1
o-Nitroacetanilide	70	33 4
Acet-α naphthalide	70	30 6
Propionanilide	70	20·6
Acet β naphthalide	70	18 8
Acetanilide	70	17 8
Acet *p*-toluidide	70	16·8
p-Bromacetanilide	70	16 5
Acet *m* toluidide	70	16·1
Acet-*o*-toluidide	70	7 4

(C) HYDROLYSIS OF ANILIDES IN ABSOLUTE ALCOHOL

TABLE X. *Reactivity of Different Anilides*

Temperature 65° C Concentration of catalyst 0 25 N

Anilide	Concentration of anilide	$K_1 \times 10^4$
	M	
Acetanilide	0·05	9·20
Benzanilide	0 01	3
Benz *p*-toluidide	0·0125	2·52
Benz-*o*-toluidide	0·0125	2·07

(D) HYDROLYSIS OF ANILIDES IN ACETIC ACID

TABLE XI *Effect of Temperature*

Concentration of catalyst 0·5 N Concentration of acetanilide 0·1

Temperature °C	$K_1 \times 10^4$
70	29·7
80	96·5
90	161·0

TABLE XII. *Effect of Change of Solvent on the Velocity of Hydrolysis*

Concentration of catalyst 0 25 N

Temp. (°C)	Anilide	Concentration of anilide	$K_1 \times 10^4$	
			In water	In 50% alcohol
30	Formanilide	0 05 M	61 3	47·5
30	Form *o*-toluidide	0 05 M	27 3	21 0
40	Form *p*-toluidide	0 025 M	103·1	67 2
70	*o*-Nitro-acetanilide	0·025 M	38 1	23·5
70	Acetanilide	0 05 M	20 1	17·7
70	Acet *m* toluidide	0 025 M	19 8	16 5

TABLE XIII *Effect of Change of Solvent on the Velocity of Hydrolysis*

Concentration of catalyst 0 25 N Concentration of acetanilide 0·05 M

Temperature 65° C

Solvent	$K_1 \times 10^4$
Water	14 36
10% alcohol	12·42
20% do	11 16
30% do	9 77
40% do	9 25
50% do	9·06
60% do	8·67
70% do	8 41
80% do	7 28
90% do	6·74
Absolute alcohol	5 72

DISCUSSION OF RESULTS

It will be seen from Table I that the velocity constant (K_1) increases as the concentration of the catalyst (b) is increased The plots of K_1 against b show that the relation between the two is a linear one The values of K_2, equal to K_1/b, were calculated and are given in the last column of Table I They are very nearly equal to each other A similar behaviour is noticed in the case of results given in Table VI

Straight lines are obtained on plotting the values of log K_1 against those of the reciprocal of the absolute temperature (1/T), indicating that the Arrhenius equation $\left(\frac{d \ln K}{dt} = \frac{Q}{RT^2}\right)$ is applicable to the reactions studied in this investigation The values of Q were calculated from the various straight lines and are given in Tables II, III, IV, VII and XI It will be

seen that the values of Q for a particular anilide are very nearly independent of the concentration of the catalyst

The effect of the concentration of the anilide was examined only in one case (*cf* Table VIII). It will be seen that the values of K_1 decrease regularly as the concentration of acetanilide is increased

The reactivity of different anilides in aqueous medium, 50%-alcohol and absolute alcohol are given in Tables V, IX and X, the order of reactivity being the same as given in these tables

Experiments were made on the determination of the effect of the solvent on the velocity constant of the hydrolysis of some anilides. The results obtained are given in Table XII It will be seen that invariably the values of K_1 in aqueous medium are greater than those in 50%-alcohol. Hence, a systematic investigation was made to determine the change in the value of K_1 with the addition of different amounts of alcohol to water. The results obtained in the case of acetanilide are given in Table XIII which show that the value of K_1 decreases systematically as the percentage of alcohol in alcohol-water mixtures is increased, the lowest value being obtained in absolute alcohol. Hence, it can be stated that the hydrolysis of anilides decreases in the following order·

Water > alcohol-water mixture > Alcohol

Summary and Conclusions

From a detailed study of the hydrolysis of sixteen different anilides in the presence of different concentrations of the catalyst (sulphuric acid), at different temperatures and with varying concentrations of the anilides, and in different solvents, it has been shown that the hydrolysis of anilides is a uni-molecular reaction. Straight lines are obtained on plotting values of log K_1 against those of 1/T, indicating that Arrhenius equation is applicable to these systems; the values of Q have been calculated from these straight lines and are found to be nearly independent of the concentration of the catalyst employed The effect of substituent groups in the anilides is in accordance with the electronic theory of valency. This is seen clearly if the velocity constants of acetanilide and benzanilide are compared. The slower hydrolysis of benzanilide, in spite of the presence of a donor group near the covalent linkage is probably to be explained by the proximity effect.

[illegible]. Printed at The Bangalore Press, Bangalore City, by G. Krishnan Rao, Superintendent, and Published by The Indian Academy of Sciences Bangalore

EQUILIBRIUM SURFACE TENSION OF AQUEOUS SOLUTIONS OF NEKAL BX AND THE EFFECT OF SALTS*

By T. Krishnappa, K. S. Gururaja Doss§ and Basrur Sanjiva Rao‖

Introduction

The study of the surface tension of aqueous solutions of wetting agents is of great interest from several points of view and has received considerable attention in recent years[1,2] Wetting agents are so highly capillary active that they may be expected to form unimolecular adsorption film with a completely close packing, even at low concentration, this makes it possible to apply Gibbs' adsorption equation for the evaluation of the molecular cross-section. Since the molecular cross-section of these substances can also be investigated by spreading on aqueous substrates[3,4] a comparative study can be made of the two methods for the determination of cross-section. The study would be of interest in correlating wetting power with surface tension, for it is known that wetting power is intimately connected with surface tension.[5] Moreover wetting agents may be expected to show the phenomenon of activated accumulation discovered in this laboratory[6,7,8] and also independently by McBain and co-workers.[9,10] Surface tension studies can be expected to throw light on the interpretation of this phenomenon.

Experimental

Purification of Nekal BX

The main impurity in commercial Nekal BX is sodium sulphate To remove this, Nekal BX was shaken well with hot benzene using a mechanical shaker. The undissolved portion was allowed to settle down. The supernatant solution was decanted out and the benzene was distilled off The residue was dried, powdered, heated in an oven at 110° C. for six hours and stored in a stoppered bottle in a desiccator over dehydrated calcium chloride.

* Part of thesis submitted by T. K in partial fulfilment of the requirements for the degree of Master of Science of the Mysore University

§ Physical Chemist, Imperial Institute of Sugar Technology, Cawnpore

‖ Principal, Central College, Bangalore

Ash content of purified Nekal BX

A known weight of purified Nekal BX was ignited in a platinum crucible. The ash was treated with dilute sulphuric acid to convert it into the sulphate, and the excess of the acid was evaporated. The residue was ignited and weighed The sodium content was found to correspond to 1·10 atoms of sodium per molecule of Nekal BX

The osmotic coefficient of Nekal BX in aqueous solution at various concentrations

The osmotic coefficient was determined by the cryoscopic method and calculated using the formula

$$\theta$$

where θ = depression of freezing point, $\nu = 2$, $\lambda = 1 \cdot 85$ and m = molal concentration of Nekal BX If we assume that aggregation of only anions occurs and that the cations are all osmotically active, the average number of anions per micelle can be calculated The values are given in Table I.

TABLE I

Concentration of Nekal BX g in 100 grams of water	θ	f	Average No. of anions aggregated to form a micelle
4 0	0 252	0 53	14 7
1 0	0·091	0·74	2 1
0 4	0 046	0·98	1·1
0 20	0 024	1·02	1 0

Preparation of flat springs of quartz

The surface tension was measured by the ring method. The determination of maximum pull was made by using a new type of silica spring prepared in the following manner. Silica fibre drawn in the usual way was attached to the steel blade of a spatula by means of a gummed label. Sharp bends were then given to the fibre at the edges of the spatula by heating with an oxy-gas flame. The blade was manipulated so as to get the fibres parallel to each other after each bend. After the winding was over the label was burnt off when the spring easily slid out of the spatula as the blade had a taper both in its width and in its thickness.

The springs that got are found to be very satisfactory. They obey Hooke's law perfectly. If from a fibre of given length, a helical spring

and a flat spring having same width are prepared, the two springs would give practically the same sensitiveness, as can be seen from the following considerations :—

The extension of a flat spring takes place by the bending of the fibres. The amount of extension x_1 can be calculated by the formula

x_1 = number of coils × displacement due to bending of each coil.

The displacement δ due to the bending of each coil can be calculated to a first approximation by considering it as equivalent to twice the displacement suffered by a horizontally cylindrical fibre fixed at one end when loaded at the other end This is given by the equation,

where w = the load, d = width of the flat spring, Y = Young's modulus, A = cross-section of the fibre and k = radius of gyration[12]

$d = 2$ R, where R is the radius of the spring whose diameter is equivalent to the width of flat spring

$$A = \Pi r^2,$$

where r = radius of the cross-section of the fibre.

$$K^2 = \frac{r^2}{2}$$

$$\delta = \frac{32\, w\, R^3}{3\, Y \pi r^4}$$

Since the number of coils in the spring $= \frac{L}{4R}$, where L is the total length of the fibre,

$$x_1 = \frac{32\, w\, R^3}{3\, Y \pi r^4} \times \frac{L}{4\, R}.$$

$$= \frac{8\, w\, R^2\, L}{3\, Y \pi r^4}.$$

For a helical spring of the total length L, radius R, the extension x_2 is given by the formula[13]

$$x_2 = \frac{2\, w\, R^2\, L}{n \pi r^4},$$

where n is the rigidity modulus.

Then,

$$\frac{x_1}{x_2} = \frac{4\, n}{3\, y}$$

For silica $n \cong 3$ and $y \cong 5$

So, $$\frac{4n}{3y} = \frac{4 \times 3}{3 \times 5} = \frac{12}{15} = 0\ 8,$$

showing that the sensitivenesses of the two types of springs are of the same order

Flat springs can easily be prepared in less than half an hour while several hours have to be spent in the preparation of the helical springs even when an automatic device is employed.[11]

It has to be pointed out, however, that if the springs are to be enclosed in narrow tubes as in sorption work it is preferable to use the helical springs since the latter are more compact for any given sensitiveness and capacity.

Flat springs were prepared out of ordinary glass fibre but were found to be totally unsatisfactory Even with pyrex glass small flow effects were noticed, especially when the springs were subjected to high loads for long intervals of time The quartz springs however showed no detectable flow effects.

The quartz spring used in the present work had a sensitiveness of 2·7 cm per gram. The travelling microscope used had an accuracy of 0 01 mm

Temperature control

The ordinary air and water thermostats were found to be unsuitable for the work since the stirring arrangements caused too much disturbance of the surface and of the spring The following arrangement was employed to overcome this difficulty The conical flasks containing the solutions were kept in a shallow circular pan which contained water kept at 30° C. ± 0·1. Water from an electrically maintained thermostat 30° C. ± 0·1° C. was fed into the pan from four points symmetrically situated at the circumference of the pan. The level of the water in the pan was kept constant by pumping the excess of water back to the thermostat by means of a circulation pump. The suction tube for this purpose was kept at the centre of the pan. The chamber in which the experiment was tried was kept at 32° C. to 34° C. by keeping two heating mats in the chamber in suitable position in order to prevent the condensation of water on the sides of the flask containing the solution The heating arrangement was also helpful in preventing a cooling of the water in the pan due to evaporation. Using this arrangement a constant temperature could be easily maintained for long periods without any special attention.

Determination of surface tension

The determination of equilibrium surface tension offers many difficulties. The method employed should be a static one, since the systems under consideration show surface aging. Of the static methods, the capillary rise method is defective on account of the friction effects that operate at the meniscus [8] The sessile bubble and pendant drop methods are by far the best from this point of view though the technique has to be very elaborate to secure accurate results The ring method is also found to be suitable for the purpose[13,14] and has been adopted in the present work The conical flasks in which solutions were kept during the measurement of surface tension, were cleaned in the following manner —

Flasks, whose rims had been ground, were treated with hot chromic acid mixture and then thoroughly cleaned with distilled water They were next dried in an air oven at 140° to 150° C., cooled and again rinsed with distilled water taking care not to wet the outside of the flask Surface-active impurities were thus eliminated. The flasks were once again dried and their necks were parafinned on the outside to eliminate any creeping in of surface-active impurities from the thermostatic bath It was observed that unless these precautions were taken for avoiding contamination from surface-active impurities the results could not be reproduced Except during the measurement of surface tension the flasks were kept covered with ground glass plates placed over the ground rims. A fresh surface of the solution was generated by running down the solution into the flask at a uniform rate by means of a fifty c c. pipette at a position just touching the centre of the bottom of the flask. This is similar in principle to the method adopted by Alexander.[15] The flasks containing the solution were arranged in a circle at the circumference of the thermostatic pan mounted on a table which could be either rotated, raised or lowered The rotatory movement was helpful in bringing one solution after another beneath the spring with minimum disturbance of the surface. The vertical movement of the table could be made very gently by a worm-gear arrangement and was employed in measuring the maximum pull. Movement of the spring to measure this pull was not practicable owing to the vibrations produced

A Du Nouy ring fixed to a nichrome wire was flamed and attached to the spring which was suspended from a glass rod fixed to an iron stand. The spring had been previously calibrated. The knob of the hook of the spring was focussed through a travelling microscope and the corresponding reading was taken as the initial reading. The flask containing the solution whose surface had been freshly made, was brought underneath the ring. The ring was then completely dipped into the solution by pulling down the

nichrome wire with the fingers On releasing the fingers the ring attached itself to the surface of the solution. The flask was then lowered and the position of the knob followed by adjusting the microscope until maximum pull was attained. It was possible to make this measurement without detaching the ring from the surface of the liquid. The values of the surface tension were obtained by applying the corrections indicated by Harkins and Jordan.[16] The following interpolation formula was derived from the data of Harkins and Jordan:

Surface tension $= 21\ 6 + 117\ 3(M - 0\ 2) + 23{\cdot}75(M - 0\ 2)^2$, where M is the maximum pull in grams This holds for dilute aqueous solutions for Du Nouy ring $\left(\frac{R}{r} = 39\ 0 \text{ and } R = 0\ 636 \text{ cm}\right)$ over a range of temperature 25° C. ± 15° C The measurements were continued until equilibrium values were got and there was no significant change for at least one week. It was found necessary to continue the observation for about a month in order to get the final values The equilibrium surface tension of solutions of Nekal BX in water, in 0·1 N sodium chloride, in 0 01 N sodium chloride, 0·01 N hydrochloric acid and 0·01 N sodium sulphate with different concentrations of Nekal BX were determined. The results are given in Tables II and III and Fig 1

TABLE II

− log C.	C = Wt of Nekal Bx in 100 c c of water	Equilibrium surface tension		
		Soln. in water at 30° C	Soln in 0 01 N NaCl at 30° C.	Soln. in 0·1 NaCl (32° ± 3° C.)
3 0000	0 0010	71·2	..	..
2·6021	0 0025	65 1	..	51 1
2 3010	0 0050	60·8	57·6	46·6
2 0000	0 0100	56 3	53·0	41 6
1 6021	0 0250	50 0	46 8	36·2
1·3010	0 0500	46·2	41·7	31·9
1·0000	0·1000	41 0	37·7	30 9
0 6979	0·2000	36 3	33·3	29·3
0·3979	0·4000	31·9	31·6	29·3
0 2218	0 6000	..	..	29·6
0·0969	0 8000	31·5	31·3	29·8

TABLE III

g. Nekal BX in 100 g. water	Equilibrium surface tension		
	Soln. 0·01 N $BaCl_2$	Soln. in 0·01 N Na_2SO_4	Soln. in 0·01 N HCl
0 005	..	55·0	49·4
0 010	33·3	49·4	43·4
0·025	32 5	43·5	38·8

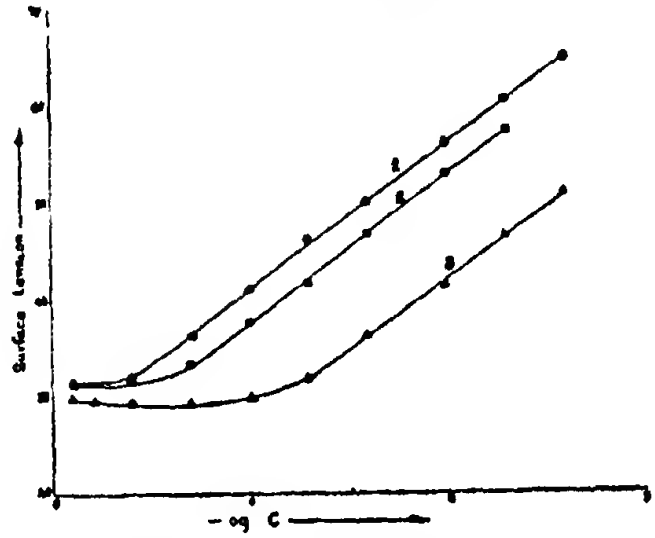

FIG. 1

Curve 1 Surface tension of Nekal B × Solution in water
Curve 2 " " " in 0 01N—NaCl
Curve 3 " " " in 0 1N—NaCl

DISCUSSION

1. *Application of Gibbs' adsorption equation*

(i) *The derivation of the usual form of Gibbs' adsorption equation.*—Gibbs derived[17] thermodynamically the important relation (for systems at constant temperature and pressure)

$$-d\sigma = \Gamma_1 d\mu_1 + \Gamma_2 d\mu_2 + \Gamma_3 d\mu_3 + \quad . \tag{1}$$

where σ is the surface tension of a solution, Γ is the Gibbs' adsorption excess and μ the chemical potential The subscripts 1, 2, 3, etc, refer to different components present in the solution. For a two-component system the equation becomes

$$-d\sigma = \Gamma_1 d\mu_1 + \Gamma_2 d\mu_2 \quad .. \tag{2}$$

Therefore,

$$-\frac{d\sigma}{d\mu_2} = \Gamma_1 \frac{d\mu_1}{d\mu_2} + \Gamma_2. \tag{3}$$

But from the properties of partial molal quantities, we have,

$$N_1 d\mu_1 + N_2 d\mu_2 = 0. \tag{4}$$

where N_1 and N_2 are mole fractions of the two components. Combining 3 and 4, we get,

$$-\frac{d\sigma}{d\mu_2} = -\Gamma_1 \frac{N_2}{N_1} + \Gamma_2. \tag{5}$$

For any position of the dividing surface, if Γ_2 is positive, Γ_1 would be expected to be negative and would be proportional to Γ_2, so that one can put,

$$\Gamma_1 = -\alpha\Gamma_2 \tag{6}$$

Combining (5) and (6), we get,

$$-\frac{d\sigma}{d\mu_2} = \Gamma_2 \left\{1 + \alpha \frac{N_2}{N_1}\right\} \tag{7}$$

It may be noted that α can be correlated with the relative dimensions of the two types of molecules, and is always positive

Equation 7, which is perfectly general for two component systems can be further simplified for the particular case of dilute solutions For if $N_1 >> N_2$ we get,

$$-\frac{d\sigma}{d\mu_2} = \Gamma_2 \tag{8}$$

Equation 8 represents the usual form in which Gibbs' adsorption equation is expressed and applies to all *dilute* solutions having two components, *irrespective of the position of the dividing surface*

(ii) *Significance of the Gibbs' adsorption excess*—Since equation (8) is true irrespective of the position of the dividing surface, one can put the dividing surface at the physical interface Thus Γ_2 would give the amount of solute present in the adsorption layer in excess over what would have been present if there were no preferential adsorption of the solute It may be pointed out that in *dilute solutions*, the quantities obtained by the moving bubble method[18] or by the highly exacting microtome technique[19] are identical with Γ_2

(iii) *Nekal BX and type III curve*—With pure Nekal BX solutions, neglecting activity coefficients, if the Gibbs' adsorption equation is applied, a unique behaviour is noticed The adsorption increases with concentration, attains a constant value of 1 60 × 10^{14} moles per sq. cm. and then abruptly falls to zero at a concentration of 0 4 per cent. Nekal BX. This corresponds to type III of McBain.[1] But the curve is very unique in one respect namely that the fall from maximum adsorption to zero adsorption is extremely steep.

Type III curve, as applied to Nekal BX, presents a paradox in the chemistry of surfaces as can be seen from the following considerations:—

(*a*) Gibbs' equation in the simplified form can be applied to this system as we are dealing with a dilute solution having a single solute. The Γ values give directly the amounts present in the surface layer.

(*b*) Whereas adsorption should increase with increase of concentration, it is found abruptly to fall to zero at a particular concentration

(*c*) If it is to be assumed that the fall is due to micelle formation, the micelles being assumed to be surface-inactive, the question yet remains as to why the surface tension of the solution is so low when compared with that of water.

(*d*) The paradox cannot be attributed to any want of equilibrium since in each case ample time was allowed for equilibrium while the attainment of equilibrium was almost immediate at higher concentrations.

(*e*) Surface-active impurities have been avoided in measuring the surface tension, by taking the precautions detailed in the appropriate section.

(*f*) The microtome method as applied to analogous cause of lauryl sulphonic acid shows a positive adsorption in the region in which Gibbs' equation predicts a zero or a negative adsorption. (Such experiments however have not been carried out with Nekal BX)

(*g*) The type of the curve remains unaltered even when the osmotic coefficients are taken into account while applying Gibbs' equation

Attempts to explain this anomaly have been made by McBain[1] and by Alexander McBain considers this problem in all its aspects and concludes that the Gibbs' adsorption equation itself is a limiting law But it is not at all clear why it should be a limiting law Alexander[2] seems to be right in his arguments in discarding the explanation of McBain, but his own explanation given to account for the curve is also unsatisfactory. Alexander considers that the whole complication is due to micelle formation In applying the Gibbs' equation he considers the Gibbs' adsorption excess as made up of two parts: Γ_s (of single molecules) and Γ_m (of micelles) Then,

$$-d\sigma = \Gamma_w\, d\mu_w + \Gamma_s\, d\mu_s + \Gamma_m\, d\mu_m \tag{1}$$

Placing the dividing surface so as $\Gamma_w = 0$ (and this is allowable in dilute solutions), we get,

$$-d\sigma = \Gamma_s^w\, d\mu_s + \Gamma_m^w\, d\mu_m \tag{2}$$

If the single molecules and micelles are in equilibrium,

$$\mu_s = \mu_m \tag{3}$$

whence

$$-d\sigma = \Gamma_s^w\, d\mu_s + \Gamma_m^w\, d\mu_s \tag{4}$$

But

$$d\mu_s = RT\, d\ln c_s f_s \tag{5}$$

where $c_s f_s$ is the activity of single molecules.

Combining 4 and 5,

Since $\frac{d\sigma}{dc} = 0$ [at higher concentrations], (c = total concentration of the solute)

either

$$\Gamma_s^w + \Gamma_m^w = 0 \tag{6}$$

or

$$\frac{d\, c_s f_s}{dc} = 0 \tag{7}$$

or

$$c_s f_s = \infty \tag{8}$$

[Alexander puts the condition in equation (8) as $c_s f_s$ being equal to zero; but this is obviously a slip]

Alexander considers that the condition in equation (7) is satisfied and not the others in order to explain the paradox.

The defect in the treatment of Alexander can be easily appreciated if one replaces equation (4) by its equivalent equation

$$-d\sigma = (\Gamma_s^w + \Gamma_m^w)\, d\mu_m \tag{9}$$

which, proceeding on lines similar to those adopted by Alexander, leads to the final conclusion

$$\frac{d\, c_m f_m}{dc} = 0.$$

It is not clear how this conclusion can be experimentally justified

The defect in Alexander's argument appears to be in that it overlooks the important fact that Gibbs' treatment is thermodynamically rigorous and does not depend on any particular constitution of the solution. *Micelle formation is therefore a supernumerary phenomenon from the point of view of the application of Gibbs' adsorption equation* As long as there is equilibrium between the micelles and the single molecules, it is unnecessary to separate either the activity or the Gibbs' adsorption excess of the single and polymer molecules. [Such a separation is tantamount to assuming single and polymer molecules as separate components; it would on the same lines be necessary to further increase the number of components taking into account the different polymers of water, the different hydrates of the solute, etc.] If the treatment is modified so as to remove this defect, the phenomenon of $\frac{d\sigma}{dc}$ becoming zero at higher concentrations, remains unexplained.

(iv) *Cross-section of Nekal BX molecule*—If one can assume that Gibbs' adsorption equation can be successfully applied at concentration below that at which Γ becomes zero, one can show that the saturation of the surface occurs at a concentration of about 0 003 per cent. and the Γ remains constant at higher concentrations up to 0·4 per cent. of Nekal BX The Γ corresponding to saturation $= 1 \cdot 60 \times 10^{14}$ molecules per sq cm · Cross-section $= 62 \cdot 5$ sq Å. The cross-section from surface film measurements[8] works out to be 53 sq Å. The lower value in the latter case is probably due to the fact that barium chloride solution was used as the substrate.

It is of interest to note that the value of cross-section of Nekal BX at the surface of 0·01 N sodium chloride solution is almost the same (62 6 sq. Å) as that at the surface of water But the cross-section got by calculating from the data obtained by working with Nekal BX solutions in 0 1 N sodium chloride works out to be 64 8 sq Å, a value which is markedly higher. This result is rather surprising since addition of salts may normally be expected to reduce the electrostatic repulsion and consequently decrease the effective cross-section, but, the opposite has been found to be the case This is presumably connected with the facts that (*a*) concentrations and not activities have been used in applying the Gibbs' equation and (*b*) with Nekal BX in 0 1 N sodium chloride, there is a three-component system

2. *The theory of Cassie and Palmer*

Cassie and Palmer[30] have given an interesting theory for explaining the effect of salts on soluble, ionised monolayers and have brought in support of their theory, the data obtained by Powney and Addison.[31] An examination of the data on Nekal BX solutions (Tables II and III) shows that a divalent cation like the barium ion has much more effect than the univalent cation on the negatively charged monolayer. This observation is qualitatively in conformity with their theory

A quantitative application however has given a different result. The values of λ^2 calculated according to equations (16 0) and (16 1) of Cassie and Palmer are given in Table IV. The results show that the value of λ^2 shows large variations unlike the corresponding values calculated from the data obtained by Powney and Addison. This shows that the theory of Cassie and Palmer is not valid in the present case. The disagreement is probably due to the wrong assumption made by Cassie and Palmer, that the surface pressure is a single valued function of Γ. That Γ need not be a single valued function of surface pressure is obvious from the work on the spreading of stearic acid on various substrates.[26] It is to be noted however, that this assumption is somewhat justifiable at high surface pressures

(for since the surface is closely packed the Γ values would not very much change with surface pressure) It is of interest to note in this connection that the data in Table IV tend to agree with the theory of Cassie and Palmer in the region of high surface pressure. The data of Powney and Addison, which are cited by Cassie and Palmer, also correspond to the same region. It is to be noted that H^+ ions bring about a much larger lowering of surface tension than Na^+ ions at an equivalent concentration. Though this is contrary to the simple considerations of Cassie and Palmer, it can be correlated with the well-known higher adsorbability of H^+ ions.[26] A quantitative examination of the effect of Ba^{++} ions has not been attempted since the theory breaks down even with 1 1 electrolytes

The effect of salts on the equilibrium surface tension can be qualitatively interpreted in the following way. The equilibrium surface tension is governed mainly by the equilibrium concentration of the Nekal BX in the surface layer The latter is determined by the rate of entry of the ions into the layer and the rate of escape of the ions into the bulk. The entry is checked by the electrical potential barrier due to the ionised monolayer.[9] The rate of escape into the bulk however would be comparatively unaffected by the electrical potential barrier Addition of salt would increase the ionic strength of the solution and thereby lower the height of the potential barrier. This would increase the rate of entry of Nekal BX into the surface but would not affect the rate of escape into the bulk The surface concentration would therefore get increased and the surface tension would get lowered Ba^{++} ions could be expected to be much more effective than Na^+ ions since the former may directly attach themselves to the monolayer and reduce the electrical charge The behaviour of sodium sulphate is of interest in this connection. Sodium sulphate is more effective than sodium chloride in reducing the surface tension at equivalent concentrations This is presumably due to the fact that sodium sulphate solution has a higher ionic strength than sodium chloride solution of an equivalent concentration. It may be pointed out that the theory of Cassie and Palmer cannot account for this behaviour of sodium sulphate

According to the theory of Cassie and Palmer,

$$\lambda^2 = \gamma_1 S_1 [S_1 + C_1] = \gamma_2 S_2 [S_2 + C_2],$$

where S_1 and S_2 are the concentrations of the surface-active electrolytes, C_1 and C_2 are the concentrations of the salt, and γ_1 and γ_2 are the activity coefficients of the corresponding solutions having the same surface tension. The values of λ^2 calculated from our data are given in Table IV and a survey of the table shows, as has been already pointed out, that the data tend to agree with their theory only at lowest surface tensions.

TABLE IV

Surface tension	Concentration of wetting agent in molarity*	Concentration of NaCl in molarity	Logarithm of activity coefficient	$\gamma^2 \times 10^2$
57·8	$2{\cdot}53 \times 10^{-4}$	0·00	$\bar{1}$·992	6
	$1{\cdot}59 \times 10^{-4}$	0·01	$\bar{1}$·950	145
53·0	$5{\cdot}54 \times 10^{-4}$	0·00	$\bar{1}$·988	30
	$3{\cdot}19 \times 10^{-4}$	0·01	$\bar{1}$·949	292
51·1	$7{\cdot}47 \times 10^{-4}$	0·00	$\bar{1}$·986	54
	$4{\cdot}20 \times 10^{-4}$	0·01	$\bar{1}$·949	388
	$7{\cdot}96 \times 10^{-4}$	0·10	$\bar{1}$·842	554
46·6	$1{\cdot}59 \times 10^{-3}$	0·00	$\bar{1}$·980	241
	$7{\cdot}96 \times 10^{-4}$	0·01	$\bar{1}$·948	763
	$1{\cdot}59 \times 10^{-4}$	0·10	$\bar{1}$·842	1106
41·6	$2{\cdot}84 \times 10^{-3}$	0·00	$\bar{1}$·973	758
	$1{\cdot}59 \times 10^{-3}$	0·01	$\bar{1}$·946	1629
	$3{\cdot}19 \times 10^{-4}$	0·10	$\bar{1}$·842	2221
36·2	$6{\cdot}37 \times 10^{-3}$	0·00	$\bar{1}$·960	3701
	$3{\cdot}92 \times 10^{-3}$	0·01	$\bar{1}$·941	4756
	$7{\cdot}96 \times 10^{-4}$	0·10	$\bar{1}$·841	5564

* Taken from the graph in Fig. 2.

3. *Application of Szyszkowski's equation*

For relating the surface tension of a solution with the concentration of the solute Szyszkowski[22] suggested empirically the equation

$$\frac{\sigma_0 - \sigma}{\sigma_0} = B \log \left(\frac{C}{A} + 1\right) \tag{1}$$

where σ_0 and σ are the surface tensions of solvent and solution respectively. C is the concentration of the solute and A and B are constants. An examination of the Bond and Puls' treatment[23] of Szyszkowski's equation has shown that the latter can be justified on the basis of the Gibbs' adsorption equation and the Langmuir theory of adsorption. The following formal derivation can be given for Szyszkowski's equation:—

Number of molecules per sq cm. in the surface layer in dilute solutions

$$= -\frac{1}{kT}\frac{d\sigma}{d\ln c} \tag{2}$$

Fraction of the total surface covered

$$= -\frac{1}{kT}\frac{d\sigma}{d\ln c}\sigma, \tag{3}$$

where α is the cross-section of the solute molecule.

V_1 = rate of escape of molecules into the bulk

$$= -\frac{1}{kT}\frac{d\sigma}{d\ln c}K_1$$

V_2 = rate of arrival of molecules into the surface

$$= K_2 c\left\{1+\frac{1}{kT}\frac{d\sigma}{d\ln c}\alpha\right\}$$

where K_1 and K_2 are constants.

At equilibrium $V_1 = V_2$ (4)

Solving the differential equation corresponding to equation (4), we get,

$$\frac{\sigma_0-\sigma}{\sigma_0} = \frac{kT}{\alpha\sigma_0}\ln\left(1+\frac{K_2}{K_1}\alpha c\right) \tag{5}$$

which is of same form as equation (1) Comparing (1) and (5), we get,

$$B = \frac{kT}{\alpha\sigma_0} \text{ and } A = \frac{K_1}{K_2\alpha}$$

It is easily seen that B is a function of α and therefore is constant for different members of the homologous series. A, however, would be proportional to K_1 and would therefore increase with decrease in chain length. This is again in agreement with Szyszkowski's observation

Other merits of the equation are

(*a*) at low concentrations the solute can be shown to behave as a perfect gaseous film;

(*b*) at high concentrations the equation reduces itself to that of Milner[8] which is found to be in agreement with experimental results; and

(*c*) at the highest concentrations a limiting area is indicated.

An application of the equation to Nekal BX solutions shows that the equation is applicable up to 0·4 per cent. Nekal BX and then it breaks

down completely; this is because the Gibbs' adsorption equation itself does not apply beyond that concentration. (It is to be noted however that even the lowest concentrations of Nekal BX employed in the present investigation correspond to the formation of a practically complete unimolecular layer)

4 *Micelle formation*

If the horizontal portion of the $\sigma - (-\log C)$ curves is interpreted as due to micelle formation, the concentration at which the micelle formation occurs may be taken as 0·4 per cent in the case of pure Nekal BX solutions, and 0·27 per cent in the case of Nekal BX solutions in 0 01 N-N. Cl

Summary

A simple technique has been described for the preparation of flat springs of quartz fibre The new type of springs are found to be very satisfactory for the measurement of surface tension by the ring method

A method for measuring the equilibrium surface tension of solutions (which show surface aging) has been described. Full details are given of the arrangement for adequate temperature control and for the prevention of contamination of solutions by surface-active impurities

The equilibrium surface tension of Nekal BX solutions of various concentrations in water and in salt solutions, has been determined.

Application of Gibbs' equation to Nekal BX solutions has been discussed. Nekal BX solutions of concentrations above 0 4 per cent have shown either no adsorption or negative adsorption, which cannot be explained on the basis of Gibbs' equation and the phenomenon therefore remains a paradox.

The arguments put forward by McBain and by Alexander to explain the type III curve have been shown to be untenable.

The cross-section of the Nekal BX molecule has been calculated on different substrates, *viz*, water, 0·01 N and 0 1 N sodium chloride.

Applicability of Cassie and Palmer's theory to unimolecular adsorption layers formed by Nekal BX solutions has been discussed.

A formal derivation of the empirical equation of Szyszkowski has been given by combining Gibbs' equation and Langmuir's theory of adsorption and its application to Nekal BX solutions has been discussed.

References

1. McBain and Mills — *Reports of Progress in Physics*, 1938, **5**, 30
2. Al xander — *Trans Far Soc*, 1942, **38**, 248
3. Venkatachala .. *Proc. First Annual Convention, Oil Technologists' Association, India*, 1944, p 11
4. Krishnappa, Doos and Rao — Unpublished
5. Bhimasena Rao and Doss — *Proc Ind Acad Sci*, 1941, **13**, 170
6. Doss .. *Curr Sci*, 1935, **4**, 405.
7. ——— . *Ibid*, 1938, **7**, 182
8. ——— . *Colloid, Z.*, 1939, **86**, 205
9. McBain and Wilson — *J Amer Chem Soc*, 1936, **58**, 379
10. ——— and Perry .. *Ind Eng Chem*, 1939, **31**, 35
11. Doss and Rao — *Proc Ind Acad Sci*, 1936, **4**, 11
12. Neuman and Searle — *The General Properties of Matter*, 1936, 121, 127
13. Nutting, Long and Harkins — *J. Amer. Chem Soc*, 1940, **62**, 1496
14. G N. Subba Rao — *M.Sc Thesis*, Mysore University, 1942
15. Alexander — *Trans Far Soc*, 1941, **38**, 15.
16. Harkins and Jordan — *J Amer Chem Soc*, 1930, **52**, 1751
17. Gibbs — *Collected Works*, 1928, **1**
18. McBain and co-workers — *J Amer Chem Soc*, 1921, **49**, 2230, *ibid*, 1929, **51**, 3534.
19. ——— and Swain — *Proc Roy Soc*, A, 1936, **154**, 608
20. Cassie and Palmer . *Trans Far Soc*, 1941, **37**, 156
21. Powney and Addison — *Ibid*, 1937, **33**, 1243
22. Szyszkowski — *Z Physik Chem.*, 1908, **64**, 385
23. Bond and Puls — *Phil. Mag*, 1937, **24**, (7), 864.
24. *Cf* Glasstone — *Recent Advances in Physical Chemistry*, Second Edition, 1933, p 325
25. *Ibid*, p 335
26. Doss — *J Indian Chem Soc*, 1933, **10**, 503

AGING OF SURFACES OF SOLUTIONS

Part VI. Surface Aging of Casein Solutions*

By G N. Subba Rao, K S Gururaja Doss† and Basrur Sanjiva Rao
(*Department of Chemistry, Central College, Bangalore, S India*)

Received January 31, 1946

Introduction

Aqueous solutions of casein are known to produce foams of great stability The foaming is due to the surface accumulation of the protein and the formation of adsorption films These adsorption films are insoluble and exhibit surface pressure in the Langmuir trough It is thus possible to study accumulation by the method developed by Doss[1] and independently by McBain and co-workers [9, 10] Surface accumulation studies on casein are of particular interest since the area occupied by a casein molecule at the surface can be determined by direct spreading measurements. The surface aging of these solutions has been investigated in the present work by studying (*a*) the rate of accumulation and (*b*) the rate of change of surface tension with time In studying the latter, a direct comparison has been made of the trough and the ring methods The variation of surface tension has been studied by Johlin[6] by the capillary rise method This method, however, is subject to many sources of error [15]

Experimental

Casein used in the present work was an isodisperse fraction prepared according to the method of Svedberg, Carpenter and Carpenter [12] The aging was studied by employing the surface film balance described previously.[8] The zero position of the float was adjusted to be vertically below the torsion wire so as to eliminate completely the effect of any changes in the vertical component of the force due to surface tension or buoyancy [14] This is very necessary in the study of the variation of surface tension with time.

Results

1. *Accumulation studies*—Casein has been found to accumulate very rapidly It is therefore very necessary to work with a highly dilute solution

* Part of Thesis submitted by G. N. S in partial fulfilment of the requirements for the degree of Master of Science of the Mysore University.

† Physical Chemist, Imperial Institute of Sugar Technology, Cawnpore

in order to obtain a measurable rate of accumulation 0·00025% solution in 0·01 M hydrochloric acid is found suitable.

The accumulated casein film is of a highly condensed type and it is therefore possible to measure the rate of accumulation by determining the area of the film The rate of accumulation was measured as follows. The trough was thoroughly cleaned using Nekal BX which gave an extremely clear trough A blank was invariably tried with distilled water before each study The extent of contamination of a surface of distilled water was measured and found to be small, being invariably within 5% of the rate of accumulation of the casein solution. The trough was filled with the casein solution The surfaces on either side of the float were swept clean by a barrier and the time noted A known area of the surface on the left-hand side of the float was allowed to age for a definite amount of time and the area of the accumulated casein was measured at 4 dynes/cm. pressure by moving the barrier towards the float At this pressure the force-area curve for spread films of casein was steep and hence area measurements were accurate Since the area occupied by a molecular of casein at 4 dynes/cm. pressure was known from direct spreading, the rate of accumulation could be computed The casein solution employed being exceedingly dilute, the process of accumulation impoverished the solution appreciably This difficulty did not arise with the studies on benzopurpurine

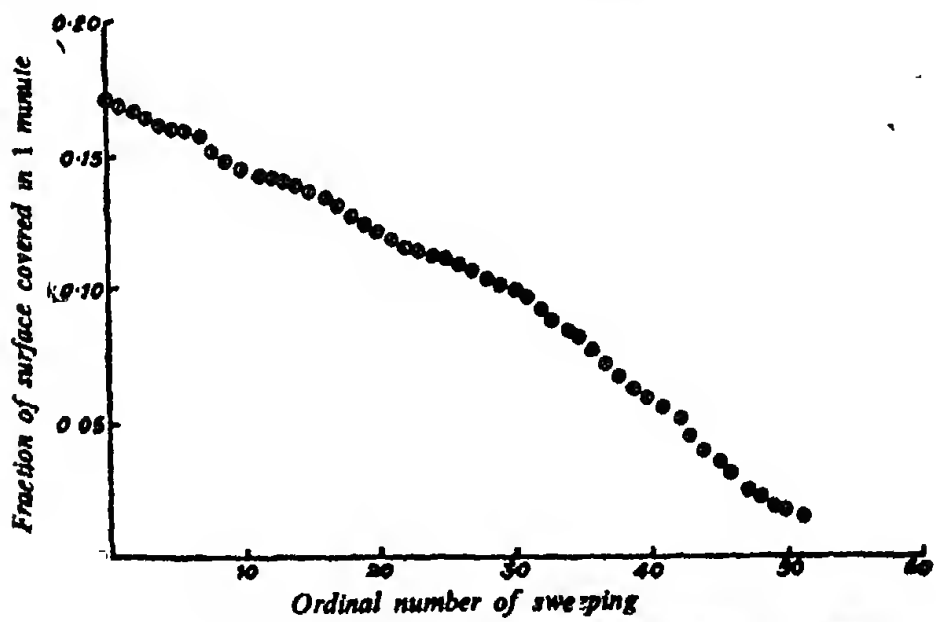

FIG. 1 Effect of repeated sweeping on the rate of accumulation of casein

10 B since comparatively strong solutions (M/250, M/500) could be employed.[6] Fig 1 illustrates this effect clearly The successive one minute-values for the area covered with the same solution against the ordinal number of the sweepings have been plotted

In order to get the time-area curve the following procedure was therefore adopted For the value corresponding to each time-interval a fresh quantity of solution was started with The surface was swept and accumulation measured thrice and the average of the three values taken The results are given in Table I

TABLE I

Time-area relationship to the accumulation of casein

0 00025 % casein in 0 01 M hydrochloric acid

Area measured at 4 dynes/cm Temperature 25° C

Time in minutes	Fraction of the surface covered
1	0 17
2	0 26
4	0 38
8	0·59
16	0·82

The effect of salts on the rate of accumulation was studied and it was found that the rate of accumulation was not altered by the addition of potassium chloride or barium chloride

The effect of temperature on the rate of accumulation was investigated. The trough was kept in a refrigerator at 13·5°C It was found that the rate of accumulation was practically the same as at 25°C, the laboratory temperature. Attempts to measure accumulation at 40° C were not successful owing to the serious disturbing effects caused by convection currents. Abnormally high accumulation was noticed—a 10° rise producing a twofold increases in the rate.

Accumulation of formolised casein—Formolised casein was prepared by mixing solutions of Hammersten casein in aqueous sodium acetate with formaldehyde[8] and allowing to stand for three days. The rate of accumulation of 0 00025% solutions in 0·01 M-hydrochloric acid was studied. The results are given in Table II.

TABLE II

Time-area relationship relating to the accumulation of formolised casein

0 00025 % formolised casein in 0 01 M hydrochloric acid
Area measured at 4 dynes/cm Temperature 25° C

Time in minutes	Fraction of the surface covered
1	0·092
2	0 12
4	0 16
8	0 26
16	0·33
32	0 46

2 *Variation of surface tension of casein solution with time* —The variation of surface tension of casein solutions was studied by methods developed by Doss [8] The reference surfaces used in the trough were (*a*) half-minute old and (*b*) fully aged These methods correspond to procedures I and II independently developed by McBain [10]

To start with, the trough was filled with the protein solution and the surfaces cleaned by barriers The right-hand surface was always cleared half a minute before taking the readings for the pressure exerted by the aging surface on the other side Thus the surface tension variation was measured using as reference the half-minute old surface The measurements were

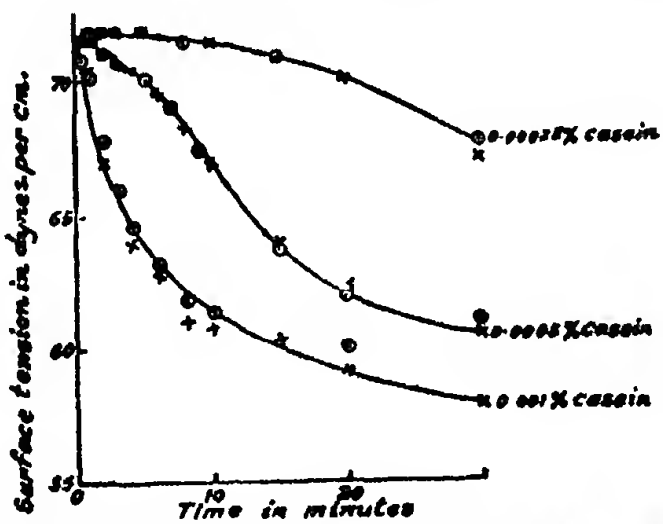

FIG. 2 Surface tension variation of casein solution in 0·01 M hydrochloric acid Temperature 25°C. ○ Reference half-minute old surface. × Reference fully aged

continued until a practically steady value was obtained Then the surface on the right-hand side was cleared and allowed to age The variation of surface tension of this surface was measured using the fully aged surface on the left as reference The surface tension of the fully aged surface was then determined directly, by the ring method using the silica spring [7] and the value employed in the calculation of the data given in Fig 2

When a fully aged surface was compressed (to 26 dynes/cm), it exhibited a rise of surface tension on aging. The rise was about 5 dynes/cm in ten minutes The rise was steep initially and the behaviour was similar to that of benzopurpurine 6 B [8]

A comparative study of the ring and trough methods was made, employing identical surfaces, and measuring the surface tension alternately by the two methods at various intervals of time In the ring method a flat spiral of silica constructed in this Laboratory[7] was used for measuring the maximum pull The results are illustrated in Fig 3, and show that comparable results can be obtained by both the methods

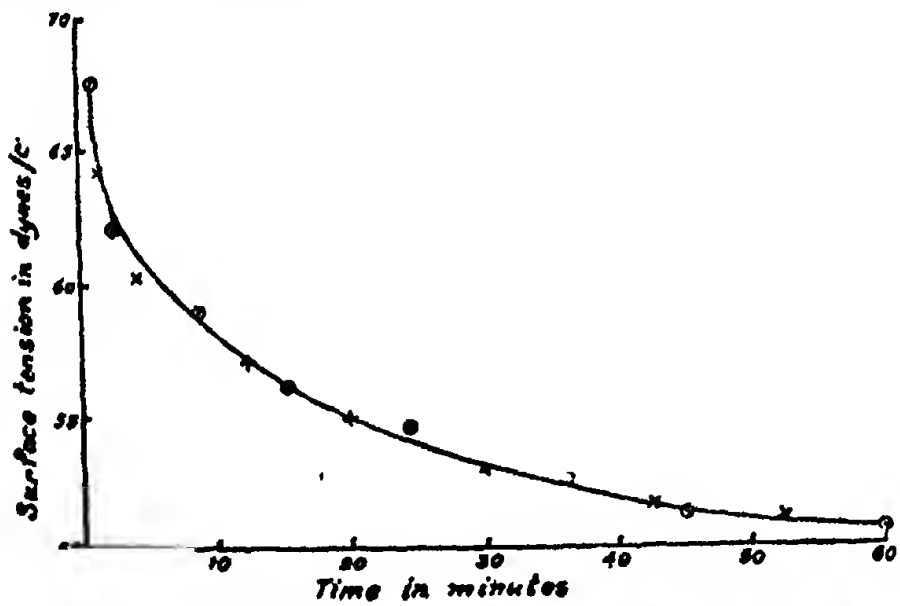

FIG. 3 Comparison of trough and ring method ⊙ Ring method × Trough method.

For 0·1% solutions, of casein, the trough method could not be used for studying the variation of surface tension since the solution wetted the paraffin and leakage past barriers occurred. The variation was therefore studied by the ring method. A two-minute old surface showed a surface

tension of 52·2 dynes/cm. Further aging caused a very slow change, the surface tension dropping to 50·8 dynes/cm after one hour.

Discussion

1 *Calculation of the theoretical rate of accumulation*—The order of time needed for covering any definite fraction of the total surface by accumulation can be estimated roughly as follows. For covering a fraction of the surface, the depth of the solution (below the surface) which is to be denuded $= \frac{\chi \times 10^{-7}}{2\ 5 \times 10^{-6}}$ or 0 04 cm (10^{-7} = No. of g of casein present per sq cm of the casein monolayer at a pressure of 4 dynes/cm on 0 01 M hydrochloric acid and $2\ 5 \times 10^{-6}$ = concentration of casein in g. per c c of solution)

Consider the Brownian displacement of the molecules parallel to the vertical direction Assuming that half the molecules move towards the surface by Brownian displacements, the distance Δ that a molecule has to cover to appear at the surface would be twice the above depth, *i e*, 0 08χ cm.

According to Einstein's equation, we have,

$$\frac{\Delta^2}{t} = \frac{RT}{N} \quad 1$$

where t is the time for the displacement Δ. R = gas constant, T = absolute temperature, η = viscosity, N = Avogadro number and r = radius of the casein molecule. r can be estimated by the equation $\frac{4}{3}\pi r^3 = \frac{M}{\rho N}$ where M and ρ are the molecular weight and density of casein respectively Substituting the appropriate values in the Einstein's equation, we get

$$\chi = 0\ 012\sqrt{t}, \text{ where } t \text{ is in seconds}$$

2. *The high rate of acculumation*—From the above equation, the fraction of the total surface covered in 60 seconds works out to be 0 091 whereas the experimentally observed value is 0 17, *i e*, nearly twice the theoretical value. A similar calculation for the later successive intervals would show that the experimental values of the accumulation are higher than the maximum possible theoretical values This is a surprising feature. All the systems studied so far by the earlier investigators[1, 11] exhibit slow accumulation. The abnormally high rate of accumulation now noticed cannot be explained on the basis of the presence in casein of any fractions of low molecular weight. For, the casein preparation used is known to be practically isodisperse. Moreover, to account for the observed high rate,

an average molecular weight of about 9,000 has to be assumed, a value which is obviously inadmissible. The observed high rate may at first sight appear to be caused by the dragging effect of the gegenions associated with the casein molecules But the experiments on the effect of neutral salts definitely show that the influence of gegenions is negligible It is of interest to note that a high rate of accumulation is not peculiar to casein It is also exhibited by egg albumin.[18] Our observations suggest that this phenomenon is caused by (*a*) undulations produced during the formation of the new surface and (*b*) existence of eddy currents near the surface which disturb the concentration gradient set up by the diffusion of protein molecules into the surface.

3 *Effect of temperature on the rate of accumulation* —The temperature coefficient of accumulation is negligible The accumulation is therefore not activated. This observation supports the other fact that the accumulation is very fast

As already stated, convection currents interfered with measurements attempted at 40° C and gave very high values Since the accumulation of casein is not of the activated type, any molecule of the protein reaching the surface by diffusion, sticks to the surface Therefore the rate of accumulation is high and one is obliged to work with very dilute solutions In such solutions accumulation causes a concentration gradient Convection currents would disturb this gradient and promote diffusion, thereby increasing the rate of accumulation. It may be pointed out that this complication does not arise with systems like benzopurpurine 10 B giving activated accumulation,[3] for, the accumulation being slow no appreciable concentration gradient can occur in such system

4. *Effect of neutral salts.*—Neutral salts have negligible influence on the rate of accumulation. This shows that there is no electrical potential barrier inhibiting accumulation.[15] It also confirms the view that the high rate of accumulation is not due to the influence of the gegenions, for, if they enhance the diffusion rate of casein molecules to the surface, neutral salts should reduce the rate of accumulation.

5. *The time-area curve.*—Langmuir's theory of adsorption can be applied to this system. The rate of increase of total surface covered by casein molecules is given by the equation

where χ is the fraction of the total surface covered by casein molecules in a time-interval t, K_1, the specific velocity of adsorption and K_2 the velocity

of desorption. As the adsorption is practically irreversible K_2 may be taken as zero (Actually K_2 may have a negative value For, χ becomes unity when the surface pressure due to accumulation becomes 4 dynes/cm., the pressure at which the area of accumulated film is measured, but even at this stage accumulation continues, increasing the surface pressure much further) The equation can then be written as

$$\frac{d\chi}{dt} = K_1 C (1 - \chi) \text{ or } K_1 = \frac{1}{(t_1 - 1)} \ln \frac{1 - \chi_1}{1 - \chi},$$

where χ_1 is the area covered in one minute In Table III the values of K_1 for the accumulation of casein are given

TABLE III

Accumulation of casein from 0 00025% *solution in* 0·01 *M hydrochloric acid*

t	K_1
2	0·050
4	0 042
8	0 044
10	0 040

In this discussion, the first minute value has not been taken into account owing to the disturbing factors that operate during the formation of a new surface The examination of the table shows that the system obeys fairly well the Langmuir's equation. This shows that (*a*) the molecules of casein at the surface hinder accumulation of other casein molecules only to the extent of the surface they occupy at the surface pressure of 4 dynes/cm. and (*b*) the eddy current effects are nearly the same in all the measurements. A totally different result has been obtained with egg albumin[18] which does not obey Langmuir's equation Molecules of albumin inhibit accumulation over an area about three times their cross-section. This is probably due to the influence of long-range electrical forces

6 *Effect of formaldehyde.*—Accumulation of casein treated with formaldehyde shows a large diminution in the rate, if the fraction of total surface covered within a definite interval of time is considered. But taking into consideration the fact that the formolised casein occupies nearly half the area occupied by untreated casein, one finds the amount (in mg per sq m. of the surface) that has accumulated is nearly the same for the ordinary as well as the treated casein. This result shows that treatment with formaldehyde does not alter the state of aggregation of the molecule.

7 *Variation of surface tension with time*—The surface tension time curves for dilute solutions of casein can be interpreted, taking into account the condensed nature of the adsorption film The accumulation starts, directly the new surface is formed But accumulated molecules form a highly condensed film, having negligible surface vapour pressure Consequently the surface tension remains constant though the accumulation proceeds. This goes on until the surface gets almost completely covered At this stage further accumulation causes a large change in surface tension At the next stage, when the surface gets highly packed up with molecules, the rate of penetration of casein molecules from the bulk solution into the surface decreases, so the slope of the surface tension-time curve decreases In more concentrated solutions, accumulation goes on so rapidly that the initial horizontal portion of the curve is not noticeable Similar behaviour has been noticed with solutions of lauric acid[16] and benzopurpurine 6 B[4]

An examination of Fig 2 shows that the values of surface tension are not so dependable when the fully aged surface is used as a reference surface This is due to the fact that the surface tension of the fully aged surface is markedly upset by the irregular movements of the float during the determination.

When the adsorption film is compressed to a high pressure the surface tension of the compressed surface exhibits a rise in surface tension with time This may be attributed either to a partial collapse of the film or to a change in the orientation of the molecules on the surface With casein films, partial collapse has been noticed at a pressure of 26 dynes/cm

Summary

1. The rate of accumulation of isodisperse casein has been investigated, employing a surface film balance The rate is found to be much higher than the value expected from theory This surprising feature, reported for the first time in the present work, has been explained

2. Neutral salts have no effect on the rate of accumulation, thus showing the absence of influence of gegenions and of any electrical potential barrier

3 Temperature coefficient of accumulation is negligible. Therefore the process is not activated.

4. Accumulation of formaldehyde-treated casein has been found to be essentially of the same order as of ordinary casein.

5. The time-area curve for casein obeys Langmuir's adsorption equation. There is no potential barrier inhibiting the accumulation.

6. Comparative study of the trough and ring methods for measuring surface tension has been made under identical conditions. The two methods are found to yield comparable results

7. Variation of surface tension with time has been studied by the trough method.

References

1	Doss	*Curr Sci*, 1935, 4, 405
2	———	*Proc Ind Acad Sci*, A, 1936, 4, 97
3	———	*Curr. Sci*, 1937, 5, 645
4	———	*Ibid*, 1938, 7, 182
5	———	*Kolloid-Z*, 1938, 84, 138.
6	Johlin	*J Phys Chem.*, 1925. 29, 271 897
7	Krishnappa, Doss and Rao	Unpublished
8	Lindstrom-Lang	*Comp rend Lab Carlsberg*, 1925, 16, 48
9	McBain and Wilson	*J Amer Chem Soc*, 1936, 58, 380
10	——— and Perry	*Ind Eng. Chem*, 1939, 31, 35
11a.	Nutting, Long and Harkins	*J Amer Chem Soc*, 1940, 62, 1500
b	——— and Long	*Ibid*, 1941, 63, 87
c	McBain, Ford and Mills	*Ibid*, 1940, 62, 1324
d	Ward and Tordai	*Nature*, 1944, 154, 146
12.	Rao, G N S, Doss and Rao, B. S	Unpublished
13.	Svedberg, Carpenter and Carpenter	*J. Amer Chem Soc*, 1930, 52, 241.
14	Venkatachala, Doss and Rao	Unpublished
15	Doss	*Kolloid-Z*, 1939, 86, 205
16	Harkins and co-workers	*Nature*, 1936, 138, 406

STUDIES IN INORGANO-ORGANIC GELS IN PINENE

Part V. Gel-Strength Measurements of Gels of Sodium Stearate in Pinene

By Mata Prasad, S S Dharmatti and G S Hattiangdi
(*Chemical Laboratories, Royal Institute of Science, Bombay*)

Received December 24, 1945

The gel-strength and modulus of elasticity have been considered to be an important and characteristic property of gels The largest data available on the subject in literature is on gels of gelatin, probably because they are "rigid", and therefore it is easier to work with them than with gels of other substances which are comparatively "soft" and exude liquid and consequently lose their shape completely on an application of a slight stress.

An important investigation on the measurement of this property of gels in non-aqueous media has been carried out by Poole[1] in the case of cellulose acetate gels in benzyl alcohol He finds that elasticity is approximately proportional to the square of the concentration, indicating that the rigid phase results from a dynamic solvation equilibrium between the cellulose acetate and the solvent He proposes a Coefficient of Inner Resistance to denote the force which is required to produce unit velocity of "creep" (the increase in deformation with time when a steady stress is applied to a gel) in a unit cube of the gel in the absence of all elastic controlling forces Lampitt and Money[2] also find that the gel-strength of gelatin gels is linearly related to the square of the concentration of the gel over a limited range.

In the present investigation the gel-strength of sodium stearate gels in pinene has been measured with a view to get some insight into the elastic properties of these soap gels in non-aqueous media. This soap was selected because it was found to give rise to stable and fairly stiff gels

Experimental

The several methods which have been proposed for measuring or comparing the gel-strengths of gels may be divided into four main classes.

(*a*) dynamometer methods, in which the forces required to twist a column of the gel through definite angles are measured;

(*b*) methods involving the breaking of a gel;

(*c*) measurement of the depression produced by a constant load; and

(*d*) measurement of the load required to produce a definite depression. Soap gels in pinene are generally weak or "soft" for they lose shape and exude liquid on the application of a slight torsion Hence dynamometric methods could not be employed to investigate the gel-strength of these gels.

Preliminary experiments made with a gel-testing apparatus similar to the one described by Oakes and Davis[3] showed that this method could be employed with advantage to measure the gel-strength of sodium stearate gels in pinene In this apparatus, the bottom of one pan of a sensitive balance is attached to a plunger made of good quality glass This is counterpoised so that the pointer rests at zero on the scale

Gel-forming solutions containing varying amounts of sodium stearate (Merck's pure product) were prepared in 10 c c of pinene as described by Prasad and Hattiangdi[4] and were immediately poured into small weighing bottles in which they were allowed to set The surface of the gel was then brought into contact with the plunger, weights were slowly added to the pan and the corresponding deflections on the scale as indicated by the pointer were noted. It was found that all small deflections of the pointer were proportional to the depression of the plunger Such readings were taken till the breaking point or the elastic limit of the gel was reached. Care was taken to see that there was no jerking or oscillation of the plunger while in contact with the gel, and that the pressure was applied perpendicularly to the surface of the gel.

According to several earlier workers, all the methods which depend upon the breaking or compression of the gel in open glasses are subject to two sources of error: (*a*) the glasses usually vary in diameter thus forming a surface of variable area, and (*b*) there is always a "skin" of greater or less thickness which interferes with the accuracy of the test. The difficulty arising from the first cause was overcome by employing bottles of the same diameter ($2r = 2\ 4$ cm.). To determine the existence, if any, of a "skin" or "surface" effect and the extent to which it vitiates the values of gel-strength, the plunger was dipped into a gel-forming solution before it was allowed to set; gel-strength measurements were carried out after the gel had set, in the same manner as described earlier

Some workers recommend the use of a flat-ended plunger in preference to the hemispherically-ended one, since the area in contact with the gel is constant in the former case instead of increasing with depression as it happens if the latter type of plunger is used. In order that a comparison

of the two types of plungers could be made, a flat-ended circular disc-type plunger having a diameter equal to that of a hemispherically-ended one ($2r = 0 \cdot 8$ cm.) was prepared, and a series of load-deflection curves were obtained

The various load-deflection results obtained for these gels are shown graphically in Figs 1–4

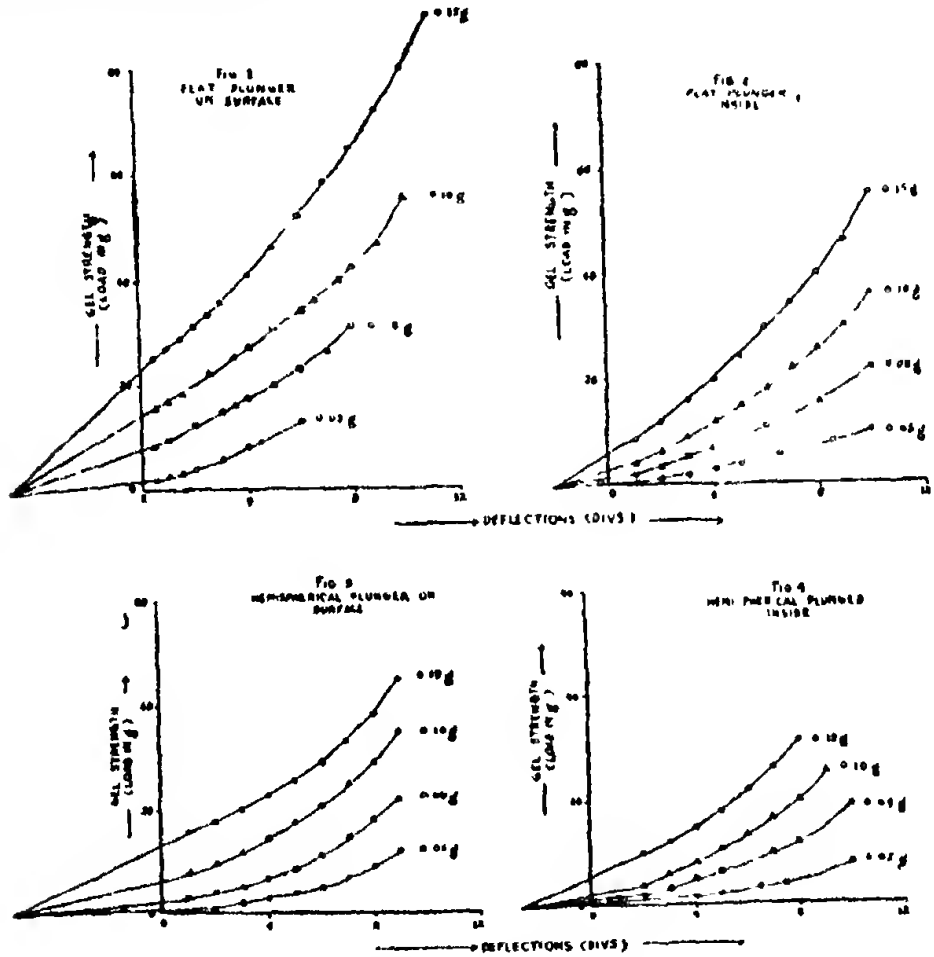

Discussion of Results

A comparison of the data obtained with the two types of plungers acting (i) on the surface of, and (ii) inside the gel, shows that

(*a*) both plungers give an almost linear loading curve until the elastic limit is exceeded;

(*b*) the deflection produced for a given load is much smaller in the case of a flat plunger than when the hemispherical plunger is used; this is due to the fact that the hemispherical plunger has a greater weight in proportion to the surface directly opposed to the gel, and is therefore better able to overcome the resistance of the gel Thus the velocity of the hemispherical plunger is assisted and a greater range for the same load is obtained;

and (*c*) the elastic limit of the gel is reached with a smaller depression (deflection) of the flat plunger than that of the hemispherically-ended one, this is a direct consequence of the observation and behaviour mentioned in (*b*)

An interesting observation was made during the actual experimentation Initially the pointer is at rest at zero on the scale when the surface of the gel is brought into contact with that of the plunger When a very small load is applied, the plunger actually rises up instead of being forced down, and the pointer immediately starts oscillating On applying small increasing loads, the upthrust of the plunger is gradually countered till a stage is reached when the pointer is once again at rest at zero, and subsequently the plunger moves downwards only if still greater loads are applied. The initial upthrust of the plunger is an evidence of the existence of a "surface" effect which behaves like an elastic membrane and whenever the loads applied are small the upward reaction is quite noticeable; in the absence of such an effect, the plunger would have pressed down against the surface of the gel on the application of even a very small load An attempt was made to determine the magnitude of this "surface" effect by increasing the load till it could just break the surface film.

In the case of a flat plunger, the expression for the tension can be mathematically derived on the considerations that the rim of the flat plunger is in contact with the film to be broken and the tension will act perpendicularly to the line of contact Usually in liquids, some angle (the angle of contact) is made with the direction of the tension and the line of contact. No angle was, however, observed when a rod was immersed vertically inside the gel, and hence the angle of contact was taken as zero. The total force acting upwards is therefore $2\pi rT_F$, where r is the radius of the plunger, and this is balanced by mg the force necessary to break the film. Therefore,

$$2\pi rT_F = mg,$$

$$\text{or} \qquad T_F = mg/2\pi r \qquad \text{(I)}$$

The expression in the case of the hemispherical plunger can be derived as follows. As increasing loads are applied, the plunger presses more and more against the surface of the gel, and near about the point when the skin is pierced the hemisphere is closely and completely surrounded by the membrane on the top of the gel At this stage the extended membrane has an area $2\pi r^2$, where r is the radius of the sphere; the area of the membrane before this extension took place was only πr^2, and therefore the increase in area due to the action of the plunger is πr^2 Therefore the surface energy is equal to $\pi r^2 T_H$ This energy is derived by the work done by the weight mg in moving through a distance r, the buoyancy effect being neglected

Hence,

$$\pi r^2 T_H = mgr,$$

$$\text{or} \qquad T_H = mg/\pi r \qquad \text{(II)}$$

The values of the tension T_F and T_H were calculated for gels of different concentrations of sodium stearate using the relations (I) and (II), and are given in columns 2 and 3 of Table I

TABLE I

Values of the Surface Effect " T "

Soap content (in g)	Determined from the limiting value of the load on the surface of the gel		Determined by the graphical method	
	Flat ended plunger T_F	Hemispherical plunger T_H	Flat ended plunger T_F'	Hemispherical plunger T_H'
0·05	1290	1169	2078	2027
0·08	3959	3945	4937	4755
0·10	6238	6238	6366	6230
0·15	8470	8055	8445	8420

The existence of the "surface" effect can be evidenced on different considerations altogether. If there were no such effect, the shear required to produce any strain should be the same wherever the plunger may be acting, on the surface or inside The various curves in Figs. 1 and 2, and 3 and 4, however, show that the load required to produce a certain deflection is larger when either type of plunger is acting on the surface than when it is inside the gel. The difference between these two values of loads can be reasonably assumed to be the force which is necessary to counter the "surface" effect. The correctness of this assumption was verified by

determining the actual magnitude of the effect as follows. If L_1 is the load required to produce a certain deflection when the plunger is acting on the surface of the gel, and if L_2 is the load which produces the same deflection when the plunger is inside the gel, then $(L_1 - L_2)\,g$ is the force required to overcome the surface effect Substituting $(L_1 - L_2)\,g$ for mg in equations (I) and (II), the values of T_F' and T_H' were calculated, and are given in columns 4 and 5 of Table I

It will be seen from Table I that (i) there is a good agreement between the values of T_F and T_H and T_F' and T_H' over the range of concentrations studied, indicating that the value of T is almost independent of the nature of the plunger used, and (ii) there is a very good agreement between the values of T_F, T_H, T_F' and T_H' for 0·10 g and 0 15 g content of sodium stearate in the gel-systems, but the two sets of values are widely divergent for lower soap contents The values obtained by the graphical method are higher than those obtained by the other method, but they are more correct for the following reasons In the graphical method the value of m taken in calculating T for any concentration is the mean of several values computed from the graphs, while in the other method only one value of m can be available for calculation and a slight variation in the value of m would considerably affect the value of T Hence the error is considerably minimised in the graphical method

The development of a skin or membrane on the surface of the gel can be, in the first instance, very clearly seen when the gel-forming solution is being cooled Further, it was observed that if the skin of a well-formed gel is pierced by a glass rod or plunger, the pierced portion of the surface appears like a fresh wound when the rod or plunger is withdrawn, and no fresh skin is formed on this spot even on keeping the gel for a sufficiently long time This shows that a skin is formed during the process of setting of the gel Its probable mode of formation is as follows When a hot homogeneous solution of sodium stearate in pinene is allowed to cool, there is a rapid radiation of heat from the surface which brings about (i) an immediate inhomogeneity in the distribution of the solute in the dispersion medium, and (ii) a quick evaporation of the pinene due to which a semi-dry skin or membrane is formed on the surface of the gel The skin or membrane is thus formed only during the process of setting of the gel, and not at any stage afterwards.

Previous workers have shown that Hooke's law holds true in the case of gels, that is the load–displacement curve is a straight line passing through the origin, and its slope is proportional to elasticity. The earlier portions

of the curves in Figs. 1–4 are straight lines, thus showing that Hooke's law is obeyed up to certain loads only; but with increasing loads these lines bend into a curve which shows that the elastic limit or the fatigue point has been exceeded If the straight lines are produced backwards, they do not meet at the origin but some point which may be taken as the true origin of the load-deflection co-ordinates The shape of these curves and the abovementioned behaviour are similar to those reported by Oakes and Davis[3] and Sheppard and Sweet[6] in the case of gelatin gels, using similar plunger methods The difference in the nature of the earlier portions of the curves in the soap–pinene systems and gelatin gels may be caused by the varying surface of contact of the plunger employed in the latter case

The gel-strength can be measured either from the slope of the straight lines which converge to a point, or by comparing the loads required for the same deflection The values of gel-strength were calculated from the slopes of the load–deflection curves shown in Figs 2 and 4, that is, when the plunger is placed inside the gel, and are given in the following table

TABLE II

Values of Gel-Strength (arbitrary units)

Soap content (in g)	Flat ended plunger	Hemispherical plunger
0 05	0 75	0 75
0 08	1 75	1 50
0 10	2 75	2 20
0 15	3 75	2 80

The above results show that the gel-strength increases as the soap content of the gels is increased; the slight variation in the actual values when the two types of plungers are used is mainly due to the fact that when the hemispherical plunger is acting, the micelles get more opportunity to orientate themselves in such a way as to reduce the resistance and to increase the strain, and hence the gel-strength values are slightly smaller Although it is an anomaly to say that a physical property like elasticity is different when different methods are used, it is not surprising to find such a behaviour in these gel systems where the binding forces between the micelles are of such a small order as could be destroyed by mere mechanical agitation

Poole and others have found that the plots of the logarithm of elasticity or gel-strength (E) against the logarithm of the concentration (C) are approximately straight lines in several cases, and the value of the slope does not

exceed 2 On plotting the values of log E against log C, obtained from the data given in Table II, it was found that the several points lie very nearly on a straight line whose slope is equal to 1·8 which closely approximates to 2 This observation is in accordance with the fibrillar theory of gel-structure developed by Poole. It has, however, to be remarked that the variation of elasticity or gel-strength as the square of the concentration, according to the theory, does not appear to hold true in the case of soap-pinene systems for higher concentrations

One of the authors (G S H) is grateful to the authorities of the University of Bombay for awarding him a University Research Scholarship, which has enabled him to carry out this investigation

Summary

The gel-strength of gels of sodium stearate in pinene has been measured by the plunger method under several conditions. The values of elasticity have been calculated from the load–deflection curves, and it is found that log E varies linearly as log C, the slope of this straight line being very nearly equal to 2 The existence of a skin or membrane on the surface of the gel which vitiates the values of gel-strength has been critically examined, and its approximate magnitude has been determined

References

1. Poole *Trans Farad Soc*, 1925, **21**, 114
2. Lampitt and Money *J Soc Chem Ind*, 1936, **55**, 88 T
3. Oakes and Davis *J Ind Eng Chem*, 1922, **14**, 706
4. Prasad and Hatliangdi *Proc Ind Acad Sci*, 1945, **21**, 1
5. Sheppard and Sweet *J Ind Eng Chem*, 1923, **15**, 571

STUDIES IN INORGANO-ORGANIC GELS IN PINENE

Part VI. Viscosity Changes with Time and Shear during the Gelation of Some Soap Systems in Pinene

By G S Hattiangdi and S P Adarkar

(*Chemical Laboratories, Royal Institute of Science, Bombay*)

Received December 24, 1945

(Communicated by Dr Mata Prasad, F A.SC)

In a recent communication, Prasad and co-workers[1] have determined the viscosity changes that take place during the setting of solutions of sodium oleate and sodium stearate in pinene when they are cooled to different temperatures, using two types of viscometers, namely, the capillary-type Ostwald viscometer and the Falling Sphere viscometer The regularities observed in the viscosity data obtained by the latter instrument during the process of gel-formation could, according to them, be expressed by the empirical relation $\eta - \eta_0 = ae^{bt}$, whereas the data obtained with the capillary viscometer obeyed the well-known Einstein's equation $\eta/\eta_0 = 1 + k\phi$ within a certain range of temperature only It is very important to determine the effect of shear on the viscosity values obtained during the sol-gel transformation An attempt in this direction was made in the case of cellulose acetate gel-forming systems in benzyl alcohol by Mardles[2] who observed that the values of the apparent viscosity decrease with increasing shear, and the nature of the viscosity-time curve changes its character with a change in the shear applied He has, however, given no satisfactory explanation for this peculiar behaviour of the gelating systems

This investigation gives the results of the measurements of the viscosity changes with time of some soap systems in pinene during the process of setting when different shears are applied The soaps used are sodium oleate, sodium stearate and sodium palmitate, and the viscosity determinations have been made by employing a rotating cylinder viscometer

Experimental

The sodium oleate and sodium palmitate used were products of the B. D. House, and sodium stearate of Messrs E Merck. The pinene used was obtained from Messrs. Eastman Kodak & Co., and was the fraction distilling at 156°.

The rotating cylinder viscometer used was manufactured by Messrs. W. G. Pye & Co., and consisted of a hollow cylinder (3·73 cm. in diameter and 10 cm. in length), which was rotated in a cylindrical vessel containing the gel-forming solution, there being a clearance of 0 678 cm between the walls of the two cylinders. The inner cylinder was rotated by means of falling weights attached to the ends of a thin tough cord which passed over frictionless pulleys The effective radius of the drum, D, round which the cord was wound was 1 91 cm The value of the viscosity was calculated from the relation

$$\eta = \frac{g\,D\,(a^2 - b^2)}{8\,\pi^2 a^2 b^2} \cdot \frac{MT}{l + k}$$

TABLE I

Sodium oleate in pinene

Soap content (in g.)	Time interval (in mts.)	Relative viscosity values at different rates of shear		
		10 g	15 g.	20 g
0 60	0	2·50	2 50	2·50
	1	2 60	2 55	2 55
	2	2 80	2·70	2·65
	3	3·25	2·93	2 34
	4	3·69	3·06	2 02
	5	3 89	3·45	3 20
	10	do	3·73	3 56
	20	do	do	do
	30	do	do	do
	40	do	do	do
	50	do	do	do
0 75	0	3·10	3 10	3·10
	1	3 40	3·25	3 20
	2	3 85	3·45	3·30
	3	4·50	3·70	3 45
	4	4·99	3 85	3·60
	5	5·29	4·00	3·73
	10	5 56	4·25	4·14
	20	do	do	4·25
	30	do	do	do
	40	do	do	do
	50	do	do	do
0 90	0	4·15	4·15	4 15
	1	4·43	4 27	4 21
	2	4·65	4 40	4 27
	3	4 98	4·65	4 35
	4	5·10	4·95	4 82
	5	5 32	5 07	4·75
	10	5·84	5 33	5·00
	20	do	do	do
	30	do	do	do
	40	do	do	do
	50	do	do	do

The radius of the outer and inner cylinders, a and b, were 2·543 cm. and 1·865 cm., respectively; M is the mass applied to the end of the cord and is proportional to shear; T is the time taken (in seconds) for one complete revolution of the cylinder; l is the length of the gel, and k the constant of the instrument ($k = 0\ 55$)

The solutions of the various sodium soaps in pinene were prepared by dissolving known amounts of the soap in 60 c.c of pinene as described by Prasad and Hattiangdi[8]; the results of the various experiments are given in Tables I to III.

TABLE II

Sodium stearate in pinene

Soap content (in g)	Time interval (in mts)	Relative viscosity value at different rates of shear						
		10 g	15 g	20 g	30 g	40 g	50 g	60 g
0·60	0	3 0	3 0	3 0	3 0	3 0	3 0	3 0
	1	3 34	3·20	3 1	3 07	3 06	3 06	3·05
	2	3·57	3 51	3 25	3 15	3·12	3 08	do
	3	3 81	3·70	3 4	3·25	3 17	3 1	do
	4	3·96	4·12	3·6	3 33	3 20	3 1	do
	5	4 12	do	3 75	3·42	3 25	3 15	do
	10	4·46	do	3 9	3 64	3·50	3 25	do
	20	4 95	do	do	do	do	do	do
	30	do	do	do	do	do	do	do
	40	do	do	do	do	do	do	do
	50	do	do	do	do	do	do	do
0·75	0	4·2	4·2	4·2	4·2	4 2	4 2	4 2
	1	4·44	4 35	4·33	4 32	4 31	4·3	4 2
	2	4 7	4 55	4 5	4 45	4 33	4 3	4·3
	3	4 95	4 8	4·75	4 64	4 45	4·41	do
	4	5·60	5·2	4·98	4 8	4 55	4 45	do
	5	6·19	6 5	5 25	4 9	4 65	4 5	do
	10	8·42	6·91	6 25	5 52	5 0	4 8	do
	20	6 91	7 76	6 6	do	do	do	do
	30	do	do	do	do	do	do	do
	40	do	do	do	do	do	do	do
	50	do	do	do	do	do	do	do
0·90	0	5·0	5·0	5·0	5 0	5 0	5 0	5 0
	1	5·25	5 15	5·07	5 06	5·06	5·06	5·06
	2	5 50	5 32	5·25	5·11	5 11	5 06	do
	3	6·0	5 54	5 32	5 24	5 15		do
	4	6·52	5·8	5·53	5 32	5·2	5 1	do
	5	6·75	6·25	5·71	5 45	5 25	5·2	do
	10	8·69	7·58	6 95	5 95	5 50	5 25	do
	20	do	do	do	do	do	do	do
	30	do	do	do	do	do	do	do
	40	do	do	do	do	do	do	do
	50	do	do	do	do	do	do	do

to these observations. The peculiar phenomenon of anomalous viscosity exhibited by the soap systems during gel-formation can be explained on the basis of the mechanism of the formation of these gels stressed by Prasad and co-workers in a number of papers. According to them, gel-formation results from (i) the gradual increase in the number and size (volume) of the soap micelles which are aggregates of small soap particles, (ii) the solvation of these micelles with the dispersion medium which is a saturated solution of soap in pinene, (iii) the fusion or aggregation of these solvated micelles into fibrils, and (iv) the enclosure of the intermicellary fluid in the interfibrillar space in an adsorbed state due to the attractive or linking forces between the fibrils. Prasad and co-workers have also shown that all the aforesaid processes take place simultaneously in the gel-forming system although some of them may take place preponderantly at one time than the others. Thus when a gel-forming solution of soap in pinene is allowed to cool to a low temperature, there will firstly be, preferably on an average, an increase in the number and size of the micelles and this will be abundantly followed by processes (ii), (iii) and (iv) described above. As a consequence, in the earlier stages of gelation, the structural gel-strength which is linked with the growth of the micelles will be weak and will become stronger as time elapses and the setting point is being approached.

The viscosity–time curves (*cf* Fig. 1) for low rates of shear bring out the above-mentioned points very clearly The slow increase in viscosity initially is caused by the increase in the number and the size of the soap micelles; the subsequent fairly rapid rise shows that the increase in viscosity with time is considerably accelerated owing to the large degree of solvation of the soap micelles and their aggregation into fibrils The very rapid rise in viscosity during the last stage is due to the formation of a structure in the gel which behaves almost like a solid and hence offers a great resistance. These observations lead to the conclusion that the aforesaid behaviour would be shown by the gel-forming systems of soap in pinene if a viscosity–time curve is obtained without the application of any shear (*cf* the curves obtained by Prasad and others[1]).

When the viscosity measurements are made with these gel-forming systems under different shear, two processes take place simultaneously, namely, (i) the occurrence of the processes described above, and (ii) the breakdown of all or some of the functions in the processes due to the shear acting in a direction opposite to the forces which come into play during the gel-formation.

The S-shaped curves obtained with increasing shear varying from 10 g. to 30 g. show that excepting for the earlier portions, the curves are lowered on increasing the shear, the latter part being lowered more than the earlier one. This shows that the application of the shear causes a general decrease in the rates of the occurrence of the four processes involved in gel-formation of soap-pinene systems, and the decrease is considerably more in the last three processes than the first one This means that there is not only a decrease in the number and volume of the micelles formed owing to the application of the shear but their extent of solvation and aggregation into fibrils is also decreased, and hence the formation of a structure which causes a gel to set is delayed This view is supported by the fact that the gel takes slightly more time to set when the shear applied is increased from 10 g to 30 g.

When the shear is increased to 40 g and 50 g, it is observed that (i) the viscosity–time curve is a straight line, that is, the acceleration in viscosity entirely disappears, and (ii) the earlier parts of the curves in the two cases are practically coincident On the basis of the theory outlined above it means that factors which tend to form the essential agents for the formation of gel-structure are prevented from getting into action by the opposing shear Since the gradients of these straight lines are less than those of the earlier parts of the curves for 10 g to 30 g, it appears that the increase in viscosity at uniform rate in these two cases takes place mostly owing to the constant rate of increase in the number and the size of the micelles, and possibly, to some extent, to their solvation This view is supported by the fact that when shears higher than 30 g are applied, the system does not set to a gel even on keeping it for a sufficiently long time after the application of the shear, probably because the structure has been very badly broken down, and it looks like a suspension of soap in pinene

On further increasing the shear to 60 g., the viscosity increases slightly in the beginning (during the first one or two minutes) and then attains a constant value. This shows that initially some micelles are formed which give the observed viscosity value to the gel-forming system; later on, the application of the high shear either destroys or prevents completely (i) the formation of more micelles and (ii) their increase either in volume, solvation, or aggregation The viscosity–time curve for 60 g. of shear therefore represents the condition of the formation of a minimum number of micelles in this particular instance which is not affected by the shear

This discussion leads us to two important conclusions regarding the application of shear, namely, (i) it can prevent or destroy the formation of gel structure which is responsible for the acceleration of viscosity with time,

and (ii) it can also decrease the rate of formation of the micelles or of the increase in their size or degree of solvation.

According to Goodeve and Whitefield[4], there is an equilibrium under certain conditions of steady shear between the rate of increase of the concentration of the micelles in a thixotropic system and their breakdown, and the apparent viscosity η of the system is given by the relation

$$\eta - \eta_0 = \frac{\theta}{s},$$

where η_0 is the residual viscosity, s the shear, and θ the coefficient of thixotropy They also report that on plotting the observed values of viscosity against the reciprocal of shear straight lines are obtained. According to Freundlich, Goodeve and others, thixotropy indicates the isothermal decrease of viscosity with increase in rate of shear. In the light of the above definition, soap gels in pinene may be considered to be thixotropic and hence may conform to the above mentioned relation This has been found to be so. On plotting the values of the apparent viscosity (η) against the reciprocal of the shear $\left(\frac{1}{s}\right)$, the curves obtained are straight lines for all the gel-forming systems studied in this investigation Further according to the relation given above, the intercepts of the straight lines on the viscosity axis must be equal to η_0, the residual viscosity of the system The values of η_0 have been determined and have been found to correspond to the state of the soap-pinene systems upto which all the $\eta - t$ curves are coincident. The residual viscosity may therefore be interpreted as the true viscosity of the colloidal system containing soap micelles which have undergone little or no solvation. Acccording to the considerations brought out in the discussion, this part of the viscosity–time curves corresponds to the soap-pinene system which contains practically only the soap micelles in a colloidal state in pinene

The authors are extremely grateful to Dr. Mata Prasad, D.Sc., F.I.C, and Dr S S Dharmatti, PH D, F INST P, for the kind interest they took while this work was under progress; one of the authors (G S H) is grateful to the authorities of the University of Bombay for awarding him a University Research Scholarship.

SUMMARY

Measurements of the viscosity changes with time taking place in the gel-forming systems of certain soaps in pinene yield $\eta - t$ curves which change their shape considerably as the shear applied is varied. It is also found that the shear applied can (i) prevent or destroy the formation of a gel structure which is responsible for the acceleration of viscosity with time,

and (ii) decrease the rate of formation of the micelles or of the increase in their size or degree of solvation. The plots of viscosity against the reciprocal of the shear are straight lines, indicating that the equation $\eta - \eta_0 = \theta/s$ is applicable to these soap-pinene systems.

References

1. Prasad, Hattiangdi and Vishvanath — *Proc Ind Acad Sci*, 1945 **21**, 90
2. Mardles — *Trans Farad Soc*, 1923 **18**, 327
3. Prasad and Hattiangdi — *Proc Ind Acad Sci*, 1945 **21**, 1
4. Goodeve and Whitefield — *Trans Farad Soc*, 1938, **34**, 511

[illegible]-46. Printed at The Bangalore Press Bangalore City by G Srinivasa Rao, Superintendent,
and Published by The Indian Academy of Sciences Bangalore

THE ELECTROLYTIC PREPARATION OF HYDROGEN PEROXIDE

Part I The Intermediate Production of Sodium Persulphate

By Dr D N Solanki and I S K Kamath
(*Chemistry Department Benares Hindu University*)

Received February 26, 1946
(Communicated by Professor S S Joshi, F A Sc)

The present investigation arose out of the work of Joshi, Solanki and Sheshadri[1] who have worked out the optimum conditions for the electro-chemical preparation of hydrogen peroxide from sulphuric acid Though simple, this method is subject to limitations owing to the fact that the current yield of the intermediately formed perdisulphuric acid, ($H_2S_2O_8$), is affected by its comparative instability under ordinary conditions It was of interest, therefore, to investigate the utilisability of aqueous sodium sulphate as a starting material instead of sulphuric acid, so that the intermediate product is the stabler sodium salt of perdisulphuric acid This on distillation under appropriate conditions yields hydrogen peroxide The preparation of hydrogen peroxide in this way may be divided into two main parts (i) the electro-chemical preparation of sodium persulphate and (ii) the distillation, concentration and stabilisation of hydrogen peroxide from sodium persulphate

A review of the literature having shown that no detailed information is available for the preparation of sodium perdisulphate except in a German Patent,[2] an investigation in some detail has been carried out on the optimum conditions for its electro-chemical preparation

Experimental

The cell consisted of a glass jar 12" × 4" fitted with a perforated stopper carrying a pair of platinum electrodes a thermometer and an exit tube for the evolved gases The electrolytic cell was cooled by immersion in a well stirred freezing mixture so that a temperature of 5 to 10° C as desired was maintained during electrolysis 50 c c of aqueous sodium sulphate of known concentration formed the bath solution, except in Expts reported in Table IX The circuit included an ammeter, an adjustable resistance and a voltmeter between the two electrodes After the cessation of electrolysis, 5 c.c. of the electrolyte was analysed for the total active oxygen, by

treatment with an excess of standard $FeSO_4$ solution in an inert atmosphere; the excess of the $FeSO_4$, was then determined by back-titration with N/20 $KMnO_4$ From this, and the quantity of electricity passed through the electrolyte the current efficiency, C E is calculated from Faraday's Law. The following is a typical calculation from Expt 1 in Table VIII

Blank-titre for 10 c c $FeSO_4$ . .	— 21 1 c c N/20 $KMnO_4$
Back-titre after treatment with 5 c c. of electrolyte .	5 4 c c ,, ,,
Active oxygen in 5. c c of the electrolyte ..	— 15·7 c c ,, ,,
Total active oxygen in 50 c c	—157 0 c.c. ,, ,,
Quantity of electricity passed	—0 25 amp hr.

Corresponding to 100% C E, the current efficiency, 26 86 amp hrs. of electricity should produce active oxygen equivalent to 1,000 c c. of N $KMnO_4$

The C.E in the above case .. $\frac{157 \times 26\ 86 \times 100}{0{\cdot}25 \times 20 \times 1000}$ 84·0%

The C E has been studied in respect of the following factors: Conc. $Na_2SO_4\ 10H_2O$ in neutral solution (Table I); conc. $Na_2SO_4\ 10H_2O$ in dil. sulphuric acid (Table II), conc. sulphuric acid (Table III), anodic and cathodic current densities (Tables IV and V), inter-electrode distance (Table VI); temperature (Table VII); duration of electrolysis (Table VIII), current concentration (Table IX), addition agents (Table X) and the use of a diaphragm

TABLE I

Influence of the Concentration of Na_2SO_4. $10H_2O$ on C E

Anodic current density .	55·2 ampa./dm²
Cathodic current density	15 0
Temperature	10°C
Duration of electrolysis	30 mins.
Current	1 amp.
Inter-electrode distance	1·5 cm.

Conc. Na_2SO_4. $10H_2O$ (gms./100 c c.)	P D. (Volts)	Total active O_2 (c c N/20 $KMnO_4$)	C E. %
10	4·5	2	0 5
20	do	4	1·1
30	do	3·5	0·9
40	do	4	1·1

TABLE II

Influence of the concentration of Na_2SO_4. $10H_2O$ in 4N H_2SO_4 on C E

Conditions same as in Table 1

Conc Na_2SO_4, $10H_2O$ (gms /100 c c)	P D (Volts)	Total active O_2 (c c N/20 $KMnO_4$)	C E %
15	4 8	155	41 6
25	do	175	47 0
45	do	203	54 5

TABLE III

Influence of Concentration of H_2SO_4 on C E

Conc of Na_2So_4 10 H_2O — 40 gms /100 c c

Other conditions same as in Table II

Conc H_2SO_4 (gms /100 c c.)	P D (Volts)	Total active O_2 (c c N/20 $KMnO_4$)	C E
5	4 5	44 1	11 6
10	4 5	74 0	19 5
20	4 6	111 0	29 2
30	4 6	157 0	41·3
40	4 7	217 0	57 1
50	4 8	235 0	62 1
60	4 8	277 0	73 1

TABLE IV

Influence of Anodic Current Density on C E

Composition of both solution | 40 gms of Na_2So_4 $10H_2O$ & 60 gms of H_2So_4/100 c c

Current varied as indicated in 1st column

Other conditions same as in Table III

Current (amps)	Anodic C. D (Amps /dm²)	P D (Volts)	Total active O_2 (cc N/20 $KMnO_4$	C E %
0·3	16·6	3 6	59	59 9
0·5	27 6	3 8	118	62 7
1·0	55 2	5·1	272	71 7
1·5	82·8	5·8	407	71 5
2·0	110·3	6·8	531	70 0
3·0	165·5	8·5	765	67 2

TABLE V

Influence of Cathodic Current Density on C.E

Anodic C D — 55 1 amps./dm²
Current 1 1 amp
Other conditions same as in Table IV

Cathodic C D (amps /dm²)	P D (Volts)	Total active O_2 (c c N/20 $KMnO_4$)	C E %
15 0	4 7	243	64 1
18 5	5 5	235	61·9
82 6	6 0	225	59·2

TABLE VI

Influence of Inter-Electrode Distance on C E

Cathodic C D — 15 0 amps /dm²
Other conditions same as in Table V

Inter Electrode distance (cm.)	P D (Volts)	Total active O_2 (c c N/20 $KMnO_4$)	C. E %
1 5	4·4	240	63 2
2·3	4 6	239	63 0
3 5	4 8	238	62·7
4 0	5 0	234	61 7

TABLE VII

Influence of Temperature on C E

Inter-Electrode distance — 3·4 cm.
Other conditions same as in Table VI

Temperature (°C)	P W (Volts)	Total active O_2 (c.c N/20 $KMnO_4$)	C. E %
5	5 8	228	60 0
10	5·0	242	63·8
15	4 8	240	63 3
20	4 7	233	61·4
30	4·3	195	51·3
40	4·0	129	33·9
50	3·8	83	21·9

TABLE VIII

Influence of Duration of Electrolysis on C E

Temperature — 10°C

Other conditions same as in Table VII

Time (mins.)	P D (Volts)	Total active O_2 (c c N/20 $KMnO_4$)	C E %
15	4 8	157	84 0
30	4 8	240	63 3
45	4 9	326	58 5
60	5·0	408	54 7
90	4 9	577	51 6
120	4 8	731	49 0
240	4 3	1379	46 3

TABLE IX

Influence of Current Concentration on C E

Duration — 30 mins

Volume of electrolyte varied as indicated

Other conditions same as in Table VIII

Vol of electrolyte (c c)	Current conc (amps./100 c c)	P D (Volts)	Total active O_2 (c c N/20 $KMnO_4$)	C E %
100	1 5	4 5	257	68 8
75	1 4	4 5	256	68·5
50	2 8	4 8	249	66 6

TABLE X

Influence of Addition Agents on C E

Temperature — 10°C

Composition of bath solution — 40 gms Na_2SO_4, 10 H_2O; 60 gms H_2SO_4 and 1 gm addition agent per 100 cc solution

Other conditions same as in Table VIII

Addition agent	P D (Volts)	Total active O_2 (c c N/20 $KMnO_4$)	C E %
$K_2Cr_2O_7$	4 7	168	45 1
$Pb(CH_3CO_2)_2$	4 6	186	50 0
$MnSO_4 \cdot 7H_2O$	4 6	195	52 4
Al_2O_3	4 7	202	54 3
$MgSO_4 \cdot 7H_2O$	4 6	216	58 0
$Fe_2(SO_4)_3$	4 8	223	59 9
CeO_2	4·7	227	61 0
$CoSO_4 \cdot 7H_2O$	4 6	240	64 5
HCl	4 8	241	64 7
Na_2HPO_4	4·7	250	67 1
$NiSO_4 \cdot 7H_2O$	4 7	273	73 3
$KClO_4$	4·6	276	74 1
HF	4 6	303	81 4

Discussion

When a neutral aqueous solution of sodium sulphate is electrolysed between platinum electrodes, the hydrogen and oxygen evolved are in the ratio 2 1 to a good approximation The characteristic smell of ozone, however, can be observed clearly even at 5° C for the bath temperature. The net result of electrolysis is apparently the decomposition of water into its elements When, however, the solution of sodium sulphate is acidified with sulphuric acid, it is observed that the evolution of oxygen at the anode is considerably lower, the actual volume of the oxygen liberated is less than half of the cathodic hydrogen This diminution in the amount of oxygen is associated with the acquirement of strong oxidising properties by the electrolyte It is due to the formation of perdisulphuric or Marshall's acid ($H_2S_2O_8$) at the anode, which depends on the concentration of sodium sulphate and sulphuric acid on the bath (*cf*, Tables II and III)

Various theories exist in literature regarding the electrolytic formation of perdisulphuric acid and its salts at the anode According to a well-worked out theory due to Richarz[3] perdisulphuric acid is formed at the anode by the polymerisation of discharged HSO_4'-ion pairs, according to the equation

$$2HSO_4' \rightarrow H_2S_2O_8 + 2 - \qquad (1)$$

It follows from (1) that the precedent condition necessary for the formation of perdisulphuric acid is a sufficient concentration of the HSO_4'-ions in the bath The rate of the polymerisation of the discharged HSO_4'-ions would also be a determining factor These deductions are in agreement with the general experimental results

It must be pointed out, however, that though the above theory explains the formation of perdisulphuric acid and its potassium and sodium salts, it fails almost completely to account for the high current yields obtained in the electrolysis of a neutral solution of ammonium sulphate, in which there are practically few HSO_4'-ions. This has been explained by assuming the polymerisation of SO_4''-ions according to the equation[4]

$$2SO_4'' \rightarrow S_2O_8'' + 2 - \qquad (2)$$

It may be suggested that the anomaly shown by ammonium sulphate may be due to the well-known peculiar structure of the ammonium ion, which has been found to show a different electro-chemical behaviour from that of the other cations.

Another theory which has been put forward by Foerster[5] and may be considered as an improvement on the view of Traube[6] that the perdisulphuric acid is produced by the oxidation of sulphuric acid by the nascent anodic

oxygen, assumes that persulphates are formed by anodic oxidation as given by the following reactions.

$$2HSO_4' + O + H_2O = H_2S_2O_8 + 2\,OH' \quad (3)$$

$$2SO_4'' + O + H_2O = S_2O_8'' + 2\,OH' \quad (4)$$

An increase in the anodic potential, on the basis of this theory would favour the per-sulphate formation, this has been experimentally verified[4] That perdisulphuric acid can be prepared by the oxidation of sulphuric acid by nascent oxygen from hydrogen peroxide[7] is an additional support of Foerster's view[8]

A more comprehensive theory of persulphate formation has been worked out by Muller,[4] who assumes that the primary anodic process is the discharge of OH'-ions which react with sulphuric acid to give perdisulphuric acid directly

$$2H_2SO_4 + 2\,OH' = H_2S_2O_8 + 2\,H_2O + 2\,- \quad (5)$$

This is followed by the secondary reactions

$$H_2S_2O_8 + H_2O = H_2SO_5 + H_2SO_4 \quad (6)$$

$$H_2SO_5 + H_2O = H_2SO_4 + H_2O_2 \quad (7)$$

$$H_2SO_5 + 2OH' = H_2SO_4 + H_2O + O_2 + 2\,- \quad (8)$$

The $H_2S_2O_8$ formed is partly hydrolysed in successive steps to permono sulphuric or Caro's acid (H_2SO_5) and hydrogen peroxide Besides, part of the Caro's acid acts as a depolariser at the anode by reacting with the discharged OH'-ions as shown in equation (8) With the progress of electrolysis the concentrations of $H_2S_2O_8$ and H_2SO_4 are greatly increased, and the main reactions taking place after some considerable time are those given by equations (5) and (8) In the case of sulphuric acid, a certain stage in the electrolysis may be reached at which the electric current is equally distributed between these two reactions so that as much $H_2S_2O_8$ as is formed by reaction (5) is converted into H_2SO_5 by reaction (7), and decomposed subsequently by the OH'-ions discharge (reaction (8)), at the anode This corresponds to a "*steady state*" at which no fresh $H_2S_2O_8$ is formed even if the electrolysis is prolonged. The principal support for Muller's hypothesis[4] is that this "steady state" has been observed by numerous workers in the case of sulphuric acid.

It may be pointed out, however, that Muller's theory is based on the assumption that the main anodic processes (5) and (8) are the result of OH'-ion discharge; it is, however, different to understand how there could be any

considerable concentration of OH'-ions in the highly acidic solutions that are required for persulphate formation

The electrolysis of neutral solutions of sodium sulphate gives very low current efficiency (*cf*, Table I) As may be expected from the modern theory of complete ionisation of electrolytes, it is likely that the concentration of the HSO_4'-ions in these solutions may be negligible, the whole of the sodium sulphate may be ionised into Na and SO_4''-ions so that the prerequisite for persulphate formation is not satisfied The observed low C Es may thus be explained It is not improbable that these low C Es. are due to the dissolved oxygen in the electrolyte Results in Tables II and III show that an increase of the concentrations of sodium sulphate and sulphuric acid improve the C E markedly. Even normally, dilute sulphuric acid contains a fair percentage of HSO_4'-ions[8] so that the addition of sulphuric acid increases the HSO_4'-ions concentration which is favourable for persulphate formation High C E, are thus observed at higher concentrations as recorded in Tables II and III

When the anodic current density is increased the rate of discharge of the HSO_4'-ions is also increased, so that these ions are in a closely packed condition immediately after the discharge This would facilitate their polymerisation and a high C E would result Moreover, the discharge potential of the HSO_4'-ion is higher than that of SO_4''-ions and oxygen[6] and therefore, high anodic current densities would be favourable for its discharge Results indicated in Table IV show that a rise in anodic current density up to 82 8 amps /dm^2 is followed by a corresponding rise in the C E At still higher current densities, however, the heating effect of the electric current probably becomes prominent and the C E consequently begins to fall

Results recorded in Table VII show that the C E falls rapidly with rise of temperature (*cf*, Table VII)

During the initial stages of the electrolysis, the concentration of the HSO_4'-ions in the electrolyte is a *maximum* It decreases steadily when more and more of it is consumed by the formation of persulphate, so that the C E also begins to decrease with longer durations Further complications due to the formation of perdisulphuric acid according to (5) and its decomposition by (6), (7) and (8) also set in These have, in general, an unfavourable influence on the C.E In the case of sulphuric acid, a 'steady state', as already indicated, is reached when a certain amount of electricity has been passed, after which, the amount of active oxygen in the electrolyte remains constant. Table VIII illustrates the influence of the duration of electrolysis on the C E and the active oxygen in the electrolysed solution.

After the passage of about two amp- -hrs of electricity the separation of solid sodium persulphate begins to take place, which increases in bulk with the progress of electrolysis Though the C E falls rapidly with greater durations, the active oxygen increases very regularly and our results do not indicate the attainment of a "steady state" This may be due to the circumstance that, instead of the whole of the persulphate formed at the anode, being quantitatively destroyed after conversion into Caro's acid, a part or even the whole of it may be precipitated as the insoluble sodium salt This is evidently not the condition which would correspond with Muller's concept of the 'steady state'

The effect of addition agents on the C E according to Muller and others,[11] would be favourable if the Caro's acid produced by reaction (6) is destroyed either chemically or by over voltage effects produced by the ions of the addition agent on the anode Increase of anodic potential would destroy Caro's acid and the reaction (8) may be inhibited, the electricity passed can thus be utilised solely for the production of $H_2S_2O_8$ The fluoride ion and the perchlorate ion have been found by Muller and Schellhaas[10] and Mizzucchelli[11] respectively, to raise the anode potential and an increase in the C E is consequently observed as recorded in Table X

Factors such as cathodic current density (Table V), interelectrode distance (Table VI) and current concentration (Table IX) are found to have negligible influence on the C E The former two factors may be ineffective due probably to the comparative stability of the sodium persulphate towards reduction by cathodic hydrogen

A diaphragm of porous material when used to separate the anolyte and catholyte is found to increase the C E to a very great extent, and in the presence of 1 gm. of HF in 100 c c of the anolyte, the C E is found to be very high (92 7%)

In conclusion the authors welcome this opportunity to express their very sincere thanks to Dr S S Joshi, D Sc (London), University Professor and Head of the Department of Chemistry, Benares Hindu University for suggesting this problem, for the keen interest taken and the valuable guidance he has given during the course of this work

Summary

The optimum conditions for the electro-chemical formation of sodium persulphate from aqueous sodium sulphate have been investigated with respect to the bath composition, anodic and cathodic current densities, interelectrode distance, temperature, duration of the electrolysis, current con-

centration, the influence of "addition agents" and the use of a diaphragm. A strongly acidic bath favours the reaction At the optimum temperature, *viz.*, 10° C high anodic current densities up to 82 2 amps./dm^2 are advantageous The process is complicated by the fact that after about 2 amp. hours the persalt tends to separate as a solid phase Our results do not support Muller's hypothesis of a '*steady state*' in the corresponding sulphuric acid electrolysis. A current efficiency as high as 92 7% has been obtained with a diaphragm, HF as 'addition agent' and special concentration (*vide infra*) of the bath solution

From a review of the various theories of persulphate formation, our results are in accord with Richardz's view, *viz*, that persulphuric acid is produced by the polymerisation of discharged HSO_4'-ions at the anode

REFERENCES

1 Joshi, Solanki and Seshadri *Proc Ind Sci Cong* 1942, Sec III, Chemistry, **11**, 12
2 L Lowenherz *Ger Pat* 77340
3 Richarz *Ber* 1888, **21**, 1672
4 Muller *A Laboratory Manual of Electro-Chemistry*, G Routledge & Sons, 1931, 252
5 Foerster *Elektrochemie Wasseriger Losungen*, 1922, 842
6 Traube *Ber*, 1893, **26**, 1471, 1886, **19**, 1115
7 Berthelot *Compt Rend* 1878, **86**, 20, 71, 277, 1892, **114**, 875
8 Mellor *A comprehensive Treatise on Inorganic and Theoretical Chemistry* Longmans, 1930, **10**, 448
9 Stark *Zeit Phys Chem* 1899, **29**, 385
10 Müller and Schellhaas *Zeit Elektrochem*, 1907, **13**, 257
11 Mazzucchelli *R Gazetta*, 1924, **54**, 1010, 1013.

STUDIES IN CHARNOCKITES FROM ST. THOMAS MOUNT, MADRAS—PART I

By C Rajagopalan M Sc

(Geology Department, Andhra University, Waltair)

Received April 5 1946

(Communicated by Prof C Mahadevan F A Sc)

Introduction

The name Charnockite, given by Sir T H Holland in 1893 for a hypersthene-granite from Mount St Thomas, Madras, was later extended by him (1900) to include a series of igneous rocks bearing a genetic relationship with the type rock from Madras Holland's own later work and that of several others such as Walker (1902), Hallows (1924), Crookshank (1938), Ghosh (1941), Rama Rao (1945), Groves (1935), Gevers and Dunne (1942) and Prider (1945) has shown the extensive distribution of this rock suite in India and elsewhere. But, these rocks, though considered as having a certain general consanguinity, have not till now been studied in much detail from the type area of Holland, in their mineralogical, chemical, and petro-provincial aspects

The scope of the present work is directed towards this objective For the purpose of the present study the type area, St Thomas Mount, Madras, was visited in the summer of 1939 and an extensive collection of representative specimens from the acid to the basic type was made The field relations of the various members of the series was carefully studied and the collection was subjected in the laboratory to detailed physical optical and chemical studies. A comparative study of results of these investigations from this area was made with the published results on charnockites and other relevant igneous rock suites from other parts of the world with a view to elucidate the differentiation tendencies of the magma on the lines initiated by Niggli.

Methods of Study

The methods of laboratory study pursued in these investigations may be classified as follows.—

1 Petrological examination—megascopic and microscopic.

2 Optical study of the important minerals by the Universal Stage

3 Chemical analysis of representative specimens from the acid to the basic types.

4 Isolation and chemical analysis of the important ferromagnesian minerals

5 Micro-metric analysis by Shand's Recording Micrometer

6. Graphical representation of the chemical analyses of rocks and minerals

7 Interpretation of the results and correlation

In the present paper the chemical and optical studies of the essential minerals are recorded In subsequent contributions the chemical and optical studies of the chief rock types and the petrochemistry and genesis of the charnockites will be given

Chemical and Optical Studies of Some of the Important Minerals

The charnockites studied belong to three fairly well marked groups, *viz*, acid, intermediate and basic In the acid varieties the constituent minerals are quartz, felspars, hypersthene, and some minor accessories In the intermediate varieties quartz is subordinate and the felspars are mainly plagioclase, with hypersthene, augite, and hornblende occurring as the other principal minerals In the basic varieties, quartz is almost entirely absent and the plagioclase is mostly labradorite, hypersthene persists with augite and hornblende The results of the chemical and optical studies of the ferromagnesian minerals, *viz*, hypersthene, augite and hornblende and the optical study of the plagioclase felspars are recorded here

Hypersthene

Chemical Analysis—The distinguishing mineral of the charnockite series is hypersthene Some of the acid rocks like $M\frac{st}{2}$ and $M\frac{st}{56}$ were crushed and after preliminary panning a concentrate of hypersthene was obtained with Thoulet solution, all magnetite having been removed by means of a bar magnet The chemical analysis of the mineral is given in Table I along with those of other hypersthenes from other localities

The chemical analysis shows that the hypersthene is an aluminous variety high in silica; FeO is slightly in excess of MgO, while lime is low

A metallic oxide in its minimum state of combination either with SiO_2 or any other metallic oxide is termed as a "Basis molecule" by Niggli (p. 299, 1936). Thus the Basis molecular composition of this mineral would be·

$$5\ Cal + 5\ 3\ Sp + 28{\cdot}2\ Fo + 23{\cdot}2\ Fa + 2{\cdot}1\ Fs + 36{\cdot}2\ Q$$

TABLE I

	A	B	C	D	E
SiO_2	56 91	53 16	55 15	54 37	45 9
Al_2O_3 ..	6 10	10 55	6 50	9 39	7 0
Fe_2O_3	1 90	4 30	2 10	0 95	2·9
FeO	18 87	17 10	17 68	18 82	18 9
MnO	0 64	Nil	0 34	0 27	
MgO	14 42	11 95	16 62	14 44	14 9
CaO	1 62	Nil	1 58	1 69	9 3
TiO_2	Trace	1 35	0 03	0 07	1·1
H_2O		2 00			
Total	100 46	100 41	100 00	100 00	100 0
si	128	127½	117	115	84½
al	8	15	8	11½	7½
fm	88	85	88	85	74
c	4	0	4	3½	18½
mg	0 55	0 50	0 60	0 54	0 55
Q	36 2	39	32 4	31 9	21 9
L	5 0	0	5 3	4·6	11 7
M ..	58 8	61	62 3	63 5	66·4
$CaSiO_3$	4 4	0	4 2	4 6	20 8
$MgSiO_3$	54 6	50	59 8	55 0	46 4
$FeSiO_3$	41 0	50	36 0	40 4	32 9

A Hypersthene from charnockite, St Thomas Mt Madras Analyst C Rajagopalan

B Hypersthene (Bidalotite) Bidaloti Mysore, Analyst E R Tirumalachar *Proc. Ind Acad Sci* 5, B p 292

C Hypersthene from charnockite, between the Hill Ihunga and Waki camp Buttaba Hoima Road, Bunyoro, Uganda Analyst A W Groves *Q J G S* XCI, p 156 1935

D Hypersthene from charnockite, same locality as (C) Analyst A W Groves *op cit*

E Hypersthene from metadolerite, four miles from Kigarohya Rest House Bunyoro, Uganda, Analyst A W Groves, *op cit*

The formula of hypersthene from the charnockite computed from the analysis following the method used by Groves* (p 213, 1937) is given below (Table II)

* The chemical analysis is arranged as shown in Table II The M P of all the constituents are first determined and recorded in the third column These values are multiplied by the number of oxygen or fluorine atoms and given in the fourth column The number of O, OH and F atoms being fixed by the formula at 24, it (twenty-four) is divided by the sum of O, OH and F for the different radicals (column 4) This, multiplied by the number of metal atoms in the molecules gives the number of metal atoms on a basis of 24 (O, OH, F) which is given in column 5 Silicon should obviously be 8 But in many cases as will be seen in augite and hornblende it will be less than 8 In such a case it is very possibly replaced by Ti or Al or both Enough of these are to be given to make Silicon 8 The rest are taken as metallic radicals

TABLE II

Computation of the formula of hypersthene

	Wt %	M P	No of (O, OH, F)	Metal atoms on the basis of 24 (O, OH, F)	
SiO_2	56 91	949	1 898	8·20	8 20
Al_2O_3	6 10	60	0·180	1 04	1·25
Fe_2O_3	1 90	12	0 036	0 21	
FeO	18 87	262	0 262	2 27	2 35
MnO	0 04	0	0 009	0 08	
MgO	14 42	361	0·361	3 12	3 12
CaO	1 62	29	0 029	0 25	0 25
Total	100 46		2 775		

$$\frac{24}{2 \cdot 775} = 8\ 65$$

1 25 $(Al, Fe)_2O_3$ 3 12 MgO, 2 35 (Fe, Mn) O, 0 25 CaO, 8 21 SiO_2 or nearly,

10 $(Al, Fe)_2O_3$, 25 MgO, 19 (Fe, Mn) O, 2 CaO, 66 SiO_2; or calculated on a lime-free basis it comes to Mg_3 (Fe, Al, Mn)$_4$ $(SiO_3)_8$ and the formula according to the molecular proportions would be

5 $(Al, Fe)_2O_3$, 25 MgO 18 (Fe, Mn) O, 2 CaO, 66 SiO_2

From the above formulæ it is easily seen that SiO_2 is in excess of the metallic oxides The proportion of MgO to FeO in a normal hypersthene is roughly 3.2 which is closely approximated by this hypersthene.

For a comparative study, when we plot this hypersthene on the Metasilicate and the Q-L-M Diagrams (Table I) it is found (Fig. 1) that this mineral, along with other hypersthenes, falls within the field of rhombic pyroxene given by Tsuboi (p 69, 1932) in the former, while in the Q-L-M Diagram (Fig 2) instead of being near about P in Niggli's field of "normal" pyroxenes (p 643, 1938) enclosed by dotted lines, it falls on the side of Q showing its siliceous nature which has already been noted in the computed formulæ

Optical Studies—In thin sections, under the microscope, the mineral shows coarse cleavage in which small plates of magnetite are usually seen. It has a characteristic pleochroism, the uniformity of which is maintained in all the types of rocks, except perhaps a slight weakening in the most acid types. A determination on the Universal Stage gave:

X: Brownish pink
Y: Pinkish yellow to pink
Z: Bluish green

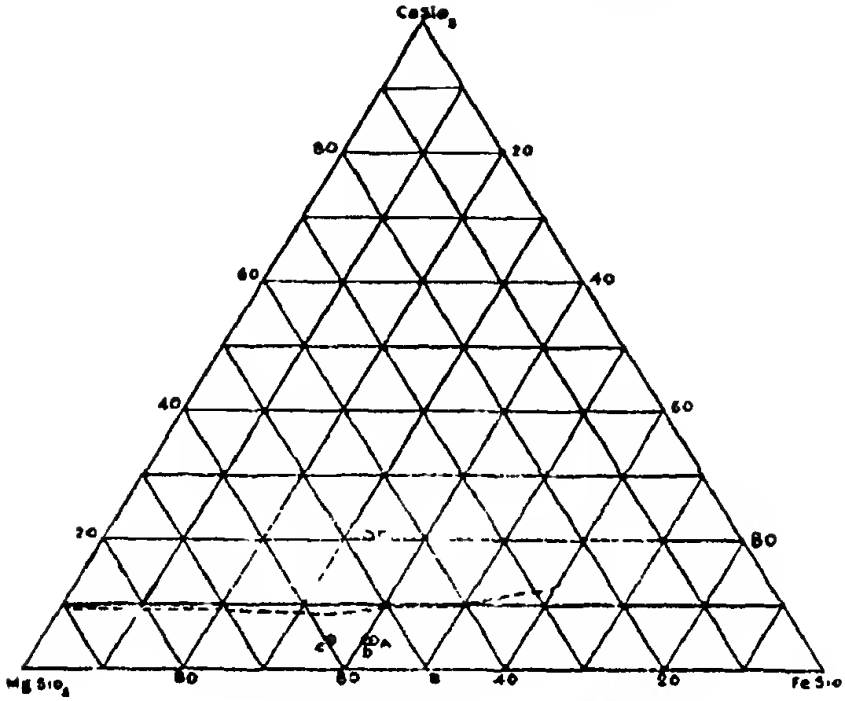

FIG 1 Metasilicate Diagram for Hypersthene

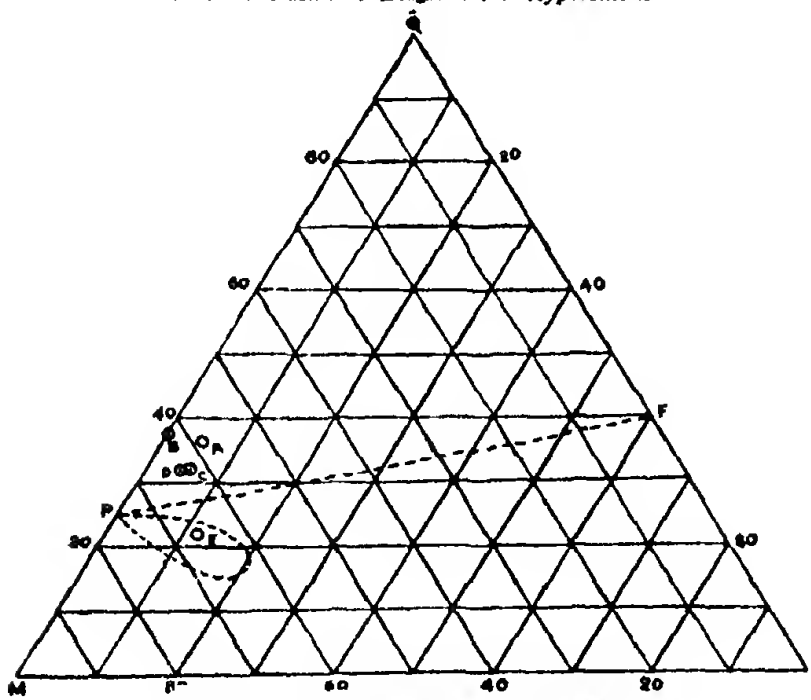

FIG. 2. Q L.M. Diagram for Hypersthene

Under crossed nicols, the mineral shows yellows and pinks of the 1st order, a marked oblique extinction even upto 36° Fifteen determinations for the measurement of 2V were taken of which nine gave values of – 60° to – 62° The remaining six gave values ranging between – 52° and –79° Such variations observed even in the same slide were also noted in hypersthenes of other rocks by Verhoogen (1937) Further, the curves given by Winchell (p 177, 1927) for the series $MgSiO_3$–$FeSiO_3$ show that slight variations in the composition is accompanied by rapid changes in the values of 2V It is therefore possible that in this hypersthene also slight changes in composition have been responsible for the variation in the optic axial angle earlier formed crystals being probably richer in FeO

Oblique extinction in hypersthene is not uncommon as several authors such as Lacroix (p 173, 1891), Sen Gupta (1916), Walker (p 17, 1902), Naidu (1943) and Ray and Roy (1944) have reported about it With a view to ascertain whether the observed inclined extinctions are due to the oblique orientation as suggested by Johannsen (p 212, 1937) or to an angle between *c* and Z I have followed the usual method of locating the ether axes with the Universal Stage and tracing the optical planes of symmetry on the Wulff's Net and then plotting the pole of the cleavage in the same stereogram If we assume that the cleavage plane is in the prism zone then, it follows that a point at right angles to the cleavage pole and the Y ether axis will give the position of the crystallographic axis *c* (since Y is parallel to *b*) By making seven such determinations it is found that *c* never coincided with Z Four of these gave values ranging from 4° to 9°, one gave 28°, another 33° and another 36°

Thus, from the foregoing, it is clear that this hypersthene from Madras charnockites cannot be identified either with Winchell's clinohypersthene (p 180, 1927) or with the artificial products of Bowen and Schairer (1935). It is yet to be ascertained whether the non-coincidence of *c* with Z in this hypersthene is just a freak confined to Madras rocks, or a serial character of the charnockites In any case it stands unique in being aluminous and giving an angle between *c* and Z at the same time having the characteristic pleochroism of rhombic pyroxene

Augite

The augite seen in these charnockites is a dark green variety usually with some opaque inclusions, chiefly of magnetite This mineral found in specimen No M $\frac{6t}{16}$ disposed as a veinlet was carefully isolated, a small piece of which was used for making a thin section for optical determinations.

Chemical Analysis —A sample part of the mineral was used for chemical analysis after treating it with Thoulet solution and separating the magnetite by magnet. The chemical analysis of the augite, along with other monoclinic pyroxenes from other localities, is given in Table III

TABLE III

Chemical analyses of monoclinic pyroxenes

	A	B	C	D	E
SiO_2	50 06	50 9	51 30	60 23	51·87
Al_2O_3	1 92	1 5	0 76	3·53	2 02
Fe_2O_3	2 00	3·2		3 41	3 50
FeO	14·62	13·3	13 92	10 63	8 98
MnO	0·05	..	0 25	0 10	0 18
MgO	13·07	10·7	14 85	12 27	16·26
CaO	17 85	18·6	20·15	17 44	15 70
Na_2O	0 36	.		1 25	0 16
K_2O	Trace	..	.	0 31	0 09
TiO_2	0·76	.		0 53	0 21
H_2O	..		0 21	0 64	1 20
Total	100·69	100 00	101·44	100 44	100 17
si	93	100	91½	97	98
al	2	2	1	4	2
fm	62	58	60½	57½	65½
c	35	40	38½	36	32
alk	1			2½	½
k	..		.	0 16	0 28
mg	0 59	0 52	0·65	0 61	0 70
Q	22 1	25 8	24 7	22 6	24·4
L	4 2	2 5	1 6	9·6	3 7
M	73 7	71 7	73 7	67·8	71 9
$CaSiO_3$	37·6	42 6	38 8	40·7	34 4
$MgSiO_3$	38·6	34·0	40·2	40·0	50·0
$FeSiO_3$	23·9	23·4	21·0	19·3	15·6

A Augite from charnockite, St Thomas Mt, Madras, Analyst C Rajagopalan

B "Monoclinic pyroxene from charnockite," from the top of Mt Wati (Ote), Uganda Analyst A W. Groves, *Q.J.G.S*, XCI, p 157, 1935

C "Diallage, Skye" Analyst · Vom Rath—*Handbuch der Mineralchemie*, p 465, 1860. Quoted from A. Harker "The Tertiary igneous rocks of Skye" *Mem G S United Kingdom*, p 108, 1904.

D Common augite from diabase, Issutschki, Südrussland. P Niggli *Geologie der Schweiz*, Geotechnische Serie XIV, Lieferung, p 17, 1930

E Pigeonite from diabase Launceston, Tasmania P Niggli, *op cit*, p. 16

From the Table it is seen that this augite is a non-aluminous, non-titaniferous and non-alkalic variety, which compares closely with that of Uganda (B). Further, it is seen that the mineral is rich in clinoenstatite

and clino-hypersthene molecules and therefore grades partially into pigeonite The Basis molecular composition of a normal augite kindly supplied by Dr K P Rode in a personal communication, is 1 Kp + 7 Ne + 2 9 Cal + 26 5 Cs + 13 5 (Fa + Fs) + 25 9 Fo + 22 8 Q + 0·2 Ru The augite from the Madras charnockite 2 0 Ne + 2 2 Cal + 25 9 Cs + 19 5 (Fa + Fs) + 27 7 Fo + 22 1 Q + 0 6 Ru shows a much higher value of (Fo + Fa + Fs) which indicates the pigeonitic nature

The computation of the formula of augite on the lines suggested by Groves (p 213, 1937) is given in Table IV

TABLE IV

Computation of the formula of augite

	Wt%	M. P	No of (O, OH, F)	Metal atoms on the basis of 24 (O, OH F)			
SiO_2 ..	50·06	834	1·668	7 60		8 0	8·0
TiO_2 ..	0 76	10	0 20	0·09			
Al_2O_3 .	1·92	19	0·057	0 35	0·31		
Fe_2O_3 .	2·00	12	0·039	0·24	0·04	0·28	5·10
FeO ..	14 62	203	0·203	1 85	1·86		
MnO .	0 05	1	0 001	0·01			
MgO ..	13 07	327	0 327	2·98	2·98		
CaO ..	17 85	319	0 319	2 90	2·90		3·01
Na_2O	0 36	6	0 006	0·11	0·11		
Total ..	100·69		2·634				

0 28 $(Al, Fe)_2O_3$, 2 98 MgO, 1·86 (Fe, Mn) O, 2·9 CaO, 0·11 Na_2O, 8·0 $(Si, Al, Ti) O_2$ or nearly,

3 $(Al, Fe)_2O_3$, 30 MgO, 18 (Fe, Mn) O, 29 CaO, Na_2O, 80 $(Si, Al, Ti) O_2$; or to put it slightly differently,

$$(Ca, Na)_3 (Mg, Fe, Al, Mn)_3 [(Si, Al, Ti) O_3)]_8$$

while that according to the molecular proportions comes to:

5 $(Al, Fe)_2O_3$, 54 MgO, 34 (Fe, Mn) O, 53 CaO, Na_2O, 141 $(Si, Ti) O_2$.

On the Q-L-M (Fig 3) Diagram the augite is seen falling just on the border of Niggli's field for "normal" pyroxenes (indicated by dotted lines); being on the M side, it indicates deficiency in SiO_2 carrying normative olivine in its composition. On the Metasilicate Diagram (Fig 4) this augite falls not within Tsuboi's field of monoclinic pyroxenes (p 69, 1932) but between the ranges of rhombic and monoclinic, though nearer to the latter. This shows its deficiency in wollastonite molecules,

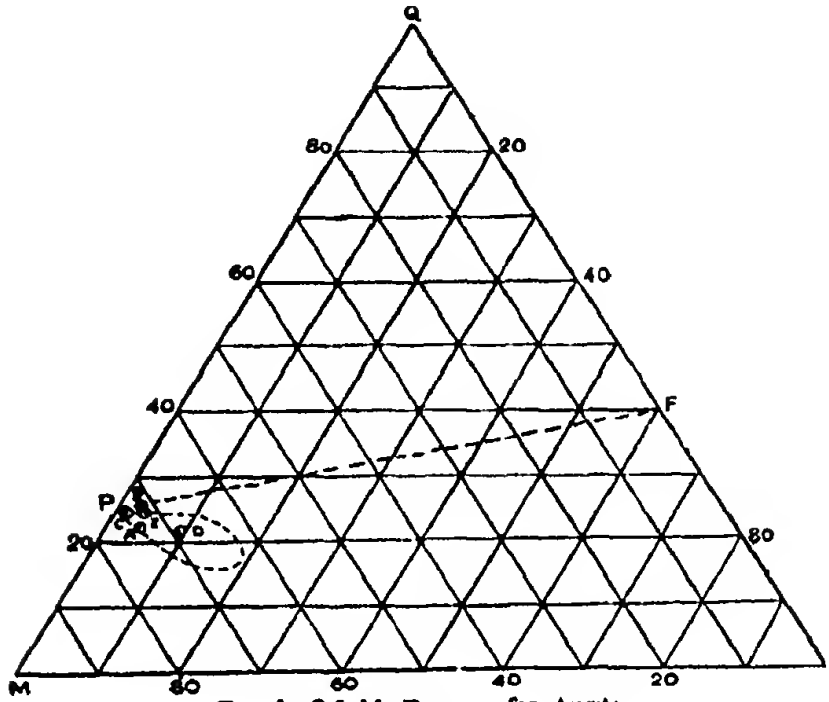

FIG 3 Q L.M Diagram for Augite

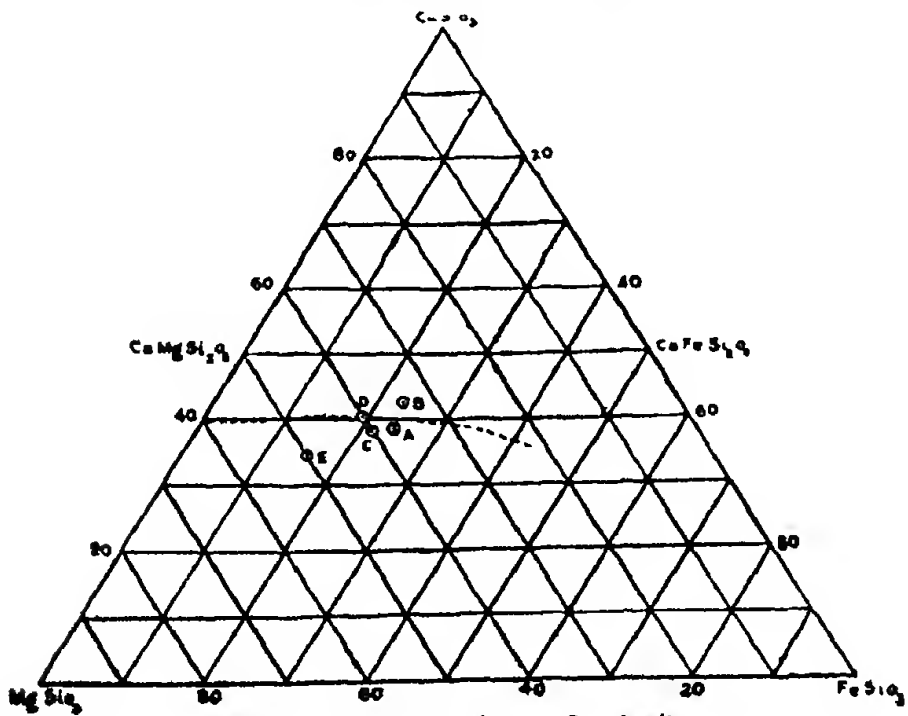

FIG. 4 Metasilicate Diagram for Augite

with higher $MgSiO_3$ and $FeSiO_3$ than normal, showing thereby its pigeonitic nature.

Optical Studies—Under the microscope the mineral is green or bluish green in thin sections, with well-developed cleavages in which, as in the case of hypersthene, small plates of magnetite are usually developed. It sometimes shows a very faint but distinct pleochroism

TABLE V

Chemical analyses of hornblende

	A	B	C	D	E
SiO_2	44 10	42·38	37 79	46 22	43 11
Al_2O_3	9·00	8 65	11·92	8·12	11 10
Fe_2O_3	6 23	8 18	6·78	9·33	4·97
FeO	16·72	13 80	15·99	15 18	13 04
MnO	0 06	.	.	..	0 43
MgO	6 56	7 53	8 37	5 20	9·35
CaO	11 15	12 07	9 76	10·08	11·76
Na_2O	1 42	1 65	1 38	2·46	1·18
K_2O	0·94	0 63	3 08	1·23	1 27
TiO_2	3 27	3 88	3 37	1 08	1·32
P_2O_5	.			.	0·10
H_2O^+	0 98	0·93	1 37	1·36	1 92
H_2O^-	0 07	0 30	0 19	..	0 16
Total	100 50	100 00	100·00	100 26	99 78
si	92	86½	73	100	86
al	11	10½	13½	10½	13
fm	60	59	60	59½	58
c	25	26½	20	23½	25
alk	4	4	6½	6½	4
k	0·30	0·18	0 59	0 24	0·41
mg	0 35	0·38	0 41	0 39	0 49
Q	21·2	19·3	12 3	21 6	20·2
L	21 5	21·6	31 1	23·5	25 1
M	57·3	59·1	56·7	54·9	54·7
$CaSiO_3$	33 5	36 3	28 8	34·7	33 6
$MgSiO_3$	27·5	31·5	34·6	25·0	37 4
$FeSiO_3$	39·0	32 2	36·6	40·3	29·0

A · Hornblende from charnockite St Thomas Mt, Madras Analyst C. Rajagopalan.

B · Hornblende from charnockite From the top of Mt. Wati (Ote), Uganda, Analyst. A W Groves, *Q J G S.* XCI, p 158, 1935

C Hornblende from charnockite From the bed of a river about 1½ miles S. W of Mt. Wati, Uganda. Analyst A W Groves. *op. cit*

D Hornblende from syenite, Biella, Piedmont, Italy, Rosenbusch . *El*, *Gest* pp 103 and 106. Quoted from Clarke . *Data of Geochemistry*, 1924, 5th Ed.

E . Common hornblende from amphibolite Palmer center, Mass., U.S.A. P. Niggli. *Geologie der Schweiz*, Geotechnische Serie XIV, p. 14.

X: Yellowish green

Y Green

Z Bluish green

Under crossed nicols, most of the pieces show thin and distinct lamillæ with different polarisation colours of 1st and 2nd orders giving the effect of multiple twining. Probably this is due to 'slips' along the planes of parting A determination on the Universal Stage gave the following results.

$$+2V = 52° \pm 4°$$

$$c \wedge Z = 45° \pm 2°$$

Though the majority were near about 50° in their optic axial angle, grains of augite are not wanting showing smaller values The low optic axial angle and the richness of the mineral in clino-enstatite and clino-hypersthene molecules, distinctly point out that this augite is a member of the pigeonite family.

Hornblende

Chemical Analysis—This mineral was isolated from rock No M $\frac{st}{53}$ in which it is found to occur in large stringers The mineral thus obtained was checked under low power microscope and treated with Thoulet solution The heavier residue was powdered and magnetite was separated by a strong magnet The purified powder thus got was analysed, the results of which are given in Table V along with the analyses of hornblendes from other localities.

From the analysis given above (Table V A) we find that this hornblende is rich in iron, which is probably responsible for its colour; TiO_2 is also fairly high and is probably the cause of the strong pleochroism exhibited by it The computation of the formula according to Grove's method is given below (Table VI)

$$1{\cdot}66\,(H, Na, K)_2O,\ 2\ 13\,(Fe, Mn)\,O,\ 1\ 5\,MgO,\ 1\ 86\,CaO$$
$$2{\cdot}33\,(Al, Fe)_2O_3\ 7\ 09\,(Si, Ti)\,O_2$$

or nearly,

$$11\,(H, Na, K)_2O,\ 14\,(Fe, Mn)\,O,\ 10\,MgO,\ 12\,CaO,\ 16\,(Al, Fe)_2O_3\ 47\,(Si, Ti)O_2$$ or better as, $H_2\,(Ca, Na, K)_5\,(Mg, Fe, Al, Mn)_{10}\,[(Si, Al, Ti)\,O_2]_{14}$ and that according to the molecular proportions comes to.

$$9\,(H, Na, K)_2O,\ 23\,(Fe, Mn)\,O,\ 16\,MgO,\ 20\,CaO,\ 13\,(Al, Fe)_2O_3,\ 76\,(Si, Ti)\,O_2.$$

TABLE VI

Computation of the formula of hornblende

	Wt%	M P	No of (O, OH, F)	Metal atoms on the basis of 24 (O, OH, F)		
SiO_2	44 10	735	1 470	6·72		8 00
TiO_2	3 27	41	0·082	0 37	0 91	
Al_2O_3	9 00	88	0 264	1 61	0 70	
Fe_2O_3	6 23	39	0 117	0 72	1 42	5 05
FeO	16 72	232	0 232	2 12	2 13	
MnO	0 06	1	0 001	0 01		
MgO	6 56	164	0 164	1·50	1·50	
CaO	11 15	200	0 200	1 86	1 86	2·46
Na_2O	1 42	23	0 23	0 42	1·66	
K_2O	0 94	10	0 10	0·18		
H_2O^+	0 98	58	0 58	1 06		1 06
H_2O^-	0 07					
Total	100 50		2 621			

From the above formulæ it is easily seen that the metallic oxides are in excess of SiO_2 This deficiency in silica is due to the partial replacement This mineral also, therefore, carries normative olivine molecules, just as augite does.

The composition of common hornblende is expressed by Groves (p 212, 1937) as

$$H_2(Ca, Na, K)_{2-3}(Mg, Fe, Al)_5[(Si, Al)O_8)]_8$$

The formula of the hornblende expressed in similar manner compares very well with the above one, except that the H_2 is deficient It is very probable that the hornblende is derived from augite with insufficient water Other chemical evidences which will be discussed in the next paper also suggest a similar conclusion

The Basis composition of this hornblende and the hornblende from quartz-gabbro and quartz-diorite (personal communication from Dr K P. Rode) is given below

Hornblende from	Basis composition
Qz-gabbro	10 2 (Kp + Ne) + 12 4 Cal + 13 1 Cs + 42 4 (Fo + Fa + Fs) + 21·9 Q
Qz-diorite	8 5 (Kp + Ne) + 9 2 Cal + 12 1 Cs + 45·4 (Fo + Fa + Fs) + 24 8 Q
Charnockite (Madras) ..	11 7 (Kp + Ne) + 9 8 Cal + 12 9 Cs + 42·0 (Fo + Fa + Fs) + 23·6 Q

From the above, it is seen that the mineral in question compares very well with the normal hornblendes characteristic of plutonic igneous rocks

When plotted in the two Trilinear Diagrams (Figs 5 and 6) it is seen that this hornblende falls in the proper field in both cases

Optical Studies—Under the microscope in thin sections, it is seen that the mineral is a greenish-brown variety and highly pleochroic with the following scheme of pleochroism as determined on the Universal Stage

X· Pale yellow to bright yellow

Y Brown.

Z Deep brownish-green

The prismatic cleavage is well developed A determination on the Universal Stage gave the following results

$$-2V = 81° \pm 1°$$

$$c \wedge Z = 8° \pm 4°$$

Though most of the grains gave the above values there were, however, a few pieces giving slightly lower or higher values both in their optic axial angle and maximum extinction angle, the variations probably being due to slight differences in composition, as in the case of hypersthene

General Relationship of the Femic Minerals

From the foregoing chemical study we find that while the FeO content of the three femic minerals is almost uniform, in augite there is relatively an enrichment of lime at the cost of alumina and silica The silica is higher in the rhombic pyroxene than in the monoclinic which in fact carries some normative olivine molecules.

As compared to the pyroxene, hornblende is richer in total iron, particularly sesqui-oxide, and to some extent alumina also, this being at the expense of MgO, CaO, and to some extent SiO_2

On the basis of microscopic study Sen Gupta (1916) considered the rhombic pyroxene to have been derived from augite A chemical study or these minerals does not, however, support such a conclusion For such a change, the impoverishment of augite in lime might be explained away by assuming it to have been drawn upon for the formation of anorthite of garnet, but then, there is no source of alumina required either by anorthite or garnet or for that matter by hypersthene itself (*vide* analysis of hypersthene and augite), since this augite is practically a non-aluminous variety.

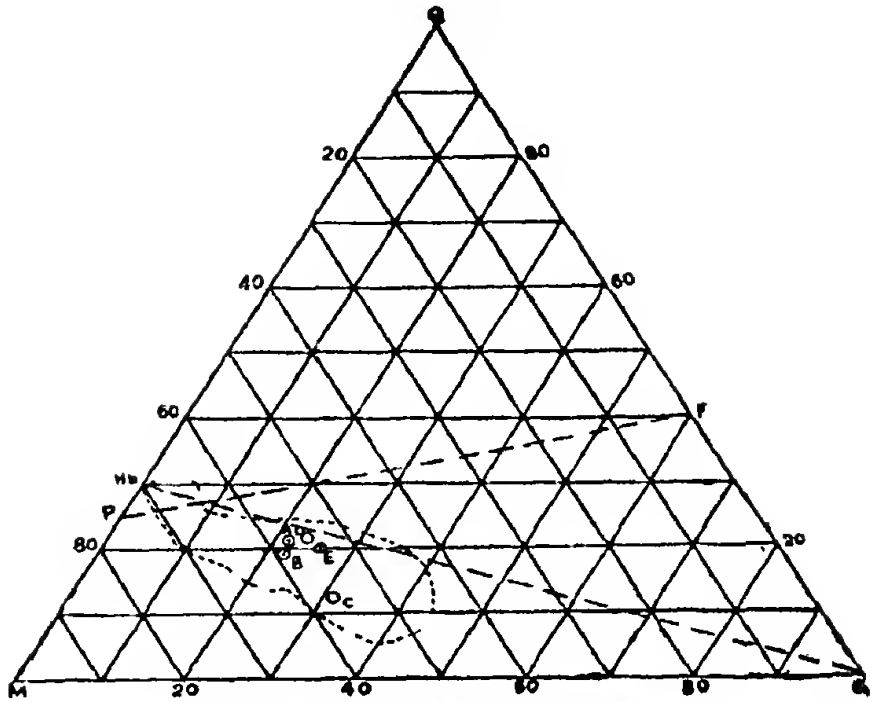

Fig 5. Q L M Diagram for Hornblende

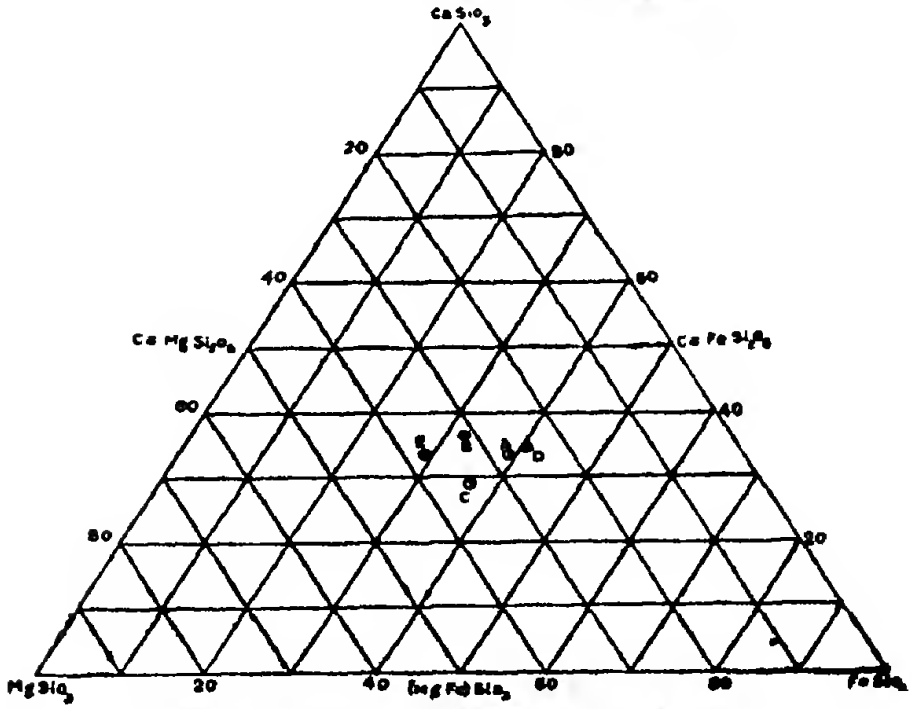

Fig. 6. Metasilicate Diagram for Hornblende

Ghosh (1941) has suggested that basic diopsidic rocks on assimilation by highly alkaline magma would give rise to hypersthene-bearing rocks (*i e.*, charnockites)·

Diopside + anorthite + silica = garnet + hypersthene

In charnockites from Madras, however, garnet which must be produced according to the above reaction is not so universally present

Tsuboi (p 73, 1932) following Barth's (1931) observations asserts that "so far as is known, the porphyritic (or plutonic) pyroxenes (*i e*, of intra-telluric crystallization) are either monoclinic approximating in composition

TABLE VI

Determination of the anorthite content of the plagioclase felspars

Slide No	2V	Deduced An%	Rock type	Min R I	Deduced An%	Twin Law	An%
M st/53 ..	+78°	50	A Ilb-Norite	1 558	55–58	Albite-ala Albite-karls	40–45 64
M st/48 ..	+82°	45	B Hy-Gabbro	1 550	43	Albite-ala Albite-karls Albite-est	40 40 35
M st/52 .	+86°	42	C. Norite	1 550	43	Aklin Manebach-ala	48–50 40
M st/23 ..	+68°	40	C Norite	1 545	35	Albite-ala Manebach-al	25–35 40
M st/55 ..	+84°	42	C. Norite	1 547	38	Albite-ala Manebach-akli Albite-karls	30–33 35–40 32
M st/23 ..	−88°	36	D. Grano-Diorite	1 545	35	Albite-ala Manebach-ala	28 29
M st/4 .	−80°	30	D Grano Diorite	1·545	35	Albite-ala Albite-ala Albite-ala	28 29–30 30
M st/26 ..	−84	32	E Granite	1 542	30–32	Albite-ala Manebach-ala	29 25
M st/17 ..	−80	30	E. Granite	1 545	35	Albite-ala Albite-ala Albite-ala	29 35 35
M st/12b ..	+86	12–13	F Hy-Granite	1·538	18	Albite-ala Albite-karls Manebach-aklin	13–15 12 15
M st/2 ..	+86	12–13	F Hy-Granite	1 533	10–12	Albite-ala Albite-ala Albite-ala	10–12 8–12 12

$CaMgSi_2O_6$—$CaFeSi_2O_6$ or rhombic approximating to $MgSiO_3$—$FeSiO_3$, but never pigeonitic " But here in these rocks we have a monoclinic pyroxene which is definitely of pigeonitic nature

Felspars

Among the invariable constituents of charnockites microcline-microperthite and perthite are the commonest alkali members. The plagioclase felspars which are present in all the types are mostly twinned The nature of the plagioclase (*i e*, the anorthite content) and the twin law was determined on the Universal Stage following the method given by Reinhard (1931) For confirming the results, the minimum refractive index determined by immersion method and the 2V were used

From the above data it is clear that the most important twin law obeyed by the plagioclase felspars of the charnockites from Madras is Albite-ala The plagioclases are usually twinned after the Albite and Pericline Laws, but here it is significant to note that the twins are dominantly after Albite-ala. The deduced values of anorthite from the minimum refractive index and 2V agree closely with those of the determined ones The blue colour of the felspars of charnockite was suggested by Jayaraman (1937) as probably due to dissemination of minute hair-like inclusions of Fe_2O_3 and TiO_2 But the possibility that the colour is due to pressure should not be overlooked

ACKNOWLEDGEMENT

In the end I wish to express my grateful thanks to Dr K. P. Rode for his guidance and help throughout the course of these investigations; to Dr Rajnath, Head of the Department of Geology, Benares Hindu University, for the facilities he gave me to carry out these investigations. to Doctors M S Krishnan, C Mahadevan and G W Crickmay for the helpful suggestions and editing; and to the Director of Geological Survey of India for supplying me with the necessary literature

REFERENCES

Barth, Tom F W — "Crystallisation of pyroxenes from Basalts," *Amer Miner*, 1931, 16, 195-208.

Bowen, N L., and Schairer, J F — "The system MgO FeO-SiO_2", *Amer. Jour Sci*, 1935, 29, 151-217

Clarke, F W — *Data of Geochemistry*, 1924 5th Ed, Washington.

Crookshank, H — "The Western Margin of the Eastern Ghats in Southern Jeypore," *Rec G S.I*, 1938, 73, pt. 3, 396-434.

Gevers, T W, and Dunne, J C — "Charnockite Rocks near Port Edward, Alfred County, Natal," *Trans Geol Soc, South Africa*, 1942, 45, 183-213

Ghosh, P. K. — "The charnockite series of Bastar State and Western Jeypore," *G.S.I. Rec*, 1941, 75.

Groves, A. W — "The charnockite series of Uganda, British East Africa," *Q J G S London*, 1935, **91**, 150-207

——— — *Silicate Analysis*, 1937

Hallows, K A K — "Basic and Ultra-basic members of the charnockite series in the Central Provinces," *Rec G S I* 1924, **25**, 254–59

Harker, A — "The Tertiary Igneous Rocks of Skye," *Mem G S United Kingdom*, 1904, 108.

Holland, T H — "The Petrology of Job charnock's Tombstone," *Jour As Soc Beng*, 1893, **62**, Pt 2, 162–64

——— — "The Charnockite Series, a group of Archean Hypersthenic Rocks in Peninsular India," *Mem G S,I*, 1900, **28**, Pt 2.

Jayaraman, N. — "A note on the blue Quartz of the Charnockite of Pallavaram, near Madras" (Abstract), *Proc Twenty-fourth Ind Sci Congr*, 1937

Johansen, A. — *Petrography* 1937 3, 212

Lacroix, A. — "Gneissose rocks of Salem and Ceylon," *Rec G,S I*, 1891, **24**, Pt 3, 173

Naidu, P R J — "Inclined extinctions in Hyperthenes of charrocxito," *Curr Sci*, 1943 **12** No 5, 158

Niggli, P — "Beitrage zur Geologie der Schweiz, Geotechnische," 1930, Serie **14**, Lieferung

——— — "Uber Molekularnormen zur Gesteinsberechnung," *Schweiz Min Petr Mitt*, 1936, Band **16**, 295–317

——— — "Die komplexe gravitative kristallisations-differentiation," *Ibid*, 1938, Band, **18**, 610–64

Prider, T R. — "Charnockitic and Related Cordierite-bearing Rocks from Dangin, Western Australia," *Geol Mag*, 1943, **82**, No 4

Rama Rao, B — "The Charnockite rocks of Mysore," *Mysore Geological Department, Bulletin*, 1945, No 18

——— and Rama Rao, L. — "On 'Bidalotite' a new orthorhombic pyroxene," *Proc Ind Acad Sci*, 1937, **5**, B, 290–95

Ray, S., and Roy, S K — "Inclined extinction in Indian hypersthenes," *Q J Geol, Min, Met Soc Ind*, 1944, **16**, No 4.

Reinhard, M — *Universaldrehtischmethoden*, 1931

Sen Gupta, K. K — "On the Hypersthenisation of Monoclinic Pyroxenes" (In charnockite) (abstract), *Jour As Soc Beng*, 1916, N. S. **12**, Proc, cxxi–cxxiii

Tsuboi, S. — "On the course of Crystallization of Pyroxenes from rockmagmas," *Jap Jour*, 1932, **10**, 67–82

Verhoogen, Jean — "A monoclinic 'Hypersthene' from the Cascade Lavas," *Amer Jour Sci*, 1937, **33**, 63

Walker, T. L. — "Geology of Kalahandi State, Central Provinces," *Mem. G S I*, 1902, **33**, Pt 3, 1–2

Winchell, A. N — *Optical Mineralogy* Pt. II, New York and London, 1927.

STUDIES IN THE NAPHTHALENE SERIES

Part XI. The Condensation of 2 Acetyl-1-naphthol and Methyl 1-hydroxy-2-naphthoate with Stearyl, Palmityl and Lauryl Chlorides

By R D Desai, F A Sc, and W S Waravdekar

(From the Department of Chemical Technology, and the Chemistry Department, St Xavier's College, Bombay)

Received March 8, 1946

In the course of exploring the best methods of preparing 4-stearyl, -4-palmityl- and 4-lauryl-1-naphthols, we condensed 2-acetyl-1-naphthol with stearyl chloride with a view to converting 4-stearyl-2-acetyl-1-naphthol (I) into 2-methyl-3-acetyl-6-stearyl 1·4-α-naphthapyrone (II) which, on alkaline hydrolysis, would give 4-stearyl-1-hydroxy-2-naphthoic acid, the decarboxylation of which would furnish 4-stearyl-1-naphthol However, as the alkaline hydrolysis of the pyrone (II) gave the original ketone (I) this synthetic route was blocked Some interesting properties of the ketone (I) have been studied Its bromination using one mol or excess of bromine gave 4-stearyl-2-bromacetyl 1-naphthol (III), as hot alkali converted it into 5-stearyl-3-keto-α-naphthacoumaranone (IV) Nitration with one mol or excess of nitric acid gave mainly 4-nitro-2-acetyl-1-naphthol with traces of 4-stearyl-2-nitro-1-naphthol The Clemmenson reduction gave 4-stearyl-2-ethyl-1-naphthol, as the same compound was obtained by condensing stearyl chloride with

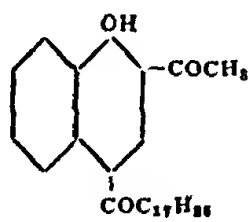

(I)

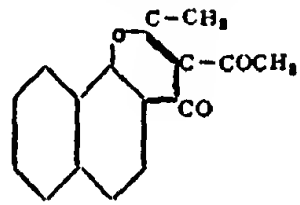

(II)

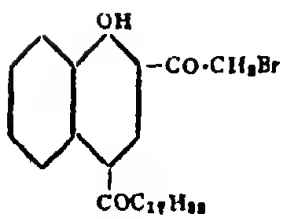

(III)

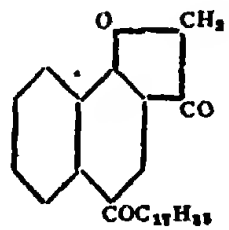

(IV)

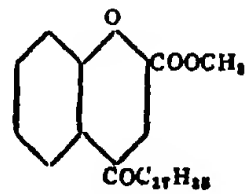

(V)

2-ethyl-1-naphthol On heating its glacial acetic acid or propionic acid solution in presence of anhydrous zinc chloride, the ketone lost the stearyl group Similar condensations of 2-acetyl-1-naphthol with palmityl and lauryl chlorides and the properties of the resulting products were studied.

The second route adopted for the synthesis of 4-stearyl-1-naphthol was the condensation of methyl-1-hydroxy-2-naphthoate with stearyl chloride with the hope of obtaining 1-hydroxy-2-carbmethoxy-4-stearyl-naphthalene (V), the corresponding carboxylic acid of which was expected to give 4-stearyl-1-naphthol on decarboxylation No doubt the product (V) was formed in nearly 40% yield, but it was accompanied by an equal amount of 2-stearyl-1-naphthol, while the decarboxylation of the acid gave the final overall yield of 25% of 4-stearyl-1-naphthol Similar condensations were carried out with palmityl and lauryl chlorides, and 4-palmityl and 4-lauryl-1 naphthols were obtained in 20% yield Other methods are being explored

EXPERIMENTAL

2-Acetyl-4-stearyl-1-naphthol

A mixture of 2-acetyl-1-naphthol (12 gm), stearyl chloride (20 gm) and zinc chloride (10 gm) in nitrobenzene (60 c c) was kept for 48 hours, decomposed by hydrochloric acid and steam-distilled The product crystallised from alcohol in white, flat needles, m p 75-76° C (Yield 75%) Its alcoholic solution gave no colouration with ferric chloride (Found C, 79 6; H, 9·7 $C_{30}H_{44}O_2$ requires C, 79 6, H, 9 6 per cent)

Kostanecki Reaction with the above ketone and the preparation of 2-methyl-3-acetyl-6-stearyl-1 4-α-naphthapyrone—The above ketone (3 gm), sodium acetate (5 gm) and acetic anhydride (30 c c) were heated in an oil-bath at 175-80° C for 12 hours The product was crystallised from alcohol in white, shining needles, m p 65-66° C depressed to 51° C by the original ketone (Found: C, 78·5, H, 8 8, $C_{34}H_{46}O_4$ requires C 78 7; H, 8 9 per cent.)

Hydrolysis of the above pyrone.—The pyrone was reacted with 10 per cent. alkali and the product after hydrolysis was crystallised from alcohol in shining needles, m p 75-76° C undepressed by 2-acetyl-4-stearyl-1-naphthol.

p-Nitrophenyl-hydrazone of the ketone was obtained from alcohol in yellowish-red, flat needles, m p 260-61° C (Found. N, 7·2; $C_{36}H_{49}O_4N_3$ requires N, 7·1 per cent.)

Clemmensen reduction of the ketone and the preparation of 2-ethyl-4-stearyl-1-naphthol.—The ketone (2 gm) with amalgamated zinc (10 gm)

and hydrochloric acid (60 c c) was refluxed for six hours and crystallised from alcohol in small plates, m p 71–72° C , depressed to 56–57° C. by the original ketone but undepressed by 2-ethyl-4-stearyl-1-naphthol prepared from stearyl chloride and 2-ethyl-1-naphthol (Found: C, 82 0; H, 10·7; $C_{30}H_{46}O_2$ requires C, 82 1 , H, 10 6 per cent.)

p-Nitrophenyl-hydrazone of 2-ethyl-4-stearyl-1-naphthol gave deep-red crystals, m p 130-31° C (Found. N, 7 5; $C_{36}H_{51}O_3N_3$ requires N, 7·3 per cent)

2-Brom-acetyl-4-stearyl-1-naphthol was prepared from the ketone (1 6 gm) and bromine (0 2 c c) in acetic acid (50 c c) and crystallised from alcohol in white, small, flat needles, m p 72–73° C The mixed m.p with the ketone was 53–54° C (Found Br, 15 1; $C_{30}H_{43}O_2$ Br, requires Br, 15·0 per cent.)

Further bromination gave the same product

Formation of 5-stearyl-3-keto-α-naphtha coumaranone —The solution of the bromo product (1 gm) in caustic soda (10%, 60 c c) was heated for three hours On acidifying, 5-stearyl-3-keto-α-naphtha-coumaranone, m p 66–67° C , depressed to 51–52° C by the original compound, was obtained (Found: C, 80 1; H, 9 3; $C_{30}H_{42}O_3$ requires C, 79 9; H, 9 4 per cent)

Nitration of 2-acetyl-4-stearyl-1-naphthol —The ketone (1 13 gm.) was nitrated with fuming nitric acid (0 1 c c , d. = 1 5) in acetic acid (45 c.c) and yellow, shining needles m p. 160° C separated out. This was found to be 4-nitro-2-acetyl-1-naphthol by comparison with an authentic sample The clear acetic acid solution, on dilution with water gave a solid which crystallised from alcohol in shining needles, m p 175–76° C , undepressed by the authentic sample, of 2-nitro-4-stearyl-1-naphthol Nitration of the ketone with excess of nitric acid gave 4-nitro-2-acetyl-1-naphthol.

Action of acetic acid and propionic acid on 2-acetyl-4-stearyl-1-naphthol in the presence of anhydrous zinc chloride —The ketone (1 gm) was added to the solution of zinc chloride (2 gm) in acetic acid (100 c c) and heated for three hours The product obtained was 2-acetyl-1-naphthol as identified with an authentic specimen Similar reaction with propionic acid gave 2-acetyl-1-naphthol

2-Acetyl-4-palmityl-1-naphthol was prepared from 2-acetyl-1-naphthol (12 gm), zinc chloride (9 gm) and palmityl chloride (18 gm) in nitrobenzene solution (60 c c). It was crystallised from alcohol in white flakes, m p 95–96° C (yield 77%) (Found: C, 79·1; H, 9 6; $C_{28}H_{46}O_3$ requires C, 79·2; H, 9·3 per cent.)

p-*Nitrophenyl-hydrazone* of this ketone gave red, shining flakes, m p. 255–56° C. (Found N, 7 6, $C_{34}H_{45}O_4N_3$ requires N, 7 5 per cent)

The *Kostanecki Reaction* of the ketone using acetic anhydride gave 2-methyl-3-acetyl-6-palmityl-1 4-α-Naphthapyrone which crystallised from alcohol in white, small plates, m p 75–76° C (Found C, 78 5, H, 8 7, $C_{33}H_{48}O_4$ requires C, 78 3, H, 8 6 per cent)

The pyrone regenerated the original ketone on alkaline hydrolysis

2-*Ethyl-4-palmityl-1-naphthol* was obtained by the Clemmenson reduction of the ketone or by the condensation of 2-ethyl-1-naphthol with palmityl chloride It crystallised from alcohol in small, shining flakes, m p 74–75° C (Found C, 81 7, H, 10 4, $C_{28}H_{48}O_2$ requires C, 81 9; H, 10 3 per cent)

The p-*nitrophenylhydrazone* crystallised from alcohol in red lustrous flakes, m p 135-36° C (Found· N, 7 6, $C_{34}H_{47}O_3N_3$ requires N, 7 7 per cent)

The nitration of the ketone gave mainly 4-nitro-2-acetyl-1-naphthol together with a small quantity of 2-nitro-4-palmityl-1-naphthol

2-*Bromacetyl-4-palmityl-1-naphthol* obtained by brominating the ketone with one mol or excess of bromine crystallised from alcohol in small, flat needles, m p 67° (Found Br, 15 8, $C_{28}H_{39}O_3$ Br, requires Br, 15 9 per cent)

5-*Palmityl-3-keto-α-naphtha-coumaranone* obtained by heating with alkali solution, crystallised from alcohol in small flakes, m p 58–59° depressed to 44–45° by the original bromo-compound (Found: C, 79 3; H, 9 2 $C_{28}H_{38}O_3$ requires C, 79 5, H, 9 1 per cent)

2-*Acetyl-4-lauryl-1-naphthol* prepared in the usual manner using lauryl chloride crystallised from alcohol in white, lustrous flakes, m p 60–61° C. (yield = 70 per cent.) (Found C, 78 1; H, 8–6 $C_{24}H_{32}O_2$ requires C, 78 2; H, 8 7 per cent)

Its alcoholic solution did not give any coloration with ferric chloride.

The p-*nitrophenylhydrazone* crystallised from alcohol in yellowish red flakes, m p 195–96° (Found: N, 8 1; $C_{30}H_{37}O_4N_3$ requires N, 8 3 per cent)

2-*Methyl-3-acetyl-6-lauryl-1·4-α-naphthapyrone* crystallised from alcohol in lustrous flakes, m p 56–57° depressed to 42°–43° by the original ketone. The alkaline hydrolysis gave back the original ketone. (Found: C, 80·4; H, 8·1. $C_{26}H_{34}O_4$ requires C, 80·3; H, 8·2 per cent.)

2-Ethyl-4-lauryl-1-naphthol obtained by the Clemmenson reduction of the ketone or by condensing 2-ethyl-1-naphthol with lauryl chloride crystallised from alcohol in lustrous plates, m p 53–54° depressed to 39–40° by the original ketone (Found C, 81 3; H, 9 7. $C_{24}H_{34}O_2$ requires C, 81 3; H, 9 6 per cent)

The p-*nitrophenyl-hydrazone of the above compound* crystallised from alcohol in red, lustrous flakes, m p 120–21° (Found N, 8 7 $C_{30}H_{49}O_2N_3$ requires N, 8 6 per cetnt)

Bromination of the ketone gave only 2-brom-acetyl-4-lauryl-1-naphthol, white flakes from alcohol, m p 56–57° C (Found: Br, 17 9; $C_{24}H_{31}O_2$ Br, requires Br, 17 8 per cent)

The bromo-product on alkali treatment gave 5-lauryl-3-keto-α-naptha cumaranone, white plates from alcohol, m p 50–51° C (Found. C, 78 7; H, 8 1 $C_{24}H_{30}O_2$ requires C, 78 6, H, 8 2 per cent)

On nitration, 2-acetyl-4-lauryl-1-naphthol gave 4-nitro-2-acetyl-1-naphthol and 2-nitro-4-lauryl-1-naphthol with one mol of nitric acid

Condensation of methyl-1-hydroxy-2-naphthoate with stearyl chloride—Preparation of 4-stearyl-1-naphthol

A mixture of the naphthoic ester (10·5 gm), anhydrous powdered zinc chloride (7 gm) and stearyl chloride (15 gm.) in nitrobenzene (60 c c) was kept for 48 hours and then decomposed with hydrochloric acid. The nitrobenzene was steam-distilled and the product was treated with 10% alkali which gave alkali-soluble and alkali insoluble compounds. The alkali insoluble product was proved to be 2-stearyl-1-naphthol (yield 40%).

Methyl-4-stearyl-1-hydroxy-2-naphthoate, the alkali-soluble product was crystallised from alcohol in white shining needles, m.p 205–06° C. (yield = 42%) (Found C, 76·7; H, 9·3 $C_{30}H_{44}O_4$ requires C, 76 9; H, 9 4 per cent.)

4-Stearyl-1-hydroxy-2-naphthoic acid—The above ester was heated with 10% alkali for four hours. The alkali solution was neutralised, and the product after purifying crystallised from alcohol in white, shining flat needles, m p 230–31° C. (yield 90%) (Found: C, 76·7, H, 9 3. $C_{28}H_{44}O_4$ requires C, 76 9; H, 9·4 per cent.)

4-Stearyl-1-naphthol—The above acid was heated in an oil-bath at 240° C. for four hours. The brown product obtained was purified through alkali and crystallised from alcohol in colourless shining needles, m.p. 160–61° C (yield 25%). (Found. C, 81 8; H, 10·2. $C_{28}H_{42}O_2$ requires C, 81·9; H, 10 2 per cent.)

Preparation of 4-palmityl-1-naphthol—A mixture of the naphthoic ester (7 5 gm.), anhydrous zinc chloride (5 gm) and palmityl chloride (10·5 gm) in nitrobenzene (60 c c) was kept for 48 hours and steam-distilled, after decomposing the product with hydrochloric acid The product on treatment with alkali gave alkali-insoluble and alkali-soluble compounds The former was 2-palmityl-1-naphthol (yield 45%) while the latter was methyl-4-palmityl-1-hydroxy-2-naphthoate which crystallised in small plates, m p 209–10° C (yield 40%) Found C, 76 1, H, 9 2, $C_{29}H_{40}O_4$ requires C, 76 4, H, 9 1 per cent)

The naphthoic ester was hydrolysed with alkali to *4-palmityl-1-hydroxy-2-naphthoic* acid which crystallised from alcohol in small flakes, m p 240–41° C (Found C, 76 2, H, 9 0 $C_{27}H_{38}O_4$ requires C, 76 0, H, 8 9 per cent)

This on decarboxylation at 250° C gave 4-palmityl-1-naphthol crystallising from alcohol in small flakes, m p 180–81° C (yield 20%) (Found C, 81 5; H, 9 7, $C_{26}H_{38}O_2$ requires C, 81 7, H, 9 9 per cent)

Preparation of 4-lauryl-1-naphthol—A mixture of the naphthoic ester (7 5 gm), zinc chloride (5 gm) an lauryl chloride (9 gm) in nitrobenzene (60 c c) was treated as before and gave alkali-insoluble 2-lauryl-1-naphthol (yield 45%) and alkali-soluble methyl-1-hydroxy-4-lauryl-2-naphthoate (yield 38%) This crystallised from alcohol in white lustrous needles, m p. 190–91° C (Found: C, 74 7, H, 8 5 $C_{24}H_{32}O_4$ requires C, 75·0, H, 8 3 per cent)

When hydrolysed with alkali, this ester gave *4-lauryl-1-hydroxy-2-naphthoic acid* which crystallised from alcohol in small, white needles, m p 209–10° C. (Found C, 74 3, H, 8 2, $C_{23}H_{30}O_4$ requires C, 74 6; H, 8 1 per cent)

4-Lauryl-1-naphthol obtained by decarboxylating the above compound at 220° C , crystallised from alcohol in white, lustrous flakes, m p 146–47° C (20% yield) (Found C, 80 8, H, 9 2 $C_{22}H_{30}O_2$ requires C, 80 9, H, 9·2 per cent.)

We take this opportunity of thanking Rev Father A M Coyne, S J, for his kind interest and provision of facilities

Summary

Two methods for the preparation of 4-stearyl, 4-palmityl and 4-lauryl-1-naphthols have been worked out One did not give the desired product but its intermediate compounds have been studied. The other method gave fairly good yields but not quite satisfactory

STUDIES IN THE NAPHTHALENE SERIES

Part XII. The Preparation and Properties of 4-Stearyl-, 4-Palmithyl- and 4-Lauryl-1-naphthols

By R D Desai, F A Sc , and W S Waravdekar

(From the Department of Chemical Technology, and the Chemistry Department, St Xavier's College, Bombay)

Received March 8, 1946

The previous methods described by the authors[1] for the syntheses of 4-stearyl-, 4-palmityl and 4-lauryl-1-naphthols being unsatisfactory in giving the yields of the desired products, we repeated the conditions of condensing stearyl chloride with α-naphthol in presence of anhydrous zinc chloride, and have obtained nearly 30 per cent yield of 4-stearyl-1-naphthol by following the details described in the experimental portion As sufficient amount of this substance was available, we have studied some of its chemical properties in order to compare them with those of 4-acetyl-1-naphthol studied by Akram and Desai [2]

4-Stearyl-1-naphthol can be easily methylated with dimethyl sulphate in presence of alkali It can be smoothly reduced by amalgamated zinc to 4-octadecyl-1-naphthol, unaccompanied by even a trace of the neutral hydroxylic compound which was formed in good quantity in the reduction of 4-acetyl-1-naphthol Bromination and nitration with one, two or three mols of bromine and nitric acid gave respectively 2-bromo-4-stearyl-1-naphthol and 2-nitro-4-stearyl-1-naphthol These reactions are in direct contrast with those of 4-acetyl-1-naphthol which gave side-chain bromination products with excess of bromine, and 2 4-dinitro-1-naphthol with excess of nitric acid due to the displacement of the acetyl group by the nitro radical

4-Stearyl-1-naphthol resembled 4-acetyl-1-naphthol in respect of the Pechmann and Nencki Reactions. Thus the condensation of 4-stearyl-1-naphthol with ethylacetoacetate in presence of concentrated sulphuric acid also gave 4-methyl-1 2-α-naphthapyrone, with the elimination of stearyl group, while on heating the solutions of this substance in glacial acetic and propionic acids in presence of anhydrous zinc chloride, 2-acetyl- and 2-propionyl-1-naphthols were obtained Identical studies were made of 4-palmityl- and 4-lauryl 4-lauryl-1-naphthols and the results were similar to those of 4-stearyl-1-naphthol

EXPERIMENTAL

Condensation of α-naphthol with stearyl chloride and the preparation of 4-stearyl-1-naphthol

A mixture of α-naphthol (15 gm), anhydrous zinc chloride (14 gm) and stearyl chloride (15 gm) in nitrobenzene (80 c c) was kept for 48 hours at the room temperature, heated on water-bath for about 10 minutes and then decomposed by dilute hydrochloric acid in the cold The nitrobenzene was steam-distilled when a brown product was obtained which on treating with 10% alkali gave alkali-soluble and alkali-insoluble products

The alkali-soluble product (yield 30%) crystallised from alcohol in colourless, shining needles, m p 160-61° C, and was identified as 4-stearyl-1-naphthol (*cf* previous paper) Its alcoholic solution gave reddish violet colouration with aqueous ferric chloride (Found C, 81 8, H, 10 2, $C_{28}H_{42}O_2$ requires C, 81 9, H, 10 2 per cent)

The alkali-insoluble product which crystallised from alcohol in small needles, m p 82° C, was identified as 2-stearyl-1-naphthol (yield 40%)

p *Nitrophenylhydrazone* of 4-stearyl-1-naphthol was obtained in yellowish red, short needles, m p 220°-21 C (Found N, 7 8, $C_{34}H_{47}O_3N_3$ requires N, 7 7 per cent)

4-Stearyl-1-methoxy-naphthalene—A mixture of 4-stearyl-1-naphthol (0 5 gm), anhydrous potassium carbonate (1 gm) and dimethyl sulphate (6 c c) in dry acetone (15 c c) was heated on water-bath under reflux per six hours The alkali-insoluble product obtained was crystallised from alcohol in white, shining needles m p 125-26° C undepressed by an authentic specimen prepared from α-naphthyl methyl ether and stearyl chloride by Desai and Waravdekar[1] (Found: C, 81 8, H, 10 2, $C_{29}H_{44}O_2$ requires C, 82·1, H, 10 4 per cent)

Clemmensen Reduction of 4-stearyl-1-naphthol and preparation of 4-octadecyl-1-naphthol—The mixture of the ketone (1 gm), amalgamated zinc (5 gm.) and hydrochloric acid (30 c c) was heated on sand-bath under reflux for six hours The product crystallised from alcohol in white, shining needles m p 240-41° C. Its alcoholic solution did not give any colouration with ferric chloride (Found: C, 84 7, H, 11 2, $C_{28}H_{44}O$ requires C, 84 4, H, 11 1 per cent)

1-Methoxy-4-octadecyl-naphthalene—The reduced product was methylated as before and crystallised from alcohol in white shining needles, m p 202-03° C., undepressed by the authentic specimen prepared by reducing

1-methoxy-4-stearyl-naphthalene. (Found· C, 84 6, H, 11 3, $C_{29}H_{46}O$ requires C, 84·9, H, 11·2 per cent)

2-Bromo-4-stearyl-1-naphthaol—Bromination of 4-stearyl-1-naphthol (3 gm) with bromine (0 4 c c) in acetic acid (40 c c) gave pale-yellow, short needles, m p 180-81° C (Found Br, 16 2, $C_{29}H_{41}O_2$ Br, requires Br, 16 3 per cent)

Further bromination with two and three mols of bromine gave the same product The bromo product was treated with 10% alkali under reflux for four hours without any change

2-Nitro-4-stearyl-1-naphthol—Fuming nitric acid (0 3 c c) in acetic acid (10 c c) was added slowly to the solution of 4-stearyl-1-naphthol (3 3 gm.) in acetic acid (40 c c) The mixture was kept overnight and then poured in water, giving a deep-yellow coloured substance which crystallised from alcohol in fine, yellow needles, m p 175-76° C (Found. N, 3 2; $C_{29}H_{41}O_4N$ requires N, 3 1 per cent) Nitration with two and three mols of fuming nitric acid gave the same product

Condensation of the ketone with ethyl acetoacetate—A mixture of ethyl aceto acetate (1 5 c c) 4-stearyl-1-naphthol (0 5 gm) in sulphuric acid (73% 15 c c) was kept overnight and then poured into water The product obtained crystallised from alcohol in yellowish white small needles, m p 172° C undepressed by the authentic sample of 4-methyl 1 2-α-naphthapyrone prepared from α-naphthol and ethyl aceto acetate

Nencki Reaction with 4-stearyl-1-naphthol using acetic acid and propionic acid—A mixture of zinc chloride (3 gm), 4-stearyl-1-naphthol (0 5 gm) in glacial acetic acid (15 c c) was heated on sand-bath under reflux for three hours and poured into water The solid crystallised from alcohol in needles, m p 100° C , undepressed by 2-acetyl-1-naphthol The experiment repeated with propionic acid gave the compound which crystallised from alcohol in small plates, m p 86° C , undepressed by 2-propionyl-1-naphthol

Preparation of 4-palmityl-1-naphthol

Palmityl chloride (14 gm.) was added to a mixture of α-naphthol (15 gm) zinc chloride (14 gm) and nitrobenzene (80 c c) and the mixture after keeping for 48 hours at the ordinary temperature was heated on water-bath for 10 minutes, decomposed and steam-distilled The product gave alkali-soluble and insoluble compounds. The alkali soluble compound crystallised from alcohol in colourless, shining, small flakes, m.p. 180-81° C. (yield

Its alcoholic solution gave reddish violet colouration with ferric chloride It remained unchanged when treated with concentrated sulphuric acid. (Found C, 81 5, H, 9 7, $C_{26}H_{38}O_2$ requires C, 81 7, H, 9 9 per cent)

The alkali-insoluble product crystallised from alcohol in white shining flakes, m p 84° C, undepressed by the authentic specimen of 2-palmityl-1-naphthol

p-Nitrophenylhydrazone of 4-1-palmityl-naphthol gave reddish, short needles, from alcohol m p 250–251° C (Found N, 8 2, $C_{32}H_{43}O_3N_3$ requires N, 8 1 per cent)

Methylation of 4-palmityl-1-naphthol gave white, shining, small needles, m p 129–30° C The mixed m p with the authentic specimen of 4-palmityl-1-methoxy-naphthalene prepared from α-naphthyl methyl ether and palmityl chloride was unaltered

4-Hexadecyl-1-naphthol—A mixture of 4-palmityl-1-naphthol (1 gm), amalgamated zinc (5 gm) and hydrochloric acid (30 c c) was refluxed for 6 hours The product crystallised from alcohol in white shining plates, m p. 250–51° C (Found C, 84 5, H, 10 5, $C_{26}H_{40}O$ requires C, 84·4, H, 10·9 per cent)

Methylation of 4-hexadecyl-1-naphthol gave 1-methoxy-4-hexadecyl naphthalene which crystallised from alcohol in white, shining, flat needles, m.p 224–25° C undepressed by the authentic specimen prepared by reducing 1-methoxy-4-palmityl-naphthalene, obtained from α-naphthyl methyl ether and palmityl chloride. (Found C, 84–6, H, 11 1 $C_{27}H_{42}O$ requires C, 84 8; H_2, 11·0 per cent)

2-Bromo-4-palmityl-1-naphthol—The ketone (3 gm) was brominated with bromine (0·4 c c) in acetic acid (50 c c) and the product obtained was crystallised from alcohol in yellowish white shining plates, m p 230–31° C It was unaffected by heating with 10% alkali This was the only product obtained with 2 and 3 mols of bromine (Found Br, 17 4; $C_{26}H_{37}O_2$ Br, requires Br, 17 3 per cent)

2-Nitro-4-palmityl-1-naphthol—Nitration of the ketone (3 gm) with fuming nitric acid (0·3 c.c) in glacial acetic acid gave the nitro derivative which crystallised from alcohol in reddish white flat needles, m p 215–16° C. (Found. N, 3·1; $C_{26}H_{37}O_4N$ requires N, 3 3 per cent)

The coumarin condensation of the ketone (0 59) with ethyl acetoacetate (1·5 c.c) in presence of sulphuric acid (73%, 15 c.c) gave 4-methyl-1 : 2-α-naphtha-pyrone identified by the mixed m.p. with an authentic specimen,

The action of acetic acid and propionic acid on 4-palmityl-1-naphthol in presence of zinc chloride gave 2-acetyl- and 2-propionyl-1-naphthols.

Preparation of 4-lauryl-1-naphthol—A mixture of lauryl chloride (12 g.), α-naphthol (15 gm) and zinc chloride (14 gm) in nitrobenzene (80 c c) was kept for 48 hours at the room temperature and heated for 10 minutes on water-bath before decomposing It was then steam-distilled, and the product was treated with alkali to separate the alkali soluble and insoluble components The alkali-soluble compound crystallised from alcohol in white, shining flakes, m p 146–47° C (yield 25%) Its alcoholic solution gave reddish violet colouration with ferric chloride (Found C, 80 8, H, 9 2; $C_{22}H_{30}O_2$ requires C, 80 9, H, 9 2 per cent)

The alkali-insoluble product was identified as 2-lauryl-1-naphthol (yield 40%)

p-*nitrophenylhydroxone* of 4-lauryl-1-naphthol gave deep-red, shining, flat needles, m p 199–200° C (Found N, 9 2, $C_{28}H_{35}O_3N_3$ requires N, 9 1 per cent)

1-*Methoxy-4-lauryl-naphthalene*—The methylation of 4-lauryl-1-naphthol gave the methyl derivative which was identical with one prepared from α-naphthyl methyl ether and lauryl chloride It crystallised from alcohol in white flakes, m p 111–12° C (Found. C, 81 0, H, 9 3 $C_{23}H_{32}O_2$ requires C, 81 2, H, 9 4 per cent)

4-*Dodecyl-1-naphthol*—4-Lauryl-1-naphthol (1 g) was reduced by amalgamated zinc (5 gm) and hydrochloric acid (30 c c) The product crystallised from alcohol in white, shining, small flakes, m p 203–04° C. It did not give any colouration with ferric chloride (Found C, 84 4; H, 10 1, $C_{22}H_{32}O$ requires C, 84 5; H, 10 3 per cent)

1-*Methoxy-4-dodecyl-naphthalene*—The reduced product was methylated with dimethyl sulphate and proved to be identical with one prepared by reducing 1-methoxy-4-lauryl-naphthalene. It crystallised from alcohol in white, lustrous flakes, m p 166° C (Found C, 84 3, H, 10 3. $C_{23}H_{34}O$ requires C, 84 5, H, 10 4 per cent)

2-*Bromo-4-lauryl-1-naphthol*—4-Lauryl-1-naphthol (2 5 gm) was treated with bromine (0 4 c c) in acetic acid (40 c.c) and the product obtained was crystallised from alcohol in yellowish, shining plates, m p 170–71° C. (Found. Br, 19 8, $C_{22}H_{29}O_2Br$, requires Br., 19 7 per cent.)

2-*Nitro-4-lauryl-1-naphthol*—Nitration of the ketone (2·5 gm.) with fuming nitric acid (0 3 c c.) in acetic acid (50 c c.) gave reddish, shining,

small flakes, m.p. 160–61° C (Found. N, 3 7; $C_{32}H_{29}O_4N$ requires N, 3·8 per cent)

The coumarin condensation of the ketone—With ethyl-acetoacetate gave -4-methyl-1 2a-naphthapyrone

Acetic acid and propionic acid—When heated separately with 4-lauryl-1-naphthol in presence of zinc chloride gave 2-acetyl-1-naphthol and 2-propionyl-1-naphthol respectively

We take this opportunity of thanking Rev Father A M Coyne, SJ, for his kind interest and provision of facilities

Summary

4-Stearyl, 4-palmityl, and 4-lauryl-1-naphthols were prepared in fairly good yield by the action of their respective acid chlorides on α-naphthol Their properties have been studied, and compared with those of 4-acetyl-1-naphthol

References

1 Desai and Waravdekar *Pro Ind Acad Sci*, 1941, 13, 39 In press
2. Akram and Desai *Ibid*, 1940, 11, 149

CHEMICAL EXAMINATION OF PLANT INSECTICIDES

Part I Chemical Components of *Derris ferugines*

By N V Subba Rao and T R Seshadri

(From the Departments of Chemistry and Chemical Technology, Andhra University, Waltair)

Received August 5, 1946

There are about 25 species of Derris indigenous to India Of these *D ferruginea* belongs to the same sub-group as *D elliptica* and bears a close resemblance to it[1], careful examination is necessary to distinguish one from the other *D ferruginea* occurs in the tropical zone of the Eastern Himalayas, particularly in Assam

While making a general survey of the rotenone-bearing plants of India, Krishna and Ghose[2] noted that a species of derris from Assam contained 0 74% of rotenone It was first mistaken to be *D elliptica*[2] but later was correctly identified as *D ferruginea*[3] In a subsequent publication[4] these authors reported that the rotenone content of *D ferruginea* varied from 0 74 to 2 4% while the ether extractives ranged from 2 5 to 4 5% and also mentioned that a sample of *D ferruginea* grown by the Silviculturist, Assam, was found to contain as much as 6·1% of ether extractives but no rotenone Thus there appeared to be two varieties of this plant, one of which was rotenone-bearing and the other rotenone-free No detailed chemical investigation of these has been done so far

Before undertaking a detailed examination of the roots of *D ferruginea* and other plant materials, we have found it highly advantageous to carry out the Durham test on cut-sections of the samples Durham himself first adopted this simple procedure to characterise plants as rotenone-bearing or rotenone-free. Later Worsley[5] applied this test for studying the distribution of rotenone in the plant cells During the earlier days of work on derris, rotenone alone was considered to give this test, but subsequently a number of other compounds closely related to rotenone have been found to respond to it. A positive Durham test, therefore, should indicate the presence of rotenoids in the plant It may here be pointed out that rotenoids like tephrosin, isotephrosin and dehydro-rotenone do not exhibit the series of colour changes in this reaction as given by the others According to the generally accepted view, however, the tephrosins do not occur in the plant

as such, but are formed from deguelin by oxidation during the process of extraction [6] Similar may be the case with the dehydro-compounds Hence in testing the plant material directly, absence of the sequence of colours (red to blue or bluish green) in the Durham test may be taken as evidence of the plant being of the non-rotenoid type This is supported by our experience of the detailed chemical investigation of a number of cases The two varieties of *D ferruginea* could be easily distinguished by this simple procedure

D ferruginea is of special interest in India, as it is the only indigenous species of derris so far known to contain a fairly good percentage of rotenone Consequently samples obtained from Assam were subjected to detailed chemical examination For extraction and separation of the components we have used in general the procedure adopted by Goodhue and Haller[7] for the study of the roots of *Tephrosia virginiana* Chloroform is employed for the initial extraction of the root and ether and 5% sodium hydroxide for separation into fractions The use of chloroform instead of ether renders the initial extraction quicker and minimises loss of solvent in the tropics The rotenoid-free variety of *D ferruginea* did not give any crystalline component though the extractives amounted to 6·5% The extracted matter was liquid in consistency and most of it was soluble in petroleum ether

The rotenoid-bearing roots gave 7 3% of extractives as a definite and clean solid of which more than 60% consisted of rotenone The alkali-soluble fraction amounted to 20%, but no crystalline solid could be isolated

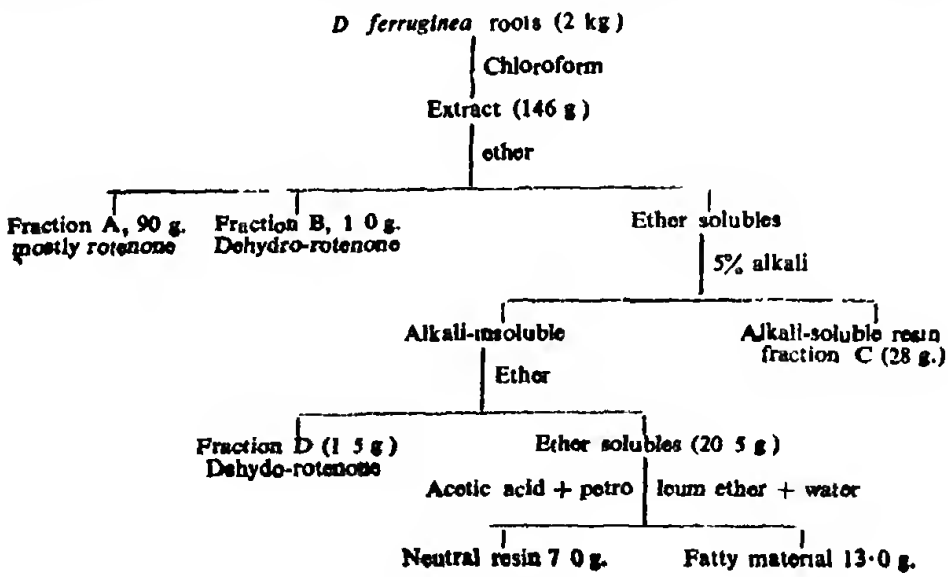

from it. From the alkali-insoluble portion only dehydro-rotenone could be obtained; attempts to get crystalline products from the other fractions by treatment with methyl alcoholic alkali or by dehydrogenation with iodine were not successful The roots appear therefore to contain only rotenone and dehydro-rotenone The scheme of extraction and separation is given above

From the results presented in this paper it appears to be possible to distinguish between *D elliptica* and *D ferruginea* roots from their chemical composition The former yields a considerably higher percentage of extractives generally and whatever may be this percentage, it is reported to contain a constant value of 40% of rotenone[8] On the other hand, *D ferruginea* yields a low percentage of extractives and rotenone amounts to more than 60% of it Again as the alkali-soluble portion *D elliptica* gives usually about 10% of the resin,[9,10] whereas nearly 20% is obtained from *D ferruginea*. Further, the neutral resin, which forms an appreciable amount (30%) of the total resin in the former species, gives deguelin and elliptone From the neutral resin of *D ferruginea* no crystalline component could be isolated. Thus there seem to be marked differences between the resins of the two species, though the differences are not so marked as between *D elliptica* and *D malaccensis*[8,9] This, no doubt, requires confirmation by examining some more samples of *D ferruginea* before it could be conclusive.

Experimental

D ferruginea (*rotenold type*).

Medium-sized roots were obtained from Assam, coarsely powdered and the powder (2 kg) was extracted five times in the cold with chloroform (5 litres each time) The combined extracts were distilled to remove the solvent The solvent-free residue (146 g), obtained as a solid, was treated with ether (350 c c) and the sparingly soluble fraction A (90 g.) was collected. By keeping the ether solution for a few days in an ice-chest, a very small amount of fraction B (1 0 g.) was obtained.

The ether solution was rapidly extracted four times with 50 c c. portions of 5% aqueous potash. The combined alkali extracts were shaken once with ether, acidified and extracted again with ether. The alkali solubles, fraction C (28 g.), were separately examined. On keeping overnight in an ice-chest, the alkali-insoluble ether solution slowly deposited a small quantity of a crystalline material. This solid, D (1·5 g.) was filtered off.

The filtrate was dried over anhydrous sodium sulphate ard after complete removal of ether, the residue was taken up in carbon tetrachloride

(50 c.c.) and kept for a week in the ice-chest with occasional stirring and shaking As no crystalline material separated from this, the solvent was removed under reduced pressure and the residue (20 5 g) taken in a small volume of ether and kept in an ice-chest No crystalline material separated even from the ether solution Therefore ether was removed and the residue was dissolved in glacial acetic acid (50 c c) Petroleum ether (50 c c) was added, followed by 5 c c of water to cause the separation of the layers The acid layer was washed with petroleum ether and the petroleum ether layer with 90 acetic acid so as to effect better separation of the components The petroleum ether layer was finally washed with alkali, evaporated and the fatty material (13 0 g) recovered The neutral resin (7 0 g) was obtained from the acetic acid solution by precipitation with water and extraction with ether This ether solution was rendered free of acetic acid by washing with 5% alkali and then washed with water free of alkali

The neutral resin was treated with dilute methyl alcoholic alkali (50 c c) and boiled for 10 minutes As no crystalline solid separated from this solution, it was acidified and the resin recovered by ether extraction Then it was taken in absolute alcohol (50 c c) and to it was added fused sodium acetate (8 g) The solution was kept gently boiling and to it was added, in small amounts, iodine (3 g) in alcohol (30 c c) After the addition was over, the solution was set aside overnight; but no crystalline material separated.

Fraction A—It formed the major bulk of the extract and was found to respond to the rotenone colour reactions It melted at about 163° and was fractionated using alcohol From 10 g of the material the following two fractions were collected.

	Yield	Melting point	Durham test	Ferric chloride colour
Fraction (i) ..	7 5 g.	163–4°	Red-blue	Nil
Fraction (ii) ..	1 8 g.	160–1°	do.	do

The two fractions were found to be identical with rotenone by mixed melting point determinations with an authentic sample

Fraction B—It had an indefinite melting point and was therefore purified by washing with petroleum ether to remove fatty impurities and then by crystallising from alcohol-chloroform mixture An yellow crystalline solid (needles), melting at 217–8°, was obtained. In the Durham test, with nitric acid it gave red colour but no blue with ammonia It did not give any ferric chloride colouration It was identified as dehydro-rotenone by taking a mixed melting point with dehydro-rotenone obtained by the dehydrogenation of rotenone.

Fraction C.—By treatment with methyl alcohol, it gave only a waxy solid melting at about 85° This solid did not give any colouration with nitric acid or ammonia in the Durham test All attempts to get a crystalline component from this fraction by treatment with various solvents were unsuccessful

Fraction D—This fraction also had an indefinite melting point and therefore was first purified by treatment with petroleum ether Then it was crystallised from alcohol The crystalline product that was sparingly soluble in alcohol was filtered It was yellow in colour (needles) and melted at 217-8°. From its properties it was identified as dehydro-rotenone The alcoholic solution on cooling gave a gelatinous product, which could not be induced to crystallise by keeping in an ice-chest or by treatment with other solvents like acetone Thus no crystalline product other than dehydro-rotenone could be obtained from this fraction

Our thanks are due to Dr S Krishna of the Forest Research Institute, Dehra Dun, for the supply of the root samples

Summary

Detailed chemical examination of the roots of *D ferruginea* has now been carried out Of the two varieties, the rotenone-free one is further characterised by not giving any crystalline component The rotenone-bearing variety yields besides rotenone (4 3%), only a small amount of dehydro-rotenone The chemical chaarcteristics of rotenone-bearing *D ferruginea* and *D elliptica* are compared It seems to be possible to use chemical composition to distinguish one from the other

References

1. Hooker — *Flora of British India*, 2, 243-6.
2. Krishna and Ghose — *Curr Sci*, 1936, 857.
3. ——— — *Ibid*, 1938, 22.
4. ——— — *Indian Forest Leaflet* No 2, 1942.
5. Worsley — *Ann. Appl Biol.*, 1937, 24, 696
6. Takei *et al* — *Ber*, 1933, 66, 1826
   La Forge and Haller — *J.A.C.S*, 1934, 56, 1620.
   Cahn and co-workers — *J. Soc Chem. Ind*, 1938, 57, 200.
7. Goodhue and Haller — *J.A C S*, 1940, 62, 2520
8. Harper — *J C.S.*, 1939, 1099.
9. Buckley — *J. Soc. Chem. Ind.*, 1936, 285 T.

5: 6: 7: 8-HYDROXY-FLAVONOLS

Part IV. A Synthesis of Calycopterin

By T R Seshadri and V Venkateswarlu

(From the Department of Chemistry, Andhra University)

Received May 18, 1946

The synthesis of calycopteretin and of its hexamethyl ether has already been reported[1] The naturally occurring derivative, calycopterin is a partial methyl ether Its constitution (III) has been established by a study of its degradation products and of its dimethyl and diethyl ethers[2, 3]. It has now been synthesised in the following manner 2-Hydroxy-ω·3.4·5:6-pentamethoxy-acetophenone (I) is condensed with the anhydride and potassium salt of *p*-benzoyloxy-benzoic acid according to the method of Allan and Robinson The product is 4'-hydroxy-3 5 6.7 8-pentamethoxy-flavone (II) which when subjected to partial demethylation using hydrobomic acid[2] yields calycopterin (III)

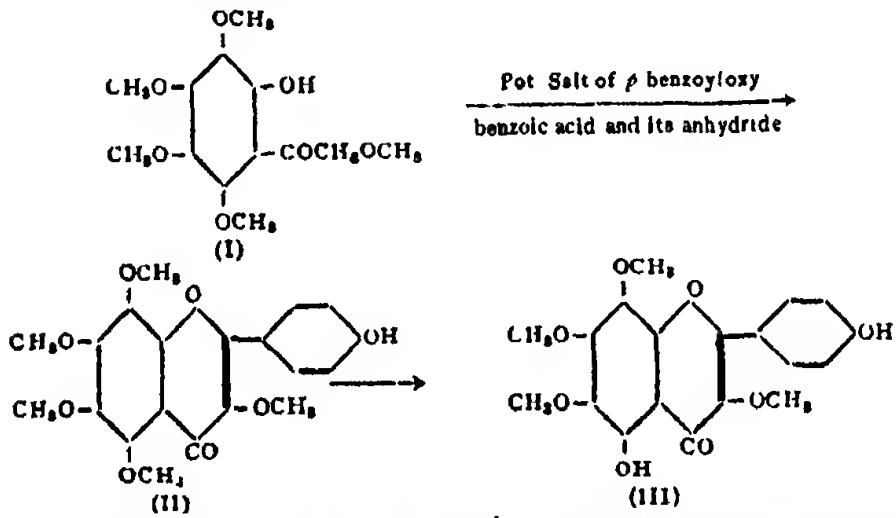

The synthetic and naturally occurring samples are identical in all their properties. The mixed melting point is undepressed While preparing the acetyl derivative for purposes of comparison it is noticed that under milder conditions a mono-acetate could be made Its properties indicate that it has the 5-hydroxyl free and that it is the 4'-acetate of calycopterin.

Experimental

p-Benzoyloxy-benzoic acid.—*p*-Hydroxy-benzoic acid (10·0 g.) was benzoylated using benzoyl chloride (10·0 c c.) and sodium hydroxide

(100 c c ; 10%) according to the Schotten-Baumann method. The solid product was filtered and crystallised from alcohol It appeared as long colourless rectangular plates and prisms and melted at 220-22°

The alkaline filtrate was acidified and the product obtained was filtered and washed with sodium carbonate solution Thus some more benzoyloxy-benzoic acid could be obtained (Found C, 69 5, H, 4 3, $C_{14}H_{10}O_4$ requires C, 69 4, H, 4 1%) The crystalline acid was sparingly soluble in cold dilute sodium hydroxide and sodium carbonate but went into solution on warming

p-Benzoyloxy-benzoic anhydride—Benzoyloxy-benzoic acid (10 g) was treated with dry carbon tetrachloride (10 c c) and finely powdered phosphorus pentachloride (10 5 g) and heated on a water-bath for 10 minutes until the evolution of hydrogen chloride ceased The solvent and phosphorus oxychloride were then distilled off under reduced pressure and the solid product washed with a small volume of dry petroleum ether in the cold When crystallised from carbon tetrachloride the acid chloride was obtained as colourless rectangular plates melting at 147-48°

The acid chloride (10 g) was dissolved in dry ether (200 c c), cooled in ice and pyridine (20 c c) added The mixture was kept at ice temperature for two hours At the end, the reaction mixture was treated with small bits of ice and the solid anhydride that separated filtered off. The ether solution was separated from the aqueous layer, washed successively with cold dilute hydrochloric acid, aqueous sodium carbonate and water, dried over anhydrous sodium sulphate and evaporated The total anhydride (7 g) was purified by crystallisation from dry benzene when it was obtained as colourless rectangular prisms melting at 155-57° (Found· C, 72 5; H, 4 2, $C_{28}H_{18}O_7$ requires C, 72 1; H, 3·9%)

3.5·6:7 8-*Pentamethoxy-4'-hydroxy-flavone* (5-O-*Methyl-calycopterin*)—An intimate mixture of 2-hydroxy-ω. 3. 4. 5. 6-pentamethoxy-acetophenone (0 75 g), the above anhydride (8 g.) and the potassium salt of *p*-benzoyloxy-benzoic acid (3 g) was heated at 175-80° for 3 hours The product was then dissolved in alcohol (75 c c.) and while boiling, a solution of potassium hydroxide (10 g. in 15 c c) added during half-an-hour and the boiling continued for another 20 minutes to decompose the anhydride The alcohol was then removed under reduced pressure and the residue dissolved in water. It was filtered and the filtrate saturated with carbon dioxide. The precipitated flavone was dried and recrystallised several times from dry ethyl acetate when it appeared as pale yellow rectangular prisms melting at 200-202° It was easily soluble in dilute

alkali to give a yellow solution and did not give any colour with alcoholic ferric chloride Yield: 0 4 g (Found C, 61 7, H, 5 4, OCH_3, 39·9; $C_{20}H_{20}O_8$ requires C, 61 9, H, 5 2 and OCH_3, 40·0%)

5, 4'-*Dihydroxy*-3 6 7 8-*tetramethoxy-flavone* (Calycopterin) —This was obtained by the demethylation of the above pentamethoxy-4'-hydroxy-flavone according to the method of Shah, Virkar and Venkataraman[2] using hydrobromic acid (50%) in acetic acid The product was purified by crystallisation from ethyl acetate when it came out as bright yellow rectangular plates melting at 226-28° It gave a green colour with alcoholic ferric chloride A mixture of it with the natural sample of calycopterin showed no depression in melting point (Found C, 61 3, H, 4 8; OCH_3, 33 4, $C_{18}H_{18}O_8$ requires C, 61 0, H, 4 8 and OCH_3, 33 2%)

The *diacetate* was prepared by boiling with acetic anhydride and six drops of pyridine, it crystallised from alcohol as colourless long needles melting at 131-32° The mixed melting point with the acetate of calycopterin from natural sources was undepressed

Mono-acetate of Calycopterin —When the synthetic or natural sample of calycopterin was boiled with acetic anhydride alone or with the addition of only a drop or two of pyridine, the monoacetate melting at 120-22° was produced It was pale yellow in colour and crystallised from alcohol in the form of rectangular plates It dissolved easily in dilute aqueous sodium hydroxide to form a yellow solution and gave a green colour with ferric chloride These reactions indicated that the free hydroxyl was in the 5-position (Found. C, 60 5, H, 5 2, $C_{21}H_{20}O_8$ requires C, 60 6 and H, 4 8%) It could be converted into the diacetate by further heating with acetic anhydride and 6-8 drops of pyridine

Summary

By the condensation of 2-hydroxy-ω 3·4·5 6-pentamethoxy-acetophenone with the anhydride and potassium salt of *p*-benzoyloxy-benzoic acid is obtained 4'-hydroxy-3 : 5·6 : 7 8-pentamethoxy-flavone which yields calycopterin by partial demethylation using hydrobromic acid

References

1. Seshadri and Venkateswarlu *Proc. Ind. Acad Sci* (A), 1946, **23**, 192
   Murti, Row and Seshadri . *Ibid.*, 1946, **23**, 233
2. Shah, Virkar and Venkataraman *J.I C S*, 1942, **19**, 135
3. Seshadri and Venkateswarlu *Proc. Ind. Acad Sci* (A) 1946, **23**, 209

COLOURING MATTER OF THE FLOWERS OF *HIBISCUS VITIFOLIUS*

By K Visweswara Rao and T. R Seshadri
(From the Department of Chemistry, Andhra University)

Received May 18, 1946

Hibiscus vitifolius is a tall annual herb common in the hotter parts of India up to a height of 3,000 ft It bears prominent flowers the petals of which are sulphur yellow in colour with purple eye spots at the base A preliminary investigation of the flower petals indicated that they are very rich in flavonols possessing high tinctorial properties

Certain interesting points should be noted regarding the extraction of these flowers When the dried flower petals were employed, complete extraction could not be achieved by repeated boiling with alcohol Considerable amount of the colouring matter could be obtained from a subsequent water extract This indicated that the components present are not so easily soluble in alcohol and are more soluble in water Consequently for complete extraction it was found necessary to use dilute alcohol Fresh flowers could be conveniently used for extraction in which case ordinary rectified spirits could be used directly, and the extraction was found to be complete in a much shorter time A good yield of a crystalline glycosidic substance separated out on concentrating the alcoholic extract and allowing it to stand for a few days It was very sparingly soluble in alcohol but could be readily crystallised from hot water It did not give any prominent colours with alkaline buffer solutions, but on hydrolysis it yielded gossypetin and glucose in equimolecular proportions The acetate of this compound could be obtained as a colourless solid but could not be crystallised. In its composition and in all the properties mentioned above the glucoside agreed closely with gossypin first isolated from the flowers of *Gossypium indicum*.[1] The important point should be noted that whereas the cotton flowers give only a poor yield of gossypin[2] and that too not consistently, the flowers of *Hibiscus vitifolius* form a rich source of this new and interesting glucoside of gossypetin Further, even for the preparation of gossypetin for various experimental purposes these flowers may be considered to be very handy and very pure specimens of the flavonol could be readily obtained.

The alcoholic mother-liquors left after the separation of gossypin were satisfactorily worked up by precipitation as the neutral lead salt. This

fraction contained besides gossypin a component sparingly soluble in water and capable of being extracted with ether This was identified as quercetin from its properties and by the preparation of its acetate It is our experience that gossypetin, the predominantly major flavonol component of these flowers, occurs entirely as the glycoside, gossypin, whereas the minor component quercetin seems to occur almost entirely free This constitutes a great advantage since the components can be readily separated, gossypin is very sparingly soluble in organic solvents and more readily soluble in water whereas quercetin exhibits just the opposite solubility characters The association of quercetin with gossypetin in the cotton flowers has been already noted The persistence of this even in *Hibiscus vitifolius* is significant in connection with the biogenesis of the flavonols as suggested in an earlier publication

EXPERIMENTAL

Extraction. First Stage (Gossypin) —

The fresh flowers with the calyx removed (2,000) were extracted twice, refluxing each time with alcohol for 3–4 hours The pigment was completely extracted by this process as was shown by the colourless residue The dark red alcoholic extract was concentrated to recover most of the solvent whereby a highly viscous dark reddish brown concentrate was left behind It was kept in the ice-chest for 3–4 days when a large amount of a yellowish brown solid separated out It was filtered and washed with a little alcohol to remove the darker coloured resinous impurities It was then dissolved in boiling water (200 c c) and the deep red solution filtered through a plug of cotton-wool to remove the waxy matter The filtrate was cooled to the room temperature, treated with an equal volume of ether and kept in the ice-chest for 24 hours The pale yellowish brown crystalline solid that separated out was filtered, washed with a little alcohol and ether and dried, yield, 8 0 g The product was purified by crystallisation from hot water thrice using a little charcoal to remove extraneous colouring matter From the clear brown filtrate gossypin came out as shining yellow crystals which appeared as narrow rectangular plates under the microscope. On heating in a capillary tube it melted with vigorous decomposition at 228–30°

When the dry flowers were used (250 g amounting to roughly 3,000 flowers) they were first moistened with water, left for a few hours and then extracted with alcohol in the above manner. The yield in this case was 10 g ; it is therefore slightly less with dry flowers

Gossypin was readily soluble in water to a golden yellow solution ; it was sparingly soluble in alcohol and pyridine and almost insoluble in ether,

acetone or ethyl acetate. It gave a dark olive green colour with alcoholic ferrric chloride and a brown precipitate separated out soon. In alcoholic solution a bright red precipitate was obtained with lead acetate It dissolved in aqueous alkali to a stable bright yellow solution With alkaline buffer solutions, a yellow solution was obtained which changed to a pale pink during the course of 3 days With *p*-benzoquinone in alcohol it did not produce any reddish brown colour or precipitate even after a long time.

The acetate was prepared by boiling gossypin (0·5 g) with acetic anhydride (5 c c.) and a few drops of pyridine for 2 hours. The white solid that separated out on pouring the reaction mixture into water was filtered and washed. It was readily soluble in alcohol or benzene to a brown solution which did not deposit the acetate on cooling. On precipitation from benzene solution by the addition of petroleum ether it could be obtained as a colourless amorphous solid and all attempts at crystallising it were unsuccessful It melted indefinitely round about 120°

Hydrolysis of the glucoside—Gossypin (1 g.) was hydrolysed by boiling with 7% sulphuric acid (30 c c) for 2 hours Bright golden yellow silky needles of the aglucone separated out during the course of the reaction. The mixture was then cooled, the aglucone filtered and washed and the filtrate preserved for the examination of the sugar The yield of the aglucone was 0 5 g

It was purified by crystallising from a mixture of ethyl acetate and benzene from which it separated out as bright yellow elongated rectangular prisms decomposing at 300–10°. It was sparingly soluble in water but it readily dissolved in alcohol, ether, acetone or ethyl acetate. In alkaline buffer solution (pH, 9 8) it formed a yellow solution which immediately changed to bright emerald green and then to pure blue; this gradually faded and finally a colourless solution was left. In alcoholic solution it gave a dark red precipitate with benzoquinone, an olive brown colour with ferric chloride and a red precipitate with lead acetate. It was identical with gossypetin in all respects.

A small quantity of the aglucone was acetylated with acetic anhydride and pyridine. The acetate was sparingly soluble in alcohol from which it crystallised in the form of rectangular prisms melting at 226–28°. The mixed melting point with an authentic sample of gossypetin hexa-acetate was not depressed.

By methylating the aglucone with dimethyl sulphate and potassium carbonate in anhydrous acetone medium the hexamethyl ether was obtained.

It was best crystallised from ethyl acetate from which it came out as colourless narrow rectangular plates melting at 170–72° The mixed melting point with gossypetin hexamethyl ether was not depressed

The acid filtrate containing the sugar was neutralised with barium carbonate, filtered and the filtrate concentrated to small bulk The syrup was diluted with a little distilled water and filtered The filtrate was treated with an excess of a mixture of phenylhydrazine hydrochloride, sodium acetate and acetic acid On heating for about 30 minutes in a boiling water-bath the osazone separated out as a yellow crystalline solid which had the characteristic crystal appearance of sheaves of needles resembling that of glucosazone When crystallised from dilute alcohol it melted with decomposition at 205°

A quantitative estimation of the products of hydrolysis of gossypin from *Hibiscus vitifolius* yielded gossypetin (monohydrate) 63 3% and glucose 33·4% Similar results were obtained with the gossypin sample from *Gossypium indicum* also

Extraction Second Stage (Gossypin) - -

The original alcoholic filtrate left after gossypin had been removed, was concentrated further in a large basin and the concentrate treated with excess of water and filtered from waxy and resinous impurities An equal volume of ether was added to the filtrate and the mixture kept in the ice-chest for a few days A small quantity of a yellow solid separated out and it was filtered and washed Yield, 1 g Its properties indicated that it was gossypin.

The filtrate was diluted with water and extracted with ether repeatedly On distilling off the ether from the extract a viscous semi-solid residue was obtained It did not crystallise. Keeping it in the ice-chest for a long time and other attempts at crystallisation using various solvents were not successful However, it gave an olive green colour with ferric chloride, a reddish brown precipitate with lead acetate and dissolved in aqueous alkali to a stable yellow solution. It seemed to contain a small amount of quercetin in a very impure condition.

Extraction. Third Stage (Gossypin and Quercetin) —

The mother-liquor left after extraction with ether was treated with excess of an aqueous solution of lead acetate when a good yield of a reddish brown precipitate was obtained. It was filtered, washed repeatedly with hot water and alcohol. The lead salt was suspended in hot water and decomposed by passing hydrogen sulphide The lead sulphide was removed

by filtration and the dark red filtrate was concentrated to small bulk, treated with an equal volume of ether and kept in the ice-chest. A small quantity of a yellow crystalline solid separated out and it was filtered and washed with a little ether It was found to be identical with gossypin. The filtrate was repeatedly extracted with ether and the combined ether extract was distilled to remove the solvent The yellow crystalline solid residue was purified by crystallisation from aqueous alcohol twice It separated out as yellow silky needles decomposing at about 300°. It was sparingly soluble in water but was readily soluble in alcohol, ether or acetone. In alcoholic solution it gave an olive green colour with ferric chloride and a red precipitate with lead acetate It dissolved in aqueous alkali to a yellow solution and the colour was fairly stable. It did not respond to the gossypetone reaction

The compound was acetylated using acetic anhydride and pyridine. The acetate was crystallised from a mixture of absolute alcohol and petroleum-ether from which it came out in the form of flat needles melting at 192-93°. The mixed melting point with an authentic sample of quercetin penta-acetate was not depressed

The filtrate from the neutral lead salt was treated with basic lead acetate. As the precipitate was very small it was not further studied.

Summary

The colouring matter of the flower petals of *Hibiscus vitifolius* consists almost entirely of gossypin along with very small amounts of quercetin. These petals form a very good source of this new and interesting glycoside and eventually of gossypetin also.

Literature References

1 Neelakantam and Seshadri *Proc Ind Acad Sci*, 1936, 4A, 54
2 Rao and Seshadri *Current Sci.*, 1938, 7, 227

THE BITTER PRINCIPLE OF *PHYLLANTHUS NIRURI*

By G V Krishnamurti and T R Seshadri
(*From the Department of Chemistry, Andhra University*)

Received May 18, 1946

During the war there was serious shortage of the cinchona alkaloids owing to the loss of Java and the ever-increasing demand of antimalarials for the fighting forces. Since synthetics were not available for civilians, attention was directed to the use of other plant drugs which had enjoyed reputation for the cure of intermittent fevers *Phyllanthus niruri* is one such. It is also considered to have a wider therapeutic application,[1] for example a decoction of the leaves administered orally cures jaundice The plant is an annual herb found as a weed all over India and all its parts and particularly the leaves are markedly bitter

As early as 1891 it was reported that Ottow[2] isolated the toxic bitter principle of *Phyllanthus niruri* in a crystalline condition, and gave it the name 'phyllanthin' and the formula $C_{29}H_{37}O_6$, but no details were available. Later Peckolt[3] recorded that he could obtain it only in an amorphous form and in a yield of 0 05% From his description of its properties it is clear that it was impure In the course of the work described in this paper successful attempts have been made to isolate phyllanthin in good yield and in a pure condition and study some of its important properties Incidentally some other components of the drug have also been examined and their properties are described.

The dried leaves were employed for the extraction. Cold chloroform or hot ligroin could successfully extract the bitter principle The first solvent was preferable. The concentrated extract contained also large amounts of wax and chlorophyll. The former was mostly left behind when the extract was taken up with a limited amount of alcohol. The alcoholic solution contained all the bitter component and a semi-solid product was obtained on removing the solvent. By treatment with petroleum-ether it could be separated into two fractions. (1) The sparingly soluble fraction was not bitter and it yielded after repeated crystallisation a colourless crystalline solid melting at 129–30°. Since it has considerable resemblance to phyllanthin in its chemical properties it is named hypophyllanthin. Hypophyllanthin and its bromoderivative are both stable to alkali, cold and hot. (2) The more soluble fraction contained the bitter principle along with

considerable amount of chlorophyll Attempts to remove the colouring matter by chromatographic adsorption were not successful Methods of fractional precipitation and crystallisation from solvents gave very poor yields and entailed considerable loss of phyllanthin But separation could finally be achieved by treatment with alcoholic potash and this method is suited for the purification of larger quantities Phyllanthin was thus obtained as a colourless crystalline substance melting at 97–98°. Its taste is extremely bitter and it is toxic to fish and frogs. It contains no nitrogen or halogen, has the approximate molecular formula $C_{21}H_{22}O_7$ and contains methoxyl and methylenedioxy groups Five methoxy groups seem to be present in the molecule It is stable to treatment with alkali and to oxidation with neutral permanganate Demethylation with hydriodic acid was

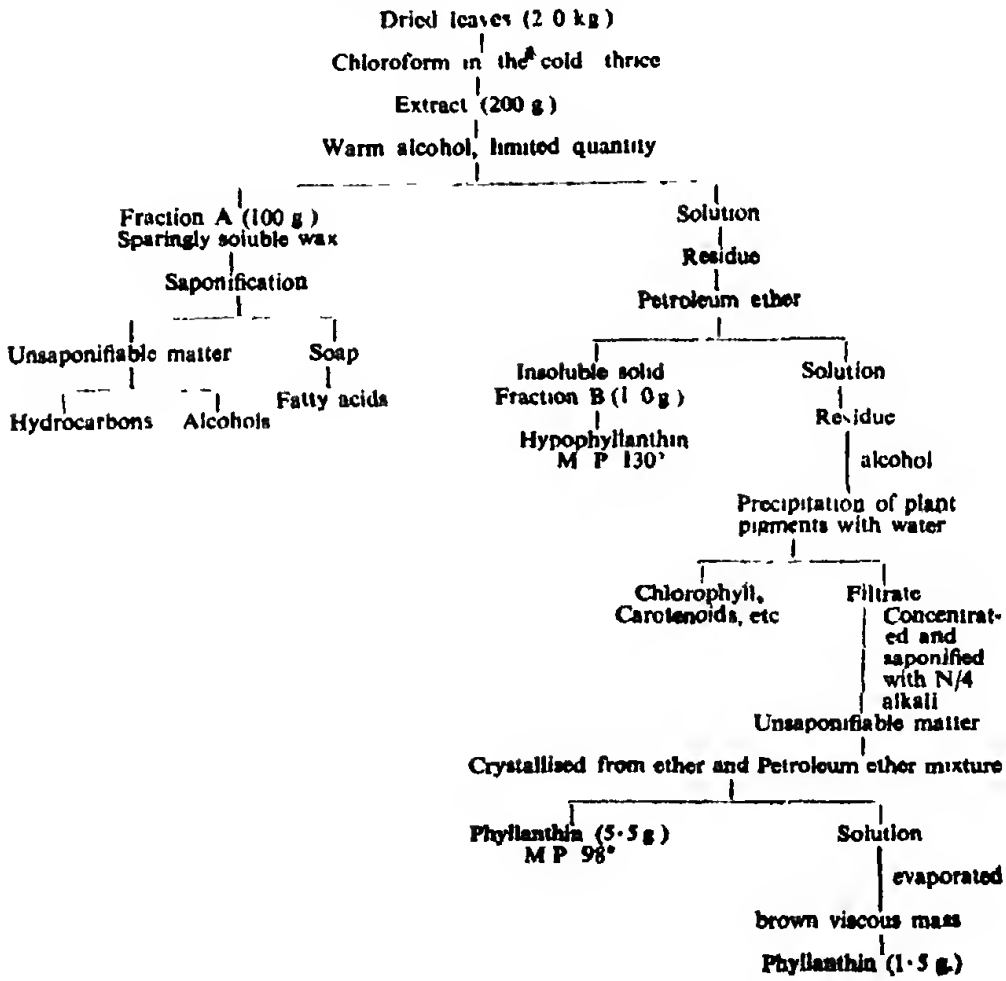

unsuccessful leading to resinous products. By the action of concentrated hydrochloric acid at 125° a phenolic substance was formed But it has not yet been obtained in a pure condition Phyllanthin yields a monobromo derivative which is also stable to alkali The properties of phyllanthin and its composition suggest that it should be aromatic The above diagram explains the stages in the isolation of phyllanthin and hypophyllanthin

EXPERIMENTAL

Fresh leaves were collected from the garden areas of Madras during the wet part of the year 1945, dried in air and powdered. 100 0 grams of the dried leaf powder were successively extracted in a Soxhlet with petroleum ether (80–100°), chloroform, acetone and alcohol using 6 hours of extraction for each solvent Details of the various fractions are given below

Solvent	Yield of extract	Nature of the product
Petroleum ether ..	7%	Dark green solid, waxy in consistency and bitter to taste Mainly chlorophyll and wax along with the bitter principle
Chloroform	3%	Green and waxy Not bitter Mostly chlorophyll and wax along with non bitter materials
Acetone ..	2%	Dark brown and resinous, contained mostly resin
Alcohol	3%	Reddish-brown and astringent to taste Mostly tannin with inorganic material

Isolation of the various fractions —

The dry leaf powder (2 0 kg) was extracted with chloroform thrice in the cold soaking each time for 24 hours. The major bulk of the solvent was recovered by ordinary distillation, the last portions being removed under reduced pressure. The residue (200 0 g) was semi-solid in consistency and dark green in colour with a faint aromatic odour. To separate the wax, the residue was taken up with warm alcohol (500 c c) and allowed to stand in the cold for a day. It was then filtered and the solid waxy matter washed with a little alcohol The filtrate was concentrated to about half the volume when some more of the wax separated. It was collected as before. The combined solid (100·0 g.) was crystallised from benzene-alcohol mixture twice when a colourless crystalline wax melting at 80° was obtained This was marked (A); yield, 88 0 g.

The alcoholic solution was distilled to recover most of the solvent. The last traces were removed under reduced pressure and a dark green waxy solid was obtained. The material was then taken up with petroleum ether

(300 c c) and allowed to stand overnight in the refrigerator when a crystalline material was deposited It was filtered and washed with a little petroleum ether when it became colourless The petroleum ether solution was then concentrated to half its volume when a little more of the same crystalline solid separated out It crystallised from alcohol as shining rectangular plates and prisms melting at 129–30° This fraction (B) is named hypophyllanthin; yield, 1 0 g

The petroleum ether solution was then distilled to recover the solvent The dark green residue was taken up with alcohol and the colouring matter eliminated to a great extent by fractional precipitation with water After filtration the aqueous alcoholic solution was distilled under reduced pressure and the solvent completely removed The green residue was then dried over concentrated sulphuric acid *in vacuo*. It was taken up in ether-petroleum ether mixture (1 10) using the minimum volume and allowed to crystallise when a small quantity of a crystalline solid separated out. This was collected and washed with a little petroleum ether When crystallised again from this solvent it came out as colourless narrow rectangular plates and prisms melting at 97–98°, yield, 0 05 g It was bitter to taste This substance (C) was given the original name, phyllanthin

The mother-liquor was still intensely bitter and crystallisations using various solvents were unsuccessful as the bitter principle had presumably the same solubility as chlorophyll Attempts at the elimination of chlorophyll were made using chromatographic adsorption on anhydrous alumina. Initially a petroleum ether solution was employed and the chromatogram developed with benzene-petrol mixture (1 8) Two coloured zones were formed, a lower orange-yellow layer, the colour being due to carotenoids and an upper greenish layer containing chlorophyll and other substances. The column was washed with the solvent mixture (benzene-petroleum ether, 1 . 6) and the washings collected in stages and examined No substance was found in the colourless solution Even when the orange-yellow zone was washed down there was no bitterness. But it was present in the chlorophyll layer and its extract contained all the bitter principle. Therefore the green extract was distilled and the solvent removed. The residue was dissolved in light petroleum and again subjected to chromatographic adsorption over a bigger column of anhydrous alumina, developed and eluted as before but a separation of chlorophyll and the bitter principle was not possible.

Recourse was then taken to eliminate chlorophyll by subjecting it to treatment with alkali The solid residue containing the bitter principle and chlorophyll was dissolved in alcohol and after adding sufficient potash to make

it 1 4% (N/4), the alcoholic solution was refluxed for half an hour The solvent was then removed and water added, whereby a pale yellow solid separated out. This was collected, washed with water and dried The dried material was crystallised from ether-petroleum ether mixture (1 10) when a white crystalline bitter solid was obtained, identical with the above sample of phyllanthin, yield, 5 5 g When the mother-liquor was evaporated, a brown viscous semi-solid appearing yellow in thin layers was left It was equally bitter On allowing to stand for several days it underwent partial crystallisation It was filtered after thinning with some ether The process was repeated and about 1 5 g more of phyllanthin obtained in a crystalline condition The total yield of phyllanthin was 0 4% of the dry leaves

Fraction A (Wax).—It was a colourless amorphous solid melting at 80°, and had acid No 17 and saponification No 92 It was saponified by boiling with 8% alcoholic potash and benzene The unsaponifiable matter was separated into two fractions by means of cold petroleum ether The less soluble portion after repeated crystallisation from ether-acetone mixture melted at 87°, and formed an acetate which crystallised from alcohol as colourless needles and melted at 72° This fraction agreed with the description of myricyl alcohol which was shown by Chibnal *et al*[4] to be a mixture of the composition 40% C_{30} 40% C_{32} and 20% C_{34} alcohols The fraction more soluble in petroleum ether consisted of a small quantity of paraffin hydrocarbons which after purification by boiling with amyl alcoholic hydrochloric acid and by treatment with concentrated sulphuric acid at 130° melted at 59° (Found: C, 85 0; H, 14 9%) The melting point corresponded to an average chain length[5] of $C_{27\cdot8}$ and hence this fraction should consist mainly of C_{27} hydrocarbon and its near homologues The fatty acid portion melted at 84° after crystallisation from alcohol Its mean molecular weight as determined by titration with N/10 alkali was 408·1 This corresponded to an average chain-length of C_{27} for the mixture and it should consist mainly of C_{26} and C_{28} acids and their near homologues. It could therefore be concluded that the wax consisted mostly of esters (about 85%) of the long-chain fatty acids and alcohols mentioned above, minor quantities of free fatty acids (about 10%) and still smaller quantities of hydrocarbons (about 5%)

Fraction B (Hypophyllanthin).—It was a snow-white solid crystallising as rectangular plates and prisms and melting at 129–30° It was tasteless and soluble in ether, benzene, chloroform and alcohol and insoluble in dilute acid or alkali. It gave no colouration with aqueous or alcoholic ferric

chloride It did not respond to Molisch test for carbohydrates and to Libermann-Burchard reaction for sterols Nitrogen, halogens or sulphur were not present in it No colour was produced when an alcoholic solution of hypophyllanthin was treated with magnesium and hydrochloric acid. It was recovered unchanged after boiling with 7% alcoholic sulphuric acid for 6 hours It did not form any derivative with 2.4-dinitro-phenylhydrazine or semi-carbazide With concentrated sulphuric acid and a little gallic acid it gave an emerald green colour on warming and thus indicated the presence of a methylene-dioxy group [Found: C, 65 6, H, 6 4 and OCH_3, 35 2%; $C_{19}H_{22}O_6$ requires C, 65 9, H, 6 4 and OCH_3(4), 35 8%]

The substance (0 5 g) was boiled under reflux with 25 c c of absolute alcoholic potash (10%) for 7 hours The solvent was later removed and water added when a solid was precipitated It was filtered, washed free of alkali and crystallised from alcohol when it was found to be identical with hypophyllanthin

Bromo-derivative—When treated with bromine under conditions described for phyllanthin, hypophyllanthin yielded a bromo-derivative which crystallises from alcohol as narrow rectangular plates and prisms melting at 112-13°

Substance C (Phyllanthin)—It was a colourless shining solid crystallising in narrow rectangular plates and prisms and melting at 97-98° It had a marked bitter taste; it was soluble in ether, chloroform, benzene and alcohol, sparingly soluble in light petroleum and almost insoluble in dilute acid or alkali No colour was produced on adding to its alcoholic solution ferric chloride or magnesium and hydrochloric acid The substance dissolved in strong sulphuric acid producing an orange-red colour which changed to purple and was not thrown out on dilution It did not contain nitrogen, sulphur or halogen. It did not give the test for sterols with the Libermann-Burchard reagent and for carbohydrates by the Molisch reaction. It was recovered unchanged after boiling with aqueous alcoholic sulphuric acid (7%) for 6 hours No derivative was obtained with either phenylhydrazine or semi-carbazide It was resistent to oxidation with neutral permanganate in acetone or with aqueous permanganate in alkaline medium. Like hypophyllanthin it gave an emerald green colour on warming with concentrated sulphuric acid and a little gallic acid and thus indicated the presence of a methylene-dioxy group. [Found: C, 66 0; H, 5 6; OCH_3, 39 6% and molecular weight, 384 (Rast's micro-method) and 380 (depression of freezing point using benzene); $C_{21}H_{22}O_7$ requires C, 65·4; H, 5·7; OCH_3(5), 40 2% and molecular weight 386]

It was toxic to fish In an aqueous solution containing 50 parts per million fresh water fish, *Haplochilus malarica* (about 1" in length and 1·0 g in weight) showed symptoms of toxicity and lost equilibrium in 10 minutes It was also toxic to frogs Frogs weighing about 35 0 g were employed for the purpose By injecting into each about 0 1 c c of an aqueous alcoholic solution containing phyllanthin sufficient to produce a concentration of 100 parts per million body weight, they showed an apparent difficulty to preserve equilibrium in water and got overturned in 30 minutes Further they turned pale and got depigmented in an hour and they regained the colour only after 20 hours

Bromo-derivative—0 5 g of the substance was dissolved in chloroform (10 c c) and a solution of bromine in chloroform (4%) added little by little till the colour of bromine persisted even after five minutes The reaction was attended with a copious evolution of hydrogen bromide gas After half an hour the chloroform solution was allowed to evaporate in an open porcelain basin at the laboratory temperature The residue was crystallised from alcohol when it came out as narrow rectangular plates and prisms melting at 139–40° (Found Br, 18 1%, $C_{21}H_{21}O_7Br$ requires Br, 17·2%)

0 5 g of phyllanthin was boiled with acetic anhydride (5 c c) and hydriodic acid (5 c c) for 30 minutes The mixture was cooled and aqueous sulphur dioxide added A resinous material was precipitated and it could not be crystallised

Phyllanthin was boiled with absolute alcoholic potash and also with 50% aqueous potash for 6 hours It did not undergo fission and was recovered unchanged

Demethylenation of phyllanthin was attempted as follows 0 5 g of phyllanthin, 1 0 g. of resorcinol and 7 c c of concentrated hydrochloric acid were placed in a sealed tube and heated in a bomb furnace for an hour at 125° The mixture containing some resin and a red coloured liquid was diluted with water and filtered. The insoluble substance was extracted with hot water several times The combined filtrate was extracted with ether and the ether solution evaporated. The residue was taken up in water and treated with a solution of lead acetate and the lead salt filtered It was decomposed with dilute hydrochloric acid and filtered The filtrate was extracted with ether. When the solvent was removed a brown oily substance was obtained. It could not be crystallised. It gave a green colouration with a solution of ferric chloride.

SUMMARY

Phyllanthin, the bitter principle of the leaves of *Phyllanthus niruri* has been isolated in a crystalline condition and in good yield It melts at 97–98°, has the molecular formula $C_{21}H_{22}O_7$ and contains methoxyl and methylene-dioxy groups Its important properties are described A related crystalline substance, hypophyllanthin, which is not bitter, has also been isolated in a small yie'd The leaves contain about 5% of wax which consists mostly of esters

REFFRENCES

1 Kirtikar and Basu *Ind Med Plants*, 1933, 3, 2225
2 Ottow *Jahresber der Pharm*, 1891, 86
3 Peckolt *Ber Pharma Gesell*, 1905, 15, 186
4 Chibnal, *et al* *Biochem J*, 1934, 28, 2197, 2202
5 Piper *et al* *Ibid*, 1931, 25, 2076, 2082
——— *Ibid*, 1934, 28, 2186

CHEMICAL EXAMINATION OF PLANT INSECTICIDES

Part II Chemical Components of *Derris scandens*

By N V Subba Rao and T R Seshadri

(From the Departments of Chemistry and Chemical Technology, Andhra University, Waltair)

Received August 5, 1946

Derris scandens is a climbing shrub occurring in Eastern Himalayas, Bengal, the Central Provinces and Madras Presidency It belongs to the sub-section Brachypterum of the genus *Derris*, to which *D robusta* also belongs. It is distributed also in Ceylon, Siam, Australia and other warmer areas The Ceylonese plant was reported to be of no insecticidal value, as it did not yield any ether extract [1]

Krishna and Ghose,[2] while making a survey of the rotenone-containing plant insecticides of India, examined the roots of *D scandens* obtained from Chanda District (Central Provinces) and reported that they contained no rotenone However, they mentioned that two crystalline substances, one melting at 185° and the other at 225°, were obtained from the ether extract Our attention was drawn to this and as we had isolated from certain *Tephrosia* species compounds having similar melting points, we arranged to procure samples of *D scandens* root from the Chanda District with a view to examine them. Due to war conditions and the shifting of the Andhra University from Waltair, the progress of work was very slow Meanwhile the publication of Clark[3] on 'Scandenin—a constituent of *D scandens*' reached us towards the middle of the year 1944

Clark examined *D. scandens* cultivated in a nursery at St. Petersburg, U S A., primarily to know whether it contained rotenone or not. By exhaustive extraction of the roots with ether, he obtained a mixture of crystalline substances none of which was identical with rotenone [3] The main component was a new compound melting at 231° and having the molecular formula, $C_{28}H_{28}O_6$. It was designated by him 'Scandenin'. A second substance which was also in appreciable amounts and gave little trouble in separation was lonchocarpic acid, previously found in *Lonchocarpus* species by Jones [4] Clark identified it by comparison with an authentic sample of lonchocarpic acid. The sample obtained from *D scandens* sintered between 200° and 205° and melted at 223°. A third substance

melting at 190° was obtained only in small quantities and that too after elaborate purification It was considered to be robustic acid[8] mainly from its behaviour in the Durham test

Though *D scandens* grows in several parts of India, the root samples were obtained from the South Chanda Division of the Central Provinces for the reason already mentioned and a detailed examination was carried out During the earlier part of this investigation, the roots were first exhausted with ether and then with chloroform By concentrating the extracts in stages several fractions were obtained and studied in detail It was easy to get a definite top fraction melting at 228-31° and this seemed to be a definite chemical entity This was designated D S I Other fractions had indefinite melting points, and their behaviour indicated that they were composed of more than one entity In order to obtain information useful for guiding the separation of the individual substances, chromatographic adsorption analysis was done using a small quantity of one of the fractions Alumina was used as the adsorbent and benzene as the solvent. For elution chloroform-benzene mixture was employed and the various fractions were crystallised from benzene or alcohol As a result of this study, it was clear that an individual substance melting at 217-18° was present This was marked D S II Since yields suffered markedly in the adsorption analysis, methods of fractional crystallisation were explored for getting this substance in quantity and they were successful

In later experiments the root powder was directly extracted with chloroform, ether being omitted By this means all the extractives were obtained in one lot (7 0% yield) and the experimental work and loss of solvents minimised. The extract was separated into fractions using first ether and subsequently other solvents Here again it was comparatively easy to separate D S I, melting at 228-31° by virtue of its sparing solubility and its being the main crystalline component of the roots D S II could also be obtained as the result of fractional crystallisation Certain of the fractions consisted of mixtures which were difficult to separate by this procedure. They could, however, be dealt with by means of acetylation and fractional crystallisation of the acetyl derivatives The sharp melting acetates were then hydrolysed. By this means a third compound melting at 196° was isolated and this was marked D.S III. Thus the presence of three crystalline entities in the root could be established.

D S I exhibited a marked tendency to crystallise and came out as colourless stout rectangular prisms and rods. When crystallised from ordinary organic solvents its melting point was only 230-31° but it could be

obtained purer with a higher melting point, 233–34° by conversion into its potassium salt and regeneration. The substance behaved as a weak acid and formed a sparingly soluble potassium salt which readily separated from the potash solution as silky crystals

It was found to be non-rotenoid in character according to the Durham test and it gave no ferric chloride colour, though soluble in alkali It did not reduce Fehling's solution nor did it respond to the magnesium-hydrochloric acid reduction test of flavo es or the colour reactions of resinols and sterols The characteristic blue colour given by the methylene-dioxy group was not obtained when the substance was warmed with gallic acid and concentrated sulphuric acid Thus it could not be placed under any known group of compounds

It had the molecular formula $C_{26}H_{28}O_6$ and formed a diacetate melting at 160–61° On methylation it gave a dimethyl ether melting at 128–29°. By a comparison with the data reported by Clark [3] it could be identified as scandenin

D S II had a crystal structure similar to that of scandenin and was soluble in alkali Further, it did not give any colour with ferric chloride and did not respond to the Durham test Like scandenin it contained one methoxyl; but it definitely differed from scandenin in being more soluble in alcohol, and in not yielding a sparingly soluble potassium salt Its melting point was 217–18° and this was considerably depressed by admixture with scandenin The composition too was different and agreed with the formula, $C_{26}H_{26}O_5$ On acetylation it gave a diacetate melting at 153–54° and on methylation a monomethyl ether melting at 116–17° Its possible identity with lonchocarpic acid was examined in view of the findings of Clark relating to the American sample of *D scandens* For comparison an authentic sample of this acid was obtained from the Bureau of Entomology and Plant Quarantine, Washington, D C Besides the difference noted in Table I, the mixed melting point with lonchocarpic acid was depressed. Though the acetates had the same melting points, the mixture melted lower Thus D S II seemed to be a new substance and was named 'Nallanin' derived from the local name of the plant 'Nalla thiga'.

D S III resembled D S II (nallanin) closely in several properties, but its melting point was lower (202°) and mixed melting points with scandenin and nallanin and also lonchocarpic acid were further lowered Again in view of the suggestion of Clark that robustic acid is probably present in the American sample of *D scandens*, D S III was compared closely with robustic acid obtained in a pure condition from *D robusta*. The two were found to

be different Consequently D.S III is also considered to be a new entity and named 'Chandanin' derived from 'Chanda District' wherefrom the plant material was obtained Chandanin melted at 201–2°, contained three methoxyls and had the molecular formula $C_{29}H_{30}O_7$. It formed a tetra-acetate and a tetramethyl ether, thereby indicating the presence of four phenolic hydroxyl groups It seemed to be extraordinary in several respects. Table I brings out briefly the salient features of the compounds mentioned in the above paras

TABLE I

Substance	Melting point	Molecular formula	Acetate m p	Methyl ether m p	Remarks
Scandenin (D S 1)	233–4°	$C_{26}H_{22}O_6$	160–1°	128–9°	Present data
Do	231°		150°	129°	Clark's data
D S II	217–8°	$C_{26}H_{28}O_5$	153–4°	116–7°	Present data
Lonchocarpic acid	221° (202°)	$C_{28}H_{26}O_6$	153–4°	154–5°	,,
D S III	201–2°	$C_{29}H_{30}O_7$	137–8°	154–5°	,,
Robustic acid	205–6°	$C_{28}H_{30}O_6$	196–7°	193–4°	,,
Do	190°	$C_{27}H_{24}O_6$	—	190°	Harper's data

It is evident from the table that of the three components isolated from the *D scandens* root, scandenin is the only one previously reported in the literature, whereas the other two appear to be new substances Thus these roots do not contain any lonchocarpic acid or robustic acid.

As none of the compounds isolated responded to the rotenoid colour reaction (Durham test), it may safely be concluded that even the Indian sample of *D scandens* does not possess rotenone or allied substances. The chief chemical component is scandenin, as in the case of the American sample, but the yields in the present case are far higher (1 5% compared to 0·5%). Nallanin and chandanin are present only in minor amounts and hence detailed work on these could not be carried out

EXPERIMENTAL

The air-dried thick roots of *D scandens* were made into thin shavings and extracted in two batches of 1,000 g each.

1st batch—It was extracted with ether (7 5 litres) by cold percolation and the extract was concentrated to small volume (300 c c.); during the course of this concentration a crystalline solid began to separate. The mixture was set aside for a few days and the solid, fraction A (10·7 g.) was then filtered off The mother-liquor on concentration to 150 c c. yielded fraction B (3 5 g.). By further concentration fraction C (1 5 g.) was obtained.

The dried marc obtained after ether extraction was extracted in the cold with chloroform The extract, after complete removal of the solvent and addition of ether (50 c c), gave fraction D (1 0 g)

Fraction A —It had a fairly sharp melting point, 225–8°, and was soluble in most of the organic solvents with the exception of ether and petroleum ether, in which it was sparingly soluble It (9 0 g) was crystallised from acetone and the following four fractions were collected fraction (i) 2 5 g , m p 227–8°, (ii) 4 0 g , m p 228–31°, (iii) 1 0 g , m p 225–8°, and (iv) 0 75 g , m p 225–7° All the fractions had the same crystal structure, rectangular prisms and rods, and they seemed to contain only one substance except for the presence of a small impurity in the last fractions The substance melting at 228–31° is henceforward designated as D S I

Fraction B —This had an indefinite melting point, softening at 184° and melting clear at 208° It was boiled with benzene (140 c c) and the sparingly soluble residue (B) collected on a filter This had a melting point of 227° (sintering at 220°), which was undepressed by admixture with the pure product obtained from fraction A

The benzene mother-liquor on cooling deposited a solid (B_2) melting at 185–206° This was crystallised with the samples, having the same melting point range, obtained from the 2nd batch

Fraction C —This also had an indefinite melting point, 165–82° On crystallisation from acetone and removal of the gelatinous impurities that separated in the beginning, a crystalline solid (C_1), m p 205–18°, was obtained The filtrate on concentration yielded a product (C_2), m p 185–206°, identical with B_2. These were put together By further concentration, fraction C_3, m p 165–80° was obtained; this seemed to have the same composition as the original fraction C, m.p. 165–82° It was therefore considered better to apply the technique of chromatography to resolve this mixture A pilot experiment was conducted starting with 170 mg of the substance using alumina as adsorbent and benzene as solvent The development and elution were carried out with chloroform-benzene mixture, the proportion of chloroform being increased in the later elutions The final elution was carried out with alcohol Several fractions were collected and the products were obtained by evaporation of the solvents and final crystallisation from benzene or alcohol The results are tabulated below.

The above results indicated the presence in the mixture of a substance melting above 225°, another melting at 217–18° and possibly a third melting

TABLE II

Fraction No	Solvent		Melting point of the product	Remarks
I	Benzene mother-liquor		Nil	Only development
II & III	Benzene-chloroform	(6 1), 20 c c	,,	
IV & V	,,	(3 1), ,,	,,	
VI	,,	(2 1), ,,	176°	Sintering earlier
VII	,,	(1 3), ,,	217-18°	Mixed m p with D S I depressed (195–220°), seemed to be a single component
VIII	Chloroform	20 c c	187–225°	Appeared to be mixtures of D.S I and fraction VIII
IX	,,	35 ,,	188–220°	
X	,,	40 ,,	,,	
XI	Chloroform ethyl alcohol (1 3),	10 ,,	,,	
XII	Ethyl alcohol	30 ,,	195–215°	

above 180°. This suggested that the fraction C_1 may be an impure form of the substance melting at 217–18° and not of D S I as it was originally considered to be Therefore C_1 was recrystallised from alcohol, when a crystalline substance melting at 214–18° was obtained (mixed melting point with D S I from fraction A was depressed). This is henceforward designated as D S II

Fraction D —This has a melting point range of 210–18° On recrystallisation from acetone, the following fractions were obtained (i) melting at 228–9°, mixed melting point with D S. I undepressed, (ii) melting at 223–9°, undepressed by D S I No other substance was obtained from this fraction.

2nd batch —The second batch was directly extracted with chloroform as this proved to be a better solvent than ether The material was exhaustively extracted with this solvent (7 5 litres) which was recovered by distillation. The last traces of the solvent were removed by evaporation, at the laboratory temperature, in an open basin. The brown, viscous, semi-solid residue (70 g.) was taken in ether (300 c c.) and set aside for a few days. Immediately after the addition of ether, a colourless crystalline solid began to separate The solid (fraction A, 16 5 g) was collected on a filter and washed with a small amount of ether The ether solution on concentration (150 c c.) yielded fraction B (2·4 g) A further fraction C (1·3 g) was obtained by concentrating the mother-liquor.

Fraction A —Though it was uniformly crystalline, it melted at 218–25° and was therefore fractionated from acetone. The following fractions were collected ·

Fraction No	Yield	Melting Point
(i) Acetone ..	8 7 g	227-9°
(ii) ,,	3 7 g.	227-9° (slight sintering earlier)
(iii) ,,	1 5 g	225-7°
(iv) Methyl alcohol + acetone	1 0 g	185-220°
(v) ,,	1 0 g	175-92°

Fraction (i) was crystallised from methyl alcohol-chloroform mixture and the following crops collected by gradual removal of solvents

Crop A 5 2 g, m p 228-31°

Crop B 3 0 g, m p 228-31°

The crops thus obtained were identical with D S I from the 1st batch

Fractions (ii) and (iii) were considered to be slightly impure forms of D S I, as they had melting point ranges above 225°

Fraction (iv) was mixed with fraction B, as it had the same melting point range as the latter

Fraction (v) had nearly the same melting point range as fraction C and therefore was examined along with it

Fraction B—This had a melting point range of 185-218° As attempts to fractionate the mixture by making use of solvents were not successful, it was acetylated with acetic anhydride and sodium acetate The crude acetate obtained was crystallised from acetic acid, when two major fractions were collected. One of them melted at 138-40° and another at 125-30° They were deacetylated with N/2 alcoholic potash, when from the former a product melting at 196-97° and from the latter a product of indefinite melting point, 190-224°, were obtained The second product, which appeared to be a mixture could be resolved into two fractions, the major one melting at about 224°, identical with D S I and the other at 196-97° The results are represented below:

Fraction B m p 185-218°)

Acetylation

Acetate (i) m p 138-40° — Acetate (ii) m p 125-30°

Deacetylation

Product I, m p. 196-97° (D S III) — Product II, m p 190-224°

D.S. I, m.p 224-28° — D.S. III, m.p 196-97°

Fraction C—This also had an indefinite melting point, 170–210° and therefore was first purified by boiling with petroleum ether to remove any fatty matter present Later it was washed with ether, crystallised from alcohol and the following fractions collected. Fraction (i) m p 195–210°, (ii) m p 212–15° and (iii) m p 175–200° Of these only fraction (ii) had a fairly sharp melting point Its mixed melting point with D S II (m p 214–18°) was not depressed

Thus *D scandens* obtained from the Central Provinces yielded three substances D S I, m p 228–31°, D S II, m p 214–18° and D S III, m p about 196° The various fractions collected from the extracts may have the following probable composition

Fraction A· Mostly D S I
" B D S I + D S III
" C D S. II + the other two substances

D S I (*Scandenin*)—It crystallised as colourless rectangular prisms and rods and exhibited a play of colours when viewed at different angles. Attempts to raise the melting point through crystallisation from solvents were not successful It was readily soluble in chloroform, hot acetone and hot alcohol, less soluble in benzene, ether and petroleum ether Though it was insoluble in water, it was found to be soluble in hot aqueous potash from which the sparingly soluble potassium salt readily separated on cooling as silky white crystals On saturating the alkali solution with carbon dioxide the original substance was reprecipitated After recrystallisation with alcohol it now melted at 233–34°

The substance dissolved in concentrated sulphuric acid forming an intense orange-red solution without any visible fluorescence In the Durham test, it did not give the rotenoid colour changes but was found to give an yellow solution with concentrated nitric acid which changed to orange-red on the addition of concentrated ammonia. The substance did not give any definite ferric chloride colouration, only an orange colour being observed Fehling's solution was not reduced by it. It did not respond to either the magnesium-hydrochloric acid test of flavones or the colour reactions of resinols and sterols. When a speck of the substance was treated with gallic acid and concentrated sulphuric acid and gently heated, no blue colour was produced, thereby indicating the absence of methylene-dioxy grouping in the molecule. (Found. C, 71·7; H, 5 9; $-OCH_3$, 7·3; $C_{26}H_{26}O_6$ requires C, 71 8, H, 6 0; $-OCH_3$, 7·2%.)

Diacetate.—D S I (0 2 g) was treated with acetic anhydride (3 c c.) and sodium acetate (0·5 g.) and gently refluxed for 3 hours in an oil-bath

at 140°. It was then poured into cold water, when a colourless crystalline solid began to separate It was filtered, washed with plenty of water and recrystallised from ethyl acetate-petroleum ether (rectangular plates) The acetate melted at 160-61°. (Found C, 69 1, H, 6 0, $C_{30}H_{30}O_8$ requires C, 69·5; H, 5 8%)

Dimethyl ether—The substance (1 0 g) in anhydrous acetone solution (75 c c) was treated with dimethyl sulphate (5 c c) and anhydrous potassium carbonate (12 g) and refluxed on a water-bath for 36 hours Then the solution was filtered from the carbonate, which was washed with sufficient quantity of dry acetone and the combined acetone solution was distilled to remove as much of the solvent as possible Water was added to the residue and the solid product was filtered and air-dried (0 85 g) The methyl ether crystallised from alcohol as long rectangular plates and needles and melted at 128-9° (Found· C, 72 3, H, 6 6; $-OCH_3$, 19 7, $C_{28}H_{30}O_6$ requires C, 72 7, H, 6 5, $-OCH_3$, 20 1%)

D S II (*Nallanin*)—On further crystallisation from alcohol, the melting point became sharper, 217-18° Under the microscope its crystal structure was similar to that of scandenin (rectangular prisms and rods); but the mixed melting point with scandenin was depressed It was compared with the sample of lonchocarpic acid obtained from Dr Jones but was again found to be different as was evidenced by the mixed melting point and also the properties of its derivatives It was more easily soluble in alcohol than scandenin In its solubility in aqueous potash it resembled scandenin, though there was no quick separation of the potassium salt In the Durham test, it also did not give the rotenoid colour changes, the change being from yellow to brick red. With concentrated sulphuric acid it formed an intense red solution without any visible fluorescence. There was no definite phenolic colour reaction with ferric chloride (Found C, 74 6, H, 6 5; $-OCH_3$, 7·8, $C_{26}H_{26}O_5$ requires C, 74 6; H, 6 2, $-OCH_3$, 7 4%)

Diacetate.—On acetylation with acetic anhydride and sodium acetate it gave a diacetate, m p. 153-4°, which crystallised as rectangular rods from ethyl acetate; the mixed m.p. with the acetate of lonchocarpic acid was depressed (Found C, 71·4; H, 6·3; $C_{30}H_{30}O_7$ requires C, 71 7, H, 6 0%)

Monomethyl ether.—The substance was methylated with methyl sulphate and potassium carbonate in anhydrous acetone medium by refluxing for 30 hours. The product crystallised from alcohol as long rectangular prisms and its melting point was 116-17°. (Found: C, 75 2, H, 6 6; $-OCH_3$, 13·8; $C_{27}H_{28}O_5$ requires C, 75 0; H, 6·5; $-OCH_3$, 14 3%)

D.S. III (*Chandanin*).—On repeated crystallisation from alcohol its melting point rose to 201-2°. It resembled D.S. II very closely in all the

colour reactions but its mixed melting points with D S. II and also with lonchocarpic acid were appreciably depressed. (Found C, 71 2, H, 6·2; $-OCH_3$ 18 6, Molecular weight (Rast). 465 $C_{29}H_{30}O_7$ requires C, 71 0; H, 6 1, $-OCH_3$, 19 0% Mol. weight, 490)

In the Durham test, the colour change was from yellow to brick red It was soluble in alkali, though no definite phenolic colouration was obtained with ferric chloride

Tetra-acetate—Chandanin was acetylated with acetic anhydride and sodium acetate and the crude product was crystallised from ethyl acetate-petroleum ether mixture. The acetate melted at 137–38° and appeared under the microscope as rectangular rods (Found. C, 66 9; H, 5·5; $C_{37}H_{38}O_{11}$ requires C, 67 4, H, 5 8%)

Tetra-methyl ether—The methyl ether was prepared as in the case of D S I and D S II It appeared under the microscope as rhombic prisms and melted at 154–55°; the mixed melting point with the methyl ether of lonchocarpic acid was depressed (Found. C, 72 8, H, 6 7, $C_{33}H_{36}O_7$ requires C, 72 5; H. 6 9%)

Our thanks are due to the Forest Officer, South Canada Division of the Central Provinces, for the supp'y of root samples and to Dr Jones for the sample of lonchocarpic acid

Summary

The roots of *Derris scandens* obtained from the Central Provinces of India have now been investigated in detail From the chloroform extractives (7·0%) three crystalline substances could be isolated and characterised. There is no rotenone The major component is scandenin, as in the case of the American sample examined by Clark; but the yield is much higher. The other two substances appear to be new compounds and are therefore named 'Nallanin' and 'Chandanin' Lonchocarpic and robustic acids are not found in the Indian roots

Nallanin has the molecular formula $C_{30}H_{28}O_6$, contains one methoxyl and two hydroxyls, one of which seems to be phenolic and the other alcoholic On the other hand, Chandanin has the molecular formula $C_{29}H_{30}O_7$ possesses three methoxyls and four phenolic hydroxyls; it seems to be rather extraordinary in its characteristics.

References

1 Holland . *Trop Agric*, Ceylon, 1932, 79, 126
2 Krishna and Ghose *Indian Forest Leaflet*, No. 20, 1942.
3 Clark . *J. Org Chem.*, 1943, 8, 489.
4. Jones .. *J.A.C.S.*, 1934, 56, 1247.
5. Harper .. *J.C.S.*, 1942, 181.

CONSTITUTION OF GOSSYPIN—PART I

By K Visweswara Rao and T R Seshadri
(*From the Department of Chemistry, Andhra University, Waltair*)

Received August 5, 1946

Gossypin, a new glucoside of gossypetin, was originally obtained from *Gossypium indicum*[1] A detailed study of this substance could not be carried out earlier owing to lack of material These cotton flowers were variable in composition and did not yield this glucoside in any appreciable amounts in later experiments. A richer and more convenient source has recently been found in the flowers of *Hibiscus vitifolius*[2] and considerable quantities of gossypin have been obtained A detailed study of it has therefore been possible now

Gossypin is markedly soluble in water and much less soluble in anhydrous organic solvents Because of this characteristic, it has not been possible to obtain it entirely free of mineral matter Consequently accurate analytical data could not be obtained, but analysis for carbon and hydrogen and estimation of the products of acid hydrolysis, glucose and gossypetin agreed satisfactorily with a monoglucoside formula for gossypin

Two significant properties which distinguish gossypin from gossypitrin are as follows: (1) it does not give any prominent colours in alkaline buffer solutions; (2) it does not respond to the gossypetone reaction These may indicate that in the linking of the sugar group a hydroxyl in the 5- or 8-position is involved, the latter being more probable In order to locate the position of the glucose group definitely gossypin has been subjected to complete methylation using dimethyl sulphate and potassium carbonate in anhydrous acetone medium. Though the substance is sparingly soluble in this solvent the suspension reacts and complete methylation eventually takes place This is indicated by the fact that the product does not give any colour with aqueous sodium hydroxide or ferric chloride. Hydrolysis of the methylated glucoside yields a monohydroxy compound (A) which yields veratric acid on fission with alcoholic potash This reaction shows that the free hydroxyl group is not in the side phenyl nucleus. Four alternative positions still left for its location are 3-, 5-, 7- and 8-. O-Pentamethyl gossypetins with a hydroxyl in the 5- and the 7-positions (formulæ III and IV) are already[3,4] known The isomeric compound with a free hydroxyl

in the 3-position (V) has now been prepared for purposes of comparison As shown in the table given below these three compounds do not agree with the degradation product of gossypin (A) in properties Mixed melting points have been taken and have been found to be depressed. Hence it should be concluded that compound (A) bears a hydroxyl in the 8-position (formula II) and that gossypin is a 8-mono-glucoside of gossypetin (I)

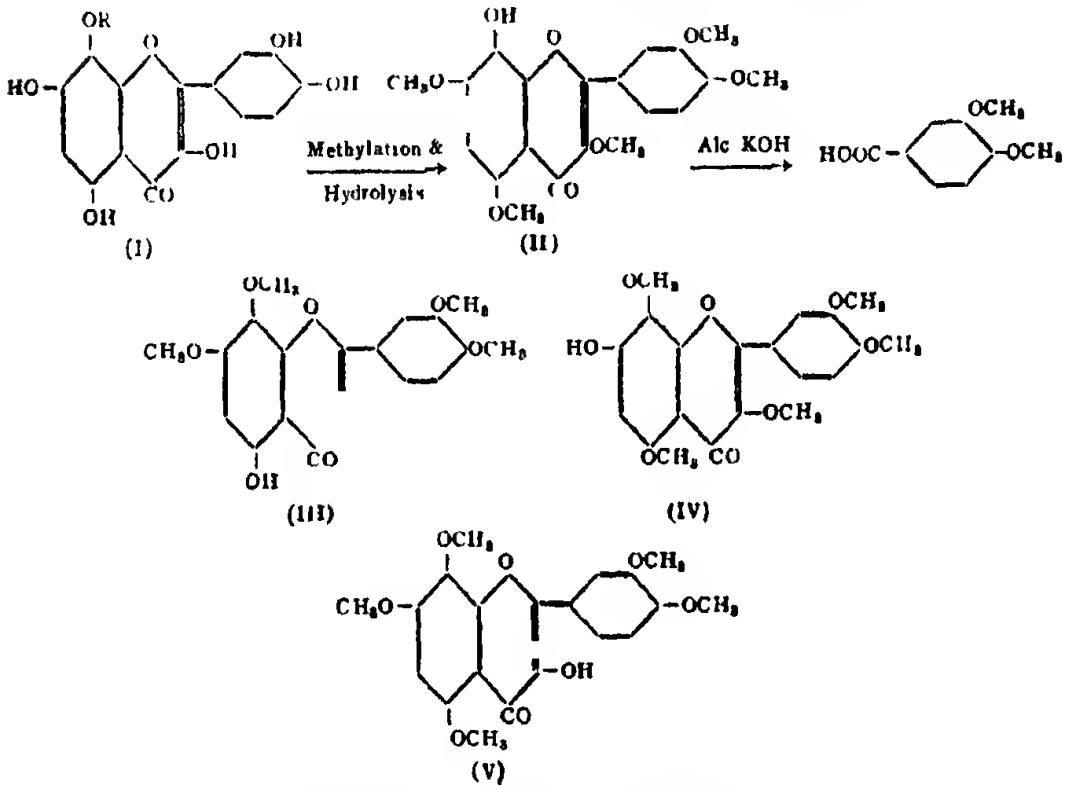

This constitution satisfactorily explains why gossypin does not respond to the gossypetone reaction with *p*-benzoquinone and why it does not exhibit marked colour changes in alkaline buffer solutions. But how the location of the sugar group in the 8-position gives rise to the markedly high solubility of gossypin in water and its marked insolubility in organic solvents is not yet clear.

Of the O-pentamethyl gossypetins required for the above comparison the 7-hydroxy compound (IV) has been obtained according to the method of Baker, Nodzu and Robinson,[6] and the 5-hydroxy compound (III) by the partial methylation of gossypetin in anhydrous acetone solution using dimethyl sulphate and anhydrous potassium carbonate. The 3-hydroxy

Name of the substance	Melting point of the substance	Melting point of the acetate	Ferric chloride colour
5-Hydroxy 3 7 8 3' 4'-pentamethoxy flavone (III)	166-68°	165-66°	Olive green
7 Hydroxy-3 5 8 3' 4' pentamethoxy flavone (IV)	253-55°	167-69°	Nil
8 Hydroxy 5 7 8 3' 4' pentamethoxy flavone (V)	228-30°	207-8°	Violet brown
Degradation product of gossypin (A)	196-98°	214-16°	Brown

compound (V) was synthesized starting from 2-hydroxy-3 4 6-trimethoxy acetophenone (VI) This ketone is best obtained according to the procedure of Baker[5] which involves Friedel and Craft's reaction on 1 2 3 5-tetramethoxy benzene Its constitution is definitely established by its preparation by an alternative method using 2 5-dimethoxy resorcinol[6] It is condensed in alkaline solution with veratric aldehyde and the resulting chalkone (VII) converted subsequently into the flavanone (VIII) and flavonol (V)

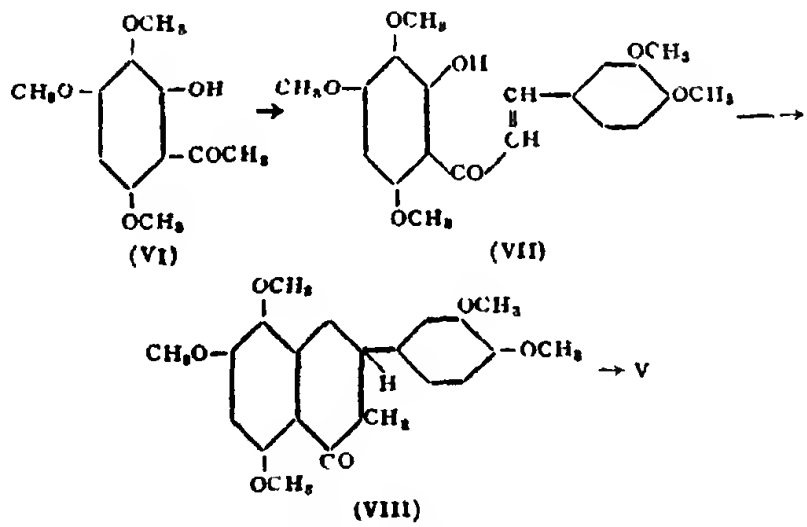

Experimental

The sample of gossypin used for the following experiments was purified by repeated crystallisation from hot water It separated out in the form of bright yellow sheaves of fine needles which melted with vigorous decomposition at 228-30° The results of analysis for carbon and hydrogen reported in an earlier paper[1] agree closely with the requirements of the formula $C_{21}H_{20}O_{12}$ than the more complex formula originally suggested.[1] (Found in air-dried sample C, 46 7, H, 4·5; loss on drying *in vacuo* at

110° for 3 hours, 10 1% $C_{21}H_{20}O_{12}$. $3H_2O$ requires C, 47 2; H, 4 9 and $3H_2O$ loss 10 1%) Quantitative estimation of glucose and gossypetin was already reported [3] This also agrees with the monoglucoside formula. (Found· Gossypetin 63 3, glucose 33 4; $C_{21}H_{20}O_{12}$, $3H_2O$ requires $C_{15}H_{10}O_8$, H_2O, 62 9 and $C_6H_{12}O_6$, 33 9%)

Though the acetyl derivative of gossypin could be obtained only as a colourless powder and could not be crystallised, it gave values for acetyl groups agreeing with the monoglucoside formula (Found $COCH_3$, 44 6%, calculated for 9 acetyl groups in $C_{39}H_{38}O_{22}$, 45 1%) It undergoes hydrolysis on keeping and turns yellow

Methylation of Gossypin—A suspension of finely powdered gossypin (1 g) in anhydrous acetone (200 c c) was treated with freshly distilled dimethyl sulphate (8 c c) and anhydrous potassium carbonate (20 g). After refluxing for 30 hours on a water-bath the potassium salts were filtered off and the residue washed with acetone The filtrate was distilled to recover the solvent When the reddish brown oily residue was treated with excess of ether a light brown amorphous solid separated out which was easily soluble in water, alcohol and acetone but not in ether or benzene The alcoholic solution did not give any colour with alkali or with ferric chloride Attempts to crystallise the methyl ether from various solvents were unsuccessful and it was therefore directly used for hydrolysis

Hydrolysis of Methylated Gossypin—The methylated product (1 g) was refluxed with 7% sulphuric acid (50 c c) for 2 hours The dark red solution was filtered hot through a plug of cotton-wool from a small amount of resinous impurity On diluting with water (200 c c) and cooling in the ice-chest fine silky needles of the hydrolytic product separated out It was filtered and washed free from acid It crystallised from alcohol in the form of pale yellow rectangular plates and prisms melting at 196–98°. (Found: C, 58 9; H, 5 3, methoxyl, 38 0, loss on drying *in vacuo* at 110–20° for 3 hours, 4 1, $C_{20}H_{20}O_8$. H_2O requires C, 59 1; H, 5 4, methoxyl, 38·2 for 5 methoxyl groups and loss on drying, 4 4%) It was easily soluble in alcohol but sparingly in benzene and ethyl acetate In alcoholic solution it gave a brown colour with a drop of ferric chloride and with a few more drops a reddish brown slimy precipitate separated With lead acetate it did not give any precipitate. In aqueous sodium hydroxide it dissolved to a reddish brown solution from which it was reprecipitated on saturation with carbon dioxide.

A small quantity of the above hydroxy compound was acetylated by boiling with acetic anhydride and few drops of pyridine for 2 hours. The

acetate crystallised from alcohol in the form of colourless narrow rectangular plates melting at 215–16° (Found C, 61 0, H, 5 4, $C_{22}H_{22}O_9$ requires C, 61 4; H, 5 1%)

On methylation with dimethyl sulphate and potassium carbonate in anhydrous acetone medium the hydroxy compound yielded the methylated product in the form of colourless narrow rectangular plates melting at 170–72° The mixed melting point with an authentic sample of gossypetin hexamethyl ether was not depressed

Alkaline hydrolysis of O-pentamethyl gossypetin (II)—The pentamethyl gossypetin (1 g) was treated with absolute alcoholic potash (30 c c of 8% solution) and the dark red solution refluxed for 6 hours in a current of hydrogen. The solvent was removed, the residue dissolved in water (30 c c) and the clear solution acidified with concentrated hydrochloric acid The solution was repeatedly extracted with ether and the ether extract shaken with aqueous sodium bicarbonate. On acidifying the bicarbonate extract a crystalline solid separated out It was filtered, washed with a little water and crystallised twice from hot water using animal charcoal when it came out in the form of colourless rectangular prisms melting at 180–82° The mixed melting point with an authentic sample of veratric acid was not depressed

The residual ether extract on evaporation gave a small quantity of a pale yellow solid which gave a greenish colour with ferric chloride. The quantity was too little for successful purification

3:7·8·3′ 4′-*O-Pentamethyl gossypetin (IV)*—The preparation of this has already been described [3] A more convenient procedure for obtaining it is as follows

Gossypetin (0 5 g.) was dissolved in a mixture of anhydrous acetone (20 c c.) and benzene (100 c c) The solution was treated with dimethyl sulphate (0 8 c c.) and potassium carbonate (5 g) and refluxed for 12 hours The potassium salts were removed by filtration and the filtrate evaporated The residual yellow solid was taken up in absolute alcohol, an equal volume of 10% absolute alcoholic potash was added and the mixture cooled in ice. The yellow crystalline solid (potassium salt) was filtered, washed with a little absolute alcohol, dissolved in water and the solution acidified On extracting it with ether and removing the solvent the pentamethyl ether was obtained as a yellow crystalline solid. It crystallised from alcohol in the form of bright yellow narrow rectangular plates melting at 166–67° It was sparingly soluble in aqueous alkali and gave a bright olive green colour with a drop of ferric chloride.

3:4.6·3' 4'-*Pentamethoxy-2-hydroxy-chalkone* (*VII*)—A mixture of veratraldehyde (9 g) and 2-hydroxy-3·4 6-trimethoxy acetophenone (3 g.) was dissolved in alcohol (25 c c) and the solution treated with a strong aqueous solution of potassium hydroxide (25 g. in 20 c c of water) with cooling Sufficient alcohol (100 c c) was then added to get a clear solution and it was left out of contact with air for 3 days The dark red reaction mixture was diluted with water (400 c c) and extracted with ether twice. The alkaline layer, on being acidified, deposited an orange yellow solid which was filtered and washed with water Yield 4 3 g After crystallisation from alcohol it separated in the form of large, orange coloured rectangular plates melting at 143–45° (Found C, 64 0, H, 5 8, $C_{20}H_{22}O_7$ requires C, 64 2, H, 5 9%)

It was readily soluble in alcohol and the alcoholic solution gave a brown colour with ferric chloride In concentrated hydrochloric acid and sulphuric acid it dissolved to form a blood-red solution

5.7 8 3' 4'-*Pentamethoxy-flavanone* (*VIII*)—A solution of the above chalkone (1 g) in aqueous alcohol (25 c c alcohol and 25 c c. water) was treated with concentrated hydrochloric acid (3 c c) After refluxing for 24 hours on a water-bath most of the alcohol was removed under reduced pressure and the residue diluted with water (300 c c) A pale brown turbid solution with some resinous solid resulted It was extracted with boiling benzene (300 c c) in 3 lots. The combined benzene extract was distilled off to recover the solvent and the residue, on the addition of ether, solidified to a light brown solid. It was macerated with dilute aqueous sodium hydroxide to remove the chalkone, filtered and washed. Yield 0·6 g. On crystallisation from ethyl acetate the flavanone separated out in the form of colourless narrow rectangular plates, melting at 172–74°. (Found: C, 63 8, H, 5·6, $C_{20}H_{22}O_7$ requires C, 64 2, H, 5 9%) The flavanone was sparingly soluble in alcohol and benzene and more soluble in ethyl acetate. It was insoluble in aqueous alkali and did not give any colour with ferric chloride. In concentrated mineral acid it dissolved to an orange yellow solution When reduced with magnesium and hydrochloric acid in alcoholic solution a pink colour resulted.

3-*Hydroxy*-5.7 8.3' 4'-*pentamethoxy flavone* (*V*)—A solution of the flavanone (0 5 g.) in alcohol (40 c.c.) was treated at 70–80° with freshly prepared isoamyl nitrite (4 c c) in small portions and concentrated hydrochloric acid (4 c c) (d. 1·19) was then slowly added little by little maintaining the above temperature. After all the acid was added, the flask was closed and left for 3 hours. It was then diluted with water (200 c.c.) and kept in

the ice-chest overnight when a yellow solid separated out. It was filtered, washed and crystallised from ethyl acetate from which it came out as pale yellow flat needles, melting at 228-30° (Found C, 61 8, H, 5 0, $C_{20}H_{20}O_8$ requires C, 61 9, H, 5 2%) It was sparingly soluble in ethyl acetate, alcohol and benzene and aqueous sodium hydroxide In alcoholic solution it gave a greenish brown colour with ferric chloride

On acetylating the compound with acetic anhydride and pyridine the acetate was obtained, it crystallised from alcohol in the form of colourless narrow rectangular plates melting at 207-08° The mixed melting point of this with the acetate of the pentamethyl gossypetin obtained from gossypin was depressed (180-90°) (Found C, 61 2, H, 5 0, $C_{22}H_{22}O_8$ requires C, 61 4, H, 5 1%)

Summary

The analytical data indicate that gossypin is a monoglucoside As a result of complete methylation and hydrolysis it yields an O-pentamethyl gossypetin. From a study of its decomposition with alcoholic potash whereby veratric acid is obtained and from a comparison of its properties with those of isomeric compounds, it is concluded that it has a free hydroxyl in the 8-position Consequently gossypin should be 8-monoglucoside of gossypetin The synthesis of O-pentamethyl gossypetin with a hydroxyl in the 3-position has been described

References

1 Neelakantam and Seshadri *Proc Ind Acad Sci*, A, 1936, **4**, 54
2 Rao and Seshadri *Ibid*, A, 1946, **24** 352
3. ———, Reddy and Seshadri *Ibid*, A, 1940, **12**, 456
4 Baker, Nodzu and Robinson *J C S*, 1929, 74
5 ——— *Ibid*, 1941, 666
6 Sastri and Seshadri *Proc Ind Acad Sci*, A, 1946, **24**, 246

STUDIES IN NAPHTHALENE SERIES

Part XIII The Preparation and Properties of 6-Acy-2-naphthols containing Short and Long Chain Alkyl Groups

By R D Desai and W S Waravdekar

(From the Department of Chemical Technology, and the Chemistry Department, St Xavier's College, Bombay)

Received May 25, 1946

We have already described the synthesis of 1-stearyl-2-naphthol by Nenckis Method in a previous communication [1] With the intention of preparing the acyl-2-naphthols having a free one position, we applied the method of Haworth and Sheldrick[2] to β-naphthol, but the resulting products were obtained in poor yields Condensation of methyl β-naphthyl ether with the requisite acid chloride followed by the demethylation with hydrogen bromide or aluminium chloride gave the desired 6-acyl-2-naphthol, in many cases

After studying the action of acetyl, propionyl, butyryl and benzoyl chlorides on methyl β-naphthyl ether, and converting the resulting methoxy into hydroxy derivatives, we condensed stearyl chloride with the above ether, 6-stearyl-2-methoxy-naphthalene was formed in good yield, but attempts to demethylate it with hydrogen bromide, hydrogen iodide or aluminium chloride led to the ejection of the stearyl group Identical results were obtained with palmityl and lauryl chlorides. However other derivatives of 6-stearyl, 6-palmityl and 6-lauryl-2-methoxy-naphthalenes were studied

Experimental

Condensation of β-naphthyl methyl ether with acetyl chloride by Friedel-Crafts method—Preparation of 2-methoxy-6-acetyl-naphthalene

A mixture of β-naphthyl methyl ether (15 g.), anhydrous zinc chloride (13 g) and acetyl chloride (8 c c) in nitro-benzene solution (70 c c) was kept for 48 hours and decomposed by dilute hydrochloric acid in cold. The nitrobenzene was steam-distilled and the product was purified and crystallised through alcohol in yellowish needles, m p 106–07° C. It was soluble in nearly all the organic solvents and its alcoholic solution did not give any colouration with ferric chloride (yield 70%) (Found: C, 78·1; H, 6·2, calculated for $C_{13}H_{12}O_2$ requires C, 78 0, H, 6 1 per cent.)

The p-*nitrophenylhydrazone* crystallised from alcohol in reddish needles, m p 239–40° C (Found. N, 12·3; $C_{19}H_{17}O_3N_3$ requires N, 12·5 per cent)

Clemmensen Reduction of 2-methoxy-6-acetyl-naphthalene and formation of 2-methoxy-6-ethyl-naphthalene

2-Methoxy-6-acetyl-naphthalene (1 g) was heated with zinc amalgam (5 g) and hydrochloric acid (30 c c) on the sand-bath under reflux for six hours The product obtained was crystallised from alcohol in yellowish needles, m p 50–51° C (Found C, 83 9, H, 7 6, $C_{13}H_{14}O$ requires C, 83 8, H, 7 6 per cent)

Demethylation of 2-methoxy-6-acetyl-naphthalene and preparation of 6-acetyl-2-naphthol

The mixture of hydrobromic acid (15 c c of 48%) 2-methoxy-6-acetyl-naphthalene (5 g) and acetic acid (35 c c) was heated on sand-bath for 6 hours The solution was poured in a large quantity of water and the product obtained was purified through alkali It crystallised from alcohol in yellowish flakes, m p 170–71° C (yield 80%) and was soluble in the usual organic solvents (Found C, 77 2, H, 5 3, $C_{12}H_{10}O_2$ requires C, 77 4; H, 5 4 per cent)

The p-*nitrophenylhydrazone* of 6-acetyl-2-naphthol gave reddish needles from alcohol m p 254–53° C (Found N 13 2, $C_{18}H_{15}O_3N_3$ requires N, 13 1 per cent)

The Clemmensen Reduction of 6-acetyl-2-naphthol gave 6-ethyl-2-naphthol which crystallised from alcohol in white small flakes, m p 93–94° C (Found C, 83 5, H, 7 1, $C_{12}H_{12}O$ requires C, 83 7, H, 7 0 per cent)

Condensation of β-naphthyl methyl ether with propionyl chloride preparation of 2-methoxy-6-propionyl-naphthalene

Propionyl chloride (8 c c), anhydrous zinc chloride (13 g) and β-naphthyl methyl ether (16 g) in nitrobenzene solution (65 c c) were well mixed and kept for 48 hours Nitrobenzene was then steam-distilled and the product formed was crystallised from alcohol in lustrous small plates, m.p. 108–09° C. (Yield 80%) It was slightly soluble in petroleum ether, but very soluble in all other organic solvents (Found C, 78 2, H, 6 4, $C_{14}H_{14}O_2$ requires C, 78 5, H, 6 5 per cent)

The p-*nitrophenyl hydrazone* of 2-methoxy-6-propionyl-naphthalene crystallised from alcohol in reddish, shining needles, m p 210–11° C (Found: N, 11 9; $C_{20}H_{19}O_3N_3$ requires N, 12 0 per cent)

2-Methoxy-6-propyl-naphthalene was obtained from 2-methoxy-6-propionyl-naphthalene (1 g) on heating with amalgamated zinc (5 gm.) and hydrochloric acid (30 c c) for six hours, and crystallised from alcohol in

white, shining plates, m.p 49–50° C (Found: C, 84 2; H, 8 1; $C_{14}H_{18}O$ requires C, 84 0, H, 8·1 per cent)

Demethylation of 2-methoxy-6-propionyl-naphthalene and preparation of 6-propionyl-2-naphthol

By heating the mixture of 2-methoxy-6-propionyl-naphthalene (5 g) and hydrobromic acid (15 c c of 48%) in acetic acid (40 c c) for four hours was obtained a brownish product which was purified through alkali and crystallised from alcohol in yellowish plates, m p 150–51° C (yield 75%) Its alcoholic solution did not give any colouration with ferric chloride. (Found C, 78 1, H, 6 2, $C_{13}H_{13}O_2$ requires C, 78 0, H, 6 0 per cent)

The p-*nitrophenylhydrazone* of 6-propionyl-2-naphthol crystallised from alcohol in deep-red needles, m p 225–26° C (Found N, 12·3, $C_{19}H_{17}N_3O_3$ requires N, 12 5 per cent)

6-*Propyl-2-naphthol*—The mixture of the hydrochloric acid (35 c c), 6-propionyl-2-naphthol (1 g) and amalgamated zinc (5 g) was heated for six hours The product was purified through alkali and crystallised from alcohol in white lustrous needles, m p 120–21° C (Found C, 83 9, H, 7 5, $C_{13}H_{14}O$ requires C, 83 8; H, 7 6 per cent)

Condensation of β-naphthyl methyl ether with butyryl chloride and preparation of 2-methoxy-6-butyryl-naphthalene

Condensation of β-naphthyl methyl ether (15 g.) with butyryl chloride (9 c.c) in presence of anhydrous zinc chloride (13 g.) in nitrobenzene solution (70 c.c) gave 2-methoxy-6-butyryl-naphthalene which crystallised from alcohol in white, lustrous flakes, m p 92–93° C (yield 60%) (Found: C, 78 8, H, 7 1, $C_{15}H_{16}O_2$ requires C, 78 9, H, 7 1 per cent)

The p-*nitrophenyl hydrazone* of 2-methoxy-6-butyryl-naphthalene crystallised from alcohol in reddish-brown plates, m p. 200-01° C. (Found N, 11 5, $C_{21}H_{21}O_3N_3$ requires N, 11 6 per cent)

The Clemmensen Reduction of 2-methoxy-6-butyryl-naphthalene (1 g) with zinc amalgam (5 g.) and hydrochloric acid (35 c.c) gave 2-methoxy-6-butyl-naphthalene which crystallised from alcohol in white, shining flakes, m p 52–53° C. (Found: C, 84 2, H, 8 3, $C_{15}H_{18}O$ requires C, 84·1: H, 8 5 per cent)

The demethylation of 2-methoxy-6-butyryl-naphthalene (5 gm.) *with hydrobromic* acid (10 c c 48%) in glacial acetic acid (40 c c) gave 6-butyryl-2-naphthol which was purified through alkali and crystallised from alcohol in white, shining small needles, m.p. 155–56° C (yield 75%). Its alcoholic

solution did not give any colouration with ferric chloride. (Found: C, 78 4; H, 6·4, $C_{14}H_{14}O_2$ requires C, 78 5; H, 6 6 per cent)

The p-*nitrophenyl hydrazone of 6-butyryl-2-naphthol* crystallised from alcohol in deep-red shining needles m p 215–16° C (Found· N, 12 1; $C_{20}H_{19}O_3N_3$ requires N, 12 0 per cent)

6-Butyl-2-naphthol was obtained by reduction of 6-butyryl-2-naphthol (1 gm.) with zinc amalgam (5 gm) and hydrochloric acid (35 c c) The product was crystallised from alcohol in white shining flakes, m p 97–98° C (Found: C, 84·1; H, 8 3, $C_{14}H_{16}O$ requires C, 84 0, H, 8 1 per cent)

Condensation of β-naphthyl methyl ether with benzoyl chloride and preparation of 2-methoxy-6-benzoyl-naphthalene

The mixture of β-naphthyl ether (15 g), anhydrous zinc chloride (12 g) and benzoyl chloride (14 c c) in nitrobenzene solution (70 c c) was kept for 48 hours and then steam-distilled The product was crystallised from alcohol in yellowish needles, m p 120–21° C (yield 75%) (Found: C, 82·5; H, 5 3, $C_{18}H_{14}O_2$ requires C, 82 4; H, 5 4 per cent)

The p-*nitrophenyl hydrazone* of 2-methoxy-6-benzoyl-naphthalene crystallised from alcohol in reddish, shining flakes, m p 180–81° C. (Found: N, 10·5; $C_{24}H_{19}O_3N_3$ requires N, 10 6 per cent)

2-Methoxy-6-benzyl-naphthalene was prepared by the reaction of 2-methoxy-6- benzoyl-naphthalene (1 g) with zinc amalgam (5 gm.) and hydrochloric acid (35 c c) and crystallised from alcohol in white, shining flakes, m p 81–82° C (Found: C, 87 1; H, 6 3, $C_{18}H_{16}O$ requires C, 87·1; H, 6 5 per cent)

Demethylation of 2-methoxy-6-benzoyl-napthalene (8 g.) was carried out with hydrobromic acid (20 c c) in acetic acid (40 c c) The crude 6-benzoyl-2-naphthol was purified through alkali and crystallised from alcohol in yellowish needles, m p 145–46° C. (yield 80%) It was freely soluble in all organic solvents but less so in petroleum ether. Its alcoholic solution gave no colouration with ferric chloride (Found. C, 82 4, H, 4 8; $C_{17}H_{12}O_2$ requires C, 82·2; H, 4 9 per cent.)

The p-*nitrophenyl hydrazone* of 6-benzoyl-2-naphthol crystallised from alcohol in reddish-brown, small needles, m p 200-01° C (Found: N, 10·9; $C_{23}H_{17}O_3N_3$ requires N, 11 0 per cent)

6-Benzyl-2-naphthol was prepared by reducing 6-benzoyl-2-naphthol (1 g.) with zinc amalgam (5 g) and hydrochloric acid (30 c.c) and

crystallised from alcohol in white, crystalline flakes, m.p. 112–13°C. (Found: C, 87 3; H, 6 2; $C_{17}H_{14}O$ requires C, 87 1; H, 6 0 per cent.)

Condensation of β-naphthyl methyl ether with stearyl chloride and preparation of 2-methoxy-6-stearyl-naphthalene

Stearyl chloride (30 g) in nitrobenzene solution (30 c c.) was slowly added to mixture of nitrobenzene (50 c c), powdered anhydrous zinc chloride (13 g) and β-naphthyl methyl ether (16 g) The mixture was kept for 48 hours at room temperature and decomposed in cold by dilute hydrochloric acid The nitrobenzene was steam-distilled and the solid was crystallised from alcohol in white shining flakes, m p 116–17°C. (yield 75%). It was soluble in usual organic solvents and its alcoholic solution gave no colouration with ferric chloride (Found C, 82 1, H, 10·4; $C_{29}H_{44}O_2$ requires C, 82 0; H, 10 5 per cent)

The p-*nitrophenyl hydrazone* of 2-methoxy-6-stearyl-naphthalene crystallised from alcohol in reddish shining flakes, m p 235–36°C (Found: N, 7 3; $C_{35}H_{49}O_3N_3$ requires N, 7 5 per cent)

Clemmensen reduction of 2-methoxy-6-stearyl-naphthalene and the formation of 2-methoxy-6-octadecyl-naphthalene

A mixture of 2-methoxy 6-stearyl-naphthalene (1 g), zinc amalgam (5 g) and hydrochloric acid (40 c c) was heated on sand-bath under reflux for eight hours The product on crystallisation from alcohol gave white, shining plates, m p 60–61°C (Found: C, 84 6; H, 11 2; $C_{29}H_{48}O$ requires C, 84 8, H, 11 3 per cent)

Demethylation of 2-methoxy-6-stearyl-naphthalene by hydrobromic acid hydroiodic acid and anhydrous aluminium chloride

A solution of-2-methoxy-6 stearyl naphthalene (5 g.) and hydrobromic acid (20 c c of 48%) in glacial acetic acid (40 c.c) was heated on sand-bath for five hours and then poured in water The solid crystallised from alcohol in white, shining plates and was identified as stearic acid by a mixed m.p. 68–69°C On keeping the 2-methoxy-6-stearyl-naphthalene with hydrobromic acid for 48 hours at room temperature with slight warming a mixture of stearic acid and the original substance was obtained Even on keeping the methoxy ketone with hydrobromic acid for 12 hours, the demethylation did not succeed

Demethylation of 2-methoxy-6-stearyl-naphthalene with hydroiodic acid in acetic acid gave only the stearic acid.

Lastly the demethylation was tried with anhydrous aluminium chloride in dry benzene but this also gave the stearic acid

2-Methoxy-6-palmityl-naphthalene the condensation of β-naphthyl methyl ether (16 g) with palmityl chloride (28 g) in presence of zinc chloride (14 g.) in nitrobenzene solution (85 c c) gave 2-methoxy-6-palmityl naphthalene which crystallised from alcohol in white, shining plates, m p 105–06° C (yield 65%) It was soluble in nearly all organic solvents and its alcoholic solution gave no colouration with ferric chloride (Found. C, 81·7, H, 10 1, $C_{27}H_{40}O_2$ requires C, 81 8, H, 10 2 per cent)

The p-*nitrophenyl hydrazone of 2-methoxy-6-palmityl-naphthalene* crystallised from alcohol in reddish, small flakes, m p 225–26° C (Found. N, 7·8; $C_{33}H_{44}O_3N_3$ requires N, 7 9 per cent)

2-Methoxy-6-hexadecyl-naphthalene was prepared by reducing 2-methoxy-6-palmityl naphthalene by zinc amalgam and the product was crystallised from alcohol in white, shining, soft needles, m p 54–55° C (Found C, 84 9; H, 11 0, $C_{27}H_{42}O$ requires C, 84 7, H, 11 1 per cent)

Demethylation of 2-methoxy-6-palmityl naphthalene with HBr, HI or anhydrous aluminium chloride did not succeed but the palmityl group was split off

2-Methoxy-6-lauryl-naphthalene was prepared by condensing lauryl chloride (28 g) in nitrobenzene (35 c c) with β-naphthyl methyl ether (16 g) and zinc chloride (14 g) in nitrobenzene (50 c c) The reaction was kept for 48 hours at room temperature and steam-distilled The solid crystallised from alcohol in white, lustrous flakes, m p 97–98° C (yield 65%) (Found. C, 81 2; H, 9·4, $C_{23}H_{32}O_2$ requires C, 81 1, H, 9 5 per cent)

The p-*nitrophenyl hydrazone* of 2-methoxy-6-lauryl-naphthalene crystallised from hot alcohol in reddish, small plates, m p 220–21° C (Found. N, 8·6; $C_{29}H_{37}O_3N_3$ requires N, 8 8 per cent)

2-Methoxy-6-dodecyl-naphthalene—The Clemmensen reduction of 2-methoxy-6-lauryl-naphthalene with zinc amalgam and hydrochloric acid gave the reduced product which crystallised from alcohol in white shining plates, m.p. 47–48° C (Found C, 84 6; H, 10 4, $C_{23}H_{34}O$ requires C, 84·6; H, 10·5 per cent.)

Demethylation of 2-methoxy-6-lauryl naphthalene with HBr, HI or anhydrous aluminium chloride did not proceed but the lauryl group was split off.

Summary

Some 6-acyl-2-naphthols such as 6-acetyl; 6-propionyl-6-butyryl; and 6-benzoyl-2-naphthols have been prepared by the demethylation 2-methoxy-6-acetyl, 2-methoxy-6-propionyl-; 2-methoxy-6-butyryl and 2-methoxy-6-benzoyl-naphthalenes. In the case of 2-methoxy-6-stearyl-; 2-methoxy-6-palmityl and 2-methoxy-6-lauryl-naphthalenes, an attempt was made to demethylate them to get the hydroxy ketones, but the stearyl, palmityl and lauryl groups were split off The properties of all the methoxy- and hydroxy-ketones have been studied

We have great pleasure in expressing our thanks to Rev Father A M. Coyne, S J., for the provision of the facilities

References

1. Desai and Waravdekar *Proc Acad Ind. Sci*, 1946
2. Haworth and Sheldrick *J*, 1934, 864.

STUDIES IN NAPHTHALENE SERIES

Part XIV. The Preparation and Properties of 2: 4-Distearyl-, 2 4-Dipalmityl- and 2 4-Dilauryl-1-naphthols

By R D Desai and W S Waravdekar

(From the Department of Chemical Technology and the Chemistry Department, St Xavier's College, Bombay)

Received May 25, 1946

The preparation and properties of 2.4-diacetyl-1-naphthol have been described by Akram and Desai [1] The present authors[2] have also studied the behaviour of 2-stearyl- and 4-stearyl-1-naphthols It was thought interesting to study the properties of 2.4-distearyl-, 2 4-dipalmityl- and 2.4-dilauryl-1-naphthols with a view to comparing their properties with those of 2·4-diacetyl-1-naphthol.

2: 4-Distearyl-1-naphthol did not give a colouration with ferric chloride. Neither did it react with bromine under any condition Nitration with excess of fuming nitric acid gave 4-nitro-2-stearyl-1-naphthol When its solution in glacial acetic acid or propionic acid was heated in the presence of anhydrous zinc chloride, only 2-stearyl-1-naphthol was obtained, as the 4-stearyl group was eliminated Vigorous acetylation by Kostanecki's method gave 2-methyl-3-hexadecyl-6-stearyl-1.4-α-naphthapyrone, which, on alkaline hydrolysis, regenerated the original ketone

Akram and Desai (*ibid*) found that 2 4-diacetyl-1-naphthol gave green colouration with ferric chloride, and reacted with bromine giving mono and tribromo derivatives Nitration of this ketone gave mixture of 4-nitro-2-acetyl-1-naphthol and 2: 4-dinitro-1-naphthol With regard to the Nencki and Kostanecki Reactions both the ketones behaved similarly. Thus it was interesting to find the long-chain ketone differing from the short-chain analogue in some of its properties,

2: 4-Palmityl- and 2: 4-dilauryl-1-naphthols which were prepared simulated the behaviour of 2: 4-distearyl-1-naphthol

Experimental

Condensation of 2-stearyl-1-naphthol with stearyl chloride by Friedel-Crafts method—Preparation of 2: 4-distearyl-1-naphthol.

A solution of 2-stearyl-1-naphthol (8 g) in nitrobenzene (50 c.c.) was added to a mixture of stearyl chloride (6 g.) and anhydrous zinc chloride

(4 g.) in nitrobenzene solution (20 c.c) The mixture was kept for 48 hours at room temperature and then decomposed by dilute hydrochloric acid in the cold The solid obtained on steam-distilling nitrobenzene, was purified and crystallised from alcohol in pale-yellow, shining, soft needles, m p 110–11° C (yield 75%) Its alcoholic solution gave no colouration with ferric chloride It was soluble in usual organic solvents but less so in petroleum ether (Found· C, 81·4, H, 11 4, $C_{46}H_{78}O_2$ requires C, 81 6; H, 11·3 per cent.)

The p-*nitrophenyl hydrazone* of 2 4-distearyl-1-naphthol crystallised from alcohol in red, shining, short needles, m p 180–81° C. (Found· N, 5 1; $C_{52}H_{81}N_3O_2$ requires N, 5 2 per cent)

Nitration of 2 4 *distearyl-1-naphthol with excess of fuming nitric acid.*

When the ketone was nitrated with one, two and three moles of fuming nitric acid the original ketone was obtained in all the cases. Therefore, the excess of fuming nitric acid (5 c.c of d. = 1 5) in acetic acid (20 c c) was added to the solution of 2 4 distearyl-1-naphthol (1 g) in acetic acid (30 c.c) The mixture was heated on water-bath for one hour and kept overnight at room temperature On pouring in water a yellowish mass separated out which was crystallised from petroleum ether in pale yellow shining needles, m.p 72° C, undepressed by the authentic sample of 4-nitro-2-stearyl-1-naphthol.

Action of acetic acid and propionic acid on 2. 4-*distearyl-1-naphthol.*

A mixture of glacial acetic acid (15 c c), anhydrous zinc chloride (3 g.) and 2 4-distearyl-1-naphthol (1 g.) was heated on sand-bath under reflux for three hours The product obtained was crystallised from alcohol in white shining small needles, m p. 82° C, undepressed by an authentic specimen of 2-stearyl-1-naphthol and no trace of 2-acetyl-1-naphthol was observed. When the reaction was repeated with propionic acid instead of acetic acid only 2-stearyl-1-naphthol and no trace of 2-propionyl-1-naphthol was obtained.

Kostanecki Reaction of 2: 4-*distearyl-1-naphthol and preparation of* 2-*methyl-*3-*hexadecyl-6-stearyl-*1 : 4-α-*naphthapyrone*

A mixture of 2.4 distearyl-1-naphthol (2 g.), powdered anhydrous sodium acetate (2 g) and acetic anhydride (20 c c.) was heated at 175–80° C. for 12 hours. The solid separated on pouring the mixture in water was crystallised from alcohol in white, lustrous flat needles, m.p. 85–86° C. It dissolved in concentrated sulphuric acid giving a brownish-yellow solution. (Found: C, 82·1; H, 10·8; $C_{46}H_{76}O_2$ requires C, 82·3; H, 10·9 per cent.)

Hydrolysis of the above pyrone with 10% alkali on water-bath for three hours gave the original ketone, m p 110–11° C, undepressed by a pure sample of 2·4 distearyl-1-naphthol

Condensation of 2-palmityl-1-naphthol with palmityl chloride and preparation of 2 4-dipalmityl-1-naphthol

2-Palmityl-1-naphthol (9 0 g) was condensed with palmityl chloride (6·5 g) in presence of zinc chloride (4 g) in nitrobenzene solution (70 c.c). The reaction was kept for 48 hours and then decomposed by hydrochloric acid On steam-distilling nitrobenzene, the solid obtained was purified and crystallised from alcohol in fine yellow lustrous flakes, m p 115–16° C (yield 72 per cent) Its alcoholic solution did not give any colouration with ferric chloride (Found C, 81 4, H, 11 1; $C_{42}H_{68}O_2$ requires C, 81 2; H, 11 0 per cent)

The p-*nitrophenylhydrazone* of 2 4-dipalmityl-1-naphthol crystallised from alcohol in yellowish-red, shining flat needles, m p 188-89° C (Found N, 5·4; $C_{48}H_{73}O_4N_3$ requires N, 5 5 per cent)

Bromination of 2 4-dipalmityl-1-naphthol did not give any bromo-product and the nitration with excess of fuming nitric acid gave 4-nitro-2-palmityl-1-naphthol

The Nencki Reaction with 2.4-dipalmityl-1-naphthol (1 g) using acetic acid (15 c c) or propionic acid gave 2-palmityl-1-naphthol.

Kostanecki Reaction with 2.4-dipalmityl-1-naphthol—Preparation of 2-methyl-3-tetradecyl-6-palmityl-1.4-α-naphthapyrone

A mixture of 2·4-dipalmityl-1-naphthol (2 g), powdered anhydrous sodium acetate (2 g) and acetic anhydride (20 c c) was heated at 175–80° C. for 12 hours The product obtained was crystallised from alcohol in white, shining plates, m p 91–92° C It was soluble in usual organic solvents with sulphuric acid and gave a brownish-yellow coloured solution (Found: C, 81 8; H, 10·7, $C_{44}H_{66}O_3$ requires C, 81 9, H, 10 6 per cent)

The above pyrone was hydrolysed with 10% caustic soda and gave back the original 2.4-distearyl-1-naphthol

2:4-*Dilauryl-1-naphthol.*

The condensation of 2-lauryl-1-naphthol (9 g.) with lauryl chloride (6 g.) in presence of zinc chloride (4 g) in nitrobenzene solution (70 c.c) gave 2:4-dilauryl-1-naphthol which was crystallised from alcohol in fine, white, shining flakes, m.p. 92–93° C. (yield 70%). It was soluble in usual

organic solvents but less soluble in petroleum ether. (Found: C, 80·5; H, 10·2; $C_{34}H_{52}O_2$ requires C, 80·3, H, 10·3 per cent.)

The p-*nitrophenylhydrazone* of 2 4-dilauryl-1-naphthol gave from alcohol yellowish red, shining, flat needles, m p 170–71° C (Found N, 6·3; $C_{40}H_{56}O_4N_2$ requires N, 6 5 per cent.) The nitration of 2·4-dilauryl-1-naphthol with excess of fuming nitric acid gave 4-nitro-2-lauryl-1-naphthol.

The action of acetic and propionic acids on 2.4-dilauryl-1-naphthol in presence of anhydrous zinc chloride gave 2-lauryl-1-naphthol only

Kostanecki Reaction with 2 4-*dilauryl*-1-*naphthol and preparation of* 2-*methyl*-3-*decyl*-6-*lauryl*-1 : 4-*a*-*naphthapyrone*

2 : 4-Dilauryl-1-naphthol (2 g), sodium acetate (2 g) and acetic anhydride (20 c c) were heated at 175–80° C for 12 hours and then poured in water The solid which separated out was crystallised from alcohol in white shining small plates, m p 62–63° C It dissolved in concentrated sulphuric acid giving a pale-brown colour (Found: C, 81·4; H, 9·4; $C_{34}H_{52}O_2$ requires C, 81 2; H, 9 8 per cent)

The pyrone on heating with 10 per cent sodium hydroxide for three hours gave 2 : 4-dilauryl-1-naphthol.

Summary

We have synthesised 2 : 4-distearyl-, 2 : 4-dipalmityl; and 2·4-dilauryl-1-naphthols from 2-stearyl; 2-palmityl; 2-lauryl-1-naphthols and stearyl, palmityl and lauryl chlorides

The properties of these diacetyl ketones have also been studied and compared with those of diacetyl-1-naphthol

We take this opportunity of thanking Rev Father A M. Coyne, S.J., for the provision of facilities.

References

1. Akram and Desai *Proc. Ind. Acad Sci.*, 1940, 11, 154
2. Desai and Waravdekar . *Ibid.*, 1940, 12, 507 . in the press.

T8-48. Printed at The Bangalore Press, Bangalore City, by G Srinivasa Rao, Superintendent, and Published by The Indian Academy of Sciences, Bangalore

ON FLUCTUATIONS OF PRESSURE AND TEMPERATURE IN THE ATMOSPHERE*

By R Ananthakrishnan

Received June 17, 1946

1 Introduction

In dealing with a fluid medium in motion such as the atmosphere, the properties of the medium not only differ from point to point at the same instant, but also undergo variations at the same point in course of time If S is any physical property of the medium which we wish to study, then S is a function of the co-ordinates x, y, z and the time t

$$S = f(x, y, z, t) \tag{1}$$

$$\begin{aligned} \frac{dS}{dt} &= \frac{\partial S}{\partial x} \cdot \frac{dx}{dt} + \frac{\partial S}{\partial y} \frac{dy}{dt} + \frac{\partial S}{\partial z} \frac{dz}{dt} + \frac{\partial S}{\partial t} \\ &= \frac{\partial S}{\partial x} u + \frac{\partial S}{\partial y} v + \frac{\partial S}{\partial z} w + \frac{\partial S}{\partial t} \end{aligned} \tag{2}$$

where u, v, w are the x, y, z components of the velocity of flow at the point under consideration. Or

$$\left(\frac{d}{dt}\right) S = \left(\frac{\partial}{\partial t} + u \frac{\partial}{\partial x} + v \frac{\partial}{\partial y} + w\right.$$

$\frac{dS}{dt}$ is the time rate of change of the property S over a particular element of the medium and is known as the *individual* variation $\frac{\partial S}{\partial t}$ is the time rate of change of the property S at the fixed point in the medium and is known as the *local* variation.

The hydrodynamical equivalent of the principle of conservation of mass is the *equation of continuity* which states that the rate of change of density at a point in the medium is equal to the net excess of inflow of mass over outflow per unit time considered over a small volume element around

* Presented at the Annual Session of the Indian Academy of Sciences, held at Udaipur, in December 1945.

that point, divided by the volume of the element Mathematically this is expressed by the equation·

$$\frac{\partial \rho}{\partial t} + \frac{\partial}{\partial x}(\rho u) + \frac{\partial}{\partial y}(\rho v) + \frac{\partial}{\partial z}(\rho w) = 0. \tag{4}$$

where ρ is the density at the point under consideration. This can also be written as.

$$\frac{\partial \rho}{\partial t} + \rho\left(\frac{\partial u}{\partial x} + \frac{\partial v}{\partial y} + \frac{\partial w}{\partial z}\right) = 0 \tag{4 a}$$

2 Atmospheric Pressure and its Variations

To a very high degree of accuracy, the pressure at a level h in the atmosphere is given by the weight per unit area of the mass of the atmosphere above the level in question

$$p = \int_h^\infty g\,\rho\,dz \tag{5}$$

The *local* variation of pressure at the level h is therefore given by.

$$\frac{\partial p}{\partial t} = \int_h^\infty g\,\frac{\partial \rho}{\partial t}\cdot dz$$

Substituting for $\frac{\partial \rho}{\partial t}$ from (4) we get·

$$\frac{\partial p}{\partial t} = -\int_h^\infty g\left[\frac{\partial}{\partial x}(\rho u) + \frac{\partial}{\partial y}(\rho v) + \frac{\partial}{\partial z}(\rho w)\right] dz$$

$$= -\int_h^\infty g\left[\frac{\partial}{\partial x}(\rho u) + \frac{\partial}{\partial y}(\rho v)\right] dz + g\,(\rho w)_h \tag{6}$$

The integral on the right-hand side represents the rate of transport of mass above the level h due to horizontal motion (advection); the second term represents the rate of change of mass above the level h due to vertical motion At the surface of the earth $w = 0$, so that.

$$\frac{\partial p_0}{\partial t} = -\int_0^\infty g\left[\frac{\partial}{\partial x}(\rho u) + \frac{\partial}{\partial y}(\rho v)\right] dz \tag{7}$$

This equation tells us that a change of surface pressure can only be brought about by horizontal advection of mass above the place of observation On the other hand, equation (6) shows that a change of pressure at

a higher level in the atmosphere can occur even in the absence of horizontal advection of mass in the atmospheric air column under consideration

3 Fluctuations of Temperature in the Atmosphere

(*a*) *General Case*—If we consider an element of air in the atmosphere, the temperature of the element can undergo changes due to two causes, *viz.*, (1) due to direct addition of heat to or removal of heat from the element, and (2) due to external work done on the element or by the element consequent on the changes of atmospheric pressure This is expressed by the well-known First Law of Thermodynamics

$$dQ = dU + dW = c_p\, dT - ART\frac{dp}{p}$$

Hence

$$\frac{dQ}{dt} = c_p\frac{dT}{dt} - \frac{ART}{p}\frac{dp}{dt}$$

Or

$$\frac{dT}{dt} = \frac{1}{c_p}\frac{dQ}{dt} + \frac{AR}{c_p}\frac{T}{p}\frac{dp}{dt} \tag{8}$$

Since we can measure only *local* changes of pressure and temperature in the atmosphere, we transform (8) with the help of (3) and get

$$\begin{aligned}\frac{\partial T}{\partial t} = \frac{1}{c_p}\frac{dQ}{dt} &+ u\left(\frac{AR}{c_p}\frac{T}{p}\frac{\partial p}{\partial x} - \frac{\partial T}{\partial x}\right)\\ &+ v\left(\frac{AR}{c_p}\cdot\frac{T}{p}\frac{\partial p}{\partial y} - \frac{\partial T}{\partial y}\right)\\ &+ w\left(\frac{AR}{c_p}\frac{T}{p}\frac{\partial p}{\partial z} - \frac{\partial T}{\partial z}\right)\\ &+ \frac{AR}{c_p}\frac{T}{p}\frac{\partial p}{\partial t}\end{aligned} \tag{9}$$

Now, if θ is the potential temperature of the element of air, we have

$$\theta = T\left(\frac{P}{p}\right)^{\frac{AR}{c_p}}$$

Hence

$$\frac{d\theta}{\theta} = \frac{dT}{T} - \frac{AR}{c_p}\frac{dp}{p}$$

Or

$$d\theta = \frac{\theta}{T}\left(dT - \frac{AR}{c_p}\cdot\frac{T}{p}\,dp\right)$$

Substituting this relation in (9) we get·

$$\frac{\partial T}{\partial t} = \frac{1}{c_p}\frac{dQ}{dt} - \frac{T}{\theta}\left(u\frac{\partial\theta}{\partial x} + v\frac{\partial\theta}{\partial y} + w\frac{\partial\theta}{\partial z}\right) + \frac{AR}{c_p}\cdot\frac{T}{p}\frac{\partial p}{\partial t} \tag{10}$$

The first term on the right-hand side of (9) or (10) represents the change of temperature resulting from direct addition of heat due to non-adiabatic processes such as radiation, condensation, etc The second and third terms involving u and v represent the changes resulting from horizontal advection in a non-uniform pressure and temperature field The fourth term involving w represents the adiabatic change of temperature due to vertical movements Since $\frac{\partial p}{\partial z} = -g\rho$ and $\frac{Ag}{c_p} = \Gamma$ (dry adiabatic lapse-rate), this term can also be written as $w(\beta - \Gamma)$, where $\beta = -\frac{\partial T}{\partial z}$ (prevailing lapse-rate in the atmosphere) The last term on the right-hand side of (9) and (10) represents the adiabatic heating or cooling effect due to local changes of pressure

(*b*) *Particular Case*—If the processes are strictly adiabatic, then $dQ = 0$, also, if the wind is geostrophic we have·

$$u\frac{\partial p}{\partial x} + v\frac{\partial p}{\partial y} = 0 \tag{11}$$

In this case, equation (9) reduces to

$$\frac{\partial T}{\partial t} = \frac{AR}{c_p}\frac{T}{p}\frac{\partial p}{\partial t} - \left(u\frac{\partial T}{\partial x} + v\frac{\partial T}{\partial y}\right) - w(\Gamma - \beta) \tag{12}$$

Under geostrophic conditions, the relation between horizontal temperature gradient and the variation of wind with height is given by the well-known equations.

$$\left.\begin{aligned} \frac{\partial}{\partial z}\left(\frac{u}{T}\right) &= -\frac{g}{2\omega\sin\phi}\frac{1}{T^2}\frac{\partial T}{\partial y} \\ \frac{\partial}{\partial z}\left(\frac{v}{T}\right) &= \frac{g}{2\omega\sin\phi}\frac{1}{T^2}\frac{\partial T}{\partial x} \end{aligned}\right\} \tag{13}$$

From this we have.

$$\begin{aligned} u\frac{\partial T}{\partial x} + v\frac{\partial T}{\partial y} &= T^2\frac{2\omega\sin\phi}{g}\left[u\frac{\partial}{\partial z}\left(\frac{v}{T}\right) - v\frac{\partial}{\partial z}\left(\frac{u}{T}\right)\right] \\ &= -T\frac{2\omega\sin\phi}{g}\left(u\frac{\partial v}{\partial z} - v\frac{\partial u}{\partial z}\right) \end{aligned} \tag{14}$$

If ψ is the angle between the direction of the horizontal wind vector and the x-axis then:

$$\tan\psi = \frac{v}{u}$$

Hence

$$\frac{\partial}{\partial z}(\tan\psi) = \sec^2\psi \frac{\partial\psi}{\partial z} = \left(1+\frac{v^2}{u^2}\right)\frac{\partial\psi}{\partial z}$$

$$\frac{\partial}{\partial z}\left(\frac{v}{u}\right) = \frac{1}{u^2}\left(u\frac{\partial v}{\partial z} - v\frac{\partial u}{\partial z}\right)$$

Or

$$u\frac{\partial v}{\partial z} - v\frac{\partial u}{\partial z} = (u^2+v^2)\frac{\partial\psi}{\partial z}$$

$$= V_h^2 \frac{\partial\psi}{\partial z}, \tag{15}$$

where V_h is the scalar value of the horizontal wind vector Substituting in (14) we get:

$$u\frac{\partial T}{\partial x} + v\frac{\partial T}{\partial y} = T\frac{2\omega\sin\theta}{g} V_h^2 \frac{\partial\psi}{\partial z} \tag{16}$$

Substituting (16) in (12) and transposing the terms we have

$$w(\Gamma-\beta) = \frac{AR}{c_p}\frac{T}{p}\frac{\partial p}{\partial t} - \frac{\partial T}{\partial t} - \frac{2\omega\sin\phi}{g} T V_h^2 \frac{\partial\psi}{\partial z} \tag{17}$$

Equation (17) enables us to calculate the vertical wind component at any level in the atmosphere if we know the rate of change of pressure and temperature at the point in question, the vertical variation of the horizontal wind vector as well as the prevailing lapse-rate The assumptions involved are that. (i) all changes are adiabatic, and (ii) the wind is geostrophic

4 Inter-Relation between Pressure and Temperature in the Atmosphere

The relation between pressure and temperature in the atmosphere is given by the well-known fundamental law of atmospheric statics:

$$dp = -g\rho\, dz = -g\frac{p}{RT}dz$$

On integration this leads to the familiar barometric formula

$$\log\frac{p}{p_0} = -\frac{g}{R}\int_0^z \frac{dz}{T} = -\frac{g}{R}\frac{z}{T_m}, \tag{18}$$

where T_m is the *mean* temperature of the air column from the surface where the pressure is p_0 to the level z where the pressure is p If we differentiate (18) keeping z constant and treating p, p_0 and T_m as variables, we get the following relation connecting the variation of pressure at the surface and

at the level z with the change in the mean temperature of the column between those two levels

$$\Delta p_0 = \Delta p \frac{p_0}{p} - \frac{gz}{RT_m^2} p_0 \Delta T_m \tag{19}$$

From (19) it follows that if $\Delta T_m = 0$, then $\Delta p_0 = \Delta p \frac{p_0}{p}$ That is, a small change of pressure at a higher level in the atmosphere would give rise to much larger changes in the surface pressure when the mean temperature of the air column remains unchanged For instance, a change of pressure of 1 mb at a level of 16 gms where $p \approx 100$ mbs would bring about a change of nearly 10 mbs in the surface pressure In the case of an incompressible medium, a change of pressure at any level would produce the same change at all levels below it, however, in the case of the atmosphere when extra mass is added above the level z to produce an increase of pressure at that level, the column below z gets compressed and part of the extra mass added sinks below that level Hence, in order to produce an increase of pressure of 1 mb at 16 kms, additional mass equivalent to 10 mbs has to be added above that level

In (19) if p and z relate to the level of the tropopause, then it will be seen that the change in the surface pressure can be *interpreted* as resulting from.

(i) Change of pressure Δp at the level of the tropopause due to addition of mass in the stratosphere;

(ii) Change of mean temperature ΔT_m of the tropospheric air column In meteorological literature (i) is sometimes designated as the *primary pressure wave*, and (ii) as the *secondary pressure wave*

One of the striking results furnished by aerological ascents is that the day-to-day variations of pressure at all levels in the troposphere are of the same order of magnitude as that observed at the surface From (19) it follows that such a result is possible only if the primary and secondary pressure waves are opposite in phase In other words, a rise of pressure at a higher level should be accompanied by a rise of temperature in the air column below that level and *vice versa* This result is strikingly borne out by the correlation coefficients worked out by W H Dines based on sounding balloon ascents over England which showed a correlation of 0 95 between the pressure at 9 kms and the mean temperature of the air column below that level. Besides this, Dines also found the following high correlation coefficients :—

(i) 0 84 between the height of the tropopause and the pressure at 9 kms ;

(ii) 0 79 between the height of the tropopause and the mean temperature of the troposphere below 9 kms

Similar results have been obtained by other investigators from observations over Europe, America and India

Various explanations have been offered to explain the high correlations discovered by Dines and subsequently confirmed by others In the first instance it is clear that in an air column in static equilibrium, increase or decrease in the temperature of the column below a particular level would give rise to expansion or contraction of the column and consequently to transport of mass upwards or downwards through the level in question resulting in a rise or fall of pressure at that level so long as there is no horizontal convergence or divergence of mass Again, if it be assumed that large-scale horizontal movements of air are possible from lower towards higher latitudes and *vice versa*, the high correlation coefficients discovered by Dines for middle latitudes can be understood That such "*horizontal oscillations*" of the atmosphere are to be expected on theoretical grounds has been shown by Bjerknes and collaborators According to the ideas developed by them, waves can be set up on the inclined surface of the tropopause over the temperate latitudes somewhat similar to the waves on the polar front The wave crests correspond to the pole-ward extension of tropical air with its high tropopause, while the wave troughs lie over regions where the polar air with its low tropopause has extended towards lower latitudes

5. Distribution of Pressure over the Northern Hemisphere in Summer and in Winter and Effect of Meridional Advection

From the observed mean values of pressure at the surface and the mean temperature distribution in the atmosphere furnished from upper air soundings, it is possible to calculate the variation of pressure with height at various latitudes in summer and in winter Such a calculation has been made by A. Wagner and the bold figures in Table I have been taken from his work. The pressure values in mms given by Wagner have been converted into mbs The figures in italics give the changes of pressure that would be produced *at the surface* at latitude ϕ if the entire atmospheric column above level h at latitude $\phi - 10°$ is bodily transported to the higher latitude by meridional advection.

TABLE I

DISTRIBUTION OF PRESSURE OVER THE NORTHERN HEMISPHERE (Mbs)

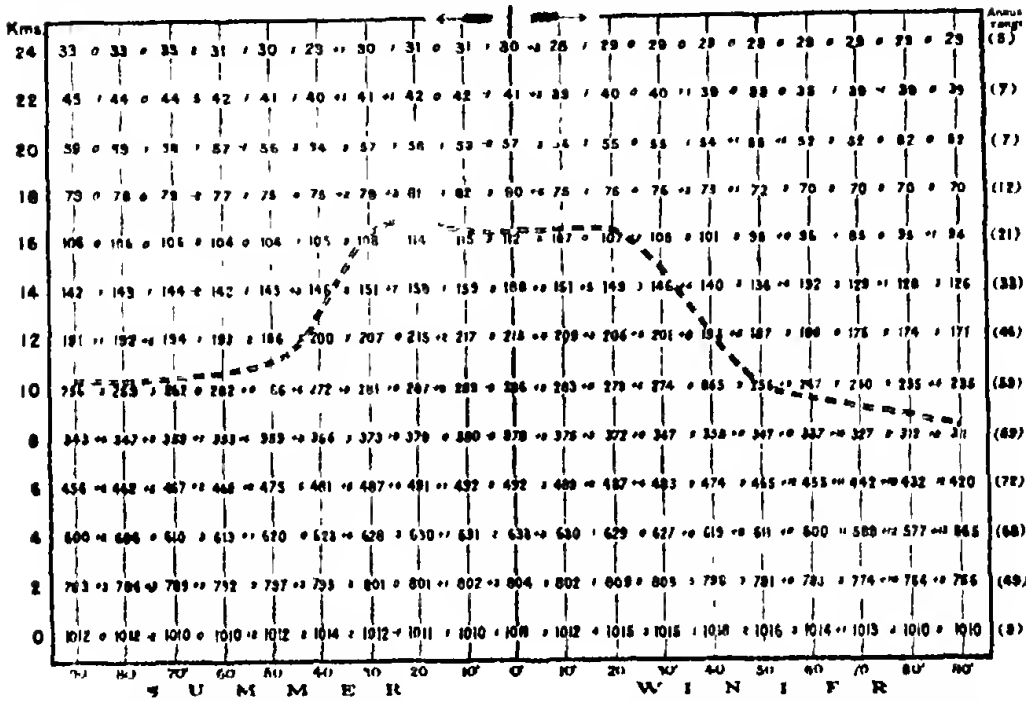

The table shows that the largest pressure gradients in the atmosphere occur in the middle and upper troposphere over polar and temperate latitudes in the winter months When it is remembered that level for level temperatures decrease towards the north in the troposphere up to 9 or 10 kms, it is clear from the table that meridional advection from lower towards higher latitudes extending throughout the atmosphere will give rise to an increase of pressure at 9 kms together with a rise in the mean temperature below that level The table also shows that the annual range of pressure is largest in the middle and upper troposphere, while the range is comparatively small at the surface of the earth and also decreases rapidly in the stratosphere above 18 kms It is interesting to see that within the tropics, horizontal advection cannot cause appreciable pressure variations especially in the summer months It will also be seen from the table that while bodily displacement of the *entire* atmospheric column at a higher latitude by a similar column from a lower latitude does not cause large changes of surface pressure, similar replacement above levels of 4 to 10 kms can produce large changes in the surface pressure For instance, if the entire atmosphere above 40° N is bodily shifted to 50° N. in winter,

there will be a rise of surface pressure of 2 mbs only at the higher latitude On the other hand, if the atmospheric column above 8 kms at latitude 40° N is transported to 50° N without effecting any change in the atmosphere below 8 kms, there will be a rise of 11 mbs in the surface pressure at latitude 50° N

6 PRESSURE AND TEMPERATURE CHANGES DUE TO ADVECTION

All changes of pressure and temperature in the atmosphere and consequently all weather phenomena are ultimately traceable to horizontal and vertical mass movements These two movements are closely inter-linked with each other and we cannot hope to gain a correct or complete insight into atmospheric processes by confining our attention only to one or other of these For instance although vertical displacements in which the transformation of potential into kinetic energy takes place play a fundamental role in phenomena such as cyclones, thunderstorms, etc, we cannot ignore horizontal convergence or divergence with which these vertical movements are intimately bound up Nevertheless, we can investigate the effect of purely horizontal mass movements and the changes which can result therefrom

The problem of the fluctuations of pressure and temperature in the atmosphere brought about by horizontal advection has been discussed by a number of investigators among whom might be mentioned Hesselberg, Exner, Steiner, Hurwitz, Rossby, Ertel, Palmén and Refsdal The problem can be stated as follows —

Consider two atmospheric air columns A and B (*vide* Fig 1) of unit cross-section extending upwards from the surface of the earth The columns are in static equilibrium to start with, the distribution of pressure and temperature being different in the two columns Horizontal advection now takes place from A towards B in one or more layers L_1, L_2, L_3, whereby the original air present in these layers in the column B is replaced by air of different density and temperature in the corresponding layers in column A As a result of this, the column B, readjusts itself to a new position of equilibrium If we have a sounding through the column B in the original state and also in the final state of equilibrium, we know the *local* changes of pressure and temperature. Is it possible to find out from the observed local changes the layer or layers in which advection has taken place and also the properties of the new samples of air brought in by advection? It is generally assumed for the sake of simplicity that all changes are adiabatic and that there is no lateral expansion or contraction of the column B as a result of the advection

The simplest and clearest solution of the problem of calculating the local changes of pressure and temperature in an atmospheric air column *below* a certain level when addition or removal of mass takes place *above* the level in question was arrived at almost simultaneously but independently by Rossby and Steiner Later, Rossby extended his theory to cover cases in which advection takes place in several layers of the column, and arrived at many interesting conclusions A couple of years later (1930), Ertel discussed the same problem and arrived at the same results as Rossby Some years after this (1935) Ertel and Sjan-zi-Li published a paper in which they claim to have discovered a " fundamental error " in Rossby's general advection theory and have worked out a new formula which they find gives more plausible results when applied to actual cases This work

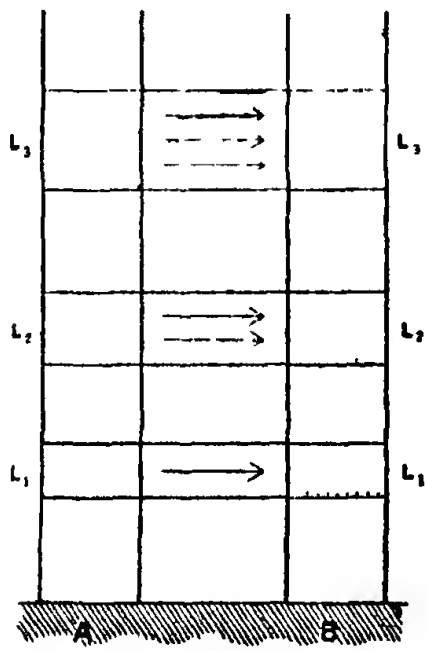

Fig 1

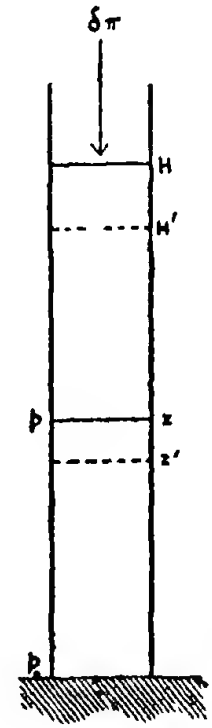

Fig. 2

has been quoted by Hurwitz in his recent book on " Dynamic Meteorology " In view of the great importance of the subject, it was considered worth while to look into the matter afresh, especially the validity of the assumptions involved and the significance of the results obtained.

7 Effect of Addition or Removal of Mass at the Top of an Atmospheric Air Column

We start with the simplest case in which an addition of mass δM equivalent to an increase of pressure $\delta\pi = g\delta M$ takes place *above* the level H due to advection in an atmospheric air column of unit cross-section What is the change of pressure and temperature at any fixed level z ($z < H$) in the column, it being assumed that there is no lateral expansion or contraction of the column from the surface to the level H?

If the atmosphere were incompressible, it is clear that the pressure at every level would increase by $\delta\pi$ However, because of the compressibility of the air, the column from the surface to the level H gets compressed under the increased pressure, and occupies only a smaller height (volume) up to H′ in the new state of equilibrium If we consider any fixed level z (Fig 2), then the air which originally occupied the space from the surface to the level z occupies only the space up to z′ after compression under the increased pressure $\delta\pi$ If p_0 be the surface pressure and p the pressure at the level z before compression then $p_0 - p$ is the weight of the air between these two levels Since after compression this air occupies only the space up to z′ the pressure difference between the surface and z′ in the new state of equilibrium is also equal to $p_0 - p$ But the surface pressure in the new state of equilibrium is $p_0 + \delta\pi$ The pressure at the level z′ is therefore $p + \delta\pi$ Hence increase in pressure over the individual element of air at z which in the new state of equilibrium occupies the position z′ is $\delta\pi$ This is the *individual* change of pressure ($\delta_i p$) The change of pressure at the fixed level z is the *local* change ($\delta_l p$) The general relation connecting local and individual variations is given by equation (3) which in this case becomes

$$\frac{dp}{dt} = u\frac{\partial p}{\partial x} + v\frac{\partial p}{\partial y} + w\frac{\partial p}{\partial z} + \frac{\partial p}{\partial t}$$

Since we assume that there is no lateral expansion or contraction of the column, $u = v = 0$ Also, $wdt = \delta z = z - z'$ Hence,

$$\delta_i p = \frac{\partial p}{\partial z}\ \delta z + \delta_l p$$

or:

$$\delta_l p = \delta_i p - \frac{\partial p}{\partial z}\ \delta z = \delta\pi - \frac{\partial p}{\partial z}\ \delta z \tag{20}$$

Similarly the relation connecting the local and individual changes of temperature is.

$$\delta_l T = \delta_i T - \frac{\partial T}{\partial z} \cdot \delta z = \delta_i T + \beta\ \delta z \tag{21}$$

The evaluation of (20) and (21) depends upon the knowledge of the quantity δz which is the decrease in height (volume) of the column brought about by compression In order to evaluate δz we have to make definite assumptions regarding the thermodynamics of the compression.

(*a*) *Isothermal Compression or Expansion*—In this case, each element of air as it changes its level retains its original temperature Let us now consider the column from the surface to the level z to be divided up into a number of thin elements Δz_1, Δz_2, Δz_n Consider the element of thickness Δz_r at the height z_r where the pressure is p_r. Since the compression is isothermal, we have

$$p_r \quad \Delta z_r = \text{constant} \tag{22}$$

Hence the decrease in thickness (volume) of the element for an increase of pressure $\delta\pi$ is given by

$$\delta(\Delta z_r) = -\delta\pi \quad \frac{\Delta z_r}{p_r}$$

The decrease in thickness of the entire column is therefore given by:

$$\sum_1^n \delta(\Delta z_r) = \delta z = -\delta\pi \int_0^z \frac{dz}{p} \tag{23}$$

Hence.

$$\delta_i p \quad \delta\pi\left[1 + \frac{\partial p}{\partial z}\int_0^z \frac{dz}{p}\right] \quad \delta\pi\left[1 - g\rho\int_0^z \frac{dz}{p}\right] \tag{24}$$

And since in this case $\delta_i T = 0$, we have:

$$\delta_i T = -\beta \quad \delta\pi \int_0^z \frac{dz}{p} \tag{25}$$

Since atmospheric movements conform more closely to adiabatic conditions, we shall now investigate this case.

(*b*) *Adiabatic Compression or Expansion*—In this case we have to replace equation (22) by.

$$p_r \cdot (\Delta z_r)^\gamma = \text{constant} \tag{26}$$

Hence·

$$\delta(\Delta z_r) = -\frac{1}{\gamma} \quad \delta\pi \frac{\Delta z_r}{p_r}$$

And so:

$$\sum_1^n \delta(\Delta z_r) = \delta z = -\frac{1}{\gamma} \quad \delta\pi \int_0^z \frac{dz}{p} \tag{27}$$

We have therefore:

$$\delta_l p = \delta\pi \left[1 - \frac{g\rho}{\gamma} \int_0^z \frac{dz}{p}\right] = \delta\pi \left[1 - \frac{g}{R\gamma} \frac{p}{T} \int_0^z \frac{dz}{p}\right] \tag{28}$$

From equation (8), the individual change of temperature for an increase of pressure $\delta\pi$ under adiabatic conditions is given by

$$\delta_l T = \frac{AR}{c_p} \frac{T}{p} \delta\pi$$

Hence:

$$\delta_l T = \frac{AR}{c_p} \frac{T}{p} \delta\pi - \frac{\beta}{\gamma} \delta\pi \int_0^z \frac{dz}{p}$$

$$= \frac{AR}{c_p} \frac{T}{p} \delta\pi \left[1 - \frac{\beta}{\Gamma} \frac{g}{R\gamma} \int_0^z \frac{dz}{p}\right] \tag{29}$$

From the hydrostatic equation, $dp = -g\rho dz$ we have

$$\frac{dz}{p} = -\frac{1}{g\rho} \frac{dp}{p} = \frac{R}{g} T \, d\left(\frac{1}{p}\right)$$

Hence:

$$\int_0^z \frac{dz}{p} = \frac{R}{g} \int_{p_0}^{p} T \, d\left(\frac{1}{p}\right) = \frac{R}{g} T_m \left(\frac{1}{p} - \frac{1}{p_0}\right).$$

where T_m is the mean temperature of the column from the surface to the level z. (This is different from the mean temperature T_m in the barometric formula)

Substituting this value of the integral in (28) and (29) we get

$$\delta_l p = \delta\pi \left[1 - \frac{1}{\gamma} \frac{T_m}{T} \left(1 - \frac{p}{p_0}\right)\right] \tag{30}$$

$$\delta_l T = \delta\pi \frac{AR}{c_p} \cdot \frac{T}{p} \left[1 - \frac{\beta}{\Gamma} \frac{1}{\gamma} \frac{T_m}{T} \left(1 - \frac{p}{p_0}\right)\right]. \tag{31}$$

These expressions give the local variations of pressure and temperature at any level where the original pressure and temperature are p and T when the column is subjected to adiabatic compression under the influence of an advection current *above* the level in question, which causes an increase of pressure $\delta\pi$ at the ground level The equations are valid only if the lower portion of the column retains its identity and there is no exchange of heat with the surroundings

All the quantities in equations (30) and (31) are readily available from two consecutive aerological ascents over a station. If from the results of

two such ascents we calculate the values of $\delta\pi$ for a number of successive levels from the known values of p, T, T_m and $\delta_l p$, then these values should be very nearly constant if the observed change of surface pressure is due to advection at very high levels, and the lower atmosphere has not been appreciably disturbed in the interval between the two soundings. Such an example has been quoted by Rossby in which he has shown that a change of surface pressure by 19 mbs at Trappes (France) between the 11th and 13th April 1912 was caused by advection above 12 kms

(*c*) *Change of Lapse-Rate*—We shall now derive an expression for the change of lapse-rate in the atmospheric air column subjected to an adiabatic compression $\delta\pi$ due to advection above the level H. Since the process is adiabatic, every individual element retains its potential temperature θ during its displacement from its original equilibrium position z where the pressure is p and temperature T to the new position z' where its pressure is $p + \delta\pi$ and temperature T′ Consider a thin layer of the column between z and $z + dz$, the corresponding potential temperatures being θ and $\theta + d\theta$. Then we have

$$\frac{d\theta}{dz} = \frac{\theta}{T}\left(\frac{dT}{dz} - \frac{AR}{c_p}\,\frac{T}{p}\,\frac{dp}{dz}\right) = \frac{\theta}{T}(\Gamma - \beta)$$

For the same element in the new position of equilibrium we have:

$$\frac{d\theta}{dz'} = \frac{\theta}{T'}\cdot(\Gamma - \beta')$$

Hence:

$$\frac{\Gamma - \beta'}{\Gamma - \beta} = \frac{T'}{T}\cdot\frac{dz}{dz'} = \frac{p + \delta\pi}{p} = 1 + \frac{\delta\pi}{p}$$

Or·

$$\beta' = \beta - \frac{\delta\pi}{p}\,(\Gamma - \beta) \tag{32}$$

From this we see that: (i) if $\beta < \Gamma$ then $\beta' < \beta$, (ii) if $\beta > \Gamma$ then $\beta' > \beta$; (iii) if $\beta = \Gamma$ then $\beta' = \beta$ Thus, stable air becomes more stable and unstable air becomes more unstable by the addition of mass to the top of the column If the air column is in neutral equilibrium, then there is no change in lapse-rate.

(*d*) *Atmosphere with Dry Adiabatic Lapse-Rate*—Equations (30) and (31) assume a comparatively simple form if we consider an atmosphere with dry adiabatic lapse-rate. In this case the potential temperature θ is a constant at all levels, and the difference of temperature between the surface and any fixed level z is the same before and after the advection. Hence $(\delta_l T)_0 = (\delta_l T)_z$; that is:

$$\frac{AR}{c_p}\,\frac{T_0}{p_0}\,\delta\pi = \frac{AR}{c_p}\cdot\frac{T}{p}\cdot\delta_l\, p$$

Hence:

$$\delta_l p = \frac{p}{p_0} \cdot \frac{T_0}{T} \quad \delta\pi = \frac{p}{p_0} \quad \left(\frac{p_0}{p}\right)^{\frac{AR}{c_p}} \quad \delta\pi$$

$$= \delta\pi \left(\frac{p}{p_0}\right)^{\frac{1}{\gamma}} \tag{33}$$

$$\delta_l T = \frac{AR}{c_p} \quad \frac{T_0}{p_0} \, \delta\pi = \frac{AR}{c_p} \cdot \frac{T}{p} \quad \delta\pi \left(\frac{p}{p_0}\right)^{\frac{1}{\gamma}} \tag{34}$$

Table II gives the values of $\delta_l p$, $\delta_l T$, $\delta_z T$ and δz for an air column with dry adiabatic lapse-rate having a surface temperature of 300°A and surface pressure of 1,000 mbs when an addition of mass equivalent to 10 mbs takes place above the level of 12 gkms

TABLE II

$$\theta = T \cdot \left(\frac{1000}{p}\right)^{\frac{AR}{c_p}} = 300°A \; ; \; p_0 = 1000 \text{ mbs} \; , \; \delta\pi = 10 \text{ mbs} \; ; \; \beta = \Gamma = 10°C/\text{gkm}$$

z (gkm)	T (A)	p (mbs)	$\left(\frac{p}{p_0}\right)^{1/\gamma}$	$\delta_l p = \delta\pi \left(\frac{p}{p_0}\right)^{1/\gamma}$ (mbs)	$\delta_l T = \frac{AR}{C_p} \frac{T_0}{p_0} \delta\pi$ (°C)	$\delta_z T = \frac{AR}{c_p} \frac{\Gamma}{\beta} \delta\pi$ (°C)	$\delta z = -\frac{R}{g} \delta\pi \frac{1}{p}\left[1 - \left(\frac{p}{p_0}\right)^{1/\gamma}\right]$ (Metres)
0	300	1000	1 0000	10 0	0 86	0 86	0 0
1	290	890	0 9204	9 2	.	0 94	7 6
2	280	785	0·8414	8·4		1 03	16 7
3	270	692	0 7691	7 7	.	1·12	26·4
4	260	610	0·7025	7 0	.	1 23	37 3
5	250	532	0 6371	6·4		1 35	50 2
6	240	461	0·5754	5·6	.	1 50	64 9
7	230	396	0·5176	5 2		1 66	82 0
8	220	344	0·4667	4 7		1 84	100 3
9	210	289	0·4121	4 1		2 09	125 4
10	200	245	0 3664	3 7	..	2·35	152 1
11	190	206	0·3236	3·2	..	2·66	182·5
12	180	170	0·2830	2·8		3 06	223 0

(*e*) *Effect of Change of Cross-Section of the Air Column.*—Hitherto we have assumed that there is no lateral expansion or contraction of the column during its readjustment after the advection. We shall now investigate the case in which a change in the cross-section of the air column takes place with advective transport of mass aloft

Consider an atmospheric air column of cross-section S Let us assume that as a result of advection above the level H, the cross-section below the level z ($z < H$) changes to $S + \delta S$ In this case we have to replace equation (26) by.

$$p_r \ (S \ \Delta \ z_r)^\gamma = \text{constant}$$

The decrease in thickness of the element Δz_r for an increase in the external pressure by $\delta\pi$ is now given by the equation:

$$\delta\pi \ p_r \ \delta S \ p_r \ \delta(\Delta \ z_r) = 0$$

Hence:

$$\delta \ (\Delta \ z_r) = -\frac{1}{\gamma} \ \delta\pi \ \frac{\Delta \ z_r}{p_r} - (r-1) \ \Delta \ z_r,$$

where $r = 1 + \frac{\delta S}{S}$, is the relative increase in the cross-section of the element. The decrease in thickness of the entire column up to the level z is therefore given by:

$$\sum_1^z \delta \ (\Delta \ z_r) = \delta z^* = -\frac{1}{\gamma} \delta\pi \int_0^z \frac{dz}{p} - \int_0^z (r-1) \ dz$$

If r is constant at all levels below z this reduces to:

$$\delta z^* = -\frac{1}{\gamma} \delta\pi \int_0^z \frac{dz}{p} - (r-1) \ z \tag{35}$$

Comparing (27) and (35) we see that δz^* is numerically greater than δz if $r > 1$. It follows, therefore, from equation (20) and (21) that the local changes of pressure and temperature are less than when there is no change in the cross-section of the column

(*f*) *Pressure and Temperature Changes due to Advection in a Saturated Atmosphere*—Hitherto we have assumed that the atmosphere is dry so that every individual element of air retains its potential temperature during its displacement from the original equilibrium position as a result of advection aloft. Let us now examine the case in which the atmosphere is saturated

either throughout its extent or in certain layers and condensation and evaporation of water take place during the displacement of the individual elements so that their changes of temperature follow the saturation adiabatic lapse-rate.

According to (27), when the atmosphere is dry, the decrease in thickness of the element Δz when the external pressure on the element is increased adiabatically from p to $p + \delta\pi$ is:

$$\delta(\Delta z) = -\frac{1}{\gamma}\ \delta\pi\ \frac{\Delta z}{p}.$$

The increase in temperature of the element as a result of the adiabatic compression is given by:

$$\delta T = \frac{AR}{c_p}\ \frac{T}{p}\ \delta\pi = \frac{R}{g}\ \frac{T}{p}\ \Gamma\ \delta\pi$$

If the element of air remains saturated throughout the process, the increase in temperature of the element is given by.

$$\delta' T = \frac{R}{g} \cdot \frac{T}{p}\ \Gamma' \cdot \delta\pi,$$

where Γ' is the saturation adiabatic lapse-rate Since $\Gamma' < \Gamma$ it follows that $\delta' T < \delta T$; that is, the increase in temperature of the element will be less in the second case Hence in order to get the decrease in thickness of the element when the air remains saturated throughout the compression, we have to add to $\delta(\Delta z)$ the decrease in thickness of the element Δz as a result of the cooling under constant pressure by the amount $\delta T - \delta' T = \frac{R}{g}\ \frac{T}{p}\ \delta\pi(\Gamma - \Gamma')$ If we denote this additional contraction in thickness by $\delta'(\Delta z)$ we have·

$$\frac{\delta'(\Delta z)}{\Delta z} = \frac{\delta T - \delta' T}{T}$$

Or:

$$\delta'(\Delta z) = \frac{R}{g} \cdot \frac{\delta\pi}{p}\ (\Gamma - \Gamma')\ \Delta z$$

Hence the total decrease in thickness of the element Δz is given by:

$$\delta(\Delta z) + \delta'(\Delta z) = -\frac{1}{\gamma}\ \delta\pi\ \frac{\Delta z}{p} - \frac{R}{g}\ \delta\pi(\Gamma - \Gamma') \cdot \frac{\Delta z}{p}.$$

The total decrease in thickness of the column from the surface to the level z is therefore given by:

$$\delta z = -\frac{1}{\gamma}\,\delta\pi \int_0^z \frac{dz}{p} - \frac{R}{g}\,\delta\pi \int_0^z (\Gamma - \Gamma') \cdot \frac{dz}{p} \qquad (36)$$

The local changes of pressure and temperature can now be readily obtained by substituting this value of δz in equation (20) and (21). It will be seen that these changes are now less than in the case of the dry atmosphere.

8 Effect of Addition or Removal of Mass on the Pressure and Temperature above the Layer of Advection

(*a*) *Advection at the Surface*—The simplest case is that in which addition of mass takes place at the surface Let an advection current at the surface of the earth cause an increase of pressure $\delta\pi$ at the surface It is assumed that the original atmospheric column is bodily lifted up by the advection current without individual pressure and temperature changes through a height δz (*vide* Fig 3) given by

$$\delta\pi = g\,\rho_a\,\delta z,$$

where ρ_a is the density of the advection current The change of pressure at the fixed level z is then given by·

$$\delta_l p = -\frac{\partial p}{\partial z}\,\delta z = \frac{p}{\rho_a}\,\delta\pi = \frac{p}{p_0}\,\frac{T_a}{T}\,\delta\pi, \tag{37}$$

where T_a is the temperature of the new air mass brought in by advection. The local change of temperature is given by:

$$\delta_l T = -\frac{\partial T}{\partial z}\cdot\delta z = \frac{\beta}{g\,\rho_a}\,\delta\pi = \frac{R\,\beta}{g}\,\frac{T_a}{p_0}\,\delta\pi \tag{38}$$

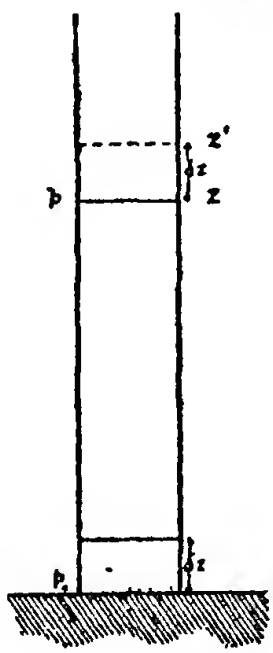

Fig 3

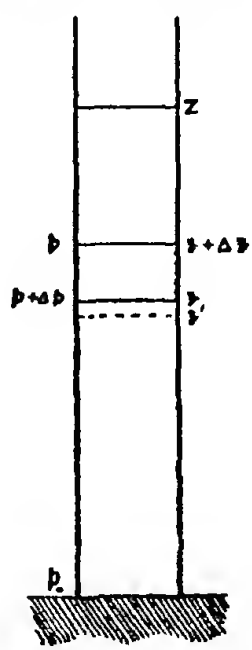

Fig 4

(*b*) *Addition of Mass at any Arbitrary Level*—We shall now consider the more general case in which the addition of mass takes place not at the surface but at some higher level Let an addition of mass ΔM equivalent to an increase of pressure $\Delta\pi = g\Delta M$ take place between the levels z and $z + \Delta z$ in an atmospheric air column originally in static equilibrium What is the local change of pressure and temperature at the level z $(z > z > 0)$?

In order to investigate this problem, let us imagine two weightless and frictionless discs in the column at z and $z + \Delta z$ which can be kept fixed or allowed to move up and down in the column as desired (*vide* Fig 4) In the initial state, the discs are in equilibrium at z and $z + \Delta z$ respectively Let $p + \Delta p$ and p be the pressures at z and $z + \Delta z$ Then

$$\Delta p = g \rho \Delta z,$$

where ρ = density of the air between z and $z + \Delta z$

Let us now imagine that the discs are kept fixed in position and the air between them replaced by a new sample of air of density ρ_a
We then have

$$\Delta p_a = g \rho_a \Delta z - \Delta p + \Delta \pi$$

Let the discs be now released so that the column readjusts itself to its new position of equilibrium What will be the new positions of the discs z and $z + \Delta z$?

The pressure on the lower surface of the disc z is $p + \Delta p$ and on its upper surface, $p + \Delta p_a = p + \Delta p + \Delta\pi$ The disc z and the column above it will therefore move down bodily compressing adiabatically the atmospheric column below it until equality of pressures is established on the two sides of the disc in its new position of equilibrium z' The distance $z - z' = \delta a$ is given by.

$$\delta a = -\frac{1}{\gamma} \Delta \pi \int_0^z \frac{dz}{p}. \tag{39}$$

Let us now consider the equilibrium position of the disc $z + \Delta z$ The pressure on its upper surface is p and on its lower surface is p_a where p_a is the pressure of the new sample of air introduced between z and $z + \Delta z$. We may now distinguish between two cases

(1) If $p_a = p$, then the disc $z + \Delta z$ will be at the same distance from the disc z in the new position of equilibrium In this case, therefore, the entire column above the disc z will sink *bodily* through the distance δa The

individual changes of pressure and temperature of any element above the layer of advection are zero, while the *local* changes are given by:

$$\left.\begin{aligned} \delta_l p &= -\frac{\partial p}{\partial z} \cdot \delta a \\ \delta_l T &= -\frac{\partial T}{\partial z} \cdot \delta a \end{aligned}\right\} \tag{40}$$

We see that when $\Delta\pi$ is positive, $\delta_l p$ and $\delta_l T$ are both negative That is, when a stratum of air in an atmospheric air column is displaced by another stratum of the same thickness but greater mass, there is an *increase* of pressure at every level *below* the layer of advection, and a *decrease* of pressure at every level *above*, provided the pressure at the upper boundary of the advection layer remains constant during the displacement.

(2) Let us now consider the case in which p_a is not equal to p The air between z and $z + \Delta z$ will then undergo adiabatic expansion if $p_a > p$ or compression if $p_a < p$, until p_a becomes equal to p In this process the column of air above $z + \Delta z$ will move bodily up or down without individual changes of pressure and temperature Let:

$$p_a - p = \delta_a p$$
$$\rho_a - \rho = \delta_a \rho$$
$$T_a - T = \delta_a T$$

If $p_a > p$, then the increase in Δz during the adiabatic expansion from p_a to p is given by.

$$\delta\beta = \frac{1}{\gamma} \quad \delta_a p \quad \frac{\Delta z}{p} \tag{41}$$

Now, we have:

$$\delta_a p = R\,(T \cdot \delta_a \rho + \rho \quad \delta_a T) \tag{42}$$

$$\Delta\pi = g\,(\rho_a - \rho) \quad \Delta z = g \quad \delta_a \rho \quad \Delta z$$

Or:

$$\delta_a \rho = \frac{1}{g} \cdot \frac{\Delta\pi}{\Delta z} = -\frac{1}{g} \cdot \frac{d\pi}{dz},$$

where π is the total increase in mass above the level z due to advection in the entire column above this level.

Hence:

$$\delta_a p = R\left(-\frac{1}{g} \cdot \frac{d\pi}{dz} \cdot T + \rho\,\delta_a T\right) \tag{43}$$

Therefore:

$$\delta\beta = -\frac{R}{g\gamma} \cdot \frac{T}{p} \cdot \frac{d\pi}{dz} \cdot \Delta z + \frac{1}{\gamma} \cdot \frac{\delta_a T}{T} \cdot \Delta z \tag{44}$$

The resultant downward displacement of the individual layer at z due to adiabatic compression of the column below z and adiabatic expansion as the stratum between z and $z + \Delta z$ is given by·

$$\delta z = \delta\alpha + \delta\beta$$

The local changes of pressure and temperature are given by:

$$\left.\begin{aligned} \delta_l p &= -\frac{\partial p}{\partial z} \cdot \delta z \\ \delta_l T &= -\frac{\partial T}{\partial z} \quad \delta z \end{aligned}\right\} \qquad (45)$$

It will be seen that when $\delta_a p = 0$, $\delta z = \delta\alpha$, so that (40) and (45) become identical In this case we see from (42) that,

$$\delta_a \rho = \rho \quad \frac{\delta_a T}{T}.$$

This means that the change of mass of the air between z and $z + \Delta z$ is brought about entirely by a change in temperature of the air at constant pressure

If $\Delta\pi$ is positive and $\delta_a p$ is also positive, we see from (39) and (41) that $\delta\alpha$ and $\delta\beta$ are opposite in sign In particular, if $\delta\alpha$ and $\delta\beta$ are numerically equal, then $\delta z = 0$; that is, there is no displacement of the individual element of air at z In this special case, therefore, the local changes of pressure and temperature at any point above the layer of advection are zero The upward displacement of the disc $z + \Delta z$ and the column above it due to the adiabatic expansion of the stratum is exactly equal in magnitude to the downward displacement of the disc z and the whole column above it due to adiabatic compression of the column below z In the final state of equilibrium, the disc z is displaced to z' while the disc $z + \Delta z$ and the column above it remain undisturbed

9 Advection in Several Layers of an Air Column

We shall now consider the case in which the atmospheric air column is traversed by arbitrary advection currents so that displacements and replacements of air take place in several layers throughout the length of the column.

In this case (*vide* Fig. 5) if we consider any individual element of air in the column at a height z above the ground, then changes of mass take place both above and below this level The final displacement of the individual element at z is the resultant of:

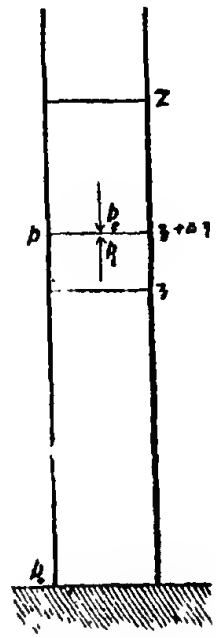

FIG 5

(1) Adiabatic compression or expansion of the individual elements in the column below z due to the change in the external pressure p_e to which the individual elements in the column are subjected as a result of advection in the entire column above the element in question;

(2) Adiabatic compression or expansion of the individual elements in the column below z due to the change in the internal pressure p_i as a result of advection in the individual elements.

Imagine the column from the surface to the level z to be divided up into a number of thin elements Δz_1, Δz_2, Δz_n. Let $\delta_a\rho_1$, $\delta_a\rho_2$, $\delta_a\rho_n$ denote the change in density in the individual elements as a result of advection; $\delta_a p_1$, $\delta_a p_2$, $\delta_a p_n$ and $\delta_a T_1$, $\delta_a T_2$ $\delta_a T_n$, the corresponding changes of pressure and temperature

The total increase of pressure over the individual element at z as a result of advection aloft is given by:

$$\pi(z) = \int_z^\infty g \cdot \delta_a \rho \cdot dz$$

The decrease in thickness of the element Δz as a result of the adiabatic increase of pressure from p to $p + \pi(z)$ is given by.

$$\delta(\Delta z) = -\frac{1}{\gamma}\ \pi(z)\frac{\Delta z}{p}.$$

The decrease in height of the column from the surface to the level z is therefore given by.

$$\alpha = \sum_{1}^{n} -\frac{1}{\gamma}\ \pi(z_r)\frac{\Delta z_r}{p_r} = -\frac{1}{\gamma}\int_0^z \pi\frac{dz}{p}. \tag{46}$$

From (41) and (44), we see that the total increase in height of the column from the surface to the level z as a result of adiabatic expansion of the individual elements due to the change in the internal pressures is given by

$$\beta = \sum_{1}^{n}\frac{1}{\gamma}\ \delta_a p_r \cdot \frac{\Delta z_r}{p_r} = \frac{1}{\gamma}\int_0^z \delta_a p\frac{dz}{p}$$

$$= \frac{1}{\gamma}\int_0^z \mathrm{R}\left(-\frac{1}{g}\frac{d\pi}{dz}\cdot \mathrm{T} + \rho\ \ \delta_a \mathrm{T}\right)\frac{dz}{p} \tag{47}$$

Hence, the resultant downward displacement of the individual layer at z is given by

$$\delta z = \alpha + \beta = -\frac{1}{\gamma}\int_0^z \pi\frac{dz}{p} - \frac{\mathrm{R}}{g\gamma}\int_0^z \frac{\mathrm{T}}{p}\frac{d\pi}{dz}\ dz + \frac{1}{\gamma}\int_0^z \frac{\delta_a \mathrm{T}}{\mathrm{T}}\ dz$$

$$= -\frac{1}{\gamma}\int_0^z \pi\frac{dz}{p} - \frac{\mathrm{R}}{g\gamma}\left[\pi\ \frac{\mathrm{T}}{p}\right]_0^z + \frac{\mathrm{R}}{g\gamma}\int_0^z \pi\left(\frac{1}{p}\ \frac{\partial \mathrm{T}}{\partial z} - \frac{\mathrm{T}}{p^2}\frac{\partial p}{\partial z}\right) dz$$

$$+ \frac{1}{\gamma}\int_0^z \frac{\delta_a \mathrm{T}}{\mathrm{T}}\ dz$$

$$= -\frac{1}{\gamma}\int_0^z \pi\frac{dz}{p} - \frac{\mathrm{R}}{g\gamma}\left(\pi\frac{\mathrm{T}}{p} - \pi_0\frac{\mathrm{T}_0}{p_0}\right) + \frac{\mathrm{R}}{g\gamma}\int_0^z \frac{\pi}{p}\ \frac{\partial \mathrm{T}}{\partial z}\ dz$$

$$+ \frac{1}{\gamma}\int_0^z \pi\ \frac{dz}{p} + \frac{1}{\gamma}\int_0^z \frac{\delta_a \mathrm{T}}{\mathrm{T}}\cdot dz$$

$$= \frac{\mathrm{R}}{g\gamma}\left(\frac{\pi_0 \mathrm{T}_0}{p_0} - \frac{\pi \mathrm{T}}{p}\right) + \frac{\mathrm{R}}{g\gamma}\int_0^z \frac{\pi}{p}\ \frac{\partial \mathrm{T}}{\partial z}\ dz + \frac{1}{\gamma}\int_0^z \frac{\delta_a \mathrm{T}}{\mathrm{T}}\cdot dz$$

where π_0, p_0, T_0 are the values of π, p, T at the surface.

The local variation of pressure at the level z is therefore given by:

$$\delta_l p = \pi - \frac{\partial p}{\partial z} \cdot \delta z = \pi + g\rho\, \delta z = \pi + \frac{g}{R} \cdot \frac{p}{T} \cdot \delta z$$

$$= \pi\left(1 - \frac{1}{\gamma}\right) + \left(\frac{1}{\gamma} \cdot \frac{\pi_0 T_0}{p_0}\right) \cdot \frac{p}{T} + \frac{1}{\gamma}\ \frac{p}{T} \int_0^z \frac{\pi}{p} \cdot \frac{\partial T}{\partial z}\ dz$$

$$+ \frac{g}{R\gamma} \cdot \frac{p}{T} \int_0^z \frac{\delta_a T}{T} \cdot dz \tag{48}$$

Let $$\phi = \int_0^z \frac{\pi}{p} \cdot \frac{\partial T}{\partial z} \cdot dz; \tag{49}$$

Then $$\frac{d\phi}{dz} = \frac{\pi}{p} \cdot \frac{\partial T}{\partial z} = -\frac{\pi}{p} \cdot \beta$$

Hence $$\pi = -\frac{p}{\beta} \cdot \frac{d\phi}{dz} \tag{50}$$

Substituting (49) and (50) in (48) and simplifying we get:

$$\frac{d\phi}{dz} - \frac{1}{\gamma - 1}\ \frac{\beta}{T} \cdot \phi$$

$$= \frac{1}{\gamma - 1} \cdot \left[\frac{\beta}{T} \cdot \frac{\pi_0 T_0}{p_0} + \frac{\beta}{T} \cdot \frac{g}{R} \int_0^z \frac{\delta_a T}{T}\ dz - \gamma\ \frac{\beta}{T}\ \delta_l p\right]$$

Let $\frac{1}{\gamma - 1} = P$, $\frac{\pi_0 T_0}{p_0} = Q$, and $\frac{g}{R} \int_0^z \frac{\delta_a T}{T}\ dz = S$

Then, we have.

$$\frac{d\phi}{dz} + P\,\frac{d}{dz}(\log T) \cdot \phi = P\left[\frac{\beta}{T}\ (Q + S) - \gamma \cdot \frac{\beta}{p}\ \delta_l p\right] \tag{51}$$

Solving this equation for ϕ we get:

$$\phi = e^{-P\int_0^z \frac{d}{dz}(\log T)\, dz} \left[\int_0^z e^{P\int_0^z \frac{d}{dz}(\log T)\, dz} \cdot P\left\{\frac{\beta}{T}(Q + S) - \gamma\ \frac{\beta}{\gamma}\, \delta_l p\right\} dz\right]$$

$$= \left(\frac{T}{T_0}\right)^{-P} \left[\int_0^z \left(\frac{T}{T_0}\right)^{P} \cdot P\left\{\frac{\beta}{T}(Q + S) - \gamma \cdot \frac{\beta}{p}\ \delta_l p\right\} dz\right] \tag{52}$$

Hence:

$$\frac{d\phi}{dz} = -\beta \cdot \frac{\pi}{p}$$

$$= P\left\{\frac{\beta}{T}(Q+S) - \gamma \cdot \frac{\beta}{p} \cdot \delta_l p\right\} - P \left(\frac{T}{T_0}\right)^{-P-1} \frac{1}{T_0} \frac{\partial T}{\partial z}$$

$$\left[\int_0^z \left(\frac{T}{T_0}\right)^P P\left\{\frac{\beta}{T}(Q+S) - \gamma \frac{\beta}{p} \delta_l p\right\} dz\right]$$

Therefore:

$$\pi = -\frac{p}{\beta} \cdot P\left\{\frac{\beta}{T}(Q+S) - \gamma \frac{\beta}{p} \cdot \delta_l p\right\}$$

$$-\frac{p}{\beta} \cdot P\left(\frac{T}{T_0}\right)^{-(P+1)} \cdot \frac{1}{T_0} \cdot \beta\left[\int_0^z \left(\frac{T}{T_0}\right)^P \cdot P\left\{\frac{\beta}{T}(Q+S) - \gamma \frac{\beta}{p} \delta_l p\right\} dz\right]$$

$$= -P(Q+S) \cdot \frac{p}{T} + P \gamma \delta_l p$$

$$+ P^2 (Q+S) \frac{p}{T^{P+1}} \int_0^z \frac{1}{p} \frac{d}{dz}(T^P)\, dz$$

$$- P^2 \gamma \frac{p}{T^{P+1}} \int_0^z \frac{\delta_l p}{p} \cdot \frac{1}{P+1} \frac{d}{dz}(T^{P+1})\, dz$$

$$= -P(Q+S)\frac{p}{T} + P \gamma \delta_l p$$

$$+ P(Q+S)\frac{p}{T^{P+1}}(T^P - T_0^P)$$

$$- P^2 \gamma \frac{p}{T^{P+1}} \frac{1}{P+1} \int_0^z \frac{\delta_l p}{p} \cdot \frac{d}{dz}(T^{P+1})\, dz$$

$$\pi = P \gamma \cdot \delta_l p - P(Q+S)\frac{p}{T} \cdot \left(\frac{T_0}{T}\right)^P - P \frac{p}{T^{P+1}} \int_0^z \left(\frac{\delta_l p}{p}\right) \cdot \frac{d}{dz}\left(\frac{T}{T_0}\right)^{P+1} \cdot dz$$

$$= P\left[\gamma \cdot \delta_l p - (Q+S) \cdot \frac{p}{T_0}\left(\frac{T_0}{T}\right)^{P+1} - p \cdot \left(\frac{T_0}{T}\right)^{P+1}\right.$$

$$\left. \cdot \int_0^z \left(\frac{\delta_l p}{p}\right) \cdot \frac{d}{dz}\left(\frac{T}{T_0}\right)^{P+1} dz\right]$$

$$= \frac{\gamma}{\gamma-1}\,\delta_l p - \frac{1}{\gamma-1}\,p\,\left(\frac{T_0}{T}\right)^{\frac{\gamma}{\gamma-1}}\left[\frac{\pi_0}{p_0} + \frac{g}{R\,T_0}\int_0^z \frac{\delta_a T}{T}\,dz + \int_0^z \left(\frac{\delta_l p}{p}\right)\cdot\frac{d}{dz}\left(\frac{T}{T_0}\right)^{\frac{\gamma}{\gamma-1}}\cdot dz\right]$$

Since:

$$\frac{\gamma}{\gamma-1} = \frac{1\cdot 4}{0\ 4} = 3\ 5;\ \frac{1}{\gamma-1} = \frac{1}{0\ 4} = 2\ 5,$$

We have:

$$\pi = 3\ 5\,\delta_l p - 2\ 5\,p\left(\frac{T_0}{T}\right)^{2\cdot 5}\left[\frac{\pi_0}{p_0} + \frac{g}{R\,T_0}\int_0^z \frac{\delta_a T}{T}\,dz + \int_0^z \left(\frac{\delta_l p}{p}\right)\ \frac{d}{dz}\left(\frac{T}{T_0}\right)^{2\cdot 5} dz\right]$$

$$= 3\ 5\,\delta_l p - 2\ 5\,p\left(\frac{T_0}{T}\right)^{3\ 5}\left[\frac{\pi_0}{p_0} + \frac{g}{R\,T_0}\int_0^z \frac{\delta_a T}{T}\,dz + \frac{\delta_l p}{p}\ \left(\frac{T}{T_0}\right)^{3\ 5} - \frac{\pi_0}{p_0} - \int_0^z \left(\frac{T}{T_0}\right)^{2\cdot 5}\frac{d}{dz}\left(\frac{\delta_l p}{p}\right) dz\right]$$

$$= \delta_l p - 2\ 5\,p\left(\frac{T_0}{T}\right)^{2\cdot 5}\left[\frac{g}{R\,T_0}\int_0^z \frac{\delta_a T}{T}\,dz - \int_0^z \left(\frac{T}{T_0}\right)^{2\cdot 5}\frac{d}{dz}\left(\frac{\delta_l p}{p}\right) dz\right] \qquad (53)$$

10. General Advection Theory of Rossby

The expression for π developed in the preceding section assumes a comparative form if we make special assumptions regarding the nature of the advection currents in the atmospheric column

Rossby assumed that at any height z the layer of thickness dz is displaced by another layer of the same thickness and that *the pressure at the upper boundary of the advection layer remains constant during the displacement.* This means that in equation (47) $\delta_a p_1$, $\delta_a p_2$, .. are each equal to zero so that $\beta = 0$. Hence:

$$\delta z = \alpha = -\frac{1}{\gamma}\int^z \pi\,\frac{dz}{p}$$

The *local* change of pressure at the level z is therefore given by :

$$\delta_l p = \pi - \frac{\partial p}{\partial z} \cdot \delta z = \pi - \frac{g}{R\gamma} \frac{p}{T} \int_0^z \pi \frac{dz}{p}$$

As has been shown by Rossby, this equation when solved for π gives :

$$\pi = \delta_l p + \frac{g}{R\gamma} \frac{1}{\theta} \int_0^z \delta_l p \frac{\theta}{T} dz \tag{54}$$

where θ is the potential temperature at the level z

It will be clear from the considerations in Section 8 that Rossby's assumption essentially means that the result of addition of mass due to advection in the atmospheric air column *below* any arbitrary level z is to produce a *bodily sinking* of the entire column above this level through a distance equal to the adiabatic compression of the column from the surface to the level z The thickness of an individual element Δz remains unchanged as a result of advection within the element, but the entire column below the element is adiabatically compressed by an amount δa given by equation (39) We thus see that *Rossby's assumption leads to the result that there is a local decrease of pressure* ($\delta_l p$ *negative*) *at all levels above the layers influenced by advection* Indeed, practically all the results derived and discussed by Rossby in the latter part of his paper are a direct outcome of this assumption

With the assumptions made by Rossby, it is also possible to derive an expression for the local change of temperature $\delta_l T$ in the atmospheric column We have

$$\delta_l T = \delta_t T - \frac{\partial T}{\partial z} \delta z = \delta_t T + \frac{\partial T}{\partial z} \frac{1}{\gamma} \int_0^z \frac{\pi}{p} dz$$

The individual change of temperature $\delta_l T$ consists of

(1) Change of temperature ($\delta_a T$) due to the replacement of the individual element of air at z with temperature T by the new element with temperature T_a brought in by advection ($\delta_a T = T_a - T$),

(2) Change of temperature ($\delta_a' T$) of the element due to adiabatic compression from p to $p + \pi$

From equation (43) we see that when $\delta_a p = 0$,

$$\delta_a T = \frac{T}{g\rho} \cdot \frac{d\pi}{dz} = \frac{R}{g} \cdot \frac{T^2}{p} \cdot \frac{d\pi}{dz}$$

Also:

$$\delta_a \cdot T = \frac{AR}{c_p} \frac{T}{p} \pi$$

Hence we have·

$$\delta_l T = \frac{R}{g} \frac{T^2}{p} \frac{d\pi}{dz} + \frac{AR}{c_p} \frac{T}{p} \pi + \frac{\partial T}{\partial z} \cdot \frac{1}{\gamma} \int_0^z \frac{\pi}{p} \cdot dz \qquad (55)$$

11 Advection Theory of Ertel and Sjan-zsi-Li

Ertel and Sjan-zsi-Li have criticised the general advection theory of Rossby because when applied to practical cases, it turns out that according to this theory, more than half the day to day variations of surface pressure have to be attributed to changes of mass above 12 to 14 kms In particular they refer to an example discussed by Thomas, relating to the results of sounding balloon ascents over Lindenberg during the period 13th to 17th January 1930. Between these two dates there was an increase of surface pressure by 35 mms. of Hg over Lindenberg When Rossby's general advection theory is applied to this case it appears that more than three-fourths of the observed increase of surface pressure has to be attributed to advection of mass above 15 kms Since the atmospheric pressure at this height is only of the order of 90 mms of Hg, such a result is highly improbable.

Ertel and Li have therefore concluded that there is a fundamental error in Rossby's general advection theory They have preceded to work out new advection theory which gives the result

$$\delta_l p = \pi (z) \left[1 - \frac{g\rho}{\gamma} \int_0^z \frac{dz}{p}\right]. \qquad (56)$$

where $\delta_l p$ is the local change of pressure at the height z and $\pi(z)$ is the advective mass transport above this level It will be seen that equation (56) is identical with equation (28) of Rossby's special advection theory, when addition of mass takes place *above* a height H, $(z < H)$ so that $\pi(z)$ is a constant for $z < H$ In general, however, $\pi(z)$ is a function of the height z

Let us now examine the assumptions implicit in the advection theory of Ertel and Li. It follows from equation (56) that when $\pi(z) = 0$, then $\delta_l p$ is also equal to zero. That is, *the pressure variation at any level z is independent of addition or removal of mass below that level.* It is clear that if we make this assumption then equation (56) follows at once from equation (28). However, this assumption is *not* generally correct. It is true only in the very special case in which the adiabatic compression of every individual element in the column at a height z $(z < z)$ due to advective increase

of mass between z and z is exactly compensated by the adiabatic expansion of the element due to change in its internal pressure as a result of advection in the element That is

$$-\frac{1}{\gamma}[\pi(z)-\pi(z)]\frac{\Delta z}{p}=\frac{1}{\gamma}\delta_a p\frac{\Delta z}{p}$$

Hence, integrating:

$$-\frac{1}{\gamma}\int_0^z[\pi(z)-\pi(z)]\frac{dz}{p}=\frac{1}{\gamma}\int_0^z\delta_a p\frac{dz}{p}$$

Or

$$-\frac{1}{\gamma}\int_0^z\pi(z)\frac{dz}{p}+\frac{1}{\gamma}\int_0^z\delta_a p\frac{dz}{p}=-\frac{1}{\gamma}\pi(z)\int_0^z\frac{dz}{p}$$

Comparing with (46) and (47), we see that the left-hand side of the above equation is equal to $\alpha+\beta=\delta z$ Hence

$$\delta_i p=\pi(z)-\frac{\partial p}{\partial z}\delta z=\pi(z)\left[1-\frac{g\rho}{\gamma}\int_0^z\frac{dz}{p}\right]$$

We thus see that the advection theory of Ertel and Li is *not* a general theory as claimed by them On the other hand, their theory is not applicable to cases of arbitrary advection

Ertel and Li have applied their theory to the example discussed by Thomas and find that the results are in agreement with the calculations made by Thomas They have remarked that his fact constitutes a strong support for their theory since they think that Thomas has tackled the problem in a different way, namely by making use of the observed equality of pressure at 15 kms on the 13th and 17th January 1930 An examination of the calculations made by Thomas shows that this is not the case Thomas has tacitly assumed in equations (8), (9) and (10) of his paper that the variation of pressure at a level is caused *entirely* by change of mass *above* that level. The assumption on which his computations are based is therefore the same as that implicit in the advection theory of Ertel and Sjan-zsi-Li Hence it is not surprising that the results of Thomas agree with the formula of Ertel and Li, and this agreement cannot be regarded as independent support for the theory

12 Some General Remarks

While the advection theory of Ertel and Li is not generally valid, the general advection theory of Rossby is perfectly correct under the assumptions

on which it is built up If the theory leads to unreasonable results then, this must be attributed to the non-validity of the assumptions made Rossby has explicitly stated the following assumptions·

(1) all movements are adiabatic, radiation, heat conduction, turbulence, condensation and evaporation phenomena being excluded;

(2) no lateral expansion or contraction of the column takes place;

(3) advection at one level is independent of simultaneous advection at other levels,

(4) a layer of thickness dz is through the advection process replaced by another layer of the same thickness

Rossby has also stated that while the first of the above assumptions is generally justified, there can be large deviations from the conditions postulated by the remaining assumptions , hence, the assumptions made restrict the applicability of the theory to a special class of advection phenomena.

As a consequence of his assumption (3) Rossby assumes that in (4) above, *the pressure at the upper boundary of the advection layer dz remains constant during the displacement* This single assumption is practically the foundation stone of Rossby's theory and as we shall show below, is responsible for the unreasonable results to which the theory leads

Referring to Fig 4, let an addition of mass $\Delta M = \frac{\Delta \pi}{g}$ take place in an air column between the levels z and $z + \Delta z$ According to Rossby's theory, the column below z will be adiabatically compressed and the individual surface z will sink through the distance:

$$\delta a = -\frac{1}{\gamma} \quad \Delta \pi \int_0^z \frac{dz}{p}$$

Rossby assumes that the entire column above z will *bodily* sink through the distance δa As we have seen in Section 8, this will be the case only if the pressure at the upper boundary of the advection layer remains unaltered, that is, if $\delta_a p = 0$ In this case we have.

$$\Delta \pi = g \cdot \delta_a \rho \cdot \Delta z = g\rho \quad \Delta z \cdot \frac{\delta_a T}{T} = g \cdot \frac{p}{RT^2} \cdot \delta_a T \cdot \Delta z$$

This means that the advective increase of mass between z and $z + \Delta z$ is caused *entirely* by the replacement of the original air by a different sample of air having the same pressure but a lower temperature According to Rossby's theory, therefore, if $\delta_a T = 0$, then $\Delta \pi = 0$

Referring to equation (6) in Section 2, we see that the general advection term responsible for change of mass in an element dz of an air column is given by

$$\frac{\partial}{\partial x}(\rho u)+\frac{\partial}{\partial y}(\rho v)$$

$$=\left(u\frac{\partial\rho}{\partial u}+v\frac{\partial\rho}{\partial y}\right)+\rho\left(\frac{\partial u}{\partial x}+\frac{\partial v}{\partial y}\right)$$

$$=u\frac{\partial}{\partial x}\left(\frac{p}{RT}\right)+v\frac{\partial}{\partial y}\left(\frac{p}{RT}\right)+\rho\left(\frac{\partial u}{\partial x}+\frac{\partial v}{\partial y}\right)$$

$$=\frac{1}{RT}\left(u\frac{\partial p}{\partial x}+v\frac{\partial p}{\partial p}\right)-\frac{p}{RT^2}\left(u\frac{\partial T}{\partial x}+v\frac{\partial T}{\partial p}\right)+\rho\left(\frac{\partial u}{\partial x}+\frac{\partial v}{\partial y}\right)$$

Thus, the advection of mass in the element can be interpreted as resulting from three causes, *viz*

(i) Advection of air of the same temperature but different pressure;

(ii) Advection of air of the same pressure but different temperature,

(iii) Horizontal convergence or divergence of velocity

Rossby's theory takes account of only (ii) above

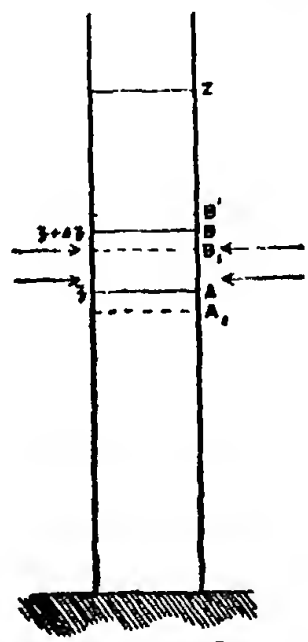

$AA_1 = BB_1 = \delta\alpha$.
$BB' = \delta\beta$
$BB' = \delta\alpha + \delta\beta$

FIG. 6

To see how Rossby's theory can give rise to erroneous results, let us assume that (i) and (ii) above are zero, and (iii) alone is operative. In this case (*vide* Fig 6), the increase of mass in the element Δz in time dt is given by:

$$\rho\left(\frac{\partial u}{\partial x}+\frac{\partial v}{\partial y}\right) dt \quad \Delta z = \frac{\Delta \pi}{g}.$$

Increase of density inside the element $(\delta_a \rho) = \frac{1}{g}\frac{\Delta \pi}{\Delta z} = -\frac{1}{g}\frac{d\pi}{dz}$.

Increase of pressure inside the element $(\delta_a p) = RT \quad \delta_a \rho = -\frac{RT}{g}\frac{d\pi}{dz}$.

As a consequence of the addition of mass, the column below z will be adiabatically compressed and the individual surface z will move downwards through the distance

$$\delta a = -\frac{1}{\gamma} \quad \Delta \pi \int_{z}^{z} \frac{dz}{p}$$

At the same time, the stratum between z and $z + \Delta z$ will expand adiabatically (*vide* Section 8) through the distance.

$$\delta_l \beta = \frac{1}{\gamma} \cdot \delta_a p \quad \frac{\Delta z}{p}.$$

The net downward displacement of the individual layer at z is given by:

$$\delta z = \delta a + \delta \beta$$

Since δa and $\delta \beta$ are opposite in sign and δa is negative, $\delta z > \delta a$ Let us assume that δz is positive This means that the entire column above z is bodily lifted up through the distance δz and so there will be a *local increase* of pressure at all levels above the layer of advection A sounding through the column before and after the advection will therefore show local increase of pressure at *all* levels. If we apply Rossby's equation (54) to this case, it will be seen that we get a finite value of π greater than $\delta_l p$ at *all* levels in the column With increasing height and decreasing values of $\delta_l p$, the value of π will tend towards a constant determined by the limiting value of the integral in Rossby's equation. We would thus be led to the obviously erroneous result that an appreciable part of the observed increase of pressure at the surface is due to addition of mass at levels at which the absolute value of pressure is small. Thus, by neglecting the effect of horizontal convergence and divergence of velocity, Rossby's theory over-emphasises the importance of the higher levels,—a feature which led Ertel and Li to seek a flaw in Rossby's theory.

The author was led to the present investigation as the result of a discussion with Diwan Bahadur Dr. K. R. Ramanathan in May 1945.

Summary

The paper contains a critical survey of the problem of pressure and temperature fluctuations in the atmosphere. If we exclude non-adiabatic processes, then changes of pressure and temperature are essentially due to horizontal and vertical movements in the atmosphere The vertical distribution of pressure over the globe shows that horizontal movements (advection) can give rise to large changes of pressure especially in the middle latitudes. The problem of identifying the layer or layers in which addition or removal of mass has taken place due to advection, from the data furnished by aerological ascents over a station has been tackled by a number of investigators Rossby considered the general problem of advection in several layers of an atmospheric air column, but his theory when applied to practical cases yields results which are often unreasonable Ertel and Sjan-zsi-Li considered the same problem some years later and claimed to have discovered a fundamental error in Rossby's theory In the present paper this problem is considered at some length It is shown that Rossby's theory is quite correct under the assumption on which it is built up while the theory of Ertel and Li is not valid for cases of arbitrary advection. It is shown that the neglect of horizontal advection of pressure and horizontal convergence and divergence of wind velocity is responsible for the obviously unreasonable results furnished by Rossby's theory when applied to actual examples

References

(*Note*—Since this investigation was completed the author has come across a paper by Geirmundur Arnason entitled "Distribution of Mass Variations in Atmospheric Air Columns," published in *Meteorologiske Annaler*, Band I, Nr 10 The theory of Ertel and Li has also been criticised by Arnason.)

1 V Bjerknes, J Bjerknes, H Solberg and T Bergeron — *Physikalische Hydrodynamik*, 1933, 741-54
2. W. H Dines — *Geophys Mem.*, 1919, No. 13, 67
3 H. Ertel — *Ger. Beit z Geophys*, 1931, 17, No 2
4. ——— and Sjan-zsi-Li — *Zeit f Phys*, 1934, 94, 222.
5. F Exner — *Köppen-Heft der Ann. d Hydrogr*, 1926
6 Th. Hesselberg — *Met Zeit*, 1915, 32, 311
7. B. Hurwitz — *Ibid*, 1927, 44, 253.
8. ——— — "*Dynamic Meteorology*", 1941.
9. E. Palmén — *Beit. z. Phys. d. frie. Atmos.*, 1934, 17, No. 2
10. A. Refsdal — *Geofys. Publik*, 1937, 11, No 13
11. C G. Rossby — *Beit z Phys d. frie Atmos*, 1927, 13, 163
12. ——— — *Ibid.*, 1928, 14, 240
13. L. Steiner — *Met Zeit*, 1926, 43, 271.
14. ——— — *Beit. z. Phys. d. frie. Atmos*, 1934, 21, 323.
15. H. Thomas — *Sitz. d Preuss Akad. d. Wiss*, 1934, 17, 222.
16. A. Wagner — *Handbuch der Klimatologie*, Band I, Teil F, *Klimatologie der frien Atmosphäre*, 1931, 67.

DETERMINATION OF THE MAGNETO-OPTIC ANOMALY OF SOME GLASSES

By S Ramaseshan

(From the Department of Physics, Indian Institute of Science, Bangalore)

Received for publication on October 16, 1946

(Communicated by Sir C V Raman, Kt, F R S, N L)

1 Introduction

Darwin and Watson (1927) have shown that in many substances the magnitude of the Faraday effect is expressible by a formula of the Becquerel type, *viz*,

$$V = \gamma \lambda \frac{dn}{d\lambda} e/2\, mc,^2$$

where V is Verdet's constant, e and m are the electronic charge and mass respectively, c is the velocity of light, λ is the wavelength of light and n the refractive index of the subtstance γ is a factor, called the magneto-optic anomaly, which is constant throughout the visible and the ultraviolet regions of the spectrum provided the contribution to the dispersive power made by the infra-red absorption bands is eliminated from the formula No reference to the data for glasses appears in the paper of Darwin and Watson The present investigation was undertaken to fill this gap in the literature and to find whether the Becquerel formula is valid for glasses and if so to ascertain how the magneto-optic anomaly depends on the composition of the glass. Most of our knowledge of the magneto-optic behaviour of glasses is due to du Bois (1894) and to Ingersol (1917) The former measured Verdet's constant for the sodium line λ 5893 in nine glasses, while the latter studied the dependence of the constant on the wavelength in five glasses The present paper records the values of Verdet's constant determined for λ 5893, λ 5461 and λ 4358 with 18 optical glasses made by the firm of Schott at Jena as well as of their dispersive powers for a test of the validity of the Becquerel formula. The results disclose the existence of interesting relationships between the composition and the magneto-optic anomaly.

2 Materials and Methods

The specimens studied formed a set of eighteen optical glasses presented to Prof. Sir C V Raman by Messrs. Schott & Co, Jena, and had the form

of rectangular blocks 3 × 3 × 2 cm having all but two of the sides polished. The thickness of each glass did not deviate by more than 0 003 cm from 2·000 cm. Table I gives the list of glasses studied, their melting numbers, approximate composition and density as supplied by the manufacturers.

TABLE I

List of Glasses Studied

Serial No	Melting No	Chemical composition		Density	n_{5893}	100γ
		More than 10%	Less than 10%			
1	25188	SiO_2, B_2O_3, Al_2O_3, K_2O	Na_2O F	2·3	1 46693	67
2	18415	SiO_2, B_2O_3, K_2O	Al_2O_3	2 3	1 49340	67
3	16776	SiO_2, K_2O	Al_2O_3, Na_2O, CaO	2 4	1 50228	73
4	23975	SiO_2, B_2O_3, ZnO	Al_2O_3, Na_2O	2 5	1 50933	72
5	24906	SiO_2 B_2O_3	Na_2O K_2O BaO	2 5	1 51714	71
6	22601	SiO_2, B_2O_3, Sb_2O_3	Al_2O_3, Na_2O, K_2O	2 7	1 52998	68 5
7	23125	SiO_2, Na_2O, PbO	ZnO	2 7	1 52686	78 7
8	22638	SiO_2, PbO	Na_2O, K_2O	2 9	1 54495	77 4
9	24464	SiO_2, ZnO, BaO	B_2O_3, Na_2O K_2O, PbO	3 1	1 57000	74
10	19510	SiO_2 PbO	Na_2O, K_2O	3 2	1 56991	77
11	23355	SiO_2, B_2O_3, BaO	Al_2O_3, Na_2O	3 3	1 58950	67 0
12	20672	SiO_2, PbO	B_2O_3, Na_2O K_2O	3 4	1 59813	77 4
13	22966	SiO_2, BaO, PbO	Na_2O, K_2O, ZnO	3 5	1 60620	76 2
14	23441	SiO_2, PbO	Na_2O, K_2O,	3 9	1 64712	77 6
15	21497	SiO_2, BaO, PbO	Na_2O, K_2O, ZnO	3 9	1 64917	77 4
16	23850	SiO_2, PbO	Na_2O, K_2O	4 4	1 7130	77
17	23590	SiO_2, PbO	Na_2O K_2O	5 1	1 7850	78
18	S1075	SiO_2 PbO	B_2O_3 K_2O, Sb_2O_3	6 7	1 8900	78

The refractive indices of the glasses were determined with the aid of a Pulfrich refractometer. The differences in refractive indices for different wavelengths could be determined with an accuracy of 2 or 3 units in the fifth place of decimals. Even so, the dispersion values were accurate only to one or two per cent. The refractive indices were determined for λ 5893, λ 5461 and λ 4358 and the constants in the dispersion formula

$$n^2 = A + B\lambda^2/(\lambda^2 - \lambda^2_0)$$

were evaluated. The values of $\lambda \frac{dn}{d\lambda}$ for different wavelengths were calculated. As the glasses 16, 17 and 18 had refractive indices much higher than the prisms supplied with the refractometer, their dispersions are not so accurate as those of the other glasses. Table II gives the refractive indices and the values of $\lambda \frac{dn}{d\lambda}$ of the glasses for different wavelengths.

An electromagnet of the Rutherford type with the distance between the polepieces 22 mm. was used in the work When 7 amperes were passed

TABLE II

Dispersion Data for Glasses

No	n_{5893}	n_{5461}	n_{4358}	$\lambda\frac{dn}{d\lambda}_{5893}$	$\lambda\frac{dn}{d\lambda}_{5461}$	$\lambda\frac{dn}{d\lambda}_{4358}$
1	1·46693	1 46868	1 47575	0 02316	0 02482	0 03897
2	1 49340	1 49522	1 50266	0 02217	0 02509	0 04130
3	1 50228	1 50430	1 51282	0 02457	0 02879	0 04649
4	1 50933	1·51138	1 51968	0 02501	0 02912	0 04578
5	1 51714	1 51910	1 52715	0·02393	0 02782	0 04356
6	1 52998	1 53249	1·54295	0 03045	0·03584	0 05892
7	1 52686	1 52939	1 53992	0 03087	0 03592	0 05614
8	1 54495	1 54782	1 55999	0 02478	0 04103	0 06814
9	1 57000	1 57243	1 58273	0 02938	0 03481	0 05891
10	1 56991	1 57320	1 58712	0 03979	0 04712	0 07945
11	1 58950	1 59183	1 60171	0 02822	0 03331	0 05637
12	1 59813	1 60190	1 61801	0 04551	0 05408	0 09317
13	1 60820	1 60962	1 62408	0 04124	0 04883	0 08279
14	1 64712	1 65182	1·67209	0 05666	0 06754	0 1174
15	1 64917	1 65335	1 67116	0 05052	0 05986	0 1023
16	1 7130	1 7191	1 7434	0·074	0 089	0·159
17	1 7850	1·7932	1·8281	0 097	0 116	0 210
18	1 8900	1 8990	1 9430	0 123	0 149	0·282

through the coils of the magnet, a field of 17200 gauss was developed A pair of wide-angle nicols were used as polariser and analyser and the angles measured were to 0 05 of a degree and this gave an accuracy of about ½%. It was considered that a greater accuracy was not necessary as the dispersions were accurate to 1% only Conductivity water whose Verdet's constant is accurately known (V_{5461} = 0 01547 at 25° C) was used as the standard for the determination of the field 1·24 cm of water gave a rotation of 3·30° when 7 amperes were passed through the coils of the magnet. The field developed was, therefore, 17200 gauss

A sodium lamp and a mercury point-o-lite lamp with suitable filters were used as the different sources of light for the measurement of the Verdet's constant of the glasses. If the glasses were kept exactly normal to the incident light, it was difficult to determine the true crossing position when the magnetic field was put on This was due to the fact that light which comes to the analyser after two reflections at the surfaces of the glass was not rotated through the same angle as that which came without any reflection. To avoid this the glasses were turned through a small angle (about ½°) away from the normal position Usually a mean of about 20 readings was taken to determine each crossing position. Table III gives the actual rotation ρ due to a field of 17200 gauss), the Verdet's constant V, and the anomaly γ for the three wavelengths λ 5893, λ 5461 and λ 4358 for the 18 glasses.

TABLE III

Magneto-optic Data for Glasses

Serial No.	λ 5893			λ 5461			λ 4358		
	ρ in degrees	V min /cm gauss	γ %	ρ in degrees	V min /cm gauss	γ %	ρ in degrees	V min /cm gauss	γ %
1	5 15	0 0149	64 2	5 80	0 0169	67 4	8 95	0 0260	66 3
2	5·10	0 0148	66 4	5 65	0 0170	67 8	9 5	0 0276	68 4
3	6 35	0 0185	74 6	7 35	0 0214	73 7	11 40	0 0332	71 0
4	6 25	0 0182	72 1	7 40	0 0215	73 3	11 25	0 0327	71 0
5	5·90	0 0172	71 2	7 00	0 0204	72 6	10 50	0 0305	69 6
6	7·25	0·0211	68 7	8 50	0 0247	68 5	13 85	0 0403	67 8
7	8 20	0 0239	76 7	9 80	0 0285	78 8	15 45	0 0449	79 4
8	9 35	0 0272	77 6	11 00	0 0320	77 4	18 25	0·0531	77 3
9	7 80	0 0227	76 6	8 95	0 0260	74 2	14 75	0 0429	72 3
10	10 65	0 0310	77 3	12 70	0 0369	77 8	21 10	0 0614	76 7
11	6 75	0 0196	69 0	7 70	0 0224	66·7	12 95	0 0377	66 3
12	12 25	0 0356	77 7	14 50	0 0422	77·4	24 80	0 0721	76 9
13	10 85	0 0316	76 0	12 95	0 0377	76 6	21·75	0 0633	75 9
14	15 10	0 0439	76·9	18 20	0 0529	77 8	31 75	0 0953	78 0
15	13 35	0 0388	76·3	16 05	0·0467	77 4	27 45	0 0799	77 5
16	19 80	0 0576	77	23 85	0 0694	77	42 25	0 123	77 0
17	26 15	0 0761	78	31 30	0 0910	78	55 45	0 164	78 0
18	33·25	0 0969	78	40 55	0 1180	78	76 75	0 223	78 0

3 DATA FOR FUSED SILICA AND QUARTZ

Cotton (1931) has determined the Verdet's constant of vitreous silica for three wavelengths, λ 5780, λ 5461 and λ 4358 The constants were redetermined for the above wavelengths as well as for λ 5893 using a plate of 8 40 mm thickness. The values obtained were within ½% of those obtained by Cotton $\lambda\, dn/d\lambda$ for this substance was calculated from the dispersion formula

$$n^2 = 1\ 36112 + \frac{0{\cdot}74655\,\lambda^2}{[\lambda^2 - (0\ 107044)^2]} - 0\ 01350\,\lambda^2,$$

where λ is expressed in microns The last term which is due to the infra-red absorption is omitted in the calculation. Table IV gives the optical and

TABLE IV

Magneto-optic Data for Fused Quartz

Wavelength in A. U	Refractive Index	Verdet's constant		γ%
		Cotton	Author	
5893	1·4585	..	0·01421	78·1
5780	1 4590	0·01479	0·01491	78·1
5461	1 4601	0·01571	0·01664	78·1
4358	1·4667	0·02602	0·02840	78·2

magneto-optical constants of vitreous silica for the four wavelengths mentioned above.

A large number of workers (1903, 1912, 1917) have devoted themselves to the study of the Verdet constant of quartz for different wavelengths in the spectrum Actual measurements extend from 20000 A° to 2000 A° $\lambda\, dn/d\lambda$ is calculated from the dispersion formula

$$n^2_w = 3\ 53445 + \frac{008067}{[\lambda^2 - 0{\cdot}00127493]} + \frac{0\ 002682}{[\lambda^2 - 0\ 000974]} + \frac{127\ 2}{[\lambda^2 - 108]},$$

where n_w is the ordinary refractive index and λ is the wavelength expressed in microns Here also the last term is omitted in the calculation. Table V gives the Verdet's constant, and for the value of γ different wavelengths

TABLE V

Magneto-optic Data for Crystalline Quartz

Wavelength	Refractive Index	Verdet's Constant	γ %
20000	1·5199	0 001266	71
16000	1 5270	0 002106	75·4
12000	1 5323	0 003727	75 1
8000	1·5383	0·008802	79·0
5893	1 5443	0·01564	78 9
5460	1 5462	0 01952	78 5
5085	1 5482	0 02257	77 1
4799 9	1·5501	0·02574	78 5
4358	1·5538	0 03081	78 5
4045	1 5572	0·03555	74 4
3612	1 5635	0 04617	74·5
2573	1·5962	0·1079	75·4
2194 6	1 6250	0 1586	69 9

4. DISCUSSION OF RESULTS

It will be seen from Table V that the Becquerel formula is obeyed by quartz for the visible spectrum There appears to be a small drop in the value of γ in the infra-red and the ultra-violet regions, but more accurate measurements are needed before the data could be accepted as indicating a real variation of γ with wavelength in quartz Although the data for fused quartz (Table IV) are not so extensive as those for crystal quartz, it is seen that γ is sensibly constant in the visible region It is worthy of remark that the values of γ for fused quartz and crystal quartz are practically identical, and this is particularly remarkable in view of the large difference in density and refractive indices of the two substances.

An examination of Table III shows that the value of γ is independent of wavelength in many of the glasses Nevertheless, there are a few glasses in the list (Nos 1, 3, 9 and 11) in which γ is apparently not constant Since these variations in γ mostly occur in glasses of low dispersive power, they may be ascribed to inaccuracies in the measurement of the refractive indices. But a more probable reason is that the dispersion due to the infra-red term has not been eliminated (as has been done in quartz and fused silica) in calculating the value of $\lambda\, dn/d\lambda$ for the glasses The variation in the value of γ in glass No 9 is probably too large to be explained on these lines In general, however, one could say that most of the glasses studied obey the Becquerel formula, the γ value of each glass being approximately constant for the visible spectrum. The mean value of γ of each glass has been incorporated in Table I.

A study of Table I reveals many interesting facts All the glasses which do not contain B_2O_3 or Al_2O_3 have values of γ lying between 76% and 78%, thus differing very little from the values for fused and crystalline quartz. This is all the more remarkable when one considers the large variations in composition, density and dispersive power of the glasses. For instance, in spite of the dispersion of glass No 18 being four times that of glass No 7 the γ factor is not appreciably different. The variations in content of PbO and ZnO—which are principally responsible for the large dispersion and high density in some of the glasses—do not appear to involve any noticeable variations in the magneto-optic anomaly.

The presence of B_2O_3 seems to have a large influence on the γ value of a glass All borate glasses have low γ values, γ being lower in glasses having a higher percentage of B_2O_3 Glass No 1 and No. 2 which contain more than 10% of B_2O_3 have lower γ values than glass No 9 which has less than 10% of B_2O_3. The results with glass 3 seem to suggest that Al_2O_3 also depresses the γ value of a glass The simultaneous presence of B_2O_3 and Al_2O_3 is obviously the cause of the very low value of γ in glasses No 2, 6 and 11 It would seem that the presence of trivalent elements not only diminishes the dispersive power of a glass but also has the effect of diminishing the magneto-optic rotation in a still greater proportion, and that on the other hand, γ is practically the same for all silicate glasses which do not contain the trivalent elements

In conclusion, the author wishes to thank Prof Sir C V Raman for his kind advice and encouragement during this investigation

5. Summary

The paper records the values of Verdet's constant determined for λ 5893, λ 5461 and λ 4358 with 18 silicate glasses made by Schott & Co., Jena. The dispersive powers of the glasses have also been measured It is found that most of the glasses obey a modified Becquerel formula, in which the multiplying factor γ is practically constant over the visible spectrum The γ factor for fused quartz and crystalline quartz for different wavelengths have also been calculated It is found that the value of γ for both the substances is about 78% All the glasses which do not contain B_2O_3 or Al_2O_3 have γ values lying between 76% and 78% in spite of large variations in composition, density and dispersive power, the presence of the heavy elements like Pb, Ba and Zn in varying proportions having no influence on the γ value. On the other hand, trivalent elements like Boron and Aluminum when present in glasses diminish γ to values between 67% and 74% depending on the amount of B_2O_3 or Al_2O_3 present

References

Borel — *Archives des Sciences Phys et nat*, 1903, 16, 24 & 157
Cotton . *Comp Rendus*, 1931, 192, 1166
Darwin & Watson — *Proc Roy Soc Lond*, 1927, 114 A, 474
Disch .. *Ann der Physik*, 1903, 12, 1153
du Bois — *Ibid*, 1894, 51, 537
Ingersol — *Phys Rev*, 1917, 9, 257
Lowry — *Phil Trans*, 1912, 212 A, 261

UMBILICAL PROJECTION*

By Sahib Ram Mandan
(*Lecturer, Fateh Chand College for Women, Lahore*)

Received February 8 1944
(Communicated by Prof B S Madhava Rao, F A SC)

The purpose of the paper is to illustrate the use of Umbilical Projection and establish a few theorems relating to certain sets of circles and families of coaxal circles in a plane by making use of a number of known results in space.

We start with a quadric Q in space and note the following correspondence:

Space S	Plane II
(i) A *plane* section of Q	A *Circle*
(ii) Two planes determine a *line*.	A *family* of coaxal circles is determined by two circles
(iii) Lines in a plane	Families *having a circle common* will be said to be "*intersecting*"
(iv) *Conjugate* planes for Q	*Orthogonal* circles
(v) Planes through a *point*	A *congruence* of circles that have *One circle common with a general family* will be said to be *linear* †
(vi) Tangent planes of a *quadric*	*A congruence of circles* that have *two circles common with a general family* will be said to be *quadric* †
(vii) Tangent planes of a *cone*	A *series of circles* that have *two circles common with a linear congruence* will be said to be *conic* †
(viii) Tangent planes of a *cubic developable*.	A *series of circles* that have *three circles* common *with a linear congruence* is said to be *cubic* †

* Read at the meeting of the Mathematical Society of the Panjab University, held on the 16th March 1942, in continuation of the paper published by the author in the *Proc. Ind Acad. Sci.*, Bangalore, 1942, 15A, No 1

† Coolidge, *A Treatise on the Circle and the Sphere*, pp 161, 157, 159

Space S.	Plane II
(ix) *Polar lines* for Q	*Conjugate families* of coaxal circles
(x) *Conjugate lines* for Q	Two families will be said to be '*polar*' when the *conjugate* of one intersects the other *The relation is mutual*
(xi) A *self-polar tetrahedron* for Q	*Four mutually orthogonal circles* will be said to form a '*self-orthogonal tetrad,*' *for the family determined by two of them is conjugate to that of the other two*
(xii) *A self-conjugate pentad* for Q	*Five circles, related in the manner that the circle orthogonal to three of them belongs to the family determined by the other two, will be said to form a 'self-orthogonal pentad'*
(xiii) *A self-conjugate hexad* for Q	*Six circles, related that the circle orthogonal to three of them and the other three belong to a linear congruence will be said to form a 'self-orthogonal hexad'*
(xiv) *Moebius Tetrads*	*Two tetrads* of circles ABCD and $A_1B_1C_1D_1$ will be said to be *Moebius* if a circle of one tetrad, say A_1 and three of the other tetrad, say B, C, D, belong to a linear congruence *The relation between the two is mutual.*
(xv) *Reciprocal Tetrahedra* for Q	*Two tetrads* of circles ABCD and A'B'C'D' will be said to be *reciprocal* if a circle of one, say A' is orthogonal to three of the other, say B, C, D and A, A'; will be said to be *corresponding circles* while BC, B'C', *Corresponding families*
(xvi) A *set of eight associated planes.*	The *eight circles* common to three independent quadric congruences will be said to form a *set of associated circles.*
(xvii) A *hexagon* ..	*Six circles* in general give rise to 15 *families that arrange into* 60 *'hexads'*

Space S	Plane II
	of the nature that every given circle belongs to *two families of a hexad* Two families of a hexad will be said to be *opposite* if the four circles determining them belong one to each of the other four families of the hexad
(xviii) *Double-six of lines*	*Two sets of six families each* will be said to form a *double-six* if five of one set are intersected by a family of the other set
(xix) *Opposite edges of a tetrahedron*	Given a *tetrad of circles*, they determine six families, two of them will be said to be *opposite* if they include all the four circles There are *three pairs of opposite families*

Now we are in a position to state the following theorems on circles in a plane without giving the details of the corresponding propositions, in space, that are hinted in brackets *wherever necessary* at the end of the theorem.

1. (i) *A linear congruence of circles is determined by three circles* in the manner that all the circles that are orthogonal to the circle orthogonal to the given three belong to it

(ii) *A family and a circle also determine a linear congruence*

(iii) Two families belonging to a linear congruence intersect

(iv) Two linear congruences have a family common

(v) Three linear congruences have a circle common

2 If A_1BCD, AB_1CD, ABC_1D, $ABCD_1$, $A_1B_1C_1D$, $A_1BC_1D_1$, $A_1B_1CD_1$ be tetrads of circles belonging to seven linear congruences respectively, A, B_1, C_1, D_1 also belong to a linear congruence (*Moebius tetrads*)

3 *If the families determined by pairs of circles AA', BB', CC' have a circle common, the circles common to the pairs of families BC, $B'C'$, CA, $C'A'$, AB, $A'B'$ are coaxal and conversely The theorem holds even if the six circles belong to a linear congruence* (*Desargue's theorem*)

4. Let A', B', C' be the circles of the families conjugate to those determined by the pairs of circles QR, RP, PQ common with the linear

congruence determined by the circles A, B, C such that the families AA', BB', CC' have a circle common, then, if P', Q', R' be the circles of the families conjugate to BC, CA, AB, common with the linear congruence PQR, the families PP', QQ', RR' have a circle common (B3*, Ex 8, p 42)

5 (i) *Two circles, one from each of two given families can be found to be coaxal with a given circle*

(ii) If OHD_1, O_1KB be circles of two families of coaxals, the three pairs of circles L, M, N, C, A, P of pairs of families OK, O_1H, HB, KD_1, D_1O_1, BO coaxal with a given circle D *belong to a linear congruence. Let B_1 be a circle of this congruence,* then the three pairs of circles L_1, M_1, A_1, P_1; N_1, C_1 of the above families coaxal with B_1 belong to *another linear congruence that will contain D The tetrads ABCD and $A_1B_1C_1D_1$ obtained here are Moebius* (B3, Ex 10, p 63)

(iii) *If the given families intersect, then the three pairs of above families also intersect and the circles common to the pairs are coaxal (Pappus' theorem)*

6 (i) Given three families of coaxal circles, there are ∞^1 families intersecting them forming a system. The aggregate of the circles of the two systems of families form a quadric congruence such that each circle belongs to two families one from each system

(ii) The circles common to a quadric congruence and a linear congruence form a conic series.

(iii) A linear congruence containing a family of a quadric congruence contains another also.

(iv) *Two quadric congruences can have two conic series, a family and a cubic series, two intersecting families and a conic series or four families common such that the two conic series have two circles common; the cubic series and the family also have two circles common*

7. (i) *There are two families of coaxal circles intersecting four general families of coaxals*

(ii) Take five arbitrary families of coaxal circles. By omitting each in turn we obtain five sets of four families each; and these four families have got two families intersecting them; we again have two circles one from each of these two families coaxal with a given circle; the ten circles so obtained belong to a linear congruence (B3, Ex 14, p. 66).

* B3 refers to H. F. Baker, *Principles of Geometry*, Vol. 3, here as well as in what follows.

(iii) If the five families intersect another family, then each set of four families has one other family intersecting them, the five families so obtained also intersect a new family We thus obtain two sets of six families each forming a *double-six* (B3, p 159)

8 If the pairs of opposite families of a *hexad determined by six given circles* be intersecting, the six families will belong to a quadric congruence in which case we shall have *six circles*, one from each family, *belonging to a conic series common* to this congruence and a linear congruence. These six circles *will also give rise to* 60 *hexads of families* With the property that *the circles common to the pairs of opposite families of a hexad are coaxal* (B3, *Dandelin's figure of six generators of a quadric forming a skew hexagon leading to Pascal's theorem for hexagon inscribed in a conic*, p 45)

9 *Given a tetrad of circles, we shall have two circles from each pair of opposite families of the tetrad coaxal with a given circle giving rise to six circles, similarly we have six other circles corresponding to another given circle The twelve circles so obtained belong to a quadric congruence.* (B3, Ex 17, p 54)

10. *If circles be drawn coaxal with a family of a given tetrad of circles passing through the points of intersection of the circles of the opposite family, the twelve circles so obtained belong to a quadric congruence.* (B3, Ex 16, p. 54)

11 *If PP', Q.Q' be pairs of orthogonal circles and f, f' be the respective conjugate families of those determined by P, P' and Q, Q', then f, f', P, P', Q, Q' belong to a quadric congruence* (B3, Ex 13, p 52)

12 (i) If ABCD, A'B'C'D' be *two reciprocal tetrads of circles, the families determined by the pairs of corresponding circles AA', BB', CC', DD' belong to a quadric congruence called* ϕ (*ABCD*) (B3, Ex 7, p 41)

(ii) Consider the twelve points of intersection of the six pairs of circles of the tetrad ABCD Three of these lying on A, B, C define a circle. We may thus, in thirty-two ways, specify four circles each of which contains three of the points, no two of these circles intersect in one of the twelve points. If we consider the family determined by D' and the circle through the three points chosen on A, B, C and the three families determined by A', B', C' taken respectively with the corresponding circles, the four families so obtained belong to a quadric congruence (B3, Ex 15, Pp 53).

13. *Cubic series of circles* (B3, pp 129, 135, 140)

(i) *Six circles in general determine the series* If seven circles of the series be common with a quadric congruence, the whole series belongs to the congruence

(ii) We can have *two series belonging to a quadric congruence having five given circles common*

(iii) Three independent, quadric congruences can be constructed to contain the six circles A, B, C, A′, B′, C′ and containing the pairs of families determined by B′ C, BC′, CA′, C′A, AB′, A′B respectively, then these quadric congruences have further a family common which has got two circles common with the series determined by the above six circles

(iv) *Given five circles and a family of circles, we can construct a series which contains the given circles and has two circles common with the family, but we cannot in general construct a series to contain four given circles and having two circles common with each of two given families unless the circles and the families belong to a quadric congruence, further a series can be constructed containing three circles, and having two circles common with each of three given families, again four families can have two circles common with a series containing two circles given*

(v) *A unique cubic series exists having two circles common with each of five given families in general and containing a given circle, infinite number of such series exist if the families are intersected by some other family*

(vi) *There exist ten families that will have two circles each common with both of two given cubic series, hence it can be shown that there exist six cubic series having each two circles common with every one of six given families in general* (B3, pp. 141–42)

14 *Set of eight associated circles* (B3, p 154)

(i) *The quadric congruences having seven circles common have an eighth common.*

(ii) *The circles of two self-orthogonal tetrads and those of Moebius tetrads form two sets, hence Moebius tetrads can consist of two self-orthogonal tetrads in a special case*

(iii) *The cubic series determined by six circles of the set will have two circles common with the family determined by the remaining circles of the set.*

(iv) If the circles of the set be denoted by 1, 2, 3, 4, 5, 6, 7, 8, the family common to the congruences (linear) determined by 123 and 567 intersects the family determined by the circles common to the family 34

and the congruence 678 and the circle common to 45 and 812, hence it follows that four families common to the pairs of congruences 123, 567, 234, 678, 345, 781, 456, 812 belong to a quadric congruence

(v) Let 2, 3, 4, 5, 7, 8 be any six circles and 1 a further circle; let P, P′, Q, Q′; R, R′ be the pairs of circles from the pairs of families 23, 57, 78, 34, 45, 82, coaxal with 1 The families QR′, RP′, PQ′ and Q′R, R′P, P′Q belong to a quadric congruence Let P_1, Q_1', R_1, P_1', Q_1, R_1' be the other circles, common with this congruence, of the families 23, 34, 45, 57, 78, 82 respectively, then the families P_1, P_1' Q_1Q_1', R_1R_1', have a circle common say 6 completing the set

15 (i) *If* $x_i = 0$ $(i = 1, 2, 3)$ *be equations*† *of three independent quadric congruences,* $\theta^2 x_1 + \theta x_2 + x_3 = 0$ *represent a system of quadric congruences out of which there are eight of a particular type* that are determined by a circle and a conic series, the eight circles determining these eight congruences form a set of associated circles* (*Math Student*, June 1942, X, Q 1809)

(ii) *If three quadric congruences of circles have a family common they have four more circles common, if they have a conic series common, they have two more circles common* (B3, Ex, 4, p 154)

16 (i) *If two pairs of opposite families of a tetrad of circles be conjugate the remaining families are also conjugate and the tetrad is self-orthogonal*

(ii) *If two pairs of opposite families of a tetrad of circles be polar, the remaining families are also polar, similarly behave the reciprocal tetrad.*

(iii) *The families determined by the corresponding pairs of circles here have a new circle common forming with either of the tetrads a self-orthogonal pentad The pairs of corresponding families are intersecting, giving six more circles that are orthogonal to the new circle obtained above We have thus got* 15 *circles in all such that each one is orthogonal to six of them that are coaxal by threes forming four families In fact, there are* 15 *circles,* 20 *families constituting* 10 *pairs of conjugate as well as polar families, and* 15 *linear congruences with the property that each circle belongs to four families and six congruences, each family contains three circles and belongs to three congruences, each congruence contains six circles and four families. The* 15 *centres of the circles are collinear by threes in* 20 *lines, four through each centre, forming* 15 *quadrilaterals whose vertices are the centres, each*

* Coolidge, *loc cit*, pp 161 and 165, Th. 54.

vertex is common to six quadrilaterals which have a line common by threes. (B3, Ex 5, p. 35)

17 As a special case we can construct *a self-orthogonal pentad consisting of three point-circles and two proper circles*· Let AB'CA'BC' be a hexagon such that every pair of adjacent sides are circular lines; if D, E, F be the meet of the opposite sides, the circles DEF, ABC and the point-circles A', B', C' or the circles DEF, A'B'C' and the point circles A, B, C form the required pentad (B3, Ex 9, p. 44)

18. If ϕ (ABCE) be a quadric congruence constructed in the manner of § 12 where E is a circle of the congruence ϕ (ABCD), the two congruences have a family common, with D' as a member and ϕ (ABCE) contains the circle D If F be the circle of ϕ (ABCE) common to the family having E as a member, intersecting the families AA', BB', CC', other than E, the *six circles ABCDEF form a self-orthogonal hexad In particular, if the circles D', E, F are coaxal, the circles A B C E F form a self-orthogonal pentad* (B3, Ex 10, p 47)

19. *A self-orthogonal tetrad or pentad taken with any other circle form a self-orthogonal pentad or hexad of circles respectively*

20 *If the circles of either a self-orthogonal tetrad, pentad or hexad belong to a quadric congruence or a cubic series, an infinite number of such sets of circles can be found to belong to the congruence or the series* (B3, Ex 12, p 50; Ex 27, p 145)

21 . *Let a, b, c be the linear congruences of circles orthogonal to the circles A, B, C respectively, and p, q, r be the families of coaxals common to the pairs of congruences b, c, c, a; a, b respectively; then the congruences Ap, Bq, Cr have a family common*

22 *If a variable family of coaxals moves about so that three fixed circles of it belong to three fixed linear congruences respectively, any fourth fixed circle of the family will then generate a quadric congruence.* (*Salmon*, Vol. I, p. 118, Ex 14).

23 *If the variable families of a hexad contain each a fixed circle and five circles of the hexad belong each to a linear congruence, the sixth circle of the hexad then generates a cubic series* (*Salmon*, Vol. I, Ex. 5, p. 145).

A CONGRUENCE PROPERTY OF $\tau(n)$

By Hansraj Gupta

(Government College, Hoshiarpur)

Received August 27, 1946

(Communicated by Prof B S Madhava Rao)

Ramanathan and, more recently, Bambah and Chowla have proved by different methods involving the use of certain relations between Ramanujan's functions P, Q and R, that

$$\tau(n) \equiv n\,\sigma_3(n) \pmod 7 \tag{1}$$

where $\tau(n)$ is defined by the relation

$$\sum_1^\infty \tau(n)\, x^n = x\,\{(1-x)(1-x^2)(1-x^3)\quad\}^{24},\ |x| < 1; \tag{2}$$

and

$$\sigma_3(n) = \sum_{d|n} d^3 \tag{3}$$

I give below a proof which is independent of such relations All congruences are modulo 7

We have

$$\sum_1^\infty \tau(n)\, x^n = x\,\{\prod_1^\infty (1-x^r)\}^{21}\,\{\prod_1^\infty (1-x^r)\}^3$$

$$\equiv x\,\{\prod_1^\infty (1-x^{7r})\}^3\,\{\prod_1^\infty (1-x^r)\}^3$$

$$\equiv x\,\{\sum_{u=0}^\infty (-1)^u (2u+1)\, x^{7u(u+1)/2}\}\,\{\sum_{v=0}^\infty (-1)^v (2v+1)\, x^{v(v+1)/2}\}.$$

Hence

$$\tau(n) \equiv \Sigma(-1)^{u+v}(2u+1)(2v+1) \tag{4}$$

where u, v run through the non-negative solutions of the equation

$$n = 1 + \frac{7u(u+1)}{2} + \frac{v(v+1)}{2}$$

which can be put in the form

$$8n = 7(2u+1)^2 + (2v+1)^2 \tag{5}$$

If $\left(\frac{n}{7}\right) = -1$, (5) has no solution Therefore

$$\tau(n) \equiv 0 \text{ when } n^3 \equiv -1. \tag{6}$$

Also if $n = 0$, then from (5)

$$2\nu + 1 = 0$$

Hence

$$\tau(7m) = 0 \tag{7}$$

Now consider the case when n is equal to an odd prime p other than 7, such that

$$\left(\frac{p}{7}\right) = 1$$

Then the equation

$$p = x^2 + 7y^2 \tag{8}$$

has a unique solution in positive integers x, y of opposite parity. If (x_1, y_1) be this solution, then

$$8p = (x_1 + 7y_1)^2 + 7(x_1 \sim y_1)^2 = (x_1 \sim 7y_1)^2 + 7(x_1 + y_1)^2 \tag{9}$$

provides the two solutions of (5), giving

$$\tau(p) = 2x_1^2 = 2p = p(p^2 + 1) \tag{10}$$

In view of the relations (6), (7) and (10), we have

$$\tau(p) = p\sigma_3(p) \tag{11}$$

for all primes $p > 2$ It holds also when $p = 2$ because

$$\tau(2) = -24 = 18 = 2\sigma_3(2)$$

Using Mordell's identity

$$\tau(p^\lambda) = \tau(p)\tau(p^{\lambda-1}) - p^{11}\tau(p^{\lambda-2}), \ \lambda \geqslant 2,$$

it is now easily shown that

Since $\tau(n)$ and $\sigma_3(n)$ are both multiplicative functions

$$\tau(n) = n\sigma_3(n).$$

SOME CONGRUENCE PROPERTIES OF THE ϕ-FUNCTION

By P Kesava Menon
(*Madras Christian College, Tambaram*)

Received August 6, 1946
(Communicated by Prof B S Madhava Rao)

Let $\phi(n)$ denote the number of numbers not greater than and prime to n. Then the following lemma can easily be proved

Lemma 1.—If a and b are prime to n and m is the least positive integer for which

$$a^m \equiv b^m \bmod n,$$

then every integer N such that

$$a^N \equiv b^N \bmod n$$

is a multiple of m, in particular $\phi(n)$ is a multiple of m

We now proceed to prove the following

Theorem 1 —If a is greater than and prime to b, then

$$\phi(a^n - b^n) \equiv 0 \bmod n$$

For, obviously

$$a^n \equiv b^n \bmod (a^n - b^n);$$

and if $r < n$, then $a^r - b^r < a^n - b^n$, so that

$$a^r \not\equiv b^r \bmod (a^n - b^n)$$

It follows from lemma 1 that n is a divisor of $\phi(a^n - b^n)$

Theorem 2 —If a is prime* to b and $n \geqslant 2$, then

$$\phi\{a^{m(n-1)} + a^{m(n-2)} b^m + a^{m(n-3)} b^{2m} + \quad + b^{m(n-1)}\} \equiv 0 \bmod mn$$

Proof—It is clear that

$$a^{mn} - b^{mn} \equiv 0 \bmod \{a^{m(n-1)} + a^{m(n-2)} b^m + \quad + b^{m(n-1)}\} \qquad (1)$$

If N is the least positive integer such that

$$a^N - b^N \equiv 0 \bmod \{a^{m(n-1)} + a^{m(n-2)} b^m + \quad + b^{m(n-1)}\} \qquad (2)$$

then, by lemma 1, N is a divisor of mn Also, for $N \leqslant m(n-1)$,

$$|a^N - b^N| < a^{m(n-1)} + a^{m(n-2)} b^m + \ldots + b^{m(n-1)}$$

* Here, as well as in what follows we shall exclude the case $a = b = 1$.

Therefore

$$mn \geqslant N \geqslant m(n-1). \tag{3r}$$

Let g be the g c d of m and N and let

$$m = gm_1,\ N = gN_1$$

Writing $a^g = \alpha$ and $b^g = \beta$ we see from (2) that N_1 is the least positive integer such that

$$\alpha^{N_1} = \beta^{N_1} \bmod \{\alpha^{m_1(n-1)} + \alpha^{m_1(n-2)}\beta^{m_1} + \quad$$

It follows that N_1 is a divisor of $m_1 n$, and since N_1 is prime to m_1, that N_1 is a divisor of n But from (3) we see that

$$N_1 \geqslant m_1(n-1) \geqslant (n-1)$$

Hence $N_1 = n$, $m_1 = 1$, and so $m = g$, $N = mn$

Therefore, by lemma 1 mn is a divisor of

$$\phi\{a^{m(n-1)} + a^{m(n-2)}b^m + \quad + b^{m(n-1)}\}$$

2 Let $n = p^a n_1$, where p is prime and n_1 is prime to p. Then if we write

$$f(m, n) = a^{m(n-1)} + a^{m(n-2)}b^m + \quad + b^{m(n-1)}$$

we have

Lemma 2 —$a^n - b^n = (a^{n_1} - b^{n_1}) \prod_{i=1}^{a} f(n/p^i, p)$

Let us further suppose that a is prime to b. Then we have

Lemma 3 —The g c d. of any two of the numbers

$$a^{n_1} - b^{n_1},\ f(n/p^i, p)\ (i = 1, 2, \quad , a)$$

is either p or 1

For, if d is a common divisor of

$$f(n/p^i, p) \text{ and } f(n/p^j, p)\ (i < j),$$

then

$$0 \equiv f(n/p^j, p)(a^{n/p^i} - b^{n/p^i})$$
$$\equiv a^{n/p^{j-1}} - b^{n/p^{j-1}} \bmod d;$$

and so

$$0 \equiv f(n/p^i, p) \equiv pa^{n(p-1)/p^j} \bmod d$$

so that, since d is prime to a,

$$d = p \text{ or } 1.$$

Similarly we can show that the g.c.d. of

$$a^{n/p^a} - b^{n/p^a} \text{ and } f(n/p^i, p)$$

is either p or 1

Lemma 4.—$f(n/p^i, p) \equiv f(n/p^a, p) \bmod p \quad (i = 1, 2, \ldots, a)$

This follows immediately from

$$a^{n/p^i} - \qquad \equiv a^{n/p^a} \bmod p$$

Lemma 5.—If $f(m, p) \equiv 0 \bmod p$, then

$$a^m \equiv b^m \bmod p$$

For,

$$0 \equiv f(m, p)(a^m - b^m) \equiv a^{mp} - b^{mp} \bmod p,$$

and

$$a^{mp} \equiv a^m \bmod p$$

$$b^{mp} \equiv b^m \bmod p$$

so that

$$0 \equiv a^{mp} - b^{mp} \equiv a^m - b^m \bmod p$$

Conversely, we have

Lemma 6.—If $a^m \equiv b^m \bmod p$, then

$$f(m, p) \equiv 0 \bmod p$$

From lemmas 2 to 6 we get

Lemma 7.—If any one of

$$a^{m_i} - b^{m_i}, \; f(n/p^i, p) \qquad (i = 1, 2, \ldots, a)$$

is prime to p, then they are all prime to each other, and

$$\phi(a^n - b^n) = \phi(a^{m_1} - b^{m_1}) \prod_{i=1}^{a} \phi\{f(n/p^i, p)\}$$

Similarly we get

Lemma 8.—If any one of $a^{m_i} - b^{m_i}, f(n/p^i, p)$ $(i = 1, 2, \ldots, a)$ is divisible by p, then so are all of them and

$$(a^{m_i} - b^{m_i})/p, \; f(n/p^i, p)/p \quad (i = 1, 2, \ldots, a)$$

are prime to each other; further, $a^n - b^n$ is divisible by p^{a+1} and

$$\phi\{(a^n - b^n)/p^{a+1}\} = \phi\{(a^{m_1} - b^{m_1})/p\} \prod_{i=1}^{a} \phi\{f(n/p^i, p)/p\}$$

Lemma 9.—None of

$$f(n/p^i, p) \quad (i = 1, 2, \ldots, a - 1)$$

is divisible by a higher power of p than the first.

If one of a, b is a multiple of p, then the other is not, and so $f(n/p^i, p)$ is clearly prime to p. Therefore we may assume that a and b are both prime to p. Then

$$a^{\frac{n}{p^i}\left(1-\frac{1}{p}\right)} \equiv 1 \bmod p^2, \ \alpha > i+1$$

i e,

$$a^{n/p^i} \equiv a^{n/p^{i+1}} \bmod p^2, \ \alpha > i+1,$$

and so

$$f(n/p^i, p) \equiv f(n/p^{i+1}, p) \bmod p^2, \ i < \alpha - 1$$

It follows that if any one of $f(n/p^i, p)$ $(i = 1, 2, \ldots, \alpha - 1)$ is divisible by p^2, then so are all the others; but this cannot be the case because of lemma 3.

We are now in a position to prove

THEOREM 3.—If $n = p^\alpha n_1$ where p is the smallest prime factor of n, and n_1 is prime to p, and a is greater than and prime to b, then

$$\phi(a^n - b^n)$$

is divisible by

$$\phi(a^{n_1} - b^{n_1})\, n^\alpha / p^{\alpha(\alpha-1)/2} \text{ if } a^n - b^n \text{ is prime to } p,$$

and by

$$\phi(a^{n_1} - b^{n_1})\,(pn)^\alpha / p^{\alpha(\alpha-1)/2} \text{ if } p \text{ is a divisor of } a^n - b^n$$

Proof.—If any one of $a^{n_1} - b^{n_1}$, $f(n/p^i, p)$ $(i = 1, 2, \ldots, \alpha)$ is prime then by lemma 7 we have

$$\phi(a^n - b^n) = \phi(a^{n_1} - b^{n_1}) \prod_{i=1}^{\alpha} \phi\{f(n/p^i, p)\}$$

But, by theorem 2,

$$\phi\{f(n/p^i, p)\} \equiv 0 \bmod n/p^{i-1},$$

and so

$$\phi(a^n - b^n) \equiv 0 \bmod \phi(a^{n_1} - b^{n_1}) \prod_{i=1}^{\alpha} n/p^{i-1}$$

If, on the other hand, $a^{n_1} - b^{n_1}$, $f(n/p^i, p)$ are all divisible by p, then by lemma 8

$$\phi\{(a^{n_1} - b^{n_1})/p^{\alpha+1}\} = \phi\{(a^{n_1} - b^{n_1})/p\} \prod_{i=1}^{\alpha} \phi\{f(n/p^i, p)/p\}.$$

But $f(n/p^i, p)/p$ being prime to p for $i < \alpha$, (by lemma 9)

$$\phi\{f(n/p^i, p)\} = \phi\{f(n/p^i, p)/p\}\, \phi(p),$$

and so, by theorem 2

$$\phi\{f(n/p^i, p)/p\} \equiv 0 \bmod n/p^{i-1}, \ i < \alpha,$$

since every prime factor of n/p^{i-1} is greater than $\phi(p) = p - 1$. Further, if the greatest power of p dividing $a^n - b^n$ be $p^{\alpha+1+r}$ $(r \geq 0)$, then either

$a^{n_1} - b^{n_1}$ or $f(n_1, p)$ is divisible by p^{r+1} and

$$\phi(a^n - b^n) = \phi(p^{a+1+r})\,\phi[(a^n - b^n)/p^{a+1+r}]$$

$$= \begin{cases} p^{a+1}\,\phi[(a^n - b^n)/p^{a+1}] & \text{if } r > 1 \\ p^a(p-1)\,\phi[(a^n - b^n)/p^{a+1}] & \text{if } r = 0, \end{cases}$$

and

$$\phi(a^{n_1} - b^{n_1}) = \phi(p^{r+1})\,\phi[(a^{n_1} - b^{n_1})/p^{r+1}]$$

$$= \begin{cases} p\,\phi[(a^{n_1} - b^{n_1})/p] & \text{if } r = 1, \\ (p-1)\,\phi[(a^{n_1} - b^{n_1})/p & \text{if } r = 0 \end{cases}$$

It follows that

$$\phi(a^n - b^n) = p^a\,\phi(a^{n_1} - b^{n_1})\,\frac{\phi[(a^n - b^n)/p^{a+1}]}{\phi[(a^{n_1} - b^{n_1})/p]}$$

$$= p^a\,\phi(a^{n_1} - b^{n_1}) \prod_{i=1}^{a} \phi\{f(n/p^i, p)/p\}$$

$$\equiv 0 \bmod p^a\,\phi(a^{n_1} - b^{n_1}) \prod_{i=1}^{a} n/p^{i-1},$$

since $\phi\{f(n_1, p)/p\}$ is certainly divisible by $n_1 p$ by Theorem 2 whether $f(n_1, p)$ is divisible by a higher power of p than the first ore not, from the fact that n_1 is prime to $\phi(p)$ This completes the proof of the theorem

From theorem 3 we get the following refinement of theorem 1

THEOREM 4.—If $n = p_1^{a_1} p_2^{a_2} \cdots p_r^{a_r}$, where $p_1 > p_2 > \cdots > p_r$ are the distinct prime factors of n, and a is greater than and prime to b, then

$$\phi(a^n - b^n) \equiv 0 \bmod \prod_{i=1}^{r} p_i^{a_i(a_1 + a_2 + \cdots + a_{i-1}) + \frac{a_i(a_i+1)}{2}}$$

Proof.—From theorem 3 we have

$$\phi(a^n - b^n) \equiv 0 \bmod \phi(a^{n/p_1^{a_1}} - b^{n/p_1^{a_1}}) \times n^{a_1}/p_1^{a_1(a_1-1)/2}.$$

Since p_2 is the least prime factor of $n/p_1^{a_1}$ we have similarly

$$\phi(a^{n/p_1^{a_1}} - b^{n/p_1^{a_1}}) \equiv 0 \bmod \phi(a^{n/p_1^{a_1} p_2^{a_2}} - b^{n/p_1^{a_1} p_2^{a_2}}) \times \left(\frac{p_1}{p_1^{a_1}}\right)^{a_2} \Big/ p_2^{a_2(a_2-1)/2}$$

and so on. Thus

$$\phi(a^n - b^n) \equiv 0 \bmod \prod_{i=1}^{r} \left(\frac{n}{p_1^{a_1} \cdots p_{i-1}^{a_{i-1}}}\right)^{a_i} \Big/ p_i^{a_i(a_i-1)}$$

which is easily seen to be theorem 4.

DETERMINATION OF MAGNESIUM AND RESIDUAL MANGANESE IN ROCKS AND MINERALS WITH 8-HYDROXY-QUINOLINE

By C Karunakaran and K Neelakantam
(Departments of Geology and Chemistry, Andhra University, Waltair)

Received September 28, 1946

Neelakantam[1] published recently procedures for the gravimetric determination of manganese, and of magnesia and residual manganese as they occur together in the analysis of rocks and minerals by means of 8-hydroxy-quinoline. In the latter case the manganese content was determined colorimetrically Satisfactory results were obtained for both magnesia and manganese This investigation was, however, carried out on pure solutions of the salts and the conditions obtaining in rock analysis were reproduced by adding oxalic acid, ammonium and sodium chlorides.

The present paper deals with the actual analyses of some rock and mineral samples, *viz*, charnockite, leptynite and garnet by the above procedures and direct comparison of the results with those obtained by the usual pyrophosphate method.

Experimental

The finely ground sample (1 0 gm.) was weighed out accurately and opened up by fusion with sodium carbonate according to the procedure described by Harwood.[2] After eliminating the silica, the R_2O_3 hydroxides and lime and strontia, the filtrate was evaporated to dryness on the water-bath. The ammonium salts and oxalic acid were oxidised by means of concentrated nitric acid in the usual manner. The residue containing magnesia and the residual manganese was taken up in 5 c c of 2N hydrochloric acid and the solution made up to volume in a measuring flask (100 c c.) with water. One aliquot (25 c c) was precipitated with ammonium phosphate according to standard procedure for Gibb's method[3] and the determination completed by ignition to the pyrophosphate and weighing. The manganese content of this residue was determined colorimetrically by the well known periodate method. An equal volume of the solution was precipitated with 8-hydroxy-quinoline according to the following procedure previously worked out by Neelakantam (*loc. cit.*).

To the solution containing magnesium and manganese, an excess of a 0·5% solution of oxine acetate (2N acetic acid) was added and heated to

60–70° C Dilute ammonia was added dropwise with stirring until alkaline to litmus Finally 3 c c. of strong ammonia was added and the precipitate digested on the water-bath for one hour and cooled to laboratory temperature The precipitate was filtered through a sintered glass crucible (No 3), washed with hot dilute ammonia (1 40), dried to constant weight at 150° C and weighed as anhydrous magnesium and manganese oxy-quinolinates For the colorimetric estimation of manganese in this residue, the oxine complex was dissolved out in hot, dilute nitric acid, the solution evaporated to dryness in a platinum dish and the residue gently ignited to destroy the organic matter, moistening with concentrated nitric acid if necessary The final residue was dissolved in a few drops of sulphurous acid, the manganese oxidised by periodate and nitric acid and estimated colorimetrically

From the values obtained for manganese in both determinations, the magnesia contents were calculated by difference The results are tabulated below:—

No	Sample	MnO%		MgO%	
		Pyrophosphate Method	Oxine Method	Pyrophosphate Method	Oxine Method
1	Leptynite	0 05	0 09	1 82	1 80
2	Charnockite	0 07	0 09	9 01	9 02
3	Garnet ..	0 18	0 29	4 48	4 50

Discussion

It is to be noted that while the results obtained for magnesia by the two methods are in good agreement, the results for manganese by the oxine method of precipitation are definitely higher than by the pyrophosphate method. The explanation is to be found in the well known fact that the precipitation of manganese as the crystalline ammonium phosphate is generally incomplete, as much as 0 2 mg or more escaping precipitation so that in accurate analyses it is customary to make final corrections based on colorimetric tests on the filtrate [4] The oxine method obviously secures complete precipitation of residual manganese along with magnesia and gives more accurate results The improvement is of considerable value in rock analysis, for the manganese content of the R_2O_3 is obtained by difference from the values for total and residual manganese and any error in its value reflects on the figure for alumina Improved accuracy in the determination of

magnesia is also rendered possible by the oxine method as it is simple and the magnesium content of the anhydrous oxine complex is only 7·78%.

Summary

The magnesia and residual manganese have been precipitated together with oxine, the content of the latter determined colorimetrically and that of the former calculated by difference in the analyses of samples of charnockite, leptynite and garnet The results obtained are compared with those obtained in parallel determinations carried out by the pyrophosphate method and improved accuracy in the estimation of residual manganese as well as magnesia claimed.

References

1. Neelakantam — *Curr Sci*, 1941, 10, 20 (details under publication elsewhere)
2. Harwood, H F — *Practical Rock Analysis for Geologists*, Imperial College of Science and Technology, London, 1933
3. Gibbs, W — *Am J. Sci*, 1867, (II), 44, 216
4. Hillebrand and Lundell — *Applied Inorganic Analysis*, 1929, pp 349

CONDITIONS OF PLANE ORBITS IN CLASSICAL AND RELATIVISTIC FIELDS

By V V Narlikar and K R Karmarkar

(Department of Mathematics, Benares Hindu University)

Received March 21, 1946

1. The classical equations for the motion of a test-particle in a field of force (X, Y, Z) are

$$\ddot{x} = X, \quad \ddot{y} = Y, \quad \ddot{z} = Z \tag{1}$$

What are the restrictions on X, Y, Z as functions of (x, y, z, t) if the orbit of the test-particle is required to be *invariably* plane? This is a simple interesting question and as it does not appear to have been investigated before we consider it here

If s denotes the distance of the current point, that is, the position of the test-particle on the orbit at time t from some fixed point on it we have

$$\begin{vmatrix} \frac{dx}{ds} & \frac{dy}{ds} & \frac{dz}{ds} \\ \frac{d^2x}{ds^2} & \frac{d^2y}{ds^2} & \frac{d^2z}{ds^2} \\ \frac{d^3x}{ds^3} & \frac{d^3y}{ds^3} & \frac{d^3z}{ds^3} \end{vmatrix} = \kappa^2 \tau, \tag{3}$$

where κ and τ are the local curvature and torsion respectively It readily follows that if the orbit is to be plane we must have everywhere on it

$$\begin{vmatrix} \dot{x} & \dot{y} & \dot{z} \\ \ddot{x} & \ddot{y} & \ddot{z} \\ \dddot{x} & \dddot{y} & \dddot{z} \end{vmatrix} = 0 \tag{3}$$

(1) and (3) lead to

$$\Sigma \dot{x}\left\{Y\left(\frac{\partial Z}{\partial x}\dot{x}+\frac{\partial Z}{\partial y}\dot{y}+\frac{\partial Z}{\partial z}\dot{z}+\frac{\partial Z}{\partial t}\right)-Z\left(\frac{\partial Y}{\partial x}\dot{x}+\frac{\partial Y}{\partial y}\dot{y}+\frac{\partial Y}{\partial z}\dot{z}+\frac{\partial Y}{\partial t}\right)\right\}=0 \tag{4}$$

The last equation can be valid at any point of the field for arbitrary values of the velocities only if

$$Y\frac{\partial Z}{\partial t}-Z\frac{\partial Y}{\partial t}=0, \quad Z\frac{\partial X}{\partial t}-X\frac{\partial Z}{\partial t}=0, \quad X\frac{\partial Y}{\partial t}-Y\frac{\partial X}{\partial t}=0, \tag{5}$$

$$Y\frac{\partial Z}{\partial x}-Z\frac{\partial Y}{\partial x}=0,\quad Z\frac{\partial X}{\partial y}-X\frac{\partial Z}{\partial y}=0,\quad X\frac{\partial Y}{\partial z}-Y\frac{\partial X}{\partial z}=0, \tag{6}$$

$$\begin{aligned} &Y\frac{\partial Z}{\partial y}-Z\frac{\partial Y}{\partial y}-X\frac{\partial Z}{\partial x}+Z\frac{\partial X}{\partial x}=0,\\ &Z\frac{\partial X}{\partial z}-X\frac{\partial Z}{\partial z}-Y\frac{\partial X}{\partial y}+X\frac{\partial Y}{\partial y}=0,\\ &X\frac{\partial Y}{\partial x}-Y\frac{\partial X}{\partial x}-Z\frac{\partial Y}{\partial z}+Y\frac{\partial Z}{\partial z}=0, \end{aligned} \tag{7}$$

From (5) and (6) it follows that:

$$\begin{aligned} X/Y &= \theta(x, y),\\ Y/Z &= \phi(y, z),\\ Z/X &= \psi(z, x), \end{aligned} \tag{8}$$

where θ, ϕ, ψ are arbitrary functions One may safely conclude that X, Y, Z are of the form

$$X = Pf(x),\ Y = Pg(y),\ Z = Ph(z), \tag{9}$$

where f, g, h are arbitrary functions of the variables concerned and P is an arbitrary function of x, y, z, t Substituting for X, Y, Z from (9) in (7) we have

$$\frac{\partial f}{\partial x}=\frac{\partial g}{\partial y}=\frac{\partial h}{\partial z} \tag{10}$$

Hence

$$f = \lambda x + \epsilon_1,\ g = \lambda y + \epsilon_2,\ h = \lambda z + \epsilon_3, \tag{11}$$

where λ, ϵ_1, ϵ_2, ϵ_3 are arbitrary constants Thus we find that the orbits are always plane in the field of force:

$$X = (\lambda x + \epsilon_1)P,\ Y = (\lambda y + \epsilon_2)P,\ Z = (\lambda z + \epsilon_3)P \tag{12}$$

It is obvious that the forces are not derivable from a potential function unless P is of the form,

$$P = P(\chi, t), \tag{13}$$

where $$\chi = \lambda(x^2 + y^2 + z^2) + 2\epsilon_1 x + 2\epsilon_2 y + 2\epsilon_3 z + \eta, \tag{14}$$

η being an arbitrary constant.

It can be easily shown that if the forces (12) are supplemented by a resisting force the orbit still remains plane.

It is interesting to notice also that the condition for plane orbits leads to what Bergmann[1] calls the classical force law.

2. The above discussion of a classical field of force suggests an interesting mathematical problem, which appears rather artificial, but which is based all the same on the established practice in general relativity.[2] For a relativistic line-element of the form,

$$ds^2 = -e^{\lambda}\, dr^2 - r^2 (d\theta^2 + \sin^2\theta d\phi^2) + e^{\nu}\, dt^2, \tag{15}$$

$$\lambda = \lambda(r, t), \quad \nu = \nu(r, t), \tag{16}$$

the geodesics provide three differential equations in r, θ, ϕ, t and the first and second order derivatives of r, θ, ϕ with respect to t If we now assume that these equations represent the motion of a test-particle in the flat space,

$$d\sigma^2 = dr^2 + r^2 d\theta^2 + r^2 \sin^2\theta d\phi^2, \tag{17}$$

the time t being regarded as Newtonian, the question naturally arises as to whether the orbit so obtained is invariably plane As regards the assumption on which the question is based it may be pointed out that the same assumption underlies the usual calculation of the motion of the perihelion of Mercury in general relativity Without discussing the justification for such an assumption, which is sanctioned by current usage, we only examine whether it leads to plane orbits invariably The vanishing of the left-hand side of (2) is now equivalent to

$$\begin{vmatrix} \lambda^1 & \lambda^2 & \lambda^3 \\ \dfrac{\delta\lambda^1}{\delta\sigma} & \dfrac{\delta\lambda^2}{\delta\sigma} & \dfrac{\delta\lambda^3}{\delta\sigma} \\ \dfrac{\delta^2\lambda^1}{\delta\sigma^2} & \dfrac{\delta^2\lambda^2}{\delta\sigma^2} & \dfrac{\delta^2\lambda^3}{\delta\sigma^2} \end{vmatrix} = 0, \tag{18}$$

where $\lambda^1, \lambda^2, \lambda^3$ stand for $dr/d\sigma$, $d\theta/d\sigma$, $d\phi/d\sigma$ respectively and $\delta\lambda^i/\delta\sigma$, $\delta^2\lambda^i/\delta\sigma^2$ are the first and second covariant[3] derivatives of λ^i with respect to σ. From the equations of the geodesics we get

$$\ddot{r} - \mathrm{P}r + \tfrac{1}{2}\lambda' r^2 - re^{-\lambda}(\theta^2 + \sin^2\theta\phi^2) + e^{\nu-\lambda}\nu' + \lambda r = 0, \tag{19}$$

$$\ddot{\theta} - \mathrm{P}\theta + \frac{2}{r} r\theta - \sin\theta\cos\theta\, r^2 = 0, \tag{20}$$

$$\ddot{\phi} - \mathrm{P}\phi + \frac{2}{r}\dot{r}\dot{\phi} + 2\cot\theta\,\dot{\theta}\dot{\phi} = 0, \tag{21}$$

where $\mathrm{P} = \tfrac{1}{2}e^{\lambda-\nu}\dot{\lambda}^2 + \nu'\dot{r} + \tfrac{1}{2}\dot{\nu}$, (22)

it being understood that $\lambda' = \partial\lambda/\partial r$, $\dot{\lambda} = \partial\lambda/\partial t$ here Thus we find

$$\lambda^1 = \dot{r}/\dot{\sigma}, \quad \lambda^2 = \theta\,\dot{\theta}/\dot{\sigma}, \quad \lambda^3 = \dot{\phi}/\sigma; \tag{23}$$

$$\frac{\delta\lambda^1}{\delta\sigma} = \frac{d^2r}{d\sigma^2} - r\left(\frac{d\theta}{d\sigma}\right)^2 - r\sin^2\theta\left(\frac{d\phi}{d\sigma}\right)^2 \tag{24}$$

$$= Q + R\dot{r}, \tag{25}$$

where

$$Q = \frac{1}{\dot{\sigma}^2}\left[-\tfrac{1}{2}\lambda' r^2 + r(e^{-\lambda}-1)(\dot{\theta}^2 + \sin^2\theta\dot{\phi}^2) + e^{\nu-\lambda}\nu' + \lambda\dot{r}\right] \tag{26}$$

$$R = P - \ddot{\sigma}/\dot{\sigma}^2 \tag{27}$$

In obtaining (25) the independent variable is changed from σ to t and (19) is used Similarly on using (20) and (21) one obtains

$$\frac{\delta\lambda^2}{\delta\sigma} = R\,\dot{\theta}, \quad \frac{\delta\lambda^3}{\delta\sigma} = R\,\dot{\phi}. \tag{28}$$

When (23), (25) and (28) are used in (18) we find that the condition for plane orbits reduces to

$$\frac{Q}{\dot{\sigma}}\begin{vmatrix} \dot{\theta} & \dot{\phi} \\ \dfrac{\delta^2\lambda^2}{\delta\sigma^2} & \dfrac{\delta^2\lambda^3}{\delta\sigma^2} \end{vmatrix} = 0, \tag{29}$$

Calculations show that

$$\frac{\delta^2\lambda^2}{\delta\sigma^2} = S\,\dot{\theta}, \quad \frac{\delta^2\lambda^3}{\delta\sigma^2} = S\,\dot{\phi} \tag{30}$$

where

$$S = \frac{1}{\sigma}\left[PR + \frac{1}{r}Q + R\right]. \tag{31}$$

Thus (29) is identically satisfied and all the orbits are invariably plane.

3 We have tried to extend the above analysis to the similar question arising out of the most general line-element,

$$ds^2 = g_{\mu\nu}\,dx^\mu\,dx^\nu. \tag{32}$$

The three equations of motion[4] with $x^4 = t$ as the independent variable are

$$\ddot{x}^i + \Gamma^i_{\alpha\beta}\,\dot{x}^\alpha\,\dot{x}^\beta - \dot{x}^i\,\Gamma^4_{\alpha\beta}\,\dot{x}^\alpha\,\dot{x}^\beta = 0, \; i = 1, 2, 3 \tag{33}$$

in the notation of general relativity. Here $\dot{x}^4$ means 1 These equations of motion may be considered, as was once suggested by Rosen,[5] with reference to any Euclidean (three-dimensional) metric,

$$d\sigma^2 = h_{ij}\,dx^i\,dx^j.$$

The condition for plane orbits turns out to be extremely complicated, and as no particular cases of interest arise we do not report here our formal result. The case treated in the second section covers the usual gravitational

questions of interest in general relativity, including that of Schwarzschild's external solution. None of the investigators responsible for discussing the motion of the perihelion of Mercury seems to have been aware that once the relativist commits himself to the use of Riemannian co-ordinates the orbit of a test-particle, or of a small planet like Mercury, can be plane only in a special artificial sense It is in the light of this special sense that we have carried out the discussion of plane orbits in relativity fields.

Summary

We have discovered the most general classical field of force for which the orbit of a test-particle is invariably plane If the relativistic equations of a test-particle are interpreted in the classical sense, a general result is obtained, of which a particular case accounts for the orbit of Mercury being plane even according to relativists

References

1. Bergmann, P. G. *Introduction to the theory of Relativity*, 1942, 11
2. Tolman, R C *Relativity, Thermodynamics and Cosmology*, 1934, 208
3. Mc Connell, A J *Applications of the Absolute Differential Calculus*, 1936, 162
4. Narlikar, V V *M N R A S* 1936, 96, 263
5. Rosen *Phys Rev*, 1940, 57, 147

CONSTITUTION OF POPULNIN

By P Ramachandra Rao and T R Seshadri
(*From the Department of Chemistry, Andhra University, Waltair*)

Received September 26, 1946

The glucoside, Populnin,[1] was obtained as the main crystalline component of the flower petals of *Thespesia populnea* and from its composition it was considered to be a monoglucoside of a tetrahydroxy-flavone which was named populnetin This has now been confirmed by the yield of glucose produced by acid hydrolysis Populnetin exhibited considerable stability to cold 50% potash and air As a matter of fact this property was used for its purification. It was therefore considered to be a flavone and not a flavonol This is now found to be incorrect Comparison of populnetin and its derivatives with synthetic samples of scutellarein[2] and 5.7 8:4-tetrahydroxy flavone[3] and their derivatives has shown that it is not one of them. The fission of the tetramethyl ether with alcoholic potash yields anisic acid and methoxy fisetol-dimethyl ether establishing definitely that populnetin is a flavonol and should be identical with kaempferol. The identity has been confirmed by comparison with authentic samples, synthetic as well as natural, of kaempferol and its derivatives It is therefore clear that the criterion of differentiation between flavones and flavonols based on stability to cold alkali and air is not reliable.

It follows from the above results that populnin is a monoglucoside of kæmpferol. In order to locate the position of the sugar group it was methylated by means of dimethyl sulphate and potassium carbonate in anhydrous acetone medium The product, when hydrolysed with mineral acid, yielded a compound melting at 283–85° It was a trimethyl ether and did not give any prominent reaction with alcoholic ferric chloride These properties indicated that the free hydroxyl was not in the 3 or 5 position. The melting points of the corresponding 4′-hydroxy and 7-hydroxy compounds as recorded in the literature are nearly the same as above. But a mixture of the degradation product with the 4′-hydroxy compound recently synthesised in this laboratory[4] melted lower and indefinitely. By elimination it should therefore be concluded that the partial methyl ether obtained from populnin has the hydroxyl group in the 7-position (II) which also indicates the position of the sugar group (I).

Name of the partial methyl ether	Melting point of hydroxy compound	Ferric chloride reaction	M.P of acetate
5:7 4′ trimethoxy 3 hydroxy flavone[2]	151–52°	Violet brown	190–91°
3 7 4′ trimethoxy 5-hydroxy flavone[2]	152–53°	Olive green	.
3 5 4′ trimethoxy 7-hydroxy flavone	283–85°	Nil	159–60°
3-5:7-trimethoxy 4′ hydroxy flavone	278–80°	Nil	147–49°

In efforts to provide confirmation of the above constitution the monohydroxy compound (II) was subjected to fission with alcoholic potash; it was found to be unaffected by this treatment It was therefore ethylated and the constitution of the ethyl ether (III) established in two ways (1) 5. 7-Dihydroxy-3 : 4′-dimethoxy-flavone (IV) obtained by the condensation of ω-methoxy phloracetophenone and the sodium salt and anhydride of anisic acid, was subjected to partial ethylation which should be normally expected to take place in the 7-position (V) Subsequently it was methylated and the final product was found to be identical with the abovementioned ethyl ether (III) obtained from the glucoside The reactions can be explained as given below.

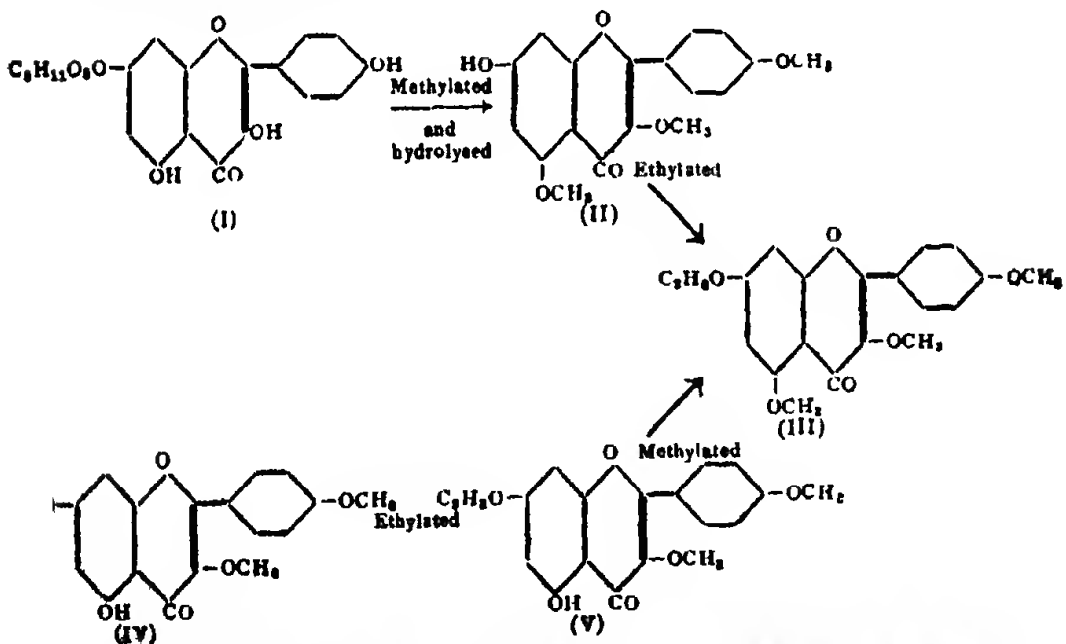

(2) The second method of confirmation involved fission of the ethyl ether (III) whereby anisic acid and a dimethyl-monoethyl phloraceto

phenone (VI) were obtained. Further ethylation of the ketonic product yielded a diethyl ether (VII) whose constitution was again established by synthesis as given below starting from ω-methoxy phloracetophenone.

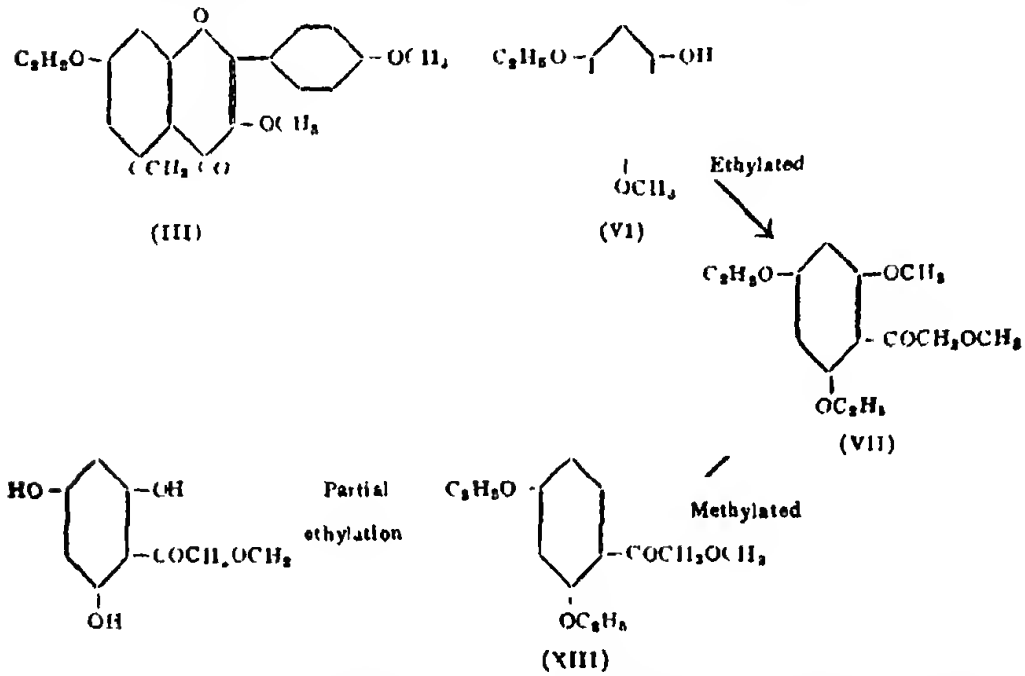

The formation of the 2 4-diethyl ether (VII) as the degradation product is possible only if in (III) the ethoxyl were in the 7-position, thus confirming that populnin is a 7-glucoside of kæmpferol (I)

A glycoside of kæmpferol with a disaccharose unit in the 7-position has been recently described by Nakamura and Hukuti [7] The 7-hydroxy compound obtained as the result of methylation and subsequent hydrolysis agrees in its properties with the compound described here in the course of the study of populnin The Japanese authors report the synthesis of this compound starting from the monomethyl ether of phloroglucinol. But they record the melting point of the acetate as 205° which is too high We get its melting point as 159–60° More recently the abstract of the paper of Zemplen and Bognar[8] on the constitution of robinin has become available. As the result of enzymic hydrolysis robinin yielded kæmpferol-7-1-rhamnoside from which by methylation and subsequent hydrolysis 3 : 5 : 4'-trimethyl ether of kæmpferol was obtained. Its melting point is given as 288-89° and that of its acetate as 157–58° These melting points agree with ours closely.

EXPERIMENTAL

Hydrolysis of Populnin—Populnin (2 g) was boiled under reflux with 7% sulphuric acid (200 c c) for two hours In about half an hour the glucoside was completely dissolved and the aglucone began to separate out within an hour The contents were filtered and the filtrate extracted with ether so as to render it free from aglucone It was then neutralised with sodium carbonate, clarified with neutral lead acetate and the sugar formed was quantitatively estimated by the method of Munson and Walker (Found: glucose, 40 2, $C_{21}H_{20}O_{11}$, H_2O requires glucose, 38 6%) The aglucone was crystallised from aqueous alcohol when it was obtained as fine needles, yellow in colour and melting at 275–76° (Found in sample dried at 120° C, 63 3, H, 3 9, $C_{15}H_{10}O_6$ requires C, 62 9, H, 3 5%) Mixed melting points of populnetin with both synthetic and natural samples of kæmpferol were undepressed Populnetin Acetate was prepared by boiling populnetin with acetic anhydride and a few drops of pyridine for two hours The product was finally recrystallised from ethyl acetate when it came out as colourless short rectangular plates When heated, the substance sintered strongly and became glassy at about 120° and melted down at 180°, a behaviour characteristic of kæmpferol acetate

Populnetin Methyl Ether—As the older method of methylation using sodium hydroxide and dimethyl sulphate was found to be not productive of good yields, the following method was adopted Populnetin (2 g) was dissolved in anhydrous acetone (50 c c), the solution was treated with anhydrous potassium carbonate (25 g) and dimethyl sulphate (8 c c.) and the mixture boiled under reflux for 30 hours A further quantity of dimethyl sulphate (4 c c) was added in small quantities during the first 24 hours The mixture was finally filtered under suction while still hot and the residue was washed with a small quantity of hot anhydrous acetone The filtrate was concentrated and on the addition of excess of water a bulky precipitate of the methyl ether was produced It was filtered and recrystallised from alcohol when it came out as long rectangular plates melting at 165–66° (Found: C, 60 5; H, 6·1; OCH_3, 32 4; and loss on drying at 120° *in vacuo* for 2 hours, 9 2, $C_{19}H_{18}O_6$, $2H_2O$ requires C, 60·3, H, 5 8, OCH_3, 32 8 and loss on drying 9 5%) The substance did not dissolve in alkali and gave no colour with ferric chloride. With concentrated sulphuric acid it gave a yellow solution with weak green fluorescence. The mixed melting point of tetramethyl populnetin with a synthetic sample of tetramethyl kæmpferol (m.p. 165–66°), obtained by methylating 5, 7-dihydroxy-3: 4′-dimethoxy flavone, was undepressed. The above partially methylated flavone was

prepared by condensing ω-methoxy-phloracetophenone with anisic anhydride and sodium anisate according to the method of Robinson and Shinoda.[9]

Decomposition of Populnetin Methyl Ether—(*a*) 50% *Aqueous potash*: O-Tetramethyl populnetin (0 5 g) was boiled under reflux in a silver flask with 20 c c of 50% aqueous potash for 8 hours. The product was then diluted and acidified with concentrated hydrochloric acid when a colourless solid separated out The contents were ether-extracted and the ether solution was washed repeatedly with 5% sodium bicarbonate solution till no more acid could be extracted The bicarbonate extract was acidified and the acid that precipitated out was filtered and recrystallised from alcohol. It was found to be identical with anisic acid The remaining ether solution contained the ketonic part but the yield of the ketone was not sufficient for identification Hence the following method of decomposition was employed

(*b*) *Absolute alcoholic potash*—O-Tetramethyl populnetin (1 0 g) was boiled under reflux with absolute alcoholic potash (30 c c , 8%) for a period of six hours At the end of the experiment, as much of alcohol as possible was removed by distillation and the residue was dissolved in water. The solution was then filtered free from any suspended insoluble impurities and the clear filtrate was acidified with dilute sulphuric acid The contents were then ether-extracted and the ether solution was repeatedly washed with 5% sodium bicarbonate solution till no more acid could be extracted. The solvent was then distilled off and the solid obtained was recrystallised from alcohol It appeared as irregular plates melting at 104–6° and was found to be identical with methoxy fisetol dimethyl ether by a mixed melting point determination with a synthetic sample obtained by partial methylation of ω-methoxy-phloracetophenone [10]

The sodium bicarbonate extract was acidified and the acid that precipitated out was filtered and recrystallised from alcohol. It was found to be identical with anisic acid

Methylation of Populnin and Hydrolysis.—Populnin (2 g) was suspended in anhydrous acetone (50 c c) and the contents were refluxed for 30 hours after adding dimethyl sulphate (10 c c) and potassium carbonate (25 g.). The mixture was finally filtered under suction while still hot and the residue was washed with a small quantity of hot anhydrous acetone. The filtrate was concentrated and finally as much of acetone as possible was evaporated off. The residue was a viscous semi-solid and it could not be crystallised even after repeated attempts. Therefore it was hydrolysed by boiling with 200 c.c of 7% sulphuric acid for 2 hours. A clear solution was first obtained

and an almost colourless bulky solid began to separate out at the end of the first half hour The product (II) was filtered and was recrystallised using a large quantity of alcohol It came out as colourless short needles melting at 283-85° (Found· C, 66 1, H, 5 2, $C_{18}H_{16}O_6$ requires C, 65 9, H, 4 9%) The substance was soluble in alkali to form a light yellow solution and gave no colour with ferric chloride in alcoholic solution It was stable to alcoholic potash and could be recovered almost completely even after refluxing with 10% absolute alcoholic potash for 8 hours The mixed melting point with 4'-hydroxy-3 5 7-trimethoxyflavone (m p 278-80°) was considerably depressed and was not sharp (235-55°) Its acetyl derivative was prepared by boiling with acetic anhydride and a few drops of pyridine It crystallised from ethyl acetate or acetone in the form of colourless flat needles and narrow rectangular plates melting at 159 60° Mixed melting point with 4'-acetoxy-3 5 7-trimethoxy flavone was considerably depressed

Ethylation of (II) —The partial methyl ether of populnetin (II) (1 0 g) was dissolved in anhydrous acetone (50 c c), ethyl iodide (5 g) and dry potassium carbonate (15 g) added and the mixture refluxed for 30 hours. At the end of the experiment, the contents were filtered while hot and the residue was washed with hot anhydrous acetone The filtrate was concentrated and was kept in an ice-chest after dilution with water The solid that separated out was filtered and washed with dilute alkali to remove any unethylated compound The product was first crystallised from alcohol when a brownish crystalline solid melting at 80° was obtained; but a colourless sample could be obtained by crystallising it from ethyl acetate The compound (III) was finally recrystallised from alcohol from which it slowly separated out as rectangular plates melting at 128-30° (Found: C, 67 5; H, 5 4; $C_{20}H_{20}O_6$ requires C, 67 4, H, 5 6%)

Decomposition of the Monoethyl-trimethyl Ether (III) —The ethylated product obtained above (1 0 g) was boiled under reflux with absolute alcoholic potash (30 c c ; 8%) for a period of 6 hours As much of alcohol as possible was then removed by distillation; the residue was dissolved in water and the clear solution was acidified with excess of dilute sulphuric acid The contents were then ether-extracted The ether solution was shaken three times with 5% sodium bicarbonate solution to extract the acid part (A).

The Ketonic Part (VI).—The remaining ether solution was then washed with water and on distilling off the solvent the residue was found to be a pale yellow viscous liquid which solidified during the course of a few hours when kept in contact with water in an ice-chest. The ketone was crystallised

from dilute alcohol when it came out as rectangular plates melting at 108–10°. It dissolved in alkali to give a bright yellow solution and gave in alcoholic solution an olive green colour with ferric chloride (Found C, 59·8; H, 7 0, $C_{12}H_{16}O_5$ requires C, 60 0, H 6 7%)

The Acid Part (A)—The bicarbonate solution on acidification with concentrated hydrochloric acid gave rise to a precipitate which on recrystallisation from alcohol was found to be identical with anisic acid

Ethylation of (VI)—The ketone (VI) (0·5 g) was dissolved in anhydrous acetone (25 c c) and after the addition of ethyl iodide (2 c c.) and anhydrous potassium carbonate (5 g) the mixture was boiled under reflux for 30 hours. The solvent was then distilled off and the residue was treated with water when an insoluble liquid separated out It was ether-extracted and the ether solution was washed with dilute alkali to remove any unethylated ketone. After washing the ether solution free from alkali and distilling off the ether, a reddish yellow viscous liquid remained behind which could not be solidified and recrystallised even after repeated attempts. It was insoluble in aqueous alkali and an alcoholic solution did not give any colour with ferric chloride Hence the 2:4-dinitrophenyl-hydrazone derivative was prepared by boiling the ketone with an alcoholic solution of 2 4-dinitrophenylhydrazine. The product was washed with dilute hydrochloric acid and was recrystallised from alcohol when it came out as deep red rhombohedral prisms melting at 198–200° (Found. C, 53 4; H, 5 0; $C_{20}H_{24}O_8N_4$ requires C, 53 6,; H, 5·4%).

7-Ethoxy-5-hydroxy-3 . 4'-dimethoxyflavone (V).—5 . 7-Dihydroxy-3 : 4'-dimethoxy flavone (IV) was prepared by condensing ω-methoxyphloracetophenone with anisic anhydride and sodium anisate according to the method of Robinson and Shinoda[8] The flavone (1 g) was dissolved in dry acetone (50 c.c), ethyl iodide (0 6 g) and anhydrous potassium carbonate (10 g.) added and the mixture boiled under reflux for 6 hours At the end of the experiment, acetone was completely distilled off and the residue was taken up with water and ether extracted. From the ether solution, the partially ethylated flavone was extracted by means of dilute aqueous alkali repeatedly until the extraction was complete. The combined alkali extracts were acidified and the precipitate was filtered and recrystallised from alcohol The 5-hydroxy compound (V) crystallised out as bright yellow rectangular plates melting at 131–32° (Found: C, 66·8, H, 5·1, $C_{19}H_{18}O_6$ requires C, 66 7, H, 5 3%). An alcoholic solution of the compound gave an olive green colour with ferric chloride.

7-Ethoxy-3 : 5 : 4'-trimethoxy flavone.—5-Hydroxy-7-ethoxy-3 . 4'-dimethoxy flavone (V) (1 0 g) was dissolved in dry acetone (30 c c) treated with anhydrous potassium carbonate (15 g) and excess of dimethyl sulphate (2 c c) and the mixture boiled under reflux for 30 hours The product was worked up in the same way as mentioned for similar cases When recrystallised from alcohol it came out as thick rectangular plates melting at 128–30° (Found C, 67 3, H, 6 0, $C_{20}H_{20}O_6$ requires C, 67 4, H, 5 6%) It was identical with compound III obtained by the degradation of populnin and the mixed melting point was undepressed

2-Hydroxy-4-ethoxy-ω 6-dimethoxy acetophenone—7-Ethoxy-3 5 4'-trimethoxy flavone (1 g) was treated with absolute alcoholic potash (2 g of potash in 30 c c of absolute alcohol) and the mixture boiled under reflux on a water-bath for about 6 hours As much of alcohol as possible was then removed by distillation, the residue dissolved in water and the solution acidified with excess of dilute sulphuric acid The product was then ether-extracted and the ether solution was washed repeatedly with sodium bicarbonate solution until anisic acid was completely removed The solvent was then distilled off and the solid obtained was recrystallised from dilute alcohol. The ketone crystallised out as rectangular plates melting at 108–10° (Found· C, 60·1; H, 6·7, $C_{12}H_{16}O_5$ requires C, 60 1; H, 6 7%). The mixed melting point with the ketone (VI) obtained from monoethyl trimethyl populnetin (III) was undepressed

2 : 4-Diethoxy-6-hydroxy-ω-methoxy acetophenone (VIII)—ω-Methoxyphloracetophenone (1 g) was dissolved in dry acetone (30 c c) and the solution refluxed for about six hours after adding ethyl iodide (1 3 c c) and anhydrous potassium carbonate (5 g) The solvent was then removed by distillation, the residue taken up with water and ether extracted From the ether extract the partially ethylated ω-methoxy-phloracetophenone was separated by extraction with alkali. The alkali solution was then acidified when an almost colourless substance precipitated out It was filtered and recrystallised from alcohol when it came out as rectangular plates and prisms melting at 110–12° (Found C, 61 3, H. 7 1; $C_{13}H_{18}O_5$ requires C, 61·4; H, 7·1%).

2 : 4-Diethoxy-ω· 6-dimethoxy acetophenone—The above ketone (0 5 g) was dissolved in acetone (30 c c.) and methylated by boiling for 30 hours, with dimethyl sulphate (2 c c.) and anhydrous potassium carbonate (5 g) The solvent was then removed by distillation and the residue treated with water when an insoluble oily product separated out, it was extracted with ether. The ether solution was washed with dilute alkali to remove any

unmethylated ketone After washing the ether solution free of alkali the solvent was distilled off; a reddish yellow viscous liquid remained behind and it could not be obtained as a solid even after repeated attempts at crystallisation. Hence the 2.4-dinitrophenylhydrazone was prepared by boiling it with an alcoholic solution of 2.4-dinitrophenylhydrazine. The product was recrystallised from alcohol when it came out as deep red rhombohedral prisms melting at 198-200° (Found: C, 53·4, H, 5 4; $C_{20}H_{24}O_8N_4$ requires C, 53 6; H, 5 4%) The mixed melting point with the dinitrophenylhydrazone of the ethylated ketone (VII) obtained from populnin was undepressed Mixed melting point with 2:4-dinitrophenylhydrazine itself was depressed.

Summary

Populnin is a monoglucoside of populnetin which is shown to be identical with kæmpferol. By the methylation and the subsequent hydrolysis of the glucoside a trimethyl ether of kæmpferol is obtained Its colour reactions and properties indicate definitely that the free hydroxyl group is not in the 3- or 5-position It has been compared with the isomeric 4'-hydroxy compound and found to be different Thus the degradation product should have the hydroxyl in the 7-position. This is confirmed by ethylation and comparison of the ethyl ether and of its alkali degradation product (ketone) with synthetic samples

References

1 Neelakantam, Rao and Seshadri *Proc Ind Acad Sci*, A, 1943, 17, 26
2 Sastri and Seshadri *Ibid.*, 1946, 23, 262
3 ——— *Ibid*, 1946, 24, 243
4 Rao and Seshadri Under publication in *J C S.*
5 Kostanecki, Lampe and Tambor *Berichte*, 1904, 2098
6 Kondo and Endo *Chem Abs*, 1930, 1396
7 Nakamura and Hukuti *B C.A* A ii, 1941, 302
8 Zemplen and Bognar *Ibid.*, A ii, 1946, 129
Berichte, 1941, 1789
9. Robinson and Shinoda *J C.S*, 1925, 1980.
10. Row and Seshadri *Proc. Ind. Acad Sci*, A, 1946, 23, 27.

CHEMICAL EXAMINATION OF PLANT INSECTICIDES

Part III Chemical Components of *Derris Robusta*

By N V Subba Rao and T R Seshadri

(From the Departments of Chemistry and Chemical Technology, Andhra University, Waltair)

Received September 26 1946

Derris Robusta is very closely related to *D scandens* botanically as both belong to the same sub-section, Brachypterum of the genus *Derris* The chief difference is that the former is an erect tree, 30–40 feet high, whereas the latter is a climber. The tree is widely distributed in the tropical areas of the world and occurs in India in the Eastern Himalayas and the Western Peninsula.

Krishna and Ghose[1] examined the roots obtained from Gauhati (Assam) and observed that they did not contain any rotenone During the course of this examination they isolated from the ether extract a crystalline solid, melting at about 190° and sent it to Rothamsted for toxicity trials; it was found to be non-toxic to *Aphis rumicis* (the bean aphid) Chemical investigation of this sample was conducted by Harper[2] who concluded that it was not a rotenoid, as shown by the Durham test and other reactions, but was a carboxylic acid akin to lonchocarpic acid isolated by Jones [3] The crystalline substance was named by him ' Robustic acid ' as it was found to possess acidic properties. He proposed the molecular formula $C_{27}H_{34}O_8$ for it from considerations of analytical values It contained two methoxyl groups, it formed a mono-methyl derivative of the same melting point as the original substance and this was considered to be the methyl ester Attempts to show the presence of a ketonic group by oximation were unsuccessful Catalytic hydrogenation gave dihydro-robustic acid He felt that the titration of the acid in hot alcohol was not a case of true neutralisation, as conflicting results were obtained and as the acid could not be recovered on acidification.

Since a detailed chemical examination of the roots of *D robusta* had not been conducted by previous workers, it was considered desirable to undertake it. Further, two recent publications, one by Clark[4] and the other by Jones and Haller[5] made this study necessary The first author reported the isolation of a substance, melting at 190°, from *D scandens* which resembled

robustic acid. As we were examining the Indian *D scandens*,[6] we needed a sample of robustic acid for purposes of identification. In the second paper, the authors showed that lonchocarpic acid was not a carboxylic acid as it was originally thought to be. This led us to the expectation that robustic acid also may not be a carboxylic acid and that it may possibly be related to the two substances, scandenin and lonchocarpic acid In this connection the close botanical relationship between *D scandens* and *D robusta* was present in our mind

The roots of *D robusta* obtained from Dr Sri Krishna of the Forest Research Institute, Dehra Dun, were extracted with ether instead of chloroform, as robustic acid was originally isolated by the previous workers from an ether extract The present sample of the roots gave 3·9% of ether extractives, which were studied on the lines outlined in an earlier publication.[7] The fraction sparingly soluble in ether gave colour reactions similar to those of robustic acid[8] but was found to have a wide melting point range extending up to 200° Therefore it was fractionated using acetone and as a result of this, a crystalline substance melting sharp at 205-6° was obtained This was designated as D R I A second crystalline substance (D R. II) which melted at 188-9° and was insoluble in alkali, was isolated by the alkali treatment of the mixture present in the more soluble portions of the ether extract. This had a crystal structure similar to that of D R I and gave similar colour reactions but differed as regards solubility in alkali. Thus the roots of *D. robusta* gave two crystalline components, one melting at 205-6° (major component) and another melting at 188-9°

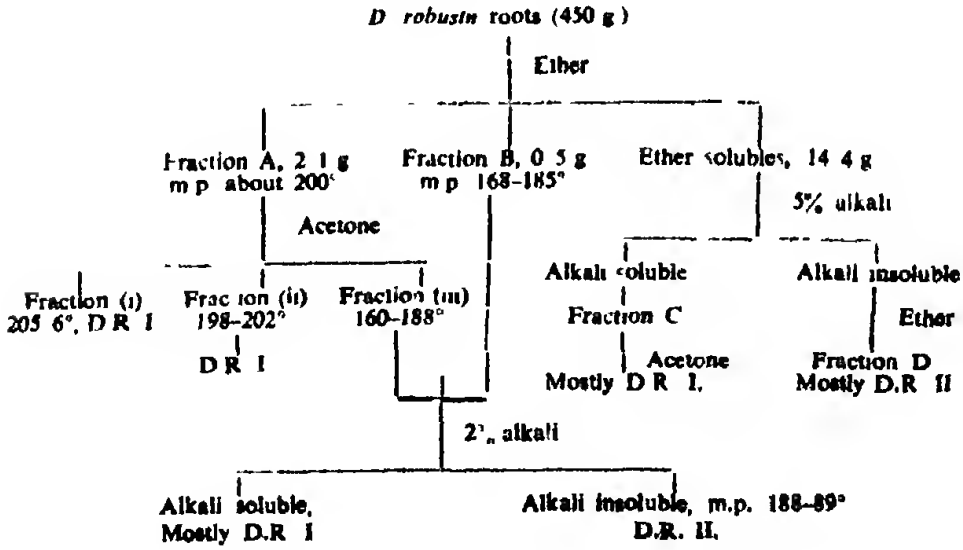

Since D R. I differed from robustic acid as described by Harper in certain of its properties, it was thought desirable to procure a sample of the acid from Dr Krishna from whom the material used by Dr Harper was also obtained and effect direct comparison The crude sample obtained from Dr Krishna had an indefinite melting point (170–90°) and was therefore purified by crystallisation from acetone The top fraction melted at 205–6° and was identical with D R I From the other fractions a sample of D R II could be obtained Consequently it could safely be concluded that D R. I is a purer sample of robustic acid than that employed by Harper for his investigation. It has a higher melting point There are differences in analytical data as well, ours has given a methoxyl content of 16 2% whereas the methoxyl value recorded by Harper was 13 1% In carbon percentage also there is a small difference

Robustic acid can be obtained in a fairly well-developed crystalline form (elongated prisms) Like scandenin, it exhibits a play of colours when viewed at different angles In solubility also, it closely resembles scandenin and forms a sparingly soluble potassium salt on treatment with aqueous alkali The substance could be precipitated from the alkali solution either by treatment with mineral acid or by passing carbon dioxide In the Durham test, it gives a green solution with nitric acid which changes to an unmistakable brilliant red colour on the addition of ammonia. It does not give any phenolic colouration with ferric chloride nor does it respond to the colour reactions of flavonols, resirols or sterols

Robustic acid contains two methoxyls, from considerations of analytical data and molecular weight determination, the molecular formula $C_{22}H_{29}O_6$ is now assigned to it Just like scandenin, it could also be titrated with alkali in alcoholic solution and the original substance recovered without any difficulty on acidifying the alkaline solution Hence the statement of Harper that the substance could not be recovered by acidification after titration with alkali does not seem to be correct This view is further supported by the observation that robustic acid is quite stable to boiling aqueous alcoholic potash. The minimum molecular weight, 397, calculated from the titration data agrees closely with that obtained by Rast's method It may be pointed out that Harper's titration values also lead to the same result

Robustic acid gives a mono-acetate, melting at 196–7° and a monomethyl ether, melting at 193–4° (*cf* Harper's m p of 'methyl ester' 190°), thereby indicating the presence of one free hydroxyl group The acetate is insoluble in alkali as is also the methyl ether. As robustic acid can be precipitated from an alkali solution by passing carbon dioxide, as it forms

an acetate which is insoluble in aqueous alkali, and as the methyl derivative does not regenerate robustic acid on treatment with alcoholic potash, it can be said with certainty that the acidic properties of robustic acid are not due to the presence of a carboxylic group as was originally thought but due to a strongly acidic hydroxyl group as in the case of scandenin and lonchocarpic acid. Hence the methyl derivative of robustic acid is a methyl ether and not a methyl ester. In all these properties there is close resemblance between robustic acid, scandenin and lonchocarpic acid. The name robustic acid should still be retained, although the substance is not a carboxylic acid, in order to avoid unnecessary confusion in the literature.

D R II has the same crystal structure as D R I (robustic acid) and also gives the same colour changes in the Durham test, but it is insoluble in alkali As it has a lower methoxyl value (17 7%) than the methyl ether of robustic acid (23·2%), it could not be considered to be identical with the latter From the analytical data, the molecular formula $C_{21}H_{20}O_6$ is assigned to it Since it appears to be a new substance, it is designated 'Robustenin'.

Experimental

The air-dried roots of medium size (450 g) obtained from the Forest Research Institute, Dehra Dun, were made into thin shavings and extracted three times with ether at the laboratory temperature soaking each time for 24 hours The combined extracts (6 litres) were concentrated and the solvent-free residue (17 g) was taken in a small volume of ether (75 c.c) The undissolved crystalline material (A) was filtered (2 1 g.) After partial concentration of the filtrate and treatment with methyl alcohol, fraction (B) (0·5 g.) separated and was filtered off.

From the filtrate the solvents were removed under reduced pressure, the residue was taken up in ether and rapidly extracted with 5% aqueous potash. The alkali-soluble portion was liberated by acidification, filtered and washed with boiling petroleum ether to remove fatty matter and was then taken in ethyl alcohol (25 c c.) and set aside. Next morning a crystalline solid (C) separated and was filtered. By concentration of the solution some more of the same solid was obtained.

The alkali-insoluble ether solution was dried over anhydrous sodium sulphate and the solvent completely removed. The solvent-free residue was taken in a small quantity of carbon tetrachloride (10 c.c.) and set aside. As no solid separated from this, the solvent was distilled under reduced pressure and the residue taken up in ether. The solid (D) that separated was collected.

From the rest of the neutral portion no other crystalline component could be obtained

Fraction A —It was colourless and crystalline in appearance It melted at about 200° (with sintering earlier) and in the Durham test gave a green colour changing to evanescent red, as described by Harper for robustic acid. As its melting point was not quite definite and was higher than that recorded for robustic acid (190°) it was fractionated Acetone was used for this purpose and the following three fractions were collected·

	Melting point	Crystal structure	Durham test	Ferric chloride colour
Fraction (i)	205-6°	Large rectangular prisms	Green to red	Negative
Do (ii)	198-202°	do	do	do
Do (iii)	160- 88°	do	do	do

Fraction (i) appeared to consist of a single entity and the melting point was not raised by further crystallisation It was therefore marked D R I. Fraction (ii) consisted essentially of this and could be purified by further crystallisation whereas fraction (iii) behaved like a mixture

Fraction B.—The solid had a wide melting point range, 168-85° but gave the colour changes in the Durham test similar to those given by D.R I. Since fraction (iii) from (A) and this solid had similar melting point ranges, they were combined and treated with 2% aqueous alkali and the mixture heated and filtered. The clear solution was acidified and the product obtained was found to have a melting point of 192-96° On crystallisation from alcohol the melting point rose and the product was found to be identical with D.R I

The alkali-insoluble solid was washed with hot water to remove any potassium salt that might have been present and then crystallised from alcohol. After two crystallisations it had a sharp melting point, 188-9° (mixed melting point with D R I depressed) In the Durham test, the colour change was from dirty green to evanescent red This substance was marked D.R. II.

Fraction C —It melted fairly sharp at 189-91° and had the same properties as D.R I. Recrystallisation raised the melting point to 193° and not further. However the mixture with D.R I also melted at the same temperature and methylation of the substance yielded a methyl ether identical with that of D R I. It was therefore concluded that this fraction consisted

mainly of D R I. The cause of the lower melting point will receive further attention when more quantities of this fraction are again obtained.

Fraction D—Its melting point was indefinite 170–80°, it was insoluble in alkali and gave in the Durham test the same colour changes as D R II. The quantity was too small to effect detailed purification

Purification of the robustic acid sample obtained from Dehra Dun—The crude sample (2 5 g, m p range 170–90°) was taken in boiling acetone (50 c c.) and the insoluole portion, which was appreciable in amount, was filtered off The first crop (0 7 g) melted at 198–202° and appeared as colourless rectangular prisms The melting point could be raised to 205–6° by another crystallisation and the mixed melting point with D.R. I was undepressed The second crop (1·3 g) had an indefinite melting point 170–88° This on treatment with alkali gave an alkali-insoluble product identical with D R II

D R I is hence forward designated robustic acid

Robustic acid—On slow crystallisation, it could be obtained in a fairly well-developed form and appeared as elongated prisms under the microscope. It was readily soluble in chloroform, boiling acetone and alcohol and less soluble in petroleum ether and benzene It had greater solubility than scandenin in ether Though it was insoluble in water, it was found to be soluble in warm aqueous potash from which the sparingly soluble potassium salt separated on cooling. On acidification of the alkali solution, the substance was reprecipitated

Robustic acid dissolved in concentrated sulphuric acid forming an intense red solution without any visible fluorescence. In the Durham test it did not give the rotenoid colour changes but gave a green colour changing to brilliant red This red colour was unmistakable and could not be missed. The compound did not respond to the sterol or resinol colour reactions. When a speck of the substance was treated with gallic acid and concentrated sulphuric acid and gently heated, no blue colour was produced, thereby indicating the absence of methylene-dioxy grouping in the molecule [Found: C, 69·2; H, 5 2; OCH_3, 16·2% Mol weight (Rast) 404, $C_{22}H_{28}O_6$ requires C, 69 5; H, 5·3, 2-OCH_3, 16·4% Mol weight 380. *Cf.* Harper's values C, 68 4; H, 5 1; OCH_3, 13 1% Mol weight (Rast) 496, 451]

Micro-titration—The substance was dissolved in hot neutralised alcohol and titrated with standard alkali using phenolphthalein as the indicator. The end point was sharp (61·0 mg. of the substance required 4 65 c.c. of 0·033 N alkali Mol. weight 397. Harper's values: 53 65 mg. required

7·05 c.c of 0 02 N. NaOH; Mol. weight 380). The substance was recovered on acidification and dilution with water.

Mono-acetate—The acetate was prepared by boiling the substance with acetic anhydride and sodium acetate The product crystallised from ethyl acetate as rectangular rods and prisms melting at 196-7°; the mixed melting point with the original substance was depressed (Found· C, 68 1, H, 5 3, $C_{24}H_{32}O_6$ requires C, 68 2, H, 5 3%)

The acetate was found to be insoluble in 5% aqueous alkali even after warming the solution, thereby indicating the absence of a carboxylic group in the substance

Mono-methyl ether—The methylation was carried out in anhydrous acetone medium using dimethyl sulphate and potassium carbonate On concentration of the acetone solution to a small volume, a crystalline solid, melting at 192-3°, was obtained; the mixed melting point with the original substance was considerably depressed It was insoluble in aqueous alkali and did not yield robustic acid on treatment with alcoholic potash. The methyl ether was recrystallised from alcohol when it came out as prismatic needles melting at 193-4° (Found OCH_3, 23 2% $C_{23}H_{32}O_6$ requires 3-OCH_3, 23 6%)

D.R II (Robustenin)—It appeared as rectangular prisms under the microscope and gave in the Durham test a dirty green colour changing to evanescent red With ferric chloride, no colouration was obtained [Found C, 68 5, H, 5 7, OCH_3, 17 7% Molecular weight (Rast) 390; $C_{21}H_{30}O_6$ requires C, 68 5, H, 5 4, (2) OCH_3, 16·9%, Molecular weight, 368] As it appeared to be a new substance, it was designated 'robustenin'

Our thanks are due to Dr. Sri Krishna of the Forest Research Institute, Dehra Dun for the supply of samples of the roots of *D robusta* and also of a sample of the crystalline component of these roots

Summary

A detailed examination of *D robusta* has now been made and two crystalline components isolated The main component (D R I) melts at 205-6° and agrees, in general, with the properties of robustic acid described by Harper except in melting point and analytical values The same substance (D R I) was also obtained from the crude sample of robustic acid supplied by the Forest Research Institute, Dehra Dun, from where Dr Harper also got his material The name robustic acid has been retained for it. The molecular formula, $C_{23}H_{30}O_6$ agrees with the results more closely. The molecule contains two methoxyls and one hydroxyl group The acid nature

of robustic acid has now been shown to be due to a phenolic hydroxyl just as in the case of scandenin and lonchocarpic acid. These three compounds seem to form a new type not having any simple relationship with rotenone

The second component now named 'robustenin' melts at 188–89°, is neutral in nature and has the probable molecular formula $C_{21}H_{20}O_6$ It contains two methoxyls

REFERENCES

1 Krishna and Ghose *Indian Forest Leaflet*, 1942, No 2
2 Harper *J C S*, 1942, 181
3 Jones *J A C S*, 1934, 56, 1247
4 Clark *J Org Chem*, 1943, 8, 489
5 Jones and Haller ——, 1943, 8, 493
6 Rao and Seshadri *Proc Ind Acad Sci*, 1946, 24, 365.
7 ——— ——, 1946, 24, 344

1188-46 Printed at The Bangalore Press Mysore Road Bangalore City, by O Srinivasa Rao, Superintendent and Published by The Indian Academy of Sciences.

A NEW BAND SYSTEM (CORDES BANDS) OF IODINE

By P Venkateswarlu, M Sc.
(Physics Department, Benares Hindu University)

Received May 13, 1946
(Communicated by Dr R K Asundi F A SC)

Cordes has recorded the absorption spectrum of iodine vapour in the region 1950 to 1500 A employing a vacuum fluorite spectrograph having a dispersion of 2 3 A/mm. at 1700 A which naturally falls rapidly on the long wavelength side He used for the absorption cell a tube 80 cm long with fluorite windows Iodine is kept in a side tube that is attached to the absorption cell By changing the temperature of the side tube the vapour pressure of iodine vapour in the absorption cell could be changed in a definite way He photographed the absorption spectrum at different pressures ranging from 3×10^{-4} mm to a pressure of 0 08 mm. The lower pressure corresponds to $-36°$ C A water-cooled hydrogen discharge tube was the source of the continuous radiation Different sets of bands were obtained at different pressures Bands about 53 in number on the shorter wavelength side which are given in Table I of Cordes paper[1] were analysed by him into eight different systems which all involve transitions from ground state to different excited electronic states above 56,000 cm^{-1} Another group of bands about 110 in number recorded in Table II of Cordes paper have not been analysed by him. He is of the opinion that they form the extension in one progression towards shorter wavelengths of Pringsheim-Rosen, Kimura-Miyanishi (P R., K. M)[2] bands which lie in the region 2700 A to 2000 A. But this is not probable because although the successive differences of the bands are of the expected order, they are completely spasmodic and do not exhibit even that small regularity of decrease which is present in P-R, K-M bands as analysed by Sponer and Watson [3] This group of about 110 bands seems to consist of two sets of bands with a gap of about 18 A in between · an extensive system of about 94 bands from 1950 to 1794 A occurring at a distance of about 2 A from one another and a few bands about 16 in number from 1776 to 1697 A Further it appears that the second set probably belongs to one of the eight systems analysed by Cordes The present paper deals with the analysis of the first extensive system of 94 bands between 1950 to 1794 A These bands make their appearance, according to Cordes, at a pressure of 3×10^{-3} mm and are completely developed at higher pressures (8×10^{-2} mm). The heads of the bands are not quite recognisable, though they appear shaded towards red at higher pressures.

The wavelengths and wave numbers of these 94 bands from Cordes paper are given in Table I. Here the wavelengths are however given correct to a tenth of an Angstrom and wave-numbers are given in whole numbers only. The bands are arranged in a V′, V″ scheme as given in Table II and are well represented by the equation·

$$\nu = 51683 + (164\ 5\,V' - 0\ 6\,V'^2 - 0\ 0035\,V'^3) - (213\ 6\,V'' - 0\ 6\,V''^2),$$

which in a physically more significant form becomes

$$\nu = 51707\ 55 + \{165\ 1\,(V' + \tfrac{1}{2}) - 0\ 595\,(V' + \tfrac{1}{2})^2 - 0\ 0035\,(V' + \tfrac{1}{2})^3\} - \{214{\cdot}2\,(V'' + \tfrac{1}{2}) -$$

The respective V′, V″ values and O − C values of all the bands are given in Table I It can be seen that some bands marked (*b*) can be placed at two places in the V′, V″ scheme Probably these values recorded by Cordes correspond to the mean value of two bands which might have caused some blending being very near to each other. This seems to be genuine because just for these bands the O − C values (Table I) and the $\Delta G_v''$ values (Table II) are abnormal For all the other bands the O − C values are reasonable if one takes into consideration the fact that the band heads are not quite recognisable, and therefore difficult to locate and measure. This may also be partly responsible for the irregularities in the ΔG_v values, but it may be mentioned that the irregularities met with can be deemed slight in comparison with those obtained in the analysis of other band systems of the molecule.

In keeping with the low temperatures at which the absorption is measured only a few vibrational levels of the ground state are excited. The V″ = 0, 1 and 2 progressions are well developed and the existence of a few bands with high V′ values involving V″ = 3 and 4 indicates the nature of the Condon parabola representing a moderate change in ω_e and r_e values.

The expression 214 2(V″ + ½) − 0 6(V″ + ½)² is very close to that of the ground state of iodine molecule[3] and this proves that Cordes bands are due to a transition from the ground state to an excited state with a frequency of 165·1 cm.⁻¹ and situated at 51683 cm.⁻¹ above the ground level. The state which gives P R and K.M. bands has $\omega_e \sim 90$ cm.⁻¹ according to Sponer and Watson.[8, 4] A preliminary attempt has shown that only a few bands if at all, on the extreme short wave side of K M. bands, can come in the V″, V′ scheme of Cordes bands with high V″ values. The above interpretation is supported by the fact that there are five groups of bands in

TABLE I

λ	ν	(V′, V″)	O−C
1948·1	51333	3 4	+ 8
1945·9	51390	2, 3	+16
1944 7	51423	1, 2	+ 1
1942·7	51475	0, 1	+ 5
1940 8	51527	3, 3	9
1938 6	51584	2, 2	− 1
1936 7	51636	1, 1	+ 1
1934 9	51683	0 0	0
1932·8	51739	3 2	− 7
1930 6	51799	2, 1	+ 2
1928 7	51849	1, 0	+ 2
1926·6	51904	4, 2	− 2
1924 7	51956	3, 1	− 2
1922 6	52013	2 0	+ 3
1920 7	52065	5, 2	0
1918 6	52120	4, 1	+ 2
1916·6	52175	3, 0	+ 4
1914·7	52227	6, 2	+ 4
1912 9	52277	5, 1	0
1911·0	52330	4, 0	− 1
1909 0	52383	7 2	+ 4
1907 1	52435	6, 1	0
1905 2	52489	5, 0	− 1
1903·5	52535	8, 2	+ 1
1901 6	52588	7, 1	− 3
1899·8	52637	6, 0	10
1897 8	52692	9, 2	+ 4
1896·0	52743	8, 1	− 3
1894 3[b]	52790	(7, 0), (11, 3)	−14, +10
1892 3	52847	10 2	+ 7
1890 8	52887	9, 1	−12
1888 9[b]	52940	(8, 0), (12 3)	−19 +11
1887 0	52994	11, 2	+ 4
1885 2	53048	10, 1	− 4
1883·7[b]	53088	(9, 0), (13, 3)	−24, +11
1881·8	53140	12, 2	0
1880·0	53193	11, 1	− 9
1878·1[b]	53248	(10, 0), (14, 3)	−16, +24
1876·4	53295	13, 2	+ 7
1874·5	53348	12, 1	− 4
1872 9[b]	53394	(11, 0), (15, 3)	−21, +26
1871·2	53442	14, 2	+ 8
1869 5	53491	13, 1	− 8
1867 5[b]	53548	(12, 0), (16, 3)	−17, +36
1866·0	53591	15, 2	+12
1864·3	53639	14, 1	− 7
1862·8[b]	53682	(13, 0), (17, 3)	−30, +28
1861 0	53733	16, 2	+11
1859·4	53782	15, 1	− 9
1857·8[b]	53827	(14, 0), (18, 3)	−32, +33
1856 1	53876	17, 2	+12
1854·5	53923	19, 3	− 9
1852 9[b]	53969	(16, 1), (21, 4)	+25, −36
1851 4	54014	18, 2	+10
1849·6	54066	20, 3	− 3
1848·2[b]	54107	(22, 4), (17, 1)	−22, +31
1846·6	54153	19, 2	+10
1845·0	54200	21, 3	− 5

TABLE 1 —(*Contd*)

λ	ν	(V′, V″)	O−C
1843 5[b]	54245	(23, 4), (18, 1)	−16, +29
1841·8	54294	17, 0	+ 5
1840·4	54337	22 3	− 2
1839·1[b]	54376	(19, 1), (24, 4)	+21, −16
1837·5[b]	54422	(18, 0), (21, 2)	− 7, +6
1836 1	54465	23 2	− 5
1834 7[b]	54505	(20, 1), (25, 4)	+13, −16
1833 2	54549	22, 2	− 1
1831 6	54597	24, 3	− 4
1830 2	54638	21, 1	+10
1828 9	54679	23 2	− 3
1827 3	54725	25, 3	− 5
1825 9	54767	22 1	+ 6
1824 6	54808	24, 2	− 4
1823 0	54854	26, 3	− 3
1821 7	54895	23, 1	+ 1
1820·1	54941	25, 2	0
1818·9	54979	22, 0	+ 5
1817 5	55021	24, 1	− 3
1816 0	55066	26, 2	− 2
1814 7	55105	23, 0	− 2
1813 3	55149	25, 1	− 4
1812 1	55185	27, 2	− 9
1810 5	55233	29, 3	+ 5
1809·3	55271	26, 1	− 9
1808 0	55311	28, 2	5
1806 7	55351	30, 3	+ 3
1805 3	55391	27, 1	−14
1804 0	55432	29, 2	− 7
1802 6	55475	31, 3	+ 9
1801 1	55522	28, 1	− 7
1798 9	55591	32, 3	+ 8
1797·6	55630	27, 0	+11
1796·6	55661	29, 1	+10
1795·6	55695	31, 2	+18
1794 3	55734	28, 0	− 8

emission with successive separation of about 165 cm^{-1}, which can only be explained due to transitions from the state at 51683 cm.$^{-1}$ having $\omega = 165$ cm^{-1}, to five different repulsive states dissociating into $^2P_{3/2} + {}^2P_{3/2}$, $^2P_{3/2} + {}^2P_{1/2}$ and $^2P_{1/2} + {}^2P_{1/2}$ iodine atoms[9]. Therefore, the Cordes bands and P.R.K M. bands come from two different states, the state giving rise to Cordes bands being the higher of the two.

Graphical extrapolation which is however a long one, gives the value 59000 ± 800 cm^{-1} or about 7·28 ± 0·18 volts, for the convergence limit of Cordes bands. The dissociation energy of the molecular state is thus 7317 ± 800 cm.$^{-1}$ Linear extrapolation for convergence gives the value 63143 cm^{-1} or about 7·8 volts which is the upper limit. The convergence limit for P.R.K.M. bands as found by Sponer and Watson[8] is also about

Table II

V″ \ V″										ΔG′
0	51683	208	51475							
	166		160							163
1	51849	214	51635	212	51423					
	164		164		161					163
2	52013	214	51799	215	51584	194	51390			
	162		157		155					158
3	52175	219	51956	217	51739	218	51527	194	51333	
	155		161		161					161
4	52330	210	52120	216	51904					
	159		157		161					159
5	52489	212	52277	212	52065					
	148		158		162					156
6	52637	202	52435	212	52227					
	153		158		156					154
7	52790[b]		52588	205	52383					
	150		155		148					151
8	52940[b]		52743	208	52535					
			144		157					150
9			52887		52692					
	160		161		155					159
10	53248[b]		53048	201	52847					
	146		145		147					146
11	53394[b]		53193	199	52994		52790[b]			
	153		155		146		150			151
12	53548[b]		53348	208	53140		52940[b]			
	134		143		145		148			143
13	53682[b]		53491		53295		53088[b]			
	145		148		147		160			147
14	53827[b]		53639	197	53442		53248[b]			
			143		149		146			146
15	..		53782		53591		53394[b]			
					142		154			148
16			53969[b]		53733		53548[b]			
			138		143		134			138
17	54204		54107[b]		53876		53682			
	128		138		138		145			137
18	54422[b]		54246[b]		54014		53827[b]			
			131		139					135
19	.		54375[b]		54153		53923			
			129				143			136
20	.		54505[b]				54066			
			133				134			134
21	..		54638		54422[b]		54200		53969[b]	
			129		127		137		138	133
22	54979	212	54767	218	54549	212	54337		54107[b]	
	126		128		130		128		138	130
23	55105	210	54895	216	54679	214	54465	220	54245[b]	
			126		129		132		130	131
24			55021	213	54808	211	54597		54376[b]	
			128		133		128		129	130
25	.		55149	208	54941	218	54725	220	54505[b]	
			122		125		129			125
26			55271	205	55066	212	54854			
			120		119					120
27	55680	239	55391	206	55185		.			
			131		126					128
28	55734	212	55522	211	55311					
			139		121					130
29	.		55661	229	55432	201	55223			
							118			118
30	..		..		.		55341			
							124			124
31	..		.		55695	220	55475			
							116			116
32	..		..		.		55591			
		214		211		210		211		

* In calculating the average ΔG″ values the abnormal ΔG″ values which are mostly to bands marked b are i

60,200 cm^{-1} or about 7 45 volts. Thus the molecular state giving rise to Cordes bands, and that giving rise to K.M P.R. bands arise from the same dissociation products

The question is what are the probable dissociation products? Now the ground state of the molecule dissociates into two normal I atoms in $^2P_{3/2}$ state at 12437 cm^{-1} (1 535 volts). The atomic term difference $^2P_{3/2} - {}^2P_{1/2}$ being 7600 cm^{-1} the dissociation level $^2P_{3/2} + {}^2P_{\frac{1}{2}}$ will therefore be at 20037 cm.$^{-1}$ and that of $^2P_{\frac{1}{2}} + {}^2P_{\frac{1}{2}}$ at 27637 cm^{-1} The resonance line $5p$, $^2P_{3/2} \longleftrightarrow 6s$, $^4P_{5/2}$ of iodine atom lies at 1830 A corresponding to an energy of 6 74 volts or 54632 cm^{-1}[14] Thus the level $^2P_{3/2} + {}^4P_{5/2}$ lies at 54632 + 12437 = 67069 cm^{-1} or 8 28 volts. If the dissociation products are to be *neutral* (though excited) atoms, there can be no level of dissociation products between 67069 and 27637 cm.$^{-1}$ The maximum value of the convergence limit of the Cordes absorption bands is 63143 cm.$^{-1}$ or 7 8 volts. Thus it is evident that the dissociation products are not neutral atoms The only other possibility is that they are I^- ($^1S_0$) + I^+ ($^3P_2$), negative and positive ions in their ground states If we assume that this is true and that the electron affinity[8] of iodine atom is 3 14 ± 0 07 volts, the ionisation potential of the iodine atom can be calculated as 8 9 ± 0 2 volts. This agrees with the ionisation potential experimentally obtained which varies from 8 to 10·5 volts according to different observers[6] Thus the possible dissociation products are very likely I^+ ($^3P_2$) + I^- ($^1S_0$) In support of this view there is the experiment of Ludlam and West[7] which shows appreciable conductivity in iodine vapour excited by wavelengths below 1850 A (above 54100 cm^{-1}) However the excitation being not monochromatic it is not possible to calculate the exact energy of the level $I^+ + I^-$ from their experiments

The next problem is to find the probable electronic terms and electronic configurations of the two molecular states Mulliken[9] has given the term scheme of the iodine molecule. The ground state of the molecule, $^1\Sigma_g^+$ or O_g^+ has the electronic configuration σ_g^2, π_u^4, π_g^4. [A transition from this to σ_g^2, π_u^4, π_g^3, σ_u (O_u^+) and (1_u) gives the visible and near infra-red absorption bands] The probable electronic configuration (as Mulliken has suggested for P R.K M. bands), for the two states that give Cordes and P.R.K M. bands seems to be σ_g, π_u^4, π_g^4, σ_u The probable electronic states from this are $^1\Sigma_u^+$ and $^3\Sigma_u^+$ if the coupling is of case (*a*) or (*b*) type and O_u^+, 1_u, O_u^- if the coupling is of case (*c*) type[9] $^1\Sigma_u^+$ of case (*a*) type is to be correlated with O_u^+ of case (*c*) type and $^3\Sigma_u^+$ of case (*a*) type to be correlated with 1_u and O_u^- of case (*c*) type. Cordes as well as Mulliken have attributed $^1\Sigma_u^+$ to the state that gives rise to P R K M. bands. The dissociation products according to Cordes are I^- ($^1S_0$) + I^+ ($^3P_2$). But the combination of these two atomic

terms gives only triplets but not singlets Thus the attribution of a singlet state $^1\Sigma_u^+$ according to strict case (*a*) or (*b*) type is not suitable. In a heavy molecule like iodine the tendency to case (*c*) type coupling is however greater than to case (*a*) or (*b*) type Then Ω becomes a good quantum number and the distinction between singlets and triplets loses its meaning As already mentioned above the probable electronic states according to case (*c*) type from the electronic configuration $\sigma_g\ \pi_u^4,\ \pi_g^4,\ \sigma_u$ are O_u^+, 1_u and O_u^- In absorption a transition cannot take place from the ground state to O_u^- because of $+ \rightarrow -$ prohibition rule Thus O_u^+ and 1_u seem to be the two electronic states that give rise to Cordes bands and K M bands respectively O_u^+ being of greater energy than 1_u O^+ and 1 states are among the states that will be possible from case (*c*) type coupling of $I^-(^1S_0) + I^+(^3P_2)$ Thus we conclude that Cordes bands belong to a transition from ground state to O_u^+ state and P R K M. bands are due to a transition from ground state to 1_u state

My thanks are due to Prof R K Asundi, for guidance and help

Summary

A new band system involving a frequency of 165 1 cm.$^{-1}$ in the excited state of the molecule is discovered in the absorption spectrum of iodine as measured by Cordes. This locates an electronic level at 51683 cm.$^{-1}$ above the ground level. The P-R, K-M bands form very probably a different system with a lower electronic level for their excited state The dissociation products of the initial states of both the systems are however identical, *viz*, $I^-(^1S_0) + I^+(^3P_2)$ The nature of the transitions giving rise to these two systems is discussed

References

1 Heinrich Cordes *Zs f Phys*, 1935, 97, 603
2 (*a*) Pringsheim and Rosen *Ibid*, 1928, 50, 1
(*b*) Kimura and Miyanishi *Scient Papers Inst of Phys and Chem. Research, Tokyo*, 1929, 10 33
(*c*) Sponer and Walson *Zs f Phys*, 1929, 56, 184
(*d*) Warren *Phys Rev*, 1935, 47, 1
(*e*) Curtis and Evans *Proc Roy Soc*, 1933, 141 A, 603
3 Sponer *Molekulspektren*, Vol I
4 Turner *Zs f Phys*, 1928, 31, 983
5 Sutton and Mayer *Journ Chem Phys.*, 1935, 3, 20
6. Fruth *Phys Rev*, 1928, 31, 614
Smith and Compton *Ibid*, 1920, 16, 501
Mulliken *Journ. Chem. Phys.*, 1934, 2, 782
7. R. S Mulliken *Phys. Rev*, 1934, 46, 549
8 Ludlam and West *Proc Roy. Soc Edinb.*, 1924, 45, 34.
9. Venkateswarlu *Proc. Ind Acad Sci* (this number).

EMISSION BANDS OF HALOGENS

Part I. Iodine Bands arising in 0_u^+ State at 51683 cm^{-1}

By P Venkateswarlu, M Sc

(Physics Department Benares Hindu University)

Received June 22, 1946

(Communicated by Dr R K Asundi, F A SC)

Introduction

In a previous communication on the emission bands of fluctuation type in the spectrum of iodine,[1] the existence of two wavenumber differences (about 214 cm^{-1} and 154 cm^{-1}) among the bands in the region 4,800 to 3,450 A was pointed out It was also suggested that the bands are probably due to the diatomic molecule I_2 Since then the bands have been further investigated with instruments of bigger dispersion and greater resolving power. In the meanwhile a new band system[2a] in the absorption spectrum of iodine recorded by Cordes[2b] has been reported. This system has for its excited electronic state a frequency of the order of 165 cm^{-1} This has led to an interpretation of such of the emission bands which involve a wavenumber difference of this order of magnitude. The present paper deals with this interpretation. General experimental details and description of the observed emission spectrum from 6700 A to 2400 A are given with wavelength data on the maxima of the bands interpreted

Experimental Details

A quartz tube 10 cm. in length and 2 cm. in diameter with fused-on clear windows, and containing some resublimed iodine crystals is attached to an evacuating apparatus. After evacuating it is excited by high frequency oscillations using tin foils as external electrodes. The tube was gently heated until no impurity spectra could be detected after which it was sealed off. The high frequency oscillations used for exciting the discharge were obtained from a modified Hartley oscillatory circuit using a Telefunken 'Re 134' valve. The frequency of the oscillations used is about 900 kc/sec. The colour of the discharge was pinkish white. In the visible region the spectrum was photographed on a constant deviation glass spectrograph and a 3-prism glass Steinheil spectrograph. In the ultraviolet region a Medium Hilger quartz spectrograph and an E_1-Hilger quartz Littrow spectrograph were employed The dispersion of the Steinheil spectrograph is about 6·5 A/mm.

at 4060 A and about 12·2 A/mm. at 4510 A. The E_1 quartz spectrograph has a dispersion of 4·2 A/mm. at 2860 A and about 11·2 A/mm. at 3920 A. Super Panchro-Press P 1200 and Process Regular B-20 Kodak plates were used. Process Regular B-20 plates proved to be more useful in the region 4500–2000 A as they gave better contrast than the other plates.

It is found that the nature of the spectrum (6700–2400 A) obtained by the above method does not differ from that obtained by exciting flowing iodine vapour through an uncondensed transformer discharge

General Description of the Spectra Obtained

In the region 6700–5000 A discrete bands degraded towards red and identical with the well-known visible absorption bands of iodine were obtained. These were, however, not followed by any continuum as in the absorption bands From 4800–2400 A, groups of diffuse bands were obtained. Of these the wavelengths and wavenumbers of the intensity maxima of the bands between 4800–3450 A only were published in *Nature* [1]

The wavelengths and wavenumbers of the intensity maxima of the bands in the region 4154–3978 A and 2712–2687 A which only will be discussed in this paper are given in Table I The intensity values given in the table

Table I

Emission as obtained in present experiments					Fluorescence	
Group	Intensity	λ in air	ν in vac	Average Δν	McLennan λ in air	Oldenberg λ in air
I	6 5 6 7 8 8 3	4154·4 4124·2 4094 6 4067·6 4044 6 4016·0 3991 1	24064 24240 24416 24578 24717 24881 25049	164 5	(4170) ? A single broad band from 4130 to 4015	4007 (10)
II	6 3	3945 6 3919·4	25338 25507	169	3925	3925 (10)
III	6 6	3879 9 3855 8	25767 25928	161	3870	3866 (8)
IV	3 4	3821 8 3796·0	26158 26322	164	3800	3813 (7)
V	4 3 4	2712·0 2699 6 2687 5	36862 37032 37198	168	2715 2697 2685	

correspond to the visually estimated relative intensities of these bands obtained on the Process Regular plate taken on the E_1 quartz spectrograph. The wavelengths of the bands between 4154 A and 3798 A correspond to mean values obtained from a number of plates taken on Steinheil, E_1 quartz and Medium quartz spectrographs So they differ slightly from the values published in *Nature*[1] which correspond to the mean values obtained from plates on Steinheil and Medium quartz spectrographs only as by that time experiments on E_1 quartz spectrograph were not done * The values of the three bands between 2712 and 2687 A are means of three readings on plates from E_1 quartz spectrograph. Plate XXV is a reproduction of the bands obtained.

Interpretation of the Bands

All these bands are diffuse and do not show any kind of structure with the instruments used. The wavenumber difference of successive bands in different groups is of the order of 165 cm^{-1} So these bands are probably due to a transition from a single electronic state with $\omega = 165$ cm.$^{-1}$ to different lower unstable states. The first group (*vide* Table I) consists of seven diffuse bands with an average wavenumber separation of 164 5 cm^{-1} The first of these bands is at 24064 cm.$^{-1}$ A new electronic level in iodine molecule with a frequency of 165 cm^{-1} has been recently reported [26] It lies at 51683 cm^{-1} above the ground level A transition from the ground state to this level gives the absorption bands recorded by Cordes in the vacuum region [26] If this electronic state is the initial state which gives rise to the seven diffuse bands of the first group, the point on the lower potential energy curve, which lies vertically below the minimum of the upper potential energy curve, will be at (51683–24064) = 27619 cm.$^{-1}$ above the ground level of I_2 Now the dissociation level of $I(^2P_{3/2}) + I(^2P_{3/2})$ which is accurately known from the visible absorption bands is at 20037 cm^{-1}[3] The atomic term difference $(^2P_{1/2} - {}^2P_{3/2})$ from Turner's[4] experiment is 7600 cm.$^{-1}$ So the dissociation level $I(^2P_{1/2}) + I(^2P_{1/2})$ lies at 27637 cm.$^{-1}$ It is thus possible to identify the lower state of the first group of seven bands as a repulsive state arising out of $I(^2P_{1/2}) + I(^2P_{1/2})$ and having a flat potential energy curve So a transition from the stable electronic state ($\omega = 165$ cm.$^{-1}$) to the flat potential energy curve that dissociates into $I(^2P_{1/2}) + I(^2P_{1/2})$ atoms gives the first group of bands.

Each of the second, third, and fourth groups (Table I) consists of two bands with wavenumber separations 169 cm.$^{-1}$, 161 cm.$^{-1}$ and 164 cm.$^{-1}$

* Grouping of the bands has also to be changed slightly because of the data available from the recent experiments.

respectively. The two bands of each group overlap one another and give the appearance of a broad continuous band with two intensity maxima. This suggests that these bands are due to transitions from the stable electronic state ($\omega = 165$ cm^{-1}) to three different repulsive curves of three unstable states. The three points on the repulsive curves, which lie vertically below the minimum of the stable potential energy curve lie at (51683–25338) = 26345 cm.$^{-1}$, (51683–25767) 25916 cm.$^{-1}$ and (51683–26158) 25525 cm.$^{-1}$ respectively above the ground level These repulsive states, which are slightly steep and almost parallel except at their common convergence limit, probably dissociate into $I(^2P_{1/2}) + I(^2P_{3/2})$ atoms whose dissoiation level lies at 20037 cm^{-1}

The three diffuse bands of the fifth group in the ultraviolet lie at 2712 0 A (36862 cm.$^{-1}$), 2699·6 A (37032 cm^{-1}), and 2687 5 A (37198 cm^{-1}) with an average wavenumber separation of 168 cm.$^{-1}$ If this state also has the above stated stable electronic level as the upper state, the point on the lower potential energy curve that lies vertically below the stable state will be at (51683–36862) = 14821 cm.$^{-1}$ This state is also a repulsive state having a nearly flat curve dissociating into $I(^2P_{3/2}) + I(^2P_{3/2})$ level at 12437 cm.$^{-1}$ or 1·535 volts.

It is indeed satisfactory to find that this interpretation is moreover in accordance with the theoretical predictions as to the number and nature of the electronic levels of I_2. The different molecular electronic states and their nature can be worked out either by combining the two iodine atoms in normal and various excited states, or from the electronic configurations of the molecule as a whole In neither case, however, can the excited energies be accurately calculated Mulliken[8] has worked out the term scheme and electronic configurations for the predicted molecular states Now the ground state of the iodine molecule is $^1\Sigma_g^+ (0^+_g)$ and the electronic configuration of the ten outer electrons is $\sigma_g^2, \pi_u^4, \pi_g^4$ The electronic state with $\omega = 165 \cdot 1$ cm.$^{-1}$ at 51683 cm^{-1} is 0_u^+ state[26] according to case (*c*) type coupling and can be correlated with $^1\Sigma_u^+$ of case (*a*) or (*b*) type The electronic configuration of this state which is the initial state of all the bands interpreted here is $\sigma_g, \pi_u^4, \pi_g^4, \sigma_u$ This dissociates into $I^-(^1S_0) + I^+(^3P_2)$ ions.

The lower state of the bands in the first group, according to the present interpretation, dissociates into $I(^2P_{1/2}) + I(^2P_{1/2})$ atoms The electronic states that are possible from the combination of such two atoms, according to case (*c*) type coupling, are 0_u^-, 1_u and 0_g^+ The only possible term out of these three, that can combine with the initial state 0_u^+, is 0_g^+. This 0_g^+ state can easily be correlated with $^1\Sigma_g^+$ of case (*a*) or (*b*) type which is one of the

states that can be derived from the electronic configuration $\sigma_g^2, \pi_u^4, \pi_g^3, \sigma_u^2$. (From this configuration the states $^1\Sigma_g^+$, $^1\Delta_g$, $^3\Sigma_g^-$ are possible)[5] Thus a transition from $\sigma_g, \pi_u^4, \pi_g^4, \sigma_u; 0^+ (^1\Sigma_u^+)$ to $\sigma_g^2, \pi_u^4, \pi_g^2, \sigma_u^2; 0^+_g (^1\Sigma^+_g)$ gives the seven diffuse bands of group I.

We have interpreted that the next three groups have their lower states dissociating into $I(^2P_{3/2}) + I(^2P_{1/2})$ The possible electronic states from the combination of these two atomic terms, according to case (*c*) type are $2_g, 2_u, 1_g, 1_u, 1_g, 1_u, 0_g^+, 0_u^+, 0_g^-, 0_u^-$ Of all these the only terms that can combine with the state 0_u^+ are 0_g^+, 1_g and 1_g. These respectively correspond to the final states of the bands in second, third and fourth groups. The first two terms 0_g^+ and 1_g which correspond to the final states of second and third groups can be correlated with $^3\Sigma_g^-$ of case (*a*) or (*b*) type[3] which can be derived from the same electronic configuration $\sigma_g^2, \pi_u^4, \pi_g^2, \sigma_u^2$, as the $^1\Sigma_g^+$ state discussed above Had it been a case (*a*) or (*b*) type coupling, however, the first two transitions would not have been possible because of $\Sigma^+ \leftarrow\!\!|\!\!\rightarrow \Sigma^-$ prohibition rule The occurrence of these two transitions is therefore a clear proof of the existence of case (*c*) type coupling in the iodine molecule, by which Ω becomes a good quantum number and Λ and Σ lose their significance The third state 1_g which is the lower state of the bands in the fourth group, can be correlated with $^1\Pi_g$ of case (*a*) type.[5] The electronic configuration of this state is $\sigma^2_g, \pi^3_u, \pi^4_g, \sigma_u$. Thus the second, third and fourth groups of bands definitely arise from the following transitions·

II Group :—$\sigma_g, \pi_u^4, \pi_g^4, \sigma_u$, $0_u^+(^1\Sigma_u^+) \rightarrow \sigma^2_g, \pi^4_u, \pi^2_g, \sigma^2_u$, $0^+_g (^3\Sigma_g^-)$

III Group :—$\sigma_g, \pi_u^4, \pi_g^4, \sigma_u$, $0_u^+(^1\Sigma_u^+) \rightarrow \sigma_g^2, \pi_u^4, \pi_u^3, \sigma_u^3$; 1_g

IV Group :—$\sigma_g, \pi_u^4, \pi_g^4, \sigma_u$; $0^+_u(^1\Sigma_u^+) \rightarrow \sigma^2_g, \pi^3_u, \pi^4_g, \sigma_u$; 1_g $(^1\Pi_g)$

The fifth group consisting of three bands has a lower state dissociating into $I(^2P_{3/2}) + I(^2P_{3/2})$. The possible electronic terms that arise from the combination of these two atomic terms are: $3_u, 2_u, 2_g, 1_u, 1_g, 1_u, 0_u^-, 0_g^+, 0_u^-$ 0_g^+. Of these, the terms that can combine with 0_u are only 0_g^+, 0_g^+, 1_g, Among these three, one 0_g^+ corresponds to the ground state of the iodine molecule The remaining two states 0_g^+ and 1_g, of which the former lies higher of the two, can be correlated with $^3\Pi_g$ of case (*a*) or (*b*) type which can be derived from the electronic configuration $\sigma_g^2, \pi_u^3, \pi_g^4, \sigma_u$. We will attribute the term $0_g^+ (^3\Pi_g)$ to the repulsive state that forms the final level of the bands of group V. The transition can be written as:

$$\sigma_g, \pi_u^4, \pi_g^4, \sigma_u \cdot 0_u^+(^1\Sigma_u^+) \rightarrow \sigma_g^2, \pi_u^3, \pi_g^4, \sigma_u \cdot 0_g^+ (^3\Pi_g).$$

Fluorescence Bands

McLennan[6] in 1913, and Oldenberg[7] in 1923 have obtained some fluorescence bands in this region by exciting iodine vapour with quartz mercury lamp According to McLennan, the Hg lines λ 1942 3 and λ 1849 6 are responsible for the ultraviolet fluorescence McLennan could get only a single broad continuous band extending from 4130 to 4015 A instead of the seven bands in the first group and one band each for the next three groups This might probably be because of the low dispersion instruments they used. The results of McLennan and Oldenberg are included in Table I. The numbers in brackets are the intensity values given in Oldenberg's paper The explanation of these fluorescence bands is now simple By illuminating the iodine vapour with wavelengths between 1950 and 1840 A, the molecules in the ground state can easily go to the stable electronic state 0_u^+ at 51683 cm^{-1} Transitions from this 0_u^+ state to different lower repulsive states, give the fluorescent bands similar to those obtained in emission

Summary

Among the diffuse fluctuation bands observed in the emission spectrum of iodine, there are five groups each of which involves a frequency difference of about 165 cm.$^{-1}$ among the component bands An interpretation of these five groups is given, which shows that they are due to transitions from a common initial level to five different final levels The initial level is identified with the newly discovered level 0_u^+ at 51683 cm^{-1} The five different final levels are identified with just those states whose energies and nature can be calculated theoretically All these are repulsive states with potential energy curves of varying slopes * The occurrence of bands (3945 6 and 3919·4 A) in the second group and of bands (3879 9 and 3855 8 A) in the third group clearly shows that the coupling conditions in I_2 are of Hund's case (*c*).

My thanks are due to Prof R K. Asundi for guidance and help and to Prof. S. P. Prasad, Science College, Patna, for permission to work on E_1 quartz spectrograph and for facilities during my stay at Patna. Thanks are also due to Lala Kamalapat Singhania Trust for the award of a scholarship.

* Fluorescence bands observed by McLennan and Oldenberg find a similar interpretation.

References

1.	Asundi and Venkateswarlu	*Nature*, 1945, 156, 452.
2 *a*	P Venkateswarlu	*Proc Ind Acad. Sci.* (in this number).
2 *b*	Cordes, H	*Zs f Phys*, 1935, 97, 603
3	Brown, W G.	*Phy. Rev.*, 1931, 38, 709
4.	Turner, L. A.	*Ibid*, 1926, 27, 397.
5	Mulliken, R. S	*Ibid.*, 1934, 46, 549.
6	McLennan, J C	*Proc Roy Soc.*, 1913, 88 A, 289
	———	*Ibid*, 1915, 91 A, 23
7	Oldenberg, O	*Zs f. Phys.*, 1923, 18, 1.

ILLUSTRATION TO PLATE

The plate shows the emission spectrum of iodine vapour excited by high frequency oscillations.

Spectrum (*a*) is taken on a 3 prism glass Steinheil spectrograph The bands of the first group (Table I) are marked

The spectra (*b*) and (*c*) are taken on an E_1 quartz spectrograph The bands of the first, second, third and fourth groups are marked in spectrum (*b*), and those of the fifth group are marked in spectrum (*c*)

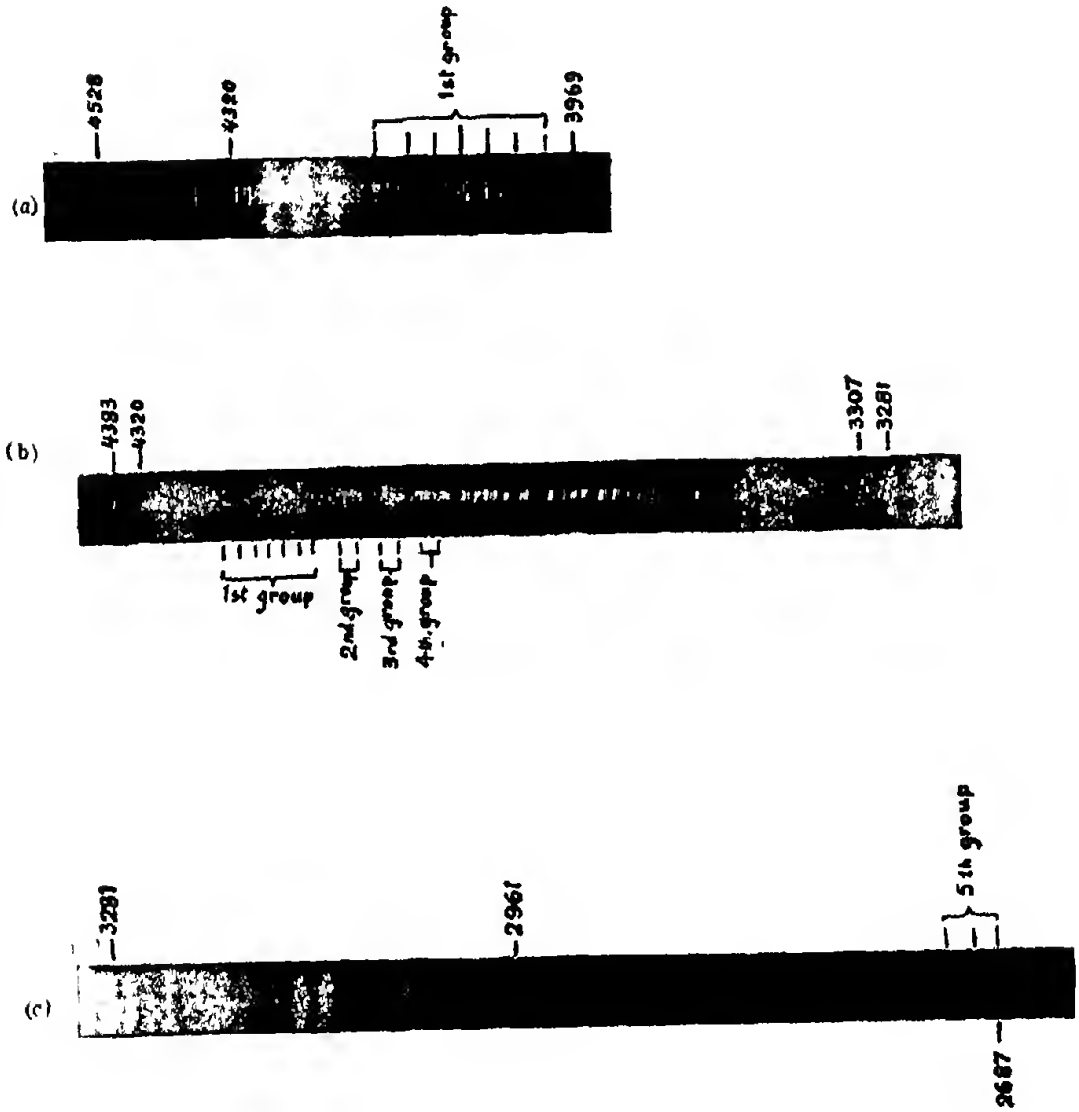
(a)
4528
4320
1st group
3969
(b)
4383
4320
1st group
2nd group
3rd group
4th group
3307
3281
(c)
3281
2961
5th group
2687

CONDENSATION OF ALDEHYDES WITH AMIDES

Part XII. Condensation of Benzaldehyde and o-Chlorobenzaldehyde

By Gur Saran Bhatnagar and Kantilal C Pandya

(*St John's College, Chemistry Laboratory, Agra*)

Received April 8, 1946

Pandya and Miss Pandya have shown that the aldehyde-malonic acid condensation is very favourably influenced by a chlorine or a bromine atom on the ring of the aldehyde.[1] In the present paper an effort is made to find out if the aldehyde-amide condensation is similarly influenced by one chlorine atom on the aromatic ring of the aldehyde In order to make the comparison good it was necessary to have definite yields from the benzaldehyde-amide condensation While this condensation, using benzaldehyde and various amides, has been studied by a host of workers in the past sixty years, the study has been carried out under very different conditions and in many cases the yields are not to be found. In the present investigation, therefore, it was necessary to have the figures of the yields of the condensations of benzaldehyde with various amides employing the same method that might be used for the chloro-benzaldehydes Some of these benzylidene-amides have been well known· others described here have been obtained for the first time.

Chlorine is found, on the whole, to increase the yield of the condensation product, though not in all cases The conclusion has to be also limited by the fact that only the *o*-chlorobenzaldehyde has been studied here, the *m*- and the *p*- ones being not available at the moment

In the condensations reported in the earlier eleven papers, it was found that heating the aldehyde and the amide alone together was one of the best of the processes· in some cases, however, the yields were distinctly improved by the use of 0·1–0·15 mol. of pyridine, though this was not so in all the cases examined. Here also pyridine has been found to improve the yield by 1 to 5%: but temperature and the time of heating had a more pronounced effect.

The products have generally been of the benzylidene-bisamide type, though, in the earlier papers, the monoamides too have been met with.[2] The aldol that must have presumably preceded the monoamide, has not so

far been obtained by any worker. Both benzaldehyde and *o*-chlorobenzaldehyde gave bisamide products. Formamide presented the usual difficulty, giving only a 13% yield with benzaldehyde. Another worker here (Mr. K K. Baslas) had obtained a 36% yield in 1942.[3]

EXPERIMENTAL

Condensation of Benzaldehyde with Amides

With Benzamide

Roth's[4] experiment as well as that of Hoffmann and Victor Meyer,[5] namely that of heating the aldehyde and the amide alone was first repeated.

i *In the Absence of Pyridine or any Condensing Agent.*—0·5 g benzaldehyde and 1 2 g benzamide (1·2 mol) were heated together in a 50 c.c. round-bottomed flask on a water-bath for six hours. The mixture first melted to a colourless liquid, which gradually passed on to a straw-yellow and a distinct yellow colour. Water vapours were seen coming out, there being no condenser After two hours the colour was yellowish brown which became brown after four hours. After six hours' heating, the flask was left overnight Next morning a dirty brown crystalline solid appeared, which was insoluble in water and in ether. The substance was taken out, crushed and shaken with 20 c c of hot water. The insoluble matter was removed by rapid filtration and washed again with hot water to remove all the remaining benzamide. It was washed with small quantities of ether to remove the unreacted aldehyde. The milky white needle-crystals were dried, and melted at 198° The product was insoluble also in chloroform and benzene, sparingly soluble in methyl alcohol and acetone, and readily soluble in hot alcohol. It was recrystallised thrice from hot dilute alcohol, when the melting point remained stationary at 217 5° (Victor Meyer obtained 218° after recrystallising it four times[5]). The yield was 0·36 g. or 21·8% of theory

ii *In the Presence of Pyridine-Trace.*—The same amounts were taken with 0 05 c.c. of pyridine (1 : 2·0·1 mol.) and heated on water-bath for six hours as before The observations and the procedure were the same. The purified product as well as the mixture of the products of the two experiments gave the same melting point The yield was 0·39 g. or 23% of theory.

iii. Another experiment with 0·5 mol. of pyridine, *i.e.*, 0·25 c.c., but treated exactly as above, gave the same yield of 23%.

iv. With 0·1 mol. of pyridine, but on reducing the heating to only two hours on water-bath, the yield decreased to 0·2 g. or 12·4% of theory.

v. Taking again no pyridine but heating at 115° for six hours gave a hard dark brown product, which gave, on purification, a good melting point, weighed 1·05 g. and was thus 63·6% in yield. This was the best yield obtained.

vi. When the molecular proportions were 1 : 1 and there was no pyridine, and the heating was carried out by the smallest flame with asbestos for two hours, the yield was only 8%.

(Found: N = 8·73%; benzylidene-bisbenzamide $C_{21}H_{18}O_2N_2$ requires 8·48%. The mono-amide would require 6·69%.) It gave no colour with concentrated sulphuric acid and did not decolorise Baeyer's reagent in the cold indicating an absence of unsaturation

Condensation with Acetamide.

i. *In the Absence of any Condensing Agent.*—1·0 g. benzaldehyde and 1·2 g. acetamide (1 : 2) were heated as above on water-bath for six hours. A solid began to separate after 3 hours. Next day a yellow crystalline solid appeared in the cold flask. It was taken out and treated with water and ether as before. Silky white needle-crystals melting at 212° were obtained, which on recrystallisation (hot alcohol) finally melted at 245°. The yield was 0·35 g. or 17% of theory, calculated as bisamide. It has been prepared by Roth,[4] and recently by Noyes and Forman,[6] who refluxed the amide and the aldehyde with acetic acid for four hours and who report the melting-point as 238° and a 48% yield.

ii. *In the Presence of Pyridine-Trace*—To the same quantities of the aldehyde and the amide, 0·1 c c. of pyridine was added (1 : 2 : 0·1 mol.), and the whole heated as before on a water-bath for six hours. The product melted at 245° and the yield was 0·39 g. or 19·5°.

iii. *Heating Without any Condensing Agent for* 18 *Hours.*—The product was hard, brown and in an increased amount. Yield = 1·1 g. or 55% of theory.

iv. *Heating at Higher Temperatures.*—The heating was at 115° for six hours. The yield was 1·0 g. or 50% of theory. (Found: N = 13·84%; benzylidene-bisacetamide $C_{11}H_{14}O_2N_2$ requires 13·59%.) Its solubility and reactions were the same as those described for the bis-benzamide derivative.

Condensation with Formamide.

This has been studied by Bülow,[7] whose experiment was repeated.

i. *In the Absence of any Condensing Agent.*—1·0 g. of benzaldehyde and 0·9 g. of formamide were taken (1 : 2 mol.) and heated on a water-bath for 24 hours (in four days). Water vapour came out and the colour changed to pale yellow and then to orange-yellow. A sticky solid also made its

appearance, which after treatment with water and ether melted at 130°. On recrystallisation from hot alcohol it became a white crystalline material melting at 148° (Bülow gives 149–50°[7]). It was soluble in hot water and hot alcohol. The yield was only 0·15 g. or 9% of theory.

ii. *In the Presence of Pyridine-Trace.*—0·1 c.c. of pyridine was added to the same amounts and the mixture was heated on as before. The yield was slightly better, 13·2% of theory.

The product was soluble in hot water and hot alcohol, and gave no reaction with Baeyer's Reagent and with concentrated sulphuric acid, and was identical with Bülow's benzylidene-bisformamide.

iii. *At Higher Temperature.*—Following Bülow, the two were kept in a flask provided with a reflux condenser and heated with a small flame on asbestos wire-gauze, so that it kept on boiling very gently. In five minutes the liquid became pale yellow, yellow and lastly dark brown. The heating was stopped after two hours. The dirty yellow amorphous product, obtained after treatment with water and ether, melted at 240°, and after recrystallisation (alcohol), at 246°, corresponding to Bülow's 246–47°. It was tetraphenylpyrazine: the yield was only 18% of theory. It decolorised bromine water and alkaline permanganate in the cold and gave a brownish colour with concentrated sulphuric acid.

Condensation with Propionamide.

0·5 G benzaldehyde and 0·7 g. propionamide were heated alone on a water-bath for three hours. Next morning a pale yellow solid appeared which did not melt on the water-bath. The flask was therefore put on an oil-bath and the bath gradually raised to 120° when the reactants again fused to a yellow liquid. The heating was continued for five hours more, when the product had a brown-yellow colour. The crystalline solid was treated with water and ether and became beautiful milk-white needle crystals, melting at 218°. Recrystallised (alcohol), the melting point rose very little, becoming 220°. (Found: N = 12·56%; the benzylidene-bispropionamide $C_{12}H_{16}N_2$ requires 11·97%.) The yield was 0·35 g. or 30·7% of theory. Its properties were similar to those of the other bisamides mentioned above.

Condensation with n-Butyramide.

0·5 G. benzaldehyde and 0·9 g. *n*-butyramide were heated on a water-bath. As only some of the amide dissolved by this time and as higher temperatures are favourable to better yields, the flask was transferred to an oil-bath at 110–15°, when complete fusion to a clear liquid took place. After

five hours the heating was stopped. Next morning plenty of aldehyde was found still left and so the temperature was raised to 115°. As all the substance did not fuse, the temperature was raised to 130° when a full melting occurred. The heating was carried on for three hours more. The brown solid product was extracted in the usual way. White needle-like crystals melting at 160° were obtained. Recrystallisation (alcohol) raised the melting point to 170°. It had the same properties as described above. (Found: N = 10·74%; benzylidene-bis-*n*-butyramide $C_{15}H_{22}O_2N_2$ requires 10·68%) The yield was 1·1 g. or 86% of theory.

Condensation with n-*Heptamide*

0·5 G. benzaldehyde and 1·3 g. *n*-heptamide (1 : 2 mol) were heated as usual on water-bath for 5 hours Next morning a yellow solid mass was seen which smelt distinctly of benzaldehyde and therefore the heating was continued, first on water-bath, later on an oil-bath at 120° when the reactants changed into a yellow liquid. After 2 hours' heating, the bath was raised to 130° and the heating continued for another four hours. The dirty brown mass was treated next morning with water and ether and gave a white crystalline product melting at 124°. Recrystallisation (alcohol) raised the meltingpoint to 128° (Found: N = 7·92%; benzylidene-bis-*n*-heptamide $C_{21}H_{34}O_2N_2$ requires 8·09%.) The yield was 0 82 g or 48·2% of theory. Its reactions were similar to those of the other bisamides above.

Condensation with Cinnamamide.

0·5 G. benzaldehyde and 1·47 g. cinnamamide (prepared in the laboratory from the acid) were heated on an oil-bath at 130°. After four hours in this way, the temperature was raised next day to 160° and the heating continued for 5 hours. Next morning the mass was found to be so hard that it could not be powdered with a glass rod. The usual treatment released a brownish powder melting at 216°. On recrystallisation the melting point rose to 238° and retained a buff colour. (Found: N = 7·26%; benzylidene-biscinnamamide requires 7·33%.) The yield was 1·5 g. or 80% of theory. It decolorised bromine water and Baeyer's reagent in the cold, on account of the unsaturation present in cinnamamide.

Condensation of o-*Chlorobenzaldehyde*

Condensation with Acetamide.

1·4 G. *o*-chlorobenzaldehyde and 1·2 g. acetamide were taken.

i. *In the Absence of any Condensing Agent.*—The two were heated on water-bath for 5 hours. A yellow and not a very hard crystalline mass

appeared in the flask next morning, melting at 240°. Recrystallisation (hot alcohol) raised the melting point to 250°. The yield was 0·95 g. or as bisamide 40% of theory.

ii. *In the Presence of Pyridine-Trace.*—0·1 c.c. of pyridine was added (1:2:0·1 mol) to the same amount of the two, and the whole was heated for five hours on water-bath. The yellow crystalline product was next day treated as usual, when it gave white needles, melting at 240°, and, after purification at 250° The yield was 1·05 g. or, as bisamide, 43·4% of theory.

iii. *Higher Temperature Without a Condensing Agent.*—The aldehyde and the amide were heated alone on an oil-bath at 110° for 5 hours. Next morning the brown product was treated as usual and was changed into white crystals melting at 241°, which on recrystallisation melted at 250°. The yield was 1·3 g. or 54·5% as bisamide. On fusion with sodium, the product showed that it contained chlorine (Found: Cl = 14·33%; *o*-chlorobenzylidenebisacetamide $C_{11}H_{12}O_2N_2Cl$ requires 14·76%. The mono-amide would require 19·55%. (Found: N = 11 48%; the above bisacetamide requires 11·22%.) Its properties were similar to those of the corresponding benzylidene-bisacetamide.

Condensation with Propionamide.

o-Chlorobenzaldehyde 1·4 g. and propionamide 1·5 g. were taken.

i. *In the Absence of any Condensing Reagent*—The two were heated alone on water-bath for 5 hours. Next day they had to be kept on an oil-bath at 115° to ensure fusion, the heating being for 5 hours. Brown hard crystalline mass soon changed to white crystals under the usual treatment, and melted at 210°, the recrystallised pure product melting at 216°. The yield was 1·8 g. or as bispropionamide 67% of theory.

ii. *In the Presence of Pyridine-Trace.*—The same amounts were heated with 0·1 c.c. of pyridine (1:2:0·1 mol.) on water-bath for 4 hours and, the next day, on an oil-bath at 115° for 5 hours. The product came out as usual, weighing 1·9 g. or as bisamide 68·3% of theory. The melting and the mixed melting points were identical, and so were its properties. (Found: Cl = 12·99%; *o*-chlorobenzylidenebispropionamide $C_{13}H_{17}O_2N_2Cl$ requires 13·22%.)

Condensation with n-*Butyramide.*

o-Chlorobenzaldehyde 1·4 g. and *n*-butyramide 1·75 g. (1:2 mol.) were taken.

i. *Heating alone at* 130°.—The two were heated on a water-bath for 4 hours on one day and the next day at 120° for another 2 hours and a

125–30° for 2 hours more. After purification the product melted at 173° and after recrystallisation the final melting point was 180°. The yield was 1·9 g. or 64·2% of theory.

ii. *Heating alone up to* 145°—The heating was for 3 hours at 130° and for 3 hours at 140–45°. The product was 2·5 g. or 86% of theory. (Found: Cl = 11·64%; the *o*-chlorobenzylidene-bis-*n*-butyramide $C_{15}H_{21}O_2N_2Cl$ requires 11·97%.)

Condensation with Benzamide.

i. *In the Absence of any Condensing Agent*—*o*-Chlorobenzaldehyde 1·4 g. and benzamide 2·4 g. were heated together first on water-bath and then on an oil-bath at 110° for about 4 hours in all. The next day the mixture was heated at 140° for 3 hours. The crude white crystals melted at 200°; recrystallised (dilute hot alcohol) the product melted at 215°. The yield was 2·5 g. or 70% of theory.

ii. *In the Presence of Pyridine-Trace.*—In the presence of 0 1 mol. of pyridine and heated at 110° for three hours and 140° for another three hours, the same product was obtained, melting at 215° after recrystallisations. The yield was 2·7 g. or 74·5% of theory. (Found: Cl = 9·39%, *o*-chlorobenzylidene-bisbenzamide $C_{21}H_{15}O_2N_2Cl$ requires 9·74%.)

Condensation with Formamide.

In the Absence of any Condensing Agent.—*o*-Chlorobenzaldehyde 1·4 g. and formamide 0·9 g. were heated alone. In one experiment, (i) on water-bath for 30 hours in 5 days. A brown sticky mass was obtained, which, by means of the usual process, gave a crude product melting at 169°. When recrystallised (alcohol), it finally melted at 176°. It was straw yellow in colour. The yield was only 8% of the theory, as bisamide. In the second experiment, (ii) the two were heated at 140° for five hours. Next morning a dark brown viscous liquid was left. It was washed with water. On treating it with ether, it was found to dissolve completely in it, leaving no insoluble solid. After the evaporation of ether, it was shaken up with a saturated solution of sodium bisulphite, when some solid derivative, possibly of the aldehyde, separated But the residue remained a liquid from which no solid derivative could be isolated. It was obvious that the heating was insufficient.

The solid obtained in (i) gave on analysis Cl = 16·3%; *o*-chlorobenzylidenebisformamide $C_9H_8O_2N_2Cl$ requires 16·70%. Its properties were similar.

Condensation with n-Heptamide.

o-Chlorobenzaldehyde 1·4 g. and *n*-heptamide 2·6 g. (1 : 2 mol.) were heated on a water-bath for two hours, when a solid began to separate. The heating was continued at 110° for four hours; more solid separated in the beginning but later on it went into solution, thus at the end of the heating there was no solid in the flask. Next morning the solid that had come out was found to contain plenty of the free aldehyde, and so the heating was continued at 125° when the solid again went in solution. After 2 hours a solid again came out which increased in amount gradually, the heating being stopped after five hours. The hard brown crystalline product found next morning, gave after the usual treatment, a white crystalline product melting at 135°, and after recrystallisation, 141°. (Found: Cl = 9·09%; *o*-chlorobenzylidene-bis-*n*-heptamide $C_{21}H_{32}O_2N_2Cl$ requires 9·32%.) The yield was 3·1 g. or 81·6% of theory. Its properties were similar.

Condensation with Cinnamamide.

o-Chlorobenzaldehyde 1·4 g. and cinnamamide 2·9 g. were heated together (1 : 2 mol.) first on water-bath and then on an oil-bath at 120° when the reactants melted to a brown liquid. After 2 hours the temperature had to be raised to 130° for 2 hours and to 140° for another 2 hours. The next day the hard dark brown mass, on the usual treatment, gave a brown powder melting at 216° which, after several recrystallisations, melted finally at 232°. It was a buff coloured substance. (Found: Cl = 8·08%; *o*-chlorobenzylidenebiscinnamamide $C_{25}H_{21}O_2N_2Cl$ requires 8·52%.) The yield was 3 g. or 72% of theory. As before in the case of the benzaldehyde compound, it decolorised bromine water and Baeyer's reagent in the cold and gave a brown colour to concentrated sulphuric acid.

	Benzaldehyde		*o*-Chloro-benzaldehyde	
Amides	Maximum yield %	Melting point	Maximum yield %	Melting point
Formamide ..	13·2	148° C.	8	176° C.
Acetamide ..	55	245° C.	54·5	250° C.
Propionamide ..	30·7	220° C.	68	210° C.
n-Butyramide ..	86	170° C.	84	180° C.
n-Heptamide ..	48·2	128° C.	81·6	141° C.
Benzamide ..	63·6	217·5° C.	74·5	215° C.
Cinnamamide ..	80	228° C.	72	240° C.

Summary

The condensation of benzaldehyde and of *o*-chlorobenzaldehyde with several amides has been studied, in the presence as well as in the absence of pyridine. The base slightly increased the yield in many cases. The rise of temperature as well as the prolongation of heating raised the yield more effectively. All the products were the corresponding bisamides. The presence of chlorine on the aromatic ring of the aldehyde, had the expected tendency to increase the yield, particularly in the condensations with benzamide, propionamide and *n*-heptamide. Condensations with formamide, as has been the general experience, did not give good yields; in all other cases, the yields were good, starting from 30% and reaching up to 86% in some cases.

References

1. Pandya and Miss Pandya . *Proc. Ind. Acad. Sci* (A), 1941, 14, 112.
2. Pandya and Sodhi *Ibid.*, 1938, 7, 361.
3. Krishna Kumar Basias . Thesis, M.Sc, Agra University, 1941.
4. Roth .. *Annal.*, 1870, 154, 72, 76.
5. Hoffmann and Victor Meyer .. *Ber.*, 1892, 25, 212.
6. W. A. Noyes and Don. B. Forman *J. Am. C. S.*, 1933, 55, 3493–6.
7. Bülow *Ber*, 1893, 26, 1972–4 *J. C. S.* (A), 1893, 1, 712.

CHEMICAL EXAMINATION OF THE FIXED OIL DERIVED FROM THE WOOD OF *PTEROCARPUS MARSUPIUM* ROXB.—PART I

By Prithwi Nath Bhargava

(*Chemistry Department, Benares Hindu*

Received September 2, 1946

(Communicated by Dr. S. Dutt, F.A.SC.)

Pterocarpus Marsupium Roxb, commonly known in Hindi and Bengali as 'Bija Sal', is a large deciduous tree, belonging to the Natural Order 'Papilionaceæ'. It grows all over India, especially in the extreme south-east corner of Kumaon, Oudh forest, Gorakhpur, Central and South India and as far as Rajmahal hills in Bihar and Ceylon.

The wood is heavy, close-grained, and yellowish-brown in colour with an aromatic smell. The heart-wood is darker than the sap-wood and often contains dark coloured streaks. The wood is very commonly used in making doorsills, doors and furniture in general as a cheap substitute for teak. Recently the Railway Board of India has been using it for sleepers with success in place of sal, because it is not affected by white-ants and other insects and does not undergo any fungous rot on storage.

According to Kirtikar and Basu[1] and K. L. Dey,[2] the wood has got interesting medicinal properties. On account of its bitter and astringent action it has been used for a long time in this country for the cure of diabetes. Generally, the patient is asked to have a cup made of the wood in which water is kept overnight and the decoction drunk next morning. This is repeated for a number of days, until the wood is exhausted, when it is thrown away and a fresh cup made. A paste made from the wood by rubbing it on a stone slab with water is used for sores, boils, etc. In the bark of this and other species of this genus are sacs filled with a red astringent oily gum, which is obtained by making incisions in the bark and sold as East Indian Kino. This Kino being an officinal is used as an astringent medicine in diarrhœa and pyrosis. Its action being milder, it is better adapted for children and delicate females.

The chemical constituents of the wood, which impart to it the medicinal properties described above, are not known, and the wood does not seem to have been chemically examined as yet. In the present investigation the

wood has been found to contain 0·52% of a fixed oil, potassium nitrate, an essential oil and 0·25% of a fine yellow colouring matter and one should not be surprised if these products are responsible for its medicinal properties. In this paper, the fixed oil obtained from the petroleum ether extract of the wood shavings has been examined.

A detailed examination of the oil has shown that the component liquid acids are oleic 41·59%, linoleic 35 91% and linolenic 3·38%. A special feature of the oil is that it contains a high percentage of the unsaponifiable matter and a low percentage of solid fatty acids. The solid fatty acids have been obtained in insufficient amount for a thorough quantitative examination. The unsaponifiable matter will be dealt in Part II of this series.

Experimental

A big lot of the authentic specimen of wood was chipped, dried in sunlight and beaten into small shavings In order to have an approximate idea regarding the solubility of the constituents of wood in different solvents, the coarsely powdered shavings were extracted in lots of 200 gm with a number of solvents and after filtration the solvent was evaporated in each case and the residue brought to a constant weight by keeping in a steam oven. The following results were obtained.

Petroleum-ether extract (0·59%).—A sweet smelling yellow oily liquid, turning yellow with caustic soda solution and reddish yellow with strong sulphuric acid.

Benzene extract (1·5%).—A yellow oily liquid soluble in hot alcoholic caustic potash solution.

Chloroform-extract (4·41%).—A reddish yellow oily substance, slightly soluble in alcohol and insoluble in water, but developing a yellow colour with caustic soda solution.

Ether extract (2·14%).—A yellow fatty and resinous substance, soluble in alcohol, yellow with caustic soda and red with strong sulphuric acid.

Ethyl acetate extract (11·01%).—A brown resinous substance, acidic to litmus, soluble in water, yellow with caustic soda, dark red with strong sulphuric acid and finally decolourising bromine water.

Alcohol extract (19·92%).—A dark brown solid, slightly acidic, soluble in water and also in caustic soda, giving a red colour with strong sulphuric acid, an orange precipitate with lead acetate and reducing Fehling's solution.

Aqueous extract (16·78%).—A brown substance soluble in caustic soda solution and giving a red colouration with ferric chloride.

For complete extraction about 15 kilos of small shavings were extracted with petroleum ether (b.p. 40–60° C.) in a five litre extraction flask. On distilling off the solvent about 80 gm. of a reddish brown oil having a characteristic smell were obtained. The oil was allowed to stand overnight but nothing was deposited. It was subjected to steam distillation, whereby the volatile oil was removed. Now there remained in the distilling flask an aqueous layer and above it an oily layer. The oily layer was separated by means of a separating funnel and dissolved in petroleum-ether. The aqueous layer was discarded. On distilling off the solvent, a dark red oil was obtained and was purified with animal charcoal and fuller's earth, having the following physical and chemical constants as recorded in Table I. The yield of the oil was 0·52% on the weight of wood shavings.

The shavings after complete extraction with petroleum-ether were further extracted with alcohol. The examination of the alcoholic extract containing the colouring matter will be the subject of communication in the next paper.

TABLE I

Specific gravity $\frac{\text{Oil } 25°\text{C.}}{\text{Water } 25°\text{C}}$	..	0·9082
Refractive index ($n_d^{25°C}$)	..	1·4648
Acid value	..	18·68
Saponification value	..	189·9
Acetyl value	..	40·5
Iodine value (Wijs)	..	105·8
Hehner value	..	94·4
Unsaponifiable matter	..	7·8%

60 gm. of the oil were saponified with 20% alcoholic caustic potash and the unsaponifiable matter extracted with ether as usual. The ethereal solution was set aside and examined in Part II of this series. The soap was then dissolved in hot water, the solution cooled and decomposed with dilute hydrochloric acid in presence of ether. The ethereal solution of the fatty acids was freed from the solvent by distillation. The fatty acids thus obtained had the following physical and chemical constants as recorded in Table II.

TABLE II

Consistency	..	Liquid
Neutralisation value	..	200·4
Saponification value	..	200·2
Mean molecular weight	..	280·1
Iodine value (Wijs)	..	117·8

The mixture of fatty acids described above was then separated into solid and liquid acids by Twitchell's[8] lead-salt alcohol process. The solid

acids were obtained in small quantities only and were insufficient for thorough quantitative examination. Hence the solid acids were examined qualitatively and the liquid acids quantitatively. The following table gives the percentage, iodine value (Wijs) and neutralisation value of the solid and liquid acids (Table III).

TABLE III

Examination of the Liquid Acids

Acids		Percentage in oil	Percentage in mixed acids	I.V.	N.V
Solid	..	6·12	7·03	0·64	202·3
Liquid	..	80·88	92·96	137·7	198·9

EXAMINATION OF THE LIQUID ACIDS

Oxidation with Potassium Permanganate.—The liquid acids on oxidation according to the method of Lapworth and Mottram[4] gave a dihydroxy stearic acid, m.p. 130° C., a tetrahydroxy stearic acid, m p 172° C., and a hexahydroxy stearic acid, m p. 202° C., showing the presence of oleic, linoleic and linolenic acids.

Bromination Method.—The constituents of the liquid acids were determined quantitatively according to the method of Eibner and Muggenthaler[5] modified by Jamieson and Baughman,[6] whereby the bromine addition products of the constituent acids were prepared at −10° C. and examined. Linolenic hexabromide, m.p. 180–81° C., and linoleic tetrabromide, m p. 113° C, were confirmed when their melting points on admixture with pure samples of linolenic hexabromide and linoleic tetrabromide respectively remained undepressed. The results are given in Table IV.

TABLE IV

Weight of liquid acids taken	..	5·2738	gm.
Weight of linolenic hexabromide	..	0·6008	,,
Percentage of bromine in the above (Piria and Schiff's) method	..	62·88	
Weight of linolenic acid	..	0·2204	,,
Weight of linoleic tetrabromide			
Percentage of bromine	..	53·08	
Weight of linoleic acid		1 8600	,,
Weight of the residue (di- and tetrabromides)		5·2716	,,
Percentage of bromine		39·51	
Weight of oleic acid		2·7117	,,
Total weight of linoleic acid		2·2415	,,

The percentage of the various acids in liquid acids, mixed acids and the oil is given in Table V.

TABLE V

Examination of the Solid Acids

Acids		Percentage in liquid acids	Percentage in mixed acids	Percentage in oil
Oleic	..	51·42	47·80	41·59
Linoleic	..	44·40	41·28	35·91
Linolenic	..	4·18	3·88	3·38

EXAMINATION OF THE SOLID ACIDS

As the solid acids were obtained in insufficient amounts for a thorough quantitative examination, these were examined qualitatively only. The crude acids melted at 57° C. On repeated crystallisation from acetone two fractions were obtained, one melting at 67–68° C. and another at 61° C. The melting points of both the fractions on admixture with pure samples of stearic acid and palmitic acid respectively remained unchanged. Thus stearic and palmitic acids were confirmed in the solid acids.

SUMMARY

The wood shavings of *Pterocarpus Marsupium* on extraction with petroleum-ether (b.p 40–60° C.) have been found to yield 0·52% of a semi-drying oil having $d^{28°}$ 0·9082, $n_d^{25° C.}$ 1·4648, acid value 18·68, sap. value 189·9, acetyl value 40·5, Hehner value 94·4, iodine value (Wijs) 105·8 and unsaponifiable matter 7·5%.

The component liquid acids on further examination have been found to give linolenic 3·38%, linoleic 35·91% and oleic 41·59%.

The solid fatty acids being insufficient for a thorough quantitative examination, have been examined qualitatively only and are found to yield palmitic and stearic acids.

REFERENCES

1. Kirtikar and Basu . *Indian Medical Plants*, 827.
2. Dey, K. L. .. *Indigenous Drugs of India*, 260.
3. Twitchell .. *J. Ind. Eng. Chem.*, 1921, 13, 806.
4. Lapworth and Mottram .. *J.C.S.*, 1925, 127, 1628.
5. Elbner and Muggenthaler .. *Chem. Tech. of Oils, etc.*, Vol. I, 568.
6. Jamieson and Baughman .. *J. Amer. Chem. Soc.*, 1920, 42, 1197.

CHEMICAL EXAMINATION OF THE FIXED OIL DERIVED FROM THE WOOD OF *PTEROCARPUS MARSUPIUM* ROXB.

Part II. Isolation of Pterocarpol A and Pterocarpol B

By Prithwi Nath Bhargava

(*Chemistry Department, Benares Hindu University*)

Received September 2, 1946

(Communicated by Dr S. Dutt, F A SC)

In the previous paper on this subject the author, in course of his investigation on the chemical constituents of the fixed oil, has referred to the ethereal solution of the unsaponifiable matter. From this ethereal solution two compounds of the nature of phytosterols (*a*) m.p 112° C. and (*b*) m p. 161° C. have been obtained after purification according to the method of Windaus and Hauth.[1] These have been named Pterocarpol A and Pterocarpol B respectively. In the present paper, the isolation as well as the systematic chemical examination of both the sterols is recorded.

A detailed examination of pterocarpol A, $C_{27}H_{46}O.\ 2H_2O$ after drying in air and $C_{27}H_{46}O$ after drying at 100° C. *in vacuo*, has shown only one hydroxy group in the molecule and it gives reactions of a phytosterol. The compound pterocarpol B, $C_{27}H_{46}O$ after drying at 110° C. *in vacuo* has been also found to contain one hydroxy group in the molecule and to give the reactions of a phytosterol. Thus pterocarpol A and pterocarpol B are obtained in an yield of 0·011% and 0·005% respectively on the weight of wood shavings.

Experimental

Isolation of pterocarpol A and pterocarpol B.—The ethereal solution of the unsaponifiable matter as described in Part I, was now distilled to recover the solvent completely. The residue was treated with benzene in which it was only partially soluble. The insoluble product was filtered and the filtrate was distilled to recover benzene. The residue after distilling benzene was repeatedly crystallised from methyl alcohol with the addition of animal charcoal in white flakes, m.p. 110° C. (Fraction I).

The benzene-insoluble product was then dissolved in chloroform. The greater part of the solvent was distilled off and the concentrated solution allowed to stand overnight, but nothing crystallised out. Hence the solvent

was completely evaporated off and the residue crystallised from methyl alcohol a number of times with the addition of animal charcoal until colourless leaflets, m.p. 158° C., were obtained (Fraction II). Both the fractions were further purified according to the method of Windaus and Hauth (*loc. cit.*).

The Fraction I (3 gm.) was acetylated as usual and crystallised from alcohol in colourless needles, m.p. 92° C. This acetyl derivative was dissolved in ether (25 c.c.) and treated with a 5% solution of bromine in glacial acetic acid (35 c.c.). The brown solution was allowed to stand overnight in a frigidaire, when a yellowish precipitate was obtained. This precipitate was filtered, washed with 75% acetic acid and dried in a vacuum over strong sulphuric acid. The dried product was crystallised from chloroform in yellow leaflets, m.p. 86° C. It was debrominated by boiling with zinc dust (2 gm.), glacial acetic acid (5 c.c.) and alcohol (40 c.c.) for three hours. The colourless solution was filtered to remove the excess of zinc, diluted with water and extracted with ether. The ethereal solution was evaporated and the residue saponified by boiling with alcoholic caustic potash. The solution was diluted with water, the residue extracted with ether and the solvent was evaporated off. The remaining residue on crystallisation from methyl alcohol gave colourless leaflets, m.p. 112° C. The yield of pterocarpol A thus obtained was 1·3 gm., *i.e.*, 0·011% on the weight of wood shavings.

The Fraction II (1·3 gm.) was acetylated, brominated and debrominated in order to get the pure sterol similarly as Fraction I. The acetyl derivative was obtained in white flakes, m.p. 120° C. The brominated product, acetyl pterocarpol B dibromide on crystallisation from chloroform gave yellow needles, m.p. 111° C. The debrominated product was saponified by boiling with alcoholic caustic potash, diluted with water and the residue extracted with ether. From this ethereal solution, the solvent was evaporated off and the remaining residue crystallised from anhydrous ether in white flakes, m.p. 161° C. The flakes were dried at 110° C. *in vacuo* and the melting point determined but it remained unchanged. Thus the yield of pterocarpol B was 0·58 gm., *i.e.*, 0·005% on the weight of wood shavings.

Pterocarpol A.—It crystallises from methyl alcohol in colourless leaflets. It is soluble in benzene, chloroform and ether, sparingly soluble in methyl alcohol and ethyl alcohol and insoluble in petroleum-ether and water. In strong sulphuric acid, it dissolves with a yellow colour, which turns intense red on warming the solution. From this solution it recovers unchanged on dilution with water like alangol.[8] It gives a positive Liebermann-Burchard's[9] test showing red, violet, blue and green colour. In Salkowski's[4] reaction, it assumes a brown colouration which turns green. It is optically active

having in chloroform a lævorotation of $[\alpha]_d^{30^\circ C.} = -27 \cdot 7^\circ$. [Found in air-dried sample: C = 76·63; H = 11·98; loss (H_2O) on drying = 8·45; M.W. by Rast's camphor method = 418, 425; $C_{27}H_{46}O$. $2H_2O$ requires C = 76·78; H = 11·85; loss (H_2O) on drying = 8·53%; M.W. = 422. Found in the sample dried at 110° C. *in vacuo*: C = 83 79; H = 12·04; M.W. by Rast's camphor method = 385, 390; $C_{27}H_{46}O$ requires C = 83 92; H = 11·92%; M W. = 386.]

Monoacetyl Pterocarpol A.—It was prepared by heating the substance (0·25 gm.) with acetic anhydride (10 c.c.) and pyridine (3 c c.) under reflux on a water-bath for an hour. The mixture was poured into water and kept overnight when a precipitate was obtained. It was filtered, washed with water and crystallised from alcohol in colourless needles, m p 92° C. The yield was 74 8% of the theoretical. (Found: C = 81·16; H = 11·34; $C_{29}H_{48}O$. $CO.CH_3$ requires C = 81·32; H = 11·21%.)

Monobenzoyl Pterocarpol A—The substance (0·2 gm.), benzoyl chloride (5 c.c.) and pyridine (10 c c) were heated under reflux on a water-bath for an hour. The product was poured into water and kept overnight. On the next day a white precipitate was obtained. It was filtered, washed with water and crystallised from alcohol in colourless prisms. The yield of this derivative, m.p 95° C., was 91·2% of the theoretical (Found: C = 83·12; H = 10·32; $C_{27}H_{46}O$ $CO.C_6H_5$ requires C = 83 28; H = 10·21%.)

Monoacetyl Pterocarpol A Dibromide—Monoacetyl pterocarpol A (0·1 gm.) was dissolved in ether (5 c.c.) and treated with a 5% solution of bromine in glacial acetic acid (10 c.c.). The brown solution was allowed to stand overnight in a frigidaire, when a yellowish precipitate was obtained. This precipitate was filtered, washed with 75% acetic acid and dried in a vacuum over strong sulphuric acid The dried product on crystallisation from chloroform gave yellow leaflets, m.p. 86° C. The yield was 0·1368 gm. (Found: Br = 26·89; $C_{29}H_{46}O_2Br_2$ requires Br = 27·2%.)

Pterocarpol A Monophenylurethane.—This was prepared by allowing a mixture of the substance (0·2 gm.), phenylisocyanate (1 gm.) and dry benzene (30 c.c.) to stand at the ordinary temperature in a stoppered flask for three days, when from the clear solution, some of the phenylurethane derivative crystallised out. More of the substance was obtained by distilling off greater part of the solvent and allowing the concentrate to crystallise for two days. The combined product was recrystallised from boiling alcohol in colourless prisms), m.p. 102° C. It was obtained in an yield of 61·2% of the theoretical. (Found: N = 2·69; $C_{27}H_{46}O.CO.NHC_6H_5$ requires

Pterocarpol A Digitonide—The substance (0·1 gm.) and digitonin (0·1 gm.) dissolved in alcohol (20 c.c.) were heated under reflux on a water-bath for two hours. On cooling the digitonide crystallised out in colourless leaflets, m.p. 188° C. and was thus obtained in practically quantitative yield of the theoretical. (Found: C = 61·39; H = 8·56; $C_{27}H_{44}O$. $C_{55}H_{94}O_{28}$ requires C = 61·51; H = 8·5%.)

Pterocarpol B.—It crystallises from ether in colourless glistening flakes. It is soluble in chloroform and pyridine, sparingly soluble in methyl alcohol and ethyl alcohol but insoluble in benzene and petroleum-ether. It gives a red coloration with strong sulphuric acid. With Liebermann-Burchard's test (*loc. cit.*), it gives pink, brown, violet and blue coloration. In Salkowski's reaction (*loc. cit.*), it gives a purple coloration which turns green finally. It gives a monoacetyl, a monoacetyl dibromide and a digitonide derivative, indicating the presence of an alcoholic hydroxy group in the molecule. (Found; C = 83·74; H = 12·1; M.W. by Rast's camphor method = 390, 392; $C_{27}H_{44}O$ requires C = 83·92; H = 11·92%; M.W. = 386.)

Monoacetyl Pterocarpol B.—The substance (0·2 gm.), acetic anhydride (10 c.c.) and pyridine (2 c.c.) were heated under reflux on a water-bath for 45 minutes and poured into water. On keeping overnight, a white precipitate was obtained. It was filtered, washed with water and crystallised from alcohol in colourless flakes, m.p. 120° C. The yield was 75·7% of the theoretical. (Found: C = 81·18; H = 11·32; $C_{27}H_{44}O.CO\,CH_3$ requires C = 81·32; H = 11·21%.)

Monoacetyl Pterocarpol B Dibromide.—Monoacetyl pterocarpol B (0·12 gm.) was dissolved in ether (5 c.c.) and treated with a 5% solution of bromine in glacial acetic acid (10 c.c.) in small quantities at a time, until the solution was brown. This solution was kept overnight in a frigidaire. On the next day, a brown precipitate was obtained. It was filtered, washed with 75% acetic acid and dried in a vacuum over strong sulphuric acid. The dried product on crystallisation from chloroform gave yellow needles, m.p. 111° C. The yield was 0·1642 gm. (Found: Br = 26·94; $C_{29}H_{46}O_3Br_2$ requires Br = 27·2%.)

Pterocarpol B Digitonide.—This was prepared by heating under reflux a mixture of the substance (0·1 gm.) and digitonin (0·1 gm.) dissolved in alcohol (20 c.c.) for three hours. On cooling the digitonide crystallised out in colourless flakes, m.p. 215° C. The yield was practically quantitative of the theoretical. (Found; C = 61·40; H = 8·54; $C_{27}H_{44}O$. $C_{55}H_{94}O_{28}$ requires C = 61·51; H = 8·5%.)

Summary

From the unsaponifiable matter of the fixed oil of the wood of *Pterocarpus marsupium*, two phytosterols have been obtained. One of these has been named 'pterocarpol A', having a molecular formula $C_{27}H_{46}O\ 2H_2O$ after drying in air and $C_{27}H_{46}O$ after drying at 100° C *in vacuo* The other phytosterol has been named 'pterocarpol B', having a molecular formula $C_{27}H_{46}O$ after drying at 110° C *in vacuo*

Both have been found to contain an alcoholic hydroxy group as these give monoacetyl derivatives Further pterocarpol A gives a monobenzoyl, a monoacetyl dibromide, a monophenylurethane and a digitonide derivative. Monoacetyl dibromide and digitonide derivatives of pterocarpol B have been also obtained.

References

1. Windaus and Hauth — *Berichte*, 1906, 39, 518
2. Bhargava, P. N., and Dutt, S — *Proc Ind. Acad Sci*, 1942, 16, 328.
3. Liebermann-Burchard — *Berichte*, 1885, 18, 1804
4. Salkowski — *Arch. Gessel Physiol*, 1872, 6, 207.

CHEMICAL EXAMINATION OF THE UNSAPONIFIABLE MATTER OF THE FAT FROM THE FLESHY ARILS OF *CELASTRUS PANICULATA*

By Prithwi Nath Bhargava
(*Chemistry Department, Benares Hindu University*)

Received September 2, 1946
(Communicated by Dr S. Dutt, F.A.SC.)

Celastrus paniculata commonly known as 'Malkangini' in Hindi and Bengali is a shrub belonging to the Natural order 'Celastraceæ'. It is cultivated in many parts of India, as far as Ceylon from the hilly districts of the Himalayas The seeds are of the size of a millet, of reddish brown colour, oily and angular like the section of a sphere and are covered by the arils on the surface

According to Dymock, Warden and Hooper[1] and Kirtikar and Basu[2] the seeds have been described to be highly medicinal in the indigenous system of medicine. Gunde and Hilditch[3] have examined the fat obtained from the husk or the arils of the seeds in detail, but not the unsaponifiable matter. Warsi,[4] however, claims to have isolated a sterol, m.p. 184° C. from the unsaponifiable matter but he has also not examined it further. In the present paper, therefore, the author has confirmed the nature of the unsaponifiable matter from which a sterol, namely 'Celastrol' and a resinous colouring matter have been isolated.

The arils on extraction with petroleum-ether (b p. 40–60° C.) gave an orange red semi-solid fat. The fat on saponification, as usual, and extraction with ether gave an unsaponifiable matter 6 46% from which a phytosterol has been isolated according to the method of Windaus and Hauth.[5] In addition to this a highly coloured resinous product is also present in the crude unsaponifiable matter but could not be isolated in a pure form for [illegible]

The phytosterol 'Celastrol' ($C_{27}H_{46}O_2$), m.p. 142° C., is quite different from that detected by Warsi (*loc. cit.*). A number of derivatives of Celastrol have been prepared, which account for only one hydroxy group in the sterol. The nature of the remaining oxygen atoms is not yet known.

EXPERIMENTAL

About 10 kilos of the authentic specimen of the seeds together with the orange red arils were obtained from the Punjab Ayurvedic Pharmacy, Amritsar. The arils were separated very carefully from the seeds by the hand-picking method, thus giving an yield of 25% on the weight of seeds. These arils were completely extracted with petroleum-ether (b p 40–60°), when an orange red semi-solid fat was obtained On purification with fuller's earth and animal-charcoal, it was obtained in an yield of 30% on the weight of arils

450 gm. of the fat were saponified in the usual manner with 20% alcoholic caustic soda and the unsaponifiable matter extracted with ether. This ethereal solution was washed with water, dehydrated with anhydrous sodium sulphate, filtered and distilled to recover the solvent. The residue on repeated crystallisation from methyl alcohol with the addition of animal-charcoal gave white flakes, m p 141–42° C, but a part of it still remained resinous. This resinous residue was highly coloured and probably consisted of the colouring matter. It was dissolved in chloroform and precipitated with acetone. The precipitate was filtered and crystallised from methyl alcohol with the addition of animal-charcoal in white flakes, m p. 141–42° C These flakes were further purified by the method of Windaus and Hauth (*loc cit.*).

The chloroform acetone solution was distilled to recover the solvent, when an orange red resinous residue was obtained. On crystallisation from methyl alcohol, two fractions were obtained but none of these could be isolated in a pure form.

The flakes obtained above were acetylated as usual and crystallised from methyl alcohol in colourless leaflets, m p. 160° C. The acetylated product was dissolved in ether (30 c c.) and treated with a 5% solution of bromine in glacial acetic acid (40 c.c) The solution was brown indicating an excess of bromine. On keeping over night in a frigidaire, a white amorphous precipitate was obtained. It was filtered, washed with 75% acetic acid and dried in a vacuum over sulphuric acid. The acetyl-sterol dibromide formed a yellowish amorphous powder and was crystallised from chloroform in yellowish flakes, m p. 81° C. It was debrominated by boiling with zinc dust (3 gm.), glacial acetic acid (10 c c) and alcohol (50 c c) for three hours. The colourless solution was filtered to remove the excess of zinc, diluted with water and extracted with ether. From the ethereal solution the solvent was evaporated and the residue saponified with alcoholic caustic potash. The solution was then diluted with water, the residue extracted with ether

and the solvent evaporated, when it gave a white product, which on crystallisation from methyl alcohol gave white flakes, m.p 142° C The yield of the product was 2 25 gm., thus giving an yield of 0·15% on the weight of arils. It has been named 'Celastrol'.

Properties—Celastrol is a white crystalline substance, m p. 142° C. It is soluble in petroleum-ether and chloroform, sparingly soluble in ethyl alcohol and methyl alcohol and insoluble in water. It remains insoluble in aqueous caustic potash and does not give any colouration with ferric chloride. In concentrated sulphuric acid, it gives a dark red colour. It assumes a red colouration in Salkowski's[6] reaction and ultimately turns green. With Liebermann-Burchard's[7] test, it turns yellow, red, brown, green and violet. Thus it gives reactions of a sterol.

It gives a monoacetyl and an acetyl dibromide derivative and forms a crystalline digitonide. [Found in air-dried sample: C = 71·18, H = 11·12; loss (H_2O) on drying = 8·05; M W by Rast's camphor method = 432, 470, $C_{27}H_{46}O_2$ $2H_2O$ requires C = 71·36; H = 11·01; loss (H_2O) on drying = 7 92%, M W. = 454 Found in the sample dried at 110° C. *in vacuo*. C = 77 39, H = 11 10; M W = 410, 431; $C_{27}H_{46}O_2$ requires C = 77 50, H = 11 01%; M W = 418]

Monoacetyl Celastrol—Celastrol (2 gm.) was dissolved in pyridine (15 c.c) and treated with acetic anhydride (40 c c.). It was refluxed for half an hour on a water-bath, poured into cold water and kept overnight, when a precipitate was obtained. This precipitate was filtered, washed with water and crystallised from alcohol in colourless silky leaflets, m p 160° C The yield was 78·7% of the theoretical (Found. C = 75·47; H = 10·56; $C_{29}H_{48}O_4$ requires C = 75 65; H = 10 43%.)

Monoacetyl Celastrol Dibromide.—Monoacetyl celastrol (1·8 gm.) was dissolved in ether (20 c.c) and treated with a 5% solution of bromine in glacial acetic acid (30 c c) in small quantities at a time, until the solution was brown. This solution was allowed to stand overnight in a frigidaire, when a yellowish amorphous precipitate was obtained. It was filtered, washed with 75% acetic acid and dried in a vacuum over strong sulphuric acid. This product on crystallisation from chloroform gave yellowish flakes, m.p 81° C. The yield was 2·4182 gm. (Found: Br = 25·47; $C_{29}H_{48}O_4Br_2$ requires Br = 25 8%.)

Celastrol Digitonide.—This was prepared by heating under reflux a mixture of celastrol (0·2 gm.) and digitonin (0·2 gm.) dissolved in alcohol (60 c.c.) for three hours. On cooling the digitonide crystallised out in

colourless prisms, m.p. 195° C. The yield was practically theoretical. (Found: C = 60 20; H = 8·39, $C_{27}H_{46}O_2$ $C_{55}H_{90}O_{29}$ requires C = 60·3; H = 8·33%.)

SUMMARY

The arils of *Celastrus paniculata* on examination have been found to give a semi-solid fat (30%), a phytosterol namely celastrol (0 15%) and a highly coloured resinous substance.

Celastrol obtained from the unsaponifiable matter has a molecular formula $C_{27}H_{46}O_4$. It contains an alcoholic hydroxy group and gives a monoacetyl, a monoacetyl dibromide and a digitonide derivative The nature of the remaining oxygen atoms has not yet been known.,

REFERENCES

1. Dymock, Warden and Hooper — *Pharmacographia Indica*, 343
2. Kirtikar and Basu — *Indian Medicinal Plants*, 574
3. Gunde and Hilditch — *J C. S*, 1938, 2, 1981
4. Warsi — *Sci. Congress Abst*, 1939
5. Windaus and Hauth — *Berichte*, 1906, 39, 518
6. Salkowski — *Arch. Gesell Physiol*, 1872, 6, 207
7. Liebermann-Burchard — *Berichte*, 1885, 18, 1804.

OVERTONE AND COMBINATION LINES IN THE RAMAN SPECTRUM OF CHLOROFORM

By M Visweswara Rao

(From the Department of Physics, Andhra University, Waltair)

Received October 28, 1946

(Communicated by Prof S Bhagavantam, F A SC)

1 Introduction

In addition to the usual lines due to the fundamental frequencies of vibration in a Raman spectrum, there are also occasionally present overtone and combination tones. According to the theory of Placzek, developed on the assumption that the polarisability can be expanded in the form of a series, the overtone lines will be either of zero or negligibly small intensity, according as the second order derivative of polarisability is zero or negligibly small. Later, Bhagavantam has shown that the anharmonic nature of an oscillation may also contribute to the intensity of its overtone in Raman scattering.

Thus, overtones and combination tones are, in general, much weaker than the fundamentals. They may yet be observed in Raman effect by using sufficiently long exposure times. It is easier to get them in infra-red absorption and using sufficiently thick absorbing layers, several instances have been recorded. Liquid chloroform is studied in this paper with a view to record combination and overtone Raman lines using a sufficiently big tube to increase the illuminated volume of the liquid and giving lengthy exposures.

2. Experimental Arrangement

Chloroform was distilled repeatedly four or five times at constant temperature, discarding the first and last portions of the distillate each time. The pure liquid thus obtained is introduced into a thoroughly cleaned and dried dust-free Raman tube suitably painted with black paint. The condenser arrangement was used to photograph the scattered spectrum. The time of exposure was about hundred hours, and very intense pictures were recorded. Five combination and overtone lines are seen in the Raman spectrum.

3. Results

The Raman frequencies obtained by the author by taking the averages of measurements on four spectrograms are given in Table I along with those recorded by some earlier investigators. The six well-known frequencies

printed in bold type represent the fundamental vibrations. In addition, there are five others which have to be explained as first overtones or binary combinations of fundamentals.

TABLE I

Raman Frequencies of Chloroform

Ganesan[1] and Venkateswaran	Langer and Meggers[2]	Dabadghao[3]	Author	Assignment
261	261	262	259	Fundamental
368	367	366	367	
..	..	.	497	$757-259=493$ (E_2-E_3)
..	.		622	$259+364=623$ (E_2-A_1)
669	668	667	664	Fundamental
762	760	762	757	
..	..		1027	$757+259=1016$ (E_2+E_3)
1218	1215	1213	1215	Fundamental
1441	.	1441	1420	$757+664=1421$ (E_2+A_1)
.	.	.	1510	$757+757=1514$ $(2E_2)$
3019	3019	3017	3018	Fundamental
..	.	3072		

The frequency at 3072 reported by Dabadghao is not confirmed by other workers. $\Delta\nu$ 1510 cm.$^{-1}$ appears to have been reported by some previous workers and assigned to be the first overtone of the fundamental at $\Delta\nu$ 757 cm^{-1} as there is a reference to it in Herzberg's book[4]

4 DISCUSSION

The six fundamental frequencies recorded are to be expected from the assumed pyramidal structure (symmetry group C_{3v}) for the molecule of chloroform. The selection rules for the occurrence of overtones and combination tones in Raman effect have been obtained by Tisza.[5] The results for chloroform are worked out and presented in Table II.

TABLE II

	A_1	A_2	E_2
A_1 ..	A_1	A_2	E_2
A_2 .		A_1	E_2
E_2 ..			$A_1+A_2+E_2$

Since A_1 and E_2 are allowed and A_2 is not allowed in Raman effect as fundamentals, all the combinations except (A_1+A_2) are allowed. E_2+E_2 is also allowed because in the term $A_1+A_2+E_2$, A_1 and E_2 are active

When the selection rules are applied to a difference band, one finds easily that it is allowed or forbidden depending on whether the corresponding summation band is allowed or forbidden. The intensity of a difference band would be expected to be much smaller than that of the corresponding summation, since the number of molecules in the initial state is much smaller, and the ratio will be governed by the Boltzmann factor Therefore, a difference band cannot be expected to appear unless the corresponding summation band makes its appearance with a greater intensity. It can be seen from Table I, where the assignment of the various Raman shifts are given, that for the difference line recorded, the corresponding summation is also recorded and it is visually observed that the latter is more intense than the former. Quantitative work on the relative intensities of the difference and summation tones will be taken up in due course. It may be mentioned here that the value of the Boltzmann factor gets smaller and smaller for higher values of the frequencies, and hence, for taking up the problem of quantitative determination of the relative intensities of summation and difference lines, liquids having low fundamental frequencies (combinations between the fundamentals being allowed) have to be specially chosen.

The possibility that the additional lines may be due to their presence in the incident exciting radiation (here, a quartz mercury arc) or to the presence of slight traces of impurities in the liquid has to be examined. The spectrum of the mercury arc is separately photographed on the same plate on which the Raman spectrum is recorded, and it is seen that there are no lines in the region of the new Raman lines. Possible impurities in chloroform are, ethyl alcohol, phosgene in solution and acetone. The strong Raman lines due to each of these are given below:

Ethyl alcohol: $\Delta\nu$ 1051, 1455, 2878, 2928 and 2972 cm.$^{-1}$

Acetone: $\Delta\nu$ 532, 788, 1425, 1708, 2922, 2965 and 3005 cm.$^{-1}$

Phosgene (liquid): $\Delta\nu$ 301, 444, 571 and 1810 cm.$^{-1}$

None of these lines coincide with the new combination lines that are recorded.

5. Summary

An intense Raman spectrum of liquid chloroform has been obtained with a Fuess glass spectrograph. Besides the six fundamentals, five lines are recorded, which are to be explained as either combination tones or overtones. Of these five, two summation bands and one difference band are recorded for the first time. Taking into consideration the selection rules for the appearance of combination tones, a table is worked and it is found that all the combination tones recorded here are allowed.

In conclusion, the author takes this opportunity of expressing his grateful thanks to Prof S. Bhagavantam, under whose direction this work was carried out.

6 References

1. Ganesan and Venkateswaran — *Ind. Jour Phy*, 1929, 4, 195
2. Langer and Meggers — *Bur of St Jour Res*, 1930, 4, 711
3. Dabadghao — *Ind. Jour Phy*, 1930, 5, 207
4. Herzberg — *Infra-Red and Raman Spectra of Polyatomic Molecules*, 1945
5. Tisza — *Zeit f Phy*, 1933, 82, 48

PRODUCTION OF *JOSHI-EFFECT* UNDER *UNI-*, AND *BI-*ELECTRODE EXCITATION

By B B Prasad

(*Chemistry Department, Benares Hindu University*)

Received October 28, 1946

(Communicated by Prof. S. S. Joshi, F.A.SC.)

The dependence[1, 2] of the magnitude of the above phenomenon Δi on factors such as the gas pressure, nature of the solid-gas interface and electrical quantities, *e.g.*, the inter-electrode capacitance, wave-form and current frequency, etc., has been emphasised by Prof. Joshi. This is observed in a striking manner in the above modes of excitation, which have besides the advantage of keeping (most) other factors unaltered.

2 Fig. 1 shows the general circuit and apparatus used. It consisted essentially of a Siemens' ozoniser filled with purified chlorine at about 300 mm.

Fig 1 Joshi-Effect in Uni-, Bi-electrode Excitation

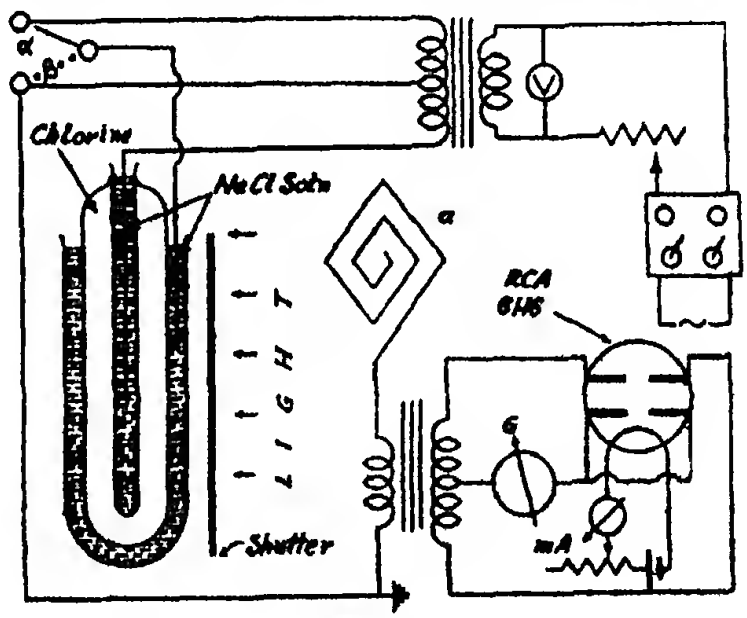

Fig. 1

pressure and excited in the range 5-9 kV of 50 cycles frequency; a frame aerial (*a*) and a double diode 6H6 (RCA). The two plates of the latter were connected to the secondaries of a Bell transformer; the aerial was connected in its primary. The cathodes were connected together and to the centre of

the secondary through a reflection galvanometer. The current i was observed in dark (i_d) and when the excited ozoniser was irradiated from an incandescent 200 watt, 220 volt (glass) bulb (i_l), under the following conditions, α and β:

(α) The inner and outer electrodes of the ozoniser were connected to the secondaries of an H T. transformer, and whose centre was earthed (*vide* α, Fig. 1).

(β) The outer electrode of the ozoniser was earthed; the corresponding secondary terminal in (α) was left unconnected. Since only half of the transformer now comes into operation, the voltage applied to the ozoniser was maintained similar to that in (α) by adjustment of the primary potential. These connections are shown by (β) in Fig 1 In the latter arrangement, *i.e.*, β, the potential of the inner electrode alternates between + V and − V; the other electrode is throughout at zero potential In (α) i is due to anti-phase excitation of the two electrodes. The results for only one typical series under (α) and (β) for the net *Joshi-effect* $i_d - i_l = \Delta i$, and its relative value $100 \times \frac{\Delta i}{i_d} = \% \Delta i$ are returned in Table I.

TABLE I

Potential-Variation of Joshi-Effect *under* Uni-, *and* Bi-*Electrode Excitation*

kV	i_{dark}	i_{light}	Δi	$\% \Delta i$
		Bi-electrode (α)		
5·3	1·4	1·3	0·1	7·1
5·6	1·6	1·4	0·2	12·5
5·9	1·8	1·5	0·3	16·7
6·4	1·9	1·7	0·2	10·5
6·8	1·9	1 7	0·2	10·5
7·2	2·2	2 0	0 2	9·1
7·5	2·3	2·1	0·2	8·7
7·9	2·4	2·2	0·2	8·3
8·2	2·5	2·3	0 2	8 0
		Uni-electrode (β)		
5·3	2·5	1·4	1·1	44·0
5·6	4·1	2·1	2 0	48·8
6·0	4 9	2·4	2 5	51·0
6·4	5·4	2·7	2·7	50·0
6·8	6·0	3·0	3·0	50·0
7·2	6·9	3·4	3·5	50·0
7·5	7·7	3·8	3·9	50·7
7·9	8·6	4·2	4·4	51·6
8·3	8·9	4·6	4·3	48·8

3. Joshi[5, 2, 6] has shown as a general result that Δi occurs predominantly in the high frequency part of the conductivity produced under the discharge. It is seen from the experimental arrangement that the current picked up by the aerial is chiefly in the H.F The fundamental significance of the threshold potential V_m (and its dependence on factors such as the structural constants of the tube, the frequency of the A.C. supply) above which only Δi occurs has been established by Joshi.[5, 6] It was interesting to observe that in the present case, V_m was found to be 4·3 kV, in both the *uni*- and the *bi*-electrode excitations, *i.e.*, in (α) and (β) respectively For the same applied potential V in (α) and (β), i should have been the same, since according to a general result due to Joshi,[7] *ceteris paribus*, i depends on $V-V_m$. The results in Table I show, however, that i in (α) is far smaller than in (β) Thus *e.g.*, at 6 kV i_d is 4·9 and 1·8 units, corresponding to (β) and (α), respectively. This disparity is explicable on the following considerations:

In (α) the bi-electrode excitation, the two electrodes, are constantly out of phase by π, with possibly a neutral zone in the discharge space corresponding to the earthed centre on the transformer secondary. As a consequence, the earth connected aerial receives two half wave trains mutually out of phase by π which are, therefore, subject to interference. Under ideal conditions the aerial current would be nil; actually, however, the two halves of the circuit are not strictly equivalent in respect of their oscillatory constants; of the position of the neutral zone due to the asymmetry of the excited system, etc. It was also remarkable to find that both the net and the relative *Joshi-effect* Δi and % Δi, are far greater in (β) as compared with (α); thus *e.g.*, at 6 kV in (α) Δi and % Δi are 0·3 and 16·7 as against 2·5 and 51 in (β), respectively. The current in *bi*-electrode excitation (α) being much smaller than that in *uni*-electrode excitation (β), it is to be anticipated that the same should hold for the corresponding Δi and % Δi in (α), since according to a general result due to Joshi,[8] both the above quantities increase with i over a certain limited range of applied potentials, and decrease thereafter.

Joshi[8] has suggested recently a following (additional) factor in the production of Δi. It is that irradiation produces a change of capacity and therefore, that of phase between the electrodes. On this view, it is easy to see that under irradiation, in effect, the interelectrode phase in the *uni*-electrode excitation shifts towards that normal in a *bi*-electrode excitation (that is, in dark); as a consequence of this phase-shift, the photo-reduction of conductivity as observed, follows. Also, since in the latter, *i.e.*, *bi*-electrode excitation neither of the electrodes has a constant characteristic

phase, like the earth electrode in the *uni*-electrode excitation, the phase-shift[6] under light at either electrode as contemplated by Joshi is less likely; the corresponding *Joshi-effect* is anticipated, therefore, to be smaller than in *uni*-electrode excitation, as observed.

In conclusion, I express my grateful thanks to Prof S S Joshi, D Sc (Lond), for suggesting the problem and for the keen interest he took during the work

Summary

Production of *Joshi-effect* Δi, *viz*, an instantaneous and reversible photo-diminution of current i in excited chlorine has been studied in an *aerial* current under *uni*-, and *bi*-electrode excitation. The current in dark, the net and relative *Joshi-effect* Δi and % Δi, in the latter, were comparatively low. Based on interference of anti-phase wave trains, together with a recently suggested *phase-shift* due to Prof. Joshi in the production of this effect, an explanation is developed for the reduced i (in dark), Δi and % Δi under *bi*-electrode excitation

References

1 Joshi *Presi Addr, Chem. Sec, Indian Sci Cong*, 1943
2. ——— . *B. H U Journ*, 1943, 8, 99
3. ——— . *Nature*, 1944 154, 147.
4. ——— *Curr Sci.*, 1944, 14, 67
5. ——— *Ibid*, 1944, 13, 253
6. ——— . *Trans Faraday Soc*, 1929, 25, 120
7 ——— *Proc Indian Acad. Sci*, 1945, 22, 389.
8 ——— *Ibid*, 1945, 22, 225.
——— *Curr. Sci*, 1945, 14, 317, 1946, 15, 281
——— .. *Proc Indian Sci Cong Phys. Sec Abst*, 26, 1945.

A NEW IDENTICAL EQUATION FOR MULTIPLICATIVE FUNCTIONS OF TWO ARGUMENTS AND ITS APPLICATIONS TO RAMANUJAN'S SUM $C_M(N)$*

By C S Venkataraman

Received September 12, 1946
(Communicated by Dr. R. Vaidyanathaswamy, F.A.SC.)

I Introduction

In his memoir[1] "The Theory of Multiplicative Arithmetic Functions," Dr. Vaidyanathaswamy establishes an identical equation,[2] for any multiplicative function $f(M_1, \ldots, M_r)$ of r arguments which in the case of functions of one argument reduces to

$f(MN) = f(M) f(N) C(M, N)$, where $C(M, N)$ is a cardinal function defined by $C(M, N) = (-1)^{\gamma} f^{-1}(MN)$ if M, N have the same γ distinct prime factors, and $C(M, N) = 0$, otherwise

But the above identical equation is not always the most suitable one, for multiplicative functions of two arguments. In this paper, I derive a new identical equation for functions of two arguments. The special interest of this equation lies in its applications to Ramanujan's function $C_M(N)$.[3]

We will require the following definitions and notations.[4]

1.1. An arithmetic function $f(M_1, \ldots, M_r)$ of r arguments is said to be multiplicative, if $f(M_1, \ldots, M_r) f(N_1, \ldots, N_r) = f(M_1N_1, \ldots M_rN_r)$ whenever the products $\prod_{i=1}^{r} M_i$ and $\prod_{i=1}^{r} N_i$ are mutually prime. (1.1.1) With the convention that unity is both prime to and a factor of every number, it follows that if $f(M_1, \ldots, M_r)$ is multiplicative in $M_1, \ldots, M_r$, then $f(1, 1, \ldots, 1) = 1$

* Some of the results of this paper were given in a thesis, for which the M.Sc. of the University of Madras, was awarded, and I am deeply indebted to Dr. wamy for his guidance.

[1] See *Trans. Amer Math. Soc.*, 33, No. 2, 579–662, 1931. The above memoir, will be hereafter, referred to as *M.F.*

[2] See *M F.*, p. 645.

[3] *Collected Papers of Srinivasa Ramanujan*, 179–80.

[4] For details ref. *M.F.*

1.2. *The generating series*—The series,

$$f_p(x_1, \ldots, x_r) = \sum_{\substack{m_i = 0 \\ (i = 1, 2, \ldots r)}}^{\infty} f(p^{m_1}, \ldots, p^{m_r})\, x_1^{m_1} \ldots x_r^{m_r}$$

is called the generating series or briefly g-series of the multiplicative function f to the prime base p. Given the g-series to all prime bases, it follows that the multiplicative function is completely determined.

1.3. *Convolution*—Let $f(M_1, \ldots, M_r)$ be a multiplicative function of $r(>1)$ arguments. Then, the process of convolving M_1, M_2 in f consists in forming the function,

$$\phi(M, M_3, \ldots, M_r) = \sum_{M_1 M_2 = M} f(M_1, M_2, \ldots, M_r)$$

ϕ can readily seen to be a multiplicative function of its $(r-1)$ arguments and its g-series to a prime base p is given by,

$$\phi_{(p)}(x, x_3, \ldots x_r) = \Sigma \Big(\sum_{m_1 + m_2 = m} a_{m_1, m_2, \ldots m_r} \Big) x^m x_3^{m_3} \ldots x_r^{m_r}$$

$$= f_{(p)}(x, x, x_3, \ldots x_r), \text{ where}$$

$$f_{(p)}(x_1, x_2, \ldots x_r) = \Sigma\, a_{m_1, m_2, \ldots m_r} x_1^{m_1} \ldots x_r^{m_r}$$

is the g-series of f to the base p. The function ϕ is called *a convolute* of f. In particular, for functions $f(M_1, M_2)$ of two arguments, *the* convolute ϕ is given by $\phi(M) = \sum_{d|M} f\left(\frac{M}{d}, d\right)$. We will denote $\phi(M)$ by $\Omega f(M_1, M_2)$.

(1.3.1) The composite of two multiplicative functions $f_1(M_1, \ldots, M_r)$, $f_2(M_1, \ldots, M_r)$ is the function $f(M_1, \ldots, M_r)$, obtained by convolving the pairs M_i, N_i in the product, $f_1(M_1, \ldots M_r) \times f_2(N_1, \ldots N_r)$. Thus $f(M_1, \ldots M_r) = \Sigma f_1\left(\frac{M_1}{d_1}, \ldots, \frac{M_r}{d_r}\right) f_2(d_1, \ldots, d_r)$ summed for all divisors d_i of M_i, $(i = 1, 2, \ldots r)$. f is denoted by $(f_1 f_2)$ and its g-series to any base p is given by, $f_{(p)}(x_1, \ldots, x_r) = f_{1(p)}(x_1, \ldots x_r) \times f_{2(p)}(x_1, \ldots, x_r)$. (1.3.2) The composite of $f(M_1, \ldots, M_i, M_{i+1}, \ldots M_r)$ and $E_0(M_1, \ldots, M_i)\, E(M_{i+1}, \ldots M_r)$ is called the *integral* of f with respect to $M_{i+1}, \ldots, M_r$, where $E_0(M_1, \ldots M_r)$ and $E(M_1, \ldots M_r)$ are functions defined by,

$$E_0(M_1, \ldots, M_r) = 1, \text{ when } M_1 = M_2 = \ldots = M_r = 1 \text{ and}$$
$$= 0, \text{ otherwise}$$

and $$E(M_1, \ldots, M_r) = 1, \text{ for all values of } M_1, \ldots M_r.$$

The composite of $f(M, N)$ with $\phi(M)$ is the same as $f(M, N) \cdot \phi(M)\, E_0(N)$.

(1.3.3) If $f_1(M_1, M_2)$ and $f_2(M_1, M_2)$ are multiplicative in M_1, M_2, then it can be easily shown that $(\Omega f_1)\ (\Omega f_2) = \Omega(f_1, f_2)$.

(1.3.4) The inverse of f denoted by f^{-1} is the unique function, determined from $f(M_1, \ldots, M_r)\ f^{-1}(M_1, \ldots, M_r) = E_0(M_1, \ldots, M_r)$. It follows readily that $f_{(p)}(x_1, \ldots, x_r) \times f_{(p)}^{-1}(x_1, \ldots, x_r) = E_{0(p)}(x_1, \ldots, x_r) = 1$.

(1.3.5) The inverses of $E_0(M)$, $E(M)$ and $I(M)$ [the function defined by $I(M) = M$], can be easily seen to be $E_0(M)$, $\mu(M)$ and $M\mu(M)$ respectively, $\mu(M)$ being the well-known Möbius function, defined thus:—

$\mu(1) = 1$, $\mu(M) = 0$ if M has a squared factor and

$\mu(p_1 p_2 \ldots p_r) = (-1)^r$ if $p_1, p_2, \ldots p_r$ are different primes.

(1.3.6) The following properties of the processes of composition and inversion will be often used in the sequel:—

(*a*) Composition is associative and commutative

(*b*) The compositional operation distributes multiplication, whenever the multiplier is a linear function

(*c*) The inverse of the composite of any number of functions is the composite of their inverses.

(*d*) The inverse of the product of functions without common argument is the product of the inverses. For *e.g.*, $[\phi(M)\,\psi(N)]^{-1}$ is $\phi^{-1}(M)\,\psi^{-1}(N)$.

(*e*) In a compositional equation, any term can be transposed from one side to the other, by replacing it by its inverse. Thus if $f_1 \cdot f_2 = \phi_1 \cdot \phi_2$, then $f_1 = \phi_1\ \phi_2\ f_2^{-1}$.

(1.3.7) The *derivate* of a function $f(M, N)$ with respect to M is defined as $f(1, N)$ and is denoted by $D_M(f)$. $D_M(f)$ is clearly multiplicative in N. Also, it can be easily seen that for two functions $f(M, N)$, $\phi(M, N)$,

$$(a)\quad D_M(f) \cdot D_M(\phi) = D_M(f \cdot \phi) \text{ and } (b)\ D_M(f^{-1}) = \{D_M(f)\}^{-1}$$

1.4. A *cardinal* function $C(M, N)$ is one for which $D_M(C) = E_0(N)$ and $D_N(C) = E_0(M)$. It is easy to show that (*a*) the composite of two cardinal functions is a cardinal function and (*b*) the inverse of a cardinal function is a cardinal function.

1.5. A *principal* function $P(M, N)$ is one which vanishes whenever M is not equal to N. The function $\psi(M) = P(M, N)$ is called the function of one argument equivalent to the principal function $P(M, N)$.

(1.5.1) If $\psi_p(x)$ be the g-series of ψ to a base p, then $P_p(x, y) = \psi_p(xy)$. Thus ψ determines $P(M, N)$ completely and we will write $P = \text{princ}\ \psi$.

(1.5.2) It can be easily seen that, (*a*) $\phi(M, N) \times \text{princ}\ \psi = \text{princ}\ [\phi(M, M) \times \psi(M)]$, $\phi(M, N)$, being any multiplicative function of M, N. and (*b*) $(\text{princ}\ \psi)^{-1} = \text{princ}\ \psi^{-1}$

2. Next, before proceeding to the main results of the paper, we will establish three lemmas which will be required later

2.1. *Lemma*—Every multiplicative function $F(M, N)$ of two arguments, possesses, with respect to each of its arguments, the following property, which may be referred to as 'quasi-multiplicative' property —

Wherever M is prime to M', $F(M, N)\, F(M', N) = F(MM', N)\, F(1, N)$.

Similarly, $F(M, N)\, F(M, N') = F(M, NN')\, F(M, 1)$ if N and N' are mutually prime.

We will prove the first part.

Proof.—Let $N = N_1 N_2 T$, where N_1 contains only all those prime factors of N, which divide M and further these prime factors occur in N_1, to the same powers, to which they occur in N; N_2 is composed of only those prime factors of N, which divide M[1] and these occur in N_2, to the same powers to which they occur in N, and, T is composed of the remaining prime factors of N (to the same powers to which they occur in N)

Such a resolution is clearly possible

Now[6] $(N_1, N_2) = (N_2, T) = (N_1, T) = 1 \qquad (M, M') = 1$

Also $(N_1, N_2T) = (MN_1, N_2T) = (MN_1, M'N_2T) = 1$

Therefore $F(M, N) = F(M, N_1 N_2 T) = F(M, N_1)\, F(1, N_2T)$

and $F(M', N) = F(M', N_1 N_2 T) = F(M', N_2T)\, F(1, N_1)$.

$$\begin{aligned}
\text{Hence } F(M, N)\, F(M', N) &= F(M, N_1)\, F(1, N_2T)\, F(M', N_2T)\, F(1, N_1) \\
&= F(M, N_1)\, F(M', N_2T)\, F(1, N_2T)\, F(1, N_1) \\
&= F(MM', N_1N_2T)\, F(1, N_1N_2T) \\
&= F(MM', N)\, F(1, N)
\end{aligned}$$

The second part can be proved similarly.

2.2. *Lemma.*—The necessary and sufficient condition that a multiplicative function $F(M, N)$ of the two arguments M, N should be multiplicative in one of the arguments (say) M is $D_M(F) = E(N)$.

Proof—The condition is necessary, for if $F(M, N)$ is to be multiplicative in M, then $F(1, N)\, F(M, N) = F(M, N)$ by (1.1.1)

[6] (a, b) denotes the greatest common divisor of a and b

or $\qquad F(1, N) = 1 = E(N)$

(*i e*) $\qquad D_M(F) = E(N)$

The sufficiency of the condition follows from lemma 2.1 since if $D_M(F) = E(N)$, then $F(M, N)\,F(M', N) = F(MM', N)$ whenever $(M, M') = 1$.

2.3 *Lemma*—If a multiplicative function $F(M_1, M_2)$ is of the form $f(M_1)f^{-1}(M_2)$ then $\Omega F(M_1, M_2) = E_0(M)$

For, $\Omega F(M_1, M_2) = \sum_{d/M} f\left(\frac{M}{d}\right) f^{-1}(d) = f.f^{-1} = E_0(M)$

We will now derive,

3 *The new identical equation for multiplicative functions of two arguments.*

Let $F(M, N)$ be multiplicative in M and N Then $F(M, 1)\,F(1, N)$ is also multiplicative in both the arguments. We know by (1.3.4) that every multiplicative function $F(M, N)$ has an inverse $F^{-1}(M, N)$ such that $F(M, N)\cdot F^{-1}(M, N) = E_0(M, N)$.

The inverse of $F(M\ 1)\,F(1, N)$, by (1.3.6) (*d*) and (1.3.7) (*b*) is $F^{-1}(M, 1)\,F^{-1}(1, N)$ and we have

$F(M, N).F^{-1}(M, N) = E_0(M, N) = F(M, 1)\,F(1, N)\cdot F^{-1}(M, 1)\,F^{-1}(1, N)$.

Therefore by (1.3 6) (*e*)

$F(M, N) = F(M, 1)\,F(1, N)\cdot\{F^{-1}(M. 1)\,F^{-1}(1, N).F(M, N)\}$

or 3.1 $\qquad F(M, N) = F(M, 1)\,F(1, N)\cdot C(M, N)$,

where $\qquad C(M, N) = F(M, N)\cdot F^{-1}(M, 1)\,F^{-1}(1, N)$.

Now $\qquad D_M(C) = F(1, N)\cdot F^{-1}(1, N) = E_0(N)$ by (1.3.7) (*a*)

Similarly $\qquad D_N(C) = E_0(M)$.

Hence $C(M, N)$ is a cardinal function. We shall refer to $C(M, N)$ as the *cardinal component* of $F(M, N)$ and the relation 3.1, as the *identical equation* of $F(M, N)$

It easily follows from 1·4 (*a*) and (*b*) that (a) *the cardinal component of the composite of two functions is the composite of their cardinal components and* (b) *the cardinal component of the inverse of a function is the inverse of its cardinal component.*

(3.1.1) THEOREM.—*The cardinal components of a cardinal function and a principal function are identical with the functions themselves.*

For, if $F(M, N)$ is cardinal or principal, then $F(M, 1) = E_0(M)$; $F(1, N) = E_0(N)$ and therefore

$F(M, N) = E_0(M)\,E_0(N)\cdot C(M, N) = E_0(M, N)\cdot C(M, N) = C(M, N)$.

When the cardinal component $C(M, N) = E_0(M, N)$, we deduce the following important result:—

(3.1.2) THEOREM—*The necessary and sufficient condition that a multiplicative function $F(M, N)$ be a product of two functions of M, N respectively is that its cardinal component $C(M, N) = F_0(M, N)$*

Proof.—Suppose $F(M, N) = F_1(M) F_2(N)$. Then clearly $F_1(M) = F(M, 1)$ and $F_2(N) = F(1, N)$, so that

$$F(M, N) = F(M, 1) F(1, N).$$

Therefore $C(M, N) = F(M, N) F^{-1}(M, 1) F^{-1}(1, N)$

$$= F(M, 1) F(1, N) F^{-1}(M, 1) F^{-1}(1, N) = E_0(M, N).$$

The sufficiency of the condition is obvious, from 3.1

Note—It follows from the above that the *cardinal component* represents in the general case, the *deviation* of $F(M, N)$ from the product-form.

(3.1.3). *The identical equation for functions of a single-argument*—If $F(M, N)$ is a function of the product of the arguments and is equal to $f(MN)$, then the new identical equation reduces to Dr Vaidyanathaswamy's identical equation for functions of a single argument.

(3.1.4) *The Busche-Ramanujan identity for functions of a single argument.*[6]—If $F(M, N) = f(MN)$ and the cardinal component is a principal function, then the new identical equation assumes the form of a Busche-Ramanujan identity for functions of a single argument

For, if $C(M, N) = \text{princ}\ \psi$, then $F(M, N) = f(MN)$

$$= f(M) f(N) C(M, N)$$

$$= \sum_{d/M} \sum_{\delta/N} f\left(\frac{M}{d}\right) f\left(\frac{N}{\delta}\right) C(d, \delta)$$

$$= \sum_{d/M, N} f\left(\frac{M}{d}\right) f\left(\frac{N}{d}\right) \psi(d)$$

(summed for common-divisors d, of M, N), which is the form of the abovementioned identity.

3.2. *The cardinal components of the Ordinal and the Modular functions*—We will next examine the nature of the cardinal components of two important types of multiplicative functions of two arguments, *viz*. (1) the Ordinal and (2) the Modular functions.

[6] See *M.F.*, p. 646.

Definitions—A multiplicative function $f(M, N)$ is called an function, if it vanishes whenever $N > M$. M, N are called the *major* and the *minor* arguments respectively, of the ordinal function.

If a multiplicative function $f(M, N)$ has its value unaltered whenever N is increased by any multiple of M, it is said to be a *modular* function. M is called the *modulus*.

I have shown elsewhere[7] that (a) *the composite of two Ordinal functions is an Ordinal function*, and (b) *corresponding to any Modular function* f (M, N), *there exists a unique Ordinal function* ψ (M, N), (*called the* primitive *of* f) *such that* f *is the integral of* ψ *with respect to its minor argument N.*

We will assume the above results in what follows:—

(3.2.1) THEOREM *The cardinal component of an Ordinal function is itself an Ordinal function*

Proof—For, let $f(M, N)$ be an Ordinal function Then $f(1, N) = E_0(N)$ since $f(1, N) = 0$ whenever $N > 1$ The identical equation of $f(M, N)$ is, by (3 1)

$$f(M, N) = f(M, 1)\, E_0(N).C(M, N), \text{ where}$$
$$C(M, N) = f(M, N)\, f^{-1}(M, 1)\, E_0(N).$$

But $f^{-1}(M, 1)\, E_0(N)$ is an Ordinal function since if $N > M$, it implies that $N > 1$ and so the function vanishes. Hence $C(M, N)$ being the composite of two Ordinal functions is Ordinal by 3.2 (*a*).

(3.2.2) THEOREM—*The cardinal component of a Modular function is Ordinal and identical with that of its primitive*

Proof—Let $f(M, N)$ be a modular function and $\psi(M, N)$ be its primitive so that $f(M, N) = \psi(M, N).E_0(M)\, E(N)$ by 3 2 (*b*).

Now $f(1, N) = f(1, 1)$, on account of the modular character of $f(M, N)$
$= E(N)$

and $D_N(f) = D_N(\psi) \cdot D_N\{E_0(M)\, E(N)\}$ by (1.3.7) (*a*)

(*i.e*), $f(M, 1) = \psi(M, 1) \cdot E_0(M) = \psi(M, 1)$.

The identical equation of $\psi(M, N)$ is given by

$$N) = \psi(M, 1)\, E_0(N) \cdot C(M, N), \text{ where } C(M, N) \text{ is Ordinal}$$
by (3.2.1).

[7] Under publication in

Therefore $f(M, N) = \psi(M, N).E_0(M)\ E(N)$

$$= \psi(M, 1)\ E_0(N).C(M, N).E_0(M)\ E(N)$$

$$= \psi(M, 1)\ E_0(N).E_0(M)\ E(N).C(M, N)$$

$$= \psi(M, 1)\ E(N)\ C(M, N)$$

$$= f(M, 1)\ E(N)\ C(M, N)$$

Hence by (3.1) it follows that the cardinal component of f is Ordinal and identical with that of its primitive

(3.2.3) We will now give some illustrations of the identical equation: *The identical equation of the elementary function* $\delta(M, N)$ This is defined by,

$$\delta(M, N) = 1 \text{ if } N/M$$

$$= 0, \text{ otherwise}$$

It is clear that $\delta(M, N) = 0$ if $N \not> M$ and can be easily shown to be multiplicative in M, N Thus it is an Ordinal function Now, the identical equation of $\delta(M, N)$ is given by,

$$\delta(M, N) = \delta(M, 1)\ E_0(N).C(M, N)$$

$$= E(M)\ E_0(N).C(M, N).$$

Therefore $C(M, N) = \delta(M, N).\mu(M)\ E_0(N)$.

Let $\delta_{(p)}(x, y)$ be the g-series of $\delta(M, N)$ to any base p so that

$$\delta_{(p)}(x, y) = \sum_{m=0}^{\infty} \sum_{n=0}^{\infty} \delta(p^m, p^n)\, x^m y^n$$

$$= \sum_{m=0}^{\infty} x^m [1 + y + \ldots + y^m]$$

Now $\mu_{(p)}(x)\, E_0(y) = 1 - x$.

Hence $C_p(x, y) = (1 - x)\left[\sum_{m=0}^{\infty} x^m (1 + y \ldots + y^m)\right]$ See (1 3 1)

$$= 1 + xy + x^2y^2 + \ldots + x^m y^m + \ldots; \text{ on reduction}$$

$$= P_p(x, y) \text{ where } P(M, N) = \text{prime } E \text{ [ref. (1.5.1)]}.$$

Therefore $C(M, N) =$ prime E and the identical equation of $\delta(M, N)$ becomes, $\delta(M, N) = E(M)\ E_0(N)$, prime E.

NOTE.—*If* $\psi(M)$ *is the convolute of* $\delta(M_1, M_2)$, *then* ψ *represents the number of square divisors of* M.

For, $\psi(M) = \Omega\,\delta(M_1, M_2) = \Omega\,[E(M_1)\,E_0(M_2).\text{princ } E]$

$= \Omega\,E(M_1)\,E_0(M_2).\Omega \text{ princ } E$, by (1.3.3)

$= E(M)\,\lambda(M)$, where $\lambda(M) = \Omega \text{ princ } E$

$= 1$ if M is a perfect square and

$= 0$, otherwise.

$= \Sigma\lambda(d^2)$, summed for the square divisors of M

= the number of square divisors of M, since $\lambda(d^2) = 1$.

(3·2 4) *The trigonometric function T (M, N)*

T (M, N) is defined as $\sum_{h=1}^{N} e^{\frac{2\pi i h M}{N}}$ and it is well known from Trigonometry that T (M, N) = N if N/M,

= 0, otherwise.

Hence $T(M, N) = N\delta(M, N)$ and is therefore multiplicative in M, N.

The identical equation of T (M, N) is thus given by

$$T(M, N) = N\delta(M, N) = N\,[E(M)\,E_0(N)\cdot\text{princ } E]$$
$$= E(M)\,N\,E_0(N).N \text{ princ } E \text{ by (1.3.6) } (b)$$
$$= E(M)\,E_0(N) \text{ princ } I \text{ by (1.5.2) } (a)$$

It can also be easily shown that $\Omega T(M_1, M_2)$ represents the sum of the square divisors of M.

4. We will next proceed to *the applications of the identical equation to Ramanujan's trigonometric sum $C_M(N)$*

This sum is defined as $C_M(N) = \sum_h e^{\frac{2\pi i h N}{M}}$, where h runs through a complete set of residues prime to M. Ramanujan expressed $C_M(N)$ in the form

$$C_M(N) = \sum_{d/M,\,N} \mu\left(\frac{M}{d}\right) d = \sum_{d/g=(M,\,N)} \mu\left(\frac{M}{d}\right) d \qquad \text{(A)}$$

and Hardy[8] has shown that

$$C_M(N)\,C_{M'}(N) = C_{MM'}(N) \text{ whenever } (M, M') = 1$$

(*i.e.*) $C_M(N)$ is multiplicative in M.

[8] *An Introduction to the Theory of Numbers*, Hardy and Wright, p. 56, Theorem 47.

But from (A) it can be easily seen that $C_M(N)\,C_{M'}(N') = C_{MM'}(NN')$ whenever $(MN, M'N') = 1$.

Hence $C_M(N)$ is multiplicative in both the arguments. Also it is clear that $C_M(N) = C_M(N + \lambda M)$

Therefore $C_M(N)$ is a modular function

Now $C_1(N) = 1 = E(N)$ Hence from Lemma (2.2) we have $C_M(N)\,C_{M'}(N) = C_{MM'}(N)$ if $(M, M') = 1$ Thus the multiplicative property of $C_M(N)$ in M, follows as a consequence of it being a modular function.

Again, $C_M(1) = \mu(M)$ from (A) and therefore by the second part of lemma (2.1),

$$C_M(N)\,C_M(N') = \mu(M)\,C_M(NN') \text{ whenever } (N, N') = 1.$$

It is also readily seen from (A) that $C_M(N) = C_M(g)$ (B)

4.1 *The identical equation of $C_M(N)$*—Because $C_M(N)$ is a multiplicative function of two arguments, by 3 1, it satisfies an identical equation given by, $C_M(N) = C_M(1)\,C_1(N)\,C(M, N)$

$$= \mu(M)\,E(N).C(M, N)$$

$$= E^{-1}(M)\,E(N).C(M, N)$$

But the right side of relation 4. (A) is the same as $E^{-1}(M)E(N)$.princ I Hence $C(M, N) =$ princ I so that the identical equation becomes,

$$C_M(N) = E^{-1}(M)\,E(N)\cdot\text{princ I}$$

We will now derive some important properties of Ramanujan's function using its identical equation.

(4.1.1) THEOREM.—$\sum C_d(N) = M$ *if* M/N

$= 0$, *otherwise,*

the summation on the left being for all the divisors of M

Proof.—For $\sum_{d/M} C_d(N) = C_M(N).E(M)\,E_0(N)$, ref. (1.3.2)

$$= E^{-1}(M)\,F(N).\text{princ I}\;E(M)\,E_0(N)$$

$$= E^{-1}(M)\,\mathcal{L}(N)\,E(M)\,E_0(N)\cdot\text{princ I using (1.3.6) (e)}$$

$$= E_0(M)\,E(N).\text{princ I}$$

$$= \sum_{d/M,\,N} E_0\left(\frac{M}{d}\right) E\left(\frac{N}{d}\right) d$$

$= M$ if M/N and 0, otherwise,

(4 1.2). THEOREM —$\Sigma C_M(r) = E_0(M)$, *where r runs through a complete set of residues mod. M.*

Proof.—We have seen, 4 (B) that $C_M(N) = C_M(g)$. Now, let $t_1 = 1, t_2, t_3 \ldots, t_k = M$ be the distinct divisors of M. Then Dr. Vaidyanathaswamy[*] has shown that the integers 1, 2,. . . .M can be divided into classes $C_1, \ldots, C_k$ such that C_i contains those numbers whose g.c.d. with M is t_i. The class C_i will contain $\phi\left(\frac{M}{t_i}\right)$ numbers, (ϕ being Euler's function).

Now $\sum_r C_M(r) = \sum_{g=1}^{M} C_M(r)$

Hence $\sum_r C_M(r) = \sum_{d/M} C_M(d)\,\phi\left(\frac{M}{d}\right) = \psi(M, M)$, where

$$\psi(M, N) = C_M(N).E_0(M)\,\phi(N) = E^{-1}(M)\,E(N)\ \text{princ I}\ E(M)\,\phi(N)$$

or $$\psi(M, N) = E^{-1}(M)\ [(\phi\, E)(N)].\text{princ I}$$

$$= \mu(M)\, I(N)\ \text{princ I} = \sum_{d/M,\,N} \mu\left(\frac{M}{d}\right)\frac{N}{d}\, d$$

$$= N \sum_{d/M,\,N} \mu\left(\frac{M}{d}\right)$$

Hence $\psi(M, M) = M \sum_{d/M} \mu\left(\frac{M}{d}\right) = M\,[E^{-1}.E] = M\,[E_0(M)] = E_0(M)$

Thus $\sum_r C_M(r) = E_0(M)$.

(4 1.3) THEOREM. *The inverse of $C_M(N)$ is a modular function with N as the modulus and satisfies the relation* $C_M^{-1}(N) = \sum_{d/M,\,N} \mu\left(\frac{N}{d}\right)\mu(d)\, d$

Proof—For, $C_M^{-1}(N) = [E^{-1}(M)\,E(N)\cdot\text{princ I}]^{-1}$

$$= [E^{-1}(M)\,E(N)]^{-1}\cdot(\text{princ I})^{-1} \text{ by (1.3.6) (c)}$$

$$= F(M)\,\mu(N)\ \text{princ I}^{-1} \text{ by (1.5.2) (b)}$$

or $$C_M^{-1}(N) = \sum_{d/M,\,N} \mu\left(\frac{N}{d}\right)\mu(d)\, d, \qquad \text{See (1.3.5)}$$

$$= \sum_{d/g=(M,\,N)} \mu\left(\frac{N}{d}\right)\mu(d)\, d$$

It follows that

$$C_M^{-1}(N) = C_{M+\lambda N}^{-1}(N) \text{ since } (M, N) = g = (M + \lambda N, N)$$

Thus $C_M^{-1}(N)$ has the modulus N.

---

* "A Remarkable property of the integers Mod. N and its bearing on Group-Theory," *Proc. Ind. Acad. Sci.*, 1937, 5, 63–75.

ERRATA

Vol XXIV, No 5, November 1946

Page 394 Equation (4*a*) *for* $\frac{\partial \rho}{\partial t}$ *read* $\frac{d\rho}{dt}$

Page 473 5th line from the top *for* $\frac{\partial \rho}{\partial u}$ *read* $\frac{\partial \rho}{\partial x}$.

7th line from the top *for* $\frac{\partial p}{\partial p}$ *read* $\frac{\partial p}{\partial y}$

7th line from the top *for* $\frac{\partial T}{\partial p}$ *read* $\frac{\partial T}{\partial y}$

(4.1.4) THEOREM

$$\sum_{d|M} C_{\frac{M}{d}}(d) = +\sqrt{M} \text{ if } M \text{ is a perfect square,}$$
$$= 0, \text{ otherwise}$$

Proof—For, $\sum_{d|M} C_{\frac{M}{d}}(d) = \Omega\, C_{M_1}(M_2) = \Omega\,[E^{-1}(M_1)\, E(M_2).\text{princ } 1]$

$= \Omega\, E^{-1}(M_1)\, E(M_2)\ \Omega \text{ princ } 1$ by (1.3.3)

$= E_0(M)\ \Omega \text{ princ } 1$ using lemma 2.3

$= \Omega \text{ princ } 1$

$= d$ if $\frac{M}{d} = d$, and 0, otherwise

Hence the result

1189-46. Printed at The Bangalore Press, Bangalore City, by S. Srinivasa Rao, Superintendent
and Published by The Indian Academy of Sciences, Bangalore

INDEX TO VOL. XXIV (A)

AUTHORS' INDEX

Achyuthan, K.	Local variations in the photoconductivity of diamond, 162
Adarkar, S. P.	*See* Hattiangdi and Adarkar
Ananthakrishnan, R.	On fluctuations of pressure and temperature in the atmosphere, 393
Bhargawa, P. N. .	Chemical examination of the fixed oil derived from the wood of *Pterocarpus Marsupium* Roxb., I, II, 496, 501
	Chemical examination of the unsaponifiable matter of the fat from the fleshy arils of *Celastrus paniculata*, 506.
Bhatnagar, G. S., and Pandya, K. C.	Condensation of aldehydes with amides, XII, 487
Chandrasekharan, K.	On multiple Fourier series, 229
Chandrasekharan, V. .	*See* Ramachandran and Chandrasekharan.
	Phosphorescence patterns in diamond, 182
	The thermoluminescence of diamond, 187
	The phosphorescence of diamond, 193
Desai, R. D., and Waravdekar, W. S.	Studies in the naphthalene series, XI, XII, XIII, XIV, 332, 333, 382, 389
Dharmatti, S. S.	*See* Prasad and others
Doss, K. S. Gururaja ..	*See* Krishnappa and others
	See Rao and others
Gupta, Hansraj .	A congruence property of τ (n), 441
Hattiangdi, G. S. ..	*See* Prasad and others
Hattiangdi, G. S., and Adarkar, S. P.	Studies in inorgano-organic gels in pinene, VI, 295.
Kamath, I. S. ..	*See* Solanki and Kamath
Karmarkar, K. R. ..	*See* Narlikar and Karmarkar.
Karunakaran, C., and Neelakantan, K.	Determination of magnesium and residual manganese in rocks and minerals with 8-hydroxy-quinoline, 448.
Karve, D. D., and Kelkar, B. W.	Kinetics of the hydrolysis of anilides, 254.
Kelkar, B. W. ..	*See* Karve and Kelkar.

Krishnamurti, G. V., and Seshadri, T. R. — The bitter principle of *Phyllanthus niruri*, 357.

Krishnan, R. S. .. — The second order Raman spectrum of diamond, 25.
Thermal expansion of diamond, 33.
Temperature variations of the Raman frequencies in diamond, 45.

Krishnappa, T., Doss, K. S. Gururaja, and Rao, Basrur Sanjiva — Equilibrium surface tension of aqueous solutions of nekal BX and the effect of salts, 261.

Mahadevan, C. .. — X-ray studies of peaty lignites and anthracitic coals, 216

Mandan, Sahib Ram . — Umbilical projection, 433.

Menon, P Kesava .. — Some congruence properties of the ϕ-function, 443.

Murti, V. V Sreerama, Row, L Ramachandra and Seshadri, T R — 5 6 · 7 8-hydroxyflavonols, Part II, 233.

Narlikar, V V, and Karmarkar, K R — Conditions of plane orbits in classical and relativistic fields, 451

Neelakantam, K — *See* Karunakaran and Neelakantam.

Pandya, K C. . — *See* Bhatnagar and Pandya

Prasad, B B — Production of *Joshi-Effect* under *Uni-* and *Bi-*electrode excitation, 514.

Prasad, Mata, Dharmatti, S. S, and Hattiangdi, G S — Studies in inorgano-organic gels in pinene, V, 287.

Rajagopalan, C . — Studies in charnockites from St. Thomas Mount, Madras, I, 315

Ramachandran, G N. — On the crystal symmetry of diamond and its X-ray reflections, 58.
On the nature and origin of the laminations observed in diamond, 65.
The luminescence of diamond excited by X-radiation, 81.
X-ray topographs of diamond, Part II, 95.

Ramachandran, G. N, and Chandrasekharan, V — Luminescence as "Forbidden" electronic transitions in diamond, 176.

Ramanathan, K. G .. — Variations in the absorption of infra-red radiation by diamond, 130.
The absorption of ultra-violet radiation by diamond, 137.

	The absorption spectrum of diamond in the visible region, 145.
	The infra-red absorption spectrum of diamond, 150.
Raman, C V., and Ramaseshan, S	The crystal forms of diamond and their significance, I.
Ramaseshan, S.	The Faraday effect in diamond, 104
	The cleavage properties of diamond, 114
	A theory of the crystal forms of diamond, 122.
	See Raman and Ramaseshan
	Determination of the magneto-optic anomaly of some glasses, 426
Rao, Basrur Sanjiva .	*See* Krishnappa and others
	See Rao and others
Rao, G. N Subba, Doss, K. S Gururaja, and Rao, Basrur Sanjiva	Aging of surfaces of solutions, VI, 277
Rao, K. Visweswara, and Seshadri, T R.	Colouring matter of the flowers of *Hibiscus vitifolius*, 352
Rao, M. Srirama	Geology and petrography of the Bezwada and Kondapalle hill ranges, I, 199
Rao, M Visweswara	Overtone and combination lines in the Raman spectrum of chloroform, 510
Rao, N. V. Subba, and Seshadri, T. R.	Chemical examination of plant insecticides, I, II, III, 344, 365, 465
Rao, P Ramachandra, and Seshadri, T. R	Constitution of populnin, 456
Rendall, G. R. .	Geometric patterns of fluorescence in diamond, 168.
Row, L. Ramachandra	*See* Murti and others
Sastri, V. D. Nageswara, and Seshadri, T R	5 . 6 7 8-hydroxyflavonols, Part III, 238
	Synthesis of 5 · 7 8-hydroxyflavones and their derivatives, 243
Seshadri, T. R. .	*See* Murti and others.
	See Sastri and Seshadri
	See Rao and Seshadri
	See Krishnamurti and Seshadri
Seshadri, T. R., and Venkateswarlu, V.	5 . 6 · 7 : 8-hydroxy-flavonols, IV, 349
Sulanki, D. N., and Kamath, L. S.	The electrolytic preparation of hydrogen peroxide, I, 305.

Venkataraman, C. S. — A new identical equation for multiplicative functions of two arguments and its applications to Ramanujan's sum C_M (N), 518.

Venkateswarlu, P. — A new band system (Cordes bands) of iodine, 473 Emission bands of halogens, I, 480.

Venkateswarlu, V. — *See* Seshadri and Venkateswarlu.

Waravdekar, W. S. — *See* Desai and Waravdekar.

TITLE INDEX

Aldehydes, condensation, with amides, XII (Bhatnagar and Pandya), 487

Anilides, hydrolysis, Kinetics (Karve and Kelkar), 254.

Atmosphere, fluctuations of pressure and temperature (Ananthakrishnan), 393.

Bezwada and Kondapalle hill ranges, geology and petrography, I (Rao), 199

Celastrus paniculata, fleshy arils, unsaponifiable matter from, chemical examination (Bhargava), 506.

Charnockites from St Thomas Mount, Madras, studies, I (Rajagopalan), 315.

Coals, peaty lignites and anthracitic, X-ray studies (Mahadevan), 216.

Congruence properties, some, of the ϕ-function (Menon), 443

Congruence property of τ (*n*) (Gupta), 441

Diamond, absorption of infra-red radiation, variations (Ramanathan), 130.

Diamond, absorption of the ultra-violet radiation (Ramanathan), 137

Diamond, absorption spectrum, in the visible region (Ramanathan), 145.

Diamond, a theory of the crystal forms (Ramaseshan), 122

Diamond, fluorescence, geometric patterns (Rendall), 168.

Diamond, infra-red absorption spectrum (Ramanathan), 150

Diamond, luminescence as "forbidden" electronic transitions (Ramachandran and Chandrasekharan), 176.

Diamond, luminescence, excited by X-radiation (Ramachandran), 81.

Diamond, phosphorescence (Chandrasekharan), 193.

Diamond, phosphorescence patterns (Chandrasekharan), 182.

Diamond, photoconductivity, local variations (Achyutan), 162.

Diamond, Raman frequencies, temperature variations (Krishnan), 45.

Diamond, the cleavage properties (Ramaseshan), 114

Diamond, the crystal forms, and their significance (Raman and Ramaseshan), 1.

Diamond, the crystal symmetry, and its X-ray reflections (Ramachandran), 58.

Diamond, the Faraday effect (Ramaseshan), 104.

Diamond, the laminations observed, on the nature and origin (Ramachandran), 65.

Diamond, thermal expansion (Krishnan), 33.

Diamond, thermo-luminescence (Chandrasekharan), 187

Diamond, the second order Raman spectrum (Krishnan), 25

Diamond, X-ray topographs, II (Ramachandran), 95

Flavones, 5 , 7 8-hydroxy-, synthesis and their derivatives (Sastri and Seshadri), 243

Flavonols, 5 6 7 8-hydroxy-, II (Murti and others), 233, III (Sastri and Seshadri), 238, IV (Seshadri and Venkateswarlu), 349

Gels, inorgano-organic, in pinene, studies, V (Prasad and others), 287, VI, (Hattiangdi and Adarkar), 295

Glasses, some, magneto-optic anomaly, determination (Ramaseshan), 426

Gossypin, constitution, I (Rao and Seshadri), 375

Halogens, emission bands, I (Venkateswarlu), 480

Hibiscus vitifolius, flowers, colouring matter (Rao and Seshadri), 352

Hydrogen peroxide, the electrolytic preparation, I (Solanki and Kamath), 305.

Iodine, a new band system (Cordes bands) of (Venkateswarlu), 473

Joshi-effect, production, under *uni-* and *bi*-electrode excitation (Prasad), 514

Magnesium and residual manganese, determination, in rocks and minerals with 8-hydroxy-quinoline Karunakaran and Neelakantam), 448

Multiple Fourier series (Chandrasekharan), 229

Multiplicative functions of two arguments, a new identical equation, and its applications to Ramanujan's sum C_m (N) (Venkataraman), 518

Naphthalene series, studies, XI, XII, XIII, XIV (Desai and Waravdekar), 332, 333, 382, 389

Phyllanthus niruri, the bitter principle (Krishnamurti and Seshadri), 357

Plane orbits, conditions, in classical and relativistic fields (Narlikar and Karmarkar), 451.

Plant insecticides, chemical examination, I, II, III (Rao and Seshadri), 344, 365, 465

Populnin, constitution (Rao and Seshadri), 456

Pterocarpus marsupium Roxb , wood, fixed oil derived from, chemical examination, I, II (Bhargava), 496, 501

Raman spectrum of chloroform, overtone and combination lines (Rao), 510

Surfaces, aging, of solutions (Rao and others), 277.

Surface tension, equilibrium, of aqueous solutions of nekal BX and the effect of salts (Krishnappa and others), 261.

Umbilical projection (Mandan), 433.